

# Enones in Visible Light Photocatalysis

By

Juana Du

A dissertation submitted in partial fulfillment of  
the requirements for the degree of

Doctor of Philosophy

(Chemistry)

at the

UNIVERSITY OF WISCONSIN-MADISON

2012

Date of final oral examination: 05/14/12

The dissertation is approved by the following members of the Final Oral Committee:

Tehshik P. Yoon, Associate Professor, Chemistry

Clark R. Landis, Professor, Chemistry

Eric R. Strieter, Assistant Professor, Chemistry

Samuel H. Gellman, Professor, Chemistry

Shannon S. Stahl, Professor, Chemistry

## Enones in Visible Light Photocatalysis

Juana Du

Under the supervision of Professor Tehshik P. Yoon

at the University of Wisconsin–Madison

Our group is interested in the development of synthetically useful methodology that employs transition metal complexes in visible light photocatalysis. The research herein describes the design and discovery of several transformations that are promoted by visible light. These include the development of an intermolecular crossed [2+2] cycloaddition of acyclic enones, which is achieved because the problematic *cis-trans* isomerization of these acyclic substrates is circumvented by the use of visible light, and the design of a photocatalytic reductive cyclization of enones that does not generate free radicals via the conventional route of reductive dehalogenation. The inability of organic molecules to absorb wavelengths of visible light has also been utilized as an effective mechanism for disabling the problematic racemic background reaction in asymmetric photocatalysis. Promising conditions for the chiral Lewis acid-mediated crossed [2+2] cycloaddition have been developed for the synthesis of chiral cyclobutanes. The underlying motivation for the work described in this thesis has been the potential for exploiting the transparency of organic molecules to wavelengths of visible light as a means for enabling novel reactivity that is not readily accessible using current thermal or photochemical methods.

## Acknowledgements

I would like to begin by thanking my advisor, Prof. Tehshik Yoon, for all that he has taught me these past five years. The enthusiasm and scientific rigor with which he approaches science has been infectious; combined with the freedom he has given me to ask my own questions, graduate school has been a true learning experience. His (blind!) faith in me has been both confounding and humbling. It has given me the courage to think seriously about dreams that I never dared to consider before and inspired me to work harder to make them a reality. Under his guidance, I have learned just as much from my mistakes as I have from my successes. I could not have asked for a better mentor and I have known that my entire graduate career. Thank you.

I would also like to thank Prof. Shannon Stahl and Prof. Clark Landis. Their insightful comments, words of advice, and unwavering support have been instrumental to my growth as a graduate student. They are the reasons that I still hope to become a little bit of an organometallic chemist one day. I would also like to thank Prof. Sam Gellman and Prof. Eric Strieter for taking the time to be on my thesis committee.

I would be remiss if I didn't thank the person who started all of my scientific endeavors, Prof. Bob Bergman, my undergraduate advisor at UC Berkeley and my "real-life chemistry hero." Through his actions, Bob has instilled in me an obligation to curiosity, a dedication to excellence, and a commitment to success achieved with kindness and grace. He was the first to know that I would be okay in graduate school, and has held on to some really big dreams for me until I was able to make them my own. Thank you, Bob, for changing my life.

I would also like to thank Dr. Tamas Benkovics. He was my mentor in graduate school and my mentor for the Midwest; I would not have made it in either without him. I would also like to thank the rest of the Yoon group, members both past and present. I'm glad we're not an overly sentimental bunch, but it has truly been a privilege to work with each of you and made for an unforgettable five years.

The individuals who run our research facilities will always have my deepest gratitude. I have personally gone to Charlie and Monika with NMR samples of mystery structures that needed elucidation, to Ilia with unknown compounds of dubious crystal-like properties, and to Martha with vials of last things that I needed for papers. They have always been able to help and their talent and patience made conducting research immeasurably easier.

Finally, I would like to dedicate this thesis to my parents, who think that five years was a really long time to spend "making drugs in Wisconsin" and becoming "not a real doctor." They obviously have no idea what I did in graduate school, but without them, none of it could have been done.



## Table of Contents

|  |     |
|--|-----|
| <b>Abstract</b>  | i   |
| <b>Acknowledgements</b>                                    | ii  |
| <b>Table of Contents</b>                                   | iv  |
| <b>List of Figures</b>                                     | ix  |
| <b>List of Schemes</b>                                     | x   |
| <b>List of Tables</b>                                      | xiv |
| <b>Chapter 1. Strategies for Asymmetric Photocatalysis</b> | 1   |
| 1.1 Introduction   | 2   |
| 1.2 Circularly polarized light (CPL)                       | 5   |
| 1.2.1 Asymmetric photodestruction                          | 6   |
| 1.2.2 Photochemical deracemization                         | 7   |
| 1.2.3 Enantioselective photofixation                       | 7   |
| 1.2.4 Concluding remarks                                   | 8   |
| 1.3 Chiral auxiliaries                                     | 9   |
| 1.3.1 [2+2] Cycloaddition                                  | 10  |
| 1.3.2 Paternò–Büchi reaction                               | 12  |
| 1.3.3 Concluding remarks                                   | 13  |
| 1.4 Chiral complexing agents                               | 13  |
| 1.4.1 Cyclodextrins  | 14  |
| 1.4.2 Biomolecules   | 15  |
| 1.4.3 Chiral small molecules                               | 15  |

|   |    |
|---|----|
|   | v  |
| 1.4.3.1 Non-covalent small molecule chiral templates  | 17 |
| 1.4.3.2 Hydrogen-bonding chiral lactam templates  | 18 |
| 1.4.4 Concluding remarks  | 24 |
| 1.5 Photosensitizers  | 25 |
| 1.6 Future directions and concluding remarks  | 28 |
| 1.7 References  | 29 |
| <b>Chapter 2. Lewis Acid-Mediated Photocatalysis: Intermolecular [2+2] Enone Cycloadditions Using Visible Light</b> | 37 |
| 2.1 Introduction  | 38 |
| 2.2 Results and discussion  | 43 |
| 2.2.1 Intermolecular [2+2] homodimerization of acyclic enones   | 43 |
| 2.2.2 Crossed intermolecular [2+2] cycloadditions of acyclic enones   | 43 |
| 2.3 Conclusions   | 49 |
| 2.4 Contributions   | 50 |
| 2.5 Experimental  | 50 |
| 2.5.1 General information   | 50 |
| 2.5.2 General procedures  | 51 |
| 2.5.3 Synthesis and characterization of new compounds   | 51 |
| 2.5.4 Large scale photocycloaddition with ambient sunlight  | 64 |
| 2.5.5 NOE correlations  | 64 |
| 2.6 References  | 64 |

|   |     |
|---|-----|
| <b>Chapter 3. Brønsted Acid-Mediated Photocatalysis: Reductive Cyclizations of Enones Using Visible Light</b> | 70  |
| 3.1 Introduction  | 71  |
| 3.2 Results and discussion  | 74  |
| 3.3 Conclusions   | 85  |
| 3.4 Contributions   | 86  |
| 3.5 Experimental  | 87  |
| 3.5.1 General information   | 87  |
| 3.5.2 General procedures  | 87  |
| 3.5.3 Synthesis and characterization of new compounds   | 88  |
| 3.5.4 Stereochemical assignments  | 125 |
| 3.6 References  | 126 |
| <b>Chapter 4. Chiral Lewis Acids in Visible Light Photocatalysis: Enantioselective [2+2] Cycloadditions</b>   | 132 |
| 4.1 Introduction  | 133 |
| 4.2 Results and discussion  | 134 |
| 4.2.1 Lewis acid and ligand screening of intramolecular [2+2] cycloaddition                                   | 134 |
| 4.2.2 Optimization of intermolecular [2+2] cycloaddition with acyl imidazole <b>4-11</b>                      | 138 |
| 4.2.3 Identification of aryl enone for intermolecular crossed [2+2] cycloaddition                             | 142 |
| 4.2.4 Ligand screening with 2-furyl enone <b>4-24</b> in crossed [2+2] cycloaddition                          | 144 |
| 4.2.5 Optimization of intermolecular [2+2] cycloaddition with phenyl enone <b>4-23</b>                        | 146 |

|   |     |
|---|-----|
| 4.2.5.1 Lewis acid and ligand optimization  | 146 |
| 4.2.5.2 Reaction optimization and scope of cycloaddition  | 149 |
| 4.2.6 Optimization of peptide ligands for intermolecular [2+2]<br>cycloaddition                     | 151 |
| 4.3 Conclusions and future outlook  | 155 |
| 4.4 Experimental  | 156 |
| 4.4.1 General considerations  | 156 |
| 4.4.2 Representative procedure  | 156 |
| 4.4.3 Reaction optimization data  | 157 |
| 4.4.4 Characterization of new compounds   | 160 |
| 4.5 References  | 160 |
| <b>Appendix A. Anion-Accelerated Copper-Catalyzed Aminohydroxylation:<br/>Mechanistic Insights</b>  | 163 |
| A.1 Introduction  | 164 |
| A.2 Results and discussion  | 165 |
| A.3 Conclusions   | 169 |
| A.4 Contributions   | 169 |
| A.5 Experimental  | 170 |
| A.5.1 General information   | 170 |
| A.5.2 Synthesis and characterization of new compounds   | 170 |
| A.6 References  | 176 |
| <b>Appendix B. <math>^1\text{H}</math> and <math>^{13}\text{C}</math> Spectra for New Compounds</b> | 178 |
| List of compounds from Chapter 2  | 179 |

|  |      |
|--|------|
|  | viii |
| List of compounds from Chapter 3               | 196  |
| List of compounds from Chapter 4               | 248  |
| List of compounds from Appendix A              | 250  |
| <b>Appendix C. SFC Traces of New Compounds</b> | 258  |
| <b>Appendix D. X-Ray Crystallographic Data</b> | 264  |
| <b>2-15</b>                                    | 266  |
| <b>3-15</b>                                    | 276  |

## List of Figures

### Chapter 1

- Figure 1-1.** Equation for the anisotropy factor,  $g_s$  5
- Figure 1-2.** Recent examples of chiral templates in asymmetric photoreactions 17
- Figure 1-3.** Chiral lactam template structure 18

### Chapter 3

- Figure 3-1.** Incompatible aliphatic enone substrates for reductive cyclization 80
- Figure 3-2.** Incompatible aryl enone substrates for reductive cyclization 81

### Chapter 4

- Figure 4-1.** Enone structures for crossed [2+2] cycloaddition 143
- Figure 4-2.** Effect of ligand structure on the crossed [2+2] cycloaddition with 2-furyl enone **4-24** 145
- Figure 4-3.** Aryl enone scope of [2+2] photocycloaddition using aminoindanol **4-45** 151
- Figure 4-4.** Sites of modification for dipeptide ligand 152
- Figure 4-5.** Substrate scope of [2+2] photocycloaddition using peptide ligand **4-55** 155

## List of Schemes

### Chapter 1

|  |    |
|--|----|
| <b>Scheme 1-1.</b> First example of an asymmetric photochemical process  | 3  |
| <b>Scheme 1-2.</b> Asymmetric photodestruction of ( $\pm$ )-camphor with R-CPL   | 7  |
| <b>Scheme 1-3.</b> Photofixation of helicenes to afford bis(aryl) arenes   | 8  |
| <b>Scheme 1-4.</b> Chiral auxiliary-assisted intermolecular [2+2] photocycloaddition   | 10 |
| <b>Scheme 1-5.</b> Chiral lactam auxiliary approach for the total synthesis of (–)-grandisol ( <b>1-17</b> )                                   | 11 |
| <b>Scheme 1-6.</b> Chiral menthone auxiliary approach for the total synthesis of (+)-grandisol ( <b>1-22</b> )                                 | 11 |
| <b>Scheme 1-7.</b> Chiral allene-enone intramolecular [2+2] photocycloadditions  | 12 |
| <b>Scheme 1-8.</b> Phenylglyoxylate auxiliary approach for the synthesis of (+)- $\beta$ -L-apio-L-furanoside ( <b>1-30</b> )                  | 13 |
| <b>Scheme 1-9.</b> Cyclodextrins as chiral hosts for [4+4] photocycloaddition  | 14 |
| <b>Scheme 1-10.</b> Biomolecules as chiral hosts for [4+4] photocycloaddition  | 15 |
| <b>Scheme 1-11.</b> Competitive racemic and stereoselective pathways in catalytic photoreactions   | 16 |
| <b>Scheme 1-12.</b> TADDOL-mediated enantioselective [3+2] photocycloaddition  | 18 |
| <b>Scheme 1-13.</b> Diastereoselective Paternò–Büchi reaction of chiral lactam template  | 19 |
| <b>Scheme 1-14.</b> Enantioselective intramolecular [2+2] photocycloaddition reactions mediated by a chiral lactam host                        | 20 |
| <b>Scheme 1-15.</b> Chiral template-mediated enantioselective [2+2] photocycloaddition in the total synthesis of (+)-meloscine ( <b>1-55</b> ) | 21 |
| <b>Scheme 1-16.</b> Catalytic enantioselective photochemical reaction driven by photoinduced electron transfer                                 | 22 |

|   |    |
|---|----|
| <b>Scheme 1-17.</b> Catalytic enantioselective [2+2] photocycloaddition using chiral receptor-sensitizer template <b>1-60</b> | 23 |
| <b>Scheme 1-18.</b> Catalytic enantioselective photoreaction using chiral sensitizer-template <b>1-64</b>                     | 23 |
| <b>Scheme 1-19.</b> Amino acid-catalyzed $\alpha$ -oxygenation of aldehydes with $^1\text{O}_2$                               | 26 |
| <b>Scheme 1-20.</b> Amino acid-catalyzed $\alpha$ -oxygenation of ketones with $^1\text{O}_2$                                 | 27 |
| <b>Scheme 1-21.</b> Visible light-promoted enantioselective $\alpha$ -alkylation of aldehydes                                 | 27 |
| <b>Scheme 1-22.</b> Enantioselective Lewis acid-mediated [2+2] photocycloaddition   | 29 |

## Chapter 2

|  |    |
|--|----|
| <b>Scheme 2-1.</b> First reported example of a photochemical [2+2] enone cycloaddition   | 38 |
| <b>Scheme 2-2.</b> Key [2+2] photocycloaddition in the synthesis of cubane ( <b>2-5</b> )  | 39 |
| <b>Scheme 2-3.</b> Synthesis of the caryophyllenes ( <b>2-9–2-10</b> ) using an intermolecular [2+2] photocycloaddition strategy | 39 |
| <b>Scheme 2-4.</b> Visible light photocatalysis of intramolecular [2+2] bis(enone) cycloadditions                                | 41 |
| <b>Scheme 2-5.</b> Proposed mechanism for [2+2] cycloaddition promoted by visible light  | 42 |
| <b>Scheme 2-6.</b> Intermolecular dimerization of aryl enones via visible light photocatalysis                                   | 43 |
| <b>Scheme 2-7.</b> Design considerations for crossed [2+2] photocycloaddition  | 44 |
| <b>Scheme 2-8.</b> Crossed intermolecular [2+2] cycloadditions via visible light photocatalysis                                  | 45 |
| <b>Scheme 2-9.</b> Unproductive reactivity upon UV irradiation of enones <b>2-18</b> and <b>2-19</b>                             | 48 |
| <b>Scheme 2-10.</b> Crossed intermolecular [2+2] cycloaddition using ambient sunlight  | 49 |



## Chapter 3

|  |    |
|--|----|
| <b>Scheme 3-1.</b> Single-electron mediated $\alpha$ -alkylation of aldehydes using organocatalysis and photoredox catalysis | 71 |
| <b>Scheme 3-2.</b> Reductive dehalogenation of alkyl halides using visible light photocatalysis                              | 72 |
| <b>Scheme 3-3.</b> Visible light-promoted addition of glycosyl halides to alkenes  | 72 |
| <b>Scheme 3-4.</b> Dual reactivity manifolds in visible light photocatalysis   | 73 |
| <b>Scheme 3-5.</b> Unproductive reductive cyclization of aryl enones to styrenes via the enol tautomer                       | 81 |
| <b>Scheme 3-6.</b> Intermolecular reductive coupling of aryl enones  | 82 |
| <b>Scheme 3-7.</b> Subjection of <i>cis</i> cyclobutane to Brønsted acid conditions for reductive cyclization                | 83 |
| <b>Scheme 3-8.</b> Deuterium labeling control experiments  | 84 |
| <b>Scheme 3-9.</b> Proposed mechanism for photocatalytic reductive cyclization   | 85 |

## Chapter 4

|   |     |
|---|-----|
| <b>Scheme 4-1.</b> Design of chiral Lewis acid-mediated [2+2] asymmetric photocycloaddition promoted by visible light               | 134 |
| <b>Scheme 4-2.</b> Photocatalytic intramolecular [2+2] cycloadditions of acyl imidazole <b>4-1</b>                                  | 135 |
| <b>Scheme 4-3.</b> Crossed intermolecular [2+2] photocycloaddition of imidazole <b>4-11</b> and methyl vinyl ketone ( <b>4-12</b> ) | 138 |
| <b>Scheme 4-4.</b> Schiff base ligands in crossed [2+2] cycloaddition with phenyl enone <b>4-23</b>                                 | 147 |

## Appendix A

|   |     |
|---|-----|
| <b>Scheme A-1.</b> Cu(TFA) <sub>2</sub> -catalyzed aminohydroxylation of olefins    | 164 |
| <b>Scheme A-2.</b> Mechanistic pathways for copper(II)-catalyzed aminohydroxylation | 165 |

|  |     |
|--|-----|
| <b>Scheme A-3.</b> Trapping experiment with CBr <sub>4</sub> ( <b>A-5</b> )  | 167 |
| <b>Scheme A-4.</b> Radical trapping experiments with cyclopropane <b>A-8</b> | 168 |

## List of Tables

### Chapter 2

|  |    |
|--|----|
| <b>Table 2-1.</b> Effect of aryl enone structure in photocatalytic crossed cycloadditions with methyl vinyl ketone ( <b>2-19</b> ) | 46 |
| <b>Table 2-2.</b> Effect of Michael acceptor structure in photocatalytic crossed cycloadditions with phenyl enone <b>2-18</b>      | 47 |

### Chapter 3

|   |    |
|---|----|
| <b>Table 3-1.</b> Effect of Brønsted acids on the reductive cyclization of bis(enone) <b>3-16</b> | 75 |
| <b>Table 3-2.</b> Scope of reductive cyclizations initiated by aryl enones                        | 77 |
| <b>Table 3-3.</b> Scope of reductive cyclizations initiated by aliphatic enones                   | 79 |

### Chapter 4

|   |     |
|---|-----|
| <b>Table 4-1.</b> Cycloaddition of imidazole <b>4-1</b> with 20 mol% Lewis acid   | 136 |
| <b>Table 4-2.</b> Cycloaddition of imidazole <b>4-1</b> with sub-stoichiometric amounts of chiral Lewis acid                                  | 137 |
| <b>Table 4-3.</b> Crossed [2+2] cycloaddition of 2-acyl imidazole <b>4-11</b> and methyl vinyl ketone ( <b>4-12</b> ) with 20 mol% Lewis acid | 139 |
| <b>Table 4-4.</b> Chiral shift reagents in the crossed [2+2] cycloaddition  | 140 |
| <b>Table 4-5.</b> Effect of the identity of the Lewis acid with Bn-pybox <b>4-14</b> in the crossed [2+2] cycloaddition                       | 141 |
| <b>Table 4-6.</b> Effect of ligand structure on the crossed [2+2] cycloaddition   | 142 |
| <b>Table 4-7.</b> Effect of oxazoline ligand structure on the crossed [2+2] cycloaddition with 2-furyl enone <b>4-24</b>                      | 144 |
| <b>Table 4-8.</b> Effect of steric and electron ligand perturbations on enantioselectivity  | 147 |
| <b>Table 4-9.</b> Effect of amino alcohol structure on enantioselectivity   | 148 |

|   |     |
|---|-----|
| <b>Table 4-10.</b> Effect of ligand to Lewis acid ratio on enantioselectivity                 | 149 |
| <b>Table 4-11.</b> Effect of Lewis acid identity on enantioselectivity                        | 150 |
| <b>Table 4-12.</b> Effect of AA <sub>1</sub> on enantioselectivity                            | 153 |
| <b>Table 4-13.</b> Effect of AA <sub>2</sub> on enantioselectivity                            | 154 |
| <b>Table 4-14.</b> Effect of solvent identity on enantioselectivity                           | 157 |
| <b>Table 4-15.</b> Effect of base on enantioselectivity                                       | 158 |
| <b>Table 4-16.</b> Effect of photocatalyst on enantioselectivity                              | 158 |
| <b>Table 4-17.</b> Effect of temperature on enantioselectivity                                | 159 |
| <b>Table 4-18.</b> Effect of steric and electronic ligand perturbations on enantioselectivity | 159 |

## Appendix A

|   |     |
|---|-----|
| <b>Table A-1.</b> Effect of additives on copper-catalyzed aminohydroxylation using 3,3-dialkyl oxaziridine <b>A-3</b> | 166 |
|---|-----|

## **Chapter 1. Strategies for Asymmetric Photocatalysis**

## 1.1 Introduction

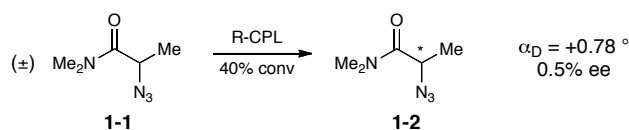
Light is an attractive reagent for chemical synthesis. Its potential as a renewable source of clean energy has been recognized for decades; the ability of sunlight to induce chemical reactivity in organic molecules was central to Ciamician's early articulation of the principles of "green chemistry" in 1912.<sup>1</sup> Photochemical processes also provide access to modes of reactivity that are often complementary to those of ground state processes, thereby enabling the construction of molecular scaffolds that would otherwise be difficult to synthesize using conventional thermal methods. As a result, the most straightforward synthetic routes to highly strained structural motifs such as cyclobutanes and oxetanes are generally photochemical processes. Thus, the development of efficient photochemical methodology continues to attract considerable interest from the synthetic community.

Because the chemical characteristics of biologically and pharmaceutically relevant molecules depend upon their three-dimensional structure, the subject of absolute and relative stereocontrol is of fundamental relevance to the development of synthetically useful methods. Asymmetric catalysis, which employs small amounts of a chiral reagent, is a particularly efficient strategy for the preparation of enantiomerically enriched compounds. Significant progress has been made in the discovery, design, and development of highly enantioselective reactions over the past several decades.<sup>2</sup> However, the vast majority of catalytic asymmetric processes reported to date are *thermally allowed* reactions; enantioselective catalytic *photochemical* transformations are relatively rare. Given that photochemical reactions enable access to novel molecular frameworks that are often difficult to obtain using thermal transformations and that the

benefits of employing light as a reagent are well established, the limited number of catalytic asymmetric photoreactions is particularly surprising.

The history of asymmetric photochemistry can be traced back to as early as 1894, when van't Hoff recognized that circularly polarized light (CPL) could potentially be used as a chiral reagent for chemical transformations.<sup>3</sup> The first conclusive evidence for this proposal was reported in 1930.<sup>4</sup> Kuhn demonstrated that the partial decomposition of racemic azide **1-1** upon irradiation with R-CPL resulted in a small but measurable optical enrichment of the remaining azide **1-2** (Scheme 1-1). This initial demonstration was soon followed by several corroborative reports,<sup>5</sup> and together, these early studies established the fundamental basis for asymmetric photochemistry. Controlling chirality in photochemical processes has been an active area of investigation ever since and several reviews summarizing this work have been published.<sup>6</sup>

**Scheme 1-1.** First example of an asymmetric photochemical process



Despite its early successes, asymmetric photochemistry can still be considered an emerging field. The use of enantioselective photochemical reactions in synthetic applications is relatively limited, and the transformations are usually narrow in scope. Furthermore, catalytic variants of these reactions are extremely rare and exist mainly as proof-of-principle paradigms. The reasons for this paucity of examples in the literature are clear when the inherent challenges of asymmetric photochemistry are considered. Key complicating issues that are unique to photochemical processes include: (1) the

short lifetimes of excited states and the number of unproductive and deactivation pathways readily available to these species; (2) the additional involvement of intermediates with different spin multiplicities; and (3) the common spectroscopic overlap of substrates, reagents, and products in the relevant wavelength regions for photochemical excitation, rendering the selective activation of a single reaction component extremely challenging. An efficient *asymmetric* photochemical transformation must address these issues while ensuring that the bond-forming process occurs exclusively in a well-defined chiral environment. Minimizing the extent of the racemic background reaction is typically the most difficult aspect in the development of a highly enantioselective photochemical method. Thus, asymmetric photocatalysis is intrinsically more difficult to achieve and these reactions must address both enantioselective thermal chemistry and photochemistry.

In spite of these challenges, significant progress has been made in the field. Numerous strategies for chiral induction have been employed with varying levels of success. This chapter will focus on enantioselective photochemical reactions in solution. In particular, topics will include the use of circularly polarized light as a chiral reagent for organic reactions and the use of chiral auxiliaries, chiral complexing agents, and photosensitizers for mediating asymmetric photochemical reactions in solution. Although solid-state approaches to asymmetric photochemical processes have been extensively investigated and these systems have been shown to be effective for a range of transformations, these studies are beyond the scope of this chapter and will not be discussed.<sup>7</sup> Particular emphasis will be given to *catalytic* enantioselective photoreactions. Reports that have promising implications for the future development of



catalytic reactions will also be mentioned and an analysis of each described approach as it pertains to asymmetric photocatalysis will be presented.

## 1.2 Circularly polarized light (CPL)

Since the early recognition that light in its chiral form might be able to serve as a physical source of chirality for asymmetric reactions,<sup>3</sup> circularly polarized light (CPL) has been studied for its relevance to the origin, control, and amplification of chirality in chemical and biological systems. Because opposite enantiomers interact differently with CPL, irradiation of a racemic mixture with CPL can afford enantiomerically enriched product. Asymmetric reactions induced by CPL irradiation are often referred to as *absolute asymmetric reactions*, since no net chirality present in the starting materials.<sup>8</sup> The optical purity of these reactions is governed primarily by the wavelength-dependent anisotropy factor  $g_\lambda$  (Figure 1-1), where  $\epsilon$  is the absorption extinction coefficient ( $M^{-1} \cdot cm^{-1}$ ).<sup>9</sup> This simple equation reflects the physical basis for enantioselective reactions with CPL: opposite enantiomers can absorb CPL with different intensities.

**Figure 1-1.** Equation for the anisotropy factor,  $g_\lambda$

$$g_\lambda = \frac{\epsilon_l - \epsilon_r}{(\epsilon_l + \epsilon_r) / 2} = \frac{\Delta\epsilon}{\epsilon}$$

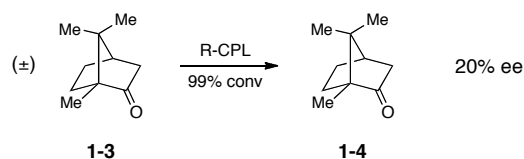
Three distinct scenarios describe the mechanism for asymmetric induction in CPL-promoted reactions. If  $g_\lambda$  is nonzero at the wavelength of irradiation, optically active compounds can be generated from a racemic mixture via pathways in which a chiral center is destroyed, preserved, or fixed upon an enantiodifferentiating interaction of the

excited state with CPL. These reactions are termed asymmetric photodestruction, photochemical deracemization, and enantioselective photofixation respectively.<sup>10</sup>

### 1.2.1 Asymmetric photodestruction

In asymmetric photodestruction, each enantiomer of a racemic mixture is consumed at a different rate upon interacting with CPL. The resulting imbalance of the two enantiomers gives rise to an enantiomerically enriched reaction mixture. For this process to occur, the following two conditions must be satisfied: (1) the substrate undergoes an irreversible photochemical transformation; and (2) the substrate does not undergo a thermal racemization.

The first reports of asymmetric photochemical reactions were examples of asymmetric photodestruction (*vide supra*).<sup>4</sup> Kagan followed the pioneering work of van't Hoff and Kuhn with some theoretical studies<sup>11</sup> and concluded that high levels of optical purity should be attainable given sufficient decomposition of the substrate.<sup>5a, 11-12</sup> Indeed, an enantiomeric purity of 20% was obtained upon photolysis of racemic camphor **1-3** (Scheme 1-2); the calculated value was 35%. This was the highest level of enantioselectivity reported at the time using CPL irradiation. Unfortunately, the requirement for high levels of enantiopurity in these systems is a significant degree of photochemical destruction and thus, asymmetric photodestruction has not been used in a synthetic context.

**Scheme 1-2.** Asymmetric photodestruction of ( $\pm$ )-camphor with R-CPL

### 1.2.2 Photochemical deracemization

Photoderacemization, also referred to as partial photoresolution or photoenantiomerization, occurs when the two enantiomers of a racemic substrate interconvert upon excitation with CPL to afford an unequal mixture of enantiomers. If the rates of all other reactions are slow relative to the rate of racemization and the final photostationary state deviates from unity, the resulting product mixture will be optically active. This process differs from asymmetric photodestruction in that the total amount of material in the system remains constant. In addition, the same photostationary state can be attained regardless of the optical purity of the starting material.

Most classic examples of CPL-induced photoderacemization involve chiral octahedral transition metal complexes bearing bidentate ligands;<sup>13</sup> for example,  $\text{Ru}(\text{bpy})_3^{2+}$  undergoes photoderacemization upon irradiation with CPL in the visible range.<sup>14</sup> Only several examples of photoderacemization exist in the literature because very few organic compounds undergo exclusive photoderacemization in the absence of any side reactions. More recent examples have been reported in the context of optical data storage<sup>15</sup> and liquid crystal-based optical switches.<sup>16</sup>

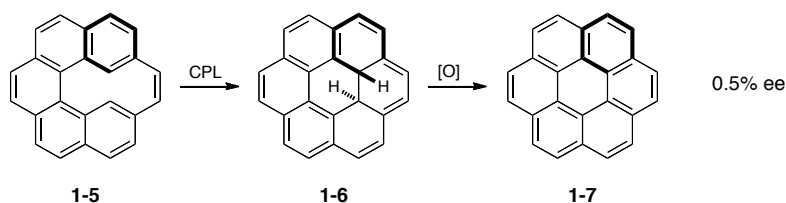
### 1.2.3 Enantioselective photofixation

Enantioselective photofixation is analogous to asymmetric photodestruction in that the rate of product formation must be significantly faster than the rates of

deactivation and racemization in the excited state. The two processes are different mechanistically because photofixation requires the presence of a rapid thermal equilibrium between substrate enantiomers such that the substrate remains racemic throughout the reaction.

Given that photoexcitation is generally much faster than thermal motion, very few chemical systems are capable of photochemical fixation. Most examples are photocyclization reactions.<sup>6b, 10, 17</sup> A classic example is the synthesis of helicenes (e.g. **1-5**) from bis(aryl) arenes (e.g. **1-6**) (Scheme 1-3).<sup>18</sup> Unfortunately, the low  $g_f$  values for enantioselective photofixation have precluded the use of these systems in synthetic applications.

**Scheme 1-3.** Photofixation of helicenes to afford bis(aryl) arenes



#### 1.2.4 Concluding remarks

CPL can provide access to enantiomerically enriched products via the partial destruction, resolution, or fixation of chiral centers. Although the low levels of observed enantioselectivity indicate that CPL is unlikely to be an efficient source of chirality for organic reactions, CPL remains an active area of investigation. A major reason for this is a fundamental interest in the possible relevance of CPL in the prebiotic origin of chirality.<sup>19</sup> One proposal suggests that the amplification of a small enantiomeric excess generated upon photolysis with CPL might be relevant to the origin of optical activity in

biologically relevant molecules.<sup>20</sup> Thus, studies of the interaction of CPL with molecules of potential prebiotic importance have been of significant interest.<sup>21</sup>

CPL has had an integral role in the field of asymmetric photochemistry. Although synthetically useful levels of enantioinduction are not obtained and asymmetric catalytic photoreactions are not possible with CPL because intense irradiation is required, studies of CPL have helped establish the field of asymmetric photochemistry. These studies will likely continue due to a curiosity pertaining to fundamental processes mediated by CPL.

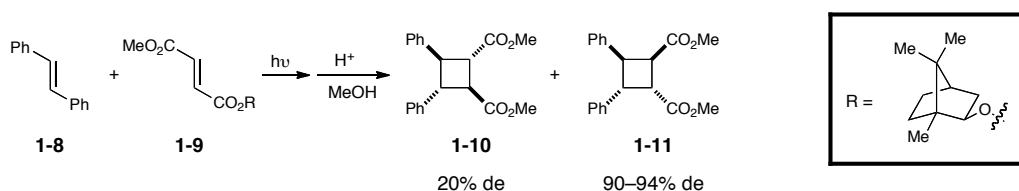
### **1.3. Chiral auxiliaries**

The use of chiral auxiliaries has been a powerful strategy in the development of enantioselective photochemical reactions. In these transformations, stereochemical information is transferred from a covalently bound source of chirality. This is one of the most successful approaches for generating highly enantioenriched product in a photochemical reaction; the levels of asymmetric induction obtained using a chiral auxiliary often rival those observed in conventional thermal reactions. A similar strategy for relaying stereochemical information from chiral substrates has also been explored. This section will cover the two most extensively studied reactions that employ chiral auxiliaries: the [2+2] cycloaddition of olefins and the related Paternò–Büchi reaction.<sup>22</sup> Methods have been selected based on their successful application to the synthesis of enantiomerically pure nature products.<sup>23</sup>

### 1.3.1 [2+2] Cycloaddition

The [2+2] photocycloaddition of olefins is an efficient strategy for the synthesis of cyclobutane structures.<sup>24</sup> While methods for directly generating chiral cyclobutanes by enantioselective catalysis are rare,<sup>25</sup> high levels of absolute stereoinduction can be obtained through the use of chiral auxiliaries. The first example of an auxiliary-assisted intermolecular [2+2] photocycloaddition was reported in 1982.<sup>26</sup> The cycloaddition of *trans*-stilbene (**1-8**) with methyl bornyl fumarate (**1-9**), followed by ester exchange with acidic methanol afforded cyclobutane products **1-10** and **1-11** (Scheme 1-4). The dramatically different levels of enantioselectivity observed for the two diastereomers was attributed to the intermediacy of a 1,4-diradical species arising from a non-concerted pathway for product formation.

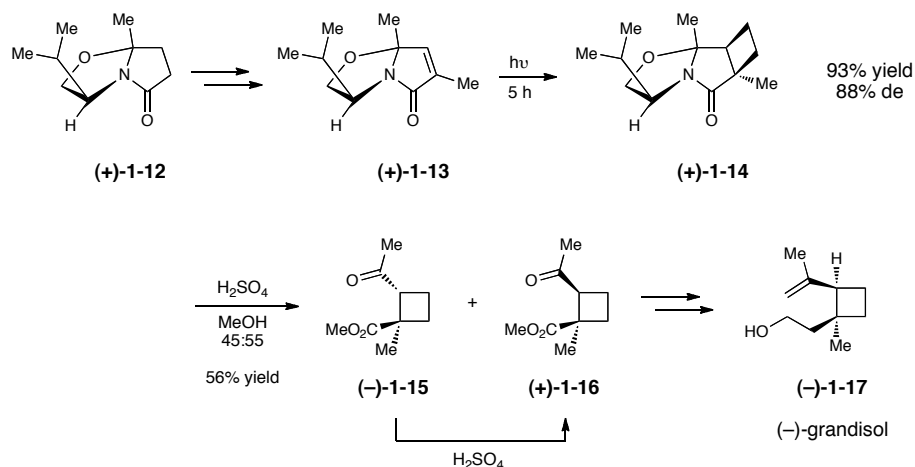
**Scheme 1-4.** Chiral auxiliary-assisted intermolecular [2+2] photocycloaddition



Meyers reported one of the first applications of a photochemical auxiliary for the synthesis of natural products in 1986.<sup>27</sup> The key [2+2] photocycloaddition employed a readily accessible chiral lactam auxiliary (+)-**1-12**<sup>28</sup> and its utility was demonstrated in the first total synthesis of enantiopure (–)-grandisol **1-17** (Scheme 1-5). Cleavage of the chiral lactam auxiliary proceeded smoothly to afford the desired cyclobutane intermediates (–)-**1-15** and (+)-**1-16**. Although enone (+)-**1-13** was the only substrate reported for the [2+2] cycloaddition, the efficient implementation of this methodology in

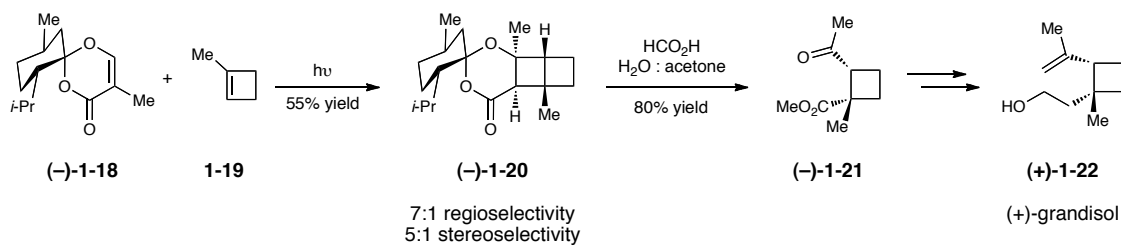
total synthesis highlights the synthetic potential of asymmetric photochemical processes.

**Scheme 1-5.** Chiral lactam auxiliary approach for the total synthesis of (–)-grandisol (**1-17**)



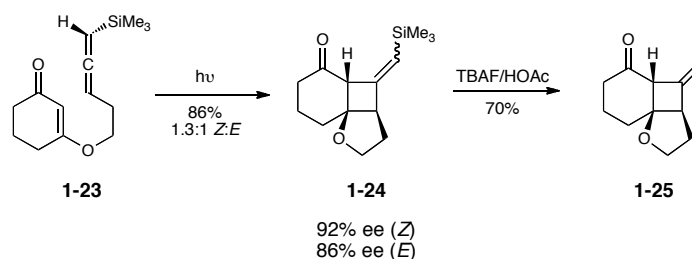
A similar approach to (+)-grandisol (**1-22**) was reported later in the same year by Demuth and co-workers.<sup>29</sup> This sequence utilized the [2+2] photocycloaddition of menthone-derived auxiliary (–)-**1-18** with alkene **1-19** to yield (–)-**1-20**. Acid hydrolysis afforded cyclobutane (–)-**1-21**, which could be converted into (+)-grandisol (**1-22**) using a previously reported protocol.<sup>30</sup> If (+)-**1-18** is employed, (–)-grandisol (**1-17**) can be obtained using an analogous sequence.

**Scheme 1-6.** Chiral menthone auxiliary approach for the total synthesis of (+)-grandisol (**1-22**)



In a similar vein, Carreira employed optically active allenes for the intramolecular [2+2] photocycloaddition of enones and enoates.<sup>31</sup> This reaction achieves high levels of asymmetric induction by exploiting the inherent chirality 1,3-disubstituted allenes.<sup>32</sup> When allenylsilanes (**1-23**) are employed, the terminal silyl moiety functions as a removable stereochemical directing group and various cyclobutane structures (**1-25**) can be obtained with high levels of enantioselectivity (Scheme 1-7).

**Scheme 1-7.** Chiral allene-enone intramolecular [2+2] photocycloadditions

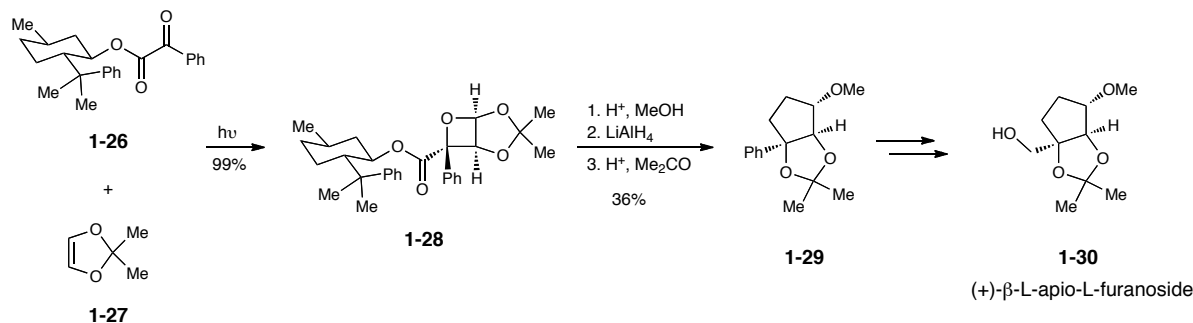


### 1.3.2 Paternò–Büchi reaction

The Paternò–Büchi reaction is a classic photochemical transformation in which an oxetane ring is formed via the [2+2] cycloaddition of a carbonyl and an alkene.<sup>33</sup> This is one of the most useful transformations in synthetic photochemistry due to the efficiency of the cycloaddition and the versatility of the four-membered photoproducts.<sup>23b, 34</sup> One synthetic application of this reaction is depicted in Scheme 1-8.<sup>35</sup> Addition of phenylglyoxylate **1-26** to electron-rich alkene **1-27**<sup>36</sup> affords oxetane **1-28**. The phenylglyoxylate auxiliary is removed using an oxidation-reduction sequence to afford intermediate **1-29** en route to (+)- $\beta$ -L-apio-L-furanoside (**1-30**). This sequence enables efficient access to branched carbohydrates from non-sugar building blocks.



**Scheme 1-8.** Phenylglyoxylate auxiliary approach for the synthesis of (+)- $\beta$ -L-apio-L-furanoside (**1-30**)



### 1.3.3 Concluding remarks

Chiral auxiliaries have been a remarkably successful method for chirality transfer in photochemical reactions. These reactions operate in an analogous fashion to their thermal counterparts: a covalent bond between the substrate and the chiral auxiliary enforces a rigid conformation that enables the reaction to proceed with high levels of stereocontrol. Because this strategy inevitably requires a stoichiometric amount of the chiral agent, it cannot be rendered catalytic. However, these studies demonstrate that sufficiently strong interactions between the substrate and the chiral entity can enable high levels of enantioselectivity in photochemical reactions and suggest that if these interactions were non-covalent, a catalytic reaction might be possible.

## 1.4. Chiral complexing agents

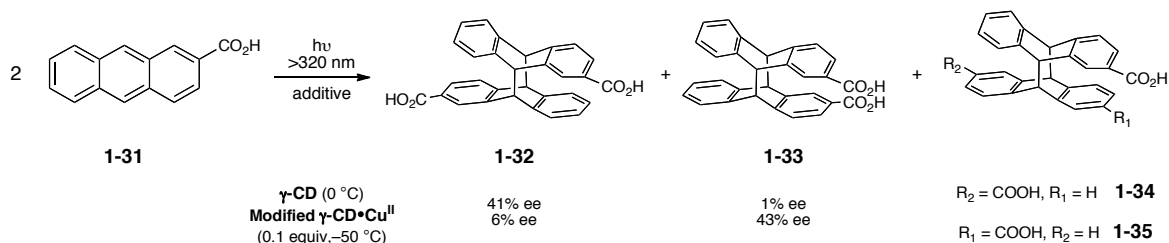
Methods involving the use of chiral complexing agents, either in a supramolecular environment or relying upon a well-defined substrate-template complex, have been relatively successful at mediating highly enantioselective photochemical processes. Unlike reactions that employ covalently bound chiral auxiliaries, these transformations utilize non-covalent interactions between the substrate and the chiral

source. This section will cover three chiral template-mediated strategies for asymmetric catalysis: (1) cyclodextrins as synthetic supramolecular hosts, (2) biomolecules as inherently chiral frameworks, and (3) small molecules as tunable chiral templates. The latter will be covered most extensively because examples of *catalytic* asymmetric photochemical reactions have been achieved using this approach.

### 1.4.1 Cyclodextrins

The chirality of cyclodextrins has intrigued chemists since their discovery.<sup>37</sup> They are known to form highly ordered chiral cavities in solution and can serve as chiral hosts for organic reactions; however, low levels of enantioselectivity are generally observed. A notable exception is shown in Scheme 1-9. The [4+4] photocyclodimerization of 2-anthracenecarboxylic acid **1-31** occurs in the presence of  $\gamma$ -cyclodextrin ( $\gamma$ -CD) to afford cycloadduct **1-32** in 41% ee.<sup>38</sup> Unfortunately, a diastereomeric chiral product **1-33** was also formed with negligible asymmetric induction.<sup>39</sup> This reaction was recently carried out using sub-stoichiometric amounts of a modified  $\gamma$ -cyclodextrin.<sup>40</sup> In the presence of copper, the metallosupramolecular host is capable of mediating the photocyclodimerization of (**1-31**); only 0.1 equivalent of the copper-cyclodextrin complex is required to achieve the maximum level of enantioselectivity.

**Scheme 1-9.** Cyclodextrins as chiral hosts for [4+4] photocycloaddition

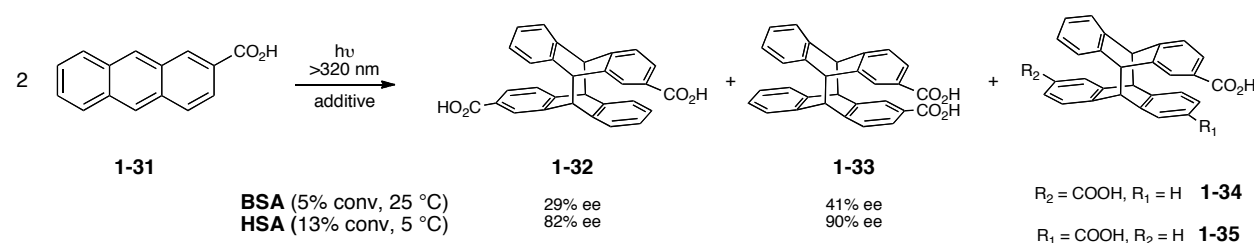


### 1.4.2 Biomolecules

Enzymes are an attractive source of chirality due to the inherent asymmetry of enzyme binding sites. Their application to enantioselective organic reactions has recently become an active area of investigation.<sup>41</sup> Use of biomolecules is a relatively new approach to asymmetric photochemistry and initial studies have primarily been focused on identifying systems that are capable of mediating enantioselective photoreactions.<sup>42</sup>

Currently, two systems are known to effect the previously described [4+4] photocycloaddition of 2-anthracenecarboxylic acid **1-31** (Scheme 1-10). Bovine serum albumin (BSA) affords the products with moderate levels of enantioselectivity.<sup>42a</sup> Superior results can be obtained with human serum albumin (HSA); *syn* head-to-tail isomer **1-32** was formed in 82% ee and *anti* head-to-head dimer **1-33** was formed in 90% ee.<sup>43</sup> In contrast to the results obtained using cyclodextrins, both enantiomers can be generated with high levels of enantioselectivity in one reaction.

**Scheme 1-10.** Biomolecules as chiral hosts for [4+4] photocycloaddition

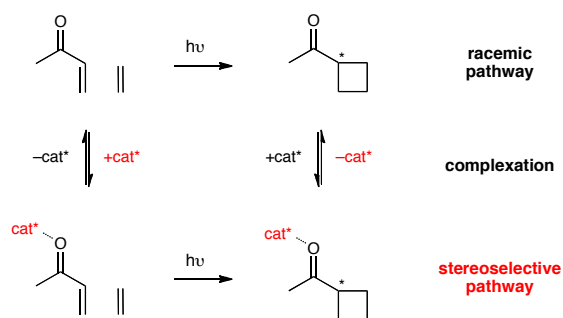


### 1.4.4 Chiral small molecules

A fundamental challenge in the development of a highly enantioselective photochemical method is the competitive racemic background reaction. Racemic

product is produced when bond formation occurs in the absence of a chiral complex, whereas enantiomerically enriched product can be obtained if bond formation occurs after complexation of the substrate to the chiral compound (Scheme 1-11). Because the wavelengths of UV light employed in photochemical reactions are unable to discriminate between the free substrate and the chiral catalyst bound substrate complex, the rate of the racemic background reaction usually occurs at a rate competitive to that of the stereoselective reaction. The extent of the background reaction is further exacerbated when a sub-stoichiometric amount of the chiral reagent is employed. The low association constant of the substrate for the chiral compound, the background reactivity of the free substrate, and the competitive binding of product to the catalyst are examples of the additional challenges that arise when a non-covalent source of chirality is used to impart stereochemical information in a photochemical reaction.

**Scheme 1-11.** Competitive racemic and stereoselective pathways in catalytic photoreactions



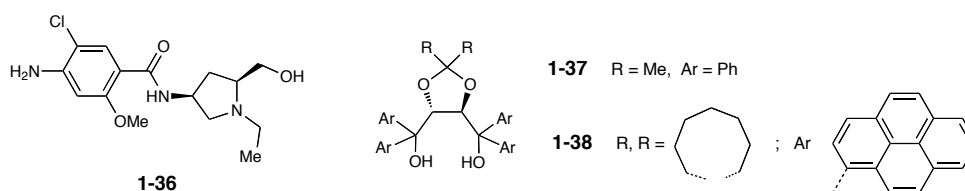
Thus, a highly enantioselective photocatalytic reaction requires that the stereoselective pathway proceed at a much faster rate than the racemic pathway. Two approaches have been taken to satisfy this criteria; both strategies effectively operate by accelerating the rate of reaction for the catalyst-bound substrate complex. One

approach relies upon altering the photophysical properties of the substrate upon binding of the chiral template. If the reaction of the bound substrate proceeds significantly faster than the reaction of the free substrate, the stereoselective pathway will predominate and formation of enantiomerically enriched product will be favored. An alternative approach employs reaction conditions in which the catalyst undergoes photexcitation but the substrate does not. This eliminates the possibility for direct formation of product from the free substrate and minimizes the number of other unproductive pathways that might be available to the photoexcited state of the substrate. Both of these strategies have been successfully employed for asymmetric photocatalysis and the remainder of this chapter will focus on the development of these systems.

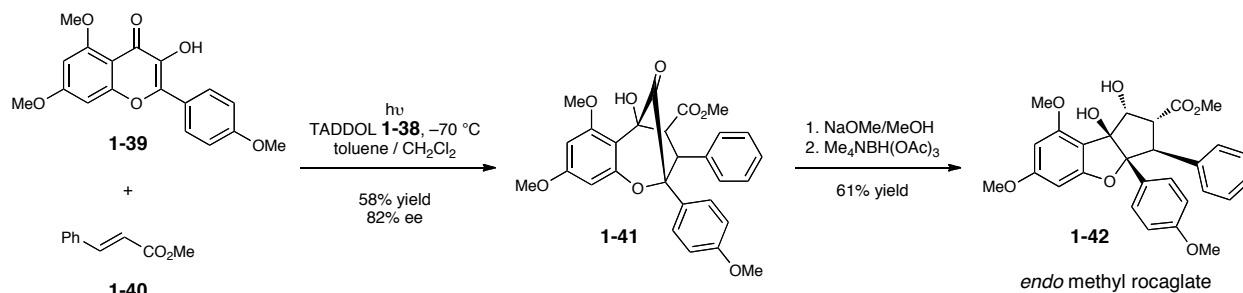
#### 1.4.3.1 Non-covalent small molecule chiral templates

A variety of chiral templates have been employed in photochemical transformations. Some recent examples are shown in Figure 1-2.

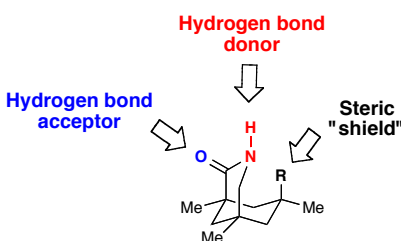
**Figure 1-2.** Chiral templates in asymmetric photoreactions



These include **1-36**, a hydroxymethylpyrrolidine derived from a gastroprokinetic agent,<sup>44</sup> and some TADDOL-based structures.<sup>45</sup> TADDOL **1-38** was employed as a chiral Brønsted acid in the synthesis of the rocaglamides (e.g. **1-42**) (Scheme 1-12).<sup>46</sup> The key enantioselective [3+2] dipolar photocycloaddition is mediated by TADDOL **1-38** through a network of hydrogen bonding interactions.

**Scheme 1-12.** TADDOL-mediated enantioselective [3+2] photocycloaddition

**1.4.3.2 Hydrogen-bonding chiral lactam templates**

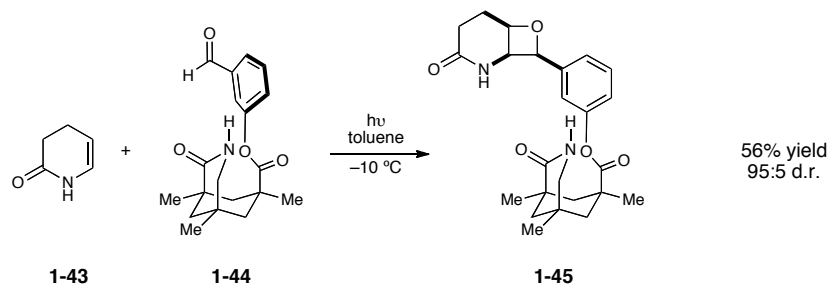
The most extensively studied chiral structures in this context are derived from Kemp's triacid (Figure 1-3).<sup>47</sup> These structures were designed to facilitate the formation of a highly ordered hydrogen bonding network; the carbonyl group and the amino group of the lactam serve as a hydrogen bond acceptor and donor, respectively. This two-point binding between the chiral template and the prochiral substrate orients the substrate such that one enantioface is effectively shielded upon proper selection of R.<sup>48</sup>

**Figure 1-3.** Design considerations for chiral lactam template structure


These structures were first employed by Bach in a photochemical context in 1999.<sup>49</sup> High levels of diastereocontrol were obtained in the Paternò–Büchi reaction of chiral lactam **1-44** to enamide **1-43** (Scheme 1-13). Because facial differentiation occurs upon binding of the chiral host to the achiral guest and is the result of a rigid hydrogen bonding environment, the remarkable stereocontrol observed in this study indicated that

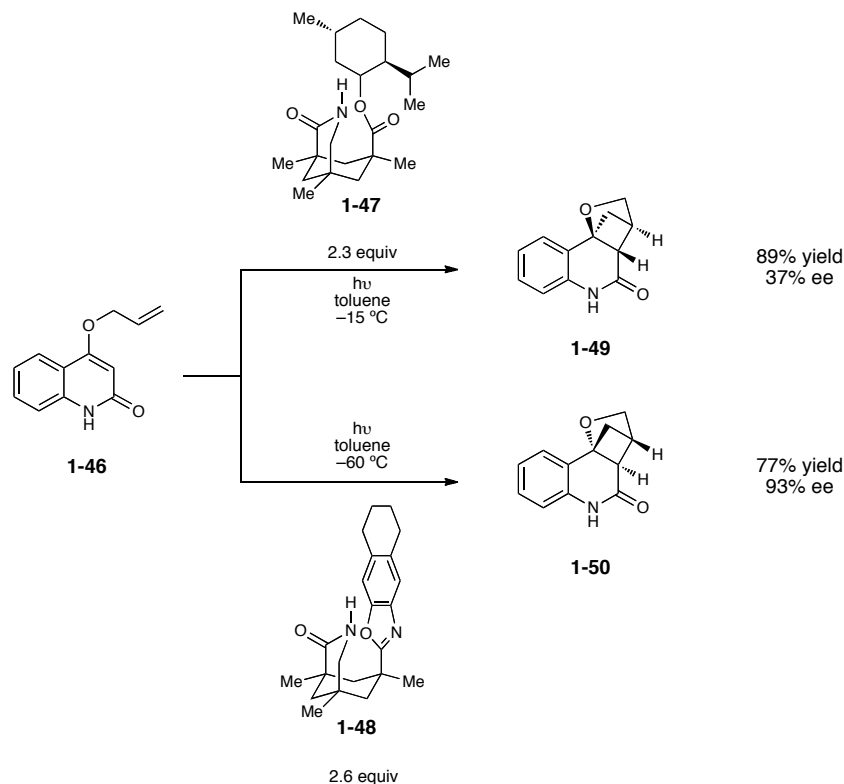
for reactions in which the host does not participate in the reaction, chiral lactam **1-44** might be an effective template for enantioselective reactions.

**Scheme 1-13.** Diastereoselective Paternò–Büchi reaction of chiral lactam template



The first enantioselective photoreaction using these chiral lactam hosts was the intramolecular [2+2] cycloaddition of **1-46** (Scheme 1-14).<sup>50</sup> Two variants of the chiral host were tested; one structure utilized menthol as the chiral unit (**1-47**) and the other contained a benzoxazole motif (**1-48**). Chiral host **1-48** provided superior levels of enantioselectivity; its efficiency as a chiral template for asymmetric induction has since been demonstrated in a variety of enantioselective photoreactions.<sup>6d, 51</sup>

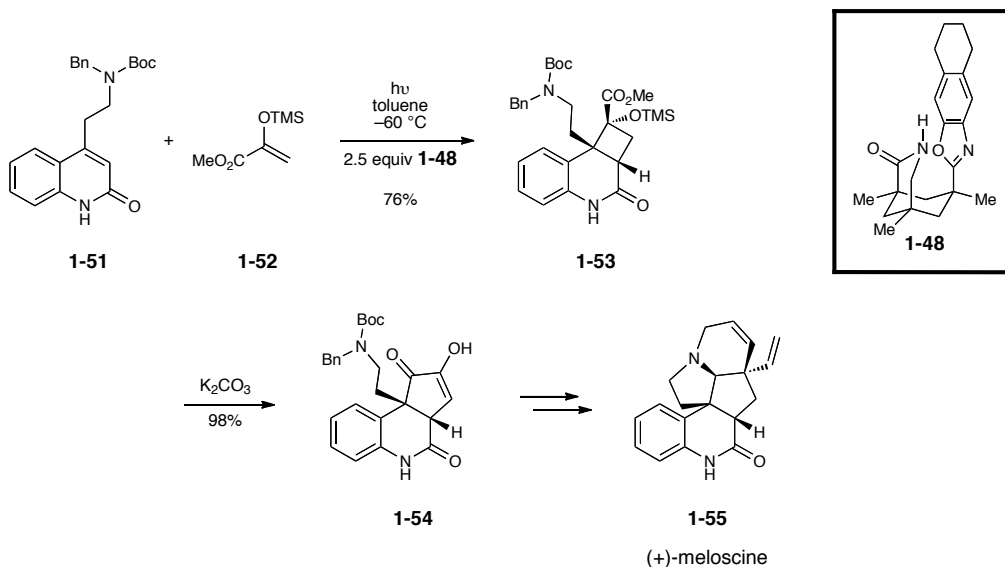
**Scheme 1-14.** Enantioselective intramolecular [2+2] photocycloaddition reactions mediated by a chiral lactam host



These complexes have also been used in the synthesis of natural products.<sup>52</sup> The intermolecular [2+2] photocycloaddition was used in the first enantioselective synthesis of (+)-meloscine (**1-55**) (Scheme 1-15).<sup>53</sup> Ring-expansion of the [2+2] cycloadduct **1-53** followed by several rearrangement steps afforded the product in 7% overall yield.



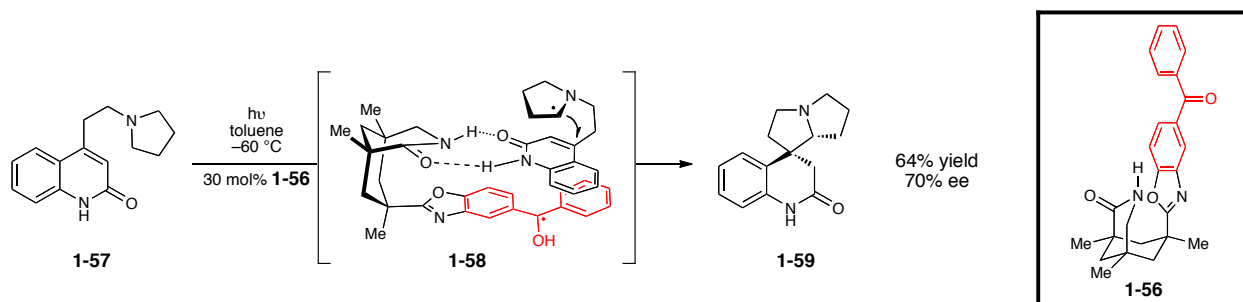
**Scheme 1-15.** Chiral template-mediated enantioselective [2+2] photocycloaddition in the total synthesis of (+)-meloscine (**1-55**)



More recently, this family of chiral hosts was applied to the development of a *catalytic* asymmetric protocol. In order to increase the rate at which the template-bound substrate reacts relative to the free substrate, a new chiral catalyst containing both a photosensitizer and an electron-accepting chiral motif (**1-56**) was designed (Scheme 1-16). Upon irradiation, the enforced proximity of these two components facilitates a photoinduced electron transfer (PET) from nitrogen to the benzophenone unit; subsequent radical cyclization affords tetracyclic product **1-59**. Rapid formation of the radical pair effectively accelerates the bond-forming process for substrate-template complexes. In addition, the chiral environment for this catalytic reaction is rigidly enforced under these conditions and relatively high levels of enantioselectivity can be obtained. Although each individual step of this transformation had previously been demonstrated, the synergy with which they occur in this system is impressive and the

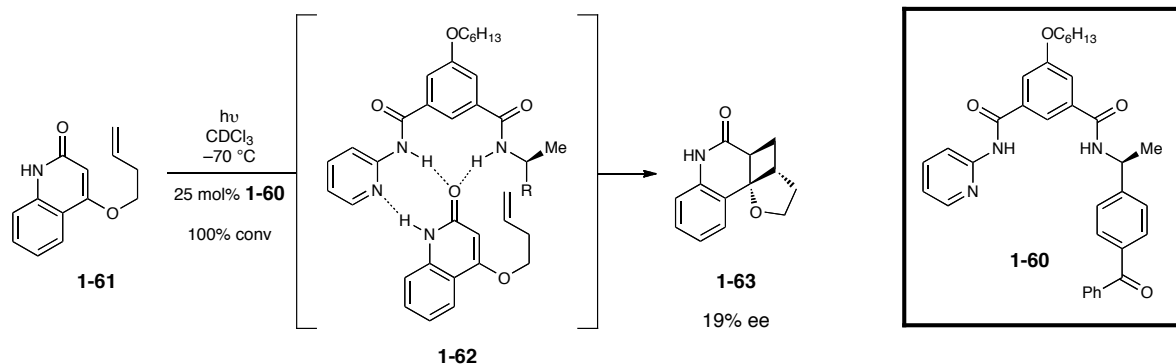
broad generality of this approach for single electron transfer sequences can be envisioned.

**Scheme 1-16.** Catalytic enantioselective photochemical reaction driven by photoinduced electron transfer



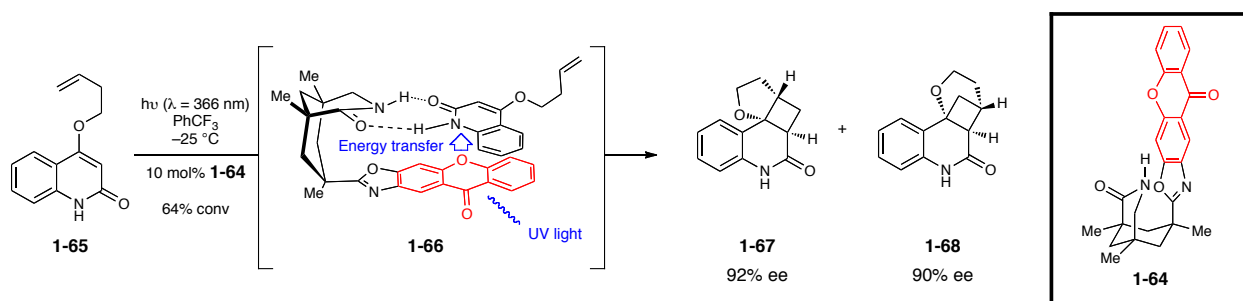
Although this represents a novel approach to asymmetric photocatalysis, this mechanism is limited to reactions that proceed via one-electron pathways. Krische reported a potentially more general approach in 2002;<sup>54</sup> molecular receptors equipped with chiral sensitizing moieties were designed to serve as catalysts for asymmetric photoreactions (Scheme 1-17). Bisamide **1-60** contains a triplet-sensitizing benzophenone moiety and three hydrogen-bonding sites to facilitate enantiodifferentiation. Because energy transfer should occur at a much higher rate for the catalyst-bound substrate due to the strong distance dependence of triplet energy transfer, this is equivalent to a binding-induced rate enhancement for the enantioselective photochemical reaction. Although high levels of enantioselectivity were not achieved in this system, the results validated the ability of **1-60** to act as a sensitizer template for asymmetric photocatalysis.

**Scheme 1-17.** Catalytic enantioselective [2+2] photocycloaddition using chiral receptor-sensitizer template **1-60**



Bach employed a similar chiral sensitizer strategy in 2009.<sup>55</sup> Based on the chiral catalyst developed for catalytic photoinduced electron transfer, organocatalyst **1-64** incorporates xanthone as the triplet sensitizer instead of benzophenone (Scheme 1-18). This new xanthone-containing catalyst **1-64** absorbs at a distinct wavelength from the quinolone substrate **1-65**, thereby combining the rate acceleration effect of triplet energy transfer with the hydrogen bonding components necessary for achieving high levels of enantiocontrol. Its improved catalytic activity was demonstrated in the [2+2] photocycloaddition of quinolone **1-65**; exceptional levels of enantioselectivity were obtained using 10 mol% of the catalyst.

**Scheme 1-18.** Catalytic enantioselective photoreaction using chiral sensitizer-template **1-64**



This report also outlined four criteria for the effective use of chiral triplet sensitizers in asymmetric photocatalysis. First, there must be small regions of spectral overlap between the substrate and the catalyst to minimize the background reaction from direct substrate excitation. Second, the triplet energy of the sensitizer must be significantly higher than the triple energy of the substrate to facilitate rapid energy transfer. Third, formation of the substrate-catalyst complex must occur readily to outcompete any possible intermolecular sensitization, and fourth, the catalyst must be an effective chiral control element for the reaction.

#### **1.4.4 Concluding remarks**

The use of complexing agents as chiral templates has been an efficient strategy for asymmetric photochemical transformations. The nature of these templates ranges from supramolecular entities such as cyclodextrins and biomolecules to small chiral molecules that operate using hydrogen bonding interactions. While promising results have been achieved in each of these systems, significant challenges still remain. Specifically, supramolecular hosts generally require low conversion for higher levels of enantioselectivity and have not been shown to participate in different types of reactions. On the other hand, well-defined substrate-template complexes require specific structural motifs and are therefore restricted to a limited substrate scope. Nevertheless, significant progress has already been made in the field and the fundamental concepts necessary for this strategy to meaningfully impact the field of asymmetric photocatalysis have been established.<sup>56</sup>

## 1.5. Photosensitizers

Since the first demonstration of enantioselective induction using energy transfer,<sup>57</sup> photoinduced electron transfer reactions have become a useful technique for asymmetric synthesis.<sup>58</sup> Because a close proximity between the donor and the acceptor is required for efficient energy transfer, the reaction of bound substrate complexes can be selectively promoted, and in the presence of a chiral sensitizer, an asymmetric reaction might be possible. These reactions require a tightly coupled photochemical excitation and enantioselective bond-forming steps (*vide supra*).

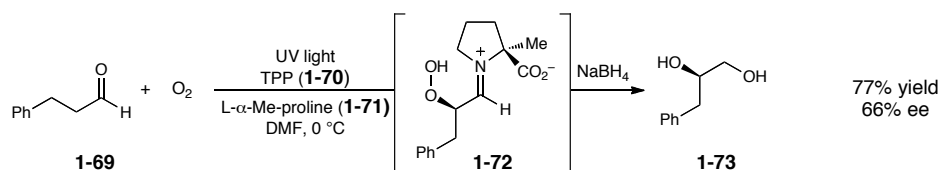
On the other hand, these two steps can be independent processes; energy transfer from the chromophore does not necessarily need to be associated with the enantioselective bond-forming process. This approach is particularly attractive because substrates that do not possess suitable chromophores for direct photochemical reactions are still viable substrates for the reactions. More importantly, these substrates can be photochemically inert and will not participate in a racemic background photochemical process.

These reactions can be carried out using a chiral photosensitizer and there has been a long-standing interest in their use in organic reactions. Generally, these systems have only resulted in modest levels of enantioselectivity (*vide supra*).<sup>59</sup> This can be rationalized by the relatively short lifetimes of molecules in their excited states. For these reactions to exhibit high levels of enantioselectivity, the substrates must adopt a highly ordered transition state and proceed extremely rapidly from the photoexcited chiral catalyst.

Asymmetric photoreactions do not require the use of a chiral photosensitizer, however, and efficient energy transfer in the presence of a chiral co-catalyst can be sufficient for asymmetric induction. Indeed, more promising results have been obtained through the use of an achiral sensitizer in combination with a chiral co-catalyst. Córdova showed that photochemically generated singlet oxygen ( $^1\text{O}_2$ ) can be incorporated into the  $\alpha$ -position of aldehydes with good levels of enantioselectivity using readily available amino acids as the source of chirality (e.g. **1-71**) (Scheme 1-19).<sup>60</sup>

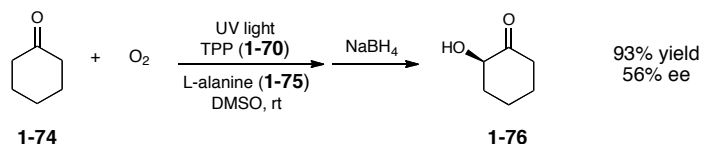
Importantly, the key photochemical and enantioselective steps in these reactions are decoupled. A photochemical process generates  $^1\text{O}_2$  from  $\text{O}_2$  and TPP (tetraphenylporphyrin, **1-70**), and a separate stereochemistry-determining bond-forming process is proposed to occur via a chiral enamine mechanism to afford the enantioenriched product.

**Scheme 1-19.** Amino acid-catalyzed  $\alpha$ -oxygenation of aldehydes with  $^1\text{O}_2$



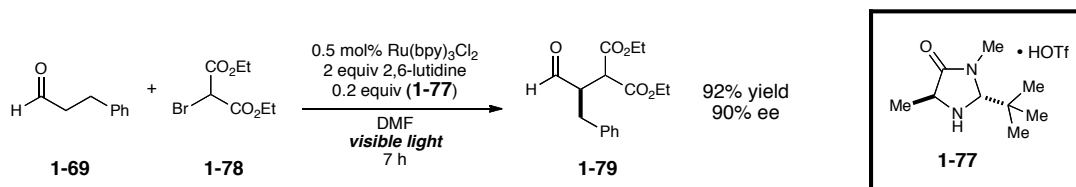
This approach was further expanded upon to include the  $\alpha$ -oxygenation of ketones (Scheme 1-20).<sup>61</sup> The  $\alpha$ -hydroxy products (**1-76**) can be obtained with good yields and reasonable levels of enantioselectivity. Despite these promising results, these systems have not been studied further.

**Scheme 1-20.** Amino acid-catalyzed  $\alpha$ -oxygenation of ketones with  $^1\text{O}_2$



More recently, a photosensitization approach employing visible light was reported.<sup>62</sup> By merging the concepts of organocatalysis and photoredox catalysis,<sup>63</sup> the enantioselective  $\alpha$ -alkylation of aldehydes was achieved with good yields and excellent enantioselectivities. This reaction employs  $\text{Ru}(\text{bpy})_3\text{Cl}_2$  (bpy = 2,2'-bipyridine) as the visible light photocatalyst and an imidazolidinone organocatalyst (**1-77**) to generate the chiral enamine intermediate (Scheme 1-21). Because the organic molecules do not absorb visible light, there is no competitive background photoreaction.

**Scheme 1-21.** Visible light-promoted enantioselective  $\alpha$ -alkylation of aldehydes



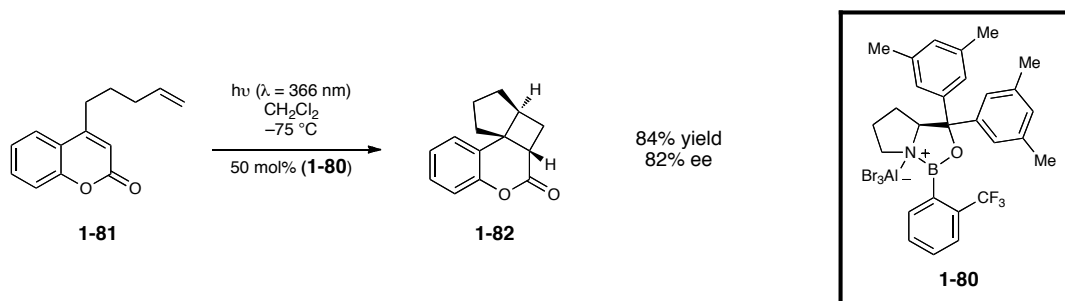
A similar protocol has been utilized for the  $\alpha$ -trifluoromethylation<sup>64</sup> and  $\alpha$ -benzylation<sup>65</sup> of carbonyl compounds. In the presence of a metal polypyridyl photocatalyst, a variety of enantioselective reactions proceed upon irradiation with visible light. Because most organic compounds are transparent to the wavelengths of visible light, this might be a useful approach for circumventing some of the traditional challenges in asymmetric photocatalysis.

## 1.6 Future directions and concluding remarks

Photochemical reactions have tremendous potential in synthetic chemistry. They enjoy the beneficial aspects of utilizing light as a reagent and provide access to unique molecular scaffolds that would be difficult to construct using thermal methods. The development of enantioselective variants of these useful transformations, however, has been relatively limited. Asymmetric photoreactions are inherently more challenging than their thermal counterparts because the short-lived excited states of molecules are more difficult to control and provide more opportunities for unproductive reactivity.

A major impediment in asymmetric photocatalysis has been the inability to employ the strategies of thermal asymmetric catalysis. Transition metals and Lewis acids have not been widely used in asymmetric photocatalysis. A rare exception was reported in 2010. In this,<sup>66</sup> a Lewis acidic  $\text{AlBr}_3$ -activated oxazaborolidine complex (**1-80**)<sup>25b, 67</sup> mediates the intramolecular [2+2] cycloaddition of coumarin **1-81** (Scheme 1-22). Although the yield and enantioselectivity diminish dramatically at lower loadings of the Lewis acid catalyst due to a background reaction of the free substrate, this study indicates that Lewis acid-catalyzed photochemical processes might be a promising future paradigm for asymmetric photocatalysis.



**Scheme 1-22.** Enantioselective Lewis acid-mediated [2+2] photocycloaddition

Nevertheless, significant progress has been made in asymmetric photochemistry. Effective strategies for asymmetric induction include the use of circularly polarized light, which produces enantioenriched product in the absence of an additional chiral source, the employment of covalently bound chiral auxiliaries and non-covalently bound chiral templates, and the use of photosensitizers. The synthetic utility of these transformations have been demonstrated in a variety of reactions and in the synthesis of complex natural products. With the recent advances in asymmetric catalytic methodology, the field of asymmetric photocatalysis is poised for a breakthrough in chemical synthesis.

## 1.7 References

1. Ciamician, G. The Photochemistry of the Future. *Science* **1912**, 36, 385-394.
2. Comprehensive Asymmetric Catalysis, Vol 1-3. Jacobsen, E. N., Pfaltz, A., Yamamoto, H., Eds. New York; Springer, 1999.
3. Van't Hoff, J. H. Die Lagerung der Atome in Raume. 2nd ed.; Vieweg: Braunschweig, 1894, 30.
4. Kuhn, W.; Knoff, E. Photochemische Erzeugung optisch aktiver Stoffe. *Naturwissenschaften* **1930**, 19, 183.
5. a) Mitchell, S. CCXXXVI.-The asymmetric photochemical decomposition of humulene nitrosite by circularly polarised light. *J. Chem. Soc.* **1930**, 1829-1834. b) Mitchell, S.;

Dawson, I. M. 121. The asymmetric photolysis of  $\beta$ -chloro- $\beta$ -nitroso- $\alpha$ -diphenylbutane with circularly polarised light. *J. Chem. Soc.* **1944**, 452-454.

6. a) Rau, H. Asymmetric photochemistry in solution. *Chem. Rev.* **1983**, 83, 535-547. b) Inoue, Y. Asymmetric photochemical reactions in solution. *Chem. Rev.* **1992**, 92, 741-770. c) Svoboda, J.; König, B. Templated Photochemistry: Toward Catalysts Enhancing the Efficiency and Selectivity of Photoreactions in Homogeneous Solutions. *Chem. Rev.* **2006**, 106, 5413-5430. d) Müller, C.; Bach, T. Chirality Control in Photochemical Reactions: Enantioselective Formation of Complex Photoproducts in Solution. *Aust. J. Chem.* **2008**, 61, 557-564.

7. a) Molecular and Supramolecular Photochemistry (v11): Chiral Photochemistry Inoue, Y., Ramamurthy, V., Eds. New York: NY; Dekker, 2004, 485-532. b) Sakamoto, M.; Kato, M.; Aida, Y.; Fujita, K.; Mino, T.; Fujita, T. Photosensitized 2+2 Cycloaddition Reaction Using Homochirality Generated by Spontaneous Crystallization. *J. Am. Chem. Soc.* **2008**, 130, 1132-1133. c) Ramamurthy, V.; Shailaja, J.; Kaanumalle, L. S.; Sunoj, R. B.; Chandrasekhar, J. Controlling chemistry with cations: photochemistry within zeolites. *Chem. Commun.* **2003**, 1987-1999. d) Toda, F. Crystalline Inclusion Complexes as Media of Molecular Recognitions and Selective Reactions. *Aust. J. Chem.* **2001**, 54, 573-582. e) Toda, F. Solid State Organic Chemistry: Efficient Reactions, Remarkable Yields, and Stereoselectivity. *Acc. Chem. Res.* **1995**, 28, 480-486. f) Ishida, Y.; Achalkumar, A. S.; Kato, S.-y.; Kai, Y.; Misawa, A.; Hayashi, Y., et al. Tunable Chiral Reaction Media Based on Two-Component Liquid Crystals: Regio-, Diastereo-, and Enantiocontrolled Photodimerization of Anthracenecarboxylic Acids. *J. Am. Chem. Soc.* **2010**, 132, 17435-17446.

8. Feringa, B. L.; van Delden, R. A. Absolute Asymmetric Synthesis: The Origin, Control, and Amplification of Chirality. *Angew. Chem. Int. Ed.* **1999**, 38, 3418-3438.

9. a) Molecular and Supramolecular Photochemistry (v11): Chiral Photochemistry Inoue, Y., Ramamurthy, V., Eds. New York: NY; Dekker, 2004, 1-44. b) Kuhn, W. The physical significance of optical rotatory power. *Trans. Faraday Soc.* **1930**, 26, 293-308. c) Riehl, J. P.; Richardson, F. S. Circularly polarized luminescence spectroscopy. *Chem. Rev.* **1986**, 86, 1-16.

10. Buchardt, O. Photochemistry with Circularly Polarized Light. *Angew. Chem. Int. Ed.* **1974**, 13, 179-185.

11. Balavoine, G.; Moradpour, A.; Kagan, H. B. Preparation of chiral compounds with high optical purity by irradiation with circularly polarized light, a model reaction for the prebiotic generation of optical activity. *J. Am. Chem. Soc.* **1974**, 96, 5152-5158.

12. Kagan, H. B.; Fiaud, J. C. Kinetic Resolution. *Top Stereochem* **1988**, 18, 249-330.

13. a) Stevenson, K. L.; Verdick, J. F. Partial photoresolution. Preliminary studies on some oxalato complexes of chromium(III). *J. Am. Chem. Soc.* **1968**, 90, 2974-2975. b)

Stevenson, K. L. Partial photoresolution. III. Tris(acetylacetonato)chromium(III) system. *J. Am. Chem. Soc.* **1972**, *94*, 6652-6654.

14. Porter, G. B.; Sparks, R. H. Photoracemization of  $\text{Ru}(\text{Bipyridine})_3^{2+}$ . *J. Photochem.* **1980**, *13*, 123-131.

15. Huck, N. P. M.; Jager, W. F.; Lange, B. d.; Feringa, B. L. Dynamic Control and Amplification of Molecular Chirality by Circular Polarized Light. *Science* **1996**, *273*, 1686-1688.

16. Zhang, Y.; Schuster, G. B. Photoresolution of an Axially Chiral Bicyclo[3.2.1]octan-3-one: Phototriggers for a Liquid Crystal-Based Optical Switch. *J. Org. Chem.* **1995**, *60*, 7192-7197.

17. Bernstein, W. J.; Calvin, M.; Buchardt, O. Absolute asymmetric synthesis. I. Mechanism of the photochemical synthesis of nonracemic helicenes with circularly polarized light. Wavelength dependence of the optical yield of octahelicene. *J. Am. Chem. Soc.* **1972**, *94*, 494-498.

18. a) Moradpour, A.; Kagan, H.; Baes, M.; Morren, G.; Martin, R. H. Photochemistry with circularly polarized light—III : Synthesis of helicenes using bis(arylvinyl) arenes as precursors. *Tetrahedron* **1975**, *31*, 2139-2143. b) Kagan, H.; Moradpour, A.; Nicoud, J. F.; Balavoine, G.; Tsoucaris, G. Photochemistry with circularly polarized light. Synthesis of optically active hexahelicene. *J. Am. Chem. Soc.* **1971**, *93*, 2353-2354.

19. Bonner, W. A. Origins of Chiral Homogeneity in Nature. *Top. Stereochem.* **1988**, *18*, 1-96.

20. Soai, K.; Shibata, T.; Morioka, H.; Choji, K. Asymmetric autocatalysis and amplification of enantiomeric excess of a chiral molecule. *Nature* **1995**, *378*, 767-768.

21. a) Shibata, T.; Yamamoto, J.; Matsumoto, N.; Yonekubo, S.; Osanai, S.; Soai, K. Amplification of a Slight Enantiomeric Imbalance in Molecules Based on Asymmetric Autocatalysis: The First Correlation between High Enantiomeric Enrichment in a Chiral Molecule and Circularly Polarized Light. *J. Am. Chem. Soc.* **1998**, *120*, 12157-12158. b) Flores, J. J.; Bonner, W. A.; Massey, G. A. Asymmetric photolysis of (RS)-leucine with circularly polarized ultraviolet light. *J. Am. Chem. Soc.* **1977**, *99*, 3622-3625. c) Breslow, R. The origin of homochirality in amino acids and sugars on prebiotic earth. *Tetrahedron Lett.* **2011**, *52*, 4228-4232. d) Breslow, R. Formation of L Amino Acids and D Sugars, and Amplification of their Enantioexcesses in Aqueous Solutions, Under Simulated Prebiotic Conditions. *Isr. J. Chem.* **2011**, *51*, 990-996.

22. Sugimura, T.; Nishiyama, N.; Tai, A.; Hakushi, T. Regio- and diastereo-chemically controlled photocycloaddition of an arene and an alkene linked by a chiral auxiliary. *Tetrahedron: Asymmetry* **1994**, *5*, 1163-1166.

23. a) Demuth, M.; Mikhail, G. New Developments in the Field of Photochemical Syntheses. *Synthesis* **1989**, 1989, 145,162. b) Bach, T. Stereoselective Intermolecular [2+2]-Photocycloaddition Reactions and Their Application in Synthesis. *Synthesis* **1998**, 1998, 683,703.
24. a) Schuster, D. I.; Lem, G.; Kaprinidis, N. A. New insights into an old mechanism: [2+2] photocycloaddition of enones to alkenes. *Chem. Rev.* **1993**, 93, 3-22. b) Fagnoni, M.; Dondi, D.; Ravelli, D.; Albini, A. Photocatalysis for the Formation of the C-C Bond. *Chem. Rev.* **2007**, 107, 2725-2756.
25. a) Narasaka, K.; Hayashi, Y.; Shimadzu, H.; Niihata, S. Asymmetric [2 + 2] cycloaddition reaction catalyzed by a chiral titanium reagent. *J. Am. Chem. Soc.* **1992**, 114, 8869-8885. b) Canales, E.; Corey, E. J. Highly Enantioselective [2+2]-Cycloaddition Reactions Catalyzed by a Chiral Aluminum Bromide Complex. *J. Am. Chem. Soc.* **2007**, 129, 12686-12687. c) Lee-Ruff, E.; Mladenova, G. Enantiomerically Pure Cyclobutane Derivatives and Their Use in Organic Synthesis. *Chem. Rev.* **2003**, 103, 1449-1484. d) Orr, R. K.; Calter, M. A. Asymmetric synthesis using ketenes. *Tetrahedron* **2003**, 59, 3545-3565.
26. Tolbert, L. M.; Ali, M. B. High optical yields in a photochemical cycloaddition. Lack of cooperativity as a clue to mechanism. *J. Am. Chem. Soc.* **1982**, 104, 1742-1744.
27. Meyers, A. I.; Fleming, S. A. Efficient asymmetric (2+2) photocycloaddition leading to chiral cyclobutanes. Application to the total synthesis of (–)-Grandisol. *J. Am. Chem. Soc.* **1986**, 108, 306-307.
28. Meyers, A. I.; Wanner, K. T. Chiral quaternary carbon compounds. II. An asymmetric synthesis of (R) or (S)-4,4-dialkyl-2-cyclopentenones. *Tetrahedron Lett.* **1985**, 26, 2047-2050.
29. Demuth, M.; Palomer, A.; Sluma, H.-D.; Dey, A. K.; Krüger, C.; Tsay, Y.-H. Asymmetric Photocycloadditions with Optically Pure, Spirocyclic Enones. Simple Synthesis of (+)- and (–)-Grandisol. *Angew. Chem. Int. Ed.* **1986**, 25, 1117-1119.
30. Rosini, G.; Marotta, E.; Petrini, M.; Ballini, R. Tereoselective total synthesis of racemic grandisol : An improved convenient procedure. *Tetrahedron* **1985**, 41, 4633-4638.
31. a) Carreira, E. M.; Hastings, C. A.; Shepard, M. S.; Yerkey, L. A.; Millward, D. B. Asymmetric Induction in Intramolecular [2+2]-Photocycloadditions of 1,3-Disubstituted Allenes with Enones and Enoates. *J. Am. Chem. Soc.* **1994**, 116, 6622-6630. b) Shepard, M. S.; Carreira, E. M. Asymmetric Photocycloadditions with an Optically Active Allenylsilane: Trimethylsilyl as a Removable Stereocontrolling Group for the Enantioselective Synthesis of *exo*-Methylenecyclobutanes. *J. Am. Chem. Soc.* **1997**, 119, 2597-2605.

32. Myers, A. G.; Finney, N. S.; Kuo, E. Y. Allene synthesis from 2-alkyn-1-ols. *Tetrahedron Lett.* **1989**, 30, 5747-5750.
33. Büchi, G.; Inman, C. G.; Lipinsky, E. S. Light-catalyzed Organic Reactions. I. The Reaction of Carbonyl Compounds with 2-Methyl-2-butene in the Presence of Ultraviolet Light. *J. Am. Chem. Soc.* **1954**, 76, 4327-4331.
34. Schreiber, S. L. [2 + 2] Photocycloadditions in the Synthesis of Chiral Molecules. *Science* **1985**, 227, 857-863.
35. Nehrings, A.; Scharf, H.-D.; Runsink, J. Photochemical Synthesis of an L-Erythrose Building Block and Its use in the Preparation of Methyl 2,3,O-Isopropylidene- $\beta$ -L-apio-L-furanoside. *Angew. Chem. Int. Ed.* **1985**, 24, 877-878.
36. Buschmann, H.; Scharf, H.-D.; Hoffmann, N.; Esser, P. The Isoinversion Principle—a General Model of Chemical Selectivity. *Angew. Chem. Int. Ed.* **1991**, 30, 477-515.
37. Takahashi, K. Organic Reactions Mediated by Cyclodextrins. *Chem. Rev.* **1998**, 98, 2013-2034.
38. Nakamura, A.; Inoue, Y. Supramolecular Catalysis of the Enantiodifferentiating [4 + 4] Photocyclodimerization of 2-Anthracenecarboxylate by  $\gamma$ -Cyclodextrin. *J. Am. Chem. Soc.* **2003**, 125, 966-972.
39. a) Yang, C.; Nakamura, A.; Wada, T.; Inoue, Y. Enantiodifferentiating Photocyclodimerization of 2-Anthracenecarboxylic Acid Mediated by  $\gamma$ -Cyclodextrins with a Flexible or Rigid Cap. *Org. Lett.* **2006**, 8, 3005-3008. b) Nakamura, A.; Inoue, Y. Electrostatic Manipulation of Enantiodifferentiating Photocyclodimerization of 2-Anthracenecarboxylate within  $\gamma$ -Cyclodextrin Cavity through Chemical Modification. Inverted Product Distribution and Enhanced Enantioselectivity. *J. Am. Chem. Soc.* **2005**, 127, 5338-5339.
40. Ke, C.; Yang, C.; Mori, T.; Wada, T.; Liu, Y.; Inoue, Y. Catalytic Enantiodifferentiating Photocyclodimerization of 2-Anthracenecarboxylic Acid Mediated by a Non-Sensitizing Chiral Metallosupramolecular Host. *Angew. Chem. Int. Ed.* **2009**, 48, 6675-6677.
41. Pordea, A.; Ward, T. R. Artificial Metalloenzymes: Combining the Best Features of Homogeneous and Enzymatic Catalysis. *Synlett* **2009**, 2009, 3225,3236.
42. a) Wada, T.; Nishijima, M.; Fujisawa, T.; Sugahara, N.; Mori, T.; Nakamura, A., et al. Bovine Serum Albumin-Mediated Enantiodifferentiating Photocyclodimerization of 2-Anthracenecarboxylate. *J. Am. Chem. Soc.* **2003**, 125, 7492-7493. b) Nishijima, M.; Pace, T. C. S.; Nakamura, A.; Mori, T.; Wada, T.; Bohne, C., et al. Supramolecular Photochirogenesis with Biomolecules. Mechanistic Studies on the Enantiodifferentiation

for the Photocyclodimerization of 2-Anthracenecarboxylate Mediated by Bovine Serum Albumin. *J. Org. Chem.* **2007**, 72, 2707-2715.

43. Nishijima, M.; Wada, T.; Mori, T.; Pace, T. C. S.; Bohne, C.; Inoue, Y. Highly Enantiomeric Supramolecular [4+4] Photocyclodimerization of 2-Anthracenecarboxylate Mediated by Human Serum Albumin. *J. Am. Chem. Soc.* **2007**, 129, 3478-3479.

44. a) Mizoguchi, J.-i.; Kawanami, Y.; Wada, T.; Kodama, K.; Anzai, K.; Yanagi, T., et al. Enantiodifferentiating Photocyclodimerization of 2-Anthracenecarboxylic Acid Using a Chiral *N*-(2-Hydroxymethyl-4-pyrrolidinyl)benzamide Template. *Org. Lett.* **2006**, 8, 6051-6054. b) Kawanami, Y.; Pace, T. C. S.; Mizoguchi, J.-i.; Yanagi, T.; Nishijima, M.; Mori, T., et al. Supramolecular Complexation and Enantiodifferentiating Photocyclodimerization of 2-Anthracenecarboxylic Acid with 4-Aminoprolinol Derivatives as Chiral Hydrogen-Bonding Templates. *J. Org. Chem.* **2009**, 74, 7908-7921.

45. Tanaka, K.; Fujiwara, T. Enantioselective [2 + 2]Photodimerization Reactions of Coumarins in Solution. *Org. Lett.* **2005**, 7, 1501-1503.

46. Gerard, B.; Sangji, S.; O'Leary, D. J.; Porco, J. A. Enantioselective Photocycloaddition Mediated by Chiral Brønsted Acids: Asymmetric Synthesis of the Rocaglamides. *J. Am. Chem. Soc.* **2006**, 128, 7754-7755.

47. Kemp, D. S.; Petrakis, K. S. Synthesis and conformational analysis of cis,cis-1,3,5-trimethylcyclohexane-1,3,5-tricarboxylic acid. *J. Org. Chem.* **1981**, 46, 5140-5143.

48. Jeong, K.-S.; Parris, K.; Ballester, P.; Rebek, J. New Chiral Auxiliaries for Enolate Alkylations. *Angew. Chem. Int. Ed.* **1990**, 29, 555-556.

49. Bach, T.; Bergmann, H.; Harms, K. High Facial Diastereoselectivity in the Photocycloaddition of a Chiral Aromatic Aldehyde and an Enamide Induced by Intermolecular Hydrogen Bonding. *J. Am. Chem. Soc.* **1999**, 121, 10650-10651.

50. Bach, T.; Bergmann, H.; Harms, K. Enantioselective Intramolecular [2+2]-Photocycloaddition Reactions in Solution. *Angew. Chem. Int. Ed.* **2000**, 39, 2302-2304.

51. a) Austin, K. A. B.; Herdtweck, E.; Bach, T. Intramolecular [2+2] Photocycloaddition of Substituted Isoquinolones: Enantioselectivity and Kinetic Resolution Induced by a Chiral Template. *Angew. Chem. Int. Ed.* **2011**, 50, 8416-8419. b) Bach, T.; Grosch, B.; Strassner, T.; Herdtweck, E. Enantioselective [6 $\pi$ ]-Photocyclization Reaction of an Acrylanilide Mediated by a Chiral Host. Interplay between Enantioselective Ring Closure and Enantioselective Protonation. *J. Org. Chem.* **2003**, 68, 1107-1116. c) Grosch, B.; Orlebar, C. N.; Herdtweck, E.; Massa, W.; Bach, T. Highly Enantioselective Diels–Alder Reaction of a Photochemically Generated o-Quinodimethane with Olefins. *Angew. Chem. Int. Ed.* **2003**, 42, 3693-3696. d) Grosch, B.; Orlebar, C. N.; Herdtweck, E.; Kaneda, M.; Wada, T.; Inoue, Y., et al. Enantioselective [4+2]-Cycloaddition Reaction of

a Photochemically Generated o-Quinodimethane: Mechanistic Details, Association Studies, and Pressure Effects. *Chem. Eur. J.* **2004**, *10*, 2179-2189.

52. Lu, P.; Bach, T. Total Synthesis of (+)-Lactiflorin by an Intramolecular [2+2] Photocycloaddition. *Angew. Chem. Int. Ed.* **2012**, *51*, 1261-1264.

53. Selig, P.; Bach, T. Enantioselective Total Synthesis of the Melodinus Alkaloid (+)-Meloscine. *Angew. Chem. Int. Ed.* **2008**, *47*, 5082-5084.

54. Cauble, D. F.; Lynch, V.; Krische, M. J. Studies on the Enantioselective Catalysis of Photochemically Promoted Transformations: "Sensitizing Receptors" as Chiral Catalysts. *J. Org. Chem.* **2002**, *68*, 15-21.

55. a) Müller, C.; Bauer, A.; Bach, T. Light-Driven Enantioselective Organocatalysis. *Angew. Chem. Int. Ed.* **2009**, *48*, 6640-6642. b) Müller, C.; Bauer, A.; Maturi, M. M.; Cuquerella, M. C.; Miranda, M. A.; Bach, T. Enantioselective Intramolecular [2 + 2]-Photocycloaddition Reactions of 4-Substituted Quinolones Catalyzed by a Chiral Sensitizer with a Hydrogen-Bonding Motif. *J. Am. Chem. Soc.* **2011**, *133*, 16689-16697.

56. a) Breitenlechner, S.; Bach, T. A Polymer-Bound Chiral Template for Enantioselective Photochemical Reactions. *Angew. Chem. Int. Ed.* **2008**, *47*, 7957-7959. b) Wessig, P. Organocatalytic Enantioselective Photoreactions. *Angew. Chem. Int. Ed.* **2006**, *45*, 2168-2171.

57. Hammond, G. S.; Cole, R. S. Asymmetric Induction during Energy Transfer. *J. Am. Chem. Soc.* **1965**, *87*, 3256-3257.

58. Hoffmann, N. Efficient photochemical electron transfer sensitization of homogeneous organic reactions. *J. Photochem. Photobiol., C: Photochem. Rev.* **2008**, *9*, 43-60.

59. a) Asaoka, S.; Kitazawa, T.; Wada, T.; Inoue, Y. Enantiodifferentiating Anti-Markovnikov Photoaddition of Alcohols to 1,1-Diphenylalkenes Sensitized by Chiral Naphthalenecarboxylates. *J. Am. Chem. Soc.* **1999**, *121*, 8486-8498. b) Inoue, Y.; Tsuneishi, H.; Hakushi, T.; Tai, A. Optically Active (E,Z)-1,3-Cyclooctadiene: First Enantioselective Synthesis through Asymmetric Photosensitization and Chiroptical Property. *J. Am. Chem. Soc.* **1997**, *119*, 472-478. c) Inoue, Y.; Yamasaki, N.; Yokoyama, T.; Tai, A. Highly enantiodifferentiating photoisomerization of cyclooctene by congested and/or triplex-forming chiral sensitizers. *J. Org. Chem.* **1993**, *58*, 1011-1018. d) Inoue, Y.; Yokoyama, T.; Yamasaki, N.; Tai, A. Temperature switching of product chirality upon photosensitized enantiodifferentiating cis-trans isomerization of cyclooctene. *J. Am. Chem. Soc.* **1989**, *111*, 6480-6482. e) Kim, J. I.; Schuster, G. B. Enantioselective catalysis of the triplex Diels-Alder reaction: addition of trans- $\beta$ -methylstyrene to 1,3-cyclohexadiene photosensitized with (-)-1,1'-bis(2,4-dicyanonaphthalene). *J. Am. Chem. Soc.* **1990**, *112*, 9635-9637. f) Kim, J. I.; Schuster,

G. B. Enantioselective catalysis of the triplex Diels-Alder reaction: a study of scope and mechanism. *J. Am. Chem. Soc.* **1992**, *114*, 9309-9317.

60. Córdova, A.; Sundén, H.; Engqvist, M.; Ibrahim, I.; Casas, J. The Direct Amino Acid-Catalyzed Asymmetric Incorporation of Molecular Oxygen to Organic Compounds. *J. Am. Chem. Soc.* **2004**, *126*, 8914-8915.

61. Sundén, H.; Engqvist, M.; Casas, J.; Ibrahim, I.; Córdova, A. Direct Amino Acid Catalyzed Asymmetric  $\alpha$  Oxidation of Ketones with Molecular Oxygen. *Angew. Chem. Int. Ed.* **2004**, *43*, 6532-6535.

62. Nicewicz, D. A.; MacMillan, D. W. C. Merging Photoredox Catalysis with Organocatalysis: The Direct Asymmetric Alkylation of Aldehydes. *Science* **2008**, *322*, 77-80.

63. a) Yoon, T. P.; Ischay, M. A.; Du, J. Visible light photocatalysis as a greener approach to photochemical synthesis. *Nature Chem.* **2010**, *2*, 527-532. b) Narayanam, J. M. R.; Stephenson, C. R. J. Visible light photoredox catalysis: applications in organic synthesis. *Chem. Soc. Rev.* **2011**, *40*, 102-113. c) Zeitler, K. Photoredox Catalysis with Visible Light. *Angew. Chem. Int. Ed.* **2009**, *48*, 9785-9789.

64. a) Nagib, D. A.; Scott, M. E.; MacMillan, D. W. C. Enantioselective  $\alpha$ -Trifluoromethylation of Aldehydes via Photoredox Organocatalysis. *J. Am. Chem. Soc.* **2009**, *131*, 10875-10877. b) Pham, P. V.; Nagib, D. A.; MacMillan, D. W. C. Photoredox Catalysis: A Mild, Operationally Simple Approach to the Synthesis of  $\alpha$ -Trifluoromethyl Carbonyl Compounds. *Angew. Chem. Int. Ed.* **2011**, *50*, 6119-6122.

65. Shih, H.-W.; Vander Wal, M. N.; Grange, R. L.; MacMillan, D. W. C. Enantioselective  $\alpha$ -Benzylation of Aldehydes via Photoredox Organocatalysis. *J. Am. Chem. Soc.* **2010**, *132*, 13600-13603.

66. Guo, H.; Herdtweck, E.; Bach, T. Enantioselective Lewis Acid Catalysis in Intramolecular [2+2] Photocycloaddition Reactions of Coumarins. *Angew. Chem. Int. Ed.* **2010**, *49*, 7782-7785.

67. a) Corey, E. J. Enantioselective Catalysis Based on Cationic Oxazaborolidines. *Angew. Chem. Int. Ed.* **2009**, *48*, 2100-2117. b) Liu, D.; Canales, E.; Corey, E. J. Chiral Oxazaborolidine-Aluminum Bromide Complexes Are Unusually Powerful and Effective Catalysts for Enantioselective Diels-Alder Reactions. *J. Am. Chem. Soc.* **2007**, *129*, 1498-1499.



## Chapter 2. Lewis Acid-Mediated Photocatalysis: Intermolecular [2+2] Enone Cycloadditions Using Visible Light

Portions of this work have previously been published:

Du, J.; Yoon, T. P. Crossed Intermolecular [2+2] Cycloadditions of Acyclic Enones via Visible Light Photocatalysis. *J. Am. Chem. Soc.* **2009**, *131*, 14604–14605.

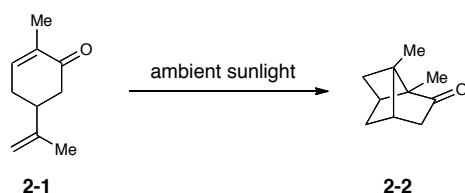
Ischay, M. A.; Anzovino, M. E.; Du, J.; Yoon, T. P. Efficient Visible Light Photocatalysis of [2+2] Enone Cycloadditions. *J. Am. Chem. Soc.* **2008**, *130*, 12886–12887.

## 2.1 Introduction

The [2+2] cycloaddition of alkenes is a powerful strategy for the synthesis of cyclobutanes.<sup>1</sup> This atom-economical reaction forms two carbon–carbon bonds and sets up to four stereogenic centers in a single step. If carried out with high levels of regio- and stereocontrol, the [2+2] cycloaddition of olefins would be an efficient method for the construction of densely functionalized cyclic structures. In addition, a number of facile ring-expansions from the strained cyclobutane-containing products can provide rapid access to orthogonal molecular scaffolds.<sup>2</sup> Given the versatility of this transformation, the development of efficient methods for the [2+2] photocycloaddition of alkenes is of particular importance.

The first example of a photoinitiated [2+2] enone cycloaddition was reported in 1908 by Ciamician and involved the clean conversion of carvone (**2-1**) to carvone-camphor (**2-2**) upon prolonged exposure to sunlight (Scheme 2-1).<sup>3</sup> Büchi and Goldman confirmed the identity of **2-2** in 1957,<sup>4</sup> sparking a renewed interest in the use of photochemical strategies for organic synthesis.<sup>5</sup>

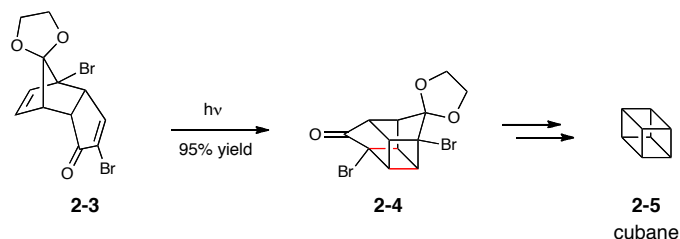
**Scheme 2-1.** First reported example of a photochemical [2+2] enone cycloaddition



Since this initial discovery, [2+2] enone cycloaddition reactions promoted by UV irradiation have been recognized as a useful strategy for generating cyclobutane-containing structures. An early demonstration of the potential of this photochemical

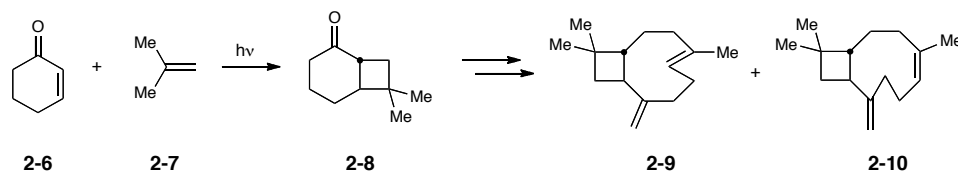
transformation was evident in the first synthesis of cubane (**2-5**) (Scheme 2-2).<sup>6</sup> This classic synthetic sequence by Eaton features a remarkably efficient intramolecular [2+2] cycloaddition to access the key intermediate (**2-4**).

**Scheme 2-2.** Key [2+2] photocycloaddition in the synthesis of cubane (**2-5**)



Pioneering studies by Corey of the intermolecular variant of this transformation and its application to the synthesis of natural products further established the synthetic utility of the photochemical [2+2] cycloaddition.<sup>7</sup> A landmark synthesis of the caryophyllenes (**2-9–2-10**) commenced with an intermolecular [2+2] photocycloaddition to generate the core cyclobutane structure (**2-8**) (Scheme 2-3). A series of subsequent ring-expansion reactions provided access to the unusual bicyclic ring system.<sup>8</sup>

**Scheme 2-3.** Synthesis of the caryophyllenes (**2-9–2-10**) using an intermolecular [2+2] photocycloaddition strategy



Despite the considerable progress that has been made in the development of methods for photochemical [2+2] cycloadditions, however,<sup>9</sup> the synthetic application of this reaction has largely been restricted to cycloadditions of cyclic enones.<sup>10</sup> Acyclic

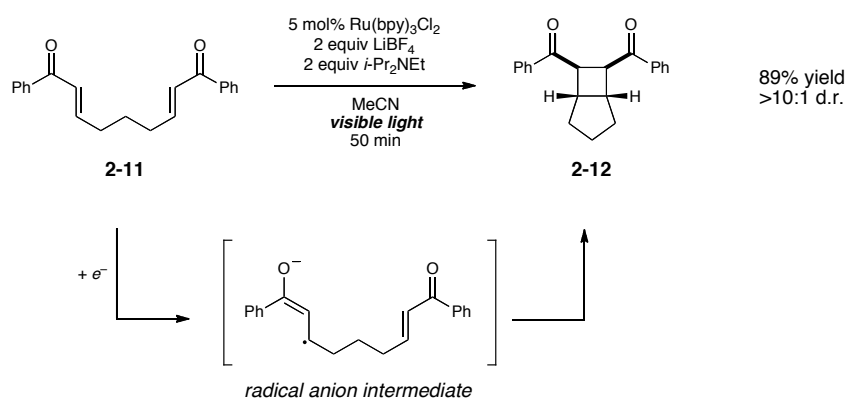
enones undergo rapid relaxation to the ground state by *cis-trans* isomerization upon UV irradiation, an energy-wasting process that dramatically diminishes the efficiency of productive cycloaddition.<sup>10</sup> As a result, these compounds are not suitable substrates for photochemical reactions that require direct UV irradiation and the efficient [2+2] photocycloadditions of acyclic enones remains a long-standing unsolved problem in synthetic chemistry.

The advantages of employing light as a reagent for chemical synthesis have been recognized for decades.<sup>11</sup> Unfortunately, the majority of organic molecules are unable to absorb visible wavelengths of light, and specialized photochemical equipment is required to safely generate the high-intensity UV light required for most organic reactions. This inconvenience has been a significant impediment in the widespread incorporation of photochemical strategies into the standard repertoire of synthetic chemists.<sup>12</sup> Thus, the development of new methods that utilize visible light is a particularly relevant endeavor.

While the visible light photochemistry of organic molecules is relatively underdeveloped, organometallic complexes that absorb strongly in the visible region have been extensively investigated.<sup>13</sup> In this context, the photochemistry of  $\text{Ru}(\text{bpy})_3^{2+}$  has been particularly well studied,<sup>14</sup> and its use in the design of systems for the conversion of solar energy into electrical current or fuel has been extensively exploited.<sup>15</sup> The use of  $\text{Ru}(\text{bpy})_3^{2+}$  in the synthesis of organic molecules, on the other hand, is relatively rare; at the beginning of our studies, only a few examples of synthetically useful organic transformations catalyzed by  $\text{Ru}(\text{bpy})_3^{2+}$  had been reported.<sup>16</sup>

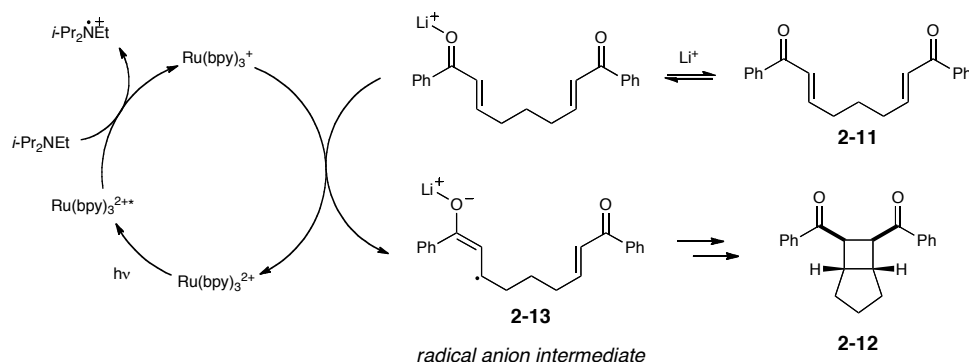
Our group has recently become interested in designing new reactions initiated by visible light photoexcitation of organometallic complexes.<sup>17</sup> As an initial goal for our investigations in visible light photocatalysis, we examined the [2+2] cycloaddition of bis(enone) **2-11**. Krische has reported that cobalt-<sup>18</sup> and copper-<sup>19</sup> catalyzed [2+2] cyclizations of bis(enone)s are initiated by one-electron reduction of the enone. The intermediacy of a radical anion in these processes is corroborated by the formation of identical [2+2] cycloadducts upon cathodic<sup>20</sup> and homogeneous<sup>21</sup> one-electron reduction. We postulated that formation of the key radical anion intermediate could be achieved through reduction of the substrate with a photoreductant generated by irradiation of Ru(bpy)<sub>3</sub><sup>2+</sup>. Indeed, we found that bis(enone) **2-11** undergoes efficient cyclization to *meso* cyclobutane **2-12** upon visible light irradiation using 5 mol% Ru(bpy)<sub>3</sub>Cl<sub>2</sub> with LiBF<sub>4</sub> and *i*-Pr<sub>2</sub>NEt as additives (Scheme 2-4).<sup>17a</sup> Given that the substrate contains at least one aryl enone component, a variety of symmetrical and unsymmetrical enones undergo cycloaddition under the optimized conditions. Importantly, the light source used in this protocol was a standard 275 W floodlight; no specialized high-pressure UV photolysis apparatus was required.

**Scheme 2-4.** Visible light photocatalysis of intramolecular [2+2] bis(enone) cycloadditions



Our proposed mechanism for the transformation is outlined in Scheme 2-5. Photoexcitation of  $\text{Ru}(\text{bpy})_3^{2+}$  with visible light produces a photoexcited complex ( $\text{Ru}(\text{bpy})_3^{2+*}$ ) that can undergo reductive quenching by  $i\text{-Pr}_2\text{NEt}$ . The resulting  $\text{Ru}(\text{bpy})_3^+$  complex is a powerful reducing agent that can transfer an electron to the lithium-activated enone, initiating the [2+2] cycloaddition and regenerating the  $\text{Ru}(\text{bpy})_3^{2+}$  photocatalyst.

**Scheme 2-5.** Proposed mechanism for [2+2] cycloaddition promoted by visible light



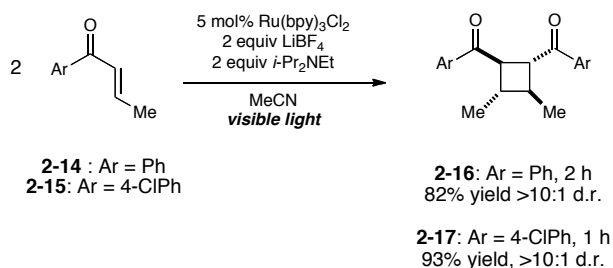
Having demonstrated that  $\text{Ru}(\text{bpy})_3\text{Cl}_2$  is an efficient visible light photocatalyst for intramolecular [2+2] enone cycloadditions, we wondered whether the development of an intermolecular variant might be possible. Because the formation of unsymmetrical cyclobutanes via the [2+2] cycloaddition of two different alkenes is arguably one of the most valuable transformations in synthetic photochemistry, a method for accessing the corresponding crossed cyclobutane products using our visible light protocol would be a synthetically useful advance.

## 2.2 Results and discussion

### 2.2.1 Intermolecular [2+2] homodimerization of acyclic enones

We first set out to probe the feasibility of an intermolecular process under the conditions of visible light photocatalysis. Because the Krische and Bauld precedent, which proceeds via an analogous stepwise mechanism to generate the requisite radical anion intermediate, is strictly limited to intramolecular reactions of tethered enones,<sup>18a, 20</sup> it was not clear at the outset that the intermolecular reaction would be possible. In contrast to this precedent, however, we discovered that intermolecular dimerizations of aryl enones proceed smoothly under our photocatalytic conditions (Scheme 2-6). Formation of the *rac* isomer from homodimerization of enone **2-15** was confirmed by single-crystal X-ray diffraction of cyclobutane **2-17**.

**Scheme 2-6.** Intermolecular dimerization of aryl enones via visible light photocatalysis

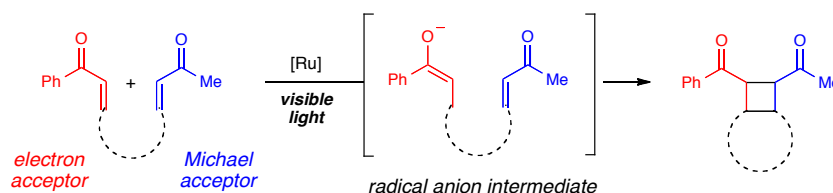


### 2.2.2 Crossed intermolecular [2+2] cycloadditions of acyclic enones

Having established the viability of the intermolecular process, we proceeded to investigate the possibility of achieving crossed intermolecular [2+2] heterodimerizations. The mechanism outlined in Scheme 2-5 suggests that there are two distinct roles for the enone substrates in the [2+2] cycloaddition. The first equivalent serves as an electron acceptor that is reduced by the photogenerated  $\text{Ru(bpy)}_3^+$  reductant, while the second

equivalent acts as a Michael acceptor that reacts with the radical anion intermediate (Scheme 2-7). Given this separation of roles, we hypothesized that the crossed product might be selectively formed if two sufficiently dissimilar enones are employed in the reaction.

**Scheme 2-7.** Design considerations for crossed [2+2] photocycloaddition

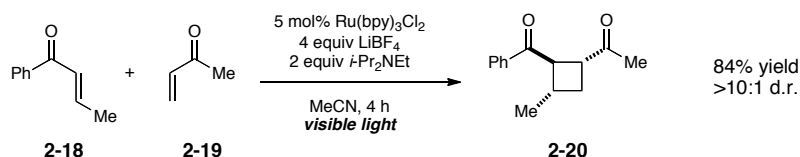


We began our studies of the heterocoupling process by studying the reaction shown in Scheme 2-8. The design of this experiment was based upon two main considerations. First, given the requirement that a reducible aryl enone serve as an electrophore in this process, we selected phenyl enone **2-18** to serve as the precursor to the key radical anion intermediate. Second, we recognized that the reaction partner must be a more reactive Michael acceptor than **2-18** to minimize the undesired homodimerization, but be less susceptible to one-electron reduction by the photocatalyst. Ultimately, we selected methyl vinyl ketone (**2-19**), which we expected should be less easily reduced than **2-18**,<sup>22</sup> but, due to the lack of a  $\beta$ -substituent, should serve as a sterically more accessible electrophilic reaction partner for the radical anion intermediate. In the event, we observed highly chemoselective formation of the crossed [2+2] cycloadduct **2-20** in 84% isolated yield with excellent diastereoselectivity (>10:1 d.r.).<sup>17b</sup> Only trace amounts of products arising from the homocoupling of **2-18** and none of the product from dimerization of **2-19** could be observed upon <sup>1</sup>H NMR analysis of



the crude reaction mixture. In addition, the cycloaddition proceeded readily upon irradiation with a standard 23 W compact fluorescent bulb; a 275 W floodlight was not necessary.

**Scheme 2-8.** Crossed intermolecular [2+2] cycloadditions via visible light photocatalysis



Next, we examined the scope of the aryl enone in the crossed cycloaddition, using methyl vinyl ketone (**2-19**) as the Michael acceptor (Table 2-1). Both electron-poor and electron-rich substrates are amenable to cycloaddition (entries 1–3), as are heteroaryl enones (entry 4). On the other hand, aliphatic enones are completely unreactive (entry 5), which is consistent with our understanding of the mechanism of this process. Variation of the  $\beta$ -substituent is also possible; however, the reaction is sensitive to steric bulk. While reactions of enones bearing primary aliphatic substituents proceed smoothly (entry 6), secondary substituents at this position retard the reaction rate (entry 7), and reactions of enones bearing tertiary alkyl substituents fail to proceed at synthetically useful rates (entry 8). On the other hand, heteroatom-bearing substituents are easily tolerated (entry 9).

**Table 2-1.** Effect of aryl enone structure in photocatalytic crossed cycloadditions with methyl vinyl ketone (**2-19**)<sup>a</sup>

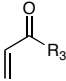
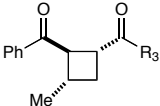
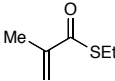
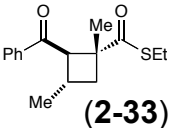
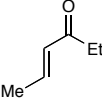
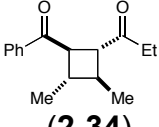
| entry          | enone  | cycloadduct | yield <sup>b</sup> | d.r. <sup>b</sup> |
|----------------|--|-------------|--------------------|-------------------|
|                |  |             |                    |                   |
| 1              | R <sub>1</sub> = Ph ( <b>2-20</b> )                  |             | 84%                | >10:1             |
| 2              | R <sub>1</sub> = 4-ClPh ( <b>2-22</b> )              |             | 82%                | >10:1             |
| 3              | R <sub>1</sub> = 4-MeOPh ( <b>2-23</b> )             |             | 53%                | >10:1             |
| 4              | R <sub>1</sub> = 2-furyl ( <b>2-24</b> )             |             | 74%                | >10:1             |
| 5              | R <sub>1</sub> = Et ( <b>2-25</b> )                  |             | 0%                 | --                |
|                |  |             |                    |                   |
| 6              | R <sub>2</sub> = Et ( <b>2-26</b> )                  |             | 70%                | 6:1               |
| 7 <sup>c</sup> | R <sub>2</sub> = <i>i</i> -Pr ( <b>2-27</b> )        |             | 64%                | >10:1             |
| 8 <sup>d</sup> | R <sub>2</sub> = <i>t</i> -Bu ( <b>2-28</b> )        |             | 8%                 | >10:1             |
| 9              | R <sub>2</sub> = CH <sub>2</sub> OBn ( <b>2-29</b> ) |             | 61%                | >10:1             |

<sup>a</sup> Unless otherwise noted, reactions conducted using 1 equiv of aryl enone, 2.5 equiv of methyl vinyl ketone (**2-19**) and 5 mol% Ru(bpy)<sub>3</sub>Cl<sub>2</sub> in the presence of 4 equiv LiBF<sub>4</sub> and 2 equiv *i*-Pr<sub>2</sub>NEt in MeCN (0.1 M). Irradiation time using a 23 W fluorescent bulb at 30 cm was 4 h. <sup>b</sup> Isolated yields and diastereomer ratios are the averaged results of two reproducible experiments. <sup>c</sup> 12 h irradiation. <sup>d</sup> 24 h irradiation.

Experiments exploring the generality of the crossed reaction with respect to the Michael acceptor are summarized in Table 2-2. A variety of aliphatic enones are good reaction partners for the crossed [2+2] cycloaddition (e.g., entries 1–2). Acrylate esters also participate, but given their reduced electrophilicity, several additional equivalents are required to outcompete homodimerization of enone **2-18** (entry 3). Thioesters, on the other hand, are excellent acceptor enones and provide high yields of the heterocoupling product (entry 4). Substrates bearing alkyl substituents at the  $\alpha$ -position

also participate and provide access to cyclobutane structures bearing all-carbon quaternary stereocenters with high selectivity (entry 5). On the other hand, as expected,  $\beta$ -substituents that sterically deactivate the Michael acceptor ability of the enone cause homodimerization of **2-18** to predominate. Nevertheless, the heterocoupling product can be isolated when a larger excess of the acceptor enone is used (entries 6–7).

**Table 2-2.** Effect of Michael acceptor structure in photocatalytic crossed cycloadditions with phenyl enone **2-18**<sup>a</sup>

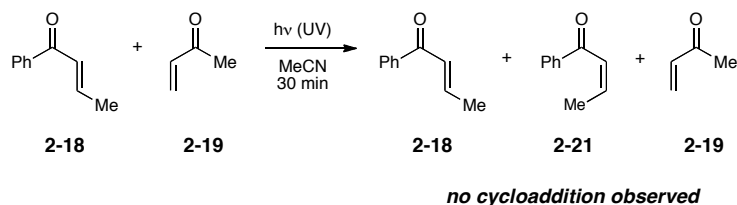
| entry            | enone   | cycloadduct   | yield <sup>b</sup> | d.r. <sup>b</sup> |
|------------------|---|---|--------------------|-------------------|
|                  |    |    |                    |                   |
| 1                | R <sub>3</sub> = Me ( <b>2-20</b> )   |   | 84%                | >10:1             |
| 2                | R <sub>3</sub> = Et ( <b>2-30</b> )   |   | 76%                | >10:1             |
| 3 <sup>c</sup>   | R <sub>3</sub> = OMe ( <b>2-31</b> )  |   | 65%                | 5:1               |
| 4                | R <sub>3</sub> = SEt ( <b>2-32</b> )  |   | 88%                | >10:1             |
| 5 <sup>c</sup>   |  |  | 57%                | 5:1               |
| 6                |  |  | 9%                 | --                |
| 7 <sup>c,d</sup> |   |   | 35%                | >10:1             |

<sup>a</sup> Unless otherwise noted, reactions conducted using 1 equiv of aryl enone **2-18**, 2.5 equiv of Michael acceptor, and 5 mol% Ru(bpy)<sub>3</sub>Cl<sub>2</sub> in the presence of 4 equiv LiBF<sub>4</sub> and 2 equiv *i*-Pr<sub>2</sub>NEt in MeCN (0.1 M). Irradiation time using a 23 W compact fluorescent bulb at 30 cm was 4 h. <sup>b</sup> Isolated yields and diastereomer ratios are the averaged results of two reproducible experiments. <sup>c</sup> 6 equiv of Michael acceptor and 12 h irradiation time. <sup>d</sup> The homodimerization product of **2-18** was isolated in 65% yield.

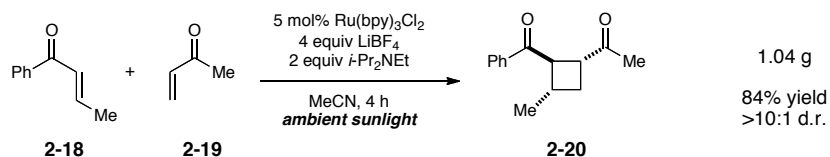
An important feature of this process is that the reaction is initiated by photoexcitation of the ruthenium catalyst and does not access electronically excited

states of the enone. By exploiting the photophysical properties of the organometallic catalyst rather than relying on direct excitation of the organic substrate, this method avoids some of the synthetic limitations of photochemical reactions conducted under standard UV photolysis conditions and enables access to cyclobutane products from *acyclic* enones. Consistent with this premise, irradiation of a solution of enones **2-18** and **2-19** in a Rayonet reactor (300 nm) does not produce any observable cycloaddition products; the only new products observed in the reaction mixture arise from *E/Z* isomerization of enone **2-18** (Scheme 2-9).

**Scheme 2-9.** Unproductive reactivity upon UV irradiation of enones **2-18** and **2-19**



Moreover, in the presence of the  $\text{Ru}(\text{bpy})_3^{2+}$  photocatalyst, the [2+2] cycloaddition proceeds upon irradiation with any visible light source. To demonstrate this principle, we conducted a gram-scale cycloaddition experiment on the roof of our laboratory building using ambient sunlight as the only source of irradiation (Scheme 2-10). The [2+2] cycloaddition between enones **2-18** and **2-19** was equally efficient in ambient sunlight as it was in our laboratory experiments and produced a single diastereomer of the crossed cycloadduct **2-20** in 84% yield. Thus, the efficiency and operational ease of this photochemical protocol represents a practical advance for enabling the use of direct sunlight in organic synthesis.

**Scheme 2-10.** Crossed intermolecular [2+2] cycloaddition using ambient sunlight

## 2.3 Conclusions

In summary, we have developed an efficient method for the crossed [2+2] cycloaddition of acyclic enones promoted by visible light. The excellent chemo- and stereoselectivity observed in this reaction represents a considerable advance in the construction of strained four-membered rings and should have a significant impact on the approach toward synthesis of cyclobutane-containing structures. More importantly, the use of visible light *enables* this reaction; the transparency of organic molecules to visible light circumvents the problematic aspects that have thus far prohibited the development of this transformation. Thus, this study illustrates the potential of visible light to serve not only as an attractive reagent for chemical synthesis, but also as a general strategy for enabling reactivity that cannot be accessed using current thermal or photochemical methods.

In addition, the success of this methodology provides corroborative evidence for our mechanistic hypothesis and establishes a solid framework for the further development of new methodology using visible light photocatalysis. Our seminal publication in this field<sup>17a</sup> was published simultaneously with MacMillan's report on the enantioselective  $\alpha$ -alkylation of aldehydes in 2008.<sup>23</sup> Since then, the field of visible light

photocatalysis<sup>24</sup> has become an active area of investigation,<sup>25</sup> particularly in the groups of Stephenson,<sup>26</sup> Gagné,<sup>27</sup> MacMillan,<sup>28</sup> and our own.<sup>17b-17i</sup>

## 2.4 Contributions

Dr. Michael A. Ischay developed the original conditions for the [2+2] cycloaddition and Prof. Tehshik P. Yoon obtained crystals for the structural determination of **2-17**.

## 2.5 Experimental

### 2.5.1 General information

Acetonitrile, CH<sub>2</sub>Cl<sub>2</sub>, and *i*-Pr<sub>2</sub>NEt were distilled from CaH<sub>2</sub> immediately prior to use. Ru(bpy)<sub>3</sub>Cl<sub>2</sub>·6H<sub>2</sub>O was purchased from Strem and used without further purification. Methyl acrylate was washed with aqueous NaOH, water, dried with CaCl<sub>2</sub> and distilled immediately prior to use. Substrates in Table 2-1, entries 1–3,<sup>29</sup> 4,<sup>30</sup> 6–8,<sup>31</sup> and Table 2-2, entry 5<sup>32</sup> were synthesized as previously described. All other chemicals were purchased from commercial suppliers and used without further purification. Flash column chromatography<sup>33</sup> was performed using Purasil 60Å silica gel (230–400 mesh). All glassware was oven-dried at 130 °C for at least 1 h or flame-dried immediately prior to use.

Diastereomer ratios for all compounds were determined by <sup>1</sup>H NMR analysis of the unpurified reaction mixtures. All NMR spectra were obtained at ambient temperature on the Varian Unity-500 and Varian Inova-500 spectrometers. Chemical shifts are reported in parts per million (δ) relative to TMS (0.0 ppm) for <sup>1</sup>H NMR data and CDCl<sub>3</sub> (77.23 ppm) for <sup>13</sup>C NMR data. IR spectral data were obtained using a Bruker Vector 22

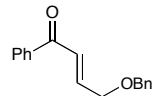
spectrometer. Mass spectrometry was performed with a Micromass LCT (electrospray ionization, time-of-flight analyzer or electron impact). These facilities are funded by the NSF (CHE-9974839, CHE-9304546), NIH (RR08389-01) and the University of Wisconsin.

### 2.5.2 General procedures

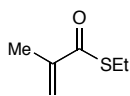
**General procedure for [2+2] homodimerizations (A):** A dry 25 mL Schlenk tube was charged with the enone (2 equiv), Ru(bpy)<sub>3</sub>Cl<sub>2</sub>•6H<sub>2</sub>O (0.05 equiv), LiBF<sub>4</sub> (2 equiv), *i*-Pr<sub>2</sub>NEt (2 equiv), and acetonitrile (0.2 M with respect to the enone) and degassed by a freeze/pump/thaw cycle (3x) under nitrogen in the dark. The reaction was then allowed to stir and irradiated by a 23 W (1380 lumen) compact fluorescent lamp at a distance of 30 cm. Upon completion, the solvent was removed *in vacuo* and the residue purified by column chromatography on silica gel.

**General procedure for crossed intermolecular [2+2] cycloadditions (B):** As per the general procedure for [2+2] homodimerizations (A), except with the following molar ratios: 1 equiv enone, 2.5 equiv Michael acceptor, 4 equiv LiBF<sub>4</sub>, and 2 equiv *i*-Pr<sub>2</sub>NEt in acetonitrile (0.1 M).

### 2.5.3 Synthesis and characterization of new compounds

 **(E)-4-(Benzyloxy)-1-phenylbut-2-en-1-one** (Table 2-1, entry 9, **2-35**). A 25 mL round-bottomed flask was charged with 2-(benzyloxy)acetaldehyde (1.0 g, 6.7 mmol), (benzoylmethylene)triphenylphosphorane (2.6 g, 6.7 mmol), and 5 mL CH<sub>2</sub>Cl<sub>2</sub> and allowed to reflux overnight. The reaction mixture was cooled to rt and

concentrated to yield a yellow oil. The resulting residue was stirred vigorously with hexane until a white precipitate was evident. The solids were washed with hexanes (5x) and the combined organics washed with brine, dried with Na<sub>2</sub>SO<sub>4</sub> and concentrated *in vacuo* to afford the crude product as a yellow oil. Further purification was carried out by chromatography using 5:1 hexanes:EtOAc as the eluent to yield the product as a pale yellow oil (1.1 g, 4.3 mmol). IR (thin film) 1627, 1469, 1382; <sup>1</sup>H NMR (500 MHz, CDCl<sub>3</sub>) δ 7.96 (dt, J = 8.1, 2.1 Hz, 2H), 7.56 (tt, J = 6.7, 1.5 Hz, 1H), 7.47 (tt, J = 9.4, 1.8 Hz, 2H), 7.38 (d, J = 4.7 Hz, 3H), 7.32 (m, 1H), 7.22 (dt, J = 15.6, 2.3 Hz, 1H), 7.08 (dt, J = 15.5, 4.1 Hz, 1H), 4.63 (s, 2H), 4.30 (dd, J = 4.1, 2.3 Hz, 2H); <sup>13</sup>C NMR (125 MHz, CDCl<sub>3</sub>) δ 190.3, 144.4, 137.7, 137.6, 132.8, 128.6, 128.6, 128.5, 127.9, 127.7, 124.9, 72.9, 72.9, 69.1; HRMS (ESI<sup>+</sup>) calc'd for [C<sub>17</sub>H<sub>16</sub>O<sub>2</sub>Na]<sup>+</sup> requires *m/z* 275.1043, found *m/z* 275.1045.

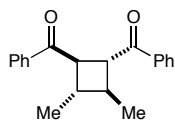


**(S)-Ethyl-2-methylprop-2-enethioate** (Table 2-2, entry 5, **2-36**). A 1 L

round-bottomed flask was charged with methacrylic acid (2.6 mL, 31 mmol), ethanethiol (2.9 mL, 39 mmol), 4-(dimethylamino)pyridine (366 mg, 3 mmol) and 45 mL CH<sub>2</sub>Cl<sub>2</sub> and cooled to 0 °C. Dicyclohexylcarbodiimide (6.6 g, 31 mmol) was added in three portions and the reaction mixture was allowed to stir and warm to rt overnight. The resulting suspension was filtered over Celite, and the filtrate washed with saturated NaHCO<sub>3</sub>, water, and brine and dried with MgSO<sub>4</sub>. Hydroquinone was added to the solution to prevent polymerization and the solvent was removed by distillation. The crude acrylate was further purified by Kugelrohr distillation at reduced pressure (5 mm Hg, 75 °C) to yield the product as yellow oil (1.3 g, 10 mmol). IR (thin film) 2971, 2930,

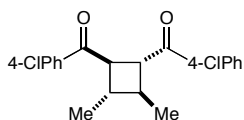


1662, 1630;  $^1\text{H}$  NMR (500 MHz,  $\text{CDCl}_3$ )  $\delta$  6.06 (s, 1H), 5.56 (q,  $J$  = 1.6 Hz, 1H), 2.93 (q,  $J$  = 7.5 Hz, 2H), 1.98 (q,  $J$  = 1.1 Hz, 3H), 1.28 (t,  $J$  = 7.2 Hz, 3H);  $^{13}\text{C}$  NMR (125 MHz,  $\text{CDCl}_3$ )  $\delta$  193.6, 143.7, 122.7, 23.2, 18.0, 14.6; HRMS ( $\text{EI}^+$ ) calc'd for  $[\text{C}_6\text{H}_{10}\text{OS}]^+$  requires  $m/z$  130.0447, found  $m/z$  130.0454.



**1,2-Dibenzoyl-3,4-dimethylcyclobutane (2-16).** Experiment 1: Prepared

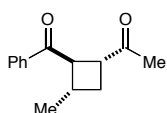
according to general procedure A using 102 mg (0.70 mmol) (*E*)-1-phenyl-2-buten-1-one, 12 mg (0.016 mmol)  $\text{Ru}(\text{bpy})_3\text{Cl}_2 \cdot 6\text{H}_2\text{O}$ , 66 mg (0.70 mmol)  $\text{LiBF}_4$ , 122  $\mu\text{L}$  *i*- $\text{Pr}_2\text{NEt}$ , and 3.3 mL acetonitrile, with an irradiation time of 2 h. Purified by chromatography using 9:1 hexanes:EtOAc to afford 81 mg (0.28 mmol, 80% yield) of the cycloadduct as a clear, colorless liquid. Experiment 2: 103 mg (0.70 mmol) (*E*)-1-phenyl-2-buten-1-one, 12 mg (0.016 mmol)  $\text{Ru}(\text{bpy})_3\text{Cl}_2 \cdot 6\text{H}_2\text{O}$ , 66 mg (0.70 mmol)  $\text{LiBF}_4$ , 122  $\mu\text{L}$  *i*- $\text{Pr}_2\text{NEt}$ , and 3.3 mL acetonitrile. Isolated 86 mg (0.29 mmol, 84% yield). IR (thin film) 1669, 1625;  $^1\text{H}$  NMR (500 MHz,  $\text{CDCl}_3$ )  $\delta$  7.98 (dt,  $J$  = 6.1, 1.8 Hz, 4 H), 7.54 (tt,  $J$  = 6.7, 1.2 Hz, 2 H), 7.44 (tt,  $J$  = 7.9 Hz, 4H), 4.04 (m, 2H), 2.15 (m,  $J$  = Hz, 2H), 1.21 (dt,  $J$  = 4.6, 2.1 Hz, 6H);  $^{13}\text{C}$  NMR (125 MHz,  $\text{CDCl}_3$ )  $\delta$  199.7, 136.3, 133.2, 128.6, 128.6, 77.3, 77.0, 76.8, 47.4, 39.4, 19.2. HRMS ( $\text{EI}^+$ ) calc'd for  $[\text{C}_{20}\text{H}_{20}\text{O}_2]^+$  requires  $m/z$  292.1458, found  $m/z$  292.1471.



**1,2-Di(4-chlorobenzoyl)-3,4-dimethylcyclobutane (2-17).**

Experiment 1: Prepared according to general procedure A using 127 mg (0.70 mmol) (*E*)-1-(4-chlorophenyl)-2-buten-1-one, 12 mg (0.016 mmol)

Ru(bpy)<sub>3</sub>Cl<sub>2</sub>•6H<sub>2</sub>O, 66 mg (0.70 mmol) LiBF<sub>4</sub>, 122  $\mu$ L *i*-Pr<sub>2</sub>NEt, and 3.3 mL acetonitrile, with an irradiation time of 1 h. Purified by chromatography using 8:1 hexanes:EtOAc to afford 119 mg (0.33 mmol, 93% yield) of the cycloadduct as a white solid. Experiment 2: 125 mg (0.70 mmol) (*E*)-1-(4-chlorophenyl)-2-buten-1-one, 12 mg (0.016 mmol) Ru(bpy)<sub>3</sub>Cl<sub>2</sub>•6H<sub>2</sub>O, 66 mg (0.70 mmol) LiBF<sub>4</sub>, 122  $\mu$ L *i*-Pr<sub>2</sub>NEt, and 3.3 mL acetonitrile. Isolated 116 mg (0.32 mmol, 93% yield). IR (neat) 1695, 1645; <sup>1</sup>H NMR (500 MHz, CDCl<sub>3</sub>)  $\delta$  7.92 (dt, *J* = 9.3, 2.4 Hz, 4H), 7.42 (dt, *J* = 9.3, 2.4 Hz, 4H), 3.96 (m, 2H), 2.13 (m, 2H), 1.2 (d, *J* = 6.4 Hz, 6H); <sup>13</sup>C NMR (125 MHz, CDCl<sub>3</sub>)  $\delta$  198.5, 140.0, 134.7, 130.2, 129.1, 77.6, 77.2, 76.8, 47.4, 39.6, 19.4. HRMS (EI<sup>+</sup>) calc'd for [C<sub>20</sub>H<sub>20</sub>O<sub>2</sub>]<sup>+</sup> requires *m/z* 292.1458, found *m/z* 292.1471. (mp = 124–129 °C).

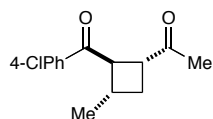


**1-((1*R*, 2*R*, 3*S*)-2-Benzoyl-3-methylcyclobutyl)ethanone** (Table 2-1,

Entry 1, **2-20**). Experiment 1: Prepared according to the general procedure

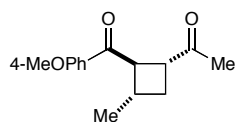
using 102 mg (0.70 mmol) (*E*)-1-phenyl-2-buten-1-one, 121 mg (1.7 mmol) 3-buten-2-one, 26 mg (0.035 mmol) Ru(bpy)<sub>3</sub>Cl<sub>2</sub>•6H<sub>2</sub>O, 261 mg (2.8 mmol) LiBF<sub>4</sub>, 243  $\mu$ L (1.4 mmol) *i*-Pr<sub>2</sub>NEt, 6.9 mL acetonitrile and irradiated for 4 h. Purified by chromatography using 6:1 hexanes:EtOAc to yield 127 mg (0.59 mmol, 84% yield) of the cycloadduct as a yellow oil. Experiment 2: 102 mg (0.70 mmol) (*E*)-1-phenyl-2-buten-1-one, 122 mg (1.7 mmol) 3-buten-2-one, 26 mg (0.035 mmol) Ru(bpy)<sub>3</sub>Cl<sub>2</sub>•6H<sub>2</sub>O, 262 mg (2.8 mmol) LiBF<sub>4</sub>, 243  $\mu$ L (1.4 mmol) *i*-Pr<sub>2</sub>NEt, and 6.9 mL acetonitrile. Isolated 125 mg (0.58 mmol, 83% yield). IR (thin film) 2957, 1709, 1674; <sup>1</sup>H NMR (500 MHz, CDCl<sub>3</sub>)  $\delta$  7.98 (dt, *J* = 8.1, 1.8 Hz, 2H), 7.57 (tt, *J* = 6.8, 1.3 Hz, 1H), 7.47 (tt, *J* = 8.0 Hz, 2H), 3.92 (t, *J* = 8.4

Hz, 1H), 3.62 (q,  $J$  = 9.3 Hz, 1H), 2.5 (m, 1H), 2.38 (m, 1H), 2.08 (s, 3H), 1.75 (q,  $J$  = 10.4 Hz, 1H), 1.18 (d, 3H);  $^{13}\text{C}$  NMR (125 MHz,  $\text{CDCl}_3$ )  $\delta$  208.2, 199.3, 136.1, 133.3, 128.6, 49.7, 43.4, 30.9, 29.2, 27.6, 20.9; HRMS ( $\text{EI}^+$ ) calc'd for  $[\text{C}_{14}\text{H}_{16}\text{O}_2]^+$  requires  $m/z$  216.1145, found  $m/z$  216.1150.



**1-((1*R*, 2*R*, 3*S*)-2-(4-Chlorobenzoyl)-3-methylcyclobutyl)ethanone**

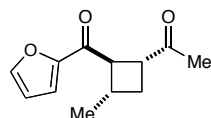
(Table 2-1, entry 2, **2-22**). Experiment 1: Prepared according to the general procedure using 126 mg (0.70 mmol) (*E*)-1-(4-chlorophenyl)-2-buten-1-one, 122 mg (1.7 mmol) 3-buten-2-one, 26 mg (0.035 mmol)  $\text{Ru}(\text{bpy})_3\text{Cl}_2 \cdot 6\text{H}_2\text{O}$ , 263 mg (2.8 mmol)  $\text{LiBF}_4$ , 243  $\mu\text{L}$  (1.4 mmol) *i*- $\text{Pr}_2\text{NEt}$ , 6.9 mL acetonitrile and irradiated for 4 h. Purified by chromatography using 6:1 hexanes:EtOAc to yield 148 mg (0.59 mmol, 84% yield) of the cycloadduct as a yellow oil. Experiment 2: 126 mg (0.70 mmol) (*E*)-1-(4-chlorophenyl)-2-buten-1-one, 122 mg (1.7 mmol) 3-buten-2-one, 27 mg (0.035 mmol)  $\text{Ru}(\text{bpy})_3\text{Cl}_2 \cdot 6\text{H}_2\text{O}$ , 263 mg (2.8 mmol)  $\text{LiBF}_4$ , 243  $\mu\text{L}$  (1.4 mmol) *i*- $\text{Pr}_2\text{NEt}$ , and 6.9 mL acetonitrile. Isolated 140 mg (0.56 mmol, 80% yield). IR (thin film) 1675, 1590, 1093;  $^1\text{H}$  NMR (500 MHz,  $\text{CDCl}_3$ )  $\delta$  7.93 (dt,  $J$  = 9.1, 2.4 Hz, 2H), 7.44 (dt,  $J$  = 9.1, 2.4 Hz, 2H), 3.88 (t,  $J$  = 8.3 Hz, 1H), 3.57 (q,  $J$  = 9.3 Hz, 1H), 2.52 (m, 1H), 2.41 (q,  $J$  = 10.4 Hz, 1H), 2.08 (s, 3H), 1.72 (q,  $J$  = 9.7 Hz, 1H), 1.17 (d, 3H);  $^{13}\text{C}$  NMR (125 MHz,  $\text{CDCl}_3$ )  $\delta$  208.0, 198.2, 139.8, 134.4, 130.1, 129.0, 49.3, 43.6, 30.6, 29.5, 27.5, 20.9; HRMS ( $\text{EI}^+$ ) calc'd for  $[\text{C}_{14}\text{H}_{15}\text{O}_2\text{Cl}]^+$  requires  $m/z$  250.0756, found  $m/z$  250.0764.



**1-((1*R*, 2*R*, 3*S*)-2-(4-Methoxybenzoyl)- 3-methylcyclobutyl)**

**ethanone** (Table 2-1, entry 3, **2-23**). Experiment 1: Prepared

according to the general procedure using 125 mg (0.71 mmol) (*E*)-1-(4-methoxyphenyl)-2-buten-1-one, 123 mg (1.7 mmol) 3-buten-2-one, 26 mg (0.035 mmol) Ru(bpy)<sub>3</sub>Cl<sub>2</sub>·6H<sub>2</sub>O, 262 mg (2.8 mmol) LiBF<sub>4</sub>, 243 μL (1.4 mmol) *i*-Pr<sub>2</sub>NEt, 6.9 mL acetonitrile and irradiated for 4 h. Purified by chromatography using 6:1 hexanes:EtOAc to yield 92 mg (0.37 mmol, 53% yield) of the cycloadduct as a yellow oil. Experiment 2: 123 mg (0.70 mmol) (*E*)-1-(4-methoxyphenyl)-2-buten-1-one, 123 mg (1.7 mmol) 3-buten-2-one, 26 mg (0.035 mmol) Ru(bpy)<sub>3</sub>Cl<sub>2</sub>·6H<sub>2</sub>O, 263 mg (2.8 mmol) LiBF<sub>4</sub>, 243 μL (1.4 mmol) *i*-Pr<sub>2</sub>NEt, and 6.9 mL acetonitrile. Isolated 86 mg (0.56 mmol, 50% yield). IR (thin film) 1794, 1664, 1600; <sup>1</sup>H NMR (500 MHz, CDCl<sub>3</sub>) δ 7.97 (dt, *J* = 9.7, 3.1 Hz, 2H), 6.94 (dt, *J* = 9.8, 2.8 Hz, 2H), 3.87 (s, 3H), 3.84 (q, *J* = 5.4 Hz, 1H), 3.61 (q, *J* = 9.1 Hz, 1H), 2.49 (m, 1H), 2.37 (q, *J* = 9 Hz, 1H), 2.07 (s, 3H), 1.74 (q, *J* = 9.3 Hz, 1H), 1.17 (d, 3H); <sup>13</sup>C NMR (125 MHz, CDCl<sub>3</sub>) δ 208.4, 197.7, 163.7, 130.9, 129.1, 113.8, 55.5, 49.5, 43.5, 30.9, 29.3, 27.7, 20.9; HRMS (EI<sup>+</sup>) calc'd for [C<sub>15</sub>H<sub>18</sub>O<sub>3</sub>]<sup>+</sup> requires *m/z* 246.1251, found *m/z* 246.1256.

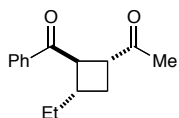


**1-((1*R*, 2*R*, 3*S*)-2-(Furan-2-carbonyl)-3-methylcyclobutyl)ethanone**

(Table 2-1, entry 4, **2-24**). Experiment 1: Prepared according to the

general procedure using 95 mg (0.70 mmol) (*E*)-1-(furan-2-yl)but-2-en-1-one, 122 mg (1.7 mmol) 3-buten-2-one, 26 mg (0.035 mmol) Ru(bpy)<sub>3</sub>Cl<sub>2</sub>·6H<sub>2</sub>O, 263 mg (2.8 mmol) LiBF<sub>4</sub>, 243 μL (1.4 mmol) *i*-Pr<sub>2</sub>NEt, 6.9 mL acetonitrile and irradiated for 4 h. Purified by chromatography using 2:1 hexanes:EtOAc to yield 106 mg (0.51 mmol, 73% yield) of

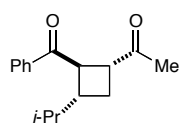
the cycloadduct as a yellow oil. Experiment 2: 95 mg (0.70 mmol) (*E*)-1-(furan-2-yl)but-2-en-1-one, 122 mg (1.7 mmol) 3-buten-2-one, 26 mg (0.035 mmol) Ru(bpy)<sub>3</sub>Cl<sub>2</sub>·6H<sub>2</sub>O, 263 mg (2.8 mmol) LiBF<sub>4</sub>, 243  $\mu$ L (1.4 mmol) *i*-Pr<sub>2</sub>NEt, and 6.9 mL acetonitrile. Isolated 106 mg (0.58 mmol, 74% yield). IR (thin film) 1708, 1665, 1467; <sup>1</sup>H NMR (500 MHz, CDCl<sub>3</sub>)  $\delta$  7.62 (dd, *J* = 1.8, 1.0 Hz, 1H), 7.27 (dd, *J* = 3.7, 0.7 Hz, 1H), 6.54 (dd, *J* = 3.8, 2.1 Hz, 1H), 3.66 (t, *J* = 8.6 Hz, 1H), 3.58 (q, *J* = 9.2 Hz, 1H), 2.54 (m, 1H), 2.37 (q, *J* = 9.8 Hz, 1H), 2.08 (s, 3H), 1.73 (q, *J* = 9.4 Hz, 1H), 1.18 (d, 3H); <sup>13</sup>C NMR (125 MHz, CDCl<sub>3</sub>)  $\delta$  209.0, 187.8, 152.1, 147.0, 118.5, 112.3, 50.1, 42.8, 30.8, 29.3, 27.5, 20.9; HRMS (EI<sup>+</sup>) calc'd for [C<sub>12</sub>H<sub>13</sub>O<sub>3</sub>]<sup>+</sup> requires *m/z* 206.0938, found *m/z* 206.0940.



**1-((1*R*, 2*R*, 3*S*)-2-Benzoyl-3-ethylcyclobutyl)ethanone** (Table 2-1, entry 6, **2-26**). Experiment 1: Prepared according to the general

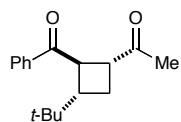
procedure using 113 mg (0.70 mmol) (*E*)-1-phenyl-2-penten-1-one, 122 mg (1.7 mmol) 3-buten-2-one, 26 mg (0.035 mmol) Ru(bpy)<sub>3</sub>Cl<sub>2</sub>·6H<sub>2</sub>O, 263 mg (2.8 mmol) LiBF<sub>4</sub>, 243  $\mu$ L (1.4 mmol) *i*-Pr<sub>2</sub>NEt, 6.9 mL acetonitrile and irradiated for 4 h. Purified by chromatography using 6:1 hexanes:EtOAc to yield 115 mg (0.50 mmol, 71% yield) of the cycloadduct as a yellow oil. Experiment 2: 106 mg (0.66 mmol) (*E*)-1-phenyl-2-penten-1-one, 116 mg (1.7 mmol), 25 mg (0.033 mmol) Ru(bpy)<sub>3</sub>Cl<sub>2</sub>·6H<sub>2</sub>O, 248 mg (2.6 mmol) LiBF<sub>4</sub>, 229  $\mu$ L (1.3 mmol) *i*-Pr<sub>2</sub>NEt, 6.5 mL acetonitrile and irradiated for 4 h. Isolated 103 mg (0.45 mmol, 68% yield). IR (thin film) 2963, 2254, 1708, 1672; <sup>1</sup>H NMR (500 MHz, CDCl<sub>3</sub>)  $\delta$  7.99 (dt, *J* = 8.5, 1.8 Hz, 2H), 7.56 (tt, *J* = 6.7, 1.3 Hz, 1H), 7.46 (tt, *J* = 7.9 Hz, 2H), 3.98 (tt, *J* = 8 Hz, 1H), 3.54 (q, *J* = 9.3 Hz, 1H), 2.4 (m, 2H), 2.07 (s,

3H), 1.72 (q,  $J = 9.3$  Hz, 1H), 1.57 (m, 1H), 1.47 (m, 1H), 0.78 (t,  $J = 7.2$  Hz, 3H);  $^{13}\text{C}$  NMR (125 MHz,  $\text{CDCl}_3$ )  $\delta$  208.1, 199.8, 136.2, 133.2, 128.6, 47.7, 44.1, 36.7, 28.5, 27.5, 27.4, 10.7; HRMS ( $\text{EI}^+$ ) calc'd for  $[\text{C}_{15}\text{H}_{18}\text{O}_2]^+$  requires  $m/z$  230.1302, found  $m/z$  230.1299.



**1-((1R, 2R, 3R)-2-Benzoyl-3-isopropylcyclobutyl)ethanone** (Table 2-

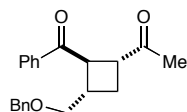
1, entry 7, **2-27**). Experiment 1: Prepared according to the general procedure using 122 mg (0.70 mmol) (E)-4-methyl-1-phenylpent-2-en-1-one, 122 mg (1.7 mmol) 3-buten-2-one, 26 mg (0.035 mmol)  $\text{Ru}(\text{bpy})_3\text{Cl}_2 \cdot 6\text{H}_2\text{O}$ , 262 mg (2.8 mmol)  $\text{LiBF}_4$ , 243  $\mu\text{L}$  (1.4 mmol)  $i\text{-Pr}_2\text{NEt}$ , 6.9 mL acetonitrile and irradiated for 12 h. Purified by chromatography using 6:1 hexanes:EtOAc to yield 108 mg (0.44 mmol, 64% yield) of the cycloadduct as a yellow oil. Experiment 2: 122 mg (0.70 mmol) (E)-4-methyl-1-phenylpent-2-en-1-one, 122 mg (1.7 mmol) 3-buten-2-one, 27 mg (0.035 mmol)  $\text{Ru}(\text{bpy})_3\text{Cl}_2 \cdot 6\text{H}_2\text{O}$ , 262 mg (2.8 mmol)  $\text{LiBF}_4$ , 243  $\mu\text{L}$  (1.4 mmol)  $i\text{-Pr}_2\text{NEt}$ , and 6.9 mL acetonitrile. Isolated 107 mg (0.44 mmol, 62% yield). IR (thin film) 2253, 1708, 1671;  $^1\text{H}$  NMR (500 MHz,  $\text{CDCl}_3$ )  $\delta$  8.04 (dt,  $J = 8.0, 2.2$  Hz, 2H), 7.56 (tt,  $J = 6.8, 1.3$  Hz, 1H), 7.46 (tt,  $J = 8$  Hz, 2H), 4.09 (tt,  $J = 8.4$  Hz, 1H), 3.31 (q,  $J = 9.2$  Hz, 1H), 2.45 (m, 1H), 2.36 (m, 1H), 2.04 (s, 3H), 1.71 (q,  $J = 9.4$  Hz, 1H), 1.55 (m, 1H), 0.83 (d,  $J = 6.9$  Hz, 3H), 0.69 (d,  $J = 6.6$  Hz, 3H);  $^{13}\text{C}$  NMR (125 MHz,  $\text{CDCl}_3$ )  $\delta$  207.8, 200.6, 136.3, 133.2, 128.6, 128.6, 45.7, 45.1, 41.2, 33.4, 27.6, 26.6, 19.5, 18.7; HRMS ( $\text{EI}^+$ ) calc'd for  $[\text{C}_{16}\text{H}_{20}\text{O}_2\text{Na}]^+$  requires  $m/z$  267.1356, found  $m/z$  267.1369.



**1-((1R, 2R, 3S)-2-Benzoyl-3-tert-butylcyclobutyl)ethanone** (Table 2-1,

entry 8). Experiment 1: Prepared according to the general procedure

using 131 mg (0.70 mmol) (*E*)-4,4-dimethyl-1-phenylpent-2-en-1-one, 122 mg (1.7 mmol) 3-buten-2-one, 26 mg (0.035 mmol) Ru(bpy)<sub>3</sub>Cl<sub>2</sub>·6H<sub>2</sub>O, 262 mg (2.8 mmol) LiBF<sub>4</sub>, 243 μL (1.4 mmol) *i*-Pr<sub>2</sub>NEt, 6.9 mL acetonitrile and irradiated for 12 h. Purified by chromatography using 6:1 hexanes:EtOAc to yield 14 mg (0.05 mmol, 8% yield) of the cycloadduct as a yellow oil. Experiment 2: 132 mg (0.70 mmol) (*E*)-4,4-dimethyl-1-phenylpent-2-en-1-one, 123 mg (1.7 mmol) 3-buten-2-one, 26 mg (0.035 mmol) Ru(bpy)<sub>3</sub>Cl<sub>2</sub>·6H<sub>2</sub>O, 262 mg (2.8 mmol) LiBF<sub>4</sub>, 243 μL (1.4 mmol) *i*-Pr<sub>2</sub>NEt, and 6.9 mL acetonitrile. Isolated 9 mg (0.05 mmol, 6% yield).

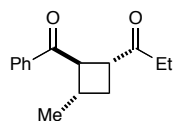


**1-((1R, 2R, 3S)-2-benzoyl-3-(benzyloxymethyl)cyclobutyl)ethanone**

(Table 2-1, entry 9, **2-29**). Experiment 1: Prepared according to the

general procedure using 176 mg (0.70 mmol) (*E*)-4-(benzyloxy)-1-phenylbut-2-en-1-one, 122 mg (1.7 mmol) 3-buten-2-one, 26 mg (0.035 mmol) Ru(bpy)<sub>3</sub>Cl<sub>2</sub>·6H<sub>2</sub>O, 263 mg (2.8 mmol) LiBF<sub>4</sub>, 243 μL (1.4 mmol) *i*-Pr<sub>2</sub>NEt, 6.9 mL acetonitrile and irradiated for 4 h. Purified by chromatography using 3:1 hexanes:EtOAc to yield 137 mg (0.42 mmol, 61% yield) of the cycloadduct as a clear oil. Experiment 2: 177 mg (0.70 mmol) (*E*)-4-(benzyloxy)-1-phenylbut-2-en-1-one, 123 mg (1.7 mmol) 3-buten-2-one, 27 mg (0.035 mmol) Ru(bpy)<sub>3</sub>Cl<sub>2</sub>·6H<sub>2</sub>O, 263 mg (2.8 mmol) LiBF<sub>4</sub>, 243 μL (1.4 mmol) *i*-Pr<sub>2</sub>NEt, and 6.9 mL acetonitrile. Isolated 140 mg (0.43 mmol, 62% yield). IR (thin film) 2254, 1673; <sup>1</sup>H NMR (500 MHz, CDCl<sub>3</sub>) δ 7.98 (d, *J* = 8.7 Hz, 2H), 7.53 (t, *J* = 7.7 Hz, 1H), 7.39 (t, *J* = 7.8 Hz, 2H), 7.31 (m, 5H), 4.52 (q, *J* = 12.1 Hz, 2H), 4.28 (t, *J* = 8.3 Hz, 1H), 3.61 (q, *J*

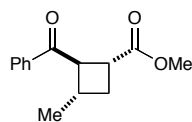
= 8.9 Hz, 1H), 3.46 (m, 2H), 2.73 (m, 1H), 2.29 (q,  $J$  = 10.2 Hz, 1H), 2.08 (s, 3H), 2.07 (m,  $J$  = Hz, 1H);  $^{13}\text{C}$  NMR (125 MHz,  $\text{CDCl}_3$ )  $\delta$  207.9, 199.3, 138.1, 135.8, 133.3, 128.7, 128.6, 128.4, 127.7, 127.6, 73.1, 71.2, 44.5, 43.8, 35.0, 27.4, 24.0; HRMS ( $\text{EI}^+$ ) calc'd for  $[\text{C}_{21}\text{H}_{22}\text{O}_3]^+$  requires  $m/z$  322.1564, found  $m/z$  322.1569.



**1-((1R, 2R, 3S)-2-Benzoyl-3-methylcyclobutyl)propan-1-one** (Table 2-

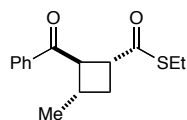
2, entry 2, **2-30**). Experiment 1: Prepared according to the general procedure using 102 mg (0.70 mmol) (*E*)-1-phenyl-2-buten-1-one, 147 mg (1.7 mmol) 1-penten-3-one, 26 mg (0.035 mmol)  $\text{Ru}(\text{bpy})_3\text{Cl}_2 \cdot 6\text{H}_2\text{O}$ , 262 mg (2.8 mmol)  $\text{LiBF}_4$ , 243  $\mu\text{L}$  (1.4 mmol) *i*- $\text{Pr}_2\text{NEt}$ , 6.9 mL acetonitrile and irradiated for 4 h. Purified by chromatography using 6:1 hexanes:EtOAc to yield 137 mg (0.59 mmol, 85% yield) of the cycloadduct as a yellow oil. Experiment 2: 102 mg (0.70 mmol) (*E*)-1-phenyl-2-buten-1-one, 147 mg (1.7 mmol) 1-penten-3-one, 26 mg (0.035 mmol)  $\text{Ru}(\text{bpy})_3\text{Cl}_2 \cdot 6\text{H}_2\text{O}$ , 262 mg (2.8 mmol)  $\text{LiBF}_4$ , 243  $\mu\text{L}$  (1.4 mmol) *i*- $\text{Pr}_2\text{NEt}$ , and 6.9 mL acetonitrile. Isolated 133 mg (0.58 mmol, 83% yield). IR (thin film) 2254, 1672, 1448;  $^1\text{H}$  NMR (500 MHz,  $\text{CDCl}_3$ )  $\delta$  7.97 (dt,  $J$  = 8.1, 1.9 Hz, 2H), 7.57 (tt,  $J$  = 6.8, 1.3 Hz, 1H), 7.47 (tt,  $J$  = 7.9 Hz, 2H), 3.94 (tt,  $J$  = 8.6 Hz, 1H), 3.61 (q,  $J$  = 8.9 Hz, 1H), 2.43 (m, 4H), 1.75 (m, 1H), 1.18 (d,  $J$  = 6.8 Hz, 3H), 1.03 (t,  $J$  = 7.3 Hz, 3H);  $^{13}\text{C}$  NMR (125 MHz,  $\text{CDCl}_3$ )  $\delta$  211.0, 211.0, 199.5, 199.5, 136.1, 133.3, 128.6, 127.9, 49.7, 42.5, 33.8, 31.0, 29.5, 20.9, 7.6; HRMS ( $\text{EI}^+$ ) calc'd for  $[\text{C}_{15}\text{H}_{19}\text{O}_2]^+$  requires  $m/z$  231.1380, found  $m/z$  231.1382.





**(1R, 2R, 3S)-Methyl-2-benzoyl-3-methylcyclobutanecarboxylate**

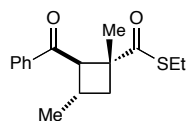
(Table 2-2, entry 3, **2-31**). Experiment 1: Prepared according to the general procedure using 102 mg (0.70 mmol) (*E*)-1-phenyl-2-buten-1-one, 361 mg (4.2 mmol) methyl acrylate, 27 mg (0.035 mmol) Ru(bpy)<sub>3</sub>Cl<sub>2</sub>·6H<sub>2</sub>O, 262 mg (2.8 mmol) LiBF<sub>4</sub>, 243 μL (1.4 mmol) *i*-Pr<sub>2</sub>NEt, 6.9 mL acetonitrile and irradiated for 12 h. Purified by chromatography using 6:1 hexanes:EtOAc to yield 103 mg (0.44 mmol, 64% yield) of the cycloadduct as a yellow oil. Experiment 2: 101 mg (0.69 mmol) (*E*)-1-phenyl-2-buten-1-one, 360 mg (4.2 mmol) methyl acrylate, 26 mg (0.035 mmol) Ru(bpy)<sub>3</sub>Cl<sub>2</sub>·6H<sub>2</sub>O, 263 mg (2.8 mmol) LiBF<sub>4</sub>, 243 μL (1.4 mmol) *i*-Pr<sub>2</sub>NEt, and 6.9 mL acetonitrile. Isolated 106 mg (0.46 mmol, 66% yield). IR (thin film) 1728, 1675; <sup>1</sup>H NMR (500 MHz, CDCl<sub>3</sub>) δ 7.96 (dt, *J* = 8.2, 2.1 Hz, 2H), 7.57 (tt, *J* = 7.1, 1.8 Hz, 1H), 7.47 (tt, *J* = 7.9, 1.9 Hz, 2H), 3.93 (t, *J* = 8.5 Hz, 1H), 3.67 (s, 3H), 3.49 (q, *J* = 9.4 Hz, 1H), 2.50 (m, 1H), 2.39 (q, *J* = 10.1 Hz, 1H), 1.88 (q, *J* = 9.4 Hz, 1H), 1.22 (d, *J* = 6.9 Hz, 3H); <sup>13</sup>C NMR (125 MHz, CDCl<sub>3</sub>) δ 198.8, 174.7, 136.1, 133.3, 128.6, 51.8, 51.1, 35.7, 31.6, 29.6, 20.9; HRMS (ESI<sup>+</sup>) calc'd for [C<sub>14</sub>H<sub>16</sub>O<sub>3</sub>]<sup>+</sup> requires *m/z* 233.1173, found *m/z* 233.1179.



**(1R, 2R, 3S)-S-Ethyl-2-benzoyl-3-methylcyclobutanecarbothioate**

(Table 2-2, entry 4, **2-32**). Experiment 1: Prepared according to the general procedure using 103 mg (0.70 mmol) (*E*)-1-phenyl-2-buten-1-one, 203 mg (1.7 mmol) (*S*)-ethyl-prop-2-enethioate, 27 mg (0.035 mmol) Ru(bpy)<sub>3</sub>Cl<sub>2</sub>·6H<sub>2</sub>O, 263 mg (2.8 mmol) LiBF<sub>4</sub>, 243 μL (1.4 mmol) *i*-Pr<sub>2</sub>NEt, 6.9 mL acetonitrile and irradiated for 4 h. Purified by chromatography using 6:1 hexanes:EtOAc to yield 159 mg (0.61 mmol, 86%

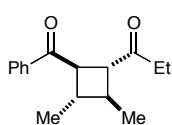
yield) of the cycloadduct as a yellow oil. Experiment 2: 102 mg (0.70 mmol) (*E*)-1-phenyl-2-buten-1-one, 203 mg (1.7 mmol) (*S*)-ethyl-prop-2-enethioate, 26 mg (0.035 mmol) Ru(bpy)<sub>3</sub>Cl<sub>2</sub>·6H<sub>2</sub>O, 262 mg (2.8 mmol) LiBF<sub>4</sub>, 243 μL (1.4 mmol) *i*-Pr<sub>2</sub>NEt, and 6.9 mL acetonitrile. Isolated 165 mg (0.63 mmol, 89% yield). IR (thin film) 2254, 1673; <sup>1</sup>H NMR (500 MHz, CDCl<sub>3</sub>) δ 7.95 (dt, *J* = 8.2, 1.7 Hz, 2H), 7.57 (tt, *J* = 6.9, 1.6 Hz, 1H), 7.47 (t, *J* = 8 Hz, 2H), 3.96 (t, *J* = 8.5 Hz, 1H), 3.68 (q, *J* = 8.8 Hz, 1H), 2.87 (q, *J* = 7.1 Hz, 2H), 2.5 (m, 1H), 2.41 (m, 1H), 1.92 (q, *J* = 9.4 Hz, 1H), 1.24 (t, *J* = 7.5 Hz, 3H), 1.21 (d, *J* = 6.8 Hz, 3H); <sup>13</sup>C NMR (125 MHz, CDCl<sub>3</sub>) δ 200.3, 198.6, 136.0, 133.3, 128.6, 128.6, 128.6, 51.3, 44.2, 31.1, 30.4, 23.2, 20.7, 14.7; HRMS (EI<sup>+</sup>) calc'd for [C<sub>15</sub>H<sub>17</sub>O<sub>2</sub>S]<sup>+</sup> requires *m/z* 262.1023, found *m/z* 262.1033.



**(1*R*, 2*R*, 3*S*)-*S*-Ethyl-2-benzoyl-1,3-dimethylcyclobutane carbothioate** (Table 2-2, entry 5, **2-33**). Experiment 1: Prepared according to

the general procedure using 103 mg (0.70 mmol) (*E*)-1-phenyl-2-buten-1-one, 546 mg (4.2 mmol) (*S*)-ethyl-2-methylprop-2-enethioate, 26 mg (0.035 mmol) Ru(bpy)<sub>3</sub>Cl<sub>2</sub>·6H<sub>2</sub>O, 262 mg (2.8 mmol) LiBF<sub>4</sub>, 243 μL (1.4 mmol) *i*-Pr<sub>2</sub>NEt, 6.9 mL acetonitrile and irradiated for 12 h. Purified by chromatography using 6:1 hexanes:EtOAc to yield 108 mg (0.39 mmol, 56% yield) of the cycloadduct as a yellow oil. Experiment 2: 102 mg (0.70 mmol) (*E*)-1-phenyl-2-buten-1-one, 547 mg (4.2 mmol) (*S*)-ethyl-2-methylprop-2-enethioate, 26 mg (0.035 mmol) Ru(bpy)<sub>3</sub>Cl<sub>2</sub>·6H<sub>2</sub>O, 262 mg (2.8 mmol) LiBF<sub>4</sub>, 243 μL (1.4 mmol) *i*-Pr<sub>2</sub>NEt, and 6.9 mL acetonitrile. Isolated 112 mg (0.40 mmol, 58% yield). IR (thin film) 2256, 1672, 1459, 1384; <sup>1</sup>H NMR (500 MHz, CDCl<sub>3</sub>) δ 7.95 (d, *J* = 8.6 Hz, 2H), 7.53 (t, *J*

= 6.5 Hz, 1H), 7.42 (t,  $J$  = 7.9 Hz, 2H), 4.18 (d,  $J$  = 8.8 Hz, 1H), 3.06 (m, 1H), 2.93 (m, 2H), 2.01 (m,  $J$  = 7.1 Hz, 2H), 1.28 (t,  $J$  = Hz, 3H), 1.21 (s, 3H), 1.13 (d,  $J$  = 6.7 Hz, 3H);  $^{13}\text{C}$  NMR (125 MHz,  $\text{CDCl}_3$ )  $\delta$  204.6, 198.8, 136.6, 133.1, 128.5, 128.5, 53.1, 51.4, 39.3, 24.4, 23.3, 20.4, 18.5, 14.7; HRMS ( $\text{EI}^+$ ) calc'd for  $[\text{C}_{16}\text{H}_{19}\text{O}_2\text{S}]^+$  requires  $m/z$  276.1179, found  $m/z$  276.1176.



**1-((1R, 2R, 3S, 4S)-2-benzoyl-3,4-dimethylcyclobutyl)propan-1-one**

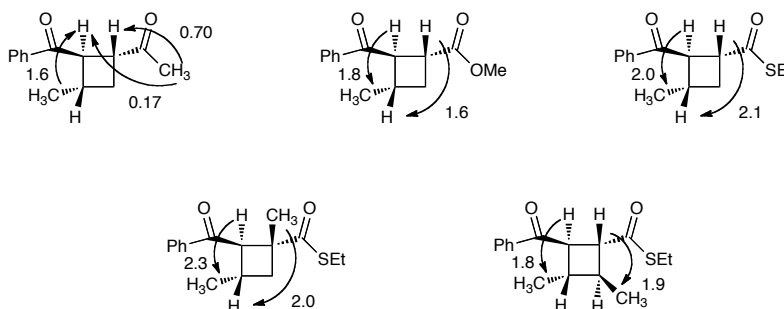
(Table 2-2, entry 6, **2-34**). Experiment 1: Prepared according to the general procedure using 102 mg (0.70 mmol) (*E*)-1-phenyl-2-buten-1-one, 412 mg (4.2 mmol) 4-hexen-3-one, 26 mg (0.035 mmol)  $\text{Ru}(\text{bpy})_3\text{Cl}_2 \cdot 6\text{H}_2\text{O}$ , 261 mg (2.8 mmol)  $\text{LiBF}_4$ , 243  $\mu\text{L}$  (1.4 mmol) *i*- $\text{Pr}_2\text{NEt}$ , 6.9 mL acetonitrile and irradiated for 12 h. Purified by chromatography using 6:1 hexanes:EtOAc to yield 60 mg (0.25 mmol, 35% yield) of the cycloadduct as a pale yellow oil. Experiment 2: 102 mg (0.70 mmol) (*E*)-1-phenyl-2-buten-1-one, 412 mg (4.2 mmol) 4-hexen-3-one, 26 mg (0.035 mmol)  $\text{Ru}(\text{bpy})_3\text{Cl}_2 \cdot 6\text{H}_2\text{O}$ , 263 mg (2.8 mmol)  $\text{LiBF}_4$ , 243  $\mu\text{L}$  (1.4 mmol) *i*- $\text{Pr}_2\text{NEt}$ , and 6.9 mL acetonitrile. Isolated 70 mg (0.27 mmol, 38% yield). IR (thin film) 1691, 1675, 1449;  $^1\text{H}$  NMR (500 MHz,  $\text{CDCl}_3$ )  $\delta$  7.97 (dt,  $J$  = 8.5, 1.3 Hz, 2H), 7.56 (tt,  $J$  = 6.8, 1.3 Hz, 1H), 7.46 (tt,  $J$  = 8.0, 1.6 Hz, 2H), 3.80 (t,  $J$  = 8.9 Hz, 1H), 3.17 (t,  $J$  = 8.8 Hz, 1H), 2.37 (dd,  $J$  = 13.9, 7.5 Hz, 1H), 2.37 (m, 1H), 1.99 (m, 2H), 1.20 (d,  $J$  = 6.7 Hz, 3H), 1.15 (d,  $J$  = 6.6 Hz, 3H), 1.03 (t,  $J$  = 7.3 Hz, 3H);  $^{13}\text{C}$  NMR (125 MHz,  $\text{CDCl}_3$ )  $\delta$  210.5, 199.6, 136.3, 133.2, 128.6, 128.6, 51.2, 47.0, 39.1, 39.0, 34.9, 19.4, 19.1, 7.5; HRMS ( $\text{ESI}^+$ ) calc'd for  $[\text{C}_{16}\text{H}_{20}\text{O}_2]^+$  requires  $m/z$  245.1537 found  $m/z$  245.1532.

### 2.5.4 Large scale photocycloaddition with ambient sunlight

A dry 100 mL Schlenk flask was charged with 846 mg (5.8 mmol) (*E*)-1-phenyl-2-buten-1-one, 1.02 g (14.6 mmol) 3-buten-2-one, 217 mg (0.29 mmol) Ru(bpy)<sub>3</sub>Cl<sub>2</sub>·6H<sub>2</sub>O, 2.18 g (23.1 mmol) LiBF<sub>4</sub>, 2.0 mL (11.5 mmol) *i*-Pr<sub>2</sub>NEt, and 57 mL acetonitrile (0.1 M) and degassed by a freeze/pump/thaw cycle (3x) under nitrogen in the dark. The Schlenk flask was then brought onto the roof and allowed to stir in direct sunlight for 4 h. Upon completion, the solvent was removed *in vacuo* and the residue purified by column chromatography on silica gel with 6:1 hexanes:EtOAc as the eluent to yield 1.05 g (4.8 mmol, 84% yield, >10:1 d.r.) of the cycloadduct as a yellow oil.

### 2.5.5 NOE correlations

NOE correlations were used to determine the relative stereochemistry of the following compounds. Subsequent assignments were made by analogy.



## 2.6 References

1. a) Schuster, D. I.; Lem, G.; Kaprinidis, N. A. New insights into an old mechanism: [2+2] photocycloaddition of enones to alkenes. *Chem. Rev.* **1993**, 93, 3-22. b) Iriondo-Alberdi, J.; Greaney, M. F. Photocycloaddition in Natural Product Synthesis. *Eur. J. Org. Chem.* **2007**, 2007, 4801-4815. c) Hoffmann, N. Photochemical Reactions as Key Steps in Organic Synthesis. *Chem. Rev.* **2008**, 108, 1052-1103. d) Fagnoni, M.; Dondi, D.;

Ravelli, D.; Albini, A. Photocatalysis for the Formation of the C–C Bond. *Chem. Rev.* **2007**, *107*, 2725-2756.

2. a) Oppolzer, W. The intramolecular [2+2] photoaddition/cyclobutane-fragmentation sequence in organic synthesis. *Acc. Chem. Res.* **1982**, *15*, 135-141. b) Winkler, J. D.; Bowen, C. M.; Liotta, F. [2+2] Photocycloaddition/Fragmentation Strategies for the Synthesis of Natural and Unnatural Products. *Chem. Rev.* **1995**, *95*, 2003-2020. c) Bach, T.; Hehn, J. P. Photochemical Reactions as Key Steps in Natural Product Synthesis. *Angew. Chem. Int. Ed.* **2011**, *50*, 1000-1045.

3. Ciamician, G.; Silber, P. Chemische Lichtwirkungen. *Chem. Ber.* **1908**, *41*, 1928-1935.

4. Büchi, G.; Goldman, I. M. Photochemical Reactions. The Intramolecular Cyclization of Carvone to Carvonecamphor. *J. Am. Chem. Soc.* **1957**, *79*, 4741-4748.

5. Crimmins, M. T. Synthetic applications of intramolecular enone-olefin photocycloadditions. *Chem. Rev.* **1988**, *88*, 1453-1473.

6. a) Eaton, P. E.; Cole, T. W. The Cubane System. *J. Am. Chem. Soc.* **1964**, *86*, 962-964. b) Eaton, P. E.; Cole, T. W. Cubane. *J. Am. Chem. Soc.* **1964**, *86*, 3157-3158.

7. Corey, E. J.; Bass, J. D.; LeMahieu, R.; Mitra, R. B. A Study of the Photochemical Reactions of 2-Cyclohexenones with Substituted Olefins. *J. Am. Chem. Soc.* **1964**, *86*, 5570-5583.

8. Corey, E. J.; Mitra, R. B.; Uda, H. Total Synthesis of d,l-Caryophyllene and d,l-Isocaryophyllene. *J. Am. Chem. Soc.* **1964**, *86*, 485-492.

9. Bach, T. Stereoselective Intermolecular [2+2]-Photocycloaddition Reactions and Their Application in Synthesis. *Synthesis* **1998**, *1998*, 683,703.

10. Morrison, H.; Rodriguez, O. Z—E photoisomerization of 3-methyl-3-penten-2-one. Evidence for non-radiative decay. *J. Photochem.* **1975**, *3*, 471-474.

11. Ciamician, G. The Photochemistry of the Future. *Science* **1912**, *36*, 385-394.

12. a) Esser, P.; Pohlmann, B.; Scharf, H.-D. The Photochemical Synthesis of Fine Chemicals with Sunlight. *Angew. Chem. Int. Ed.* **1994**, *33*, 2009-2023. b) Oelgemöller, M.; Jung, C.; Mattay, J. Green photochemistry: Production of fine chemicals with sunlight. *Pure Appl. Chem.* **2007**, *79*, 1939-1947. c) Pfoertner, K. H. Photochemistry in industrial synthesis. *J. Photochem.* **1984**, *25*, 91-97.

13. Lewis, N. S.; Nocera, D. G. Powering the planet: Chemical challenges in solar energy utilization. *Proc. Natl. Acad. Sci. U.S.A.* **2006**, *103*, 15729-15735.

14. Juris, A.; Balzani, V.; Barigelletti, F.; Campagna, S.; Belser, P.; von Zelewsky, A. Ru(II) polypyridine complexes: photophysics, photochemistry, electrochemistry, and chemiluminescence. *Coord. Chem. Rev.* **1988**, *84*, 85-277.
15. Kalyanasundaram, K. Photophysics, photochemistry and solar energy conversion with tris(bipyridyl)ruthenium(II) and its analogues. *Coord. Chem. Rev.* **1982**, *46*, 159-244.
16. a) Cano-Yelo, H.; Deronzier, A. Photocatalysis of the Pschorr reaction by tris-(2,2'-bipyridyl)ruthenium(II) in the phenanthrene series. *J. Chem. Soc., Perkin Trans. II* **1984**, 1093-1098. b) Cano-Yelo, H.; Deronzier, A. Photo-oxidation of some carbinols by the Ru(II) polypyridyl complex-aryl diazonium salt system. *Tetrahedron Lett.* **1984**, *25*, 5517-5520. c) Zen, J.-M.; Liou, S.-L.; Kumar, A. S.; Hsia, M.-S. An Efficient and Selective Photocatalytic System for the Oxidation of Sulfides to Sulfoxides. *Angew. Chem. Int. Ed.* **2003**, *42*, 577-579.
17. a) Ischay, M. A.; Anzovino, M. E.; Du, J.; Yoon, T. P. Efficient Visible Light Photocatalysis of [2+2] Enone Cycloadditions. *J. Am. Chem. Soc.* **2008**, *130*, 12886-12887. b) Du, J.; Yoon, T. P. Crossed Intermolecular [2+2] Cycloadditions of Acyclic Enones via Visible Light Photocatalysis. *J. Am. Chem. Soc.* **2009**, *131*, 14604-14605. c) Ischay, M. A.; Lu, Z.; Yoon, T. P. [2+2] Cycloadditions by Oxidative Visible Light Photocatalysis. *J. Am. Chem. Soc.* **2010**, *132*, 8572-8574. d) Lu, Z.; Shen, M.; Yoon, T. P. [3+2] Cycloadditions of Aryl Cyclopropyl Ketones by Visible Light Photocatalysis. *J. Am. Chem. Soc.* **2011**, *133*, 1162-1164. e) Du, J.; Ruiz Espelt, L.; Guzei, I. A.; Yoon, T. P. Photocatalytic reductive cyclizations of enones: Divergent reactivity of photogenerated radical and radical anion intermediates. *Chem. Sci.* **2011**, *2*, 2115-2119. f) Hurlley, A. E.; Cismesia, M. A.; Ischay, M. A.; Yoon, T. P. Visible light photocatalysis of radical anion hetero-Diels–Alder cycloadditions. *Tetrahedron* **2011**, *67*, 4442-4448. g) Lin, S.; Ischay, M. A.; Fry, C. G.; Yoon, T. P. Radical Cation Diels–Alder Cycloadditions by Visible Light Photocatalysis. *J. Am. Chem. Soc.* **2011**, *133*, 19350-19353. h) Tyson, E. L.; Farney, E. P.; Yoon, T. P. Photocatalytic [2 + 2] Cycloadditions of Enones with Cleavable Redox Auxiliaries. *Org. Lett.* **2012**, *14*, 1110-1113. i) Parrish, J. D.; Ischay, M. A.; Lu, Z.; Guo, S.; Peters, N. R.; Yoon, T. P. Endoperoxide Synthesis by Photocatalytic Aerobic [2+2+2] Cycloadditions. *Org. Lett.* **2012**, *14*, 1640-1643.
18. a) Baik, T.-G.; Luis, A. L.; Wang, L.-C.; Krische, M. J. A Diastereoselective Metal-Catalyzed [2+2] Cycloaddition of Bis-enones. *J. Am. Chem. Soc.* **2001**, *123*, 6716-6717. b) Wang, L.-C.; Jang, H.-Y.; Roh, Y.; Lynch, V.; Schultz, A. J.; Wang, X., et al. Diastereoselective Cycloreductions and Cycloadditions Catalyzed by Co(dpm)<sub>2</sub>-Silane (dpm = 2,2,6,6-tetramethylheptane-3,5-dionate): Mechanism and Partitioning of Hydrometallative versus Anion Radical Pathways. *J. Am. Chem. Soc.* **2002**, *124*, 9448-9453.
19. Yang, J.; Cauble, D. F.; Berro, A. J.; Bauld, N. L.; Krische, M. J. Anion Radical [2+2] Cycloaddition as a Mechanistic Probe: Stoichiometry- and Concentration-Dependent

Partitioning of Electron-Transfer and Alkylation Pathways in the Reaction of the Gilman Reagent  $\text{Me}_2\text{CuLi}\cdot\text{LiI}$  with Bis(enones). *J. Org. Chem.* **2004**, 69, 7979-7984.

20. Roh, Y.; Jang, H.-Y.; Lynch, V.; Bauld, N. L.; Krische, M. J. Anion Radical Chain Cycloaddition of Tethered Enones: Intramolecular Cyclobutanation and Diels–Alder Cycloaddition. *Org. Lett.* **2002**, 4, 611-613.

21. Yang, J.; Felton, G. A. N.; Bauld, N. L.; Krische, M. J. Chemically Induced Anion Radical Cycloadditions: Intramolecular Cyclobutanation of Bis(enones) via Homogeneous Electron Transfer. *J. Am. Chem. Soc.* **2004**, 126, 1634-1635.

22. House, H. O.; Huber, L. E.; Umen, M. J. Empirical rules for estimating the reduction potential of  $\alpha,\beta$ -unsaturated carbonyl compounds. *J. Am. Chem. Soc.* **1972**, 94, 8471-8475.

23. Nicewicz, D. A.; MacMillan, D. W. C. Merging Photoredox Catalysis with Organocatalysis: The Direct Asymmetric Alkylation of Aldehydes. *Science* **2008**, 322, 77-80.

24. For reviews of recent developments in visible light photoredox catalysis, see: a) Zeitler, K. Photoredox Catalysis with Visible Light. *Angew. Chem. Int. Ed.* 2009, 48, 9785-9789. b) Yoon, T. P.; Ischay, M. A.; Du, J. Visible light photocatalysis as a greener approach to photochemical synthesis. *Nature Chem.* 2010, 2, 527-532. c) Narayanam, J. M. R.; Stephenson, C. R. J. Visible light photoredox catalysis: applications in organic synthesis. *Chem. Soc. Rev.* 2011, 40, 102-113.

25. a) Chen, Y.; Kamlet, A. S.; Steinman, J. B.; Liu, D. R. A biomolecule-compatible visible-light-induced azide reduction from a DNA-encoded reaction-discovery system. *Nature Chem.* **2011**, 3, 146-153. b) Su, Y.; Zhang, L.; Jiao, N. Utilization of Natural Sunlight and Air in the Aerobic Oxidation of Benzyl Halides. *Org. Lett.* **2011**, 13, 2168-2171. c) Kalyani, D.; McMurtrey, K. B.; Neufeldt, S. R.; Sanford, M. S. Room-Temperature C–H Arylation: Merger of Pd-Catalyzed C–H Functionalization and Visible-Light Photocatalysis. *J. Am. Chem. Soc.* **2011**, 133, 18566-18569. d) Koike, T.; Akita, M. Photoinduced Oxyamination of Enamines and Aldehydes with TEMPO Catalyzed by  $[\text{Ru}(\text{bpy})_3]^{2+}$ . *Chem. Lett.* **2009**, 38, 166-167. e) Zou, Y.-Q.; Chen, J.-R.; Liu, X.-P.; Lu, L.-Q.; Davis, R. L.; Jørgensen, K. A., et al. Highly Efficient Aerobic Oxidative Hydroxylation of Arylboronic Acids: Photoredox Catalysis Using Visible Light. *Angew. Chem. Int. Ed.* **2012**, 51, 784-788. f) Maity, S.; Zhu, M.; Shinabery, R. S.; Zheng, N. Intermolecular [3+2] Cycloaddition of Cyclopropylamines with Olefins by Visible-Light Photocatalysis. *Angew. Chem. Int. Ed.* **2012**, 51, 222-226.

26. a) Narayanam, J. M. R.; Tucker, J. W.; Stephenson, C. R. J. Electron-Transfer Photoredox Catalysis: Development of a Tin-Free Reductive Dehalogenation Reaction. *J. Am. Chem. Soc.* **2009**, 131, 8756-8757. b) Tucker, J. W.; Narayanam, J. M. R.; Krabbe, S. W.; Stephenson, C. R. J. Electron Transfer Photoredox Catalysis: Intramolecular Radical Addition to Indoles and Pyrroles. *Org. Lett.* **2009**, 12, 368-371. c)

Condie, A. G.; González-Gómez, J. C.; Stephenson, C. R. J. Visible-Light Photoredox Catalysis: Aza-Henry Reactions via C–H Functionalization. *J. Am. Chem. Soc.* **2010**, *132*, 1464-1465. d) Furst, L.; Matsuura, B. S.; Narayanam, J. M. R.; Tucker, J. W.; Stephenson, C. R. J. Visible Light-Mediated Intermolecular C–H Functionalization of Electron-Rich Heterocycles with Malonates. *Org. Lett.* **2010**, *12*, 3104-3107. e) Dai, C.; Narayanam, J. M. R.; Stephenson, C. R. J. Visible-light-mediated conversion of alcohols to halides. *Nature Chem.* **2011**, *3*, 140-145. f) Nguyen, J. D.; Tucker, J. W.; Konieczynska, M. D.; Stephenson, C. R. J. Intermolecular Atom Transfer Radical Addition to Olefins Mediated by Oxidative Quenching of Photoredox Catalysts. *J. Am. Chem. Soc.* **2011**, *133*, 4160-4163. g) Furst, L.; Narayanam, J. M. R.; Stephenson, C. R. J. Total Synthesis of (+)-Gliocladin C Enabled by Visible-Light Photoredox Catalysis. *Angew. Chem. Int. Ed.* **2011**, *50*, 9655-9659. h) Tucker, J. W.; Stephenson, C. R. J. Tandem Visible Light-Mediated Radical Cyclization–Divinylcyclopropane Rearrangement to Tricyclic Pyrrolidinones. *Org. Lett.* **2011**, *13*, 5468-5471. i) Freeman, D. B.; Furst, L.; Condie, A. G.; Stephenson, C. R. J. Functionally Diverse Nucleophilic Trapping of Iminium Intermediates Generated Utilizing Visible Light. *Org. Lett.* **2011**, *14*, 94-97. j) Tucker, J. W.; Zhang, Y.; Jamison, T. F.; Stephenson, C. R. J. Visible-Light Photoredox Catalysis in Flow. *Angew. Chem. Int. Ed.* **2012**, *51*, 4144-4147.

27. a) Andrews, R. S.; Becker, J. J.; Gagné, M. R. Intermolecular Addition of Glycosyl Halides to Alkenes Mediated by Visible Light. *Angew. Chem. Int. Ed.* **2010**, *49*, 7274-7276. b) Andrews, R. S.; Becker, J. J.; Gagné, M. R. Investigating the Rate of Photoreductive Glucosyl Radical Generation. *Org. Lett.* **2011**, *13*, 2406-2409. c) Andrews, R. S.; Becker, J. J.; Gagné, M. R. A Photoflow Reactor for the Continuous Photoredox-Mediated Synthesis of C-Glycoamino Acids and C-Glycolipids. *Angew. Chem. Int. Ed.* **2012**, *51*, 4140-4143.

28. a) Shih, H.-W.; Vander Wal, M. N.; Grange, R. L.; MacMillan, D. W. C. Enantioselective  $\alpha$ -Benzylation of Aldehydes via Photoredox Organocatalysis. *J. Am. Chem. Soc.* **2010**, *132*, 13600-13603. b) Nagib, D. A.; Scott, M. E.; MacMillan, D. W. C. Enantioselective  $\alpha$ -Trifluoromethylation of Aldehydes via Photoredox Organocatalysis. *J. Am. Chem. Soc.* **2009**, *131*, 10875-10877. c) Pham, P. V.; Nagib, D. A.; MacMillan, D. W. C. Photoredox Catalysis: A Mild, Operationally Simple Approach to the Synthesis of  $\alpha$ -Trifluoromethyl Carbonyl Compounds. *Angew. Chem. Int. Ed.* **2011**, *50*, 6119-6122. d) McNally, A.; Prier, C. K.; MacMillan, D. W. C. Discovery of an  $\alpha$ -Amino C–H Arylation Reaction Using the Strategy of Accelerated Serendipity. *Science* **2011**, *334*, 1114-1117. e) Nagib, D. A.; MacMillan, D. W. C. Trifluoromethylation of arenes and heteroarenes by means of photoredox catalysis. *Nature* **2011**, *480*, 224-228.

29. Pitts, M. R.; Harrison, J. R.; Moody, C. J. Indium metal as a reducing agent in organic synthesis. *J. Chem. Soc., Perkin Trans. I* **2001**, 955-977.

30. Villalobos, J. M.; Srogl, J.; Liebeskind, L. S. A New Paradigm for Carbon–Carbon Bond Formation: Aerobic, Copper-Templated Cross-Coupling. *J. Am. Chem. Soc.* **2007**, *129*, 15734-15735.



31. Chong, J. M.; Shen, L.; Taylor, N. J. Asymmetric Conjugate Addition of Alkynylboronates to Enones. *J. Am. Chem. Soc.* **2000**, *122*, 1822-1823.
32. Keck, G. E.; Boden, E. P.; Mabury, S. A. A useful Wittig reagent for the stereoselective synthesis of trans- $\alpha,\beta$ -unsaturated thiol esters. *J. Org. Chem.* **1985**, *50*, 709-710.
33. Still, W. C.; Kahn, M.; Mitra, A. Rapid chromatographic technique for preparative separations with moderate resolution. *J. Org. Chem.* **1978**, *43*, 2923-2925.

### **Chapter 3. Brønsted Acid-Mediated Photocatalysis: Reductive Cyclizations of Enones Using Visible Light**

Portions of this work have previously been published:

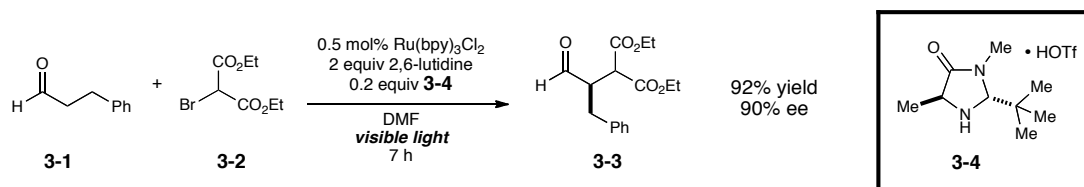
Du, J.; Ruiz Espelt, L. Yoon, T. P. Photocatalytic reductive cyclizations of enones: Divergent reactivity of photogenerated radical and radical anion intermediates. *Chem. Sci.* **2011**, 2, 2115–2119.

### 3.1 Introduction

Over the past several decades, the synthetic utility of free radicals has become increasingly apparent.<sup>1,2</sup> These highly reactive species often display reactivity that is orthogonal to that of polar reactive intermediates and thus enable the synthesis of complex molecular scaffolds that would otherwise be difficult to construct. The generation of free radicals, however, typically requires toxic or hazardous additives such as tin compounds, trialkylboranes, and peroxides. As a result, alternative methods for generating radical intermediates without the use of these unattractive reagents are of practical interest.

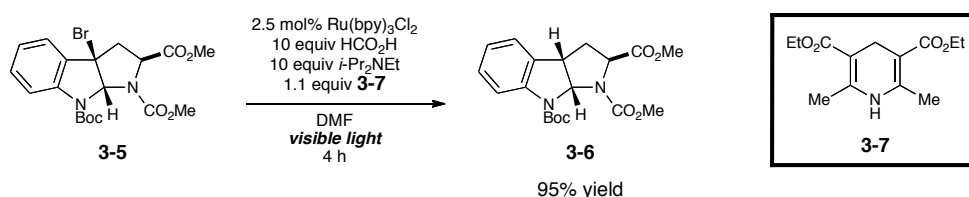
Visible light photoredox catalysis has recently emerged as a promising strategy for initiating single electron transfer processes.<sup>3</sup> Several groups have reported photocatalytic conditions for the generation of carbon-centered free radicals via the reductive dehalogenation of electron-deficient haloalkanes. In this context, MacMillan was the first to describe conditions for the asymmetric  $\alpha$ -alkylation of aldehydes (Scheme 3-1);<sup>4</sup> a number of enantioselective photoredox reactions have since been developed.<sup>5</sup> In these systems, formation of the radical species occurs via single-electron transfer from the photogenerated  $\text{Ru}(\text{bpy})_3^+$  complex to the alkyl halide.

**Scheme 3-1.** Single-electron mediated  $\alpha$ -alkylation of aldehydes using organocatalysis and photoredox catalysis



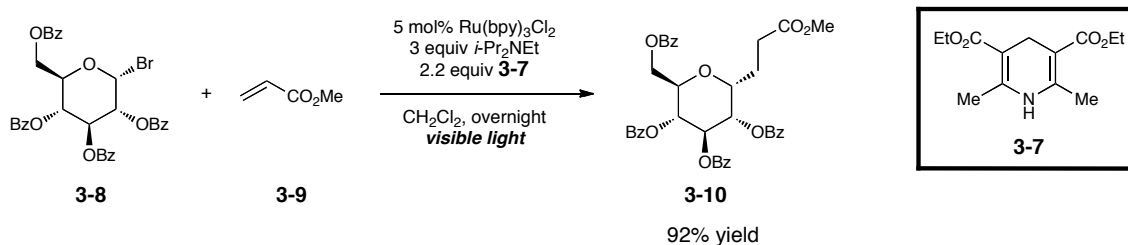
Stephenson has employed photoredox catalysis as a strategy for accessing traditional radical reactivity in organic synthesis. This was first demonstrated in the development of a tin-free photocatalytic method for reductive dehalogenation (Scheme 3-2);<sup>6</sup> a range of transformations have been reported since and its use in the synthesis of natural products has been demonstrated.<sup>7</sup> Under these conditions, the alkyl radical is generated upon reduction of the carbon–halogen bond by the  $\text{Ru}(\text{bpy})_3^+$  photoreductant.

**Scheme 3-2.** Reductive dehalogenation of alkyl halides using visible light photocatalysis



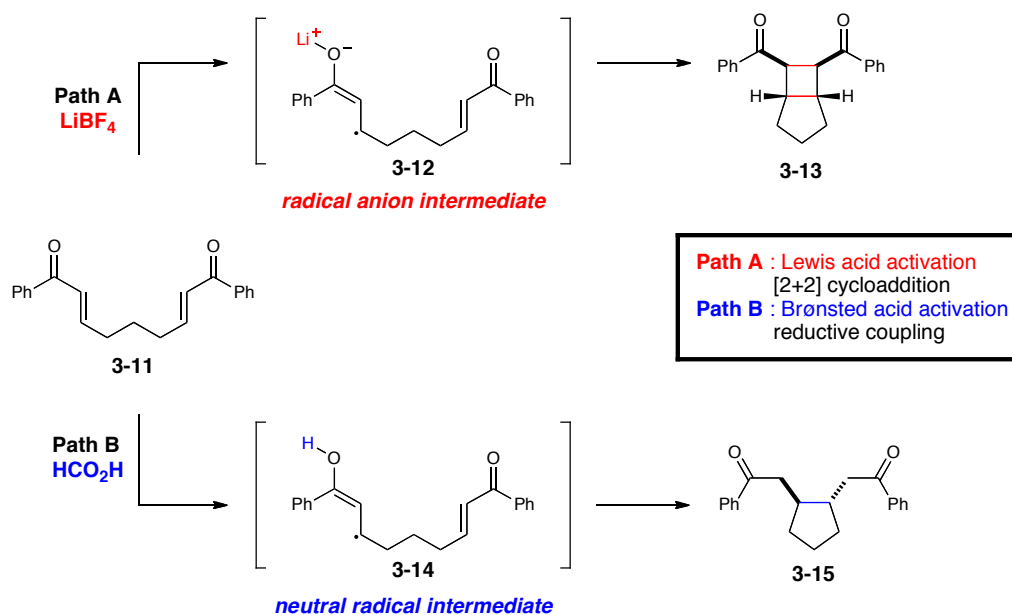
Inspired by these results, Gagné has applied the strategy of visible light photoredox catalysis to the development of conditions for the conjugate addition of glycosyl halides into activated olefins (Scheme 3-3).<sup>8</sup> This method is a marked improvement from the tin-mediated approaches that have previously been used for this transformation. Again, the radical species is proposed to arise from electron transfer from the photogenerated  $\text{Ru}(\text{bpy})_3^+$  to the glycosyl halide substrate.

**Scheme 3-3.** Visible light-promoted addition of glycosyl halides to alkenes



Our initial studies in visible light photocatalysis involved a superficially similar system for the [2+2] cycloaddition of aryl enones (e.g. **3-11**) upon irradiation with visible light in the presence of  $\text{Ru}(\text{bpy})_3\text{Cl}_2$  (Scheme 3-4, path A).<sup>9</sup> The key intermediate in these cycloadditions is the radical anion (**3-12**) formed upon one-electron reduction of the enone substrate in the presence of the Lewis acidic lithium additive. The role of the Lewis acid co-catalyst is presumably to activate the enone and stabilize the resulting radical anion intermediate. It quickly became clear to us that the nature of this reactive intermediate was quite different than that of the neutral radicals involved in MacMillan, Stephenson, and Gagné's systems. The presence of both a charge and an unpaired spin in the enone radical anion appeared to be necessary for formation of the cyclobutane product, as the cycloaddition pathway was discordant with the 5-exo-trig cyclization reactivity that would typically be expected from a neutral radical species.<sup>10</sup>

**Scheme 3-4.** Dual reactivity manifolds in visible light photocatalysis



Our realization that these two classes of reactive intermediates might exhibit fundamentally different characteristic reactivity led us to consider how we might be able to access neutral radical intermediates instead of radical anions from the photocatalytic reduction of bis(enone) substrates. In particular, activation of bis(enone) **3-11** with a Brønsted acid would afford a cationic oxocarbenium species, reduction of which should produce a neutral radical (**3-14**, Scheme 3-4, path B). This intermediate would then be poised to undergo 5-exo-trig cyclization<sup>11,12,13</sup> rather than the [2+2] cycloaddition preferred by the radical anion.

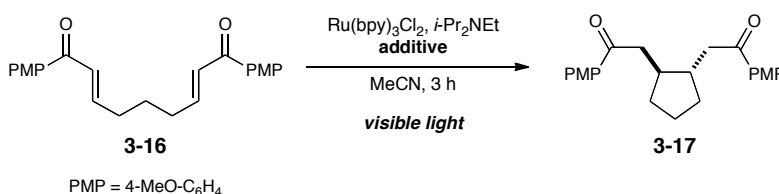
### 3.2 Results and discussion

We began our investigation of the effect of Brønsted acid additives on the photocatalytic one-electron reduction of bis(enone) **3-16** (Table 3-1). The substrate is unchanged in the absence of an acid co-catalyst (entry 1). In the presence of a variety of Brønsted acid additives, however, **3-16** undergoes reductive cyclization to produce the cyclized diketone **3-17** (entries 2–6). In all cases, *trans*-**3-17** is the major product formed, and *only traces of products arising from [2+2] cycloaddition could be observed*. In our survey of Brønsted acids, formic acid showed particular promise for promoting reductive cyclization (entry 4). Further optimization studies revealed that the reaction rate increases in the presence of a larger excess of acid (entry 7), and that lowering the photocatalyst loading to 2.5 mol% produced the desired cycloadduct in 95% yield as a single *trans*-diastereomer (entry 8).

Pandey has previously described a photocatalytic system for the reductive cyclizations of enones that utilizes 9,10-dicyanoanthracene (DCA) as a photosensitizer

along with  $\text{PPh}_3$  as a co-reductant.<sup>14</sup> The optimized conditions required relatively high loadings of the photosensitizer (20 mol%) and the use of a 450 W mercury arc lamp. We have argued<sup>9</sup> that the longer excited state lifetime (600 ns vs. 15 ns) and broader visible absorption of  $\text{Ru}(\text{bpy})_3^{2+}$  compared to DCA allow for lower catalyst loadings and lower-intensity light sources to be used in photocatalytic applications.<sup>15,16</sup> Indeed, in comparison experiments using DCA as the photocatalyst, either in place of  $\text{Ru}(\text{bpy})_3^{2+}$  in our optimized protocol (entry 9) or using a 23 W compact fluorescent bulb in place of the 450 W Hanovia lamp in Pandey's protocol (entry 10), we observe no reductive cyclization products after 3 h of irradiation. Thus, the use of  $\text{Ru}(\text{bpy})_3^{2+}$  as a photocatalyst, which results in complete conversion to **3-17** in the same timeframe, affords a significant improvement over this previous approach to photochemical reductive cyclization.

**Table 3-1.** Effect of Brønsted acids on the reductive cyclization of bis(enone) **3-16**<sup>a</sup>



| entry | conditions  | yield <sup>b</sup> |
|-------|---|--------------------|
| 1     | 5 mol% $\text{Ru}(\text{bpy})_3\text{Cl}_2$ , no acid, 4 equiv $i\text{-Pr}_2\text{NEt}$                          | <5%                |
| 2     | 5 mol% $\text{Ru}(\text{bpy})_3\text{Cl}_2$ , 2 equiv $\text{H}_2\text{SO}_4$ , 4 equiv $i\text{-Pr}_2\text{NEt}$ | <5%                |
| 3     | 5 mol% $\text{Ru}(\text{bpy})_3\text{Cl}_2$ , 2 equiv TFA, 4 equiv $i\text{-Pr}_2\text{NEt}$                      | 13%                |
| 4     | 5 mol% $\text{Ru}(\text{bpy})_3\text{Cl}_2$ , 2 equiv $\text{HCO}_2\text{H}$ , 4 equiv $i\text{-Pr}_2\text{NEt}$  | 58%                |
| 5     | 5 mol% $\text{Ru}(\text{bpy})_3\text{Cl}_2$ , 2 equiv $\text{BzOH}$ , 4 equiv $i\text{-Pr}_2\text{NEt}$           | 43%                |
| 6     | 5 mol% $\text{Ru}(\text{bpy})_3\text{Cl}_2$ , 2 equiv $\text{AcOH}$ , 4 equiv $i\text{-Pr}_2\text{NEt}$           | 36%                |
| 7     | 5 mol% $\text{Ru}(\text{bpy})_3\text{Cl}_2$ , 5 equiv $\text{HCO}_2\text{H}$ , 10 equiv $i\text{-Pr}_2\text{NEt}$ | 66%                |

|                 |  |                        |
|-----------------|--|------------------------|
| <b>8</b>        | <b>2.5 mol% Ru(bpy)<sub>3</sub>Cl<sub>2</sub>, 5 equiv HCO<sub>2</sub>H, 10 equiv <i>i</i>-Pr<sub>2</sub>NEt</b> | <b>95%<sup>c</sup></b> |
| 9               | 2.5 mol% DCA, 5 equiv HCO <sub>2</sub> H, 10 equiv <i>i</i> -Pr <sub>2</sub> NEt                                 | <5%                    |
| 10 <sup>d</sup> | 20 mol% DCA, 60 mol% Ph <sub>3</sub> P   | <5%                    |

<sup>a</sup> Reactions were irradiated using a 23 W compact fluorescent bulb. <sup>b</sup> Yields were determined by <sup>1</sup>H NMR analysis against CH<sub>2</sub>Br<sub>2</sub> as an internal standard. <sup>c</sup> Isolated yield. <sup>d</sup> Other than the light source and reaction time, this entry uses the optimized conditions from ref. 14b.

We next proceeded to examine the scope of reductive cyclization for a series of structurally varied aryl enones under our optimized conditions (Table 3-2). Symmetrical bis(enone)s bearing electron-donating and -withdrawing substituents are excellent substrates (entries 1–3), as are heteroaryl enones (entry 4). Unsymmetrical enones with one aryl component also react smoothly (entries 5 and 6).  $\alpha$ -Substituted enoates readily undergo cyclization, although the configuration of the newly formed  $\alpha$ -stereocenter is not controlled under these conditions (entry 7). A variety of heteroatomic, substituted, and extended tethering moieties can also be utilized (entries 8–11). Furthermore, as is the case with most radical-mediated cyclization reactions, the presence of acidic heteroatomic functionalities on the substrate is not problematic (entries 12 and 13). Unlike tin-mediated radical cyclizations and the aforementioned visible light-mediated processes, however, we find that unactivated alkyl bromides are easily tolerated (entry 14), enabling the unique construction of products containing this useful synthetic handle for further manipulation.



**Table 3-2.** Scope of reductive cyclizations initiated by aryl enones<sup>a,b</sup>

| entry | substrate  | product | time  | yield <sup>c</sup> | d.r. <sup>d</sup> |
|-------|--|---------|-------|--------------------|-------------------|
|       |  |         |       |                    |                   |
| 1     | R <sub>1</sub> = R <sub>2</sub> = Ph ( <b>3-15</b> )                                 |         | 2.5 h | 82%                | >10:1             |
| 2     | R <sub>1</sub> = R <sub>2</sub> = PMP ( <b>3-17</b> )                                |         | 3 h   | 95%                | >10:1             |
| 3     | R <sub>1</sub> = R <sub>2</sub> = 4-Cl-C <sub>6</sub> H <sub>4</sub> ( <b>3-44</b> ) |         | 1.5 h | 76%                | >10:1             |
| 4     | R <sub>1</sub> = R <sub>2</sub> = 2-furyl ( <b>3-45</b> )                            |         | 4 h   | 69%                | >10:1             |
| 5     | R <sub>1</sub> = PMP, R <sub>2</sub> = <i>t</i> -Bu ( <b>3-46</b> )                  |         | 6 h   | 95%                | >10:1             |
| 6     | R <sub>1</sub> = PMP, R <sub>2</sub> = SEt ( <b>3-47</b> )                           |         | 9 h   | 79%                | 10:1              |
| 7     |  |         | 12 h  | 75%                | 1:1               |
|       |  |         |       |                    |                   |
| 8     | X = O ( <b>3-49</b> )  |         | 3.5 h | 93%                | >10:1             |
| 9     | X = NTs ( <b>3-50</b> )  |         | 4 h   | 83%                | >10:1             |
| 10    | X = CMe <sub>2</sub> ( <b>3-51</b> )   |         | 3 h   | 73%                | >10:1             |
| 11    | X = CH <sub>2</sub> CH <sub>2</sub> ( <b>3-52</b> )                                  |         | 6 h   | 92%                | >10:1             |
|       |  |         |       |                    |                   |
| 12    | X = OH ( <b>3-53</b> )   |         | 5 h   | 74%                | >10:1             |
| 13    | X = NHBoc ( <b>3-54</b> )  |         | 3.5 h | 92%                | >10:1             |
| 14    |  |         | 3 h   | 64%                | 10:1              |

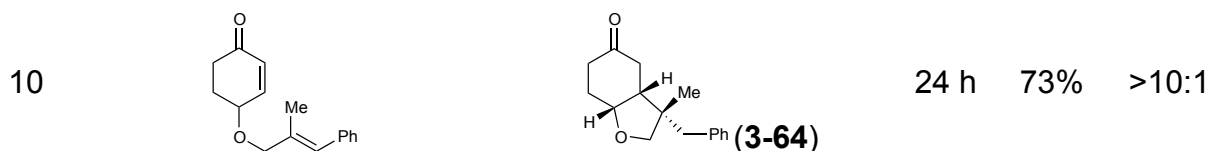
<sup>a</sup> Reactions conducted with 2.5 mol% Ru(bpy)<sub>3</sub>Cl<sub>2</sub> in the presence of HCO<sub>2</sub>H (5 equiv) and *i*-Pr<sub>2</sub>NEt (10 equiv) in MeCN (0.05 M). Reactions were irradiated using a 23 W compact fluorescent bulb. <sup>b</sup> PMP = 4-MeO-C<sub>6</sub>H<sub>4</sub>. <sup>c</sup> Data represent the averaged isolated yields from two

reproducible experiments. <sup>d</sup> Diastereomer ratios determined by <sup>1</sup>H NMR analysis of the unpurified reaction mixtures.

We also became interested in exploring the reductive cyclization of aliphatic enones. These compounds are less easily reduced than aryl enones,<sup>17</sup> and [2+2] cycloadditions were not successful with these substrates under the lithium-promoted conditions that we previously reported. We were thus pleased to discover that aliphatic bis(enone)s underwent reductive cyclization in high yields using Brønsted acid activators, although these substrates required extended reaction times (Table 3-3, entry 1). We speculated that the use of a more strongly reducing photocatalyst might increase the rate of the cyclization. Indeed, the use of Ir(dtb-bpy)(ppy)<sub>2</sub>(PF<sub>6</sub>),<sup>18</sup> which MacMillan<sup>5a</sup> and Stephenson<sup>7a</sup> have shown to be more effective photocatalysts in reductive dehalogenation processes, enabled the desired cycloadduct to be formed in good yields in only 12 h (entry 2).

A variety of other Michael acceptors, including acrylate esters (entry 3), vinyl nitriles (entry 4), and alkynoate esters are good reaction partners for reductive coupling with aliphatic enones as well (entry 5). We were particularly interested in examining cyclization reactions with styrenic acceptors. In our previous studies of the lithium-promoted [2+2] cycloadditions, we had observed that only Michael acceptors bearing strongly electron-withdrawing groups would react with the photogenerated radical anion intermediates to afford cyclobutane products. However, the neutral radical intermediates we presumed to be involved in these reductive couplings should be able to react with a broader range of less activated alkenes, including styrenic olefins. Indeed, we were delighted to discover that the reductive couplings of linear aliphatic enones with

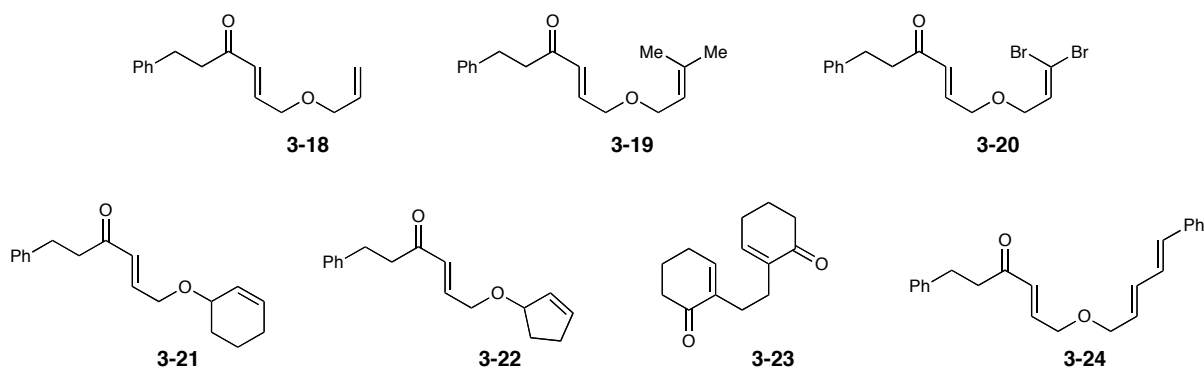




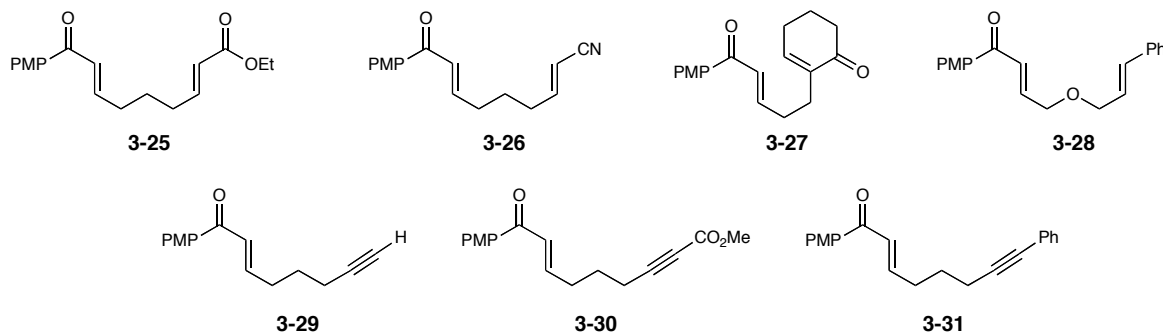
<sup>a</sup> Unless otherwise noted, reactions conducted with 2.5 mol% Ir(dtb-bpy)(ppy)<sub>2</sub>(PF<sub>6</sub>) in the presence of HCO<sub>2</sub>H (5 equiv) and *i*-Pr<sub>2</sub>NEt (10 equiv) in MeCN (0.05 M). Reactions were irradiated using a 23 W compact fluorescent bulb. <sup>b</sup> Data represent the averaged isolated yields from two reproducible experiments. <sup>c</sup> Diastereomeric ratios determined by <sup>1</sup>H NMR analysis of the upurified reaction mixtures. <sup>d</sup> Ru(bpy)<sub>3</sub>Cl<sub>2</sub> was used instead of Ir(dtb-bpy)(ppy)<sub>2</sub>(PF<sub>6</sub>). <sup>e</sup> A 2:1 *trans*:*cis* mixture of the vinyl nitrile was used for this entry.

Reactions involving unactivated olefins, however, were not high-yielding. The major product observed in these reactions resulted from reduction of the aliphatic enone without productive cyclization (Figure 3-1).

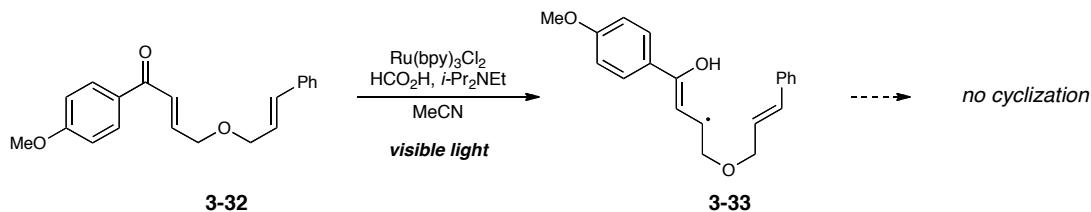
**Figure 3-1.** Incompatible aliphatic enone substrates for reductive cyclization



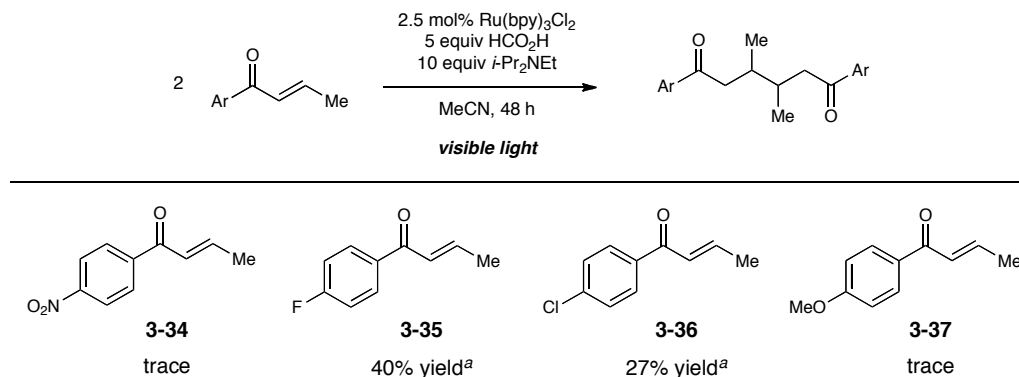
In addition, only aliphatic enones were amenable to cyclization with this broader scope of Michael acceptors. When the Michael acceptor is tethered to an aryl enone, no productive cyclization was observed using either Ru(bpy)<sub>3</sub><sup>2+</sup> or Ir(dtb-bpy)(ppy)<sub>2</sub><sup>+</sup> (Figure 3-2).

**Figure 3-2.** Incompatible aryl enone substrates for reductive cyclization

We rationalize this observation by proposing that cyclization occurs via the enol tautomer of the intermediate. The radical produced from the aryl enone would be stabilized by delocalization into the aromatic ring and thus presumably be less reactive towards cyclization (Scheme 3-5).

**Scheme 3-5.** Unproductive reductive cyclization of aryl enones to styrenes via the enol tautomer

Also in contrast to the Lewis acid-mediated conditions for [2+2] cycloadditions, the intermolecular variant of this process does not proceed efficiently. Efforts to optimize the reaction conditions were undertaken; however, in all cases, the reaction does not proceed to completion (Scheme 3-6).

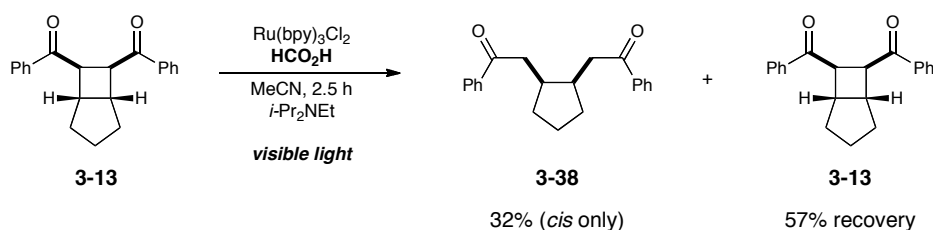
**Scheme 3-6.** Intermolecular reductive coupling of aryl enones


<sup>a</sup> Yields were determined by <sup>1</sup>H NMR analysis against CH<sub>2</sub>Br<sub>2</sub> as an internal standard.

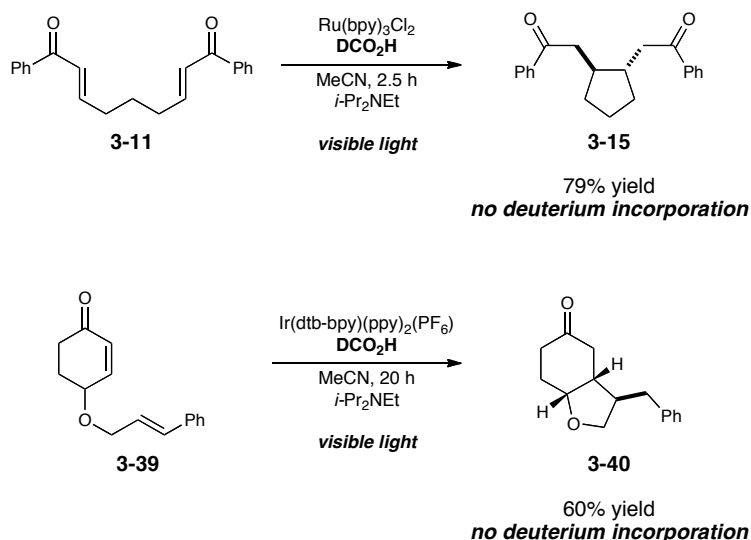
From these results, it is clear that the Brønsted acid-mediated radical cyclization is fundamentally different from the Lewis acid-induced radical anion cyclobutanation we had previously reported, for several reasons. First, the scope of each reaction is quite distinct. While neither aliphatic enones nor styrenes participate in the radical anion [2+2] cycloaddition, they are excellent reaction partners in the radical-mediated reductive cyclization process. Second, the two cyclization events favor divergent stereochemical outcomes; while the [2+2] cycloaddition requires a *cis* ring junction, the reductive cyclizations of enones are generally *trans* selective. Control experiments preclude the possibility that the reductive cyclization product might arise from initial [2+2] cycloaddition followed by reductive scission of the α-α' bond. When the *cis* [2+2] cycloadduct **3-13** is independently synthesized and subjected to the conditions for direct reductive cyclization, the reductive cleavage product (**3-38**) produced is exclusively *cis* and is formed in only 32% yield (Scheme 3-7). Thus, the cyclobutane is incompetent to

be a kinetically relevant intermediate in the reductive cyclization. Moreover, the stereochemistry of the reductive cleavage product is opposite to that observed in the direct reductive cyclization of **3-11**, which further rules out the intermediacy of cyclobutane **3-13** in this process.

**Scheme 3-7.** Subjection of *cis* cyclobutane **3-13** to Brønsted acid conditions for reductive cyclization



A third major difference between these processes is the redox balance of the overall transformation. The reductive cyclization constitutes a two-electron reduction of the enone substrate, while the [2+2] cycloadditions are net redox-neutral. Under the optimized conditions for reductive cyclization, either the amine base additive or the formate moiety could potentially serve as the terminal reductant for this process. To probe the feasibility of these two possibilities, we conducted reductive cyclizations using monodeuterated DCO<sub>2</sub>H as the Brønsted acid component. These experiments did not result in any measurable amount of deuterium incorporation, either under the Ru(bpy)<sub>3</sub><sup>2+</sup> or Ir(dtb-bpy)(ppy)<sub>2</sub><sup>+</sup> conditions (Scheme 3-8).

**Scheme 3-8.** Deuterium labeling control experiments

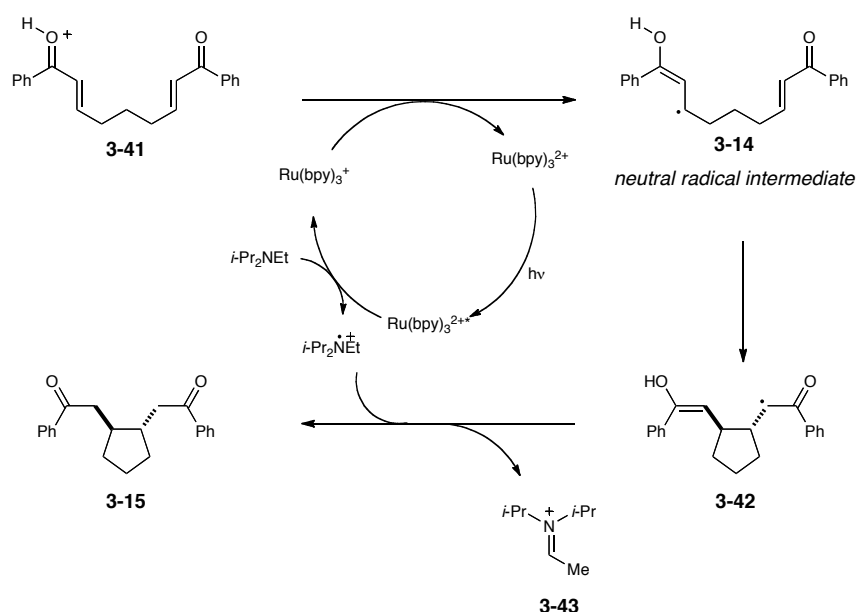
Thus, formic acid is presumably serving solely as a Brønsted acid, and the amine base additive, not the formate moiety, is the terminal reductant in this process. This is in contrast to a report by the Stephenson group,<sup>6</sup> who observed deuterated products in reductive dehalogenation reactions using  $\text{DCO}_2\text{H}$  and  $i\text{-Pr}_2\text{NEt}$ . The formation of acetaldehyde is also observed in our reactions as a by-product, which is consistent with oxidation of the *N*-ethyl group of  $i\text{-Pr}_2\text{NEt}$ . We cannot rule out the possibility that oxidation of the isopropyl group also occurs; however, the decomposition of trialkylamine radical cations has been studied, and oxidation of the least substituted *N*-substituent is commonly observed.<sup>19</sup>

The mechanism outlined in Scheme 3-9 is consistent with all of the experimental evidence we have collected to date. Visible light irradiation of  $\text{Ru(bpy)}_3^{2+}$  produces a photoexcited state ( $\text{Ru(bpy)}_3^{2+*}$ ) that can be reductively quenched by  $i\text{-Pr}_2\text{NEt}$  to afford an amine radical cation ( $i\text{-Pr}_2\text{NEt}^{\bullet+}$ ) and a  $\text{Ru(bpy)}_3^+$  complex. This photogenerated reductant can transfer an electron to the protonated oxocarbenium ion **3-41** to produce



the key neutral radical intermediate **3-14**, which undergoes 5-exo-trig cyclization to yield  $\alpha$ -ketoradical **3-42**. Hydrogen atom transfer from the photogenerated amine radical cation, either in a single atom transfer step or by sequential electron- and proton-transfer steps, would then afford the reductive cyclization product **3-15**.

**Scheme 3-9.** Proposed mechanism for photocatalytic reductive cyclization



### 3.3 Conclusions

In summary, we have developed a highly efficient method for the photocatalytic generation of radicals from enones upon irradiation with visible light. The use of a Brønsted acid activator in conjunction with a metal polypyridyl photocatalyst enables the reduction of a variety of aryl and alkyl enones, and the resulting radicals can cyclize with enones and styrenic olefins to produce reductive cyclization products. This represents an attractive method for the initiation of radicals without the need for unattractive

stoichiometric toxic reagents and introduces a novel strategy for the tin-free generation of  $\beta$ -ketoradicals that react with high diastereoselectivity and with the high functional group compatibility typical of radical cyclization reactions.

More importantly, this study underscores the versatility of transition metal polypyridyl photocatalysts in organic synthesis. Photocatalytic reactions of enones using metal polypyridyl complexes proceed by very different reaction manifolds in the presence of either Lewis or Brønsted acid additives. The same catalysts enable the facile conversion of enones either to radical anions, which participate in an overall redox-neutral [2+2] cycloaddition, or to neutral radicals, which result in a net two-electron reductive coupling reaction. The reactivities of these two intermediates are quite distinct from one another, as manifested in the different connectivity and oxidation states of their products, their divergent stereochemical outcomes, and the distinct substrate scopes of their transformations, and the appropriate choice of Brønsted or Lewis acidic additive can control the partitioning between these two reaction manifolds. This indicates that the scope of reactions that may be accessible via this approach to visible light photocatalysis is remarkably broad.

### 3.4 Contributions

Laura Ruiz Espelt conducted the experiments for Table 3-2, entries 6–7, 9–10, and 12–13 and Table 3-3, entries 3–4.

## 3.5 Experimental

### 3.5.1 General information

Acetonitrile and  $\text{CH}_2\text{Cl}_2$  were purified by elution through alumina as described by Grubbs.<sup>20</sup> *i*-Pr<sub>2</sub>NEt was distilled from  $\text{CaH}_2$  immediately prior to use.  $\text{Ru}(\text{bpy})_3\text{Cl}_2 \cdot 6\text{H}_2\text{O}$  was purchased from Strem and used without further purification. Formic acid was passed through a silica plug immediately prior to use. All other chemicals were purchased from commercial suppliers and used without further purification. Flash column chromatography was performed using Silicycle silica gel (230–400 mesh).<sup>21</sup> All glassware was oven-dried at 130 °C for at least 1 h or flame-dried immediately prior to use.

Diastereomer ratios for all compounds were determined by  $^1\text{H}$  NMR analysis of the unpurified reaction mixtures. All NMR spectra were obtained at ambient temperature on the Varian Unity-500 and Varian Inova-500 spectrometers. Chemical shifts ( $\delta$ ) are reported in parts per million relative to TMS (0.0 ppm) for  $^1\text{H}$  NMR data and  $\text{CDCl}_3$  (77.23 ppm) for  $^{13}\text{C}$  NMR data. IR spectral data were obtained using a Bruker Vector 22 spectrometer. Mass spectrometry was performed with a Micromass LCT (electrospray ionization, time-of-flight analyzer or electron impact). These facilities are funded by the NSF (CHE-8813550, CHE-9629688), NIH (RR04981-01) and the University of Wisconsin.

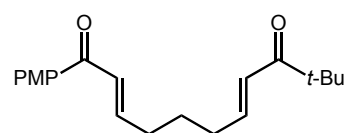
### 3.5.2 General procedures

**General procedure for reductive cyclizations of aryl enones (A):** A dry 25 mL Schlenk tube was charged with the aryl enone (1 equiv),  $\text{Ru}(\text{bpy})_3\text{Cl}_2 \cdot 6\text{H}_2\text{O}$  (0.025

equiv), HCO<sub>2</sub>H (5 equiv), *i*-Pr<sub>2</sub>NEt (10 equiv), and acetonitrile (0.05 M) and degassed in the dark using three freeze/pump/thaw cycles under nitrogen. The reaction was then stirred vigorously and irradiated with a 23 W (1380 lumen) compact fluorescent lamp. Upon completion of the reaction, the solvent was removed *in vacuo* and the residue purified by column chromatography on silica gel.

**General procedure for reductive cyclizations of aliphatic enones (B):** A dry 25 mL Schlenk tube was charged with the aliphatic enone (1 equiv), [Ir(ppy)<sub>2</sub>(dtb-bpy)][PF<sub>6</sub>] (0.025 equiv), HCO<sub>2</sub>H (5 equiv), *i*-Pr<sub>2</sub>NEt (10 equiv), and acetonitrile (0.05 M) and degassed in the dark using three freeze/pump/thaw cycles under nitrogen. The reaction was then stirred vigorously and irradiated with a 23 W (1380 lumen) compact fluorescent lamp. Upon completion of the reaction, the solvent was removed *in vacuo* and the residue purified by column chromatography on silica gel.

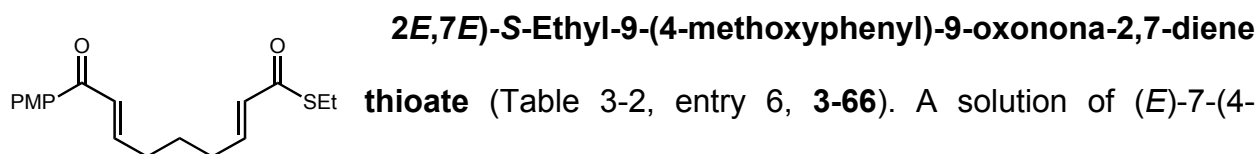
### 3.5.3 Synthesis and characterization of new compounds



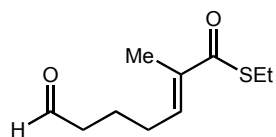
**(2E,7E)-1-(4-Methoxyphenyl)-10,10-dimethylundeca-2,7-diene-1,9-dione** (Table 3-2, entry 5, **3-65**). A solution of (*E*)-7-

(4-methoxyphenyl)-7-oxohept-5-enal<sup>22</sup> (1.89 g, 8.1 mmol) in 6.5 mL CH<sub>2</sub>Cl<sub>2</sub> was placed in a 50 mL round-bottomed flask. 3,3-Dimethyl-1-(triphenylphosphoranylidene) butan-2-one<sup>23</sup> (3.20 g, 8.9 mmol) in 20 mL CH<sub>2</sub>Cl<sub>2</sub> was added dropwise. The resulting solution was allowed to stir for 7 d, after which the reaction was concentrated *in vacuo* to afford a yellow residue. Purification by chromatography on silica gel using 5:1 hexanes:EtOAc as the eluent afforded the product as a yellow solid (1.27 g, 4.0 mmol, 51% yield). IR (thin film) 1687, 1666, 1622, 1600; <sup>1</sup>H NMR (500 MHz, CDCl<sub>3</sub>) δ 7.95 (dt, *J* = 9.1, 2.9

Hz, 2H), 7.02 (dt,  $J = 15.3, 6.9$  Hz, 1H), 6.95 (dt,  $J = 6.7, 2.1$  Hz, 2H), 6.91 (m, 1H), 6.53 (dt,  $J = 15.3, 1.7$  Hz, 1H), 3.88 (s, 3H), 2.35 (q,  $J = 7.8$  Hz, 2H), 2.29 (q,  $J = 7.3$  Hz, 2H), 1.71 (m, 2H), 1.16 (s, 9H);  $^{13}\text{C}$  NMR (125 MHz,  $\text{CDCl}_3$ )  $\delta$  204.2, 188.8, 163.3, 147.5, 146.3, 130.8, 130.7, 126.0, 124.8, 113.7, 55.5, 42.9, 32.1, 31.8, 26.8, 26.2; HRMS ( $\text{ESI}^+$ ) calc'd for  $[\text{C}_{20}\text{H}_{26}\text{O}_3\text{Na}]^+$  requires  $m/z$  337.1775, found  $m/z$  337.1760. (mp = 60–64 °C).

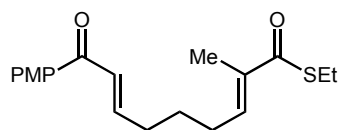


A solution of (*E*)-7-(4-methoxyphenyl)-7-oxohept-5-enal (0.96 g, 4.1 mmol) in 2.0 mL  $\text{CH}_2\text{Cl}_2$  was placed in a 25 mL round-bottomed flask. S-Ethyl-2-(triphenylphosphoranylidene)ethanethioate<sup>24</sup> (1.5 g, 4.14 mmol) in 3.0 mL  $\text{CH}_2\text{Cl}_2$  was added dropwise. The resulting solution was allowed to stir for 24 h, after which the reaction was concentrated *in vacuo* to afford a yellow residue. Purification by chromatography on silica gel using 7:3 hexanes:EtOAc as the eluent afforded the product as a yellow oil (0.60 g, 1.9 mmol, 46% yield). IR (thin film) 2932, 1666, 1620, 1599;  $^1\text{H}$  NMR (500 MHz,  $\text{CDCl}_3$ )  $\delta$  7.95 (dt,  $J = 9.0, 2.1$  Hz, 2H), 7.01 (m, 1H), 6.95 (dt,  $J = 9.2, 2.6$  Hz, 2H), 6.89 (m, 2H), 6.13 (dt,  $J = 15.7, 1.4$  Hz, 1H), 3.87 (s, 3H), 2.94 (q,  $J = 7.2$  Hz, 2H), 2.34 (q,  $J = 7.8$  Hz, 2H), 2.26 (q,  $J = 8.4$  Hz, 2H), 1.71 (m, 2H), 1.28 (t, 3H);  $^{13}\text{C}$  NMR (125 MHz,  $\text{CDCl}_3$ )  $\delta$  189.9, 188.7, 163.3, 147.3, 144.0, 130.8, 130.7, 129.3, 126.1, 113.8, 55.5, 32.0, 31.5, 26.5, 23.1, 14.8; HRMS ( $\text{ESI}^+$ ) calc'd for  $[\text{C}_{18}\text{H}_{23}\text{O}_3\text{S}]^+$  requires  $m/z$  319.1363, found  $m/z$  319.1347.



**(E)-S-Ethyl 2-methyl-7-oxohept-2-enethioate (3-67).** A

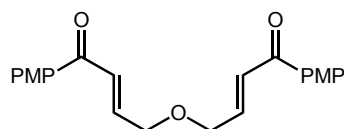
suspension of NaH (35 mg, 8.9 mmol) in 34 mL THF was placed in a 50 mL round-bottomed flask and cooled to 0 °C. S-Ethyl 3-(diethoxyphosphoryl)-2-methylpropanethioate (2.1 g, 8.2 mmol) was added dropwise and the resulting suspension stirred for 30 min, after which 5,5-dimethoxypentanal<sup>25</sup> (1.0 g, 6.8 mmol) was added dropwise. The reaction was allowed to stir for an additional 40 min, after which the organic layer was separated, dried over MgSO<sub>4</sub>, and concentrated *in vacuo*. The crude product was then dissolved in 16 mL THF and treated with 1 M HCl. After 1 h, the aqueous layer was separated, neutralized with sat. NaHCO<sub>3</sub> and extracted with EtOAc (x3). The combined organics were then washed with brine, dried over MgSO<sub>4</sub> and concentrated *in vacuo*. Purification by chromatography on silica gel using 9:1 hexanes:EtOAc as the eluent afforded the product as a yellow oil (429 mg, 2.1 mmol, 33% yield). IR (thin film) 2722, 1720, 1652; <sup>1</sup>H NMR (500 MHz, CDCl<sub>3</sub>) δ 9.79 (s, 1H), 6.67 (td, J = 7.1, 1.0 Hz, 1H), 2.92 (q, J = 7.1 Hz, 2H), 2.49 (td, J = 7.3, 1.1 Hz, 2H), 2.25 (q, J = 7.4 Hz, 2H), 1.87 (s, 3H), 1.81 (quintet, J = 7.2 Hz, 2H), 1.27 (t, J = 7.5 Hz, 3H); <sup>13</sup>C NMR (125 MHz, CDCl<sub>3</sub>) δ 201.9, 193.8, 138.7, 137.0, 43.2, 27.8, 23.3, 20.9, 14.7, 12.4; HRMS (ESI<sup>+</sup>) calc'd for [C<sub>10</sub>H<sub>16</sub>O<sub>2</sub>SNa]<sup>+</sup> requires *m/z* 223.0764, found *m/z* 223.0775.



**(2E,7E)-S-Ethyl-9-(4-methoxyphenyl)-2-methyl-9-oxonona-**

**2,7-diene thioate** (Table 3-2, entry 7, **3-68**). A solution of (E)-7-(4-methoxyphenyl)-7-oxohept-5-enal (429 mg, 2.14 mmol), S-ethyl 2-(triphenylphosphoranylidene)propanethioate (1.32 g, 3.2 mmol) and 10 mL CH<sub>2</sub>Cl<sub>2</sub> was

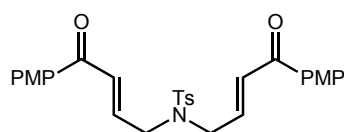
placed in a 25 mL round-bottomed flask and allowed to stir for 72 h, after which the reaction mixture was concentrated to yield a yellow oil. Purification by chromatography on silica gel using 4:1 hexanes:EtOAc as the eluent afforded the product as a yellow oil (503 mg, 1.5 mmol, 71% yield). IR (thin film) 2931, 1665, 1654, 1618;  $^1\text{H}$  NMR (500 MHz,  $\text{CDCl}_3$ )  $\delta$  7.95 (dt,  $J$  = 9.0, 2.6 Hz, 2H), 7.03 (dt,  $J$  = 15.3, 7.0 Hz, 1H), 6.95 (dt,  $J$  = 8.9, 2.0 Hz, 2H), 6.92 (dt,  $J$  = 15.1, 1.3 Hz, 1H), 6.72 (tq,  $J$  = 7.3, 1.2 Hz, 1H), 3.88 (s, 3H), 2.92 (q,  $J$  = 7.6 Hz, 2H), 2.36 (q,  $J$  = 7.9 Hz, 2H), 2.27 (q,  $J$  = 7.2 Hz, 2H), 1.88 (s, 3H), 1.72 (m, 2H), 1.27 (t, 3H);  $^{13}\text{C}$  NMR (125 MHz,  $\text{CDCl}_3$ )  $\delta$  193.8, 188.8, 163.4, 147.5, 139.4, 136.7, 130.8, 130.7, 126.1, 113.8, 55.4, 32.2, 28.0, 27.1, 23.2, 14.7, 12.5; HRMS ( $\text{ESI}^+$ ) calc'd for  $[\text{C}_{19}\text{H}_{24}\text{O}_3\text{SNa}]^+$  requires  $m/z$  355.1339, found  $m/z$  355.1340.



**(2E,2'E)-4,4'-Oxybis(1-(4-methoxyphenyl)but-2-en-1-one)**

(Table 3-2, entry 8, **3-69**). Prepared using a modification of a procedure by Montgomery.<sup>26</sup> A solution of 2,5-dihydrofuran (568 mg, 8.1 mmol) in 27 mL  $\text{CH}_2\text{Cl}_2$  was placed in a 100 mL three-necked flask and cooled to  $-78^\circ\text{C}$ . Ozone was passed through the reaction mixture until a blue coloration persisted, at which point  $\text{N}_2$  was bubbled through the solution to remove excess dissolved ozone. The ozonide was then quenched with 1.2 mL dimethylsulfide and 1-(4-methoxyphenyl)-2-(triphenylphosphoranylidene) ethanone (10 g, 23 mmol) was added in one portion. The resulting solution was warmed to room temperature and allowed to stir for 16 h. Concentration *in vacuo* and purification by chromatography on silica gel using 2:1 hexanes:EtOAc as the eluent afforded the product as a white solid (1.1 g, 3.0 mmol, 37% yield). IR (thin film) 1668, 1623, 1600;  $^1\text{H}$  NMR (500 MHz,  $\text{CDCl}_3$ )  $\delta$  7.99 (dt,  $J$  =

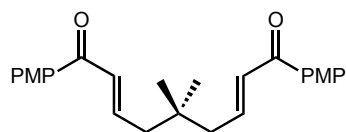
8.9, 2.9 Hz, 4H), 7.24 (dt,  $J = 15.1, 1.8$  Hz, 2H), 7.06 (dt,  $J = 15.4, 4.1$  Hz, 2H), 6.95 (dt,  $J = 8.9, 2.9$  Hz, 4H), 4.36 (dd,  $J = 4.1, 2.0$  Hz, 4H), 3.88 (s, 6H);  $^{13}\text{C}$  NMR (125 MHz,  $\text{CDCl}_3$ )  $\delta$  188.3, 163.5, 142.7, 130.9, 130.5, 124.9, 113.8, 70.0, 55.5; HRMS ( $\text{ESI}^+$ ) calc'd for  $[\text{C}_{22}\text{H}_{22}\text{O}_5\text{Na}]^+$  requires  $m/z$  389.1360, found  $m/z$  389.1367. (mp = 81–86 °C).



***N,N*-Bis((*E*)-4-(4-methoxyphenyl)-4-oxobut-2-en-1-yl)-4-methylbenzenesulfonamide** (Table 3-2, entry 9, **3-70**). A

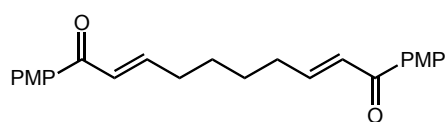
solution of *N,N*-diallyl-*p*-toluenesulfonamide<sup>27</sup> (1.0 g, 4.0 mmol) in 13 mL  $\text{CH}_2\text{Cl}_2$  was placed in a 100 mL three-necked flask and cooled to  $-78$  °C. Ozone was passed through the reaction mixture until a blue coloration persisted, at which point  $\text{N}_2$  was bubbled through the solution to remove excess dissolved ozone. The ozonide was then quenched with 1.2 mL dimethylsulfide and warmed to room temperature. 1-(4-Methoxyphenyl)-2-(triphenylphosphoranylidene)ethanone (3.5 g, 8.5 mmol) was added in one portion and the resulting solution was allowed to stir for 2 d. Concentration *in vacuo* and purification by chromatography on silica gel using 1:1 hexanes:EtOAc as the eluent afforded the product as a white solid (555 mg, 1.1 mmol, 26% yield). IR (thin film) 1669, 1624, 1599;  $^1\text{H}$  NMR (500 MHz,  $\text{CDCl}_3$ )  $\delta$  7.87 (dt,  $J = 8.9, 2.8$  Hz, 4H), 7.76 (d,  $J = 8.2$  Hz, 2H), 7.32 (d,  $J = 8$  Hz, 2H), 6.99 (d,  $J = 15.5$  Hz, 2H), 6.91 (dt,  $J = 8.9, 2.5$  Hz, 4H), 6.76 (dt,  $J = 15.2, 5.4$  Hz, 2H), 4.12 (d,  $J = 5.5$  Hz, 4H), 3.87 (s, 6H), 2.4 (s, 3H);  $^{13}\text{C}$  NMR (125 MHz,  $\text{CDCl}_3$ )  $\delta$  187.8, 163.7, 144.0, 140.3, 136.7, 131.0, 130.0, 130.0, 128.0, 127.3, 113.9, 55.5, 48.7, 21.5; HRMS ( $\text{ESI}^+$ ) calc'd for  $[\text{C}_{29}\text{H}_{29}\text{NO}_6\text{SNa}]^+$  requires  $m/z$  542.1608, found  $m/z$  542.1597. (mp = 72–79 °C).





**(2E,7E)-1,9-Bis(4-methoxyphenyl)-5,5-dimethylnona-2,7-diene-1,9-dione** (Table 3-2, entry 10, **3-71**). Prepared using a

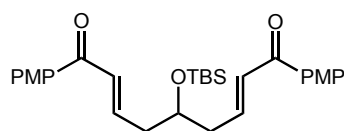
modification of a procedure by Montgomery.<sup>26</sup> To a solution of 3,3-dimethylglutaraldehyde<sup>28</sup> (0.1 g, 0.8 mmol) in 10 mL CH<sub>2</sub>Cl<sub>2</sub> was added 1-(4-methoxyphenyl)-2-(triphenyl phosphoranylidene)ethanone (0.8 g, 2.0 mmol). The resulting solution was allowed to stir for 3 d, after which the reaction was concentrated *in vacuo* to afford a yellow residue. Purification on silica gel using 4:1 hexanes:EtOAc as the eluent afforded a yellow oil that was recrystallized from hexanes:EtOAc to yield the product as a white solid (98 mg, 0.3 mmol, 32% yield). IR (thin film) 1663, 1617, 1257; <sup>1</sup>H NMR (500 MHz, CDCl<sub>3</sub>) δ 7.95 (dt, J = 8.9, 3.1 Hz, 4H), 7.09 (m, 2H), 6.93 (m, 6H), 3.86 (s, 6H), 2.28 (dd., J = 7.8, 1.0 Hz, 4H), 1.05 (s, 6H); <sup>13</sup>C NMR (125 MHz, CDCl<sub>3</sub>) δ 188.9, 163.7, 145.0, 130.8, 128.2, 113.9, 55.4, 45.3, 34.9, 27.1; HRMS (ESI<sup>+</sup>) calc'd for [C<sub>25</sub>H<sub>28</sub>O<sub>4</sub>Na]<sup>+</sup> requires *m/z* 415.1873, found *m/z* 415.1880. (mp = 51–57 °C).



**(3E,9E)-1,12-Bis(4-methoxyphenyl)dodeca-3,9-diene-1,12-dione** (Table 3-2, entry 11, **3-72**).

Prepared using a modification of a procedure by Montgomery.<sup>26</sup> A solution of cyclohexenone (756 mg, 9.2 mmol) in 23 mL CH<sub>2</sub>Cl<sub>2</sub> was placed in a 100 mL three-necked flask and cooled to –78 °C. Ozone was passed through the reaction mixture until a blue coloration persisted, at which point N<sub>2</sub> was bubbled through the solution to remove excess dissolved ozone. The ozonide was then quenched with 5.3 mL dimethylsulfide and warmed to room temperature. 1-(4-Methoxyphenyl)-2-(triphenylphosphoranylidene) ethanone (9.4 g, 22 mmol) was added in one portion and

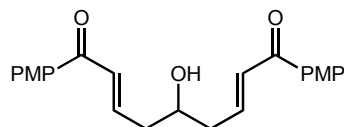
the resulting solution was allowed to stir for 2 d. Concentration *in vacuo* and purification by chromatography on silica gel using 2:1 hexanes:EtOAc as the eluent afforded the product as a white solid (1.0 g, 2.8 mmol, 30% yield). IR (thin film) 1664, 1617, 1258, 1170;  $^1\text{H}$  NMR (500 MHz,  $\text{CDCl}_3$ )  $\delta$  7.95 (d,  $J$  = 8.7 Hz, 4H), 7.04 (dt,  $J$  = 15.2, 6.9 Hz, 2H), 6.93 (m, 4H), 3.87 (s, 6H), 2.35 (m, 4H), 1.61 (m, 4H);  $^{13}\text{C}$  NMR (125 MHz,  $\text{CDCl}_3$ )  $\delta$  189.0, 163.3, 148.1, 130.8, 130.7, 125.8, 113.7, 55.4, 32.5, 27.8; HRMS ( $\text{ESI}^+$ ) calc'd for  $[\text{C}_{22}\text{H}_{26}\text{O}_4]^+$  requires  $m/z$  378.1826, found  $m/z$  378.1829. (mp = 83–88 °C).



**(2E,7E)-5-((*tert*-Butyldimethylsilyl)oxy)-1,9-bis(4-methoxyphenyl) nona-2,7-diene-1,9-dione (3-73).** Prepared using a

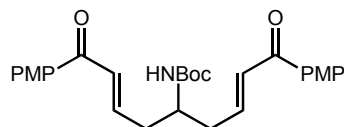
modification of a procedure by Montgomery.<sup>26</sup> A solution of *tert*-butyl(hepta-1,6-dien-4-yloxy)dimethyl silane<sup>29</sup> (2.0 g, 8.9 mmol) in 30 mL  $\text{CH}_2\text{Cl}_2$  was placed in a 100 mL three-necked flask and cooled to  $-78$  °C. Ozone was passed through the reaction mixture until a blue coloration persisted, at which point  $\text{N}_2$  was bubbled through the solution to remove excess dissolved ozone. The ozonide was then quenched with 2.6 mL dimethylsulfide and warmed to room temperature. 1-(4-Methoxyphenyl)-2-(triphenylphosphoranylidene)ethanone (7.7 g, 19 mmol) was added in one portion and the resulting solution was allowed to stir for 4 d. Concentration *in vacuo* and purification by chromatography on silica gel using 3:2 hexanes:EtOAc as the eluent afforded the product as a yellow oil (2.8 g, 5.7 mmol, 64% yield). IR (thin film) 2931, 1619, 1599, 1258, 1170;  $^1\text{H}$  NMR (500 MHz,  $\text{CDCl}_3$ )  $\delta$  7.95 (dt,  $J$  = 8.7, 2.9 Hz, 4H), 7.05 (m, 2H), 6.95 (tt,  $J$  = 7.0, 2.9 Hz, 6H), 4.05 (m, 1H), 3.87 (s, 6H), 2.51 (m, 4H), 0.88 (s, 9H), 0.06

(s, 6H);  $^{13}\text{C}$  NMR (125 MHz,  $\text{CDCl}_3$ )  $\delta$  188.5, 163.3, 144.1, 130.8, 130.6, 127.9, 113.6, 70.3, 55.3, 40.6, 25.7, 17.9; HRMS ( $\text{ESI}^+$ ) calc'd for  $[\text{C}_{29}\text{H}_{38}\text{O}_5\text{SiNa}]^+$  requires  $m/z$  517.2381, found  $m/z$  517.2396.



**(2E,7E)-5-Hydroxy-1,9-bis(4-methoxyphenyl)nona-2,7-diene-1,9-dione** (Table 3-2, entry 12, **3-74**). Prepared using a

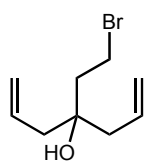
modification of a procedure by Shioiri.<sup>30</sup> (2E,7E)-5-((*tert*-Butyldimethylsilyl)oxy)-1,9-bis(4-methoxy phenyl)nona-2,7-diene-1,9-dione (2.5 g, 5.1 mmol) was allowed to stir in 50 mL of a 13:7:3  $\text{AcOH}:\text{H}_2\text{O}:\text{THF}$  mixture. After 2.5 h, the reaction was concentrated, dissolved in  $\text{Et}_2\text{O}$  and washed with  $\text{H}_2\text{O}$ . Purification of the resulting residue by chromatography on silica gel using 3:2 hexanes: $\text{EtOAc}$  as the eluent afforded the product as a white solid (638 mg, 1.7 mmol, 33% yield). IR (thin film) 3454, 1600, 1260, 1172;  $^1\text{H}$  NMR (500 MHz,  $\text{CDCl}_3$ )  $\delta$  7.94 (dt,  $J$  = 8.8, 2.4 Hz, 4H), 7.04 (m, 4H), 6.92 (dt,  $J$  = 8.8, 3.6 Hz, 4H), 4.06 (m, 1H), 3.85 (s, 6H), 2.83 (d,  $J$  = 4.8 Hz, 1H), 2.56 (m, 4H);  $^{13}\text{C}$  NMR (125 MHz,  $\text{CDCl}_3$ )  $\delta$  188.7, 163.5, 143.8, 130.9, 130.5, 128.2, 113.8, 69.4, 55.5, 40.4; HRMS ( $\text{ESI}^+$ ) calc'd for  $[\text{C}_{23}\text{H}_{24}\text{O}_5\text{Na}]^+$  requires  $m/z$  403.1516 found  $m/z$  403.1523. (mp = 110–113  $^\circ\text{C}$ ).



***tert*-Butyl((2E,7E)-1,9-bis(4-methoxyphenyl)-1,9-dioxonona-2,7-dien-5-yl)carbamate** (Table 3-2, entry 13, **3-75**).

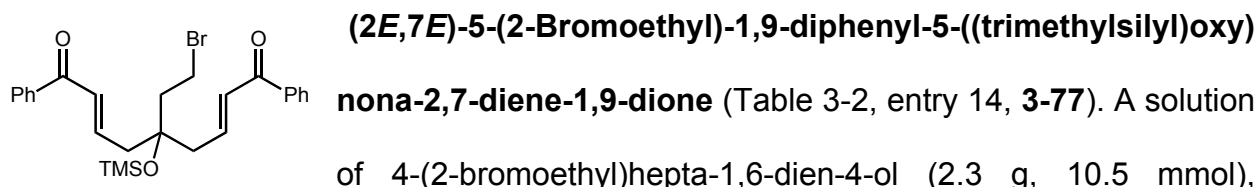
Prepared using a modification of a procedure by Montgomery.<sup>26</sup> To a solution of 3-amino-1,6-heptadiene (1.5 g, 14 mmol) in 15 mL  $\text{H}_2\text{O}$  was added di-*t*-butyldicarbonate (3.4 g, 16 mmol). The suspension was allowed to stir for 30 min, after which the reaction

was extracted with  $\text{CH}_2\text{Cl}_2$  and concentrated to afford the crude product as a yellow solid.<sup>31</sup> The resulting crude diene was dissolved in 34 mL  $\text{CH}_2\text{Cl}_2$  in a 100 mL three-necked round-bottomed flask and cooled to  $-78\text{ }^\circ\text{C}$ . Ozone was passed through the reaction mixture until a blue coloration persisted, at which point  $\text{N}_2$  was bubbled through the solution to remove excess dissolved ozone. The ozonide was then quenched with 3.0 mL dimethylsulfide and warmed to room temperature. 1-(4-Methoxyphenyl)-2-(triphenylphosphoranylidene)ethanone (8.9 g, 22 mmol) was added in one portion and the resulting solution was allowed to stir for 2 d. Concentration *in vacuo* and purification by chromatography using 3:2 hexanes:EtOAc as the eluent afforded the product as a yellow solid (1.3 g, 2.6 mmol, 30% yield). IR (thin film) 3366, 1675, 1259, 1170;  $^1\text{H}$  NMR (500 MHz,  $\text{CDCl}_3$ )  $\delta$  7.95 (dt,  $J = 9.1, 2.7\text{ Hz}$ , 4H), 6.99 (m, 4H), 6.94 (dt,  $J = 9.1, 2.9\text{ Hz}$ , 4H), 4.58 (m, 1H), 4.04 (m, 1H), 3.87 (s, 6H), 2.56 (m, 4H), 1.41 (s, 9H);  $^{13}\text{C}$  NMR (125 MHz,  $\text{CDCl}_3$ )  $\delta$  188.4, 163.5, 155.2, 143.1, 130.9, 130.5, 128.3, 113.8, 55.5, 37.6, 28.3; HRMS ( $\text{ESI}^+$ ) calc'd for  $[\text{C}_{28}\text{H}_{33}\text{NO}_6\text{Na}]^+$  requires  $m/z$  480.2381 found  $m/z$  480.2387. (mp =  $118\text{--}121\text{ }^\circ\text{C}$ ).



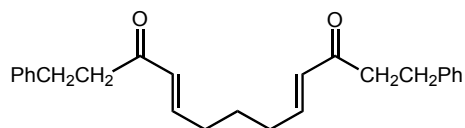
**4-(2-Bromoethyl)hepta-1,6-dien-4-ol (3-76).** Prepared using a modification of a procedure by Wang.<sup>32</sup> Allyl bromide (7.0 mL, 81 mmol) was added dropwise to a suspension of zinc dust (6.1 g, 93 mmol) in 26 mL THF. The suspension was allowed to stir for 10 min, after which ethyl 3-bromopropionate (2.6 mL, 20 mmol) was added slowly. The reaction was then stirred for 2 h, quenched with sat.  $\text{NH}_4\text{Cl}$ , extracted with  $\text{Et}_2\text{O}$  (x3), washed with brine, dried over  $\text{MgSO}_4$  and concentrated *in vacuo* to yield a clear oil. Purification by chromatography on silica gel using 9:1

hexanes:EtOAc as the eluent afforded the product as a clear oil (3.7 g, 17 mmol, 83% yield). IR (thin film) 3454, 1640, 1446;  $^1\text{H}$  NMR (500 MHz,  $\text{CDCl}_3$ )  $\delta$  5.83 (ddt,  $J = 17.3$ , 10.1, 7.0 Hz, 2H), 5.16 (dd,  $J = 16.8$ , 1.4 Hz, 4H), 3.49 (dd,  $J = 8.6$ , 7.8 Hz, 2H), 2.24 (m, 4H), 2.08 (dd,  $J = 8.4$ , 8.1 Hz, 2H), 1.73 (s, 1H);  $^{13}\text{C}$  NMR (125 MHz,  $\text{CDCl}_3$ )  $\delta$  132.8, 119.6, 73.7, 43.7, 42.6, 27.7; HRMS ( $\text{EI}^+$ ) calc'd for  $[\text{C}_6\text{H}_{11}\text{BrO}]^+$  requires  $m/z$  176.9910, found  $m/z$  176.9903.



acrolein (6.9 mL, 103 mmol), and 2<sup>nd</sup> generation Grubbs catalyst<sup>33</sup> (446 mg, 0.53 mmol) in 42 mL  $\text{CH}_2\text{Cl}_2$  was allowed to stir for 48 h.<sup>34</sup> The brown suspension was then concentrated *in vacuo*, treated with pyridine (1.7 mL, 21 mmol) and TMSCl (2.0 mL, 15.8 mmol), and allowed to stir overnight at 35 °C. The resulting reaction mixture was eluted through two consecutive plugs of silica gel using 2:1 hexanes:EtOAc to completely remove the catalyst and then concentrated *in vacuo* to yield a yellow oil.<sup>35</sup> The crude aldehyde was then dissolved in 0.3 mL THF and cooled to 0 °C. Phenyl magnesium bromide (1.0 M in THF, 0.56 mL, 0.56 mmol) was added dropwise and the resulting solution was allowed to stir for 1h, after which the reaction was quenched with water, extracted with ether (x3), washed with sat.  $\text{NaHCO}_3$ , dried over  $\text{Na}_2\text{SO}_4$ , and concentrated *in vacuo* to yield 527 mg (1.0 mmol, 10% yield) of the crude diol as a yellow residue.<sup>36</sup> The diol and 2-iodoxybenzoic acid<sup>37</sup> (730 mg, 2.6 mmol) were dissolved in 11 mL  $\text{CH}_2\text{Cl}_2$  and allowed to stir for 24 h. The reaction mixture was then

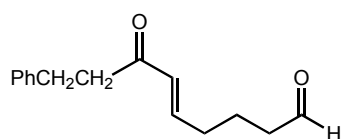
diluted with  $\text{CH}_2\text{Cl}_2$ , washed with 5%  $\text{NaHCO}_3$  (x2), water, brine, dried over  $\text{Na}_2\text{SO}_4$ , and concentrated to yield a yellow residue. Purification by chromatography on silica gel using 7:1 hexanes:EtOAc as the eluent afforded the product as a clear oil (332 mg, 0.66 mmol, 64% yield). IR (thin film) 1671, 1620, 1279;  $^1\text{H}$  NMR (500 MHz,  $\text{CDCl}_3$ )  $\delta$  7.93 (d,  $J$  = 8.5 Hz, 4H), 7.57 (t,  $J$  = 7.3 Hz, 2H), 7.46 (t,  $J$  = 8 Hz, 4H), 7.06 (m, 2H), 6.98 (d,  $J$  = 15.3 Hz, 2H), 3.64 (dd,  $J$  = 7.9, 7.8 Hz, 2H), 2.59 (m, 4H), 2.10 (dd,  $J$  = 7.9, 8.1 Hz, 2H), 0.20 (s, 9H);  $^{13}\text{C}$  NMR (125 MHz,  $\text{CDCl}_3$ )  $\delta$  189.8, 143.4, 137.5, 132.9, 129.0, 128.6, 128.5, 53.4, 43.6, 43.3, 39.6, 31.6, 22.5, 14.1, 2.5; HRMS ( $\text{ESI}^+$ ) calc'd for  $[\text{C}_{26}\text{H}_{31}\text{BrO}_3\text{SiNa}]^+$  requires  $m/z$  521.1119, found  $m/z$  521.1109.



**(4E,9E)-1,13-Diphenyltrideca-4,9-diene-3,11-dione**

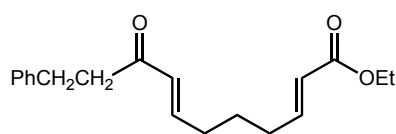
(Table 3-3, entry 1, **3-78**). A solution of glutaraldehyde (2.0 g, 10 mmol) and 4-phenyl-1-(triphenyl phosphoranylidene)butan-2-one (10.2 g, 25 mmol) in 34 mL  $\text{CH}_2\text{Cl}_2$  was placed in a 100 mL round-bottomed flask and allowed to stir for 24 h, after which the reaction mixture was concentrated to yield a clear oil. Purification by chromatography on silica gel using 4:1 hexanes:EtOAc as the eluent afforded the product as a white solid (1.13 g, 3.1 mmol, 31% yield). IR (thin film) 1701, 1669, 1629;  $^1\text{H}$  NMR (500 MHz,  $\text{CDCl}_3$ )  $\delta$  7.27 (dt,  $J$  = 7.4, 3.6 Hz, 4H), 7.20 (d,  $J$  = 7 Hz, 6H), 6.77 (dt,  $J$  = 15.9, 7.0 Hz, 2H), 6.10 (dt,  $J$  = 15.9, 1.4 Hz, 2H), 2.93 (dt,  $J$  = 7.0, 2.8 Hz, 4H), 2.86 (m, 4H), 2.21 (q,  $J$  = 6.6 Hz, 4H), 1.6 (m, 2H);  $^{13}\text{C}$  NMR (125 MHz,  $\text{CDCl}_3$ )  $\delta$  199.2, 146.1, 141.2, 130.7, 128.5, 128.3, 126.1, 41.8, 31.7, 30.0, 26.4;

HRMS (ESI<sup>+</sup>) calc'd for [C<sub>25</sub>H<sub>28</sub>O<sub>2</sub>Na]<sup>+</sup> requires *m/z* 383.1982, found *m/z* 383.1985. (mp = 40–44 °C).



**(E)-7-Oxo-9-phenylnon-5-enal (3-79).** A solution of 5,5-

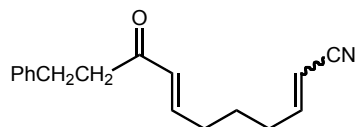
dimethoxypentanal (1 g, 6.8 mmol) and 4-phenyl-1-(triphenylphosphoranylidene)butan-2-one (3.6 g, 7.5 mmol) in 23 mL CH<sub>2</sub>Cl<sub>2</sub> was placed in a 50 mL round-bottomed flask and allowed to stir for 72 h, after which the reaction mixture was concentrated to yield a yellow oil. The residue was dissolved in 20 mL THF and treated with 1M HCl. After 1 h, the aqueous layer was separated, neutralized with sat. NaHCO<sub>3</sub> and extracted with EtOAc (x3). The combined organic layers were washed with brine, dried over MgSO<sub>4</sub>, and concentrated *in vacuo*. Purification by chromatography on silica gel using 4:1 hexanes:EtOAc as the eluent afforded the product as a yellow oil (401 mg, 1.7 mmol, 26% yield). IR (thin film): 2934, 2724, 1719, 1670, 1628; <sup>1</sup>H NMR (500 MHz, CDCl<sub>3</sub>) δ 9.76 (t, *J* = 1.1 Hz, 1H), 7.28 (m, 2H), 7.19 (m, 3H), 6.76 (dt, *J* = 15.8, 7.1 Hz, 1H), 6.11 (dt, *J* = 15.8, 1.6 Hz, 1H), 2.93 (td, *J* = 8.3, 2.0 Hz, 2H), 2.86 (m, 2H), 2.46 (td, *J* = 7.5, 1.4 Hz, 2H), 2.24 (qd, *J* = 7.1, 1.4 Hz, 2H), 1.79 (m, 2H); <sup>13</sup>C NMR (125 MHz, CDCl<sub>3</sub>) δ 201.5, 199.3, 145.8, 141.2, 130.9, 128.5, 128.4, 126.1, 42.9, 41.7, 31.5, 30.0, 20.3; HRMS (EI<sup>+</sup>) calc'd for [C<sub>15</sub>H<sub>18</sub>O<sub>2</sub>]<sup>+</sup> requires *m/z* 230.1302, found *m/z* 230.1306.



**(2E,7E)-Ethyl 9-oxo-11-phenylundeca-2,7-dienoate**

(Table 3-3, entry 3, **3-80**). A solution of (E)-7-oxo-9-phenylnon-5-enal (333 mg, 1.4 mmol) and ethyl 2-(triphenyl phosphoranylidene)acetate (750 mg, 2.2 mmol) in 5.0 mL CH<sub>2</sub>Cl<sub>2</sub> was placed in a 25 mL round-bottomed flask and

allowed to stir for 48 h, after which the reaction mixture was concentrated to yield a yellow oil. Purification by chromatography on silica gel using 4:1 hexanes:EtOAc as the eluent afforded the product as a yellow oil (362 mg, 1.2 mmol, 84% yield). IR (thin film) 1715, 1655;  $^1\text{H}$  NMR (500 MHz,  $\text{CDCl}_3$ )  $\delta$  7.28 (m, 2H), 7.19 (dt,  $J$  = 15.5, 7.1 Hz, 3H), 6.92 (dt,  $J$  = 15.5, 7.1 Hz, 1H), 6.78 (dt,  $J$  = 15.8, 6.9 Hz, 1H), 6.11 (dt,  $J$  = 15.9, 1.3 Hz, 1H), 5.82 (dt,  $J$  = 15.8, 1.6 Hz, 1H), 4.19 (q,  $J$  = 6.8 Hz, 2H), 2.93 (m, 2H), 2.86 (m, 2H), 2.22 (m, 4H), 1.63 (m, 2H), 1.29 (t, 3H);  $^{13}\text{C}$  NMR (125 MHz,  $\text{CDCl}_3$ )  $\delta$  199.3, 166.5, 147.9, 146.3, 141.2, 130.7, 128.5, 128.3, 126.1, 122.0, 60.2, 41.8, 31.7, 31.4, 30.0, 26.3, 14.2; HRMS ( $\text{ESI}^+$ ) calc'd for  $[\text{C}_{19}\text{H}_{24}\text{O}_3\text{Na}]^+$  requires  $m/z$  323.1618, found  $m/z$  323.1615.

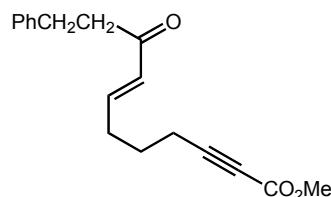


**(2E,7E)-9-Oxo-11-phenylundeca-2,7-dienitrile** (Table 3-3, entry 4, **3-81**). A solution of (*E*)-7-oxo-9-phenylnon-5-enal

(276 mg, 1.2 mmol) and 2-(triphenylphosphoranylidene)acetonitrile (540 mg, 1.8 mmol) in 10 mL  $\text{CH}_2\text{Cl}_2$  was placed in a 25 mL round-bottomed flask and allowed to stir for 72 h, after which the reaction mixture was concentrated to yield a yellow oil. Purification by chromatography on silica gel using 70:30 hexanes:EtOAc as the eluent afforded the product as a yellow oil and a 1:1 mixture of *trans:cis* isomers (285 mg, 1.1 mmol, 95% yield). IR (thin film) 2934, 2221, 1670, 1631;  $^1\text{H}$  NMR (500 MHz,  $\text{CDCl}_3$ )  $\delta$  7.28 (m, 2H), 7.20 (m, 3H), 6.73 (m, 2H), 6.45 (dt,  $J$  = 10.9, 7.6 Hz, 1H, minor isomer), 6.12 (m, 1H), 5.33 (dt,  $J$  = 10.9, 1.2 Hz, 1H, major isomer), 2.93 (m, 2H), 2.87 (m, 2H), 2.45 (qd,  $J$  = 7.5, 1.3 Hz, 2H, minor isomer), 2.23 (m, 4H), 1.63 (m, 2H),  $^{13}\text{C}$  NMR (125 MHz,

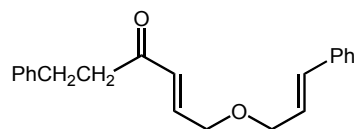


$\text{CDCl}_3$ )  $\delta$  199.2, 154.7, 153.8, 145.5, 141.2, 130.9, 128.5, 128.4, 126.1, 117.2, 115.8, 100.5, 41.9, 32.5, 31.6, 31.5, 31.2, 30.0, 26.6, 26.0; HRMS ( $\text{ESI}^+$ ) calc'd for  $[\text{C}_{23}\text{H}_{26}\text{O}_4\text{Na}]^+$  requires  $m/z$  276.1357, found  $m/z$  276.1359.



**(E)-Methyl-4-((4-oxo-6-phenylhex-2-en-1-yl)oxy)but-2-ynoate** (Table 3-3, entry 5, **3-82**). A solution of methyl 7-oxohept-2-ynoate<sup>38</sup> and 4-phenyl-1-

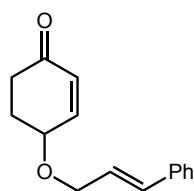
(triphenylphosphoranylidene)butan-2-one in 19 mL  $\text{CH}_2\text{Cl}_2$  was placed in a 25 mL round-bottomed flask and allowed to stir for 48 h, after which the reaction mixture was concentrated to yield a yellow residue. Purification by chromatography on silica gel using 4:1 hexanes: EtOAc as the eluent afforded the product as a yellow oil (1.42 g, 5.0 mmol, 84% yield). IR (thin film) 2235, 1707, 1670, 1630;  $^1\text{H}$  NMR (500 MHz,  $\text{CDCl}_3$ )  $\delta$  7.28 (m, 2H), 7.19 (m, 2H), 6.76 (dt,  $J$  = 15.9, 6.9 Hz, 1H), 6.14 (dt,  $J$  = 15.8, 1.5 Hz, 1H), 3.76 (s, 3H), 2.94 (m, 2H), 2.87 (m, 2H), 2.36 (t, 3H), 2.32 (dt,  $J$  = 7 Hz, 1H), 1.74 (m, 2H);  $^{13}\text{C}$  NMR (125 MHz,  $\text{CDCl}_3$ )  $\delta$  199.2, 154.1, 145.3, 141.1, 131.0, 128.5, 126.2, 88.3, 73.8, 52.6, 41.7, 31.2, 25.7, 18.0; HRMS ( $\text{EI}^+$ ) calc'd for  $[\text{C}_{18}\text{H}_{20}\text{O}_3]^+$  requires  $m/z$  284.1407, found  $m/z$  284.1407.



**(E)-6-(Cinnamyloxy)-1-phenylhex-4-en-3-one** (Table 3-3, entry 6, **3-83**). To a  $-78^\circ\text{C}$  solution of oxalyl chloride (0.55

mL, 6.4 mmol) in 24 mL  $\text{CH}_2\text{Cl}_2$  was added DMSO (0.54 mL, 7.6 mmol) in 1.6 mL  $\text{CH}_2\text{Cl}_2$ . The reaction was stirred for 30 min, after which 2-(cinnamyloxy)ethanol<sup>39</sup> (565 mg, 3.2 mmol) in 3.2 mL  $\text{CH}_2\text{Cl}_2$  was added dropwise. The suspension was allowed to

stir for 30 min, after which Et<sub>3</sub>N (2.2 mL, 16 mmol) was added. The reaction was stirred at –78 °C for 30 min, warmed to room temperature and stirred for an additional 30 min. The reaction was poured onto H<sub>2</sub>O and the product extracted with CH<sub>2</sub>Cl<sub>2</sub> (x3). The combined organics were washed with brine, dried over MgSO<sub>4</sub> and concentrated to yield a yellow oil. The crude aldehyde was dissolved in 9.4 mL CH<sub>2</sub>Cl<sub>2</sub> and treated with 2-(triphenylphosphoranylidene)acetonitrile (2.4 g, 5.8 mmol). The reaction was stirred for 2 d, after which the reaction mixture was concentrated to yield a yellow residue. Purification by chromatography on silica gel using 4:1 hexanes:EtOAc as the eluent afforded the product as a pale yellow oil (890 mg, 2.9 mmol, 91% yield). IR (thin film) 1670, 1636 <sup>1</sup>H NMR (500 MHz, CDCl<sub>3</sub>) δ 7.39 (d, J = 7.7 Hz, 2H), 7.32 (t, J = 7.3 Hz, 2H), 7.27 (m, 3H), 7.20 (m, 3H), 6.84 (dt, J = 15.7, 4.1 Hz, 1H), 6.62 (d, J = 16.2 Hz, 1H), 6.39 (dt, J = 15.8, 1.7 Hz, 1H), 6.28 (dt, J = 15.8, 5.8 Hz, 1H), 4.19 (m, 4H), 2.96 (m, 2H), 2.89 (m, 2H); <sup>13</sup>C NMR (125 MHz, CDCl<sub>3</sub>) δ 199.0, 142.3, 141.1, 136.4, 133.0, 129.2, 128.6, 128.5, 128.3, 127.8, 126.5, 126.1, 125.3, 71.4, 68.7, 42.2, 29.9; HRMS (ESI<sup>+</sup>) calc'd for [C<sub>21</sub>H<sub>22</sub>O<sub>2</sub>]<sup>+</sup> requires *m/z* 306.1615, found *m/z* 306.1619.

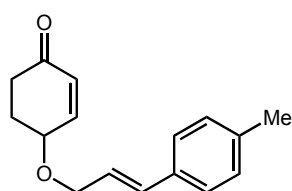


**4-(Cinnamyloxy)cyclohex-2-enone** (Table 3-3, entry 7, **3-84**). Prepared

using a modification of a procedure by Kibayashi.<sup>40</sup> A 25 mL round-

bottomed flask was charged with 4-hydroxycyclohex-2-enone<sup>41</sup> (52 mg, 0.45 mmol), cinnamyl bromide (125 mg, 0.63 mmol), Ag<sub>2</sub>O (207 mg, 0.89 mmol), and 0.87 mL CH<sub>2</sub>Cl<sub>2</sub>. The suspension was allowed to stir overnight and concentrated *in vacuo* to yield a black residue. Purification by chromatography on silica gel using 3:1 hexanes:EtOAc as the eluent afforded the product as a clear oil (16 mg, 0.071 mmol,

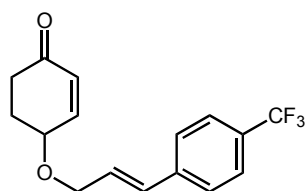
16% yield). IR (thin film) 3027, 1683, 1075;  $^1\text{H}$  NMR (500 MHz,  $\text{CDCl}_3$ )  $\delta$  7.40 (d,  $J$  = 7.1 Hz, 2H), 7.33 (t,  $J$  = 7.4 Hz, 2H), 7.27 (m, 1H), 7.00 (d,  $J$  = 9.2 Hz, 1H), 6.65 (d,  $J$  = 16.1 Hz, 1H), 6.31 (dt,  $J$  = 15.9, 6.4 Hz, 1H), 3.01 (d,  $J$  = 10.1 Hz, 1H), 4.29 (m, 3H), 2.62 (dt,  $J$  = 18.6, 3.9 Hz, 1H), 2.38 (m, 2H), 2.05 (m, 1H);  $^{13}\text{C}$  NMR (125 MHz,  $\text{CDCl}_3$ )  $\delta$  198.7, 150.5, 136.4, 133.0, 129.7, 128.6, 127.9, 126.5, 125.4, 72.4, 69.7, 35.3, 29.2; HRMS (ESI $^+$ ) calc'd for  $[\text{C}_{15}\text{H}_{16}\text{O}_2]^+$  requires  $m/z$  228.1145, found  $m/z$  228.1144.



**(E)-4-((3-(*p*-Tolyl)allyl)oxy)cyclohex-2-enone** (Table 3-3, entry 8, **3-85**). Prepared using a modification of a procedure by Kibayashi.<sup>40</sup> Phosphorous tribromide (0.48 mL, 5.1 mmol) was

added dropwise to a solution of (*E*)-3-(*p*-tolyl)prop-2-en-1-ol<sup>42</sup> (690 mg, 4.6 mmol) in 6.2 mL  $\text{Et}_2\text{O}$ . The resulting yellow solution was allowed to stir at 0 °C for 2.5 h, after which the reaction was quenched with ice and extracted with  $\text{Et}_2\text{O}$  (x3). The combined organics were washed with  $\text{H}_2\text{O}$ , dried over  $\text{Na}_2\text{SO}_4$ , and concentrated to yield the bromide as a white solid.<sup>43</sup> To the crude bromide was added 4-hydroxycyclohex-2-enone (379 mg, 3.4 mmol),  $\text{Ag}_2\text{O}$  (1.57 g, 6.8 mmol), and 6.6 mL  $\text{CH}_2\text{Cl}_2$ . The resulting suspension was allowed to stir overnight and concentrated *in vacuo* to yield a black residue. Purification by chromatography on silica gel using 2:1 hexanes: $\text{EtOAc}$  as the eluent afforded the product as a clear oil (93 mg, 0.38 mmol, 11% yield). IR (thin film) 1686, 1512, 969;  $^1\text{H}$  NMR (500 MHz,  $\text{CDCl}_3$ )  $\delta$  7.30 (d,  $J$  = 8.1 Hz, 2H), 7.14 (d,  $J$  = 7.9 Hz, 2H), 7.00 (dd,  $J$  = 8.8, 1.5 Hz, 1H), 6.61 (d,  $J$  = 15.8 Hz, 1H), 6.25 (dt,  $J$  = 15.9, 5.9 Hz, 1H), 6.01 (dd,  $J$  = 10.0, 1.2 Hz, 1H), 4.27 (m, 3H), 2.62 (dt,  $J$  = 16.3, 4.0 Hz, 1H),

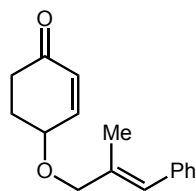
2.34 (m, 4H), 2.34 (s, 3H), 2.04 (m, 1H);  $^{13}\text{C}$  NMR (125 MHz,  $\text{CDCl}_3$ )  $\delta$  198.7, 150.6, 137.8, 133.5, 133.1, 129.7, 129.3, 126.4, 124.3, 72.3, 69.7, 35.3, 29.3, 21.2; HRMS ( $\text{EI}^+$ ) calc'd for  $[\text{C}_{16}\text{H}_{18}\text{O}_2]^+$  requires  $m/z$  242.1302, found  $m/z$  242.1312.



**(E)-4-((3-(4-(Trifluoromethyl)phenyl)allyl)oxy)cyclohex-2-**

**enone** (Table 3-3, entry 9, **3-86**). Prepared using a modification of a procedure by Kibayashi.<sup>40</sup>

A 25 mL round-bottomed flask was charged with 4-hydroxycyclohex-2-enone (450 mg, 4.0 mmol), (*E*)-1-(3-bromoprop-1-en-1-yl)-4-(trifluoromethyl) benzene<sup>44</sup> (1.48 g, 5.6 mmol),  $\text{Ag}_2\text{O}$  (1.85 g, 8.0 mmol), and 7.8 mL  $\text{CH}_2\text{Cl}_2$ . The suspension was allowed to stir overnight and concentrated *in vacuo* to yield a black residue. Purification by chromatography on silica gel using 1:1 hexanes:EtOAc as the eluent afforded the product as a clear oil (678 mg, 0.57 mmol, 57% yield). IR (thin film) 1687, 1615, 1326, 1120;  $^1\text{H}$  NMR (500 MHz,  $\text{CDCl}_3$ )  $\delta$  7.58 (d,  $J$  = 8.3 Hz, 2H), 7.49 (d,  $J$  = 8.1 Hz, 2H), 7.00 (dt,  $J$  = 10 Hz, 1H), 6.69 (d,  $J$  = 15.8 Hz, 1H), 6.40 (dt,  $J$  = 15.7, 5.6 Hz, 1H), 6.02 (d,  $J$  = 10.2 Hz, 1H), 4.30 (m, 3H), 2.63 (m, 1H), 2.37 (m, 2H), 2.06 (m, 1H);  $^{13}\text{C}$  NMR (125 MHz,  $\text{CDCl}_3$ )  $\delta$  198.5, 150.1, 139.9, 139.9, 131.0, 129.9, 128.3, 126.6, 125.6, 125.6, 125.5, 125.5, 72.8, 69.2, 35.2, 29.2; HRMS ( $\text{ESI}^+$ ) calc'd for  $[\text{C}_{16}\text{H}_{15}\text{F}_3\text{O}_2]^+$  requires  $m/z$  296.1019, found  $m/z$  296.1018.

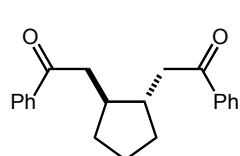


**(E)-4-((2-Methyl-3-phenylallyl)oxy)cyclohex-2-enone** (Table 3-3, entry

10, **3-87**). Prepared using a modification of a procedure by Kibayashi.<sup>40</sup>

A 25 mL round-bottomed flask was charged with 4-hydroxycyclohex-2-enone (645 mg, 5.8 mmol), (*E*)-(3-bromo-2-methylprop-1-en-1-yl)benzene (1.7 g, 8.1

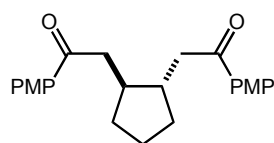
mmol), Ag<sub>2</sub>O (2.7 g, 12 mmol), and 11 mL CH<sub>2</sub>Cl<sub>2</sub>. The suspension was allowed to stir overnight and concentrated *in vacuo* to yield a black residue. Purification by chromatography on silica gel using 3:1 hexanes:EtOAc as the eluent afforded the product as a yellow oil (290 mg, 1.2 mmol, 21% yield). IR (thin film) 1683, 1379, 1087; <sup>1</sup>H NMR (500 MHz, CDCl<sub>3</sub>) δ 7.35 (m, 2H), 7.30 (m, 2H), 7.23 (t, J = 5.9 Hz, 1H), 7.01 (d, J = 10.3 Hz, 1H), 6.55 (s, 1H), 6.01 (d, J = 9.9 Hz, 1H), 4.27 (m, 1H), 4.16 (q, J = 12.3 Hz, 2H), 2.62 (dt, J = 15.7, 3.5 Hz, 1H), 2.37 (m, 2H), 2.07 (m, 1H), 1.94 (s, 3H); <sup>13</sup>C NMR (125 MHz, CDCl<sub>3</sub>) δ 198.7, 150.6, 137.2, 134.7, 129.7, 128.9, 128.2, 127.6, 126.7, 75.3, 72.3, 35.3, 29.2, 15.6; HRMS (ESI<sup>+</sup>) calc'd for [C<sub>16</sub>H<sub>28</sub>O<sub>2</sub>]<sup>+</sup> requires *m/z* 242.1302, found *m/z* 242.1303.



**2,2'-((1S, 2S)-Cyclopentane-1,2-diyl)bis(1-phenylethanone)** (Table

3-2, entry 1, **3-15**). Experiment 1: Prepared according to general procedure A using 77 mg (0.25 mmol) (*E,E*)-1,7-dibenzoyl-1,6-heptadiene, 5.0 mg (0.0067 mmol) Ru(bpy)<sub>3</sub>Cl<sub>2</sub>·6H<sub>2</sub>O, 50 μL (1.3 mmol) HCO<sub>2</sub>H, 446 μL *i*-Pr<sub>2</sub>NEt (1.3 mmol), 5.1 mL acetonitrile and irradiated for 2.5 h. Purified by chromatography using 8:1 hexanes:EtOAc to yield 63 mg (0.21 mmol, 81% yield) of the cycloadduct as a yellow oil. Experiment 2: Prepared according to general procedure A using 77 mg (0.25 mmol) (*E,E*)-1,7-dibenzoyl-1,6-heptadiene, 4.9 mg (0.0065 mmol) Ru(bpy)<sub>3</sub>Cl<sub>2</sub>·6H<sub>2</sub>O, 50 μL (1.3 mmol) HCO<sub>2</sub>H, 446 μL *i*-Pr<sub>2</sub>NEt (2.6 mmol), 5.1 mL acetonitrile and irradiated for 2.5 h. Isolated 64 mg (0.21 mmol, 82% yield). IR (thin film) 2950, 1683, 1448; <sup>1</sup>H NMR (500 MHz, CDCl<sub>3</sub>) δ 7.94 (dt, J = 8.5, 1.7 Hz, 4H), 7.54 (tt, J

= 7.3, 1.3 Hz, 2H), 7.44 (t,  $J$  = 7.9 Hz, 4H), 3.20 (dd,  $J$  = 16.5, 4.3 Hz, 2H), 2.94 (dd,  $J$  = 16.5, 8.2 Hz, 2H), 2.19 (m, 2H), 1.99 (m, 2H), 1.63 (m, 2H), 1.28 (m, 2H);  $^{13}\text{C}$  NMR (125 MHz,  $\text{CDCl}_3$ )  $\delta$  200.2, 137.2, 132.9, 128.6, 128.1, 44.0, 41.6, 32.5, 23.7; HRMS ( $\text{ESI}^+$ ) calc'd for  $[\text{C}_{21}\text{H}_{23}\text{O}_2]^+$  requires  $m/z$  307.1693, found  $m/z$  307.1708. (mp = 112–116 °C).

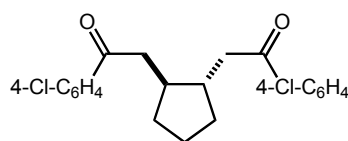


**2,2'-((1S,2S)-Cyclopentane-1,2-diyl)-bis(1-(4-methoxyphenyl)**

**ethanone)** (Table 3-2, entry 2, **3-17**). Experiment 1: Prepared

according to general procedure A using 95 mg (0.26 mmol) (*E,E*)-

1,7-(4-methoxybenzoyl)-1,6-heptadiene, 5.0 mg (0.0067 mmol)  $\text{Ru}(\text{bpy})_3\text{Cl}_2 \cdot 6\text{H}_2\text{O}$ , 50  $\mu\text{L}$  (1.3 mmol)  $\text{HCO}_2\text{H}$ , 454  $\mu\text{L}$  *i*- $\text{Pr}_2\text{NEt}$  (2.6 mmol), 5.2 mL acetonitrile and irradiated for 3 h. Purified by chromatography using 3:1 hexanes:EtOAc to yield 90 mg (0.24 mmol, 94% yield) of the cycloadduct as a white solid. Experiment 2: Prepared according to general procedure A using 95 mg (0.26 mmol) (*E,E*)-1,7-(4-methoxybenzoyl)-1,6-heptadiene, 5.1 mg (0.0068 mmol)  $\text{Ru}(\text{bpy})_3\text{Cl}_2 \cdot 6\text{H}_2\text{O}$ , 50  $\mu\text{L}$  (1.3 mmol)  $\text{HCO}_2\text{H}$ , 454  $\mu\text{L}$  *i*- $\text{Pr}_2\text{NEt}$  (2.6 mmol), 5.2 mL acetonitrile and irradiated for 3 h. Isolated 92 mg (0.25 mmol, 96% yield). IR (thin film) 1671, 1601, 1258, 1171;  $^1\text{H}$  NMR (500 MHz,  $\text{CDCl}_3$ )  $\delta$  7.93 (dt,  $J$  = 9.0, 2.2 Hz, 4H), 6.92 (dt,  $J$  = 8.9, 2.1 Hz, 4H), 3.86 (s, 6H), 3.13 (dd,  $J$  = 16.1, 4.8 Hz, 2H), 2.87 (dd,  $J$  = 16.1, 8.5 Hz, 2H), 2.15 (m, 2H), 1.96 (m, 2H), 1.62 (m, 2H), 1.27 (m, 2H);  $^{13}\text{C}$  NMR (125 MHz,  $\text{CDCl}_3$ )  $\delta$  198.8, 163.3, 130.4, 130.3, 113.7, 55.4, 43.6, 41.9, 32.5, 23.7; HRMS ( $\text{ESI}^+$ ) calc'd for  $[\text{C}_{23}\text{H}_{26}\text{O}_4\text{Na}]^+$  requires  $m/z$  389.1724, found  $m/z$  389.1709. (mp = 117–122 °C).



**2,2'-((1S,2S)-Cyclopentane-1,2-diyl)bis(1-(4-chlorophenyl)**

**ethanone)** (Table 3-2, entry 3, **3-44**). Experiment 1: Prepared

according to general procedure A using 97 mg (0.26 mmol)

(*E,E*)-1,7-(4-chlorobenzoyl)-1,6-heptadiene, 5.2 mg (0.0069 mmol) Ru(bpy)<sub>3</sub>Cl<sub>2</sub>·6H<sub>2</sub>O,

50 μL (1.3 mmol) HCO<sub>2</sub>H, 453 μL *i*-Pr<sub>2</sub>NEt (2.6 mmol), 5.2 mL acetonitrile and irradiated

for 1.5 h. Purified by chromatography using 12:1 hexanes:EtOAc to yield 73 mg (0.19

mmol, 75% yield) of the cycloadduct as a yellow oil. Experiment 2: Prepared according

to general procedure A using 97 mg (0.26 mmol) (*E,E*)-1,7-(4-chlorobenzoyl)-1,6-

heptadiene, 5.0 mg (0.0067 mmol) Ru(bpy)<sub>3</sub>Cl<sub>2</sub>·6H<sub>2</sub>O, 50 μL (1.3 mmol) HCO<sub>2</sub>H, 454 μL

*i*-Pr<sub>2</sub>NEt (2.6 mmol), 5.2 mL acetonitrile and irradiated for 1.5 h. Isolated 75 mg (0.20

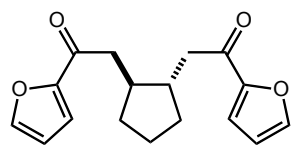
mmol, 77% yield). IR (thin film) 1676, 1588; <sup>1</sup>H NMR (500 MHz, CDCl<sub>3</sub>) δ 7.88 (tt, J =

8.4, 2.6 Hz, 4H), 7.42 (tt, J = 8.7, 2.3 Hz, 4H), 3.16 (dd, J = 16.7, 5.0 Hz, 2H), 2.92 (dd,

J = 16.3, 7.9 Hz, 2H), 2.17 (m, 2H), 1.98 (m, 2H), 1.64 (m, 2H), 1.28 (m, 2H); <sup>13</sup>C NMR

(125 MHz, CDCl<sub>3</sub>) δ 198.9, 139.4, 135.4, 129.5, 128.9, 44.0, 41.4, 32.6, 23.7; HRMS

(ESI<sup>+</sup>) calc'd for [C<sub>21</sub>H<sub>20</sub>O<sub>2</sub>Na]<sup>+</sup> requires *m/z* 397.0733, found *m/z* 397.0719.



**2,2'-((1S,2S)-Cyclopentane-1,2-diyl)bis(1-(furan-2-yl)**

**ethanone)** (Table 3-2, entry 4, **3-45**). Experiment 1: Prepared

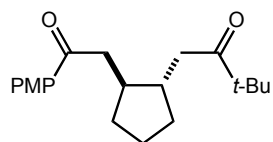
according to general procedure A using 73 mg (0.26 mmol) (*E,E*)-

1,7-(2-furoyl)-1,6-heptadiene, 4.7 mg (0.0063 mmol) Ru(bpy)<sub>3</sub>Cl<sub>2</sub>·6H<sub>2</sub>O, 50 μL (1.3

mmol) HCO<sub>2</sub>H, 447 μL *i*-Pr<sub>2</sub>NEt (2.6 mmol), 5.1 mL acetonitrile and irradiated for 4 h.

Purified by chromatography using 2:1 hexanes:EtOAc to yield 50 mg (0.18 mmol, 69%

yield) of the cycloadduct as a yellow oil. Experiment 2: Prepared according to general procedure A using 91 mg (0.32 mmol) (*E,E*)-1,7-(2-furoyl)-1,6-heptadiene, 6.0 mg (0.0080 mmol) Ru(bpy)<sub>3</sub>Cl<sub>2</sub>·6H<sub>2</sub>O, 61 μL (1.6 mmol) HCO<sub>2</sub>H, 552 μL *i*-Pr<sub>2</sub>NEt (3.2 mmol), 6.3 mL acetonitrile and irradiated for 4 h. Isolated 64 mg (0.22 mmol, 69% yield). IR (thin film) 1670, 1568, 1467; <sup>1</sup>H NMR (500 MHz, CDCl<sub>3</sub>) δ 7.57 (d, *J* = 1.3 Hz, 2H), 7.19 (d, *J* = 3.3 Hz, 2H), 6.53 (dd, *J* = 3.2, 2.1 Hz, 2H), 3.01 (dd, *J* = 15.6, 4.7 Hz, 2H), 2.79 (dd, *J* = 15.8, 8.7 Hz, 2H), 2.13 (m, 2H), 1.95 (m, 2H), 1.63 (m, 2H), 1.29 (m, 2H); <sup>13</sup>C NMR (125 MHz, CDCl<sub>3</sub>) δ 189.2, 152.9, 146.3, 117.1, 112.2, 43.5, 41.7, 32.2, 23.5; HRMS (ESI<sup>+</sup>) calc'd for [C<sub>17</sub>H<sub>18</sub>O<sub>4</sub>]<sup>+</sup> requires *m/z* 286.1200, found *m/z* 286.1192.

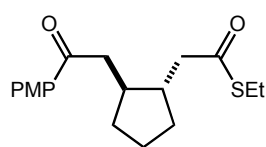


**1-((1S, 2S)-2-(2-(4-Methoxyphenyl)-2-oxoethyl)cyclopentyl)-3,3-dimethyl butan-2-one** (Table 3-2, entry 5, **3-46**). Experiment 1:

Prepared according to general procedure A using 75 mg (0.24 mmol) (2*E*,7*E*)-1-(4-methoxyphenyl)-10,10-dimethylundeca-2,7-diene-1,9-dione, 4.5 mg (0.0060 mmol) Ru(bpy)<sub>3</sub>Cl<sub>2</sub>·6H<sub>2</sub>O, 46 μL (1.2 mmol) HCO<sub>2</sub>H, 416 μL *i*-Pr<sub>2</sub>NEt (2.4 mmol), 4.8 mL acetonitrile and irradiated for 6 h. Purified by chromatography using 5:1 hexanes:EtOAc to yield 69 mg (0.22 mmol, 92% yield) of the cycloadduct as a clear oil. Experiment 2: Prepared according to general procedure A using 79 mg (0.25 mmol) (2*E*,7*E*)-1-(4-methoxyphenyl)-10,10-dimethylundeca-2,7-diene-1,9-dione, 5.0 mg (0.0067 mmol) Ru(bpy)<sub>3</sub>Cl<sub>2</sub>·6H<sub>2</sub>O, 49 μL (1.3 mmol) HCO<sub>2</sub>H, 443 μL *i*-Pr<sub>2</sub>NEt (2.5 mmol), 5.1 mL acetonitrile and irradiated for 6 h. Isolated 77 mg (0.24 mmol, 97% yield). IR (thin film) 1701, 1671, 1601; <sup>1</sup>H NMR (500 MHz, CDCl<sub>3</sub>) δ 7.94 (dt, *J* = 8.7, 2.0 Hz, 2H), 6.93 (dt, *J*



= 8.9, 1.9 Hz, 2H), 3.87 (s, 3H), 3.06 (dd,  $J$  = 16.1, 4.1 Hz, 1H), 2.85 (dd,  $J$  = 16.2, 8.7 Hz, 1H), 2.62 (dd,  $J$  = 17.8, 4.5 Hz, 1H), 2.52 (dd,  $J$  = 17.6, 8.3 Hz, 1H), 2.05 (m, 2H), 1.92 (m, 2H), 1.5 (m, 2H), 1.22 (m, 1H), 1.12 (s, 9H), 1.08 (m, 1H);  $^{13}\text{C}$  NMR (125 MHz,  $\text{CDCl}_3$ )  $\delta$  215.9, 198.9, 163.3, 130.3, 113.6, 55.4, 44.1, 43.6, 42.0, 41.5, 40.9, 32.6, 26.4, 23.7; HRMS ( $\text{ESI}^+$ ) calc'd for  $[\text{C}_{20}\text{H}_{29}\text{O}_3]^+$  requires  $m/z$  317.2112, found  $m/z$  317.2121.

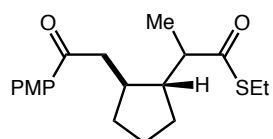


**S-Ethyl-2-((1S,2S)-2-(2-(4-methoxyphenyl)-2-oxoethyl)cyclopentyl)ethane thioate** (Table 3-2, entry 6, **3-47**). Experiment 1:

Prepared according to general procedure A using 141 mg (0.44 mmol) (2*E*,7*E*)-*S*-ethyl 9-(4-methoxyphenyl)-9-oxonona-2,7-dienethioate, 8.2 mg (0.0101 mmol)  $\text{Ru}(\text{bpy})_3\text{Cl}_2 \cdot 6\text{H}_2\text{O}$ , 79  $\mu\text{L}$  (2.1 mmol)  $\text{HCO}_2\text{H}$ , 766  $\mu\text{L}$  *i*- $\text{Pr}_2\text{NEt}$  (4.4 mmol), 9.0 mL acetonitrile and irradiated for 9 h. Purified by chromatography using 4:1 hexanes:ether to yield 113 mg (0.35 mmol, 80% yield) of the cycloadduct as a clear oil.

Experiment 2: Prepared according to general procedure A using 141 mg (0.44 mmol) (2*E*,7*E*)-*S*-ethyl 9-(4-methoxyphenyl)-9-oxonona-2,7-dienethioate, 8.2 mg (0.0101 mmol)  $\text{Ru}(\text{bpy})_3\text{Cl}_2 \cdot 6\text{H}_2\text{O}$ , 79  $\mu\text{L}$  (2.1 mmol)  $\text{HCO}_2\text{H}$ , 766  $\mu\text{L}$  *i*- $\text{Pr}_2\text{NEt}$  (4.4 mmol), 9.0 mL acetonitrile and irradiated for 9 h. Isolated 110 mg (0.34 mmol, 78% yield). IR (thin film) 1676, 1600, 1509;  $^1\text{H}$  NMR (500 MHz,  $\text{CDCl}_3$ )  $\delta$  7.94 (dt,  $J$  = 8.8, 3.0 Hz, 2H), 6.93 (dt,  $J$  = 8.9, 2.9 Hz, 2H), 3.87 (s, 3H), 3.09 (dd,  $J$  = 16.3, 4.4 Hz, 1H), 2.87 (q,  $J$  = 7.5 Hz, 2H), 2.82 (dd,  $J$  = 15.8, 8.8 Hz, 1H), 2.75 (dd,  $J$  = 14.7, 5.1 Hz, 1H), 2.49 (dd,  $J$  = 14.9, 8.7 Hz, 1H), 2.04 (m, 2H), 1.92 (m, 2H), 1.61 (m, 2H), 1.32 (m, 1H), 1.25 (m, 1H), 1.24 (t,

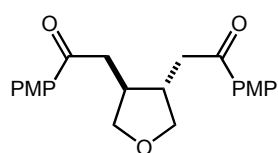
3H);  $^{13}\text{C}$  NMR (125 MHz,  $\text{CDCl}_3$ )  $\delta$  199.3, 198.5, 163.4, 130.4, 130.2, 113.7, 55.4, 49.0, 43.4, 42.8, 41.5, 32.3, 31.9, 23.5, 23.3, 14.7; HRMS ( $\text{ESI}^+$ ) calc'd for  $[\text{C}_{18}\text{H}_{24}\text{O}_3\text{SNa}]^+$  requires  $m/z$  343.1339, found  $m/z$  343.1342.



**(R)-S-Ethyl-2-((1R,2S)-2-(2-(4-methoxyphenyl)-2-oxoethyl)cyclopentyl) propanethioate** (Table 3-2, entry 7, **3-48**). Experiment 1:

Prepared according to general procedure A using 90 mg (0.27 mmol) (2*E*,7*E*)-*S*-ethyl 9-(4-methoxyphenyl)-2-methyl-9-oxonona-2,7-dienethioate, 5.1 mg (0.0068 mmol)  $\text{Ru}(\text{bpy})_3\text{Cl}_2 \cdot 6\text{H}_2\text{O}$ , 49  $\mu\text{L}$  (1.4 mmol)  $\text{HCO}_2\text{H}$ , 472  $\mu\text{L}$  *i*- $\text{Pr}_2\text{NEt}$  (2.7 mmol), 5 mL acetonitrile and irradiated for 12 h. Purified by chromatography using 4:1 hexanes:EtOAc to yield 68 mg (0.20 mmol, 75% yield) of the cycloadduct as an inseparable 1:1 mixture of diastereomers as a yellow oil. Experiment 2: Prepared according to general procedure A using 90 mg (0.27 mmol) (2*E*,7*E*)-*S*-ethyl 9-(4-methoxyphenyl)-2-methyl-9-oxonona-2,7-dienethioate, 5.1 mg (0.0068 mmol)  $\text{Ru}(\text{bpy})_3\text{Cl}_2 \cdot 6\text{H}_2\text{O}$ , 49  $\mu\text{L}$  (1.4 mmol)  $\text{HCO}_2\text{H}$ , 472  $\mu\text{L}$  *i*- $\text{Pr}_2\text{NEt}$  (2.7 mmol), 5 mL acetonitrile and irradiated for 12 h. Isolated 67 mg (0.20 mmol, 74% yield). IR (thin film) 2961, 1678, 1600, 1258;  $^1\text{H}$  NMR (500 MHz,  $\text{CDCl}_3$ )  $\delta$  7.92 (m,  $\text{H}_\text{A}$  = 2H,  $\text{H}_\text{B}$  = 2H), 6.91 (m,  $\text{H}_\text{A}$  = 2H,  $\text{H}_\text{B}$  = 2H), 3.87 (s,  $\text{H}_\text{A}$  = 3H), 3.86 (s,  $\text{H}_\text{B}$  = 3H), 3.14 (dd,  $J$  = 14.3, 3.3 Hz,  $\text{H}_\text{B}$  = 1H), 3.06 (dd,  $J$  = 15.8, 3.8 Hz,  $\text{H}_\text{A}$  = 1H), 2.91 (q,  $J$  = 7.5 Hz,  $\text{H}_\text{B}$  = 2H), 2.84 (q,  $J$  = 7.2 Hz,  $\text{H}_\text{A}$  = 2H), 2.76 (dd,  $J$  = 15.8, 9.9 Hz,  $\text{H}_\text{A}$  = 1H), 2.63 (m,  $\text{H}_\text{A}$  = 1H,  $\text{H}_\text{B}$  = 1H), 2.55 (m,  $\text{H}_\text{B}$  = 1H), 2.47 (dd,  $J$  = 14.0, 12.1 Hz,  $\text{H}_\text{B}$  = 1H), 2.24 (m,  $\text{H}_\text{A}$  = 1H,  $\text{H}_\text{B}$  = 1H), 2.17 (s,  $\text{H}_\text{A}$  = 3H,  $\text{H}_\text{B}$  = 3H), 1.98 (m,  $\text{H}_\text{A}$  = 1H), 1.87 (m,  $\text{H}_\text{A}$  = 2H), 1.8 (m,  $\text{H}_\text{B}$  = 2H), 1.56 (m,  $\text{H}_\text{B}$  = 2H), 1.24 (m,  $\text{H}_\text{A}$  = 3H,  $\text{H}_\text{B}$  = 6H), 1.16 (d,  $\text{H}_\text{A}$  = 3H);  $^{13}\text{C}$  NMR (125 MHz,

CDCl<sub>3</sub>) 203.8, 203.5, 199.0, 198.5, 163.3, 163.2, 130.5, 130.4, 113.6, 55.4, 52.2, 50.3, 48.3, 47.1, 44.3, 39.4, 37.9, 37.5, 32.6, 30.9, 30.3, 29.2, 27.7, 23.9, 23.1, 23.1, 21.4, 18.5, 15.0, 14.9, 14.7; HRMS (ESI<sup>+</sup>) calc'd for [C<sub>19</sub>H<sub>26</sub>O<sub>3</sub>SNa]<sup>+</sup> requires *m/z* 357.1495, found *m/z* 357.1483.



**2,2'-((3S,4S)-Tetrahydrofuran-3,4-diyl)bis(1-(4-methoxyphenyl)**

**ethanone)** (Table 3-2, entry 8, **3-49**). Experiment 1: Prepared

according to general procedure A using 92 mg (0.25 mmol)

(*2E,2'E*)-4,4'-oxybis(1-(4-methoxyphenyl)but-2-en-1-one), 4.8 mg (0.0064 mmol)

Ru(bpy)<sub>3</sub>Cl<sub>2</sub>·6H<sub>2</sub>O, 49 μL (1.3 mmol) HCO<sub>2</sub>H, 437 μL *i*-Pr<sub>2</sub>NEt (2.5 mmol), 5.0 mL

acetonitrile and irradiated for 3.5 h. Purified by chromatography using 1:1

hexanes:EtOAc to yield 85 mg (0.23 mmol, 92% yield) of the cycloadduct as a clear oil.

Experiment 2: Prepared according to general procedure A using 92 mg (0.25 mmol)

(*2E,2'E*)-4,4'-oxybis(1-(4-methoxyphenyl)but-2-en-1-one), 4.7 mg (0.0063 mmol)

Ru(bpy)<sub>3</sub>Cl<sub>2</sub>·6H<sub>2</sub>O, 49 μL (1.3 mmol) HCO<sub>2</sub>H, 437 μL *i*-Pr<sub>2</sub>NEt (2.5 mmol), 5.1 mL

acetonitrile and irradiated for 3.5 h. Isolated 87 mg (0.24 mmol, 94% yield). IR (thin film)

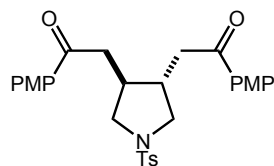
1669, 1601, 1508; <sup>1</sup>H NMR (500 MHz, CDCl<sub>3</sub>) δ 7.93 (dt, *J* = 9.0, 2.7 Hz, 4H), 6.93 (dt, *J*

= 9.2, 2.7 Hz, 4H), 4.15 (dd, *J* = 8.8, 6.7 Hz, 2H), 3.87 (s, 6H), 3.48 (dd, *J* = 8.8, 5.8 Hz,

2H), 3.31 (dd, *J* = 17.5, 5.1 Hz, 2H), 3.04 (dd, *J* = 17.4, 8.2 Hz, 2H), 2.54 (m, 2H); <sup>13</sup>C

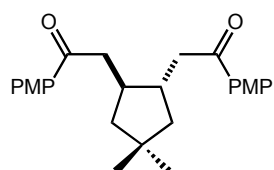
NMR (125 MHz, CDCl<sub>3</sub>) δ 197.6, 163.5, 130.3, 129.9, 113.7, 73.4, 55.5, 42.2, 40.8;

HRMS (ESI<sup>+</sup>) calc'd for [C<sub>22</sub>H<sub>24</sub>O<sub>5</sub>Na]<sup>+</sup> requires *m/z* 391.1516, found *m/z* 391.1527.



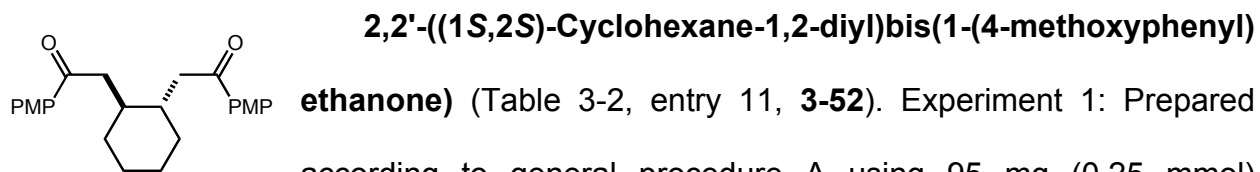
**2,2'-((3S,4S)-1-Tosylpyrrolidine-3,4-diyl)bis(1-(4-methoxyphenyl)ethanone)** (Table 3-2, entry 9, **3-50**). Experiment 1:

Prepared according to general procedure A using 74 mg (0.14 mmol) *N,N*-bis((*E*)-4-(4-methoxyphenyl)-4-oxobut-2-en-1-yl)-4-methyl benzene sulfonamide, 2.7 mg (0.0036 mmol) Ru(bpy)<sub>3</sub>Cl<sub>2</sub>·6H<sub>2</sub>O, 26 μL (0.7 mmol) HCO<sub>2</sub>H, 251 μL *i*-Pr<sub>2</sub>NEt (1.4 mmol), 2.8 mL acetonitrile and irradiated for 4 h. Purified by chromatography using 3:2 hexanes:EtOAc to yield 59 mg (0.11 mmol, 80% yield) of the cycloadduct as a yellow oil. Experiment 2: Prepared according to general procedure A using 77 mg (0.15 mmol) *N,N*-bis((*E*)-4-(4-methoxyphenyl)-4-oxobut-2-en-1-yl)-4-methyl benzenesulfonamide, 2.7 mg (0.0037 mmol) Ru(bpy)<sub>3</sub>Cl<sub>2</sub>·6H<sub>2</sub>O, 26 μL (0.7 mmol) HCO<sub>2</sub>H, 257 μL *i*-Pr<sub>2</sub>NEt (1.5 mmol), 2.9 mL acetonitrile and irradiated for 4 h. Isolated 66 mg (0.13 mmol, 86% yield). IR (thin film) 1673, 1600, 1259, 1160; <sup>1</sup>H NMR (500 MHz, CDCl<sub>3</sub>) δ 7.83 (dt, J = 9.3, 2.8 Hz, 4H), 7.70 (d, J = 8.5 Hz, 2H), 7.28 (d, J = 7.7 Hz, 2H), 6.91 (dt, J = 9.3, 3.2 Hz, 4H), 3.87 (s, 6H), 3.63 (dd, J = 2, 10.3, 6.9 Hz, 2H), 3.09 (dd, J = 17.5, 4.5 Hz, 2H), 2.94 (dd, J = 10.5, 6.6 Hz, 2H), 2.80 (dd, J = 17.8, 8.1 Hz, 2H), 2.47 (m, 2H), 2.39 (s, 3H); <sup>13</sup>C NMR (125 MHz, CDCl<sub>3</sub>) δ 196.7, 163.7, 143.5, 133.0, 130.2, 129.7, 129.6, 127.7, 113.8, 55.5, 52.9, 41.4, 39.4, 30.9, 21.5; HRMS (ESI<sup>+</sup>) calc'd for [C<sub>29</sub>H<sub>31</sub>NO<sub>6</sub>SN<sup>+</sup>]<sup>+</sup> requires *m/z* 544.1765, found *m/z* 544.1741. (mp = 128 °C (dec.)).



**2,2'-((1S,2S)-4,4-Dimethylcyclopentane-1,2-diyl)bis(1-(4-methoxyphenyl)ethanone)** (Table 3-2, entry 10, **3-51**).

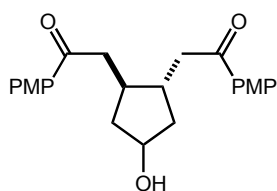
Experiment 1: Prepared according to general procedure A using 90 mg (0.23 mmol) (2*E*,7*E*)-1,9-bis(4-methoxyphenyl)-5,5-dimethylnona-2,7-diene-1,9-dione, 4.3 mg (0.0060 mmol) Ru(bpy)<sub>3</sub>Cl<sub>2</sub>·6H<sub>2</sub>O, 41 μL (1.2 mmol) HCO<sub>2</sub>H, 400 μL *i*-Pr<sub>2</sub>NEt (2.3 mmol), 4.6 mL acetonitrile and irradiated for 3 h. Purified by chromatography using 3:1 hexanes:EtOAc to yield 65 mg (0.16 mmol, 72% yield) of the cycloadduct as a white solid. Experiment 2: Prepared according to general procedure A using 92 mg (0.23 mmol) (2*E*,7*E*)-1,9-bis(4-methoxyphenyl)-5,5-dimethylnona-2,7-diene-1,9-dione, 4.4 mg (0.0058 mmol) Ru(bpy)<sub>3</sub>Cl<sub>2</sub>·6H<sub>2</sub>O, 42 μL (1.2 mmol) HCO<sub>2</sub>H, 406 μL *i*-Pr<sub>2</sub>NEt (2.3 mmol), 4.7 mL acetonitrile and irradiated for 3 h. Isolated 68 mg (0.17 mmol, 74% yield). IR (thin film) 1674, 1600, 1256; <sup>1</sup>H NMR (500 MHz, CDCl<sub>3</sub>) δ 7.92 (dt, *J* = 9.0, 2.0 Hz, 4H), 6.93 (dt, *J* = 8.9, 1.9 Hz, 4H), 3.87 (s, 6H), 3.11 (dd, *J* = 15.6, 4.5 Hz, 2H), 2.88 (dd, *J* = 16.1, 8.5 Hz, 2H), 2.33 (m, 2H), 1.82 (dd, *J* = 12.8, 6.9 Hz, 2H), 1.16 (dd, *J* = 13.0, 9.7 Hz, 2H), 1.02 (s, 6H); <sup>13</sup>C NMR (125 MHz, CDCl<sub>3</sub>) δ 198.9, 163.5, 130.3, 113.7, 55.3, 48.1, 43.4, 41.6, 37.2, 31.0; HRMS (ESI<sup>+</sup>) calc'd for [C<sub>19</sub>H<sub>26</sub>O<sub>3</sub>SN<sup>+</sup>Na]<sup>+</sup> requires *m/z* 417.2025, found *m/z* 417.2037. (mp = 102–109 °C).



(3*E*,9*E*)-1,12-bis(4-methoxyphenyl)dodeca-3,9-diene-1,12-dione, 4.7 mg (0.0063 mmol) Ru(bpy)<sub>3</sub>Cl<sub>2</sub>·6H<sub>2</sub>O, 49 μL (1.3 mmol) HCO<sub>2</sub>H, 437 μL *i*-Pr<sub>2</sub>NEt (2.5 mmol), 5.0 mL acetonitrile and irradiated for 6 h. Purified by chromatography using 3:1 hexanes:EtOAc

to yield 87 mg (0.23 mmol, 90% yield) of the cycloadduct as a white residue.

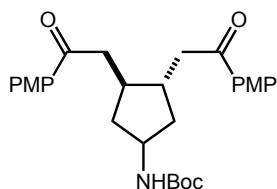
Experiment 2: Prepared according to general procedure A using 95 mg (0.25 mmol) (3*E*,9*E*)-1,12-bis(4-methoxyphenyl)dodeca-3,9-diene-1,12-dione, 4.8 mg (0.0064 mmol) Ru(bpy)<sub>3</sub>Cl<sub>2</sub>·6H<sub>2</sub>O, 49 μL (1.3 mmol) HCO<sub>2</sub>H, 437 μL *i*-Pr<sub>2</sub>NEt (2.5 mmol), 5.0 mL acetonitrile and irradiated for 6 h. Isolated 90 mg (0.23 mmol, 93% yield). IR (thin film) 1669, 1600, 1168; <sup>1</sup>H NMR (500 MHz, CDCl<sub>3</sub>) δ 7.91 (d, *J* = 8.5 Hz, 4H), 6.91 (d, *J* = 8.8 Hz, 4H), 3.86 (s, 6H), 3.01 (dd, *J* = 16.0, 3.8 Hz, 2H), 2.77 (dd, *J* = 16.0, 7.5 Hz, 2H), 1.97 (m, 2H), 1.76 (d, *J* = 13.3 Hz, 2H), 1.66 (m, 2H), 1.28 (m, 2H), 1.12 (m, 2H); <sup>13</sup>C NMR (125 MHz, CDCl<sub>3</sub>) δ 199.1, 163.3, 130.5, 130.4, 113.6, 55.4, 43.2, 39.1, 33.2, 26.0; HRMS (ESI<sup>+</sup>) calc'd for [C<sub>24</sub>H<sub>28</sub>O<sub>4</sub>Na]<sup>+</sup> requires *m/z* 403.1880, found *m/z* 403.1877.



**2,2'-((1*S*,2*S*)-4-Hydroxycyclopentane-1,2-diyl)bis(1-(4-methoxyphenyl)ethanone)** (Table 3-2, entry 12, **3-53**). Experiment 1:

Prepared according to general procedure A using 95 mg (0.25 mmol) (2*E*,7*E*)-5-hydroxy-1,9-bis(4-methoxyphenyl)nona-2,7-diene-1,9-dione, 4.7 mg (0.0063 mmol) Ru(bpy)<sub>3</sub>Cl<sub>2</sub>·6H<sub>2</sub>O, 50 μL (1.3 mmol) HCO<sub>2</sub>H, 446 μL *i*-Pr<sub>2</sub>NEt (1.3 mmol), 5.0 mL acetonitrile and irradiated for 5 h. Purified by chromatography using 2:3 hexanes:EtOAc to yield 73 mg (0.20 mmol, 76% yield) of the cycloadduct as a white solid. Experiment 2: Prepared according to general procedure A using 95 mg (0.25 mmol) (2*E*,7*E*)-5-Hydroxy-1,9-bis(4-methoxyphenyl)nona-2,7-diene-1,9-dione, 4.7 mg (0.0063 mmol) Ru(bpy)<sub>3</sub>Cl<sub>2</sub>·6H<sub>2</sub>O, 50 μL (1.3 mmol) HCO<sub>2</sub>H, 446 μL *i*-Pr<sub>2</sub>NEt (2.6

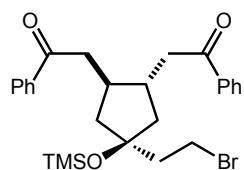
mmol), 5.0 mL acetonitrile and irradiated for 5 h. Isolated 69 mg (0.18 mmol, 72% yield). IR (thin film) 3442, 1664, 1616, 1258;  $^1\text{H}$  NMR (500 MHz,  $\text{CDCl}_3$ )  $\delta$  7.92 (t,  $J$  = 8.5 Hz, 4H), 6.91 (dd,  $J$  = 8.9, 3.6 Hz, 4H), 4.35 (s, 1H), 3.86 (s, 3H), 3.86 (s, 3H), 3.20 (dd,  $J$  = 33.7, 16.7 Hz, 1H), 3.19 (dd,  $J$  = 33.9, 16.8 Hz, 1H), 3.07 (dd,  $J$  = 16.8, 8.5 Hz, 1H), 2.88 (dd,  $J$  = 16.1, 8.5 Hz, 1H), 2.55 (m, 1H), 2.35 (m, 1H), 2.24 (m, 1H), 2.01 (m, 1H), 1.53 (m, 1H), 1.38 (m, 1H);  $^{13}\text{C}$  NMR (125 MHz,  $\text{CDCl}_3$ )  $\delta$  198.8, 198.5, 163.4, 163.4, 130.4, 130.2, 130.1, 113.7, 113.7, 72.5, 55.5, 43.8, 43.5, 42.8, 42.0, 40.0, 39.4; HRMS (ESI $^+$ ) calc'd for  $[\text{C}_{23}\text{H}_{26}\text{O}_5\text{Na}]^+$  requires  $m/z$  405.1656, found  $m/z$  405.1673. (mp = 88–93 °C).



***tert*-Butyl-((3*S*,4*S*)-3,4-bis(2-(4-methoxyphenyl)-2-oxoethyl)cyclopentyl) carbamate** (Table 3-2, entry 13, **3-54**). Experiment

1: Prepared according to general procedure A using 120 mg (0.25 mmol) *tert*-butyl ((2*E*,7*E*)-1,9-bis(4-methoxyphenyl)-1,9-dioxonona-2,7-dien-5-yl)carbamate, 4.7 mg (0.0063 mmol)  $\text{Ru}(\text{bpy})_3\text{Cl}_2 \cdot 6\text{H}_2\text{O}$ , 50  $\mu\text{L}$  (1.3 mmol)  $\text{HCO}_2\text{H}$ , 446  $\mu\text{L}$  *i*-Pr $_2\text{NEt}$  (1.3 mmol), 5.0 mL acetonitrile and irradiated for 3.5 h. Purified by chromatography using 3:2 hexanes:EtOAc to yield 111 mg (0.23 mmol, 92% yield) of the cycloadduct as a white solid. Experiment 2: Prepared according to general procedure A using 120 mg (0.25 mmol) *tert*-butyl ((2*E*,7*E*)-1,9-bis(4-methoxyphenyl)-1,9-dioxonona-2,7-dien-5-yl)carbamate, 4.7 mg (0.0063 mmol)  $\text{Ru}(\text{bpy})_3\text{Cl}_2 \cdot 6\text{H}_2\text{O}$ , 50  $\mu\text{L}$  (1.3 mmol)  $\text{HCO}_2\text{H}$ , 446  $\mu\text{L}$  *i*-Pr $_2\text{NEt}$  (2.6 mmol), 5.0 mL acetonitrile and irradiated for 3.5 h. Isolated 110 mg (0.23 mmol, 91% yield). IR (thin film) 3345, 1599, 1259, 1171;  $^1\text{H}$

NMR (500 MHz, CDCl<sub>3</sub>)  $\delta$  7.91 (d, *J* = 8.7 Hz, 4H), 6.92 (d, *J* = 9.1 Hz, 4H), 4.60 (m, 1H), 4.01 (m, 1H), 3.87 (s, 6H), 3.15 (ddd, *J* = 30.2, 15.9, 5.0 Hz, 2H), 2.92 (dd, *J* = 16.8, 8.4 Hz, 2H), 2.41 (m, 2H), 2.20 (m, 1H), 1.84 (m, 1H), 1.71 (m, 1H), 1.42 (s, 9H), 1.15 (m, 1H); <sup>13</sup>C NMR (125 MHz, CDCl<sub>3</sub>)  $\delta$  198.2, 198.2, 163.5, 130.3, 130.2, 113.7, 55.5, 43.4, 43.3, 40.3, 39.9, 39.2, 28.4; HRMS (ESI<sup>+</sup>) calc'd for [C<sub>28</sub>H<sub>35</sub>NO<sub>6</sub>]<sup>+</sup> requires *m/z* 482.2538, found *m/z* 482.2517. (mp = 107–111 °C).

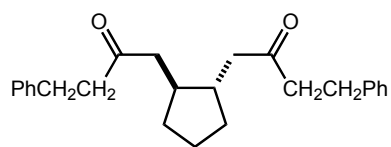


**2,2'-((1S,2S)-4-(2-Bromoethyl)-4-((trimethylsilyl)oxy)cyclopentane-1,2-diyl)bis (1-phenylethanone, 3-55)** (Table 3-2, entry 14). Experiment 1: Prepared according to general procedure A using

99 mg (0.20 mmol) (2*E*,7*E*)-5-(2-bromoethyl)-1,9-diphenyl-5-((trimethylsilyl)oxy)nona-2,7-diene-1,9-dione, 3.8 mg (0.0051 mmol) Ru(bpy)<sub>3</sub>Cl<sub>2</sub>·6H<sub>2</sub>O, 38  $\mu$ L (1.0 mmol) HCO<sub>2</sub>H, 345  $\mu$ L *i*-Pr<sub>2</sub>NEt (2.6 mmol), 4.0 mL acetonitrile and irradiated for 3 h. Purified by chromatography using 7:1 hexanes:EtOAc to yield 64 mg (0.13 mmol, 64% yield) of the cycloadduct as a yellow oil. Experiment 2: Prepared according to general procedure A using 120 mg (0.25 mmol) (2*E*,7*E*)-5-(2-bromoethyl)-1,9-diphenyl-5-((trimethylsilyl)oxy)nona-2,7-diene-1,9-dione, 4.1 mg (0.0055 mmol) Ru(bpy)<sub>3</sub>Cl<sub>2</sub>·6H<sub>2</sub>O, 43  $\mu$ L (1.1 mmol) HCO<sub>2</sub>H, 384  $\mu$ L *i*-Pr<sub>2</sub>NEt (2.2 mmol), 4.4 mL acetonitrile and irradiated for 3 h. Isolated 72 mg (0.14 mmol, 65% yield). IR (thin film) 1685, 1597, 1448, 1251 <sup>1</sup>H NMR (500 MHz, CDCl<sub>3</sub>)  $\delta$  7.94 (t, *J* = 7.0 Hz, 4H), 7.56 (m, 2H), 7.46 (m, 4H), 3.58 (m, 1H), 3.28 (m, 2H), 3.12 (dd, *J* = 16.9, 8.5 Hz, 1H), 2.95 (dd, *J* = 16.8, 9.0 Hz, 1H), 2.54 (m, 1H), 2.33 (m, 1H), 2.22 (dd, *J* = 11.8, 5.2 Hz, 1H), 21.2 (m, 1H), 2.02 (m, 2H), 1.56



(m, 1H), 1.31 (m, 2H), 0.15 (s, 1H);  $^{13}\text{C}$  NMR (125 MHz,  $\text{CDCl}_3$ )  $\delta$  200.1, 199.9, 137.3, 137.2, 133.3, 128.8, 128.3, 128.2, 83.3, 47.6, 46.8, 45.8, 44.9, 43.9, 40.9, 39.9, 39.9, 2.5; HRMS ( $\text{ESI}^+$ ) calc'd for  $[\text{C}_{26}\text{H}_{33}\text{BrO}_3\text{SiNa}]^+$  requires  $m/z$  523.1275, found  $m/z$  523.1291.



**1,1'-((1S,2S)-Cyclopentane-1,2-diyl)bis(4-phenylbutan-**

**2-one)** (Table 3-3, entry 1, **3-56**). Experiment 1: Prepared

according to general procedure A using 90 mg (0.25 mmol)

(4*E*,9*E*)-1,13-diphenyltrideca-4,9-diene-3,11-dione, 4.6 mg (0.0061 mmol)

$\text{Ru}(\text{bpy})_3\text{Cl}_2 \cdot 6\text{H}_2\text{O}$ , 48  $\mu\text{L}$  (1.3 mmol)  $\text{HCO}_2\text{H}$ , 435  $\mu\text{L}$  *i*- $\text{Pr}_2\text{NEt}$  (2.5 mmol), 5.0 mL

acetonitrile and irradiated for 36 h. Purified by chromatography using 4:1 hexanes:ether

to yield 85 mg (0.24 mmol, 94% yield) of the cycloadduct as a clear oil. Experiment 2:

Prepared according to general procedure A using 90 mg (0.25 mmol) (4*E*,9*E*)-1,13-

diphenyltrideca-4,9-diene-3,11-dione, 4.9 mg (0.0065 mmol)  $\text{Ru}(\text{bpy})_3\text{Cl}_2 \cdot 6\text{H}_2\text{O}$ , 48  $\mu\text{L}$

(1.3 mmol)  $\text{HCO}_2\text{H}$ , 435  $\mu\text{L}$  *i*- $\text{Pr}_2\text{NEt}$  (2.5 mmol), 5.0 mL acetonitrile and irradiated for 36

h. Isolated 83 mg (0.23 mmol, 92% yield). Experiment 3: Prepared according to general

procedure B using 90 mg (0.25 mmol) (4*E*,9*E*)-1,13-diphenyltrideca-4,9-diene-3,11-

dione, 5.8 mg (0.0063 mmol)  $[\text{Ir}(\text{ppy})_2(\text{dtb-bpy})][\text{PF}_6]$ , 48  $\mu\text{L}$  (1.3 mmol)  $\text{HCO}_2\text{H}$ , 435  $\mu\text{L}$

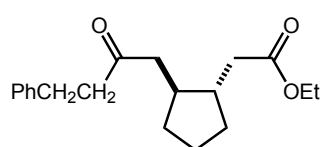
*i*- $\text{Pr}_2\text{NEt}$  (2.5 mmol), 5.0 mL acetonitrile and irradiated for 12 h. Isolated 84 mg (0.23

mmol, 93% yield). Experiment 4: Prepared according to general procedure B using 90

mg (0.25 mmol) (4*E*,9*E*)-1,13-diphenyltrideca-4,9-diene-3,11-dione, 5.8 mg (0.0063

mmol)  $[\text{Ir}(\text{ppy})_2(\text{dtb-bpy})][\text{PF}_6]$ , 48  $\mu\text{L}$  (1.3 mmol)  $\text{HCO}_2\text{H}$ , 435  $\mu\text{L}$  *i*- $\text{Pr}_2\text{NEt}$  (2.5 mmol),

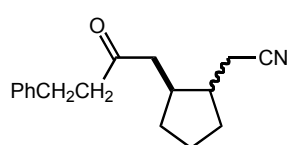
5.0 mL acetonitrile and irradiated for 12 h. Isolated 82 mg (0.23 mmol, 91% yield). IR (thin film) 1711, 1647;  $^1\text{H}$  NMR (500 MHz,  $\text{CDCl}_3$ )  $\delta$  7.27 (dt,  $J$  = 7.9, 1.7 Hz, 4H), 7.18 (m, 6H), 2.81 (t,  $J$  = 7.7 Hz, 4H), 2.7 (m, 4H), 2.49 (dd,  $J$  = 16.7, 4.3 Hz, 2H), 2.28 (dd,  $J$  = 16.5, 7.6 Hz, 2H), 1.84 (m, 4H), 1.54 (m, 2H), 1.1 (m, 2H);  $^{13}\text{C}$  NMR (125 MHz,  $\text{CDCl}_3$ )  $\delta$  209.9, 141.1, 128.4, 128.3, 126.1, 48.2, 44.6, 40.8, 32.3, 29.7, 23.5; HRMS (ESI $^+$ ) calc'd for  $[\text{C}_{25}\text{H}_{30}\text{O}_2]^+$  requires  $m/z$  362.2241, found  $m/z$  362.2238.



**Ethyl 2-((1S,2S)-2-(2-oxo-4-phenylbutyl)cyclopentyl)acetate**

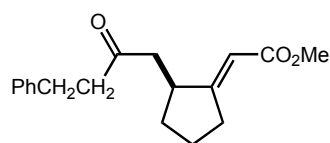
(Table 3-3, entry 3, **3-57**). Experiment 1: Prepared according to general procedure B using 99 mg (0.33 mmol) (2*E*,7*E*)-ethyl 9-oxo-11-phenylundeca-2,7-dienoate, 7.5 mg (0.0082 mmol)  $[\text{Ir}(\text{ppy})_2(\text{dtb-bpy})][\text{PF}_6]$ , 71  $\mu\text{L}$  (1.5 mmol)  $\text{HCO}_2\text{H}$ , 574  $\mu\text{L}$   $i\text{-Pr}_2\text{NEt}$  (3.3 mmol), 6.6 mL acetonitrile and irradiated for 24 h. Purified by chromatography using 9:1 hexanes:EtOAc to yield 76 mg (0.25 mmol, 77% yield) of the cycloadduct as a yellow oil. Experiment 2: Prepared according to general procedure B using 90 mg (0.30 mmol) (2*E*,7*E*)-ethyl 9-oxo-11-phenylundeca-2,7-dienoate, 6.8 mg (0.0074 mmol)  $[\text{Ir}(\text{ppy})_2(\text{dtb-bpy})][\text{PF}_6]$ , 54  $\mu\text{L}$  (1.4 mmol)  $\text{HCO}_2\text{H}$ , 519  $\mu\text{L}$   $i\text{-Pr}_2\text{NEt}$  (3.0 mmol), 6.0 mL acetonitrile and irradiated for 24 h. Isolated 69 mg (0.23 mmol, 76 % yield). IR (thin film) 2254, 1716, 1646;  $^1\text{H}$  NMR (500 MHz,  $\text{CDCl}_3$ )  $\delta$  7.27 (m, 2H), 7.19 (m, 3H), 4.11 (q,  $J$  = 7.0 Hz, 2H), 2.89 (m, 2H), 2.72 (m, 2H), 2.56 (dd,  $J$  = 15.4, 4.3 Hz, 1H), 2.41 (dd,  $J$  = 14.4, 6.9 Hz, 1H), 2.30 (dd,  $J$  = 14.9, 7.4 Hz, 1H), 1.89 (m, 4H), 1.58 (m, 2H), 1.25 (m, 4H), 1.13 (m, 1H);  $^{13}\text{C}$  NMR (125 MHz,  $\text{CDCl}_3$ )  $\delta$  209.7, 173.2, 141.1, 128.5, 128.3, 126.1, 60.2, 48.2, 44.6, 42.0, 40.8, 39.3, 32.3, 32.0,

29.8, 23.4; HRMS (ESI<sup>+</sup>) calc'd for [C<sub>19</sub>H<sub>26</sub>O<sub>3</sub>Na]<sup>+</sup> requires *m/z* 325.1775, found *m/z* 325.1769.



**2-((2S)-2-(2-Oxo-4-phenylbutyl)cyclopentyl)acetonitrile** (Table

3-3, entry 4, **3-58**). Experiment 1: Prepared according to general procedure B using 120 mg (0.47 mmol) (2*E*,7*E*)-9-oxo-11-phenylundeca-2,7-dienenitrile, 10.8 mg (0.0012 mmol) [Ir(ppy)<sub>2</sub>(dtb-bpy)][PF<sub>6</sub>], 85 μL (2.4 mmol) HCO<sub>2</sub>H, 824 μL *i*-Pr<sub>2</sub>NEt (4.7 mmol), 9.5 mL acetonitrile and irradiated for 9 h. Purified by chromatography using 4:1 hexanes:EtOAc to yield 97 mg (0.38 mmol, 80% yield) of the cycloadduct as an inseparable 1:1 mixture of diastereomers as a yellow oil. Experiment 2: Prepared according to general procedure B using 120 mg (0.47 mmol) (2*E*,7*E*)-9-oxo-11-phenylundeca-2,7-dienenitrile, 10.8 mg (0.0012 mmol) [Ir(ppy)<sub>2</sub>(dtb-bpy)][PF<sub>6</sub>], 85 μL (2.4 mmol) HCO<sub>2</sub>H, 824 μL *i*-Pr<sub>2</sub>NEt (4.7 mmol), 9.5 mL acetonitrile and irradiated for 9 h. Isolated 97 mg (0.38 mmol, 81 % yield). IR (thin film) 3027, 2953, 2244, 1712, 1453; <sup>1</sup>H NMR (500 MHz, CDCl<sub>3</sub>) δ 7.26 (m, 2H), 7.17 (m, 3H), 2.88 (m, 4H), 2.72 (m, 2H), 2.52 (dd, *J* = 17.1, 5.9 Hz, 1H), 2.38 (m, 2H), 2.26 (dd, *J* = 16.9, 7.7 Hz, 1H), 2.16 (dd, *J* = 16.4, 6.1 Hz, 1H), 2.01 (dd, *J* = 16.8, 8.3 Hz, 1H), 1.91 (m, 1H), 1.70 (m, 1H), 1.60 (m, 1H), 1.19 (m, 1H); <sup>13</sup>C NMR (125 MHz, CDCl<sub>3</sub>) δ 209.2, 208.9, 140.9, 140.9, 128.5, 128.3, 126.2, 126.1, 119.6, 119.2, 48.0, 44.4, 44.3, 43.5, 41.8, 40.1, 38.2, 37.5, 32.6, 32.0, 30.7, 30.3, 29.8, 23.5, 22.2, 21.8, 18.3; HRMS (ESI<sup>+</sup>) calc'd for [C<sub>17</sub>H<sub>21</sub>ONNa]<sup>+</sup> requires *m/z* 278.1516, found *m/z* 278.1517.



**(*S,E*)-Methyl-2-(2-(2-oxo-4-phenylbutyl)cyclopentylidene)**

**acetate** (Table 3-3, entry 5, **3-59**). Experiment 1: Prepared

according to general procedure B using 101 mg (0.36 mmol) (*E*)-methyl 9-oxo-11-phenylundec-7-en-2-ynoate, 8.2 mg (0.0090 mmol) [Ir(ppy)<sub>2</sub>(dtb-bpy)][PF<sub>6</sub>], 69 μL (1.8 mmol) HCO<sub>2</sub>H, 621 μL *i*-Pr<sub>2</sub>NEt (3.6 mmol), 7.1 mL acetonitrile and irradiated for 12 h. Purified by chromatography using 6:1 hexanes:EtOAc to yield 69 mg (0.24 mmol, 70% yield) of the cycloadduct as a clear oil. Experiment 2: Prepared according to general procedure B using 102 mg (0.36 mmol) bisenone, 8.2 mg (0.0090 mmol) [Ir(ppy)<sub>2</sub>(dtb-bpy)][PF<sub>6</sub>], 70 μL (1.8 mmol) HCO<sub>2</sub>H, 628 μL *i*-Pr<sub>2</sub>NEt (3.6 mmol), 7.2 mL acetonitrile and irradiated for 12 h. Isolated 68 mg (0.24 mmol, 66% yield). IR (thin film) 1712, 1650, 1201; <sup>1</sup>H NMR (500 MHz, CDCl<sub>3</sub>) δ 7.28 (t, *J* = 7.2 Hz, 2H), 7.19 (m, 3H), 5.61 (q, *J* = 2.3 Hz, 1H), 3.68 (s, 3H), 2.97 (m, 1H), 2.92 (t, *J* = 7.4 Hz, 3H), 2.74 (q, *J* = 7.7 Hz, 3H), 2.73 (m, 1H), 2.64 (dd, *J* = 17.0, 5.0 Hz, 1H), 2.44 (dd, *J* = 16.9, 8.5 Hz, 1H), 1.96 (m, 1H), 1.80 (m, 1H), 1.62 (m, 1H), 1.20 (m, 1H); <sup>13</sup>C NMR (125 MHz, CDCl<sub>3</sub>) δ 208.3, 171.1, 167.2, 140.8, 128.5, 128.3, 126.2, 111.1, 50.9, 47.0, 44.7, 41.7, 32.8, 32.2, 29.8, 24.1; HRMS (ESI<sup>+</sup>) calc'd for [C<sub>18</sub>H<sub>22</sub>O<sub>3</sub>]<sup>+</sup> requires *m/z* 286.1564, found *m/z* 286.1575.

**1-((3*S*)-4-benzyltetrahydrofuran-3-yl)-4-phenylbutan-2-one**

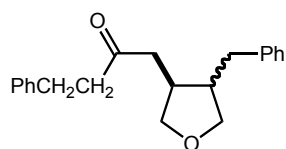
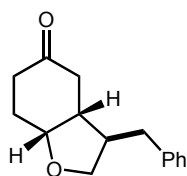


(Table 3-3, entry 6, **3-60**). Experiment 1: Prepared according to

general procedure B using 100 mg (0.32 mmol) (*E*)-6-(cinnamyloxy)-1-phenylhex-4-en-3-one, 7.5 mg (0.0082 mmol) [Ir(ppy)<sub>2</sub>(dtb-bpy)][PF<sub>6</sub>], 63 μL (1.6 mmol) HCO<sub>2</sub>H, 483 μL *i*-Pr<sub>2</sub>NEt (2.8 mmol), 6.5 mL acetonitrile and irradiated

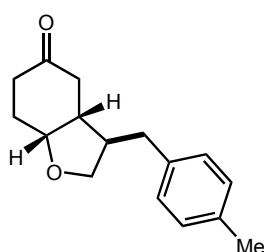
for 12 h. Purified by chromatography using 5:1 hexanes:EtOAc to yield 65 mg (0.21 mmol, 65% yield) of the cycloadduct as a clear oil. Experiment 2: Prepared according to general procedure B using 99 mg (0.32 mmol) (*E*)-6-(cinnamyloxy)-1-phenylhex-4-en-3-one, 7.5 mg (0.0082 mmol) [Ir(ppy)<sub>2</sub>(dtb-bpy)][PF<sub>6</sub>], 63  $\mu$ L (1.6 mmol) HCO<sub>2</sub>H, 483  $\mu$ L *i*-Pr<sub>2</sub>NEt (2.8 mmol), 6.5 mL acetonitrile and irradiated for 12 h. Isolated 63 mg (0.20 mmol, 63% yield). Major diastereomer: IR (thin film) 3027, 1713, 1453; <sup>1</sup>H NMR (500 MHz, CDCl<sub>3</sub>)  $\delta$  7.27 (m, 4H), 7.19 (m, 4H), 7.13 (d, *J* = 7.3 Hz, 2H), 3.97 (dd, *J* = 8.3, 6.9 Hz, 1H), 3.74 (dd, *J* = 8.1, 6.2 Hz, 1H), 3.51 (dd, *J* = 8.9, 5.5 Hz, 1H), 3.47 (dd, *J* = 8.2, 6.0 Hz, 1H), 2.89 (t, *J* = 7.7 Hz, 2H), 2.73 (m, 3H), 2.61 (m, 3H), 2.44 (m, 2H); <sup>13</sup>C NMR (125 MHz, CDCl<sub>3</sub>)  $\delta$  208.7, 140.8, 140.1, 128.6, 128.5, 128.3, 126.2, 72.7, 71.9, 44.5, 42.5, 41.2, 37.0, 33.9, 29.8; HRMS (ESI<sup>+</sup>) calc'd for [C<sub>21</sub>H<sub>24</sub>O<sub>2</sub>]<sup>+</sup> requires *m/z* 308.1771, found *m/z* 308.1757. Minor diastereomer: IR (thin film): 1710, 1603, 1495, 1453; <sup>1</sup>H NMR (500 MHz, CDCl<sub>3</sub>)  $\delta$  7.27 (m, 4H), 7.19 (m, 2H), 7.14 (m, 4H), 4.09 (dd, *J* = 8.7, 6.7 Hz, 1H), 3.82 (dd, *J* = 8.9, 7.2 Hz, 1H), 3.46 (dd, *J* = 8.6, 7.1 Hz, 1H), 3.32 (dd, *J* = 8.9, 5.8 Hz, 1H), 2.84 (t, *J* = 7.7 Hz, 2H), 2.75 (dd, *J* = 13.6, 6.6 Hz, 1H), 2.62 (m, 3H), 2.43 (m, 1H), 2.34 (m, 2H), 2.07 (m, 1H); <sup>13</sup>C NMR (125 MHz, CDCl<sub>3</sub>) 208.9, 140.8, 140.2, 128.7, 128.5, 128.3, 126.2, 126.2, 73.6, 72.8, 46.7, 46.6, 44.2, 40.1, 38.9, 29.7; HRMS (ESI<sup>+</sup>) calc'd for [C<sub>21</sub>H<sub>24</sub>O<sub>2</sub>]<sup>+</sup> requires *m/z* 308.1771, found *m/z* 308.1787.



**(3a*S*,7a*R*)-3-benzylhexahydrobenzofuran-5(6*H*)-one** (Table 3-3, entry 7, **3-61**). Experiment 1: Prepared according to general procedure B using 104 mg (0.46 mmol) 4-(cinnamyloxy)cyclohex-2-enone, 10.6 mg (0.011

mmol)  $[\text{Ir}(\text{ppy})_2(\text{dtb-bpy})][\text{PF}_6]$ , 88  $\mu\text{L}$  (2.3 mmol)  $\text{HCO}_2\text{H}$ , 794  $\mu\text{L}$   $i\text{-Pr}_2\text{NEt}$  (4.6 mmol), 9.1 mL acetonitrile and irradiated for 20 h. Purified by chromatography using 2:1 hexanes:EtOAc to yield 62 mg (0.27 mmol, 59% yield) of the cycloadduct as a clear oil.

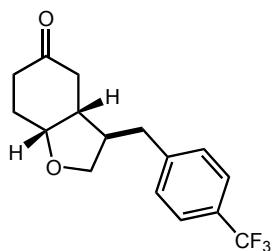
Experiment 2: Prepared according to general procedure B using 85 mg (0.37 mmol) 4-(cinnamyloxy)cyclohex-2-enone, 8.5 mg (0.0093 mmol)  $[\text{Ir}(\text{ppy})_2(\text{dtb-bpy})][\text{PF}_6]$ , 72  $\mu\text{L}$  (1.9 mmol)  $\text{HCO}_2\text{H}$ , 649  $\mu\text{L}$   $i\text{-Pr}_2\text{NEt}$  (3.7 mmol), 7.4 mL acetonitrile and irradiated for 20 h. Isolated 52 mg (0.22 mmol, 60% yield). IR (thin film): 2921, 1714;  $^1\text{H}$  NMR (500 MHz,  $\text{CDCl}_3$ )  $\delta$  7.29 (t,  $J$  = 7.4 Hz, 2H), 7.22 (d,  $J$  = 7.4 Hz, 1H), 7.13 (d,  $J$  = 6.9 Hz, 2H), 4.31 (m, 1H), 3.99 (dd,  $J$  = 8.9, 6.7 Hz, 1H), 3.41 (t,  $J$  = 8.8 Hz, 1H), 2.77 (dd,  $J$  = 13.5, 6.4 Hz, 1H), 2.65 (dd,  $J$  = 13.8, 8.5 Hz, 1H), 2.42 (ddd,  $J$  = 18.0, 10.8, 5.0 Hz, 1H), 2.34 (m, 2H), 2.19 (m, 2H), 2.09 (m, 2H), 2.01 (m, 1H);  $^{13}\text{C}$  NMR (125 MHz,  $\text{CDCl}_3$ ) 212.1, 139.5, 128.6, 128.5, 126.4, 75.6, 72.3, 48.5, 42.5, 41.5, 38.3, 34.6, 30.9, 26.4; HRMS ( $\text{EI}^+$ ) calc'd for  $[\text{C}_{15}\text{H}_{18}\text{O}_2]^+$  requires  $m/z$  230.1302, found  $m/z$  230.1392.



**(3a*S*,7a*R*)-3-(4-Methylbenzyl)hexahydrobenzofuran-5(6*H*)-one**

(Table 3-3, entry 8, **3-62**). Experiment 1: Prepared according to general procedure B using 90 mg (0.37 mmol) (*E*)-4-((3-(*p*-tolyl)allyl)oxy)cyclohex-2-enone, 8.5 mg (0.0093 mmol)  $[\text{Ir}(\text{ppy})_2(\text{dtb-bpy})][\text{PF}_6]$ , 72  $\mu\text{L}$  (1.9 mmol)  $\text{HCO}_2\text{H}$ , 647  $\mu\text{L}$   $i\text{-Pr}_2\text{NEt}$  (3.7 mmol), 7.4 mL acetonitrile and irradiated for 20 h. Purified by chromatography using 1:1 hexanes:EtOAc to yield 69 mg (0.28 mmol, 76% yield) of the cycloadduct as a yellow oil. Experiment 2: Prepared according to general procedure B using 85 mg (0.35 mmol)

(*E*)-4-((3-(*p*-tolyl)allyl)oxy)cyclohex-2-enone, 8.0 mg (0.0088 mmol) [Ir(ppy)<sub>2</sub>(dtb-bpy)][PF<sub>6</sub>], 68  $\mu$ L (1.8 mmol) HCO<sub>2</sub>H, 611  $\mu$ L *i*-Pr<sub>2</sub>NEt (3.5 mmol), 7.0 mL acetonitrile and irradiated for 20 h. Isolated 69 mg (0.28 mmol, 80% yield). IR (thin film) 2253, 908, 738, 651; <sup>1</sup>H NMR (500 MHz, CDCl<sub>3</sub>)  $\delta$  7.09 (d, *J* = 7.7 Hz, 2H), 7.02 (d, *J* = 7.9 Hz, 2H), 4.3 (m, 1H), 3.99 (dd, *J* = 8.9, 6.8 Hz, 1H), 3.40 (t, *J* = 8.6 Hz, 1H), 2.73 (dd, *J* = 13.7, 6.8 Hz, 1H), 2.61 (dd, *J* = 13.7, 8.5 Hz, 1H), 2.42 (m, 1H), 2.32 (s, 3H), 2.21 (m, 2H), 2.08 (m, 2H), 1.99 (m, 1H); <sup>13</sup>C NMR (125 MHz, CDCl<sub>3</sub>)  $\delta$  212.2, 136.4, 135.9, 129.3, 128.4, 75.6, 72.4, 48.6, 42.4, 41.6, 37.8, 34.6, 26.4, 21.0; HRMS (EI<sup>+</sup>) calc'd for [C<sub>16</sub>H<sub>20</sub>O<sub>2</sub>]<sup>+</sup> requires *m/z* 244.1458 found *m/z* 244.1446.

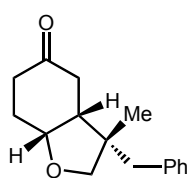


**(3a*S*,7a*R*)-3-(4-(Trifluoromethyl)benzyl)hexahydrobenzofuran-5(6*H*)-one** (Table 3-3, entry 9, **3-63**). Experiment 1: Prepared

according to general procedure B using 104 mg (0.35 mmol) (*E*)-4-((3-(4-(trifluoromethyl)phenyl)allyl)oxy)cyclohex-2-enone, 8.0 mg

(0.0088 mmol) [Ir(ppy)<sub>2</sub>(dtb-bpy)][PF<sub>6</sub>], 68  $\mu$ L (1.8 mmol) HCO<sub>2</sub>H, 611  $\mu$ L *i*-Pr<sub>2</sub>NEt (3.5 mmol), 7.0 mL acetonitrile and irradiated for 20 h. Purified by chromatography using 1:1 hexanes:EtOAc to yield 95 mg (0.32 mmol, 91% yield) of the cycloadduct as a clear oil. Experiment 2: Prepared according to general procedure B using 130 mg (0.43 mmol) (*E*)-4-((3-(4-(trifluoromethyl)phenyl)allyl)oxy)cyclohex-2-enone, 9.9 mg (0.011 mmol) [Ir(ppy)<sub>2</sub>(dtb-bpy)][PF<sub>6</sub>], 85  $\mu$ L (2.2 mmol) HCO<sub>2</sub>H, 764  $\mu$ L *i*-Pr<sub>2</sub>NEt (4.4 mmol), 8.8 mL acetonitrile and irradiated for 20 h. Isolated 121 mg (0.40 mmol, 92% yield). IR (thin film) 1715, 1325, 1116; <sup>1</sup>H NMR (500 MHz, CDCl<sub>3</sub>)  $\delta$  7.55 (d, *J* = 8.1 Hz, 2H), 7.25 (d, *J*

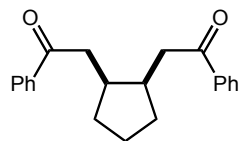
= 6.8 Hz, 2H), 4.32 (m, 1H), 3.97 (dd,  $J$  = 8.6, 6.6 Hz, 1H), 3.40 (t,  $J$  = 9 Hz, 1H), 2.86 (dd,  $J$  = 14.0, 6.5 Hz, 1H), 2.69 (dd,  $J$  = 13.8, 8.7 Hz, 1H), 2.39 (m, 3H), 2.22 (m, 2H), 2.10 (m, 2H), 2.01 (m, 1H);  $^{13}\text{C}$  NMR (125 MHz,  $\text{CDCl}_3$ )  $\delta$  211.7, 128.8, 125.6, 125.6, 75.6, 72.1, 48.2, 42.5, 41.5, 38.1, 34.5, 30.9, 26.3; HRMS ( $\text{EI}^+$ ) calc'd for  $[\text{C}_{16}\text{H}_{17}\text{F}_3\text{O}_2]^+$  requires  $m/z$  298.1176, found  $m/z$  298.1175.



**(3a*S*,7a*R*)-3-Benzyl-3-methylhexahydrobenzofuran-5(6*H*)-one** (Table

3-3, entry 10, **3-64**). Experiment 1: Prepared according to general procedure B using 91 mg (0.37 mmol) (*E*)-4-((2-methyl-3-phenylallyl)oxy)cyclohex-2-enone, 8.6 mg (0.0094 mmol)  $[\text{Ir}(\text{ppy})_2(\text{dtb-bpy})][\text{PF}_6]$ , 73  $\mu\text{L}$  (1.9 mmol)  $\text{HCO}_2\text{H}$ , 659  $\mu\text{L}$  *i*-Pr<sub>2</sub>NEt (3.7 mmol), 7.6 mL acetonitrile and irradiated for 24 h. Purified by chromatography using 2:1 hexanes:EtOAc to yield 68 mg (0.28 mmol, 73% yield) of the cycloadduct as an off-white solid. Experiment 2: Prepared according to general procedure B using 78 mg (0.32 mmol) (*E*)-4-((2-methyl-3-phenylallyl)oxy)cyclohex-2-enone, 7.6 mg (0.0083 mmol)  $[\text{Ir}(\text{ppy})_2(\text{dtb-bpy})][\text{PF}_6]$ , 63  $\mu\text{L}$  (1.6 mmol)  $\text{HCO}_2\text{H}$ , 564  $\mu\text{L}$  *i*-Pr<sub>2</sub>NEt (3.2 mmol), 6.5 mL acetonitrile and irradiated for 24 h. Isolated 58 mg (0.24 mmol, 73% yield). IR (thin film) 1642, 1447, 1250;  $^1\text{H}$  NMR (500 MHz,  $\text{CDCl}_3$ )  $\delta$  7.29 (m, 2H), 7.24 (m, 1H), 7.13 (d,  $J$  = 8.3 Hz, 2H), 4.4 (m, 1H), 3.68 (d,  $J$  = 8.8 Hz, 1H), 3.55 (d,  $J$  = 8.8 Hz, 1H), 2.71 (m, 2H), 2.45 (m, 1H), 2.38 (m, 1H), 2.27 (dd,  $J$  = 15.1, 9.4 Hz, 1H), 2.12 (m, 4H), 0.94 (s, 3H);  $^{13}\text{C}$  NMR (125 MHz,  $\text{CDCl}_3$ )  $\delta$  212.7, 137.9, 130.2, 128.2, 126.5, 46.9, 45.7, 44.1, 38.8, 34.7, 26.5, 19.4; HRMS ( $\text{EI}^+$ ) calc'd for  $[\text{C}_{16}\text{H}_{20}\text{O}_2]^+$  requires  $m/z$  244.1458, found  $m/z$  244.1458. (mp = 96–100 °C).





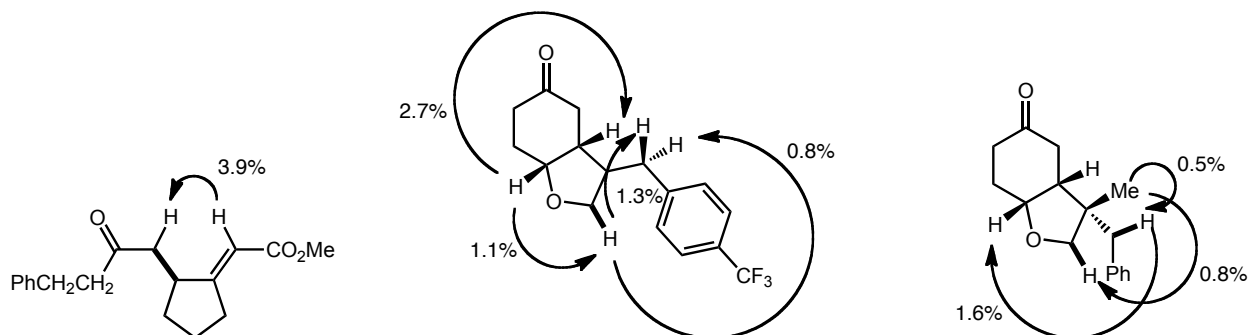
**2,2'-((1R,2S)-Cyclopentane-1,2-diyl)bis(1-phenylethanone) (3-38).**

A dry 25 mL Schlenk tube was charged with (1*R*,5*S*,6*R*,7*S*)-bicyclo[3.2.0]heptane-6,7-diylbis(phenylmethanone) (76 mg, 0.25 mmol), 4.7 mg (0.0063 mmol) Ru(bpy)<sub>3</sub>Cl<sub>2</sub>·6H<sub>2</sub>O, 45 μL (1.3 mmol) HCO<sub>2</sub>H, 436 μL *i*-Pr<sub>2</sub>NEt (2.5 mmol) and 5.0 mL acetonitrile and degassed in the dark using three freeze/pump/thaw cycles under nitrogen. The reaction was then stirred vigorously and irradiated with a 23 W (1380 lumen) compact fluorescent lamp for 2.5 h. The solvent was removed *in vacuo* and the residue purified by column chromatography on silica gel using 9:1 hexanes:EtOAc to yield 25 mg (0.08 mmol, 32% yield) of the cycloadduct as a yellow oil and 39 mg of the starting cycloadduct (0.13 mmol, 52% yield). IR (thin film) 2950, 1682, 1448; <sup>1</sup>H NMR (500 MHz, CDCl<sub>3</sub>) δ 7.94 (dd, *J* = 7.1, 1.4 Hz, 4H), 7.56 (dt, *J* = 7.4, 2.1 Hz, 2H), 7.46 (dt, *J* = 8.0, 1.6 Hz, 4H), 3.08 (dd, *J* = 15.4, 6.1 Hz, 2H), 2.80 (dd, *J* = 15.9, 7.9 Hz, 2H), 2.67 (m, 2H), 1.86 (m, 2H), 1.74 (m, 1H), 1.62 (m, 1H), 1.41 (m, 2H); <sup>13</sup>C NMR (125 MHz, CDCl<sub>3</sub>) δ 200.4, 137.0, 133.0, 128.6, 128.1, 39.6, 38.5, 30.7, 22.4; HRMS (ESI<sup>+</sup>) calc'd for [C<sub>21</sub>H<sub>22</sub>O<sub>2</sub>Na]<sup>+</sup> requires *m/z* 329.1512 found *m/z* 329.1501.

### 3.5.4 Stereochemical assignments

The stereochemistry of the major isomer of the reductive cyclization product in Table 3-2, entry 1 was established by single-crystal X-ray diffraction. The stereochemistry of the major isomers generated in Table 3-2, entries 2–14, and Table 3-3, entries 1–4, were assigned by analogy. NOE correlations were used to determine the

relative stereochemistry for the following compounds. Subsequent assignments were made by analogy.



### 3.6 References

1. a) Davies, D. I.; Parrott, M. J. *Free Radicals in Organic Synthesis*; Springer-Verlag: Germany, 1978. b) Giese, B. *Radicals in Organic Synthesis: Formation of Carbon–Carbon Bonds*; Pergamon Press: New York, 1986. c) Fossey, J.; Lefort, D.; Sorba, J. *Free Radicals in Organic Chemistry*; Wiley: New York, 1995. d) Zard, S. Z. *Radical Reactions in Organic Synthesis*; Oxford University Press: Oxford, 2003.
2. Hart, D. J. Free-Radical Carbon–Carbon Bond Formation in Organic Synthesis. *Science* **1984**, 223, 883-887.
3. a) Zeitler, K. Photoredox Catalysis with Visible Light. *Angew. Chem. Int. Ed.* **2009**, 48, 9785-9789. b) Yoon, T. P.; Ischay, M. A.; Du, J. Visible light photocatalysis as a greener approach to photochemical synthesis. *Nature Chem.* **2010**, 2, 527-532. c) Narayanam, J. M. R.; Stephenson, C. R. J. Visible light photoredox catalysis: applications in organic synthesis. *Chem. Soc. Rev.* **2011**, 40, 102-113.
4. Nicewicz, D. A.; MacMillan, D. W. C. Merging Photoredox Catalysis with Organocatalysis: The Direct Asymmetric Alkylation of Aldehydes. *Science* **2008**, 322, 77-80.
5. a) Nagib, D. A.; Scott, M. E.; MacMillan, D. W. C. Enantioselective  $\alpha$ -Trifluoromethylation of Aldehydes via Photoredox Organocatalysis. *J. Am. Chem. Soc.* **2009**, 131, 10875-10877. b) Shih, H.-W.; Vander Wal, M. N.; Grange, R. L.; MacMillan, D. W. C. Enantioselective  $\alpha$ -Benzylation of Aldehydes via Photoredox Organocatalysis. *J. Am. Chem. Soc.* **2010**, 132, 13600-13603. c) Pham, P. V.; Nagib, D. A.; MacMillan, D. W. C. Photoredox Catalysis: A Mild, Operationally Simple Approach to the Synthesis of  $\alpha$ -Trifluoromethyl Carbonyl Compounds. *Angew. Chem. Int. Ed.* **2011**, 50, 6119-6122.

6. Narayanam, J. M. R.; Tucker, J. W.; Stephenson, C. R. J. Electron-Transfer Photoredox Catalysis: Development of a Tin-Free Reductive Dehalogenation Reaction. *J. Am. Chem. Soc.* **2009**, *131*, 8756-8757.
7. a) Tucker, J. W.; Nguyen, J. D.; Narayanam, J. M. R.; Krabbe, S. W.; Stephenson, C. R. J. Tin-free radical cyclization reactions initiated by visible light photoredox catalysis. *Chem. Commun.* **2010**, *46*, 4985-4987. b) Furst, L.; Matsuura, B. S.; Narayanam, J. M. R.; Tucker, J. W.; Stephenson, C. R. J. Visible Light-Mediated Intermolecular C-H Functionalization of Electron-Rich Heterocycles with Malonates. *Org. Lett.* **2010**, *12*, 3104-3107. c) Condie, A. G.; González-Gómez, J. C.; Stephenson, C. R. J. Visible-Light Photoredox Catalysis: Aza-Henry Reactions via C-H Functionalization. *J. Am. Chem. Soc.* **2010**, *132*, 1464-1465. d) Nguyen, J. D.; Tucker, J. W.; Konieczynska, M. D.; Stephenson, C. R. J. Intermolecular Atom Transfer Radical Addition to Olefins Mediated by Oxidative Quenching of Photoredox Catalysts. *J. Am. Chem. Soc.* **2011**, *133*, 4160-4163.
8. a) Andrews, R. S.; Becker, J. J.; Gagné, M. R. Intermolecular Addition of Glycosyl Halides to Alkenes Mediated by Visible Light. *Angew. Chem. Int. Ed.* **2010**, *49*, 7274-7276. b) Andrews, R. S.; Becker, J. J.; Gagné, M. R. Investigating the Rate of Photoreductive Glucosyl Radical Generation. *Org. Lett.* **2011**, *13*, 2406-2409. c) Andrews, R. S.; Becker, J. J.; Gagné, M. R. A Photoflow Reactor for the Continuous Photoredox-Mediated Synthesis of C-Glycoamino Acids and C-Glycolipids. *Angew. Chem. Int. Ed.* **2012**, *51*, 4140-4143.
9. a) Ischay, M. A.; Anzovino, M. E.; Du, J.; Yoon, T. P. Efficient Visible Light Photocatalysis of [2+2] Enone Cycloadditions. *J. Am. Chem. Soc.* **2008**, *130*, 12886-12887. b) Du, J.; Yoon, T. P. Crossed Intermolecular [2+2] Cycloadditions of Acyclic Enones via Visible Light Photocatalysis. *J. Am. Chem. Soc.* **2009**, *131*, 14604-14605.
10. a) Dalko, P. I. Redox induced radical and radical ionic carbon-carbon bond forming reactions. *Tetrahedron* **1995**, *51*, 7579-7653. b) Schmittel, M.; Burghart, A. Understanding Reactivity Patterns of Radical Cations. *Angew. Chem. Int. Ed.* **1997**, *36*, 2550-2589. c) Sperry, J. B.; Wright, D. L. The application of cathodic reductions and anodic oxidations in the synthesis of complex molecules. *Chem. Soc. Rev.* **2006**, *35*, 605-621.
11. a) Enholm, E. J.; Kinter, K. S. Free radical cyclizations promoted by allylic O-stannyl ketyls: the intramolecular coupling of the  $\beta$ -carbons of activated alkenes. *J. Am. Chem. Soc.* **1991**, *113*, 7784-7785. b) Enholm, E. J.; Xie, Y.; Abboud, K. A. Free Radical Approach to Directed Aldol-Type Reactions Promoted by Allylic O-Stannyl Ketyls. *J. Org. Chem.* **1995**, *60*, 1112-1113. c) Enholm, E. J.; Kinter, K. S. Cyclization Reactions of Allylic O-Stannyl Ketyls. *J. Org. Chem.* **1995**, *60*, 4850-4855. d) Hays, D. S.; Fu, G. C. Organotin Hydride Catalyzed Carbon-Carbon Bond Formation: Radical-Mediated Reductive Cyclization of Enals and Enones. *J. Org. Chem.* **1996**, *61*, 4-5. e) Savchenko, A. V.; Montgomery, J. Organozinc/Nickel(0)-Promoted Cyclizations of Bis-Enones. *J. Org. Chem.* **1996**, *61*, 1562-1563. f) Montgomery, J.; Oblinger, E.; Savchenko, A. V.

Nickel-Catalyzed Organozinc-Promoted Carbocyclizations of Electron-Deficient Alkenes with Tethered Unsaturation. *J. Am. Chem. Soc.* **1997**, *119*, 4911-4920.

12. Krische observed reductive cyclization products as components of complex mixtures upon electrochemical reduction of aromatic bis(enone)s. See ref 11.

13. a) Baik, T.-G.; Luis, A. L.; Wang, L.-C.; Krische, M. J. A Diastereoselective Metal-Catalyzed [2+2] Cycloaddition of Bis-enones. *J. Am. Chem. Soc.* **2001**, *123*, 6716-6717. b) Roh, Y.; Jang, H.-Y.; Lynch, V.; Bauld, N. L.; Krische, M. J. Anion Radical Chain Cycloaddition of Tethered Enones: Intramolecular Cyclobutanation and Diels-Alder Cycloaddition. *Org. Lett.* **2002**, *4*, 611-613. c) Yang, J.; Felton, G. A. N.; Bauld, N. L.; Krische, M. J. Chemically Induced Anion Radical Cycloadditions: Intramolecular Cyclobutanation of Bis(enones) via Homogeneous Electron Transfer. *J. Am. Chem. Soc.* **2004**, *126*, 1634-1635.

14. a) Pandey, G.; Hajra, S. A Novel Photosystem for Harvesting Visible Light to Drive Photoinduced Electron Transfer (PET) Reductions:  $\beta$ -Activation of  $\alpha$ ,  $\beta$ -Unsaturated Ketones for Radical Cyclizations. *Angew. Chem. Int. Ed.* **1994**, *33*, 1169-1171. b) Pandey, G.; Hajra, S.; Ghorai, M. K.; Kumar, K. R. Designing Photosystems for Harvesting Photons into Electrons by Sequential Electron-Transfer Processes: Reversing the Reactivity Profiles of  $\alpha,\beta$ -Unsaturated Ketones as Carbon Radical Precursor by One Electron Reductive  $\beta$ -Activation. *J. Am. Chem. Soc.* **1997**, *119*, 8777-8787. c) Pandey, G.; Ghorai, M. K.; Hajra, S. A new strategy for the construction of carbo- and oxycycles by intramolecular reductive coupling of  $\alpha,\beta$ -unsaturated esters. *Tetrahedron Lett.* **1998**, *39*, 1831-1834. d) Pandey, G.; Hajra, S.; Ghorai, M. K.; Kumar, K. R. Visible Light Initiated Photosensitized Electron Transfer Cyclizations of Aldehydes and Ketones to Tethered  $\alpha,\beta$ -Unsaturated Esters: Stereoselective Synthesis of Optically Pure C-Furanosides†. *J. Org. Chem.* **1997**, *62*, 5966-5973.

15. For an overview of the photophysical properties of Ru(bpy)<sub>3</sub><sup>2+</sup>, see: Kalyanasundaram, K. Photophysics, photochemistry and solar energy conversion with tris(bipyridyl)ruthenium(II) and its analogues. *Coord. Chem. Rev.* **1982**, *46*, 159-244.

16. For the photophysical properties of DCA, see: Gould, I. R.; Ege, D.; Moser, J. E.; Farid, S. Efficiencies of photoinduced electron-transfer reactions: role of the Marcus inverted region in return electron transfer within geminate radical-ion pairs. *J. Am. Chem. Soc.* **1990**, *112*, 4290-4301.

17. House, H. O.; Huber, L. E.; Umen, M. J. Empirical rules for estimating the reduction potential of  $\alpha,\beta$ -unsaturated carbonyl compounds. *J. Am. Chem. Soc.* **1972**, *94*, 8471-8475.

18. Slinker, J. D.; Gorodetsky, A. A.; Lowry, M. S.; Wang, J.; Parker, S.; Rohl, R., et al. Efficient Yellow Electroluminescence from a Single Layer of a Cyclometalated Iridium Complex. *J. Am. Chem. Soc.* **2004**, *126*, 2763-2767.

19. a) Pandey, G.; Reddy, P. Y.; Bhalerao, U. T. Regiocontrolled set promoted photocyclisation of 2-alkyl-1-piperidine and pyrrolidine propanols: stereoselective synthesis of cis- $\alpha, \alpha'$ -dialkyl piperidines and pyrrolidines via tetrahydro-1,3-oxazines. *Tetrahedron Lett.* **1991**, 32, 5147-5150. b) Allen, J. M.; Lambert, T. H. Tropylium Ion Mediated  $\alpha$ -Cyanation of Amines. *J. Am. Chem. Soc.* **2011**, 133, 1260-1262.
20. Pangborn, A. B.; Giardello, M. A.; Grubbs, R. H.; Rosen, R. K.; Timmers, F. J. Safe and Convenient Procedure for Solvent Purification. *Organometallics* **1996**, 15, 1518-1520.
21. Still, W. C.; Kahn, M.; Mitra, A. Rapid chromatographic technique for preparative separations with moderate resolution. *J. Org. Chem.* **1978**, 43, 2923-2925.
22. Jang, H.-Y.; Huddleston, R. R.; Krische, M. J. Reductive Generation of Enolates from Enones Using Elemental Hydrogen: Catalytic C-C Bond Formation under Hydrogenative Conditions. *J. Am. Chem. Soc.* **2002**, 124, 15156-15157.
23. Ohkuma, T.; Sandoval, C. A.; Srinivasan, R.; Lin, Q.; Wei, Y.; Muñiz, K., et al. Asymmetric Hydrogenation of tert-Alkyl Ketones. *J. Am. Chem. Soc.* **2005**, 127, 8288-8289.
24. Keck, G. E.; Boden, E. P.; Mabury, S. A. A useful Wittig reagent for the stereoselective synthesis of trans- $\alpha, \beta$ -unsaturated thiol esters. *J. Org. Chem.* **1985**, 50, 709-710.
25. Lévesque, F. o.; Bélanger, G. A Versatile Cascade of Intramolecular Vilsmeier-Haack and Azomethine Ylide 1,3-Dipolar Cycloaddition toward Tricyclic Cores of Alkaloids†. *Org. Lett.* **2008**, 10, 4939-4942.
26. Montgomery, J.; Savchenko, A. V.; Zhao, Y. Convenient preparation of bis-enones and bis-enoates from cycloalkenes. *J. Org. Chem.* **1995**, 60, 5699-5701.
27. Terada, Y.; Arisawa, M.; Nishida, A. Cycloisomerization Promoted by the Combination of a Ruthenium-Carbene Catalyst and Trimethylsilyl Vinyl Ether, and its Application in The Synthesis of Heterocyclic Compounds: 3-Methylene-2,3-dihydroindoles and 3-Methylene-2,3-dihydrobenzofurans. *Angew. Chem. Int. Ed.* **2004**, 43, 4063-4067.
28. Chandler, C. L.; List, B. Catalytic, Asymmetric Transannular Aldolizations: Total Synthesis of (+)-Hirsutene. *J. Am. Chem. Soc.* **2008**, 130, 6737-6739.
29. Austin, K. A. B.; Banwell, M. G.; Willis, A. C. A Formal Total Synthesis of Platencin. *Org. Lett.* **2008**, 10, 4465-4468.

30. Kawai, A.; Hara, O.; Hamada, Y.; Shioiri, T. Stereoselective synthesis of the hydroxy amino acid moiety of Al-77-B, a gastroprotective substance from *Bacillus pumilus* Al-77. *Tetrahedron Lett.* **1988**, *29*, 6331-6334.
31. Ma, S.; Ni, B. Double Ring-Closing Metathesis Reaction of Nitrogen-Containing Tetraenes: Efficient Construction of Bicyclic Alkaloid Skeletons and Synthetic Application to Four Stereoisomers of Lupinine and Their Derivatives. *Chem. Eur. J.* **2004**, *10*, 3286-3300.
32. Wei, Y.-J.; Ren, H.; Wang, J.-X. Solvent- and catalyst-free gem-bisallylation of carboxylic acid derivatives with allylzinc bromide. *Tetrahedron Lett.* **2008**, *49*, 5697-5699.
33. Scholl, M.; Ding, S.; Lee, C. W.; Grubbs, R. H. Synthesis and Activity of a New Generation of Ruthenium-Based Olefin Metathesis Catalysts Coordinated with 1,3-Dimesityl-4,5-dihydroimidazol-2-ylidene Ligands. *Org. Lett.* **1999**, *1*, 953-956.
34. Randl, S.; Connon, S. J.; Blechert, S. Ring opening-cross metathesis of unstrained cycloalkenes. *Chem. Commun.* **2001**, 1796-1797.
35. Moreau, C.; Rouessac, F.; Conia, J. M. La thermocyclisation des alcenylphenols. *Tetrahedron Lett.* **1970**, *11*, 3527-3528.
36. Fleming, F. F.; Gudipati, S.; Vu, V. A.; Mycka, R. J.; Knochel, P. Grignard Reagents: Alkoxide-Directed Iodine-Magnesium Exchange at sp<sup>3</sup> Centers. *Org. Lett.* **2007**, *9*, 4507-4509.
37. Frigerio, M.; Santagostino, M.; Sputore, S. A User-Friendly Entry to 2-Iodoxybenzoic Acid (IBX). *J. Org. Chem.* **1999**, *64*, 4537-4538.
38. Marino, J. P.; Nguyen, H. N. Electrotelluration: A New Approach to Tri- and Tetrasubstituted Alkenes. *J. Org. Chem.* **2002**, *67*, 6291-6296.
39. Li, G.-Y.; Che, C.-M. Highly Selective Intra- and Intermolecular Coupling Reactions of Diazo Compounds to Form cis-Alkenes Using a Ruthenium Porphyrin Catalyst. *Org. Lett.* **2004**, *6*, 1621-1623.
40. Suzuki, H.; Yamazaki, N.; Kibayashi, C. Enantioselective Synthesis of (R)- and (S)-4-Benzyloxy-2-cyclohexen-1-one. *J. Org. Chem.* **2001**, *66*, 1494-1496.
41. O'Byrne, A.; Murray, C.; Keegan, D.; Palacio, C.; Evans, P.; Morgan, B. S. The thio-adduct facilitated, enzymatic kinetic resolution of 4-hydroxycyclopentenone and 4-hydroxycyclohexenone. *Organic & Biomolecular Chemistry* **2010**, *8*, 539-545.
42. Rai, G.; Sayed, A. A.; Lea, W. A.; Luecke, H. F.; Chakrapani, H.; Prast-Nielsen, S., et al. Structure Mechanism Insights and the Role of Nitric Oxide Donation Guide the

Development of Oxadiazole-2-Oxides as Therapeutic Agents against Schistosomiasis. *J. Med. Chem.* **2009**, 52, 6474-6483.

43. Kim, D. D.; Lee, S. J.; Beak, P. Asymmetric Lithiation–Substitution Sequences of Substituted Allylamines. *J. Org. Chem.* **2005**, 70, 5376-5386.

44. van Zijl, A. W.; Arnold, L. A.; Minnaard, A. J.; Feringa, B. L. Highly Enantioselective Copper-Catalyzed Allylic Alkylation with Phosphoramidite Ligands. *Adv. Synth. Catal.* **2004**, 346, 413-420.

**Chapter 4. Chiral Lewis Acids in Visible Light Photocatalysis:  
Enantioselective [2+2] Cycloadditions**



## 4.1 Introduction

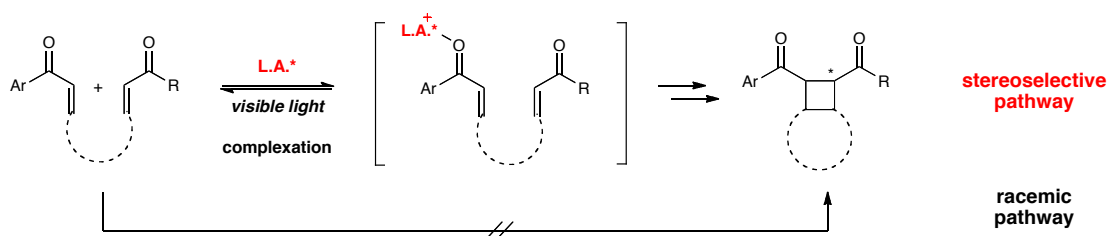
Enantioselective photochemical reactions are inherently more challenging than their thermal counterparts. The UV irradiation necessary for the majority of organic photoreactions is unable to differentiate between free substrate and substrate bound in a chiral environment. As a result, all substrate molecules are excited uniformly and the racemic reaction always occurs competitively with the stereoselective process. An ideal asymmetric photochemical method should therefore involve selective photoactivation of the catalyst-substrate complex under conditions in which the free substrate is photochemically inert (i.e., in which the rate of the racemic pathway is insignificant).

One possible solution to this problem would be to utilize visible light instead of UV light.<sup>1</sup> Because organic molecules are generally transparent to the wavelengths of visible light, this approach circumvents the direct photoexcitation of any substrate complex in solution. It may, therefore, be possible to selectively engage the catalyst-bound substrate in a stereoselective reaction.

According to this design principle, our visible light protocol for the Lewis acid-mediated [2+2] cycloaddition of enones is uniquely suited for this strategy (Scheme 4-1). Based on its necessity in the [2+2] cycloaddition, we hypothesize that the Lewis acid should be involved in the transition state for the stereochemistry-determining step of the cycloaddition. This suggests that reduction of the enone in the presence of a chiral Lewis acid should generate the key radical anion intermediate in an asymmetric environment that could relay stereochemical information to the subsequent carbon–carbon bond-forming steps. Since no reaction occurs in the absence of a Lewis acid,

the racemic pathway should be effectively disabled when a chiral Lewis acid is employed.

**Scheme 4-1.** Design of chiral Lewis acid-mediated [2+2] asymmetric photocycloaddition promoted by visible light



Given the small number of useful methods for enantioselective [2+2] cycloadditions,<sup>2</sup> the development of an asymmetric variant of this transformation should be of significant synthetic interest. A protocol requiring a stoichiometric amount of the chiral controller would be of synthetic value due to the difficulty of constructing this chiral motif; a method that uses a catalytic amount of chiral Lewis acid would obviously be more attractive. In addition, this chiral Lewis acid-mediated approach to asymmetric photocatalysis could potentially serve as a general platform for the design of efficient enantioselective photocatalytic processes.

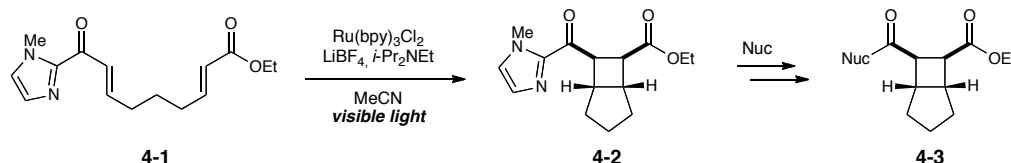
## 4.2 Results and Discussion

### 4.2.1 Lewis acid and ligand screening of intramolecular [2+2] cycloaddition

We began our studies toward the development of an enantioselective Lewis acid-mediated photochemical method by studying the intramolecular [2+2] cycloaddition of 2-acylimidazole **4-1** (Scheme 4-2). Acyl imidazole **4-1** is an attractive substrate for several reasons. First, previous work in our group has shown that **4-1** readily undergoes

[2+2] cycloaddition to afford **4-2** upon irradiation with visible light in the presence of  $\text{Ru}(\text{bpy})_3^{2+}$ ; optimized conditions have been identified for this transformation.

**Scheme 4-2.** Photocatalytic intramolecular [2+2] cycloadditions of acyl imidazole **4-1**

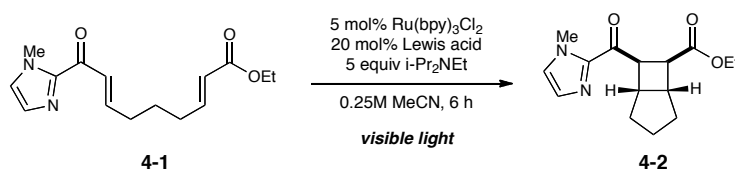


In addition, the 2-acyl imidazole moiety is a common motif in highly enantioselective reactions. This structure has been shown to chelate effectively to metal bis(oxazoline) complexes and can provide good levels of enantioselectivity in a range of cycloaddition<sup>3</sup> and conjugate addition reactions.<sup>4</sup> Because bidentate chelation has been extensively exploited as a design element in a variety of asymmetric catalytic transformations for its ability to provide high levels of transition state organization, we reasoned that these types of substrates might also be advantageous for our reaction. The acyl imidazole is also a versatile motif for diversification; it can be easily transformed into a range of useful carbonyl derivatives (**4-3**), including esters, acids, amides, aldehydes, and ketones upon reaction with an appropriate nucleophile. These conditions can be applied to the cycloadducts produced in our methodology,<sup>5</sup> thereby enabling the construction of cyclobutane structures that are not directly accessible from cycloaddition of the corresponding  $\alpha,\beta$ -unsaturated carbonyl compounds.

We first set out to probe the feasibility of a catalytic method for the enantioselective [2+2] cycloaddition by investigating whether sub-stoichiometric amounts of Lewis acid are sufficient to promote the intramolecular reaction (Table 4-1).

Experiments probing the effect of different Lewis acids at 20 mol% percent revealed that turnover could be achieved with several different Lewis acids. The observation that a variety of metal centers showed turnover was promising because it indicated that catalyst structures based upon the identity of many different metals might be potential candidates for the asymmetric transformation.

**Table 4-1.** Cycloaddition of imidazole **4-1** with 20 mol% Lewis acid



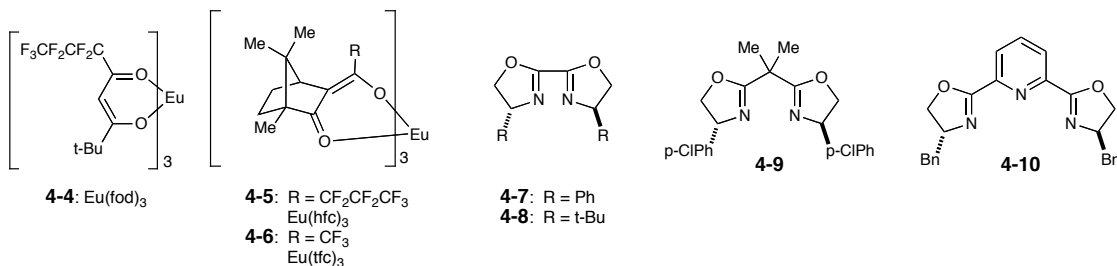
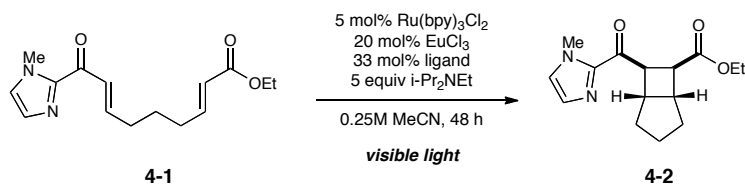
| entry | Lewis acid                         | yield <sup>a</sup> | d.r. <sup>a</sup> |
|-------|------------------------------------|--------------------|-------------------|
| 1     | LiBF <sub>4</sub>                  | 90%                | >10:1             |
| 2     | Mg(ClO <sub>4</sub> ) <sub>2</sub> | 56%                | >10:1             |
| 3     | Zn(OTf) <sub>2</sub>               | <5%                | --                |
| 4     | Sn(OTf) <sub>2</sub>               | <5%                | --                |
| 5     | La(OTf) <sub>3</sub>               | 38%                | >10:1             |
| 6     | Yb(OTf) <sub>3</sub>               | 42%                | >10:1             |

<sup>a</sup> Yields and diastereomer ratios were determined by <sup>1</sup>H NMR analysis against 1,4-bis(trimethylsilyl)benzene as an internal standard.

This study indicated that lanthanides are competent promoters of the [2+2] cycloaddition. Because the structure of the Lewis acid can be modified without affecting the photophysical properties of the Ru(bpy)<sub>3</sub><sup>2+</sup> photocatalyst, we wondered whether we could obtain an early proof-of-principle by employing commercially available chiral shift reagents<sup>6</sup> as the Lewis acid (Table 4-2). From a small screen of camphor-based europium complexes, we discovered that Eu(hfc)<sub>3</sub> afforded the cyclobutane product **4-2**

with modest but statistically significant levels of enantioselectivity (entry 2). These results, in combination with a brief survey of chiral europium–bis(oxazoline) ligands,<sup>7</sup> provided early validation for the viability of our approach; the observed enantioinduction verifies the participation of the Lewis acid in the stereodetermining bond-forming steps of the cycloaddition.

**Table 4-2.** Cycloaddition of imidazole **4-1** with sub-stoichiometric amounts of chiral Lewis acid



| entry          | ligand      | % conversion <sup>a</sup> | d.r. <sup>a</sup> | % ee <sup>b</sup> |
|----------------|-------------|---------------------------|-------------------|-------------------|
| 1 <sup>c</sup> | <b>4-4</b>  | 100                       | >10:1             | --                |
| 2 <sup>c</sup> | <b>4-5</b>  | 97                        | 5:1               | 9/--              |
| 3 <sup>c</sup> | <b>4-6</b>  | 100                       | 6:1               | 0/--              |
| 4              | <b>4-7</b>  | 89                        | 4:1               | 6/20              |
| 5              | <b>4-8</b>  | 84                        | 5:1               | 6/50              |
| 6              | <b>4-9</b>  | 74                        | 5:1               | 13/30             |
| 7              | <b>4-10</b> | 90                        | 4:1               | 4/53              |

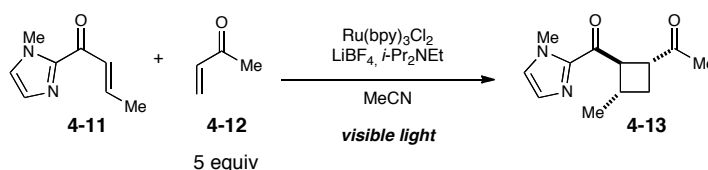
<sup>a</sup> Conversions and diastereomer ratios were determined by <sup>1</sup>H NMR analysis against 1,4-bis(trimethylsilyl)benzene as an internal standard. <sup>b</sup> Values for ee are reported as a ratio of two diastereomers (major/minor). <sup>c</sup> 20 mol% of the europium catalyst was used. No exogenous ligand was added.

### 4.2.2 Optimization of intermolecular [2+2] cycloaddition with acyl imidazole **4-11**

Although 2-acyl imidazole **4-1** helped validate our chiral Lewis acid approach to asymmetric photocatalysis, it quickly became apparent that its use as a model substrate would not be ideal due to its facile decomposition under the reaction conditions. The mass balance in these reactions was generally poor and the potential for generating up to four diastereomers in a reaction further complicated reaction analysis. Furthermore, **4-1** is not trivial to synthesize on large scale and is not amenable to long term storage.

Thus, subsequent studies have focused on the intermolecular [2+2] cycloaddition. In addition to addressing a number of practical limitations of the intramolecular variant, the intermolecular reaction is a synthetically and conceptually more interesting transformation. It provides efficient access to a diverse variety of unsymmetrical cyclobutane structures and there are currently no examples of enantioselective [2+2] photocycloadditions of *acyclic* enones.<sup>8</sup> We began our investigations with the crossed [2+2] cycloaddition between the analogous 2-acyl imidazole **4-11** and methyl vinyl ketone (**4-12**) (Scheme 4-3). The conditions for this transformation have also previously been optimized in our group.<sup>5</sup>

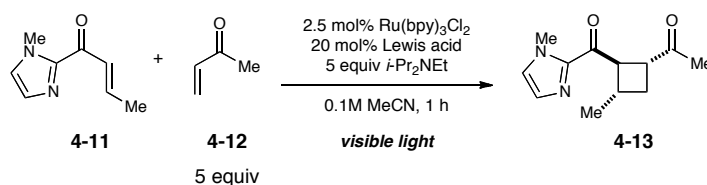
**Scheme 4-3.** Crossed intermolecular [2+2] photocycloaddition of imidazole **4-11** and methyl vinyl ketone (**4-12**)



Initial studies to confirm the feasibility of employing sub-stoichiometric amounts of Lewis acid for this transformation were conducted (Table 4-3). Consistent with our

observations in the intramolecular reaction, lanthanides were particularly efficient Lewis acids for the intermolecular cycloaddition; only one diastereomer of the product is observed in the crude  $^1\text{H}$  NMR spectrum (entries 8–10). The counter-ion also appears to have a role in the efficiency of the transformation (entries 2–3). This may be a consequence of the attenuated Lewis acidity of the cation or it may arise from other factors. This effect has not yet been investigated in our laboratories. A notable feature of these reaction conditions is the absence of homodimerization of aryl enone **4-11**. Although the reasons for this are currently not well understood, this observation is synthetically useful and mechanistically intriguing.

**Table 4-3.** Crossed [2+2] cycloaddition of 2-acyl imidazole **4-11** and methyl vinyl ketone (**4-12**) with 20 mol% Lewis acid

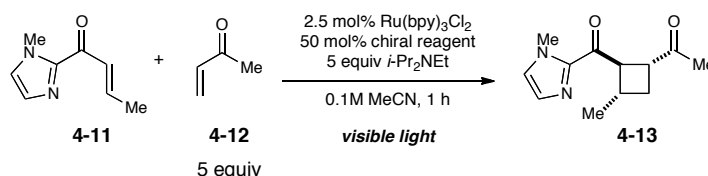


| entry | Lewis acid                  | yield <sup>a</sup> | entry | Lewis acid                | yield <sup>a</sup> |
|-------|-----------------------------|--------------------|-------|---------------------------|--------------------|
| 1     | $\text{Zn}(\text{OTf})_2$   | 15%                | 6     | $\text{Er}(\text{OTf})_3$ | 75%                |
| 2     | $\text{Mg}(\text{OTf})_2$   | 66%                | 7     | $\text{Y}(\text{OTf})_3$  | 66%                |
| 3     | $\text{Mg}(\text{ClO}_4)_2$ | 50%                | 8     | $\text{La}(\text{OTf})_3$ | >95%               |
| 4     | $\text{Al}(\text{OTf})_3$   | 0%                 | 9     | $\text{Eu}(\text{OTf})_3$ | >95%               |
| 5     | $\text{Sc}(\text{OTf})_3$   | 50%                | 10    | $\text{Gd}(\text{OTf})_3$ | >95%               |

<sup>a</sup> Yields were determined by  $^1\text{H}$  NMR analysis against 1,4-bis(trimethylsilyl)benzene as an internal standard

The ability of chiral shift reagents to mediate the intermolecular reaction was also examined (Table 4-4). Eu(tfc)<sub>3</sub> afforded the highest levels of enantioselectivity for the major diastereomer that had been observed up to this point in our studies (entry 4).

**Table 4-4.** Chiral shift reagents in the crossed [2+2] cycloaddition



| entry | chiral shift reagent <sup>a</sup> | % ee |
|-------|-----------------------------------|------|
| 1     | Yb(hfc) <sub>3</sub>              | 6    |
| 2     | Yb(tfc) <sub>3</sub>              | 4    |
| 3     | Pr(tfc) <sub>3</sub>              | 4    |
| 4     | Eu(tfc) <sub>3</sub>              | 20   |
| 5     | Eu(hfc) <sub>3</sub>              | 0    |

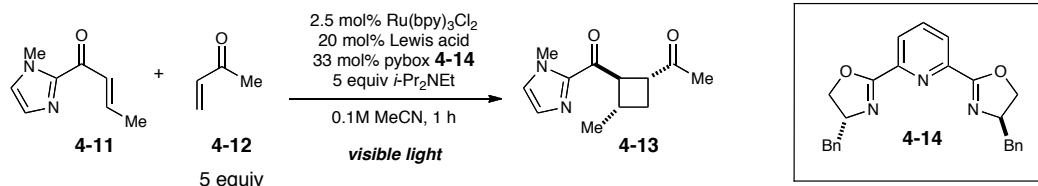
<sup>a</sup> See Table 4-2 for ligand abbreviations.

Having verified the viability of our approach for the intermolecular reaction, we began a more systematic investigation of the enantioselective transformation. Our initial screen of Lewis acids employed chiral Bn-pybox **4-14** as the ligand (Table 4-5). From the results of this study, Gd(OTf)<sub>3</sub> was selected as the Lewis acid for further studies based upon its clean conversion to product with relatively high levels of enantioselectivity (entry 11). The large discrepancy between consumption of starting material and conversion to the desired product in most reactions was troubling, however. These data indicated that two different scenarios were responsible for the consumption of starting material. Some Lewis acids do not interact deleteriously with



the substrate (entries 1–2), whereas other Lewis acids consume starting material unproductively (e.g. entries 9–11).

**Table 4-5.** Effect of the identity of the Lewis acid with Bn-pybox **4-14** in the crossed [2+2] cycloaddition



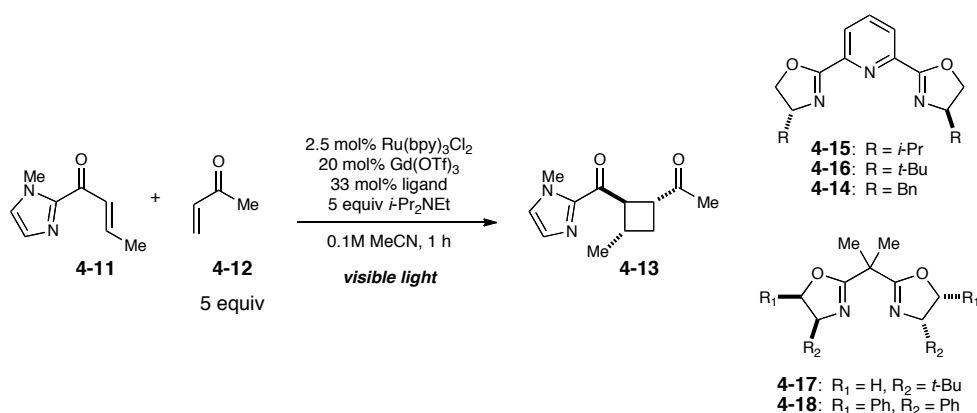
| entry | Lewis acid                         | SM yield <sup>a</sup> | [2+2] yield <sup>a</sup> | % ee |
|-------|------------------------------------|-----------------------|--------------------------|------|
| 1     | Zn(OTf) <sub>2</sub>               | 100%                  | --                       | --   |
| 2     | Al(OTf) <sub>3</sub>               | 97%                   | --                       | --   |
| 3     | Sc(OTf) <sub>3</sub>               | 55%                   | 2%                       | --   |
| 4     | Mg(OTf) <sub>2</sub>               | 38%                   | 7%                       | --   |
| 5     | Mg(ClO <sub>4</sub> ) <sub>2</sub> | 29%                   | 18%                      | 4    |
| 6     | Er(OTf) <sub>3</sub>               | 16%                   | 24%                      | 9    |
| 7     | La(OTf) <sub>3</sub>               | 7%                    | 24%                      | 10   |
| 8     | Y(OTf) <sub>3</sub>                | 19%                   | 43%                      | 8    |
| 9     | Eu(OTf) <sub>3</sub>               | 2%                    | 28%                      | 3    |
| 10    | LiOTf                              | --                    | 54%                      | 2    |
| 11    | Gd(OTf) <sub>3</sub>               | --                    | 26%                      | 18   |

<sup>a</sup> Yields were determined by <sup>1</sup>H NMR analysis against 1,4-bis(trimethylsilyl)benzene as an internal standard

Nevertheless, we were encouraged by the enantioselectivity observed with **4-14**. Because the choice of Bn-pybox **4-14** as a chiral ligand was somewhat arbitrary,<sup>9</sup> we tested several other gadolinium–bis(oxazoline) structures (Table 4-6). The enantioselectivity was slightly higher using *i*-Pr-pybox **4-15** (entry 1), but the results were not promising enough for extensive optimization. Furthermore, an increase in the

steric bulk of the ligand results in racemic product (entry 2). These results, taken together with the observation that an unproductive reaction between the Lewis acid and enone **4-11** rapidly decomposes the starting material, indicated that a different model system would be necessary for the development of a useful enantioselective photochemical method.

**Table 4-6.** Effect of ligand structure on the crossed [2+2] cycloaddition



| entry | ligand      | [2+2] yield <sup>a</sup> | % ee |
|-------|-------------|--------------------------|------|
| 1     | <b>4-15</b> | 24%                      | 23%  |
| 2     | <b>4-16</b> | 26%                      | 0%   |
| 3     | <b>4-14</b> | 26%                      | 18%  |
| 4     | <b>4-17</b> | 85%                      | 0%   |
| 5     | <b>4-18</b> | 87%                      | 0%   |

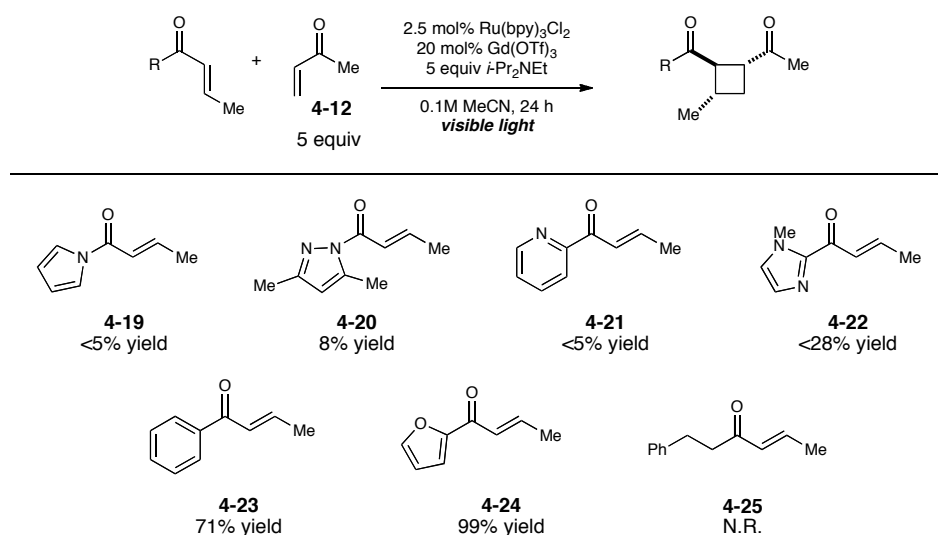
<sup>a</sup> Yields were determined by <sup>1</sup>H NMR analysis against 1,4-bis(trimethylsilyl)benzene as an internal standard

#### 4.2.3 Identification of aryl enone for intermolecular crossed [2+2] cycloaddition

Although incorporation of the 2-acyl imidazole substructure was logical at the outset of these studies, its incompatibility with Lewis acids made the development of a Lewis acid-mediated reaction extremely challenging. Thus, we wondered if a more

robust substrate might be advantageous at this point in our investigations. We initially considered substrates that would be capable of bidentate chelation to the metal center.<sup>10</sup> However, this two-point binding had not been shown to be necessary for enantioinduction and a broader survey of substrates<sup>5, 11</sup> was examined in the crossed [2+2] reaction with methyl vinyl ketone (**4-12**) in the presence of  $\text{Gd}(\text{OTf})_3$  (Figure 4-1).

**Figure 4-1.** Enone structures for crossed [2+2] cycloaddition



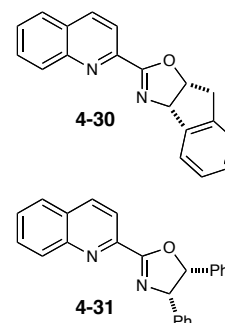
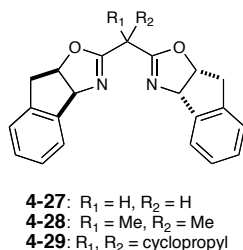
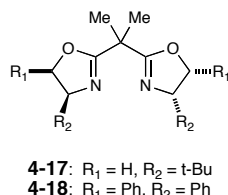
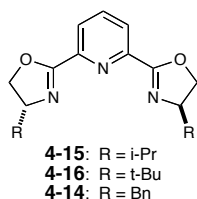
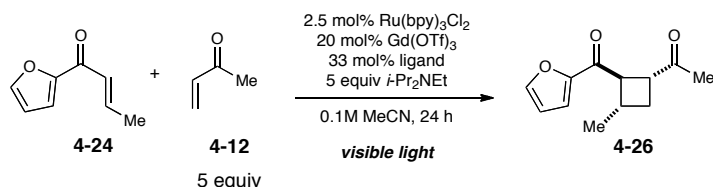
<sup>a</sup> Yields were determined by  $^1\text{H}$  NMR analysis against 1,4-bis(trimethylsilyl)benzene as an internal standard

Unfortunately, only a small number of aryl enones produced the [2+2] cycloadduct under our visible light conditions with catalytic amounts of  $\text{Gd}(\text{OTf})_3$ . Despite the limited success of this study, the high yields observed with phenyl enone **4-23** and 2-furyl enone **4-24** were encouraging. We elected to assess 2-furyl enone **4-24** as a substrate for the catalytic [2+2] cycloaddition with methyl vinyl ketone (**4-12**).

#### 4.2.4 Ligand screening with 2-furyl enone **4-24** in crossed [2+2] cycloaddition

Our initial ligand screen focused on the bis(oxazoline) structures we had examined previously. Unfortunately, all reactions with 2-furyl enone **4-24** produced racemic product (Table 4-7).

**Table 4-7.** Effect of oxazoline ligand structure on the crossed [2+2] cycloaddition with 2-furyl enone **4-24**

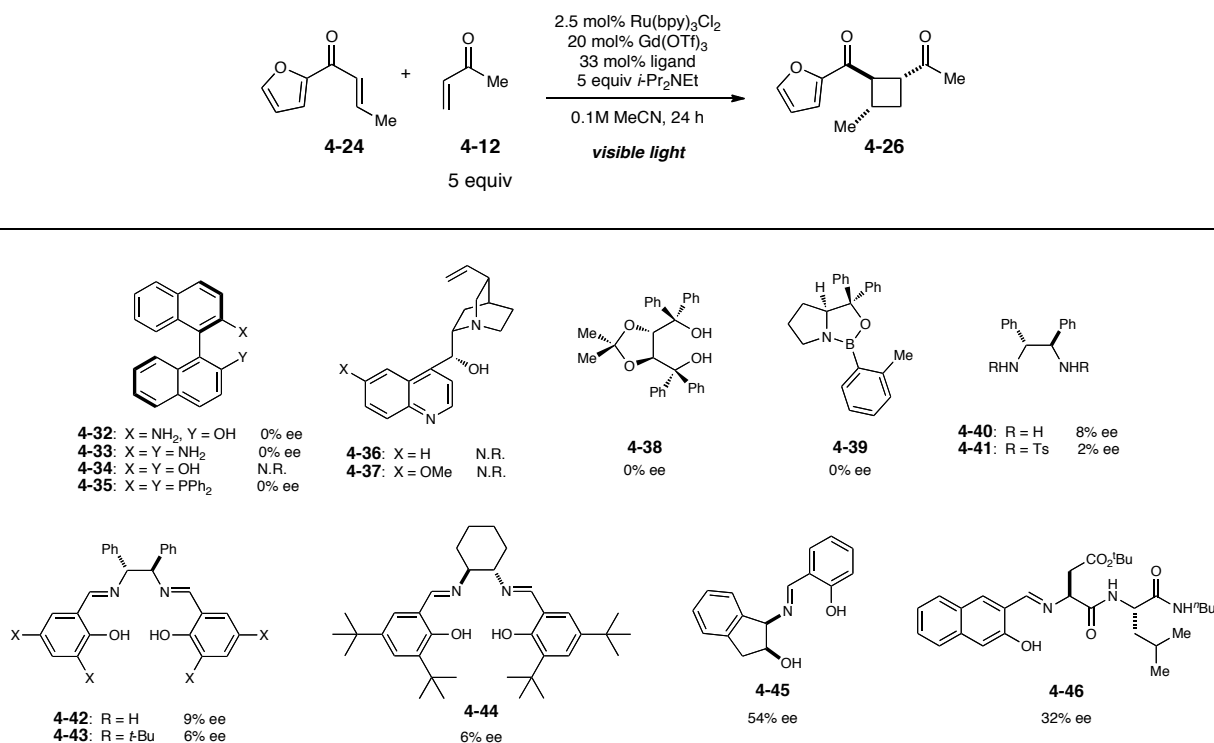


| entry | ligand      | [2+2] yield <sup>a</sup> | % ee |
|-------|-------------|--------------------------|------|
| 1     | <b>4-15</b> | 59%                      | 5    |
| 2     | <b>4-16</b> | 70%                      | 0    |
| 3     | <b>4-14</b> | 77%                      | 3    |
| 4     | <b>4-17</b> | 43%                      | 0    |
| 5     | <b>4-18</b> | 56%                      | 3    |
| 6     | <b>4-27</b> | 47%                      | 1    |
| 7     | <b>4-28</b> | 31%                      | 1    |
| 8     | <b>4-29</b> | 17%                      | 1    |
| 9     | <b>4-30</b> | 13%                      | 0    |
| 10    | <b>4-31</b> | 24%                      | 1    |

<sup>a</sup> Yields were determined by <sup>1</sup>H NMR analysis against 1,4-bis(trimethylsilyl)benzene as an internal standard

Thus, the bis(oxazoline) ligand framework did not appear to be a suitable scaffold for the reaction. An interesting trend in asymmetric catalysis is the existence of privileged structures for chiral catalysts;<sup>7</sup> several classes of synthetic catalysts have been shown to induce high levels of enantioselectivity for a wide range of transformations; the bis(oxazoline) structure is one prominent example of a privileged ligand framework. Given the disappointing results from the oxazoline-based ligands, we decided to examine some other privileged ligand structures in our reaction (Figure 4-2).

**Figure 4-2.** Effect of ligand structure on the crossed [2+2] cycloaddition with 2-furyl enone **4-24**



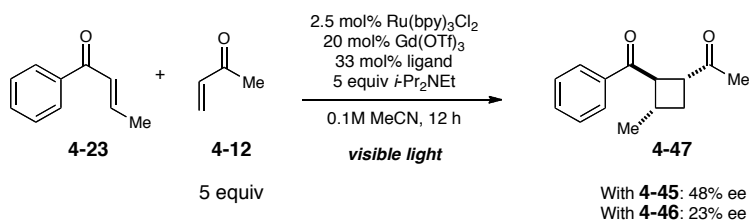
The results of this screen were particularly encouraging because several promising ligand frameworks emerged as potential lead results. First, simple salen ligands afforded the products with measurable levels of enantioselectivity (e.g. **4-42**).

Metal salen complexes are known to be efficient chiral auxiliaries for a variety of atom transfer reactions;<sup>12</sup> their ease of synthesis and the ready availability of their components make them attractive ligand frameworks for asymmetric catalysis. Tridentate Schiff base ligands also appeared to be a favorable motif for this reaction (**4-45** and **4-46**). Chiral Schiff base ligands comprised of *cis*-1-amino-2-indanol and a salicylaldehyde (**4-45**) form complexes with chromium that can mediate a variety of highly enantioselective reactions,<sup>13</sup> and small Schiff base-containing peptides (**4-46**) have begun to emerge as highly modular chiral ligands for asymmetric catalysis.<sup>14</sup>

#### 4.2.5 Optimization of intermolecular [2+2] cycloaddition with phenyl enone **4-23**

##### 4.2.5.1 Lewis acid and ligand optimization

The crossed [2+2] cycloaddition of phenyl enone **4-23** and methyl vinyl ketone **4-12** also proceeded with promising levels of enantioselectivity using either gadolinium-Schiff base catalyst (Scheme 4-4). Given that **4-23** does not contain any additional Lewis basic sites to enable bidentate chelation, two-point binding does not appear to be necessary for the transfer of stereochemical information. We chose to continue our studies with phenyl enone **4-23** to eliminate the possibility of a stereochemistry-determining transition state involving any additional substrate preorganization; this should help facilitate the development of a reaction that can accommodate a more general substrate scope.

**Scheme 4-4.** Schiff base ligands in crossed [2+2] cycloaddition with phenyl enone **4-23**

Structurally, aminoindanol **4-45** and dipeptide **4-46** are relatively similar. Because our goal was to quickly assess the effect on enantioselectivity from steric and electronic perturbations of the Schiff base component, we focused our initial studies on ligands derived from *cis*-1-amino-2-indanol due to their shorter synthetic sequence. Our evaluation of ligand efficiency has thus far been based solely on their ability to afford high levels of asymmetric induction; therefore, only %ee values are reported in this chapter.

First, a series of ligands featuring systematic modifications to the salicylaldehyde motif were synthesized and subjected to the reaction conditions with  $\text{Gd}(\text{OTf})_3$  (Table 4-8). Unfortunately, both increasing the steric bulk (entries 2–3) and perturbing the electronics (entries 4–5) were detrimental to the enantioselectivity.

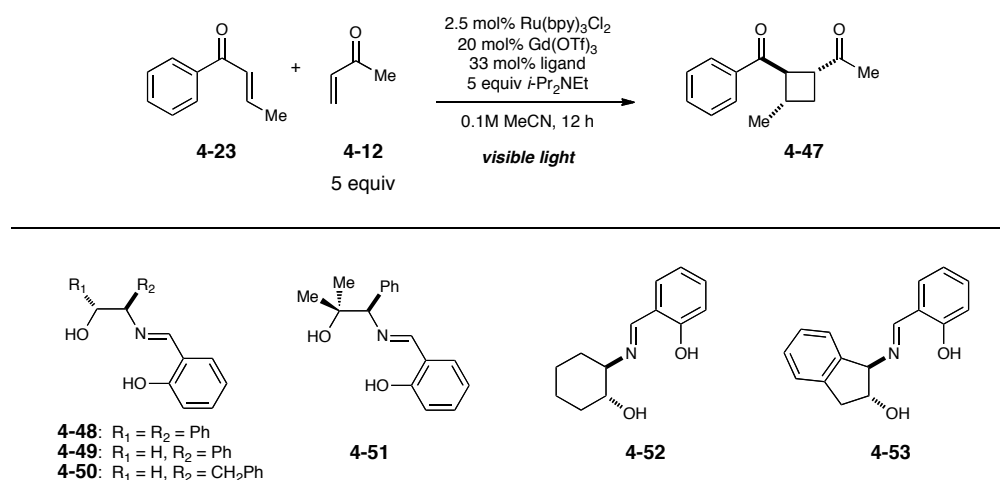
**Table 4-8.** Effect of steric and electronic ligand perturbations on enantioselectivity

| entry | X            | Y            | % ee |
|-------|--------------|--------------|------|
| 1     | H            | H            | 48   |
| 2     | <i>t</i> -Bu | <i>t</i> -Bu | 22   |

|   |   |             |    |
|---|---|-------------|----|
| 3 | H | 2-adamantyl | 19 |
| 4 | H | Cl          | 19 |
| 5 | H | OMe         | 40 |

We next considered the possibility that ligands derived from other amino alcohols might provide superior levels of enantioinduction (Table 4-9). This was not observed to be the case (entries 1–5). Notably, use of the ligand derived from *trans*-1-amino-2-indanol (**4-53**) significantly lowers the enantioselectivity (entry 6).

**Table 4-9.** Effect of amino alcohol structure on enantioselectivity



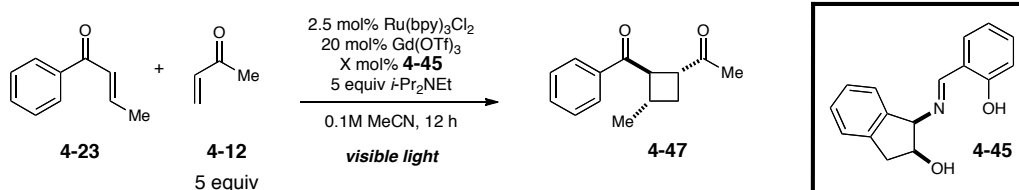
| entry | ligand      | % ee |
|-------|-------------|------|
| 1     | <b>4-48</b> | 4    |
| 2     | <b>4-49</b> | 16   |
| 3     | <b>4-50</b> | 0    |
| 4     | <b>4-51</b> | 19   |
| 5     | <b>4-52</b> | 0    |
| 6     | <b>4-53</b> | 30   |



#### 4.2.5.2 Reaction optimization and scope of cycloaddition

Because no improvements in the enantioselectivity were obtained from ligand modifications, we turned our attention to the effect of other variables. We first examined the ratio of ligand to Lewis acid (Table 4-10); a ratio of 1.6:1 had been employed at the beginning of our studies to ensure complete formation of the 1:1 chiral ligand–Lewis acid complex.<sup>15</sup> This study indicated that a 3:1 ratio of ligand to Lewis acid led to a slight improvement in enantioselectivity. Subsequent studies have employed this ratio.

**Table 4-10.** Effect of ligand to Lewis acid ratio on enantioselectivity

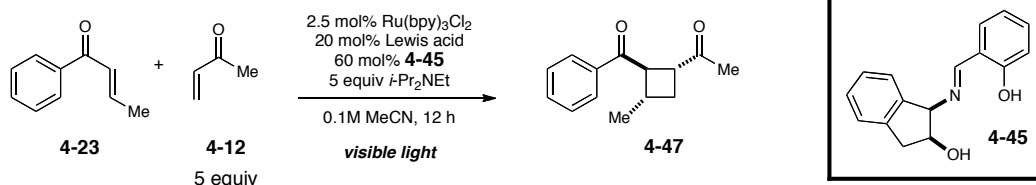


| entry | ligand : Lewis acid | % ee |
|-------|---------------------|------|
| 1     | 0.5 : 1             | 2    |
| 2     | 1 : 1               | 13   |
| 3     | 1.6 : 1             | 48   |
| 4     | 3 : 1               | 55   |
| 5     | 5 : 1               | 54   |

An extensive Lewis acid screen was carried out with this new ratio of ligand to Lewis acid (Table 4-11); lanthanides were again found to be superior Lewis acids for the reaction. Surprisingly, no product was observed using Ca(OTf)<sub>2</sub>, Mg(OTf)<sub>2</sub>, Zn(OTf)<sub>2</sub>, NaPF<sub>6</sub>, Sc(OTf)<sub>3</sub>, Al(OTf)<sub>3</sub>, Sn(OTf)<sub>2</sub>, or Yb(OTf)<sub>3</sub>. Although Eu(OTf)<sub>3</sub> gave slightly higher levels of enantioselectivity (entry 1), the poor mass balance of the reaction led us

to continue our studies with gadolinium.  $\text{Gd}(\text{OTf})_3$  was found to be the optimal source of gadolinium (entries 8–10);  $\text{Gd}_2(\text{SO}_4)_3$ ,  $\text{Gd}_2(\text{CO}_3)_3$ ,  $\text{Gd}(\text{OAc})_3$ , and  $\text{GdF}_3$  did not promote the reaction. In addition, consistent with our mechanistic understanding of the process, no product is formed in the absence of a Lewis acid (entry 11).

**Table 4-11.** Effect of Lewis acid identity on enantioselectivity



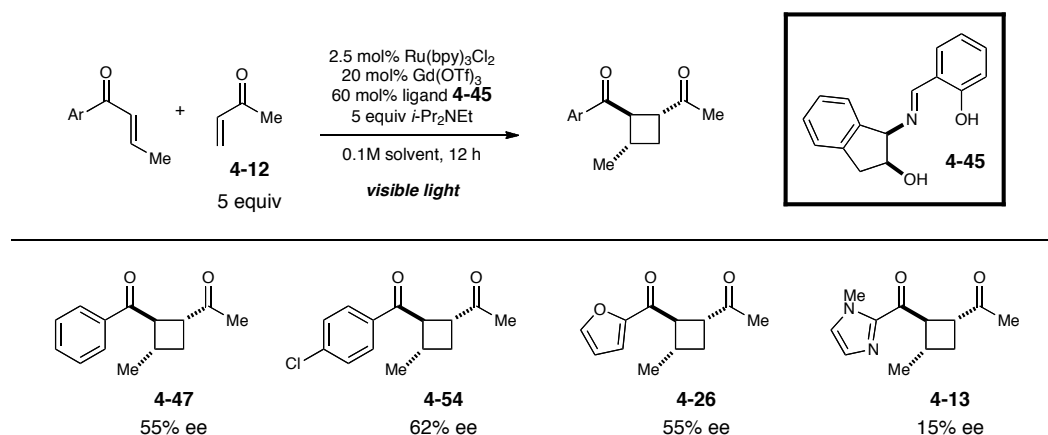
| entry | Lewis acid                 | % ee |
|-------|----------------------------|------|
| 1     | $\text{Eu}(\text{OTf})_3$  | 59   |
| 2     | $\text{Sm}(\text{OTf})_2$  | 55   |
| 3     | $\text{Dy}(\text{OTf})_3$  | 27   |
| 4     | $\text{La}(\text{OTf})_3$  | 26   |
| 5     | $\text{Nd}(\text{OTf})_3$  | 19   |
| 6     | $\text{Er}(\text{OTf})_3$  | 10   |
| 7     | $\text{Pr}(\text{OTf})_3$  | 4    |
| 8     | $\text{Gd}(\text{NO}_3)_2$ | 42   |
| 9     | $\text{GdCl}_3$            | 26   |
| 10    | $\text{Gd}(\text{acac})_3$ | 22   |
| 11    | none                       | --   |

An optimization of the other reaction variables for enantioselectivity was also carried out. These variables include solvent (Table 4-14), the identity of the base (Table 4-15), the photocatalyst (Table 4-16),<sup>1b</sup> and the effect of temperature (Table 4-17). A more extensive ligand screen was also conducted (Table 4-18). The results of these

experiments are available at the end of this chapter. Unfortunately, no improvement in the enantioselectivity for this reaction was achieved.

The optimized reaction conditions and a preliminary scope are shown in Figure 4-3. Although the results are modest, they are promising for the development of a *general* enantioselective photoreaction. Several enones participate in the reaction without significantly diminished levels of enantioselectivity.

**Figure 4-3.** Aryl enone scope of [2+2] photocycloaddition using aminoindanol **4-45**



#### 4.2.6 Optimization of peptide ligands for intermolecular [2+2] cycloaddition

The results obtained with aminoindanol **4-45** indicated that modest levels of enantioselectivity could be obtained in the [2+2] cycloaddition using chiral Lewis acids. However, ligand optimization was disappointing; any perturbation to the ligand structure or metal center had a deleterious effect on enantioselectivity. Thus we decided to examine our second lead result, peptide ligand **4-46**. The highly modular nature of this Schiff base ligand was expected to be advantageous for enantioselectivity.

Our approach to ligand optimization is outlined in Figure 4-4. Assuming that the metal interacts with the Schiff base of the ligand, we reasoned that the amino acid in closer proximity to this terminus (AA<sub>1</sub>) would have the largest effect on enantioselectivity. Therefore, beginning with AA<sub>1</sub>, we envisioned employing an iterative positional optimization approach.<sup>16</sup> For practical reasons, we simplified the salicylaldehyde component to salicylaldehyde itself.

**Figure 4-4.** Sites of modification for dipeptide ligand

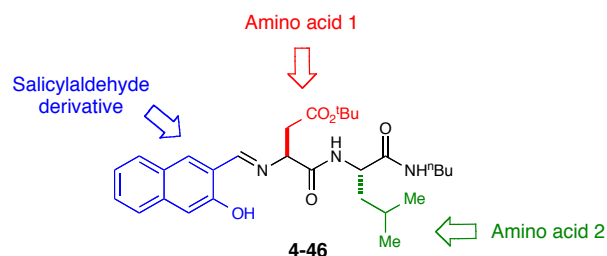
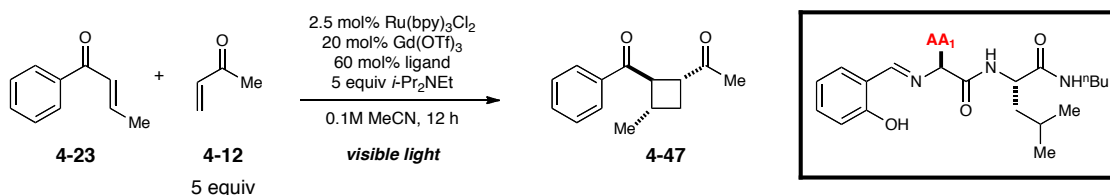


Table 4-12 shows the effect on enantioselectivity as the identity of AA<sub>1</sub> is varied. It should be noted that the use of salicylaldehyde significantly increases the enantioselectivity (entry 1). With respect to AA<sub>1</sub>, steric bulk at this position appears to be advantageous (e.g. entries 2–5); however, this effect quickly reaches a maximum level (entry 7). In addition, the presence of two peptide structures is necessary to achieve high levels of enantioselectivity (entry 12). In the absence of a second amino acid, a significant amount of enone **4-23** remains after 12 h. This indicates that the dipeptide motif is critical for achieving high levels of both reactivity and selectivity. From these studies, valine was selected as AA<sub>1</sub>.

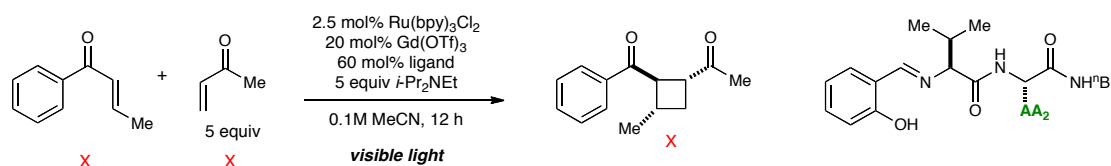
**Table 4-12.** Effect of AA<sub>1</sub> on enantioselectivity

| entry | AA <sub>1</sub>             | % ee |
|-------|-----------------------------|------|
| 1     | Asp( <i>O</i> <i>t</i> -Bu) | 50   |
| 2     | Gly                         | 39   |
| 3     | Ala                         | 47   |
| 4     | Leu                         | 44   |
| 5     | Val                         | 55   |
| 6     | Ile                         | 52   |
| 7     | Tle                         | 43   |
| 8     | Phg                         | 14   |
| 9     | Phe                         | 54   |
| 10    | Tyr( <i>t</i> -Bu)          | 55   |
| 11    | Trp(Boc)                    | 47   |
| 12    | none                        | 19   |

With the knowledge that the second amino acid is critical to the enantioselectivity, we proceeded to optimize the identity of AA<sub>2</sub> (Table 4-13). The data seem to indicate that the role of AA<sub>2</sub> is primarily conformational; the reaction is relatively insensitive to steric bulk at that position (entries 1 and 6), but substitution of L-valine with D-valine results in a significant drop in enantioselectivity (entries 3–4). If the main role of AA<sub>2</sub> is indeed to help adopt or enforce a conformational orientation, then structural variations at this position should have a dramatic effect on enantioselectivity.

Proline is often employed as an amino acid in these ligand structures. Its cyclic framework enforces significantly different structural conformations from that of its linear counterparts and its ability to act as a “turn element” is often exploited in the design of small peptide ligands.<sup>17</sup> Indeed, use of L-proline leads to a significant increase in enantioselectivity (entry 9); D-Proline affords the cycloadduct with drastically diminished enantiomeric excess (entry 10).

**Table 4-13.** Effect of AA<sub>2</sub> on enantioselectivity

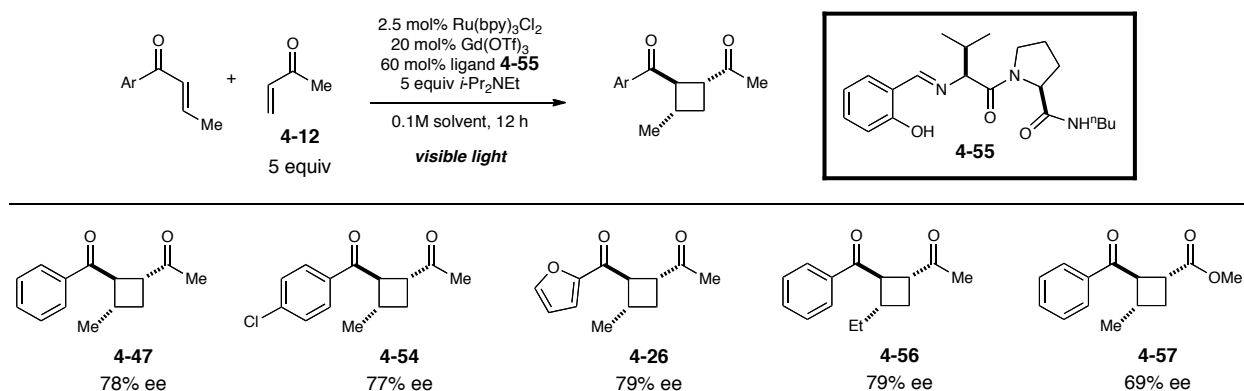


| entry | AA <sub>2</sub> | % ee |
|-------|-----------------|------|
| 1     | Ala             | 55   |
| 2     | Leu             | 55   |
| 3     | L-Val           | 56   |
| 4     | D-Val           | 41   |
| 5     | Ile             | 54   |
| 6     | Tle             | 51   |
| 7     | Phg             | 53   |
| 8     | Trp(Boc)        | 52   |
| 9     | L-Pro           | 78   |
| 10    | D-Pro           | 9    |

### 4.3 Conclusions and future outlook

Given that AA<sub>1</sub> has been shown to significantly affect the enantioselectivity and that the nature of the salicylaldehyde component has not yet been investigated, good to excellent levels of enantioselectivity should be obtainable for the crossed [2+2] photocycloaddition using these highly modular peptide ligands. Preliminary studies indicate that the substrate scope of this reaction should be sufficiently broad; variation of both the aryl enone and Michael acceptor is tolerated and reasonable levels of enantioselectivity can be obtained using a relatively unoptimized ligand (**4-55**) (Figure 4-5). Given that catalytic asymmetric photochemical methods are extremely rare and that Lewis acids have not been sufficiently demonstrated to be efficient promoters of asymmetric photochemical transformations, this work represents a promising general strategy for enantioselective photocatalysis.

**Figure 4-5.** Substrate scope of [2+2] photocycloaddition with peptide ligand **4-55**



## 4.4 Experimental

### 4.4.1 General considerations

Acetonitrile,  $\text{CH}_2\text{Cl}_2$ , and *i*- $\text{Pr}_2\text{NEt}$  were distilled from  $\text{CaH}_2$  immediately prior to use.  $\text{Ru}(\text{bpy})_3\text{Cl}_2 \cdot 6\text{H}_2\text{O}$  was purchased from Strem and used without further purification. 3-buten-2-one and methyl acrylate were distilled immediately prior to use. All other chemicals were purchased from commercial suppliers and used without further purification. Flash column chromatography<sup>18</sup> was performed using Purasil 60Å silica gel (230–400 mesh). All glassware was oven-dried at 130 °C for at least 1 h or flame-dried immediately prior to use.

Diastereomer ratios for all compounds were determined by  $^1\text{H}$  NMR analysis of the unpurified reaction mixtures. All NMR spectra were obtained at ambient temperature on the Varian Unity-500 and Varian Inova-500 spectrometers. Chemical shifts are reported in parts per million ( $\delta$ ) relative to TMS (0.0 ppm) for  $^1\text{H}$  NMR data and  $\text{CDCl}_3$  (77.23 ppm) for  $^{13}\text{C}$  NMR data. IR spectral data were obtained using a Bruker Vector 22 spectrometer. Optical rotations were obtained using a Rudolph Autopol III polarimeter. Mass spectrometry was performed with a Micromass LCT (electrospray ionization, time-of-flight analyzer or electron impact). These facilities are funded by the NSF (CHE-9974839, CHE-9304546), NIH (RR08389-01) and the University of Wisconsin.

### 4.4.2 Representative procedure

A dry 25 mL Schlenk tube is charged with the ligand (0.60 equiv),  $\text{Gd}(\text{OTf})_3$  (0.20 equiv) and half the amount of required solvent and allowed to stir for 1 h.<sup>15</sup> To the chiral catalyst is then added  $\text{Ru}(\text{bpy})_3\text{Cl}_2 \cdot 6\text{H}_2\text{O}$  (0.025 equiv), enone (1 equiv), Michael

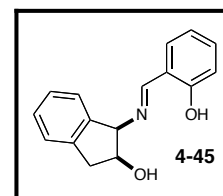
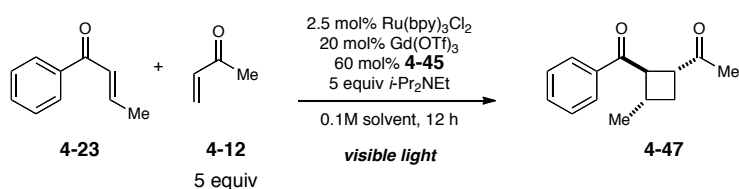


acceptor (5 equiv), *i*-Pr<sub>2</sub>NEt (5 equiv) and the remaining amount of solvent (0.1 M) and degassed by a freeze/pump/thaw cycle (3x) under nitrogen in the dark. The reaction is then allowed to stir and irradiated by a 23 W (1380 lumen) compact fluorescent bulb for 12 h, after which the reaction is run through a small plug of silica and concentrated to afford the crude reaction mixture. The residue is purified by column chromatography on silica gel.

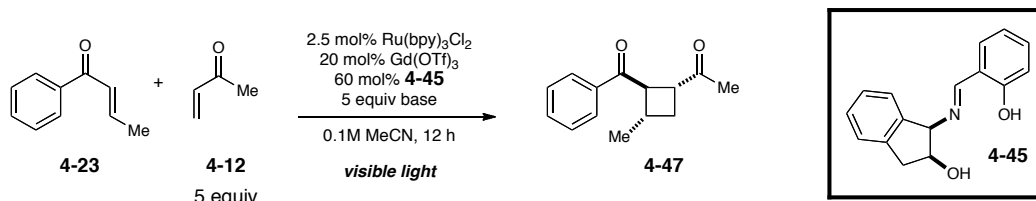
### 4.4.3 Reaction optimization data

#### 4.4.3.1 Effect of reaction variables on the [2+2] cycloaddition of phenyl enone **4-23**

**Table 4-14.** Effect of solvent identity on enantioselectivity

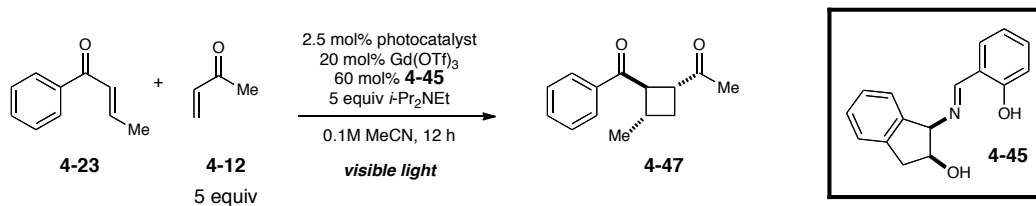


| entry | solvent                            | % ee |
|-------|------------------------------------|------|
| 1     | acetone                            | 32   |
| 2     | EtOAc                              | 31   |
| 3     | CH <sub>2</sub> Cl <sub>2</sub>    | 29   |
| 4     | CHCl <sub>3</sub>                  | --   |
| 5     | toluene                            | --   |
| 6     | <i>p</i> -CF <sub>3</sub> -toluene | --   |

**Table 4-15.** Effect of base on enantioselectivity

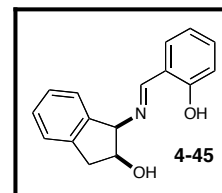
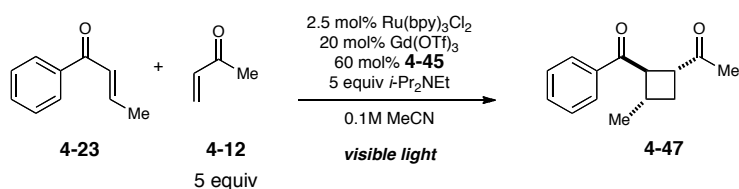
| entry          | base                            | % ee |
|----------------|---------------------------------|------|
| 1              | NEt <sub>3</sub>                | 51   |
| 2              | Cy <sub>2</sub> NEt             | 53   |
| 3              | 1,1,2,2,6-pentamethylpiperidine | 55   |
| 4              | 1-methylpiperidine              | 52   |
| 5 <sup>a</sup> | cinchonidine                    | --   |
| 6 <sup>a</sup> | quinine                         | --   |
| 7 <sup>a</sup> | PPh <sub>3</sub>                | --   |

<sup>a</sup> No cycloadduct was observed under these conditions

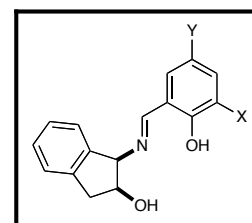
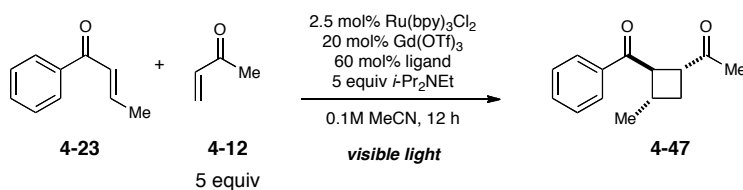
**Table 4-16.** Effect of photocatalyst on enantioselectivity

| entry          | photocatalyst  | % ee |
|----------------|--|------|
| 1 <sup>a</sup> | [Ir(ppy) <sub>2</sub> (dtb-bpy)][PF <sub>6</sub> ]   | 49   |
| 2              | Ru(bpy) <sub>3</sub> (PF <sub>6</sub> ) <sub>2</sub> | 57   |

<sup>a</sup> ppy = 2-phenylpyridine; dtb-bpy = 4,4'-di-*tert*-butyl-bpy

**Table 4-17.** Effect of temperature on enantioselectivity

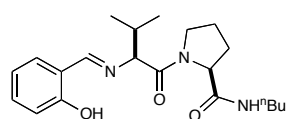
| entry | temperature | time | % ee |
|-------|-------------|------|------|
| 1     | 0 °C        | 24 h | 53   |
| 2     | 40 °C       | 12 h | 51   |

**Table 4-18.** Effect of steric and electronic ligand perturbations on enantioselectivity

| entry           | X           | Y          | % ee |
|-----------------|-------------|------------|------|
| 1               | Me          | H          | 20   |
| 2               | 2-adamantyl | Me         | 19   |
| 3               | H           | OMe        | 40   |
| 4               | H           | Me         | 49   |
| 5               | H           | H          | 55   |
| 6               | H           | Ph         | 40   |
| 7               | H           | Br         | 9    |
| 8               | H           | Cl         | 19   |
| 9               | H           | 1-naphthyl | 7    |
| 10 <sup>a</sup> | H           | 2-naphthyl | --   |

<sup>a</sup> No cycloaddition product was observed under these conditions

#### 4.4.3 Characterization of new compounds



**(S)-N-butyl-1-((S)-2-((E)-(2-hydroxybenzylidene)amino)-3-methylbutanoyl)pyrrolidine-2-carboxamide (4-55).** IR (thin film)

1732, 1390, 908;  $^1\text{H}$  NMR (500 MHz,  $\text{CDCl}_3$ )  $\delta$  13.16 (s, 1H), 8.4 (s, 1H), 7.34 (td,  $J$  = 8.4, 104 Hz, 1H), 7.27 (d,  $J$  = 9.2 Hz, 1H), 7.06 (s, 1H), 6.98 (d,  $J$  = 8.3 Hz, 1H), 6.89 (t,  $J$  = 7.3 Hz, 1H), 4.62 (dd,  $J$  = 8.0, 2.3 Hz, 1H), 3.93 (d,  $J$  = 8.2 Hz, 1H), 3.69 (td,  $J$  = 9.0, 3.2 Hz, 1H), 3.54 (q,  $J$  = 9.2 Hz, 1H), 3.22 (q,  $J$  = 6.8 Hz, 2H), 2.4 (m, 2H), 2.18 (m, 1H), 1.97 (m, 1H), 1.81 (m, 1H), 1.47 (m, 2H), 1.34 (m, 2H), 1.00 (d,  $J$  = 7 Hz, 2H), 0.96 (d,  $J$  = 6.5 Hz, 2H), 0.91 (t, 3H);  $^{13}\text{C}$  NMR (125 MHz,  $\text{CDCl}_3$ )  $\delta$  170.9, 170.8, 166.2, 161.4, 133.0, 131.9, 118.9, 118.7, 117.4, 76.4, 60.2, 47.6, 39.4, 32.0, 31.8, 26.9, 25.4, 20.3, 19.8, 18.9, 13.9; HRMS ( $\text{ESI}^+$ ) calc'd for  $[\text{C}_{21}\text{H}_{30}\text{N}_3\text{O}_3]^-$  ( $\text{M}-\text{H}$ ) $^-$  requires  $m/z$  372.2297, found  $m/z$  327.2291.

#### 4.5 References

1. a) Nicewicz, D. A.; MacMillan, D. W. C. Merging Photoredox Catalysis with Organocatalysis: The Direct Asymmetric Alkylation of Aldehydes. *Science* **2008**, 322, 77-80. b) Nagib, D. A.; Scott, M. E.; MacMillan, D. W. C. Enantioselective  $\alpha$ -Trifluoromethylation of Aldehydes via Photoredox Organocatalysis. *J. Am. Chem. Soc.* **2009**, 131, 10875-10877. c) Shih, H.-W.; Vander Wal, M. N.; Grange, R. L.; MacMillan, D. W. C. Enantioselective  $\alpha$ -Benzylation of Aldehydes via Photoredox Organocatalysis. *J. Am. Chem. Soc.* **2010**, 132, 13600-13603.
2. a) Bach, T.; Bergmann, H.; Harms, K. Enantioselective Intramolecular [2+2]-Photocycloaddition Reactions in Solution. *Angew. Chem. Int. Ed.* **2000**, 39, 2302-2304. b) Bach, T.; Bergmann, H. Enantioselective Intermolecular [2 + 2]-Photocycloaddition Reactions of Alkenes and a 2-Quinolone in Solution. *J. Am. Chem. Soc.* **2000**, 122, 11525-11526. c) Guo, H.; Herdtweck, E.; Bach, T. Enantioselective Lewis Acid Catalysis in Intramolecular [2+2] Photocycloaddition Reactions of Coumarins. *Angew. Chem. Int. Ed.* **2010**, 49, 7782-7785. d) Canales, E.; Corey, E. J. Highly Enantioselective [2+2]-Cycloaddition Reactions Catalyzed by a Chiral Aluminum Bromide Complex. *J. Am. Chem. Soc.* **2007**, 129, 12686-12687.

3. Evans, D. A.; Song, H.-J.; Fandrick, K. R. Enantioselective Nitron Cycloadditions of  $\alpha,\beta$ -Unsaturated 2-Acyl Imidazoles Catalyzed by Bis(oxazoliny)pyridine–Cerium(IV) Triflate Complexes. *Org. Lett.* **2006**, *8*, 3351-3354.
4. a) Evans, D. A.; Fandrick, K. R.; Song, H.-J. Enantioselective Friedel–Crafts Alkylations of  $\alpha,\beta$ -Unsaturated 2-Acyl Imidazoles Catalyzed by Bis(oxazoliny)pyridine–Scandium(III) Triflate Complexes. *J. Am. Chem. Soc.* **2005**, *127*, 8942-8943. b) Evans, D. A.; Fandrick, K. R. Catalytic Enantioselective Pyrrole Alkylations of  $\alpha,\beta$ -Unsaturated 2-Acyl Imidazoles. *Org. Lett.* **2006**, *8*, 2249-2252. c) Evans, D. A.; Fandrick, K. R.; Song, H.-J.; Scheidt, K. A.; Xu, R. Enantioselective Friedel–Crafts Alkylations Catalyzed by Bis(oxazoliny)pyridine–Scandium(III) Triflate Complexes. *J. Am. Chem. Soc.* **2007**, *129*, 10029-10041.
5. Tyson, E. L.; Farney, E. P.; Yoon, T. P. Photocatalytic [2 + 2] Cycloadditions of Enones with Cleavable Redox Auxiliaries. *Org. Lett.* **2012**, *14*, 1110-1113.
6. Parker, D. NMR determination of enantiomeric purity. *Chem. Rev.* **1991**, *91*, 1441-1457.
7. Yoon, T. P.; Jacobsen, E. N. Privileged Chiral Catalysts. *Science* **2003**, *299*, 1691-1693.
8. a) Schuster, D. I.; Lem, G.; Kaprinidis, N. A. New insights into an old mechanism: [2+2] photocycloaddition of enones to alkenes. *Chem. Rev.* **1993**, *93*, 3-22. b) Fagnoni, M.; Dondi, D.; Ravelli, D.; Albini, A. Photocatalysis for the Formation of the C–C Bond. *Chem. Rev.* **2007**, *107*, 2725-2756.
9. Desimoni, G.; Faita, G.; Quadrelli, P. Pyridine-2,6-bis(oxazolines), Helpful Ligands for Asymmetric Catalysts. *Chem. Rev.* **2003**, *103*, 3119-3154.
10. Johnson, J. S.; Evans, D. A. Chiral Bis(oxazoline) Copper(II) Complexes: Versatile Catalysts for Enantioselective Cycloaddition, Aldol, Michael, and Carbonyl Ene Reactions. *Acc. Chem. Res.* **2000**, *33*, 325-335.
11. Du, J.; Yoon, T. P. Crossed Intermolecular [2+2] Cycloadditions of Acyclic Enones via Visible Light Photocatalysis. *J. Am. Chem. Soc.* **2009**, *131*, 14604-14605.
12. a) Katsuki, T. Some Recent Advances in Metallosalen Chemistry. *Synlett* **2003**, *2003*, 0281,0297. b) Jacobsen, E. N.; Zhang, W.; Muci, A. R.; Ecker, J. R.; Deng, L. Highly enantioselective epoxidation catalysts derived from 1,2-diaminocyclohexane. *J. Am. Chem. Soc.* **1991**, *113*, 7063-7064.
13. Ruck, R. T.; Jacobsen, E. N. Asymmetric Catalysis of Hetero-Ene Reactions with Tridentate Schiff Base Chromium(III) Complexes. *J. Am. Chem. Soc.* **2002**, *124*, 2882-2883.

14. a) Sigman, M. S.; Jacobsen, E. N. Schiff Base Catalysts for the Asymmetric Strecker Reaction Identified and Optimized from Parallel Synthetic Libraries. *J. Am. Chem. Soc.* **1998**, *120*, 4901-4902. b) Shimizu, K. D.; Cole, B. M.; Krueger, C. A.; Kuntz, K. W.; Snapper, M. L.; Hoveyda, A. H. Search for Chiral Catalysts Through Ligand Diversity: Substrate-Specific Catalysts and Ligand Screening on Solid Phase. *Angew. Chem. Int. Ed.* **1997**, *36*, 1704-1707. c) Davie, E. A. C.; Mennen, S. M.; Xu, Y.; Miller, S. J. Asymmetric Catalysis Mediated by Synthetic Peptides. *Chem. Rev.* **2007**, *107*, 5759-5812. d) Shimizu, K. D.; Snapper, M. L.; Hoveyda, A. H. High-Throughput Strategies for the Discovery of Catalysts. *Chem. Eur. J.* **1998**, *4*, 1885-1889. e) Hoveyda, A. H.; Hird, A. W.; Kacprzynski, M. A. Small peptides as ligands for catalytic asymmetric alkylations of olefins. Rational design of catalysts or of searches that lead to them? *Chem. Commun.* **2004**, 1779-1785.
15. Sammis, G. M.; Danjo, H.; Jacobsen, E. N. Cooperative Dual Catalysis: Application to the Highly Enantioselective Conjugate Cyanation of Unsaturated Imides. *J. Am. Chem. Soc.* **2004**, *126*, 9928-9929.
16. Kuntz, K. W.; Snapper, M. L.; Hoveyda, A. H. Combinatorial catalyst discovery. *Curr. Opin. Chem. Biol.* **1999**, *3*, 313-319.
17. Francis, M. B.; Jamison, T. F.; Jacobsen, E. N. Combinatorial libraries of transition-metal complexes, catalysts and materials. *Curr. Opin. Chem. Biol.* **1998**, *2*, 422-428.
18. Still, W. C.; Kahn, M.; Mitra, A. Rapid chromatographic technique for preparative separations with moderate resolution. *J. Org. Chem.* **1978**, *43*, 2923-2925.

## Appendix A. Anion-Accelerated Copper-Catalyzed Aminohydroxylation: Mechanistic Insights

Portions of this work have previously been published:

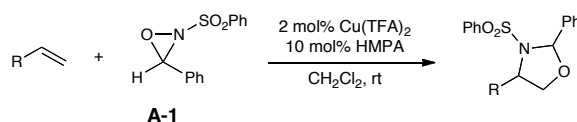
Benkovics, T.; Du, J.; Guzei I. A.; Yoon, T. P. Anionic Halocuprate(II) Complexes as Catalysts for the Oxaziridine-Mediated Aminohydroxylation of Olefins. *J. Org. Chem.* **2009**, 74, 5545–5552.

## A.1 Introduction

The 1,2-aminoalcohol motif is ubiquitous in biologically active and pharmaceutically relevant molecules. Its prevalence in medicinally important compounds, its versatility as a substructure to various molecular scaffolds, and its prominence as a chiral reagent for stereoselective synthesis have attracted continued interest in strategies for its construction. The osmium-catalyzed aminohydroxylation reported by Sharpless in 1976 remains the preferred protocol for the synthesis of 1,2-aminoalcohols.<sup>1</sup> Due to the high cost and toxicity of osmium compounds, however, the development of alternative methods is of practical importance.<sup>2</sup>

Our group is interested in employing oxaziridines as the terminal oxidant for new oxidative transformations.<sup>3</sup> In this context, we have developed a copper(II)-catalyzed method for the formal aminohydroxylation of activated olefins using *N*-sulfonyl oxaziridines (**A-1**) (Scheme A-1).<sup>3a</sup> This regioselective protocol accommodates a wide range of styrenes and 1,3-dienes and is a useful complement to the osmium-catalyzed reaction.<sup>3b</sup>

### Scheme A-1. Cu(TFA)<sub>2</sub>-catalyzed aminohydroxylation of olefins

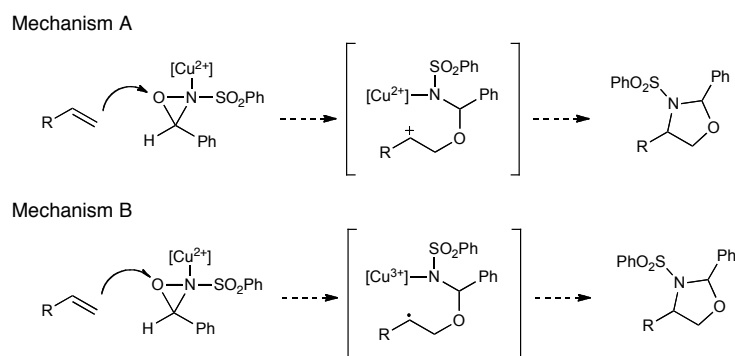


Based upon several preliminary experiments, a two-step cationic mechanism in which the copper catalyst serves as a Lewis acid that activates the oxaziridine toward nucleophilic attack was initially proposed for the transformation (Scheme A-2, Mechanism A). An alternative pathway involving a homolytic reaction of the olefin with



the copper(II)-activated oxaziridine could not be ruled out (Scheme A-2, Mechanism B). However, the requirement of a highly oxidized copper(III) intermediate in the absence of a stabilizing ligand environment led us to initially disfavor this mechanism.

**Scheme A-2.** Mechanistic pathways for copper(II)-catalyzed aminohydroxylation



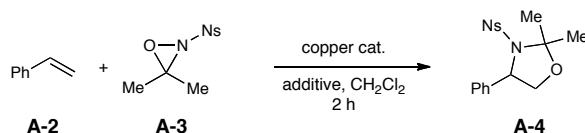
In the course of developing a more reactive catalyst system for the copper(II)-catalyzed aminohydroxylation, we discovered a significant increase in the efficiency of aminohydroxylation upon the addition of salts with coordinating anions. This seemed to suggest that an anionic halocuprate(II) complex formed upon coordination of the anionic additive to CuCl<sub>2</sub> constituted a more reactive catalyst for the aminohydroxylation than the neutral CuCl<sub>2</sub> species itself, which was inconsistent with our mechanistic hypothesis. This contradictory observation at the outset of our studies indicated that a better mechanistic understanding of the aminohydroxylation would be necessary for the development of new copper-catalyzed oxidative functionalization reactions.

## A.2 Results and discussion

Table A-1 shows the effect of salts with coordinating anions on the efficiency of aminohydroxylation using oxaziridine **A-3**. In the presence of CuCl<sub>2</sub> and Bu<sub>4</sub>N<sup>+</sup>Cl<sup>-</sup>, the

reaction proceeded to completion in 2 h (entry 1). Control experiments showed that no reaction occurs in the absence of copper(II) additives (entry 2), which rules out the possibility that the aminohydroxylation could be catalyzed by the halide alone.<sup>4</sup> Reactions using tetrabutylammonium salts of non-coordinating anions were inefficient (entry 3), whereas a variety of additives possessing coordinating anions were also capable of increasing the rate of aminohydroxylation (entries 4 and 5). These results suggest that a more active halocuprate(II) complex is formed upon coordination of an anionic additive to  $\text{CuCl}_2$ . However, it seemed unlikely that the anionic  $\text{CuCl}_3^-$  fragment would be a more powerful Lewis acid than a neutral  $\text{CuCl}_2\cdot\text{HMPA}$  complex. Thus, we wondered if the observed anion acceleration effect suggested a redox-non-innocent role for the copper catalyst and if a different mechanism involving the intermediacy of a radical species might be operative instead.

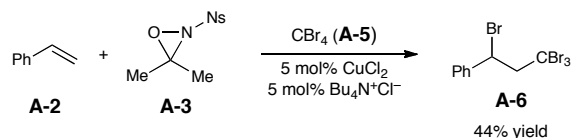
**Table A-1.** Effect of additives on copper-catalyzed aminohydroxylation using 3,3-dialkyl oxaziridine **A-3**



| entry | copper source          | additive                                     | yield |
|-------|------------------------|--|-------|
| 1     | 5 mol% $\text{CuCl}_2$ | 6 mol% $\text{Bu}_4\text{N}^+\text{Cl}^-$    | 80%   |
| 2     | none                   | 6 mol% $\text{Bu}_4\text{N}^+\text{Cl}^-$    | <5%   |
| 3     | 5 mol% $\text{CuCl}_2$ | 6 mol% $\text{Bu}_4\text{N}^+\text{ClO}_4^-$ | <5%   |
| 4     | 5 mol% $\text{CuCl}_2$ | 6 mol% $\text{Bu}_4\text{N}^+\text{Br}^-$    | 59%   |
| 5     | 5 mol% $\text{CuCl}_2$ | 6 mol% $\text{Bu}_4\text{N}^+\text{OAc}^-$   | 70%   |

To probe the feasibility of a radical mechanism, we first investigated the possibility that an exogenous trapping reagent might intercept the putative benzylic radical intermediate. The strongly oxidizing conditions of the aminohydroxylation severely limited the options for a radical trap; most standard trapping agents such as TEMPO and trialkyltin hydrides are rapidly oxidized by the oxaziridine under the reaction conditions. Ultimately, we found that carbon tetrabromide, although stable to both the oxaziridine and the copper(II) catalyst alone, could inhibit formation of the aminohydroxylation product. In the presence of excess  $\text{CBr}_4$  (**A-5**), we observed exclusive formation of Kharasch addition product **A-6** (Scheme A-3).<sup>5</sup> No reaction was observed in the absence of the oxaziridine. These data are consistent with interception of a short-lived benzylic radical intermediate by carbon tetrabromide, which would generate tribromomethyl radical and initiate the radical chain addition of  $\text{CBr}_4$  across the styrenic bond. This experiment provides strong evidence that a radical species is indeed generated under the reaction conditions, although we could not demonstrate that this radical was a productive intermediate en route to the aminohydroxylation product.

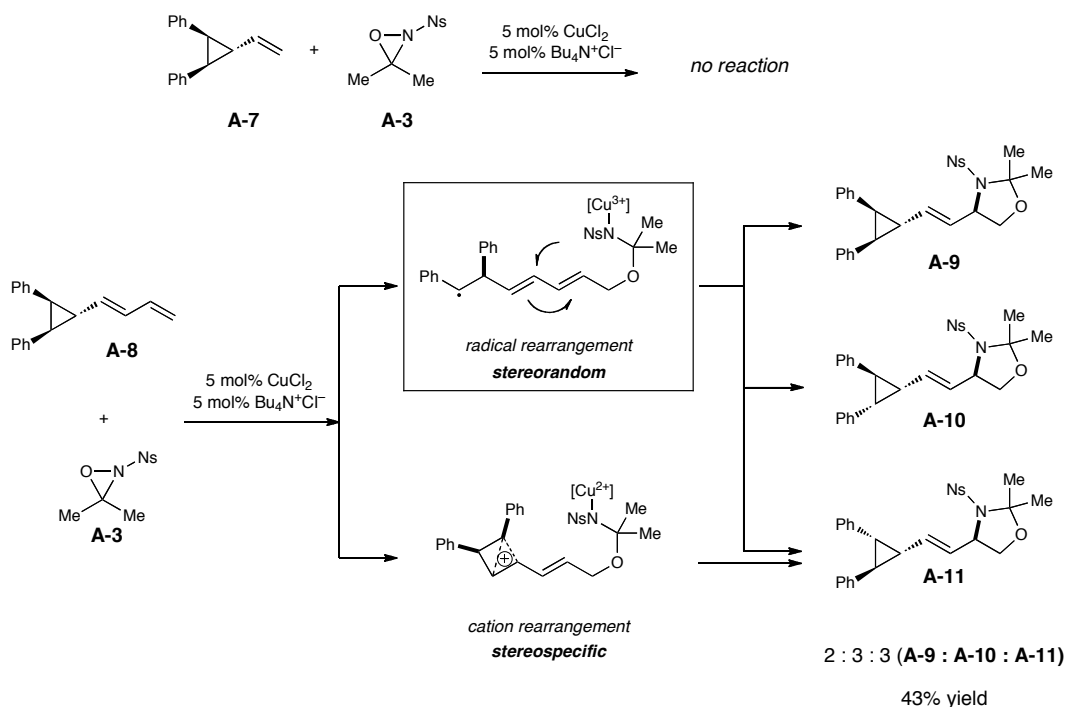
**Scheme A-3.** Trapping experiment with  $\text{CBr}_4$  (**A-5**)



We next examined the aminohydroxylation of cyclopropane-substituted alkenes in an attempt to observe products arising from ring opening of a cyclopropylcarbonyl radical (Scheme A-4). *cis*-1,2-Diphenyl-3-vinylcyclopropane **A-7** was unreactive under our optimized reaction conditions. On the other hand, the analogous 1-(*cis*-2,3-

diphenylcyclopropyl)butadiene **A-8** reacted smoothly under the same conditions and produced the aminohydroxylation products in 43% isolated yield. Surprisingly, we obtained a 2:3:3 mixture of three diastereomeric products (**A-9–A-11**) possessing varying stereochemistry about the cyclopropane. Control reactions indicated that the stereochemical fidelity of the *cis*-diphenylcyclopropane unit was preserved when diene substrate **A-8** was subjected to the copper catalyst and when the isomerically pure product **A-9** was isolated and resubjected to the reaction conditions. Stereomutation of the cyclopropane must therefore occur at an intermediate en route to the aminohydroxylation products.

**Scheme A-4.** Radical trapping experiments with cyclopropane **A-8**



These studies provide strong evidence for a radical intermediate, as proposed in Mechanism B. The diastereomeric mixture of products obtained in this experiment is

consistent with ring-opening of a cyclopropylcarbinyl radical to afford an acyclic intermediate where the stereochemical fidelity of the cyclopropane ring is lost. This is in contrast to cyclopropylcarbinyl *cations*, which are nonclassical;<sup>6</sup> their rearrangements are stereospecific in nature.<sup>7</sup> Therefore, the lack of stereochemical integrity in this experiment seems inconsistent with cationic Mechanism A and is better explained by radical Mechanism B.

### A.3 Conclusions

The oxaziridine-mediated copper-catalyzed aminohydroxylation reaction recently developed in our laboratories is significantly accelerated in the presence of anionic additives. The discovery that anionic halocuprate(II) complexes are the catalytically active species responsible for the increased reactivity under these conditions led us to re-evaluate our mechanistic proposal for the aminohydroxylation. On the basis of a variety of radical trapping experiments, we now propose a modified mechanism that involves homolytic reaction of the olefin with a copper(II)-activated oxaziridine. Together, the observation that anionic additives dramatically increase the oxidizing ability of oxaziridines and the recognition of the radical nature of reactions of oxaziridines under these conditions suggest that a variety of new oxidative transformations catalyzed by halocuprate(II) complexes should be possible.<sup>8</sup>

### A.4 Contributions

Dr. Tamas Benkovics discovered the anion-acceleration effect and optimized reaction conditions for the aminohydroxylation reaction with oxaziridine **A-3**.

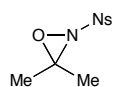
## A.5 Experimental

### A.5.1 General information

Acetonitrile and  $\text{CH}_2\text{Cl}_2$  were distilled from  $\text{CaH}_2$  immediately prior to use. Toluene was distilled from sodium immediately prior to use. Diethyl ether was distilled from sodium metal and benzophenone immediately before use. Oxaziridine **A-3** was prepared as previously described.<sup>9</sup> Anhydrous tetrabutylammonium salts were prepared by azeotropic removal of water from toluene solutions of the commercially available hydrates. Styrene and  $\text{Et}_3\text{N}$  were distilled prior to use. Flash column chromatography<sup>10</sup> was performed using Purasil 60 Å silica gel (230–400 mesh). All glassware was oven-dried at 130 °C for at least 1 h or flame-dried immediately prior to use.

Diastereomer ratios for all compounds were determined by  $^1\text{H}$  NMR analysis of the unpurified reaction mixtures. All NMR spectra were obtained at ambient temperature on the Varian Unity-500 and Varian Inova-500 spectrometers. Chemical shifts are reported in parts per million ( $\delta$ ) relative to TMS (0.0 ppm) for  $^1\text{H}$  NMR data and  $\text{CDCl}_3$  (77.23 ppm) for  $^{13}\text{C}$  NMR data. IR spectral data were obtained using a Bruker Vector 22 spectrometer. Mass spectrometry was performed with a Micromass LCT (electrospray ionization, time-of-flight analyzer or electron impact). These facilities are funded by the NSF (CHE-9974839, CHE-9304546), NIH (RR08389-01) and the University of Wisconsin.

### A.5.2 Synthesis and characterization of new compounds



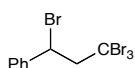
***N*-(4-Nitrobenzenesulfonyl)-3,3-dimethyloxaziridine (A-3).** Prepared using a modification of the method of Jennings.<sup>11</sup> A dry 250 mL round-bottomed

flask was charged with 4-nitrophenyl disulfide (20 g, 65 mmol), a stirbar, 30 mL CH<sub>2</sub>Cl<sub>2</sub>, anhydrous acetic acid (8.2 mL, 143 mmol) and cooled to 0 °C. Sulfuryl chloride (27 mL, 320 mmol) was added dropwise over 45 min via an addition funnel and the resulting slurry stirred for 1 h at 0 °C, at rt for 1 h, and finally at reflux for 7.5 h. The solvent was then removed *in vacuo* and the resulting red solid placed under vacuum overnight.

To the sulfinyl chloride was added 210 mL of ether and the reaction mixture vigorously stirred under nitrogen until all of the solids were dissolved. A separate dry 1 L round-bottomed flask was charged with acetone oxime (9.34 g, 128 mmol), 280 mL ether, Et<sub>3</sub>N (18 mL, 128 mmol) a stirbar and cooled to 0 °C. To this dissolved oxime solution was added the dissolved sulfinyl chloride dropwise, followed by an additional 210 mL of ether. Upon completion of the addition, the reaction was warmed to rt and allowed to stir for 4 h. The solids were then removed by filtration and washed with ether and toluene. The filtrates were concentrated *in vacuo* to yield the *N*-nitrobenzenesulfonyl acetone imine in toluene as a yellow solution and immediately subjected to oxidation.

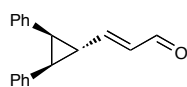
A 4 L Erlenmeyer flask, equipped with a mechanical stirrer and charged with a solution of K<sub>2</sub>CO<sub>3</sub> (150 g, 1.09 mol) in 1 L water, was cooled to 0 °C. The imine solution in toluene (~0.9 L) and a solution of Oxone<sup>®</sup> (150 g, 243 mmol) in 1 L water were added simultaneously to the reaction via addition funnel over 5 min with vigorous stirring. After 15 min, the phases were separated and the aqueous layer extracted with toluene. The combined organics were washed with water, dried over MgSO<sub>4</sub> and concentrated. Purification with chromatography with 4:1 hexanes:EtOAc followed by recrystallization (1:1 hexanes:EtOAc) yielded the oxaziridine as pale yellow crystals (16.7 g, 64.8 mmol,

50% yield). IR (neat) 3118, 1538, 1351, 1305, 1172;  $^1\text{H}$  NMR (500 MHz,  $\text{CDCl}_3$ )  $\delta$  8.43 (dt,  $J$  = 9.2, 2.4 Hz, 2H), 8.20 (dt,  $J$  = 9.5, 2.4 Hz, 2H), 2.11 (s, 3H), 1.6 (s, 3H);  $^{13}\text{C}$  NMR (125 MHz,  $\text{CDCl}_3$ )  $\delta$  151.2, 143.7, 129.8, 124.6, 88.6, 77.5, 77.3, 77.2, 77.1, 77.0, 26.1, 19.5; HRMS ( $\text{EI}^+$ ) calc'd for  $[\text{C}_9\text{H}_{10}\text{N}_2\text{O}_5\text{SNa}]^+$  requires  $m/z$  281.0203, found  $m/z$  281.0208. (mp = 120–121 °C (dec.)).



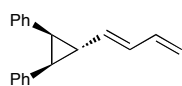
**Carbon tetrabromide radical trap experiment.** In a nitrogen-atmosphere glovebox, a 2 dram vial was charged with copper(II) chloride (3.3 mg, 0.025 mmol) and tetrabutylammonium chloride (7.0 mg, 0.025 mmol). The vial was capped with a septum and transferred out of the glovebox. 0.25 mL of  $\text{CH}_2\text{Cl}_2$  was added and the reaction mixture allowed to stir under argon for 30 min. Styrene (48.7 mg, 0.47 mmol) was then added via syringe and the septum was removed quickly to add *N*-nitrobenzenesulfonyl 3,3-dimethyloxaziridine (199 mg, 0.77 mmol),  $\text{CBr}_4$  (1.32 g, 3.98 mmol) and 0.75 mL of  $\text{CH}_2\text{Cl}_2$ . The vial was flushed with argon, sealed, and allowed to stir for 6 h. Upon completion of the reaction, the remaining oxaziridine was quenched with dimethyl sulfide, the solvent removed by rotary evaporation, and the resulting residue loaded directly onto silica for purification by flash column chromatography with 20:1 hexanes:EtOAc as the eluent to yield (1,3,3,3-tetrabromopropyl)benzene (**A-6**) as a white solid (84 mg, 0.20 mmol, 44% yield).  $^1\text{H}$  NMR (300 MHz,  $\text{CDCl}_3$ )  $\delta$  7.48 (m, 2H), 7.34 (m, 3H), 5.32 (dd,  $J$  = 7.5, 4.3 Hz, 1H), 4.08 (AB,  $J$  = 7.5, 4.3 Hz, 2H);  $^{13}\text{C}$  NMR (75 MHz,  $\text{CDCl}_3$ )  $\delta$  141.1, 129.3, 129.2, 128.5, 66.8, 50.4, 35.4 HRMS ( $\text{EI}^+$ ) calc'd for  $[\text{C}_9\text{H}_8\text{Br}_4]^+$  requires  $m/z$  431.7354, found  $m/z$  431.7344.





***trans*-2, *trans*-3-Diphenylcyclopropane vinyl aldehyde.**

A dry round-bottomed flask was charged with *trans*-2, *trans*-3-diphenylcyclopropane carboxaldehyde (710 mg, 3.2 mmol), (triphenylphosphoranylidene)acetaldehyde (922 mg, 3.0 mmol), and benzene (19 mL). The orange suspension was heated to reflux for 8 h, concentrated and purified by flash column chromatography on silica gel with 4:1 hexanes:EtOAc as the eluent to yield 675 mg of the product as a yellow solid (2.72 mmol, 90% yield). IR (neat) 3030, 2829, 1678, 1632, 1496;  $^1\text{H}$  NMR (500 MHz,  $\text{CDCl}_3$ )  $\delta$  9.54 (d,  $J$  = 8.2 Hz, 1H), 7.14 (m, 6H), 6.93 (dd,  $J$  = 7.9, 2.1 Hz, 4H), 6.71 (dd,  $J$  = 15.5, 9.6 Hz, 1H), 6.36 (dd,  $J$  = 15.2, 7.6 Hz, 1H), 2.84 (d,  $J$  = 5 Hz, 2H), 2.60 (dt,  $J$  = 9.8, 5.6 Hz, 1H);  $^{13}\text{C}$  NMR (125 MHz,  $\text{CDCl}_3$ )  $\delta$  193.2, 160.6, 135.9, 131.2, 129.0, 128.3, 126.8, 35.4, 30.4; HRMS ( $\text{EI}^+$ ) calc'd for  $[\text{C}_{18}\text{H}_{16}\text{O}]^+$  requires  $m/z$  248.1196, found  $m/z$  248.1198. (mp = 105–107 °C).

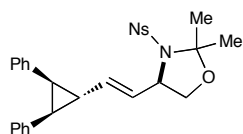


***trans*-2, *trans*-3-Diphenylcyclopropane 1-butadiene (A-8).**

A dry round-bottomed flask was charged with methyltriphenylphosphonium bromide (267 mg, 0.75 mmol) and THF (2.6 mL) and cooled to 0 °C. *n*-Butyllithium (0.75 mL, 0.87 mmol) was then added dropwise. To the resulting yellow suspension was added *trans*-2, *trans*-3-diphenylcyclopropane carboxaldehyde (186 mg, 0.75 mmol) in THF (5.3 mL) dropwise and the reaction was allowed to warm to rt. After 2 h, the reaction mixture was concentrated and purified by flash column chromatography on silica gel with 9:1 hexanes:EtOAc as the eluent to yield 150 mg of the product as a yellow oil (0.61 mmol, 81% yield). IR (thin film) 3085, 3026, 1648, 1603, 1496, 1446;  $^1\text{H}$  NMR (500 MHz,  $\text{CDCl}_3$ )  $\delta$  7.1 (m, 6H), 6.92 (dt,  $J$  = 6.7, 1.4 Hz, 4H), 6.35 (m, 2H), 5.67

(dd,  $J = 14.8, 8.3$  Hz, 1H), 5.15 (dd,  $J = 16.0, 1.9$  Hz, 1H), 5.00 (dd,  $J = 9.8, 2.3$  Hz, 1H), 2.56 (d,  $J = 5.6$  Hz, 2H), 2.33 (dt,  $J = 8.3, 5.9$  Hz, 1H);  $^{13}\text{C}$  NMR (125 MHz,  $\text{CDCl}_3$ ) 137.6, 137.0, 136.6, 130.2, 129.1, 128.0, 126.1, 115.3, 33.5, 29.6; HRMS ( $\text{EI}^+$ ) calc'd for  $[\text{C}_{19}\text{H}_{18}]^+$  requires  $m/z$  246.1404, found  $m/z$  246.1405.

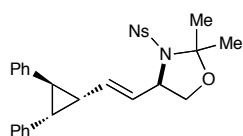
**Aminohydroxylation of *trans*-2, *trans*-3-diphenylcyclopropane 1-butadiene **A-8**.** In a nitrogen-atmosphere glovebox, a 2 dram vial was charged with 3.0 mg (0.22 mmol) copper(II) chloride, 7.0 mg (0.25 mmol) tetrabutylammonium chloride, and a stirbar. The vial was capped with a septum and transferred out of the glovebox. 0.92 mL  $\text{CH}_2\text{Cl}_2$  was added and the reaction mixture was allowed to stir under argon for 30 min. 115 mg (0.47 mmol) *trans*-2, *trans*-3-Diphenylcyclopropane 1-butadiene **A-8** was added and the vial flushed with argon, sealed and allowed to stir for 5 h. Upon completion of the reaction, the remaining oxaziridine was quenched with dimethyl sulfide, the reaction mixture concentrated, and the resulting residue purified by flash column chromatography on silica gel with 9:1:1 hexanes:EtOAc:acetone as the eluent to yield 103.5 mg (0.21 mmol, 44% yield) of a mixture of diastereomers (2:3:3 **A-9:A-10:A-11**) as an off-white oil. Multiple purification attempts resulted in the isolation of the three diastereomers characterized below.



***N*-(4-Nitrobenzensulfonyl)-4-[*cis*-(*trans*-2,*trans*-3-diphenylcyclopropylvinyl)]-2,2-dimethyl-1,3-oxazoline (**A-9**).** Isolated as a yellow semi-solid. IR (thin film) 3027, 2986, 1530, 1329, 1162;  $^1\text{H}$

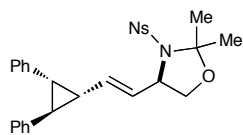
NMR (500 MHz,  $\text{CDCl}_3$ )  $\delta$  8.02 (dd,  $J = 22.9, 9.1$  Hz, 4H), 7.11 (m, 6H), 6.83 (dd,  $J =$

25.3, 6.4 Hz, 4H), 5.53 (dd,  $J = 14.9, 8.5$  Hz, 1H), 5.29 (dd,  $J = 15.5, 9.4$  Hz, 1H), 4.44 (m, 1H), 4.19 (dd,  $J = 9.2, 6.4$  Hz, 1H), 3.78 (dd,  $J = 8.8, 3.3$  Hz, 1H), 2.43 (m, 2H), 2.07 (m, 1H), 1.72 (d,  $J = 3.5$  Hz, 6H);  $^{13}\text{C}$  NMR (125 MHz,  $\text{CDCl}_3$ )  $\delta$  149.9, 148.0, 137.7, 136.7, 136.6, 129.3, 129.1, 128.6, 128.3, 128.2, 126.6, 126.5, 126.4, 124.1, 98.8, 69.6, 62.0, 33.1, 33.1, 28.3, 28.1, 26.9; HRMS ( $\text{EI}^+$ ) calc'd for  $[\text{C}_{28}\text{H}_{28}\text{N}_2\text{O}_5\text{SNa}]^+$   $[\text{M}+\text{Na}]^+$  requires  $m/z$  527.1612, found  $m/z$  527.1600.



***N*-(4-Nitrobenzensulfonyl)-4-[*trans*-(*trans*-2,*cis*-3-diphenylcyclopropylvinyl)]-2,2-dimethyl-1,3-oxazoline (A-10).** IR (thin film)

1529, 1349, 1161;  $^1\text{H}$  NMR (500 MHz,  $\text{CDCl}_3$ )  $\delta$  7.91 (s, 4H), 7.38 (t,  $J = 7.1$  Hz, 2H), 7.29 (m, 6H), 7.15 (d,  $J = 7.1$  Hz, 2H), 5.22 (dd,  $J = 15.2, 9.0$  Hz, 1H), 5.14 (dd,  $J = 15.3, 9.3$  Hz, 1H), 4.24 (m, 1H), 4.05 (dd,  $J = 9.0, 6.3$  Hz, 1H), 3.64 (dd,  $J = 8.8, 3.4$  Hz, 1H), 2.71 (dd,  $J = 9.0, 5.9$  Hz, 1H), 2.47 (t,  $J = 5.7$  Hz, 1H), 1.94 (td,  $J = 9.0, 4.7$  Hz, 1H), 1.63 (d,  $J = 9.2$  Hz, 6H);  $^{13}\text{C}$  NMR (125 MHz,  $\text{CDCl}_3$ )  $\delta$  143.3, 136.6, 131.6, 131.5, 131.0, 130.5, 129.3, 128.2, 126.4, 100.9, 97.4, 71.9, 64.4, 36.3, 35.3, 33.2, 30.4, 29.3; HRMS ( $\text{EI}^+$ ) calc'd for  $[\text{C}_{28}\text{H}_{28}\text{N}_2\text{O}_5\text{SNa}]^+$   $[\text{M}+\text{Na}]^+$  requires  $m/z$  527.1612, found  $m/z$  527.1590. (mp = 123–127 °C). The structure was confirmed by X-ray crystallographic analysis.



***N*-(4-Nitrobenzensulfonyl)-4-[*trans*-(*cis*-2,*trans*-3-diphenylcyclopropylvinyl)]-2,2-dimethyl-1,3-oxazoline (A-11).** Isolated as a

white solid. IR (thin film) 2253, 907;  $^1\text{H}$  NMR (500 MHz,  $\text{CDCl}_3$ )  $\delta$  8.12 (d,  $J = 9.1$  Hz,

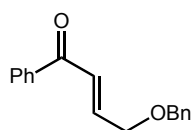
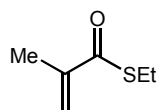
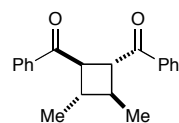
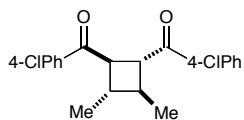
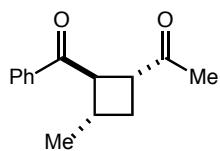
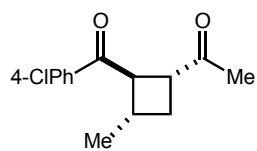
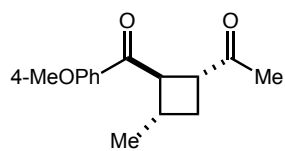
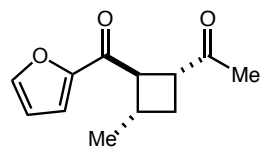
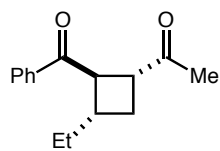
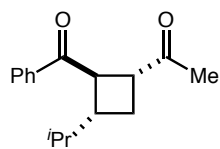
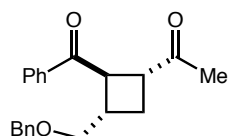
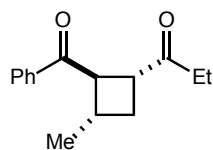
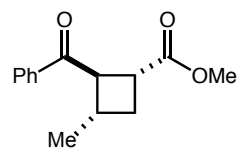
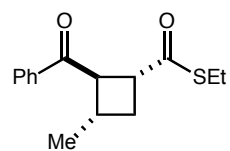
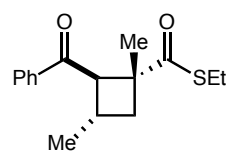
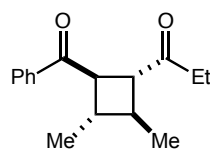
2H), 7.73 (d,  $J$  = 8.9 Hz, 2H), 7.35 (m, 6H), 7.19 (m, 4H), 5.41 (dd,  $J$  = 15.0, 8.1 Hz, 1H), 5.18 (dd,  $J$  = 15.4, 9.6 Hz, 1H), 3.94 (m,  $J$  = Hz, 2H), 3.60 (dd,  $J$  = 8.6, 4.6 Hz, 1H), 2.76 (dd,  $J$  = 9.5, 6.5 Hz, 1H), 2.45 (t,  $J$  = 5.5 Hz, 1H), 2.10 (td,  $J$  = 9.3, 5.1 Hz, 1H), 1.62 (s, 3H), 1.57 (s, 3H);  $^{13}\text{C}$  NMR (125 MHz,  $\text{CDCl}_3$ )  $\delta$  146.5, 141.0, 137.8, 132.8, 129.2, 129.1, 128.8, 128.7, 128.1, 126.9, 126.5, 126.2, 124.1, 98.9, 69.6, 61.8, 33.9, 32.7, 30.4, 29.9, 28.6, 26.2, 0.2; HRMS ( $\text{EI}^+$ ) calc'd for  $[\text{C}_{28}\text{H}_{28}\text{N}_2\text{O}_5\text{SNa}]^+$   $[\text{M}+\text{Na}]^+$  requires  $m/z$  527.1612, found  $m/z$  527.1590. (mp = 128–133 °C).

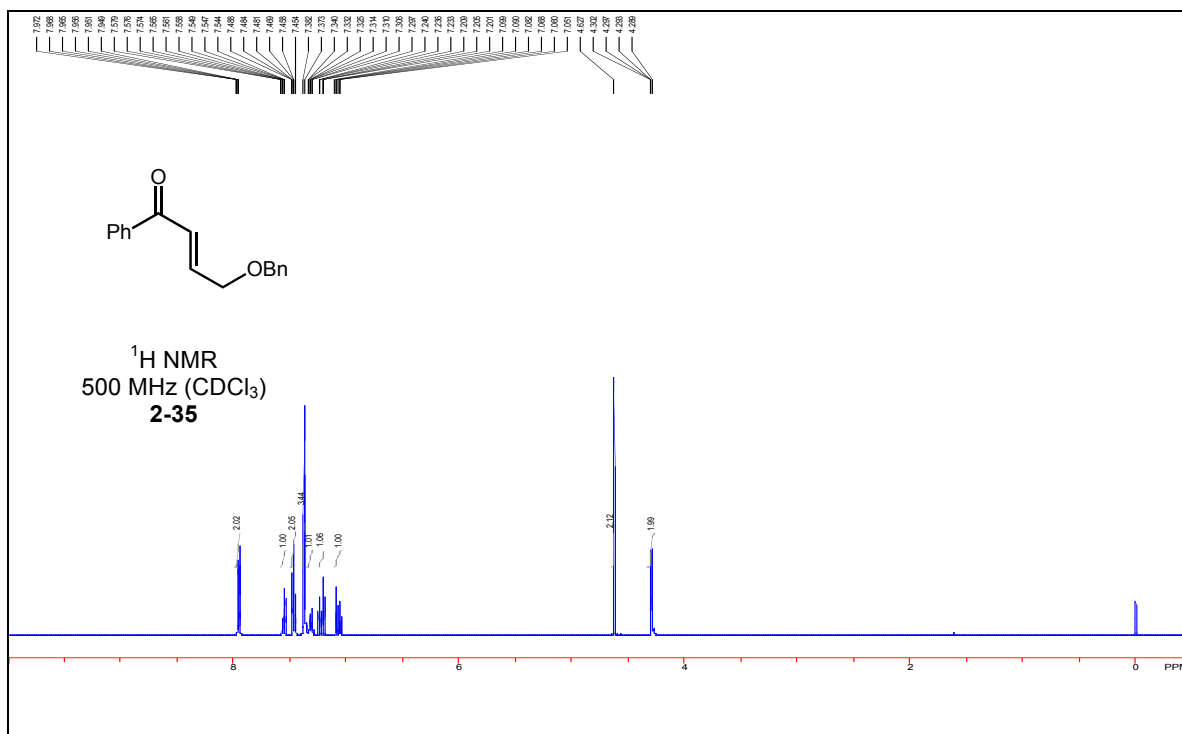
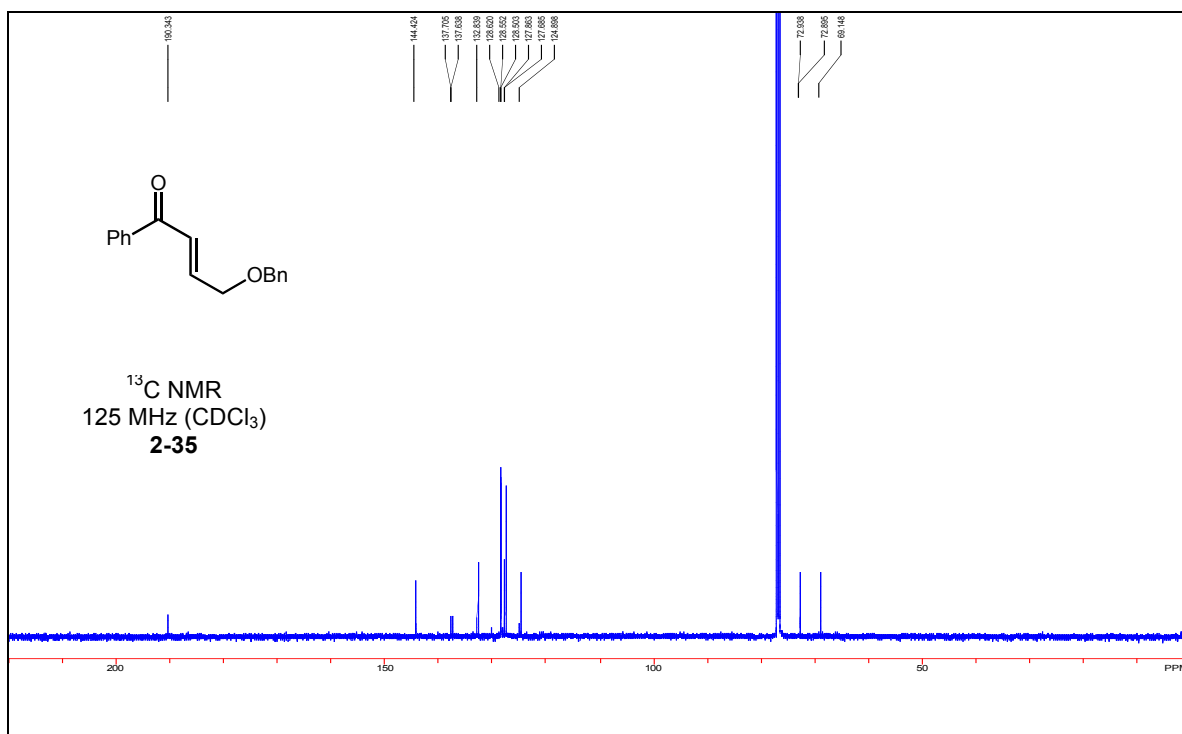
## A.6 References

1. Sharpless, K. B.; Chong, A. O.; Oshima, K. Osmium-catalyzed vicinal oxyamination of olefins by Chloramine-T. *J. Org. Chem.* **1976**, *41*, 177-179.
2. a) Alexanian, E. J.; Lee, C.; Sorensen, E. J. Palladium-Catalyzed Ring-Forming Aminoacetoxylation of Alkenes. *J. Am. Chem. Soc.* **2005**, *127*, 7690-7691. b) Liu, G.; Stahl, S. S. Highly Regioselective Pd-Catalyzed Intermolecular Aminoacetoxylation of Alkenes and Evidence for *cis*-Aminopalladation and  $\text{S}_{\text{N}}2$  C–O Bond Formation. *J. Am. Chem. Soc.* **2006**, *128*, 7179-7181. c) Noack, M.; Gottlich, R. Copper(I) catalysed cyclisation of unsaturated *N*-benzoyloxyamines: an aminohydroxylation *via* radicals. *Chem. Commun.* **2002**, 536-537.
3. a) Michaelis, D. J.; Shaffer, C. J.; Yoon, T. P. Copper(II)-Catalyzed Aminohydroxylation of Olefins. *J. Am. Chem. Soc.* **2007**, *129*, 1866-1867. b) Michaelis, D. J.; Ischay, M. A.; Yoon, T. P. Activation of *N*-Sulfonyl Oxaziridines Using Copper(II) Catalysts: Aminohydroxylations of Styrenes and 1,3-Dienes. *J. Am. Chem. Soc.* **2008**, *130*, 6610-6615. c) Partridge, K. M.; Anzovino, M. E.; Yoon, T. P. Cycloadditions of *N*-Sulfonyl Nitrones Generated by Lewis Acid Catalyzed Rearrangement of Oxaziridines. *J. Am. Chem. Soc.* **2008**, *130*, 2920-2921. d) Partridge, K. M.; Guzei, I. A.; Yoon, T. P. Carbonyl Imines from Oxaziridines: Generation and Cycloaddition of  $\text{N}=\text{O}=\text{C}$  Dipoles. *Angew. Chem. Int. Ed.* **2010**, *49*, 930-934. e) Williamson, K. S.; Yoon, T. P. Iron-Catalyzed Aminohydroxylation of Olefins. *J. Am. Chem. Soc.* **2010**, *132*, 4570-4571.
4. Jeong, J. U.; Tao, B.; Sagasser, I.; Henniges, H.; Sharpless, K. B. Bromine-Catalyzed Aziridination of Olefins. A Rare Example of Atom-Transfer Redox Catalysis by a Main Group Element. *J. Am. Chem. Soc.* **1998**, *120*, 6844-6845.
5. Kharasch, M. S.; Jensen, E. V.; Urry, W. H. Addition of Carbon Tetrabromide and Bromoform to Olefins. *J. Am. Chem. Soc.* **1946**, *68*, 154-155.

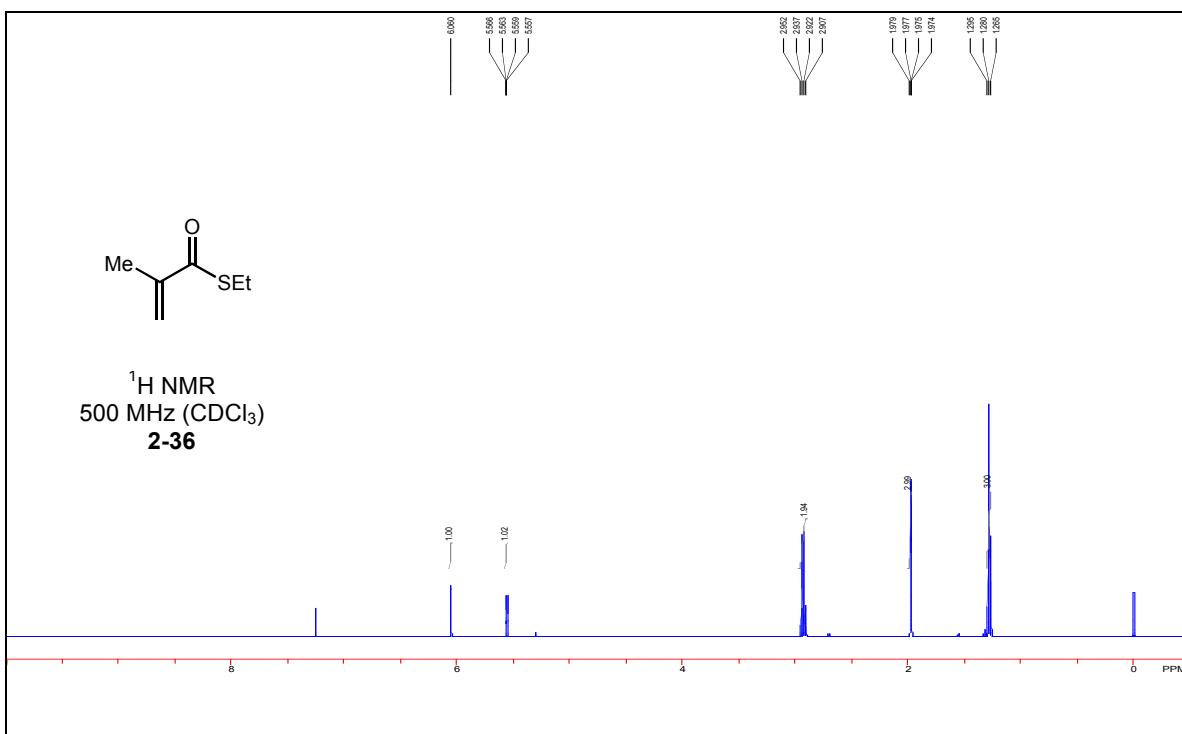
6. Olah, G. A.; Reddy, V. P.; Prakash, G. K. S. Long-lived cyclopropylcarbinyl cations. *Chem. Rev.* **1992**, *92*, 69-95.
7. a) Wiberg, K. B.; Szeimies, G. Stereochemistry of the cyclopropylcarbinyl-cyclopropylcarbinyl rearrangement. *J. Am. Chem. Soc.* **1968**, *90*, 4195-4196. b) Wiberg, K. B.; Szeimies, G. Acid-catalyzed solvolyses of bicyclobutane derivatives. Stereochemistry of the cyclopropylcarbinyl-cyclopropylcarbinyl and related rearrangements. *J. Am. Chem. Soc.* **1970**, *92*, 571-579. c) Schleyer, P. v. R.; Majerski, Z. Stereochemistry of cyclopropylcarbinyl rearrangements. Synthesis and solvolysis of cyclopropylcarbinyl-1,1',1'-*trans*-2,3,3-d<sub>6</sub> methanesulfonate. *J. Am. Chem. Soc.* **1971**, *93*, 665-671.
8. Allen, C. P.; Benkovics, T.; Turek, A. K.; Yoon, T. P. Oxaziridine-Mediated Intramolecular Amination of sp<sup>3</sup>-Hybridized C-H Bonds. *J. Am. Chem. Soc.* **2009**, *131*, 12560-12561.
9. Davis, F. A.; Jenkins Jr, R.; Yocklovich, S. G. 2-Arenesulfonyl-3-aryloxaziridines: A new class of aprotic oxidizing agents (oxidation of organic sulfur compounds). *Tetrahedron Lett.* **1978**, *19*, 5171-5174.
10. Still, W. C.; Kahn, M.; Mitra, A. Rapid chromatographic technique for preparative separations with moderate resolution. *J. Org. Chem.* **1978**, *43*, 2923-2925.
11. Jennings, W. B.; Watson, S. P.; Boyd, D. R. 3,3-Disubstituted 2-sulphonyloxaziridines: synthesis and observation of isomeric nitrogen invertomers. *J. Chem. Soc., Chem. Commun.* **1988**, 931-932.

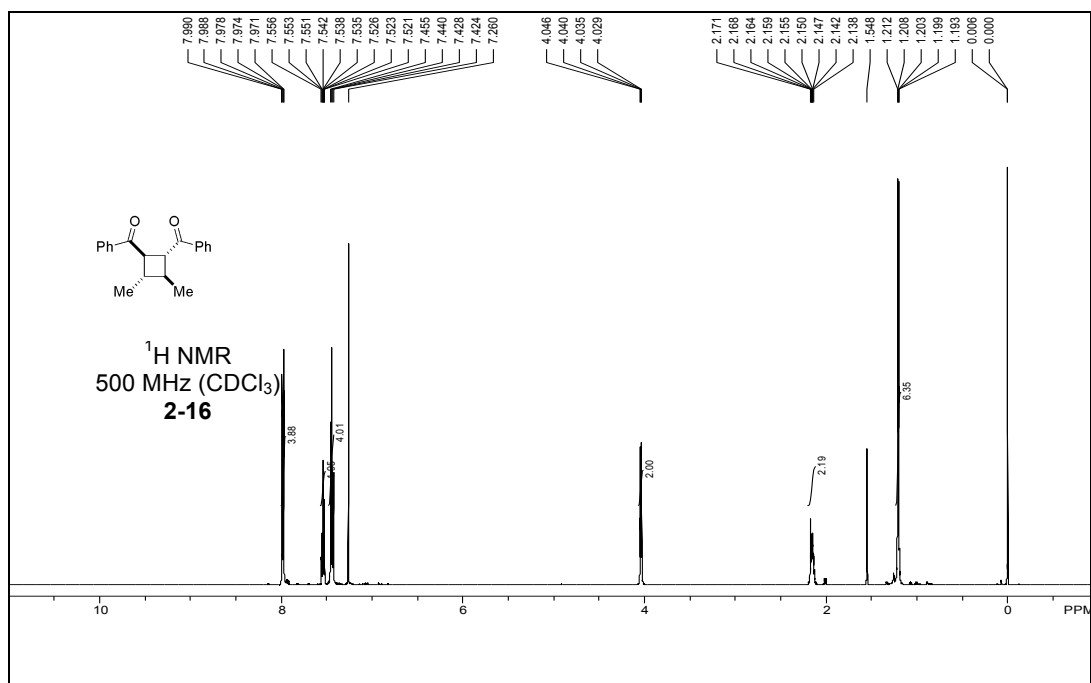
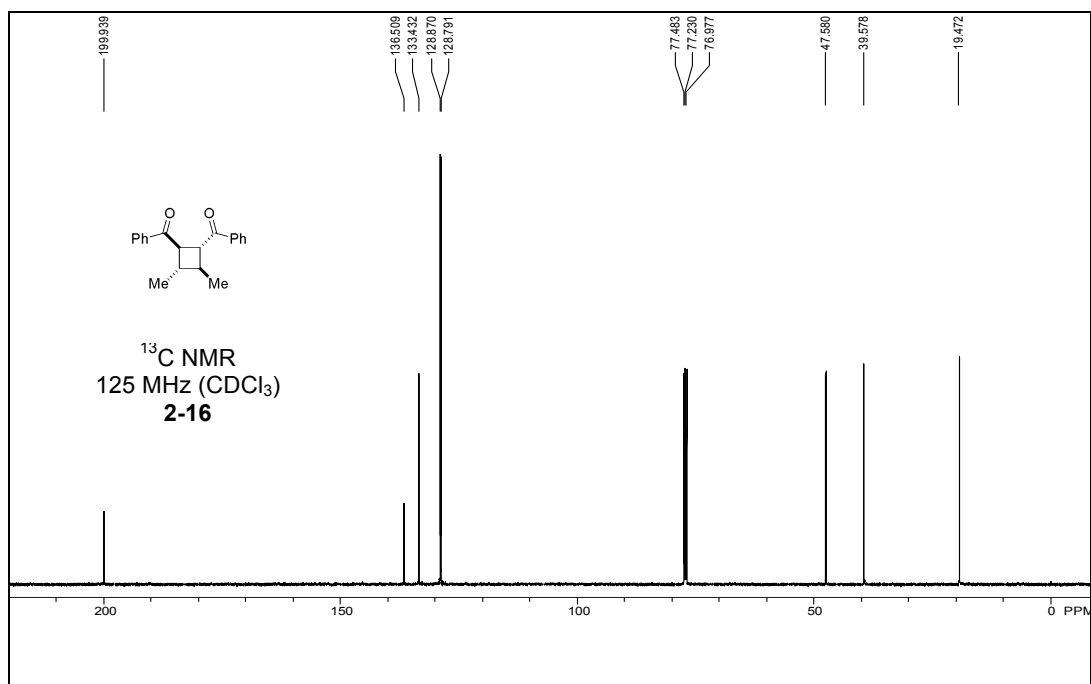
## **Appendix B. $^1\text{H}$ and $^{13}\text{C}$ Spectra for New Compounds**

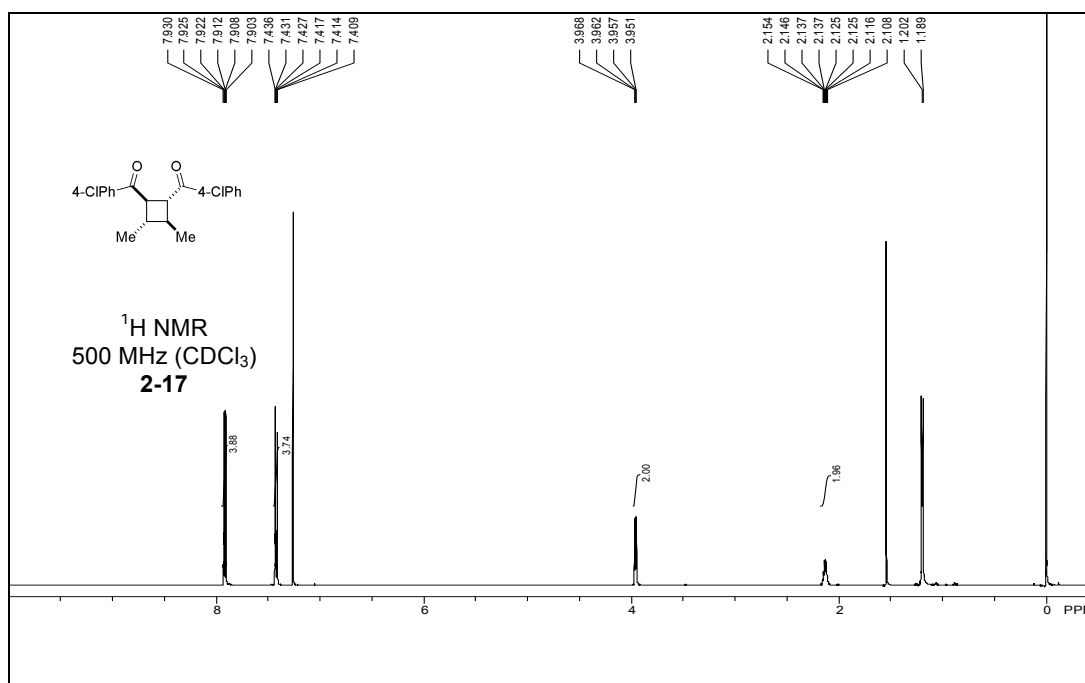
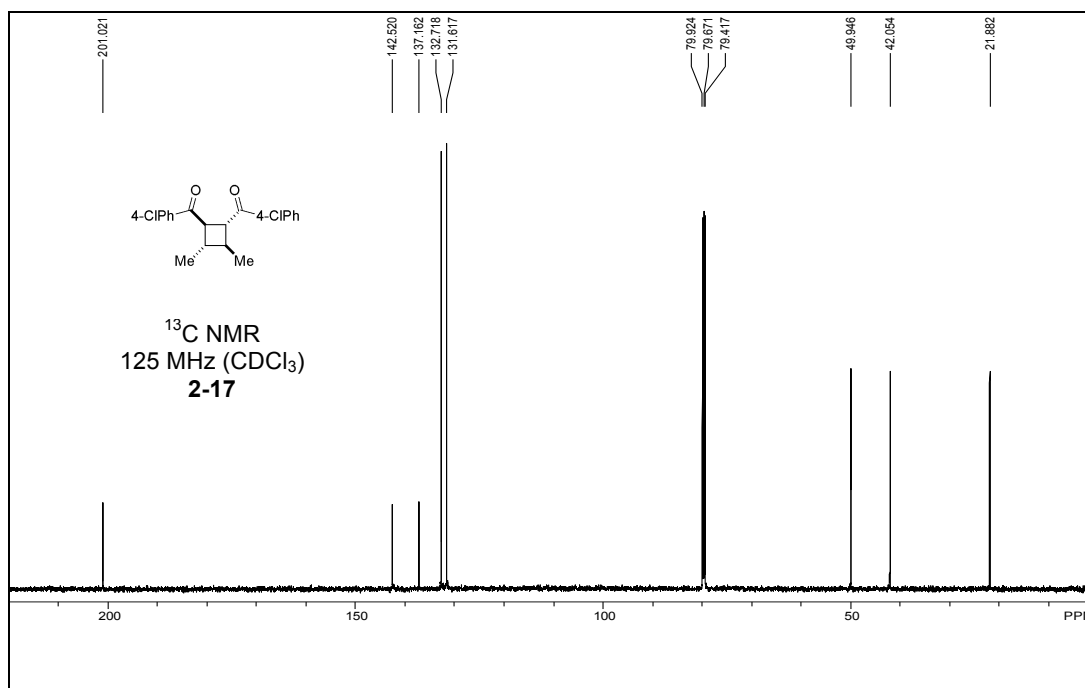
**2-35****2-36****2-16****2-17****2-20****2-22****2-23****2-24****2-26****2-27****2-29****2-30****2-31****2-32****2-33****2-34**

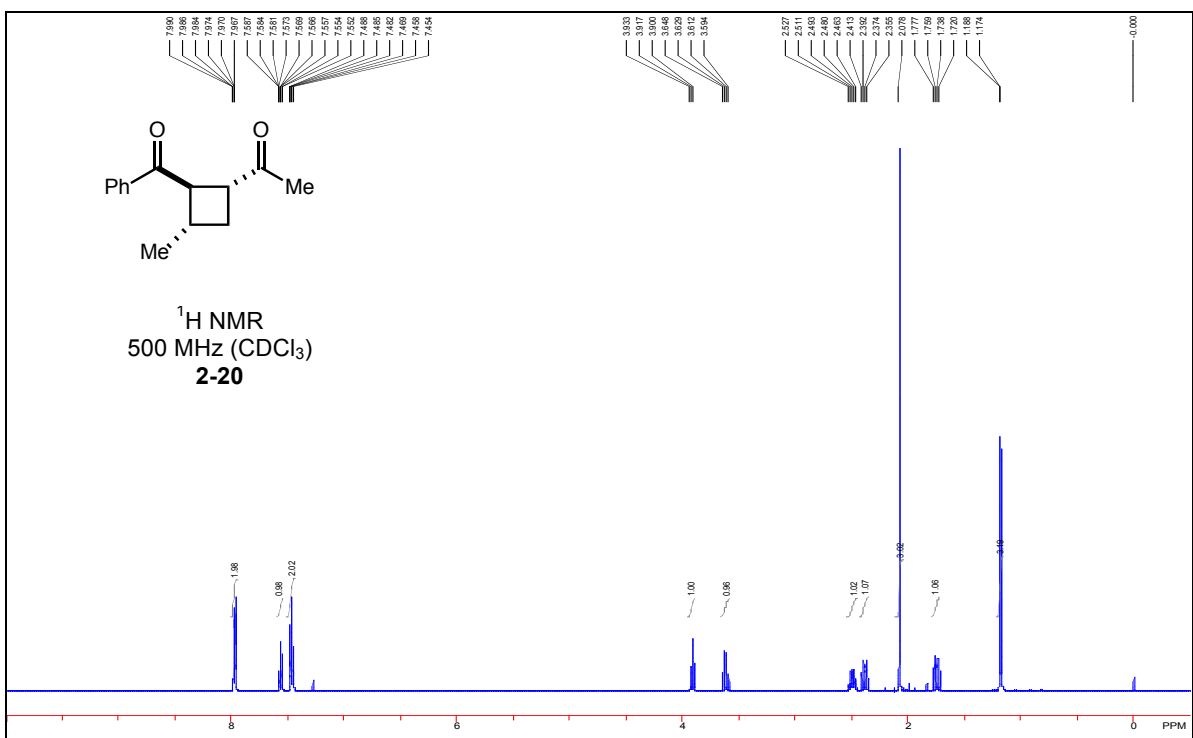


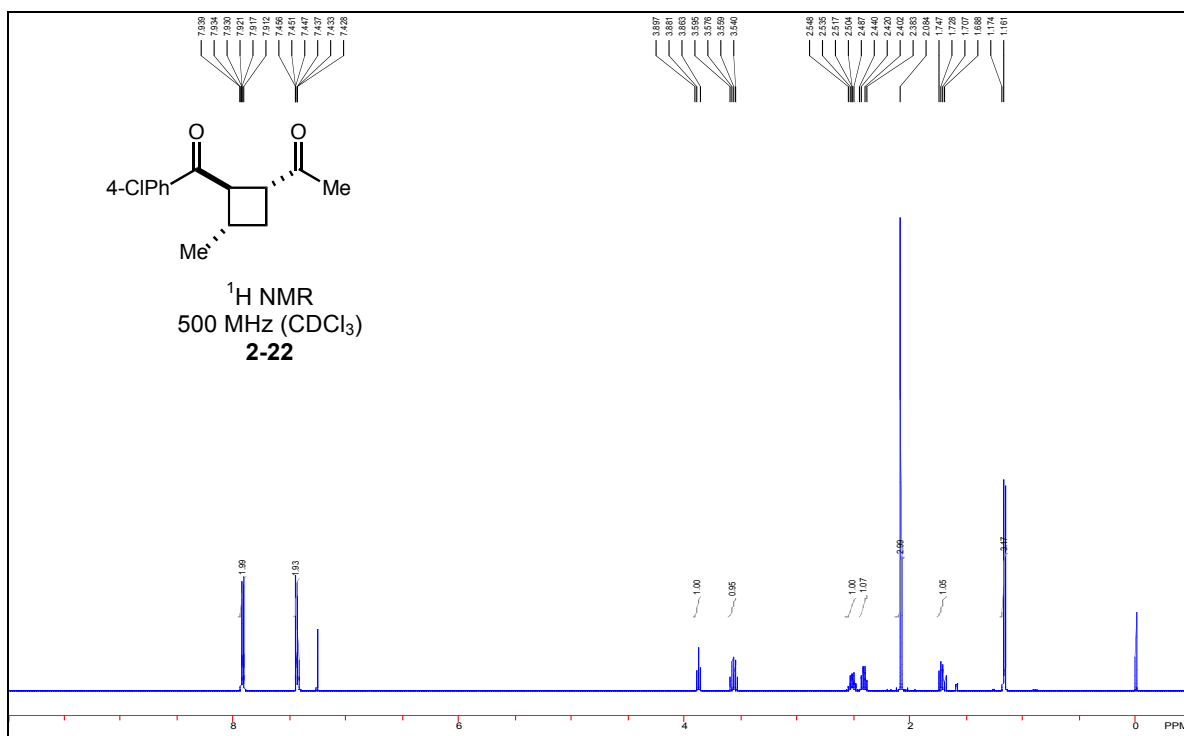
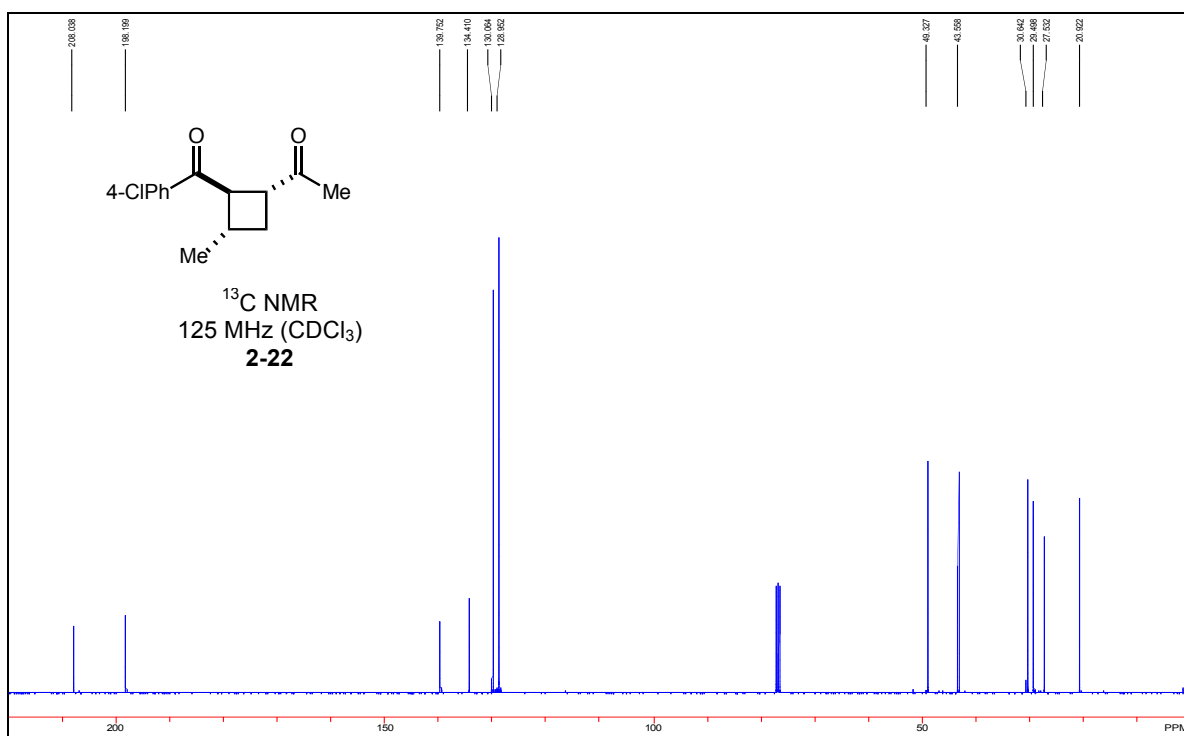


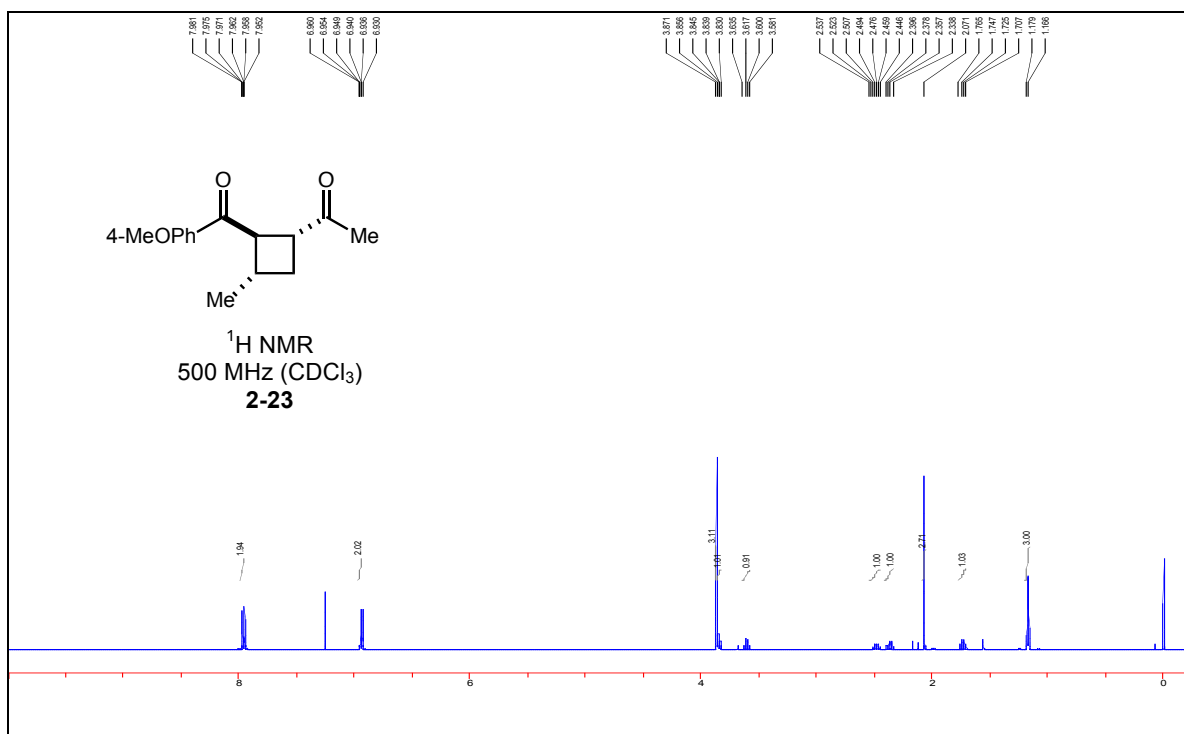
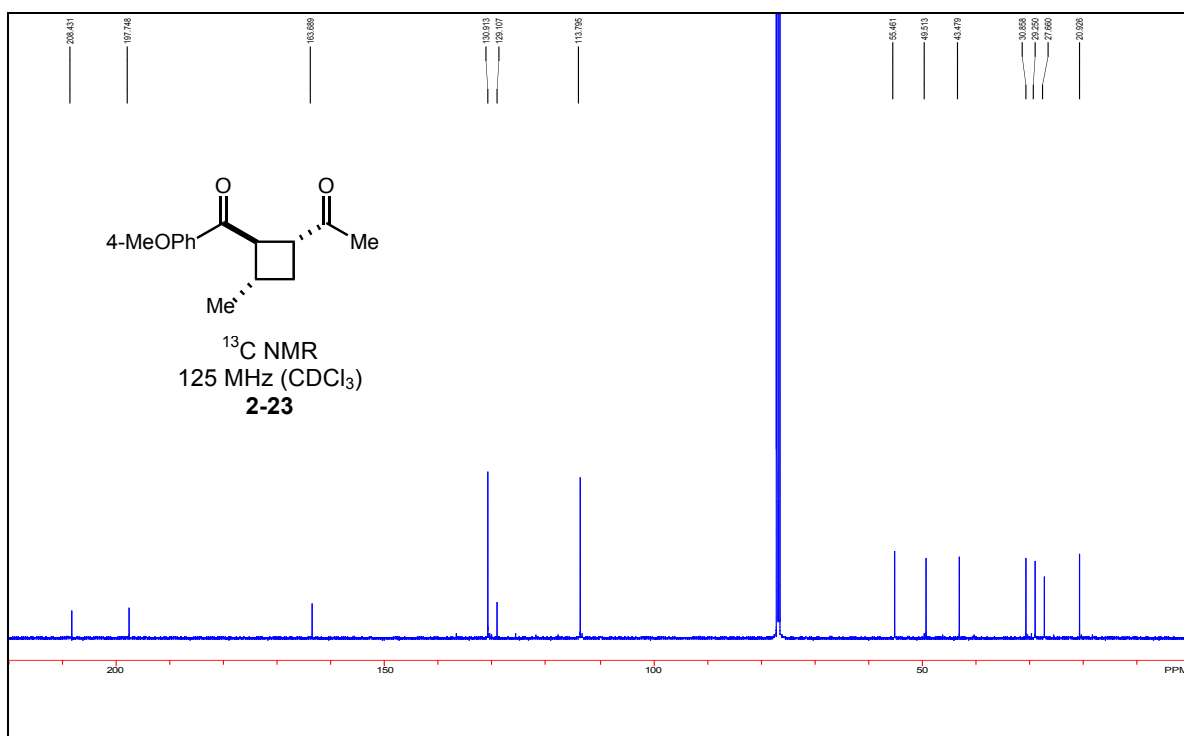


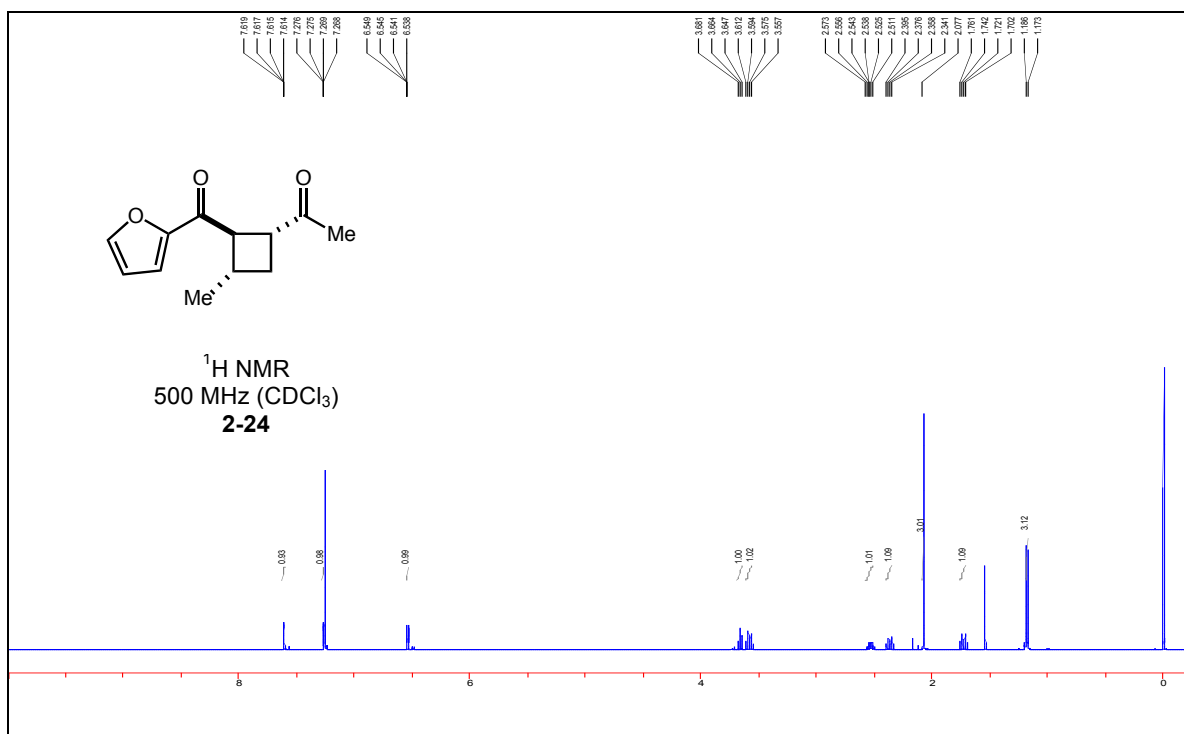
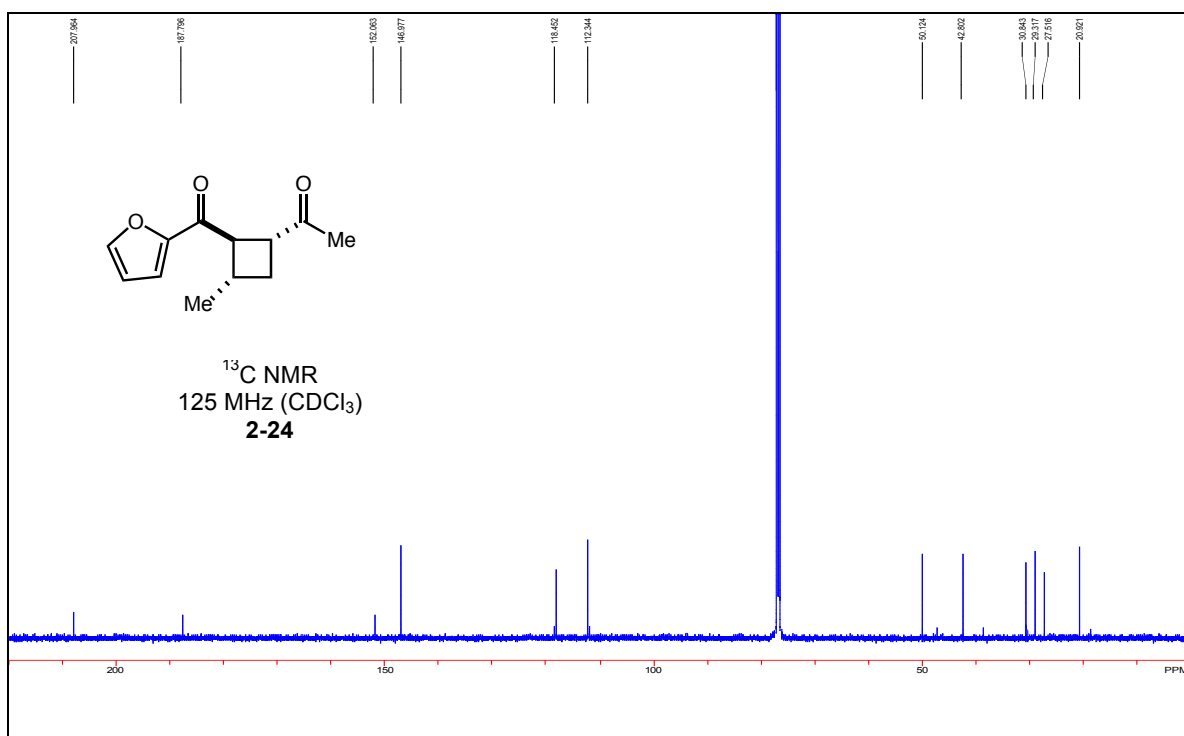


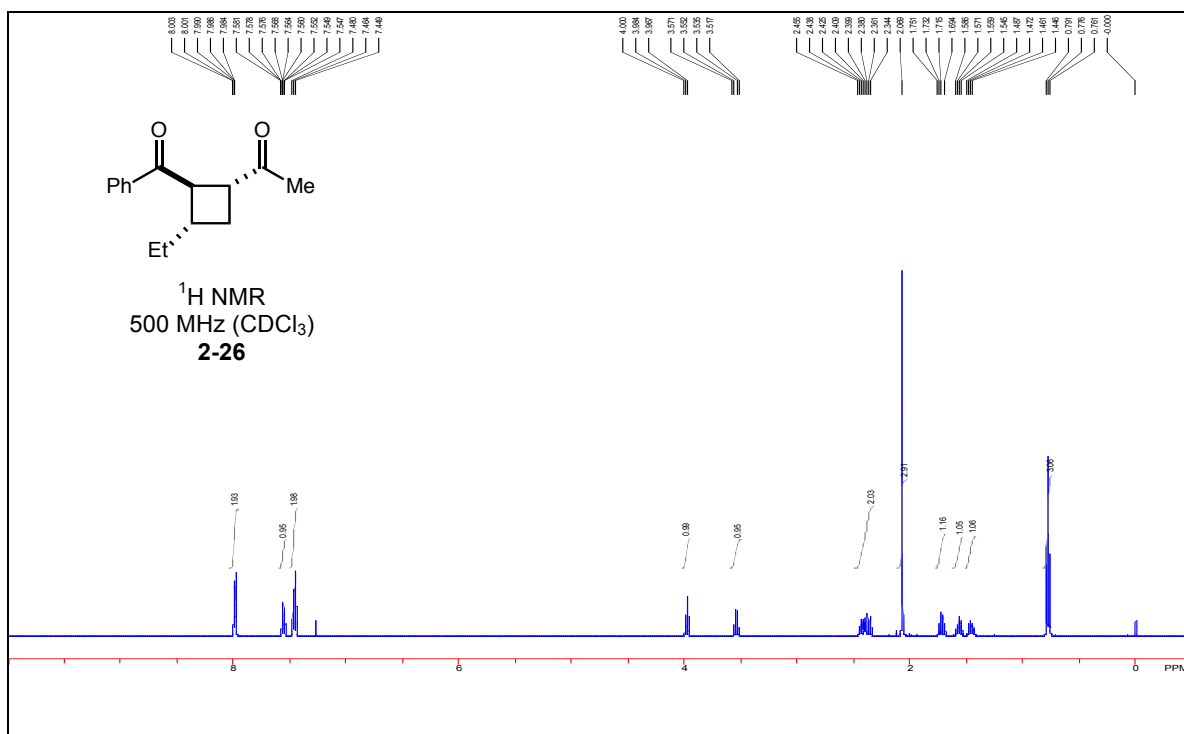
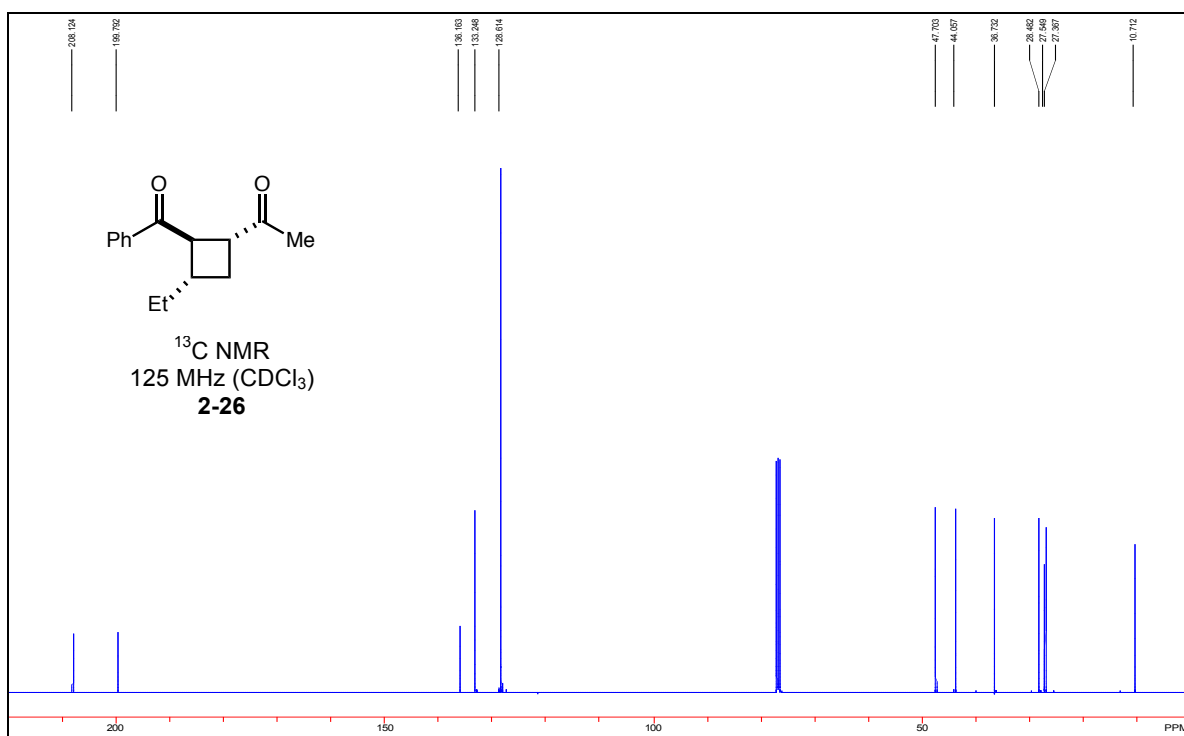




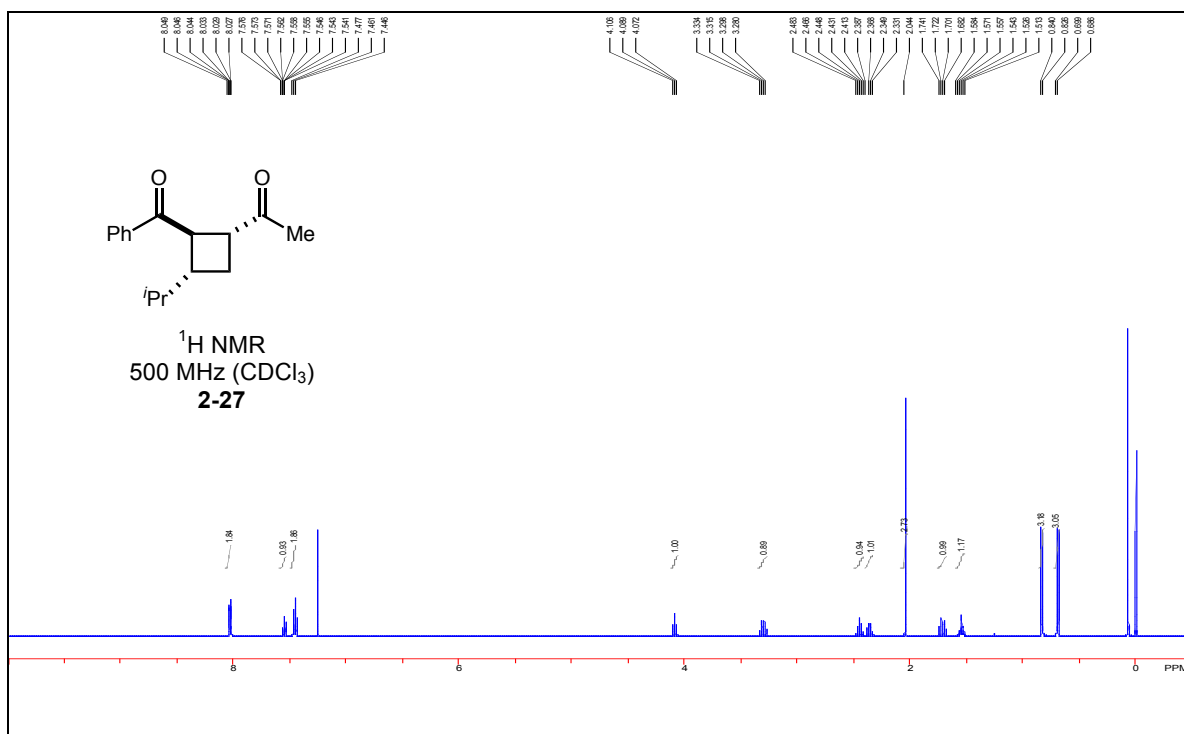
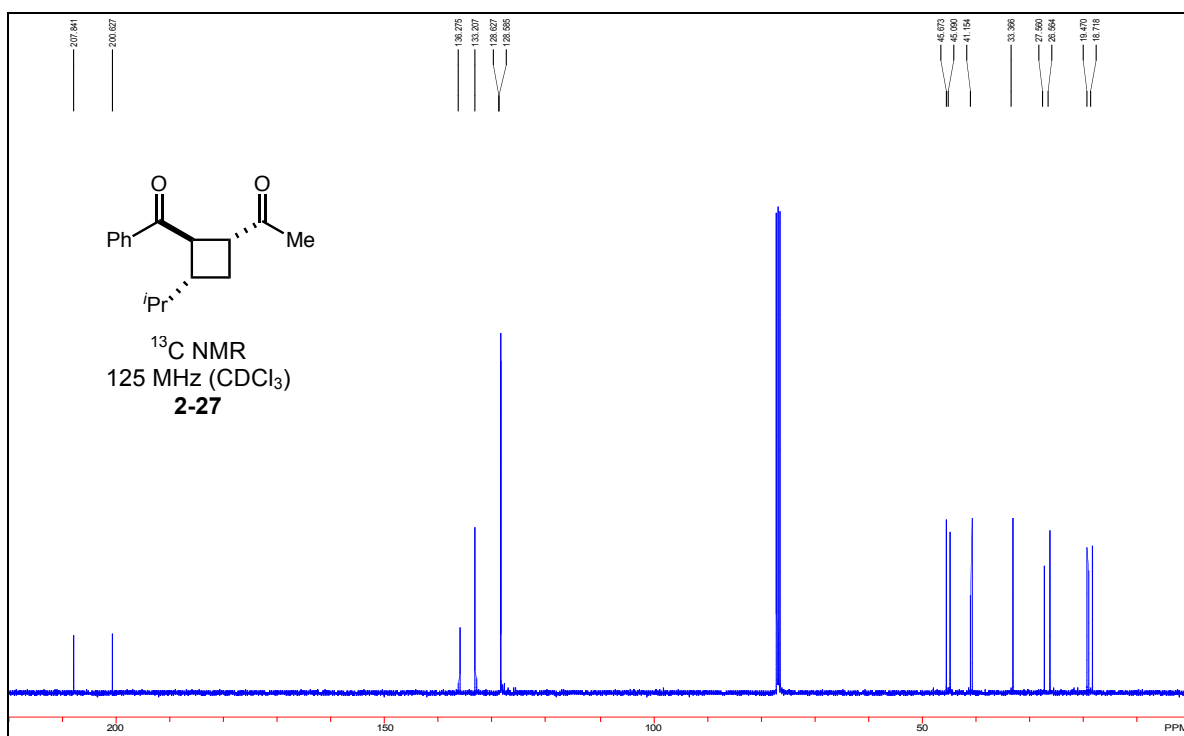


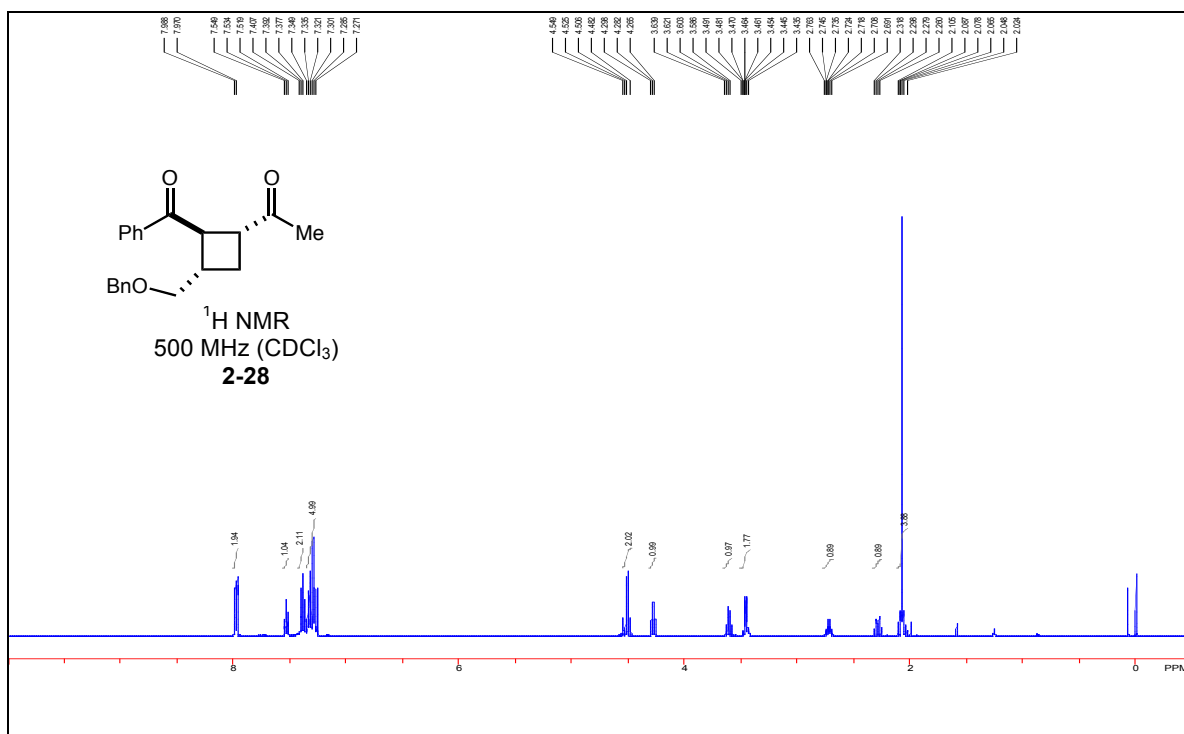
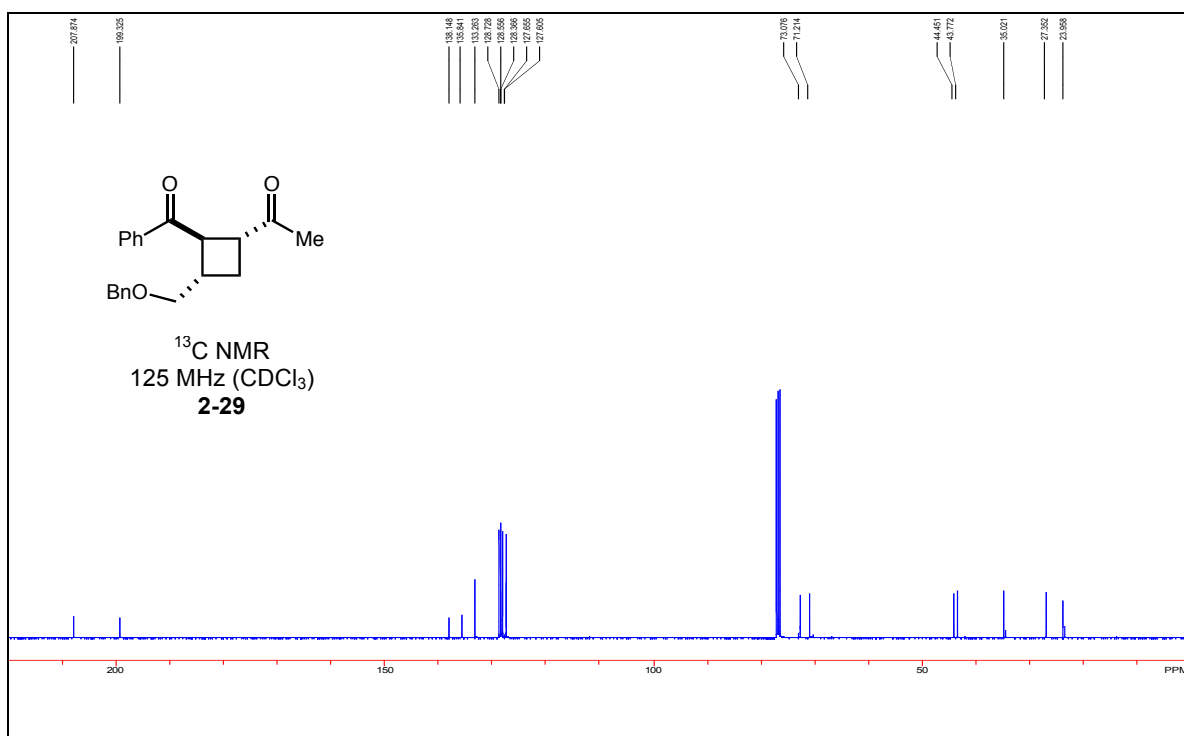


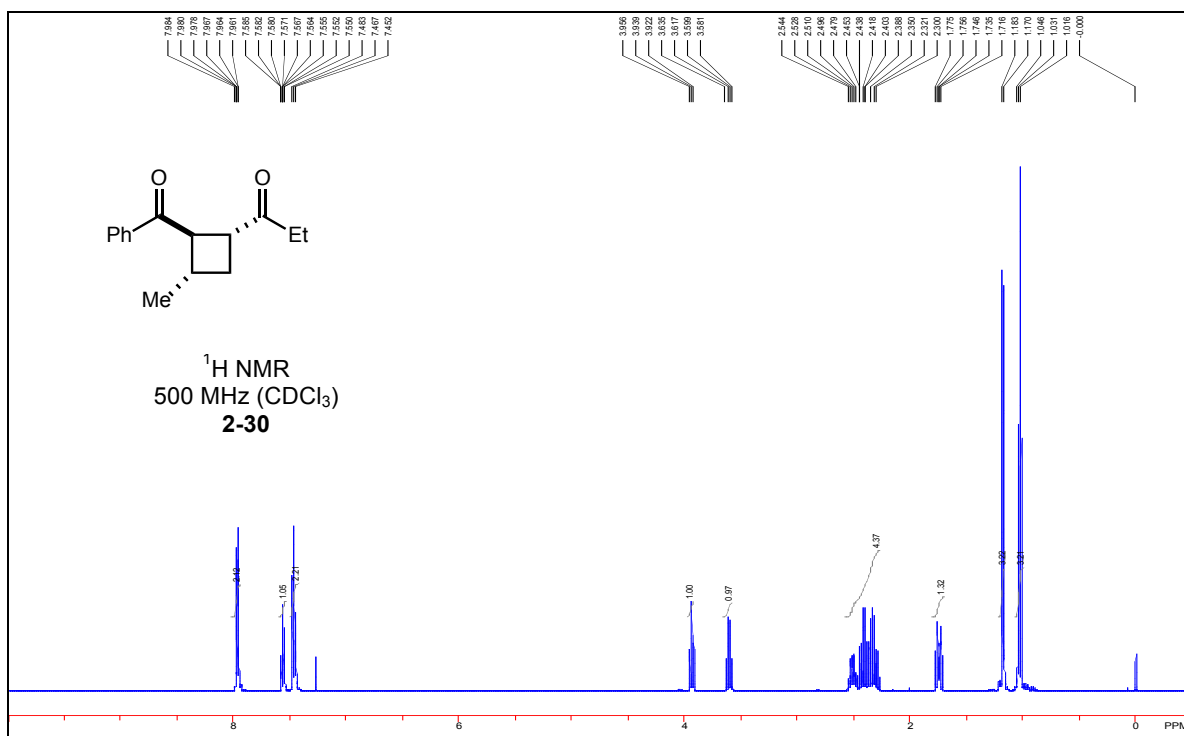
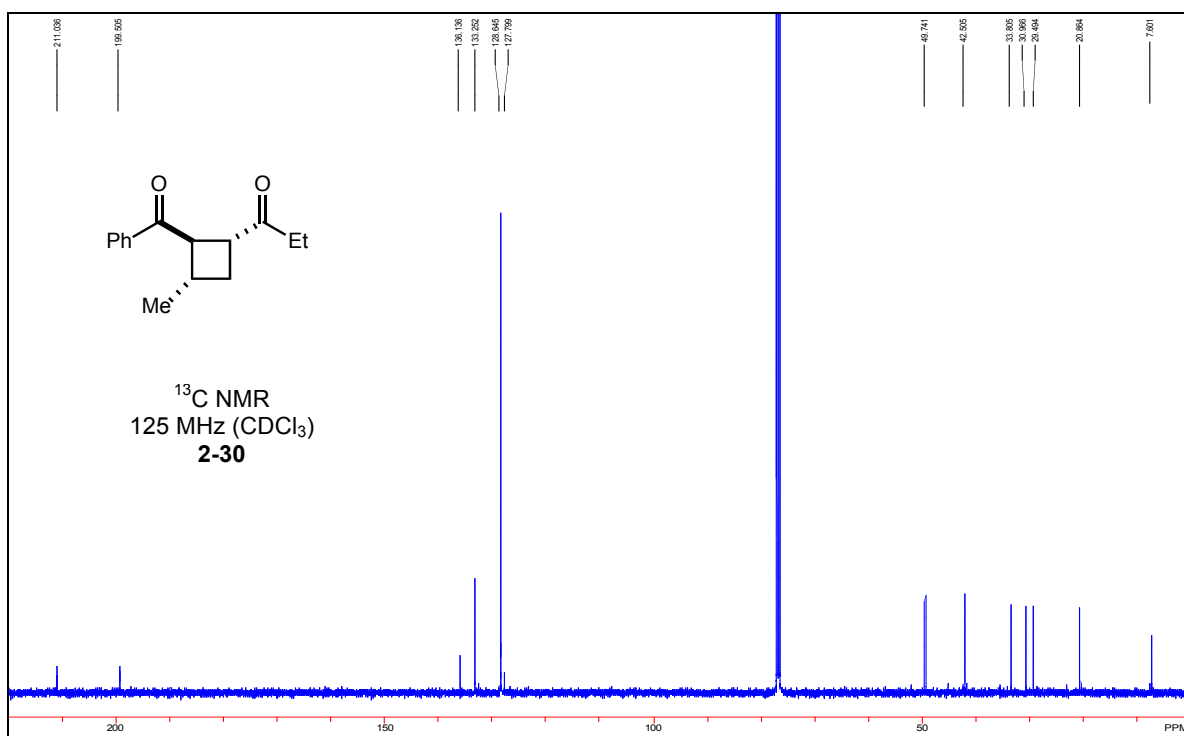


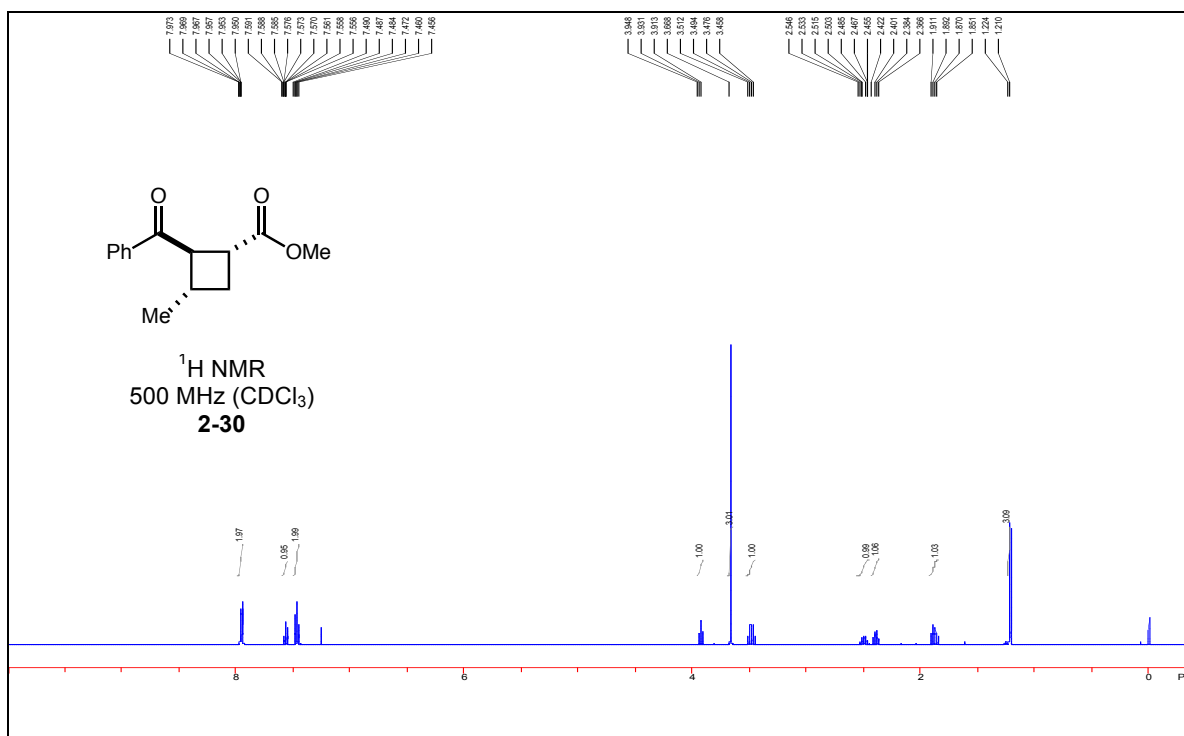
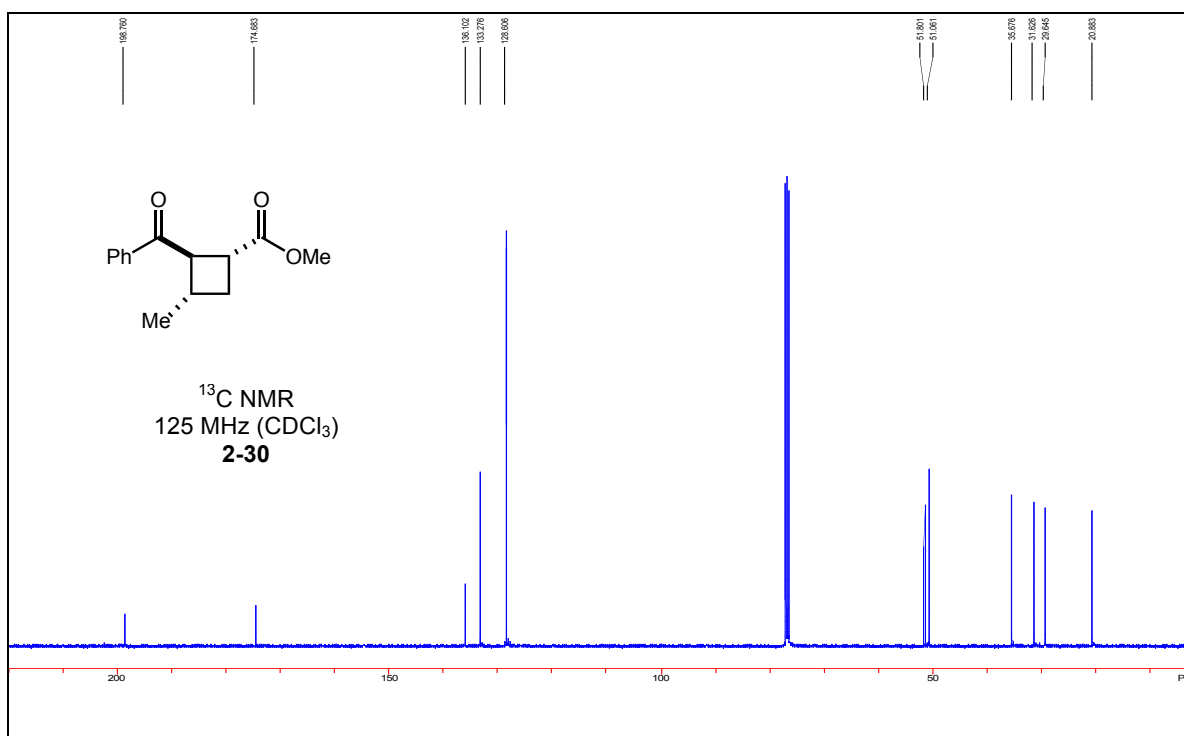


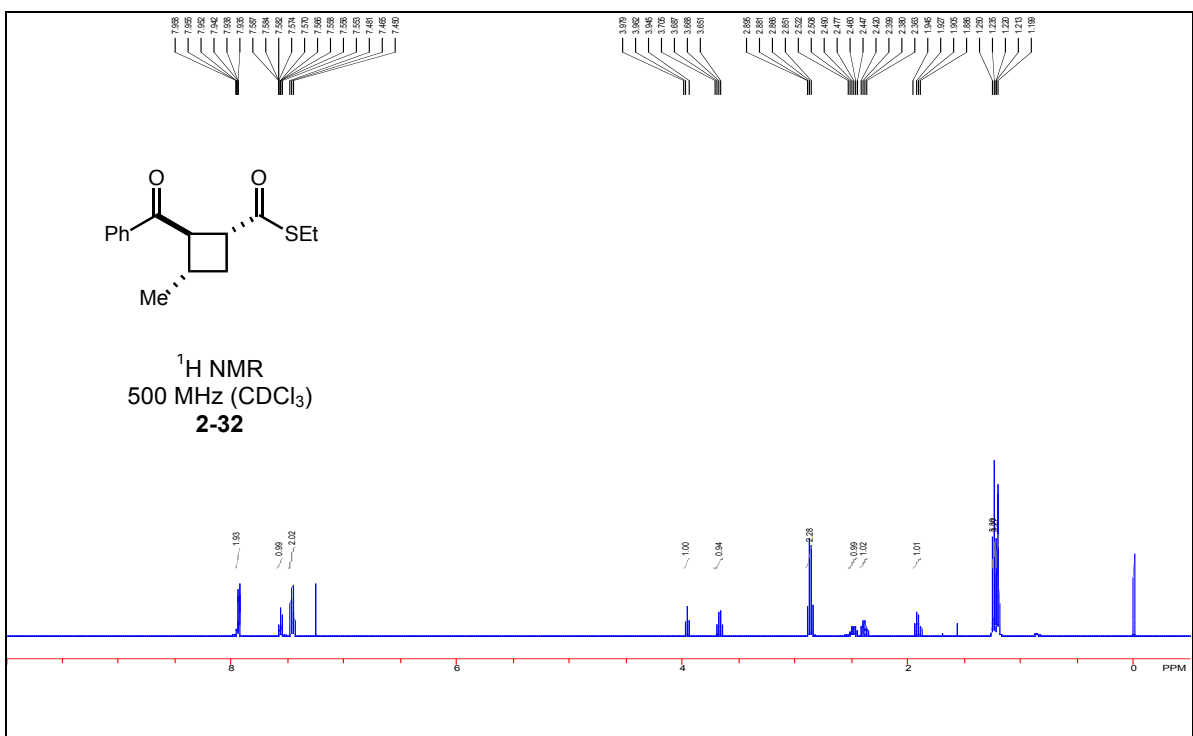


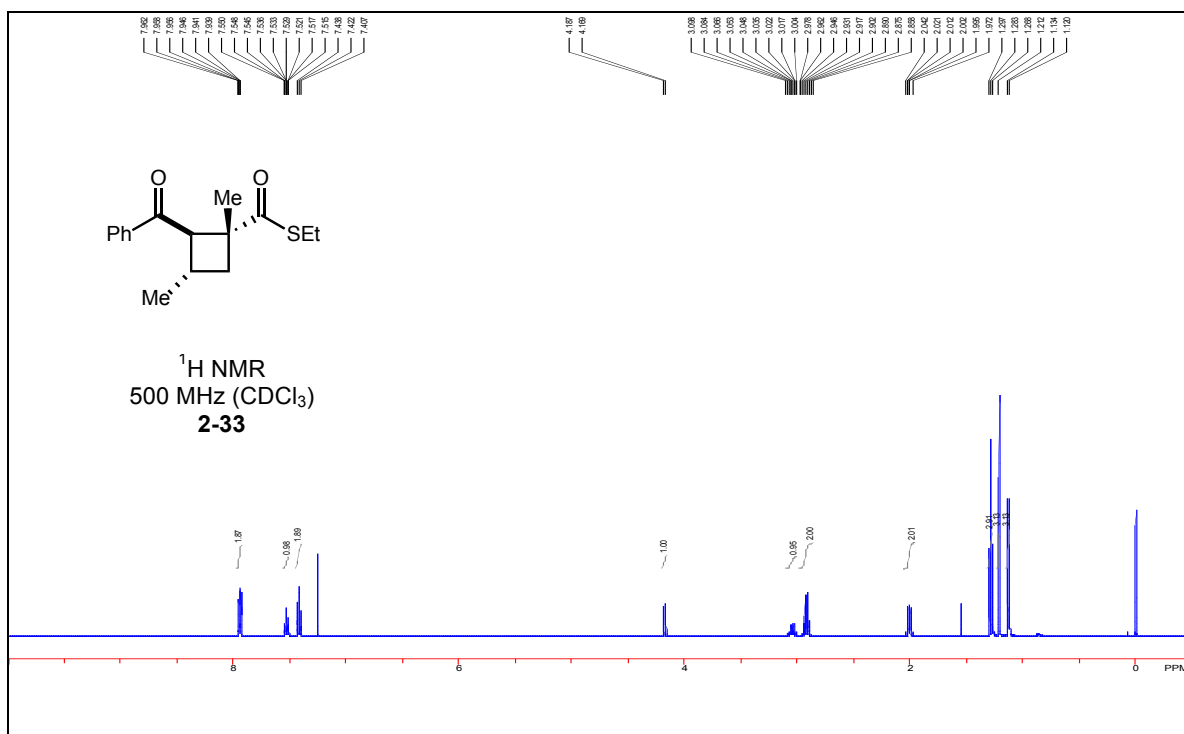
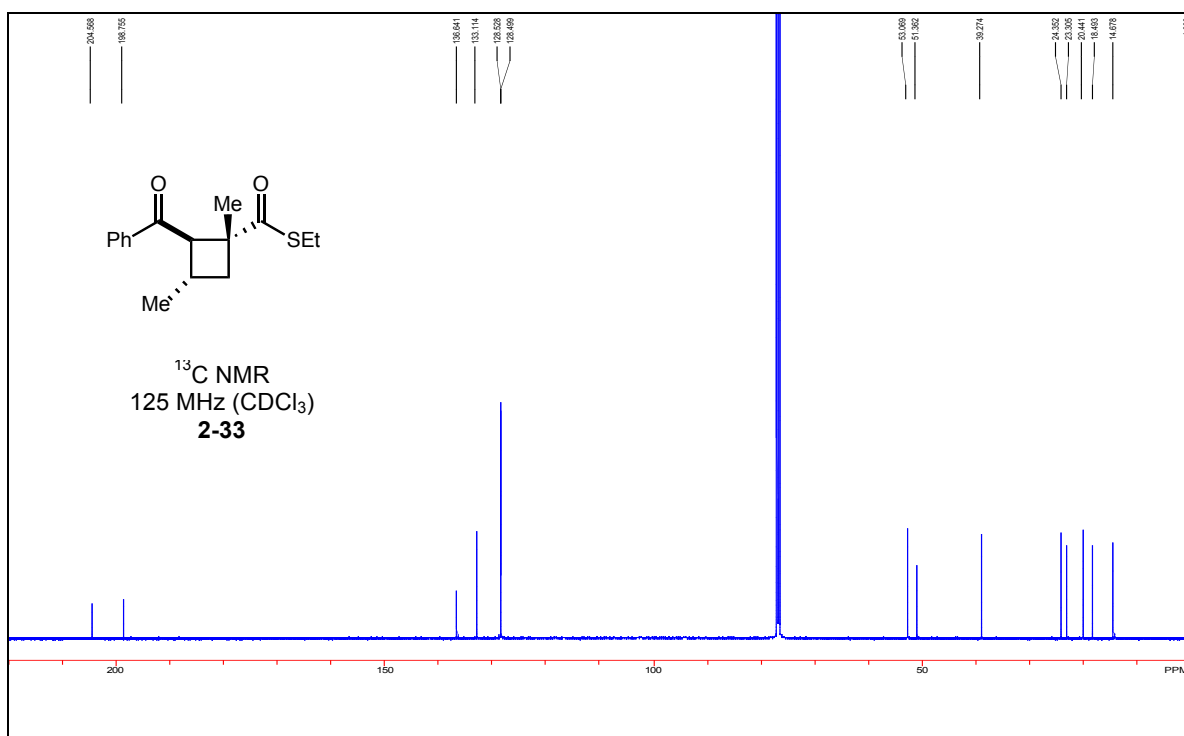


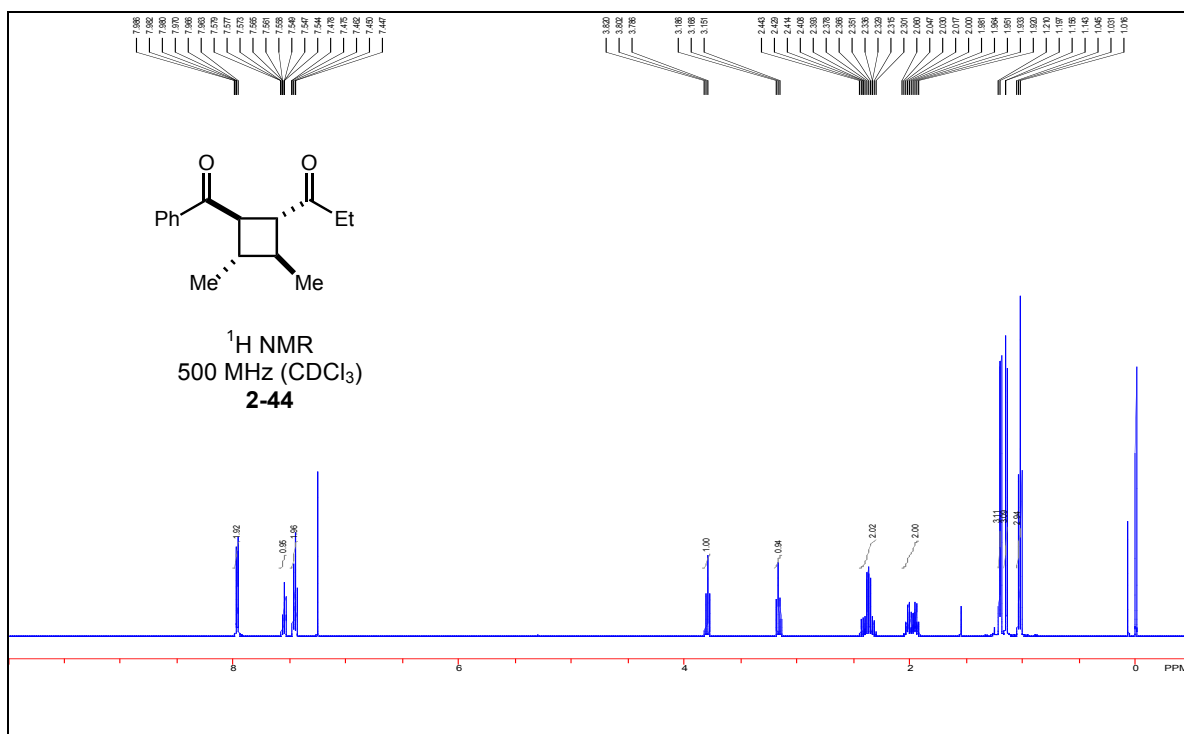
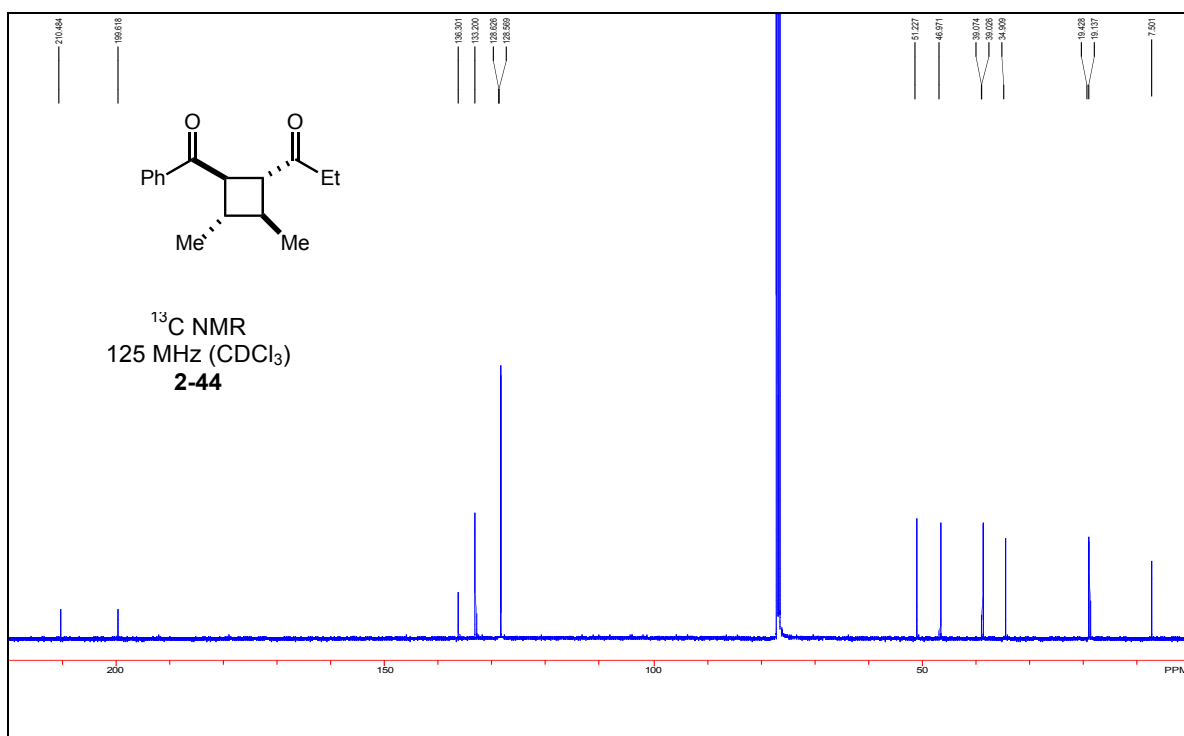


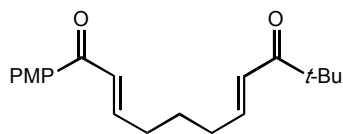
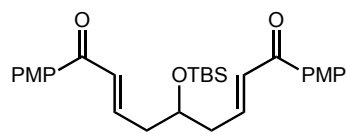
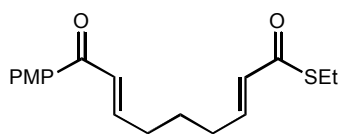
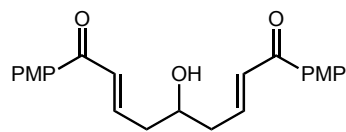
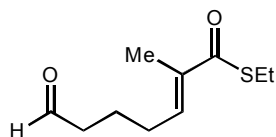
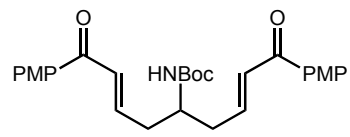
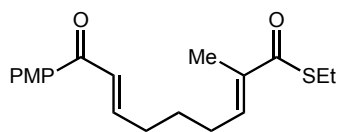
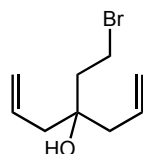
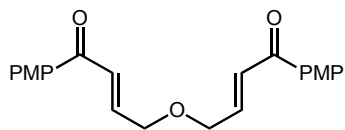
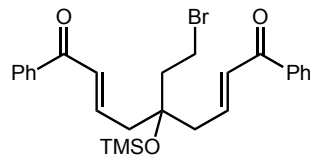
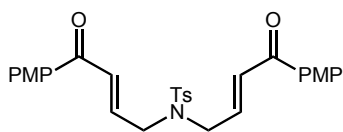
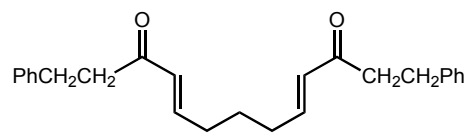
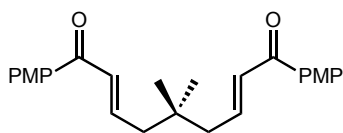
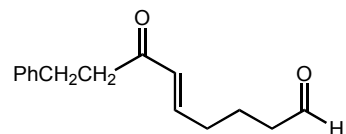
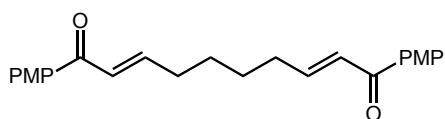
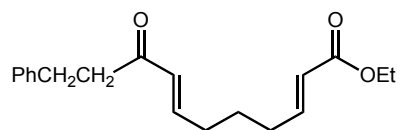




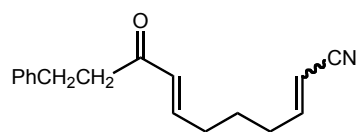
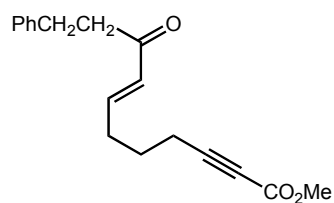
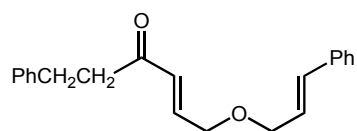
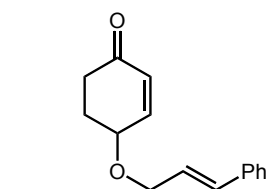
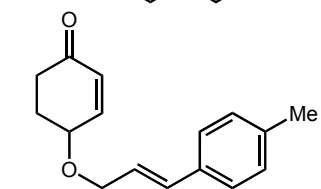
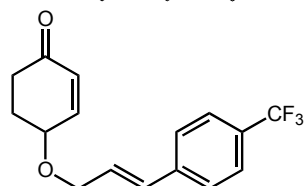
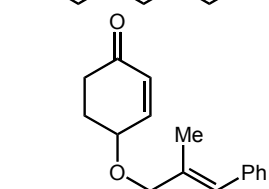
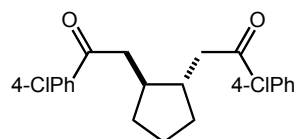
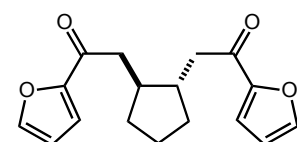
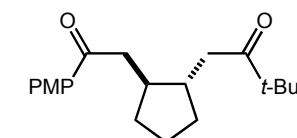
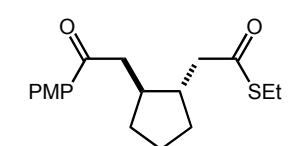
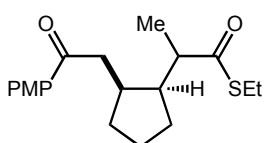
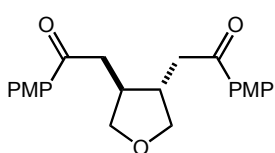
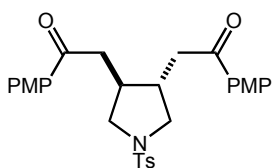


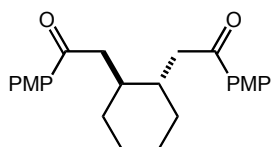
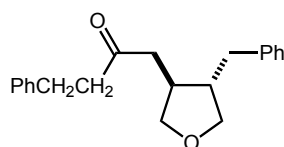
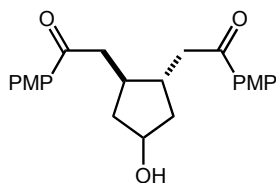
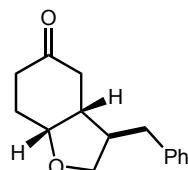
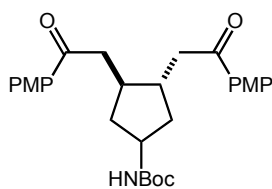
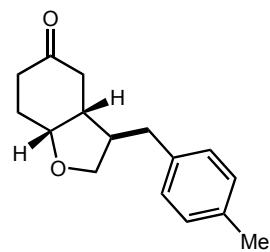
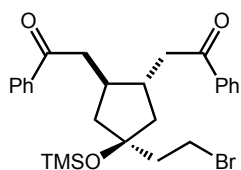
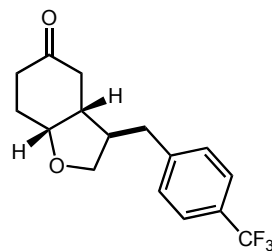
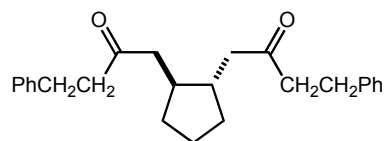
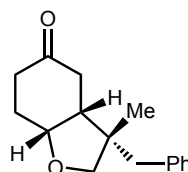
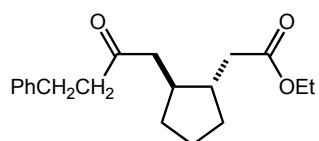
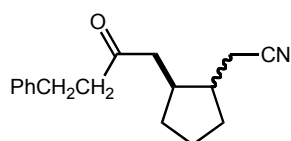


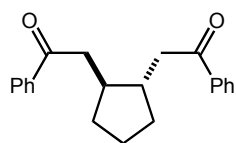
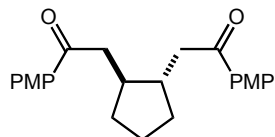
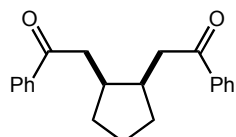
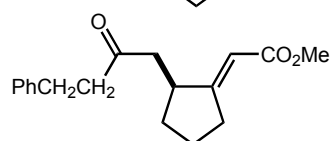
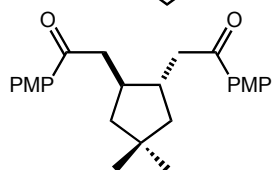


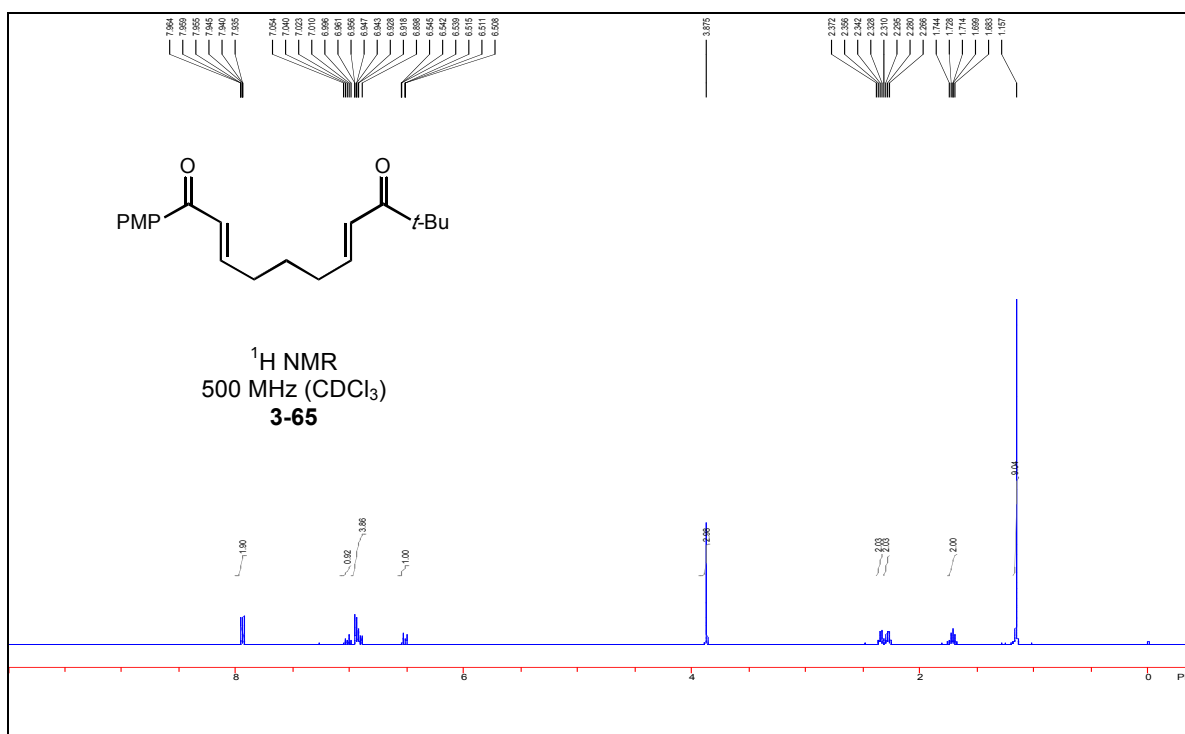
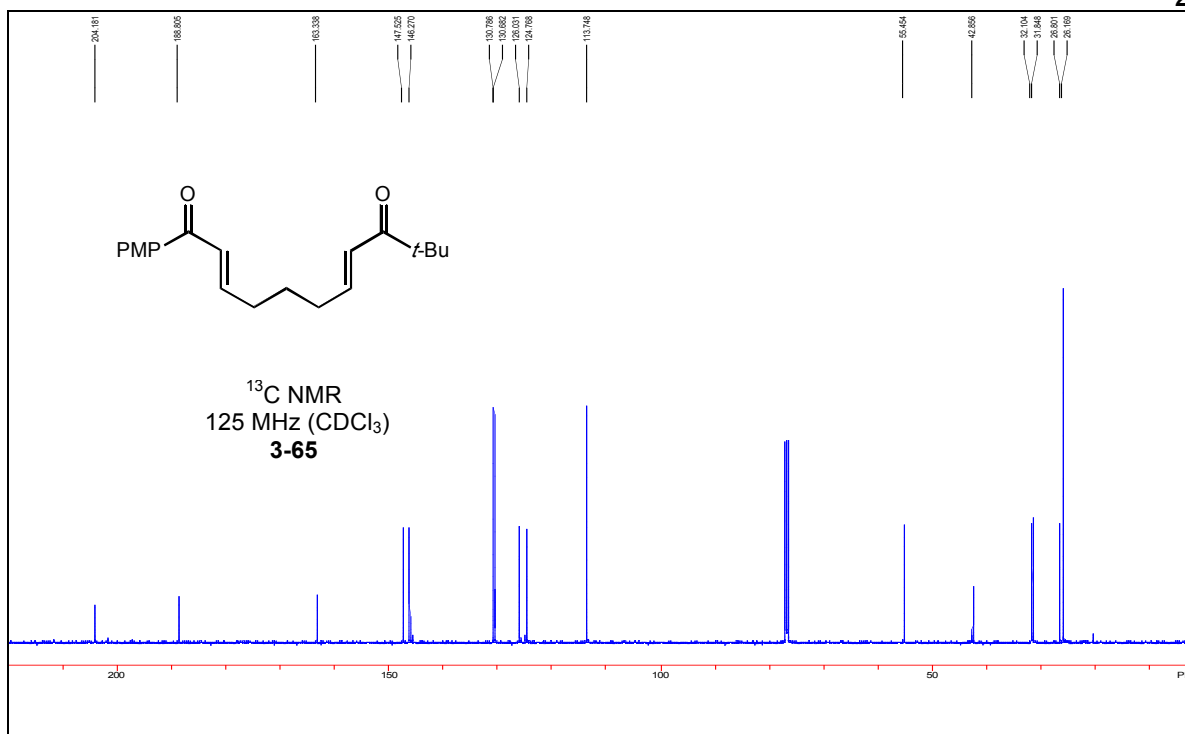
**3-65****3-73****3-66****3-74****3-67****3-75****3-68****3-76****3-69****3-77****3-70****3-78****3-71****3-79****3-72****3-80**

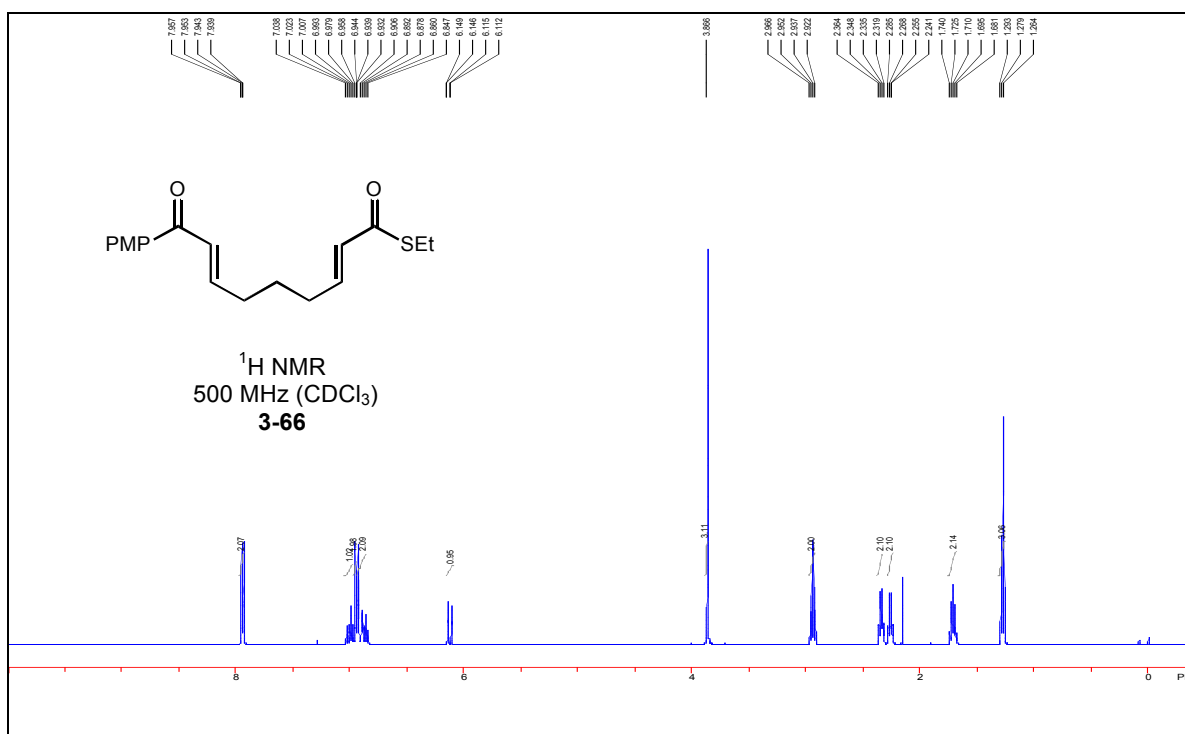
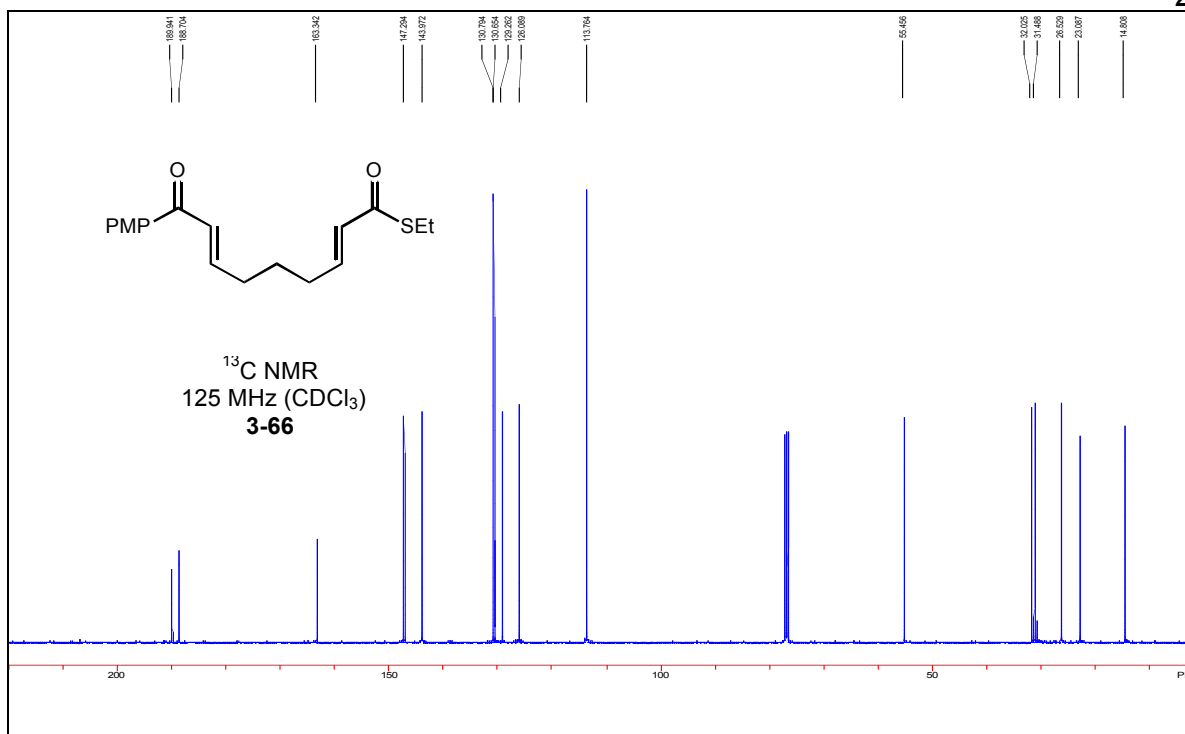


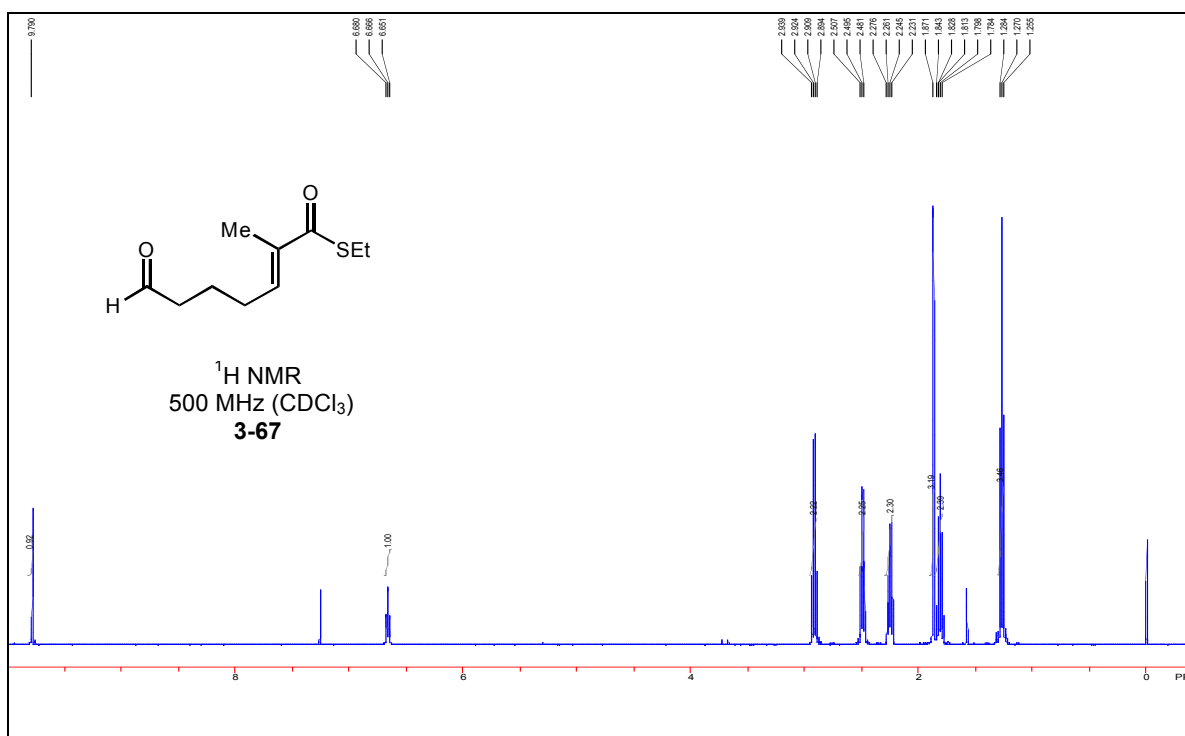
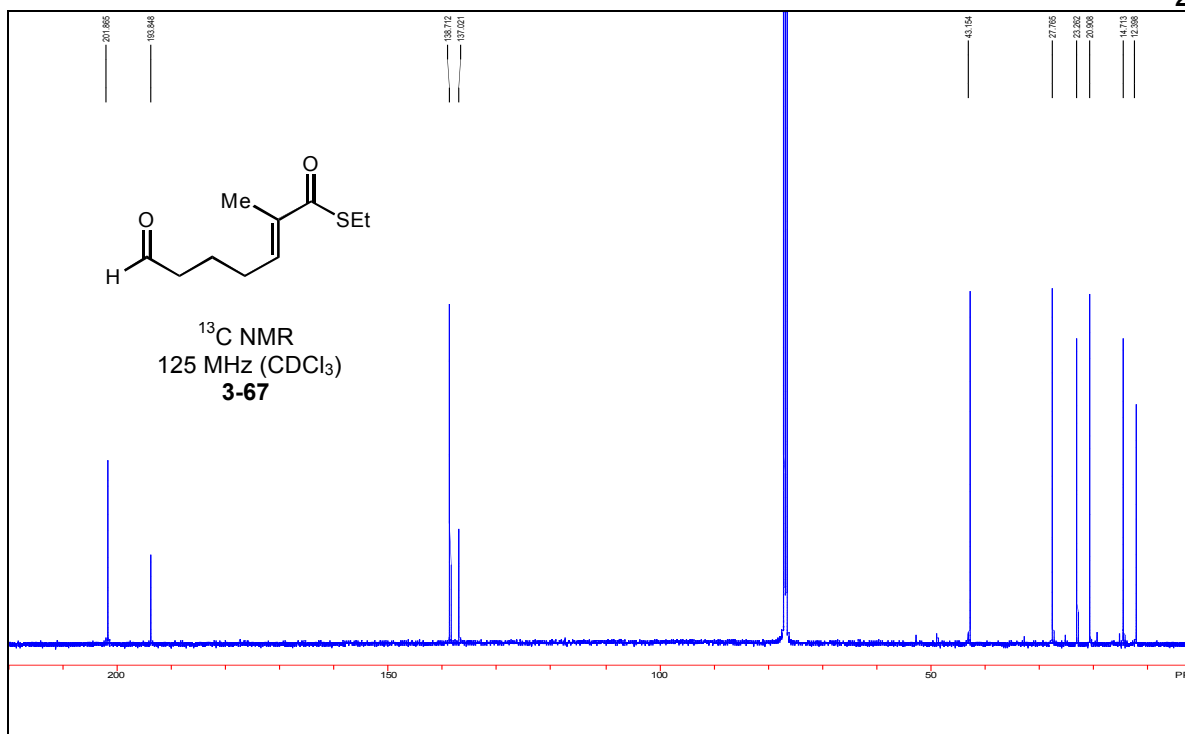
**3-81****3-82****3-83****3-84****3-85****3-86****3-86****3-44****3-45****3-46****3-47****3-48****3-49****3-50**

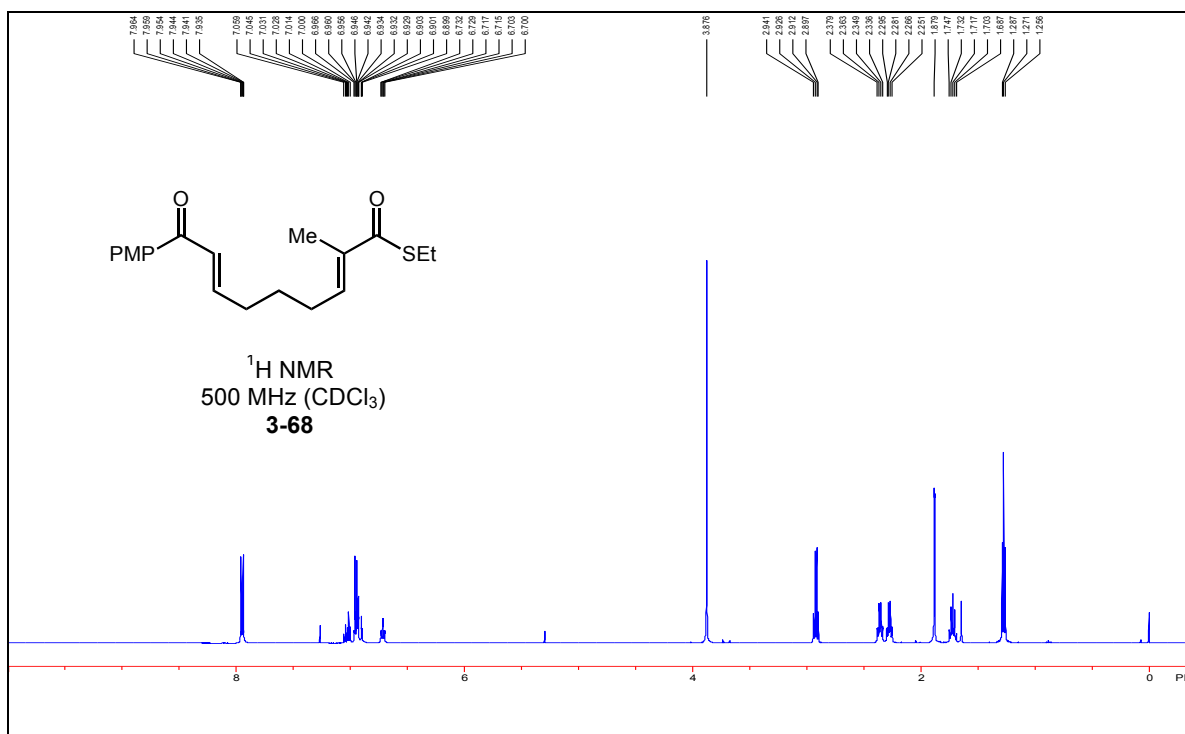
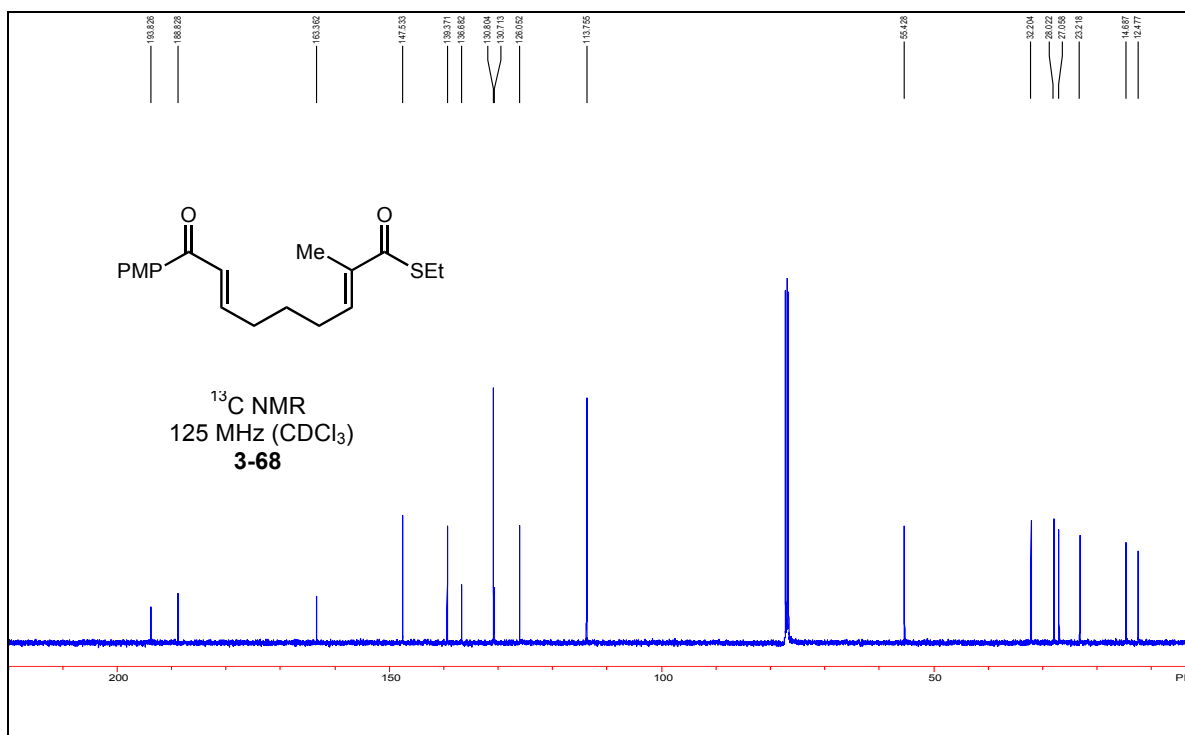
**3-52****3-60****3-53****3-61****3-54****3-62****3-55****3-63****3-56****3-64****3-57****3-58**

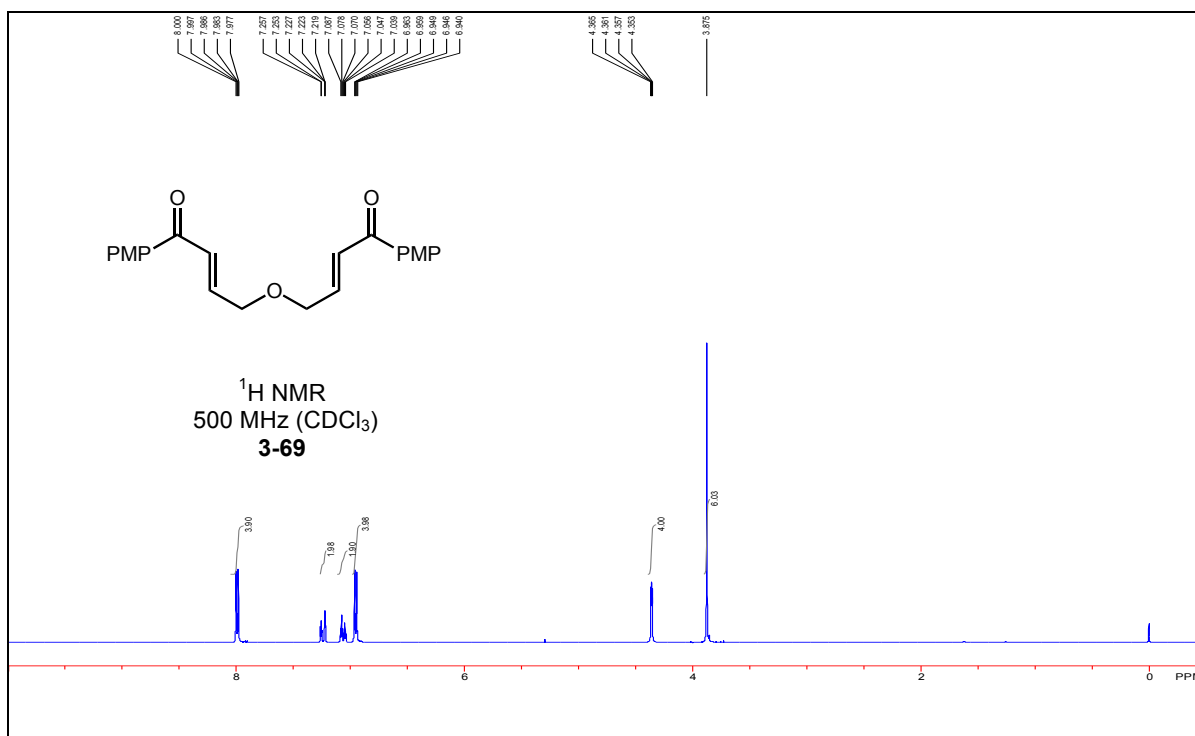
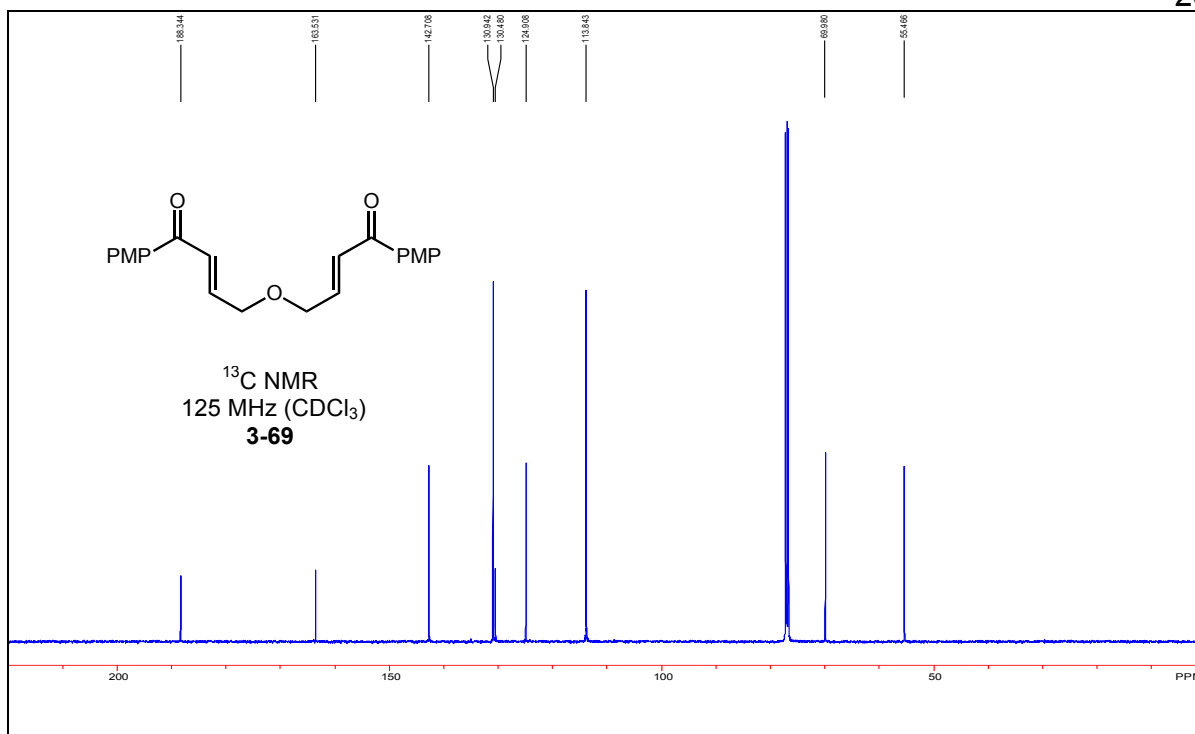
**3-15****3.17****3.38****3.59****3-51**



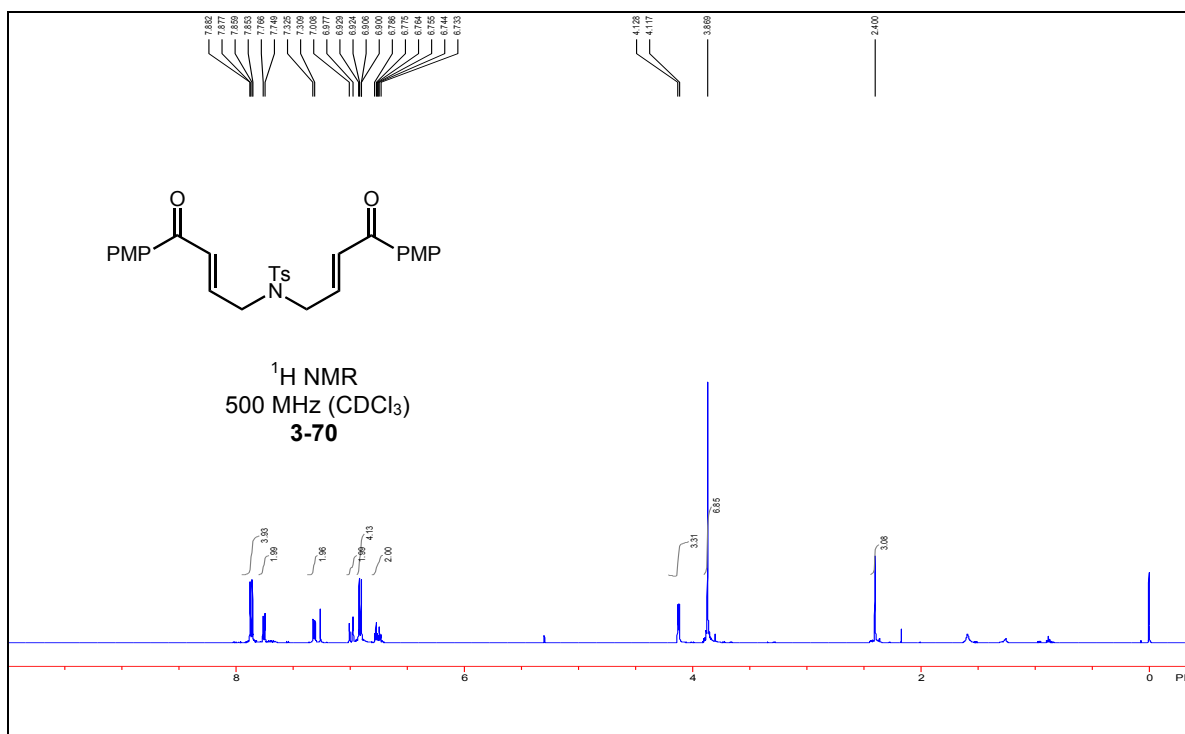
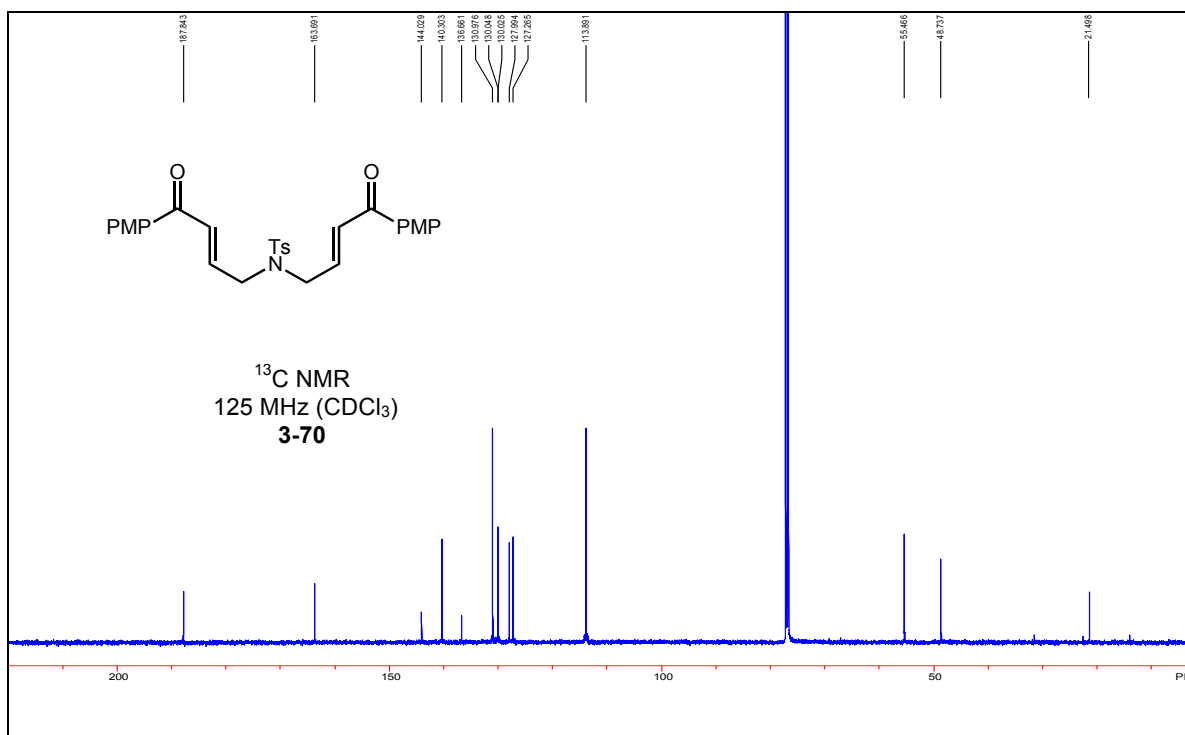


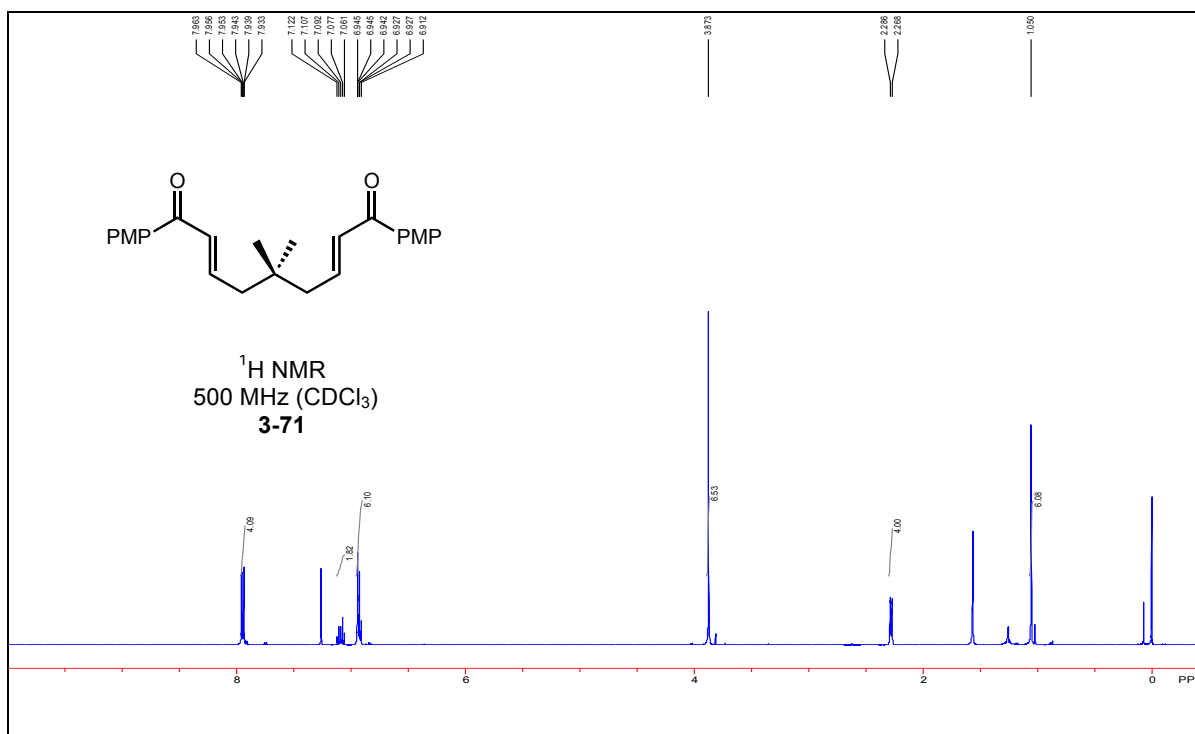
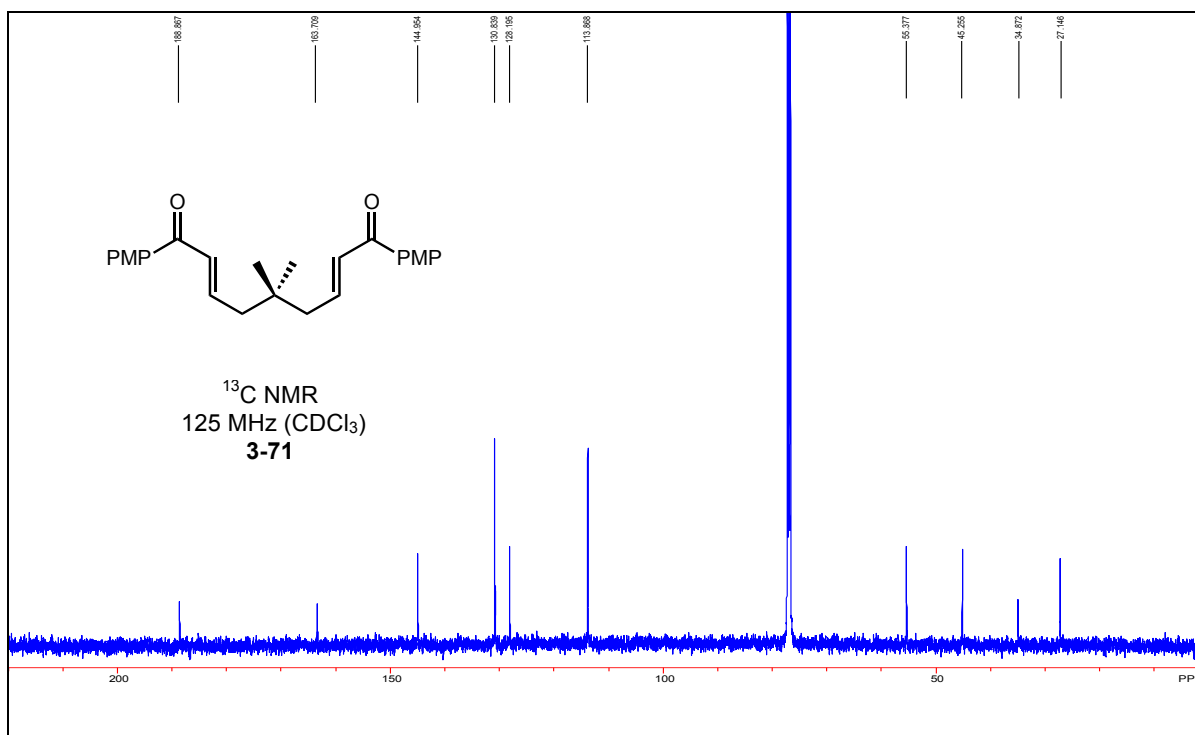


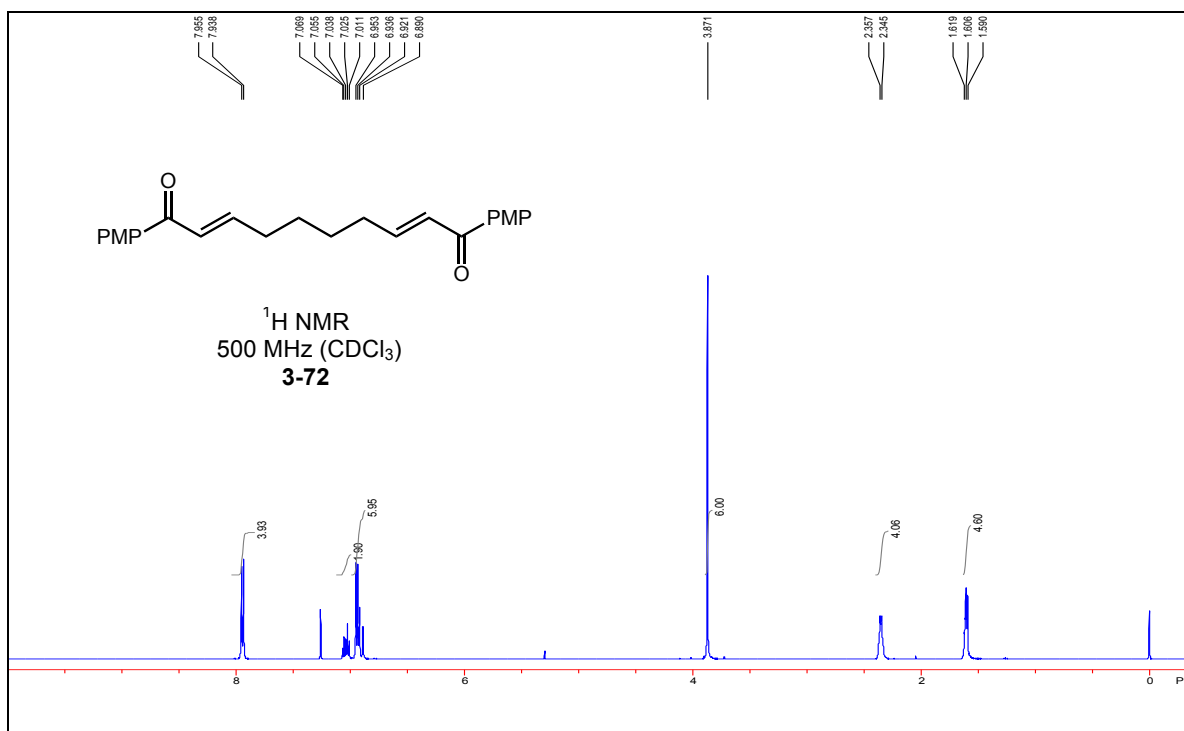
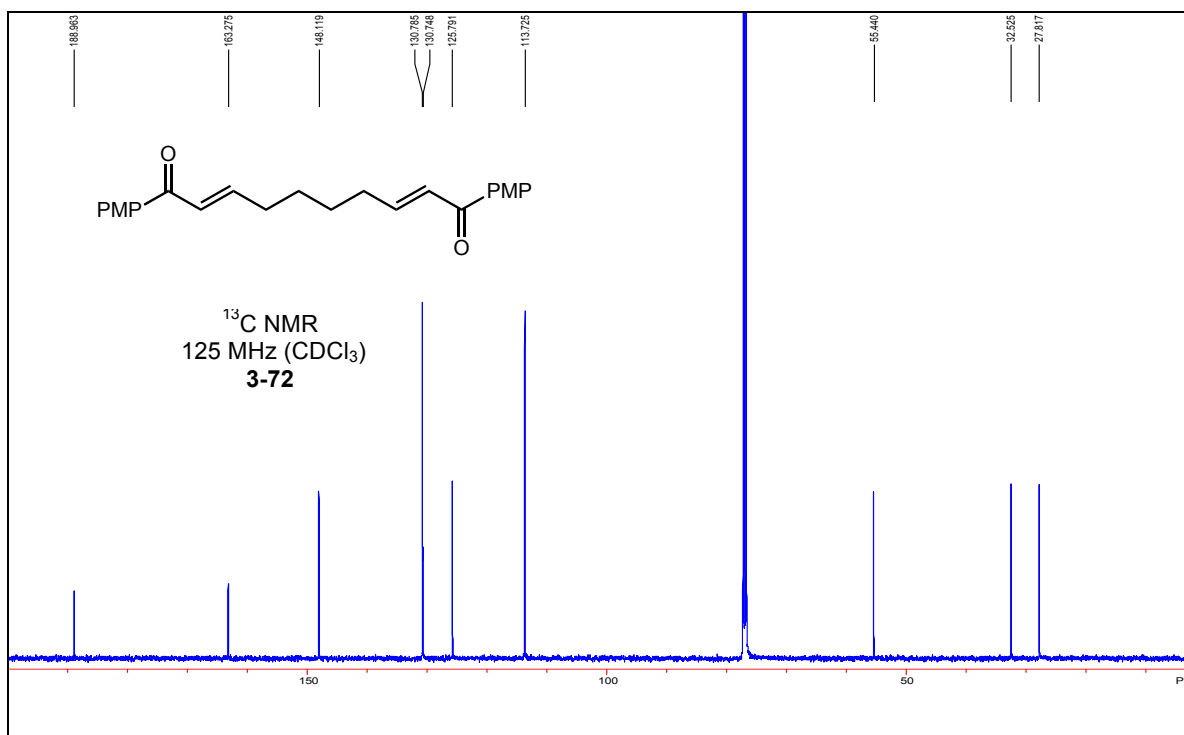


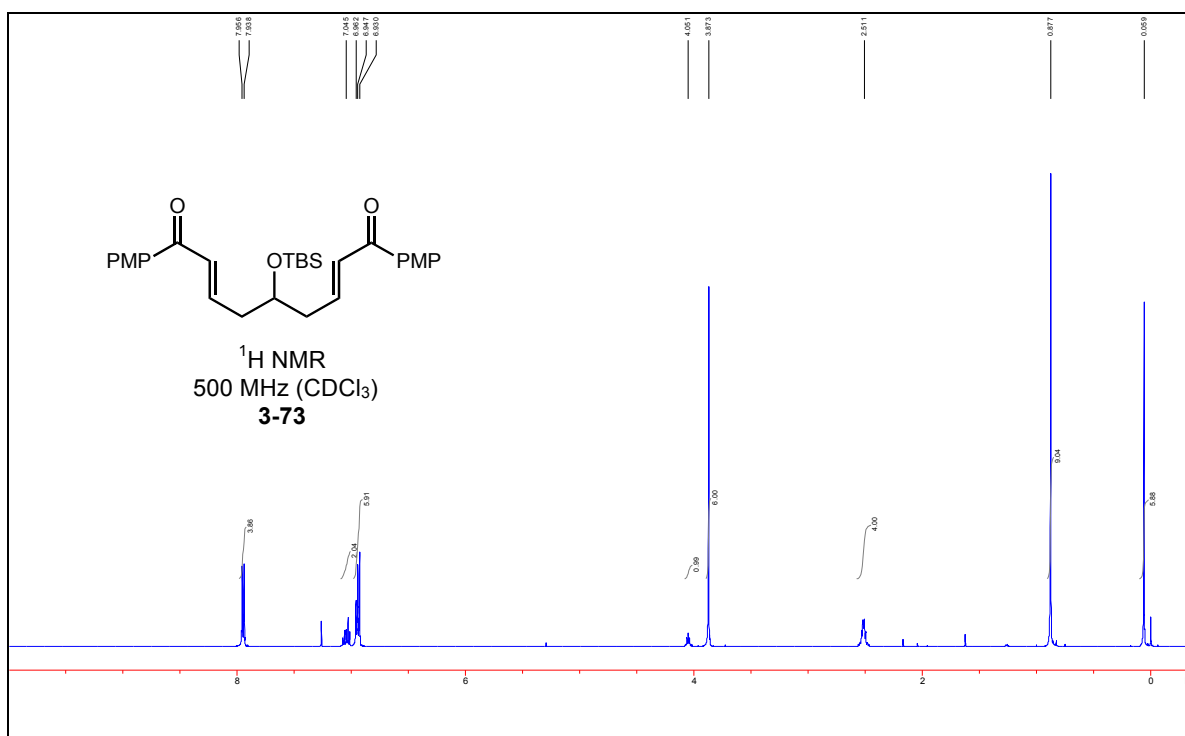
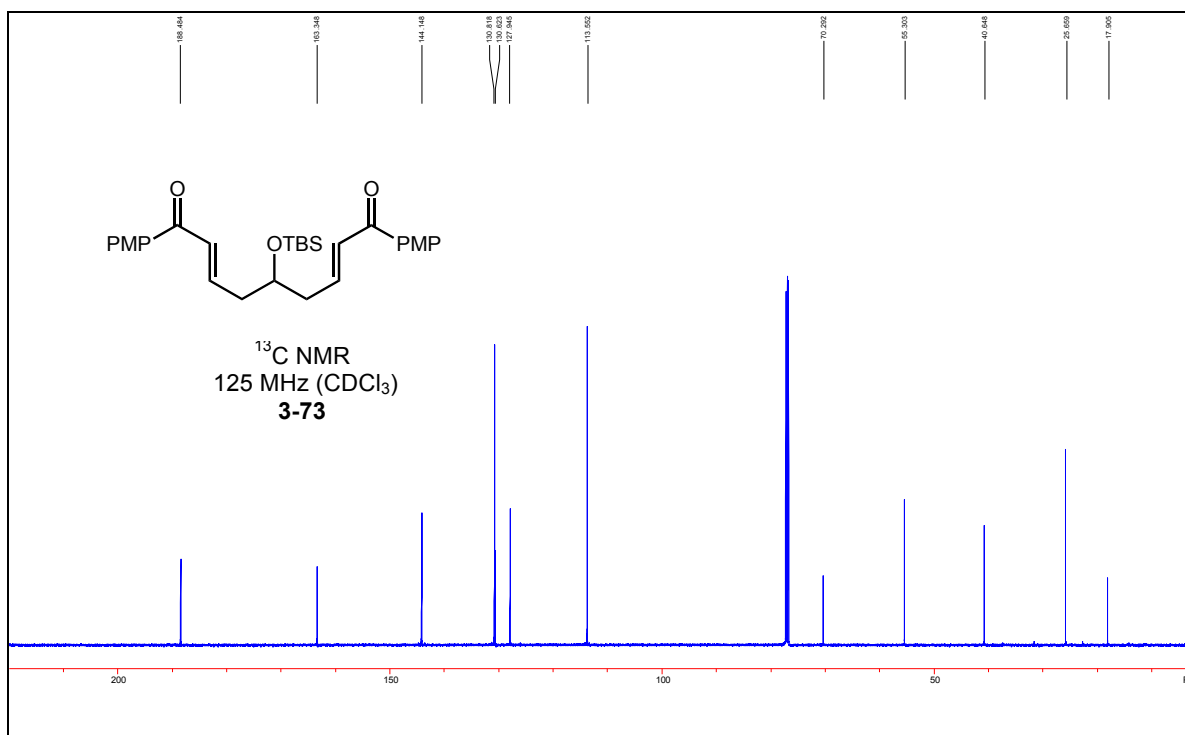


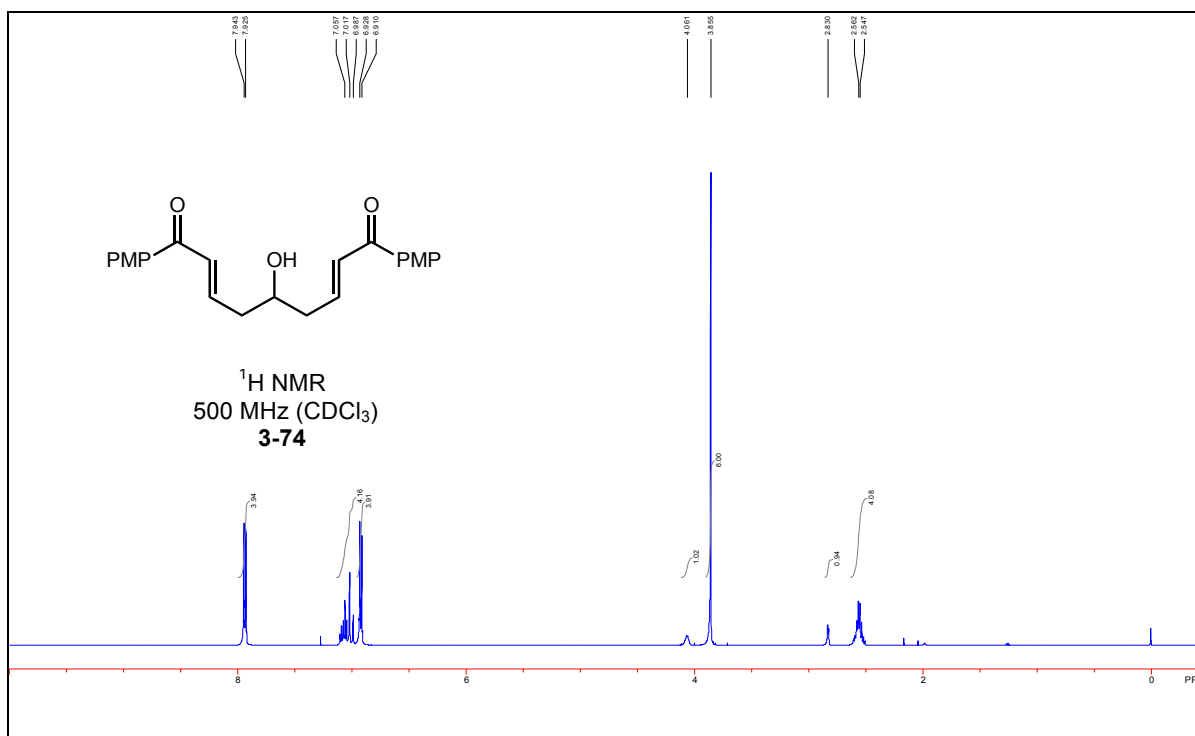
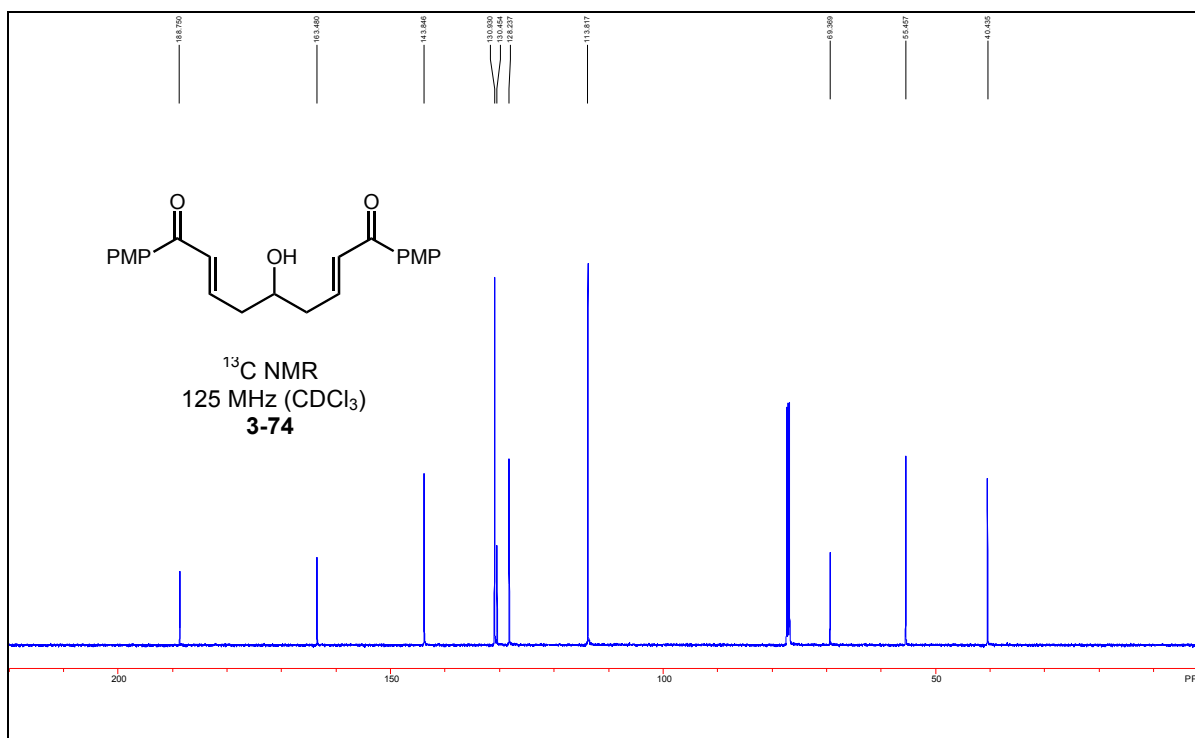


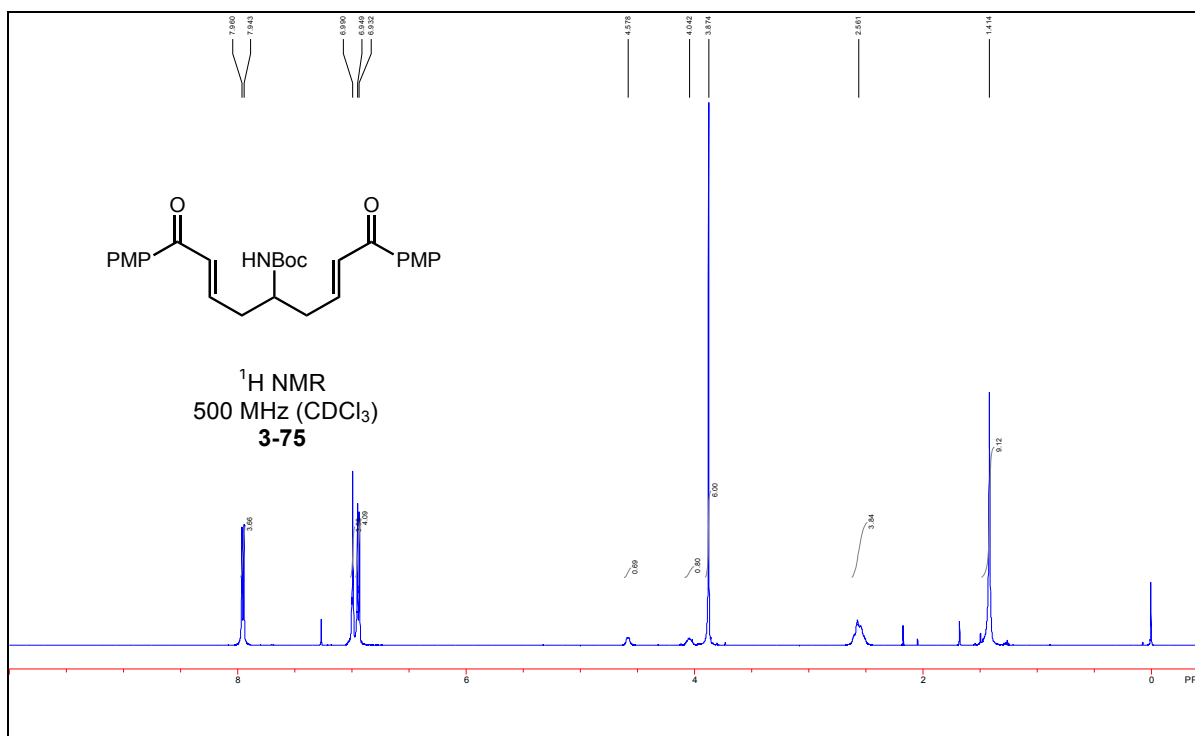
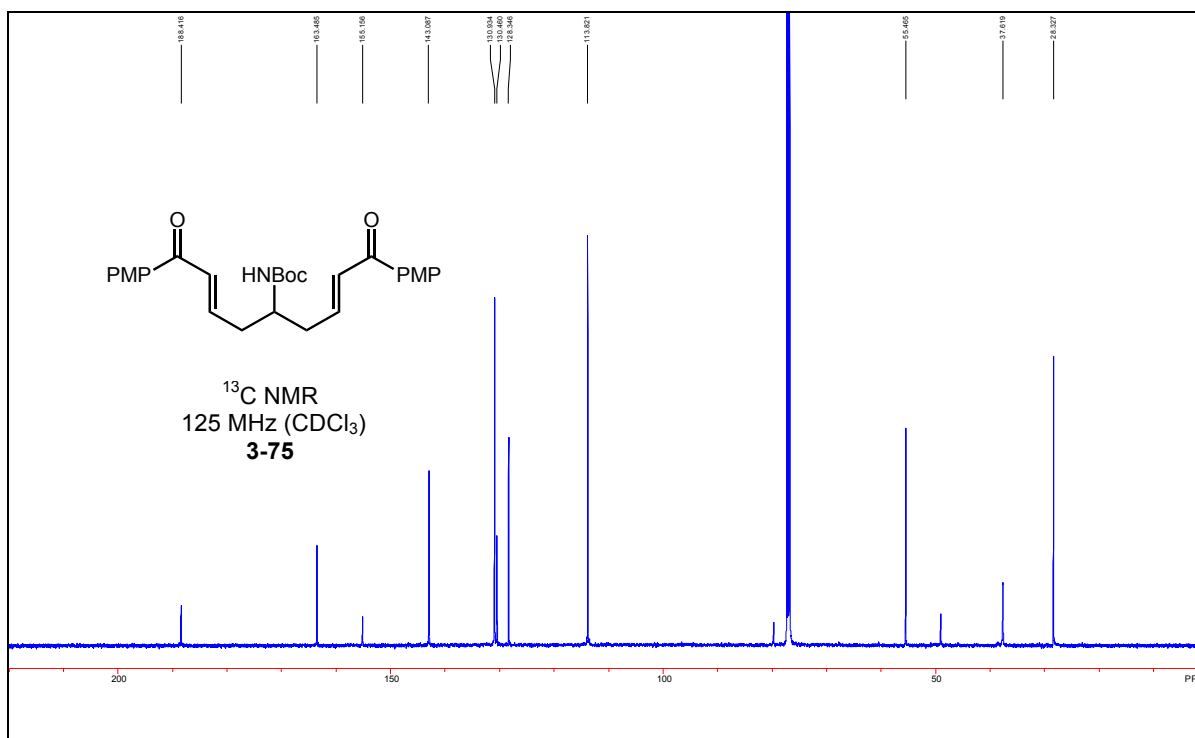


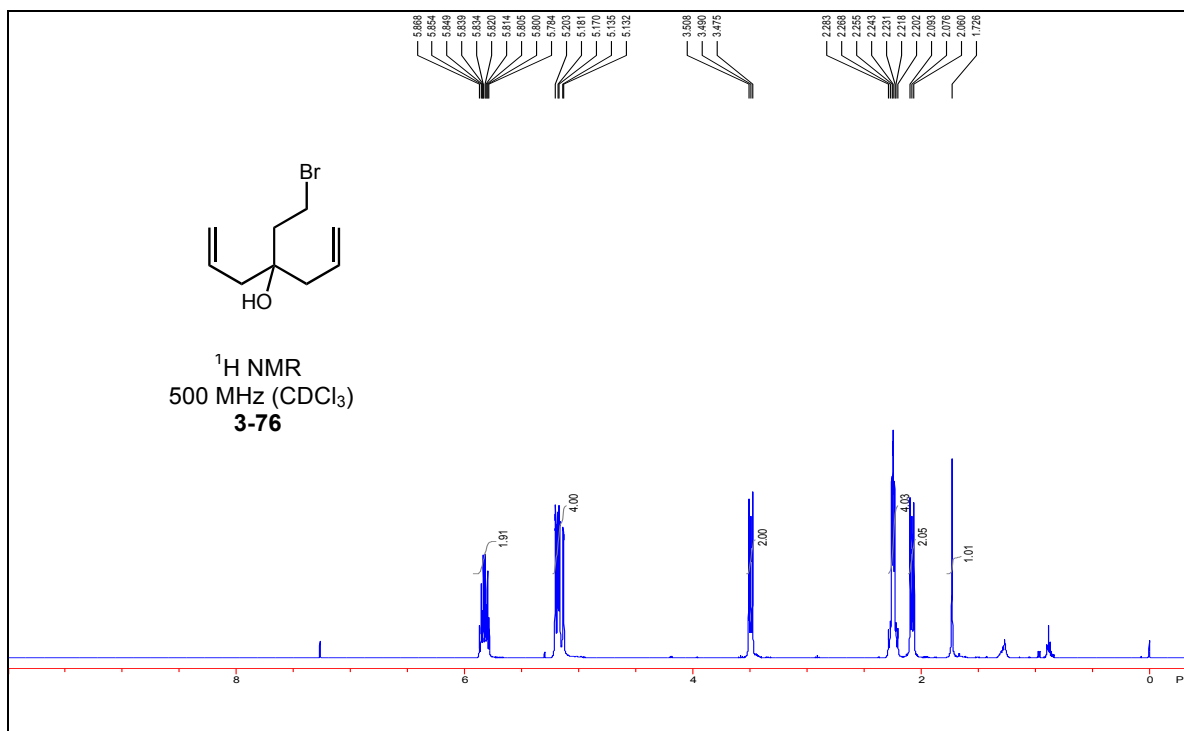
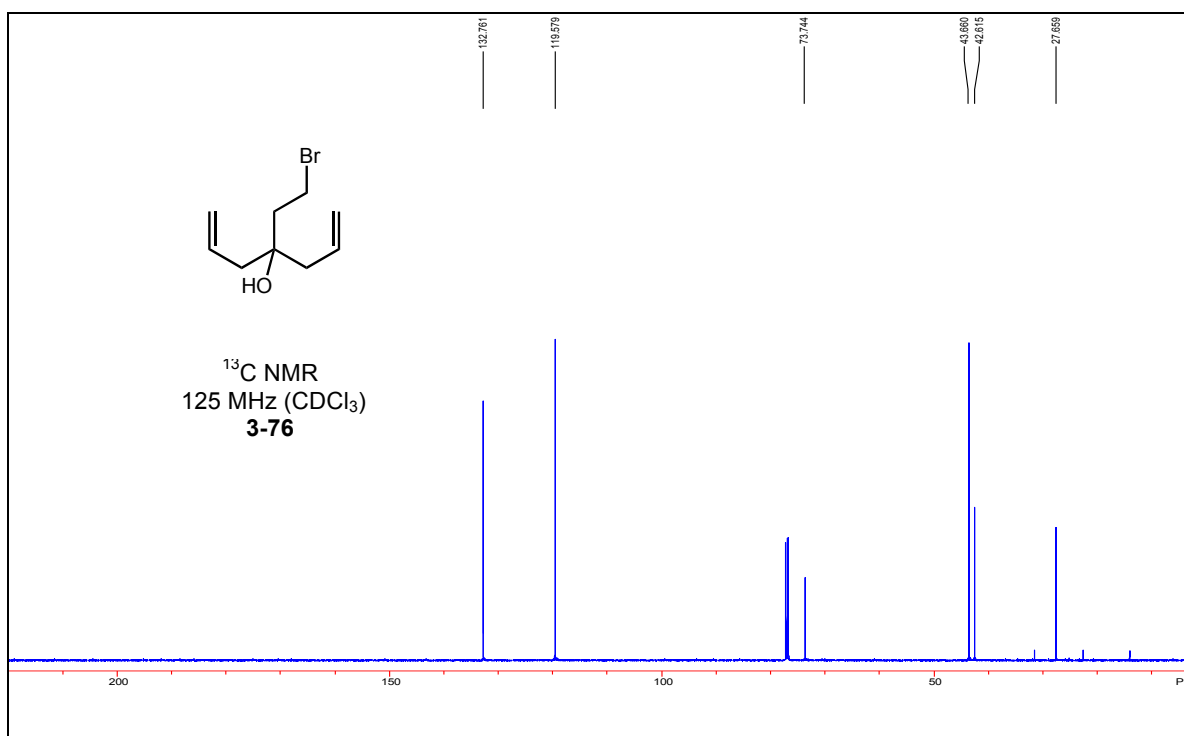


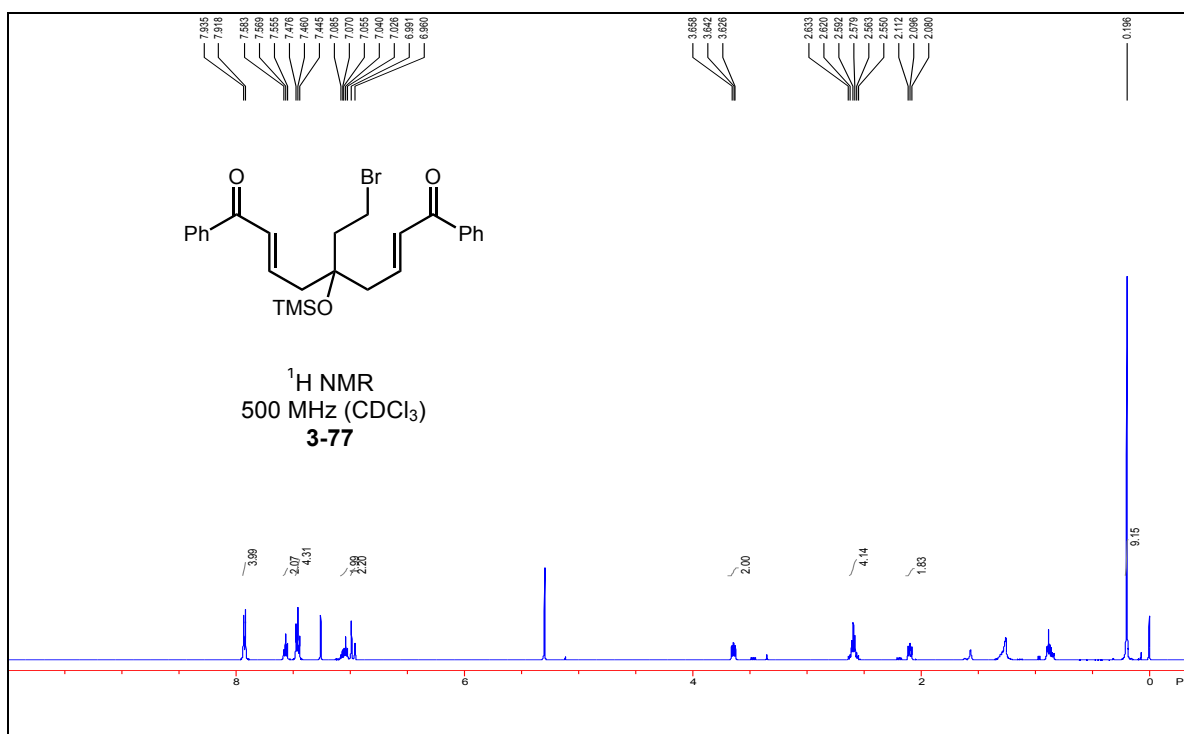
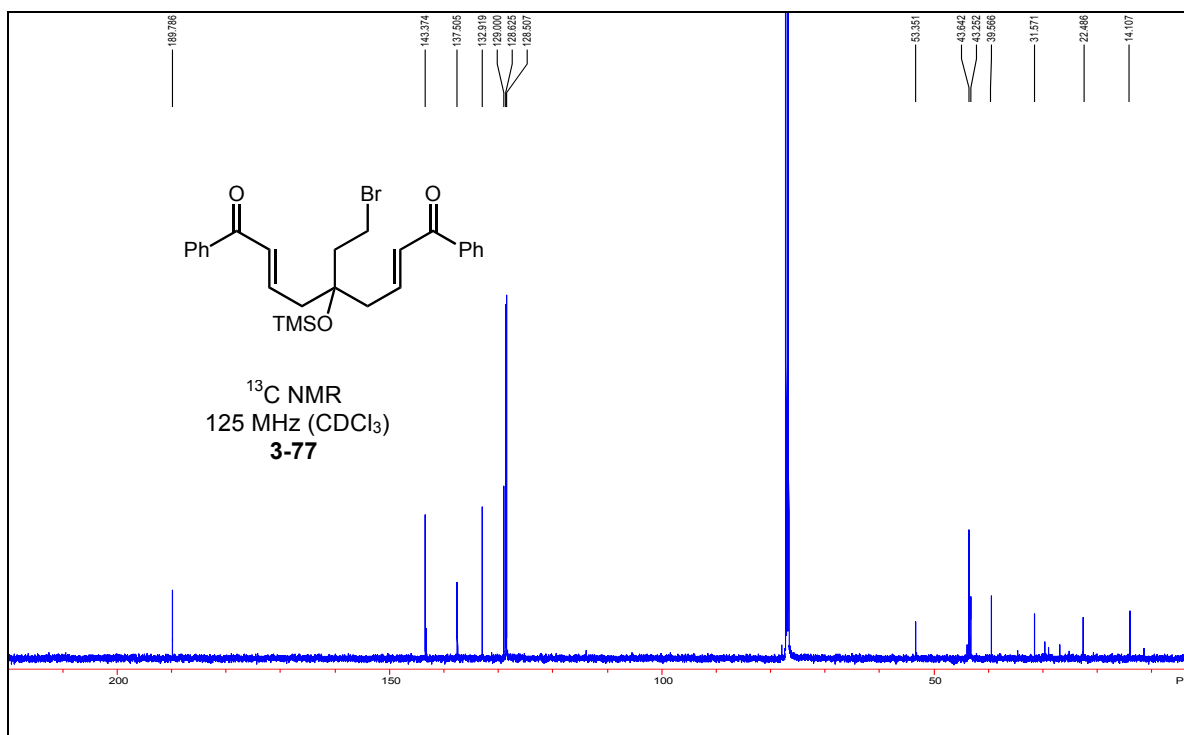




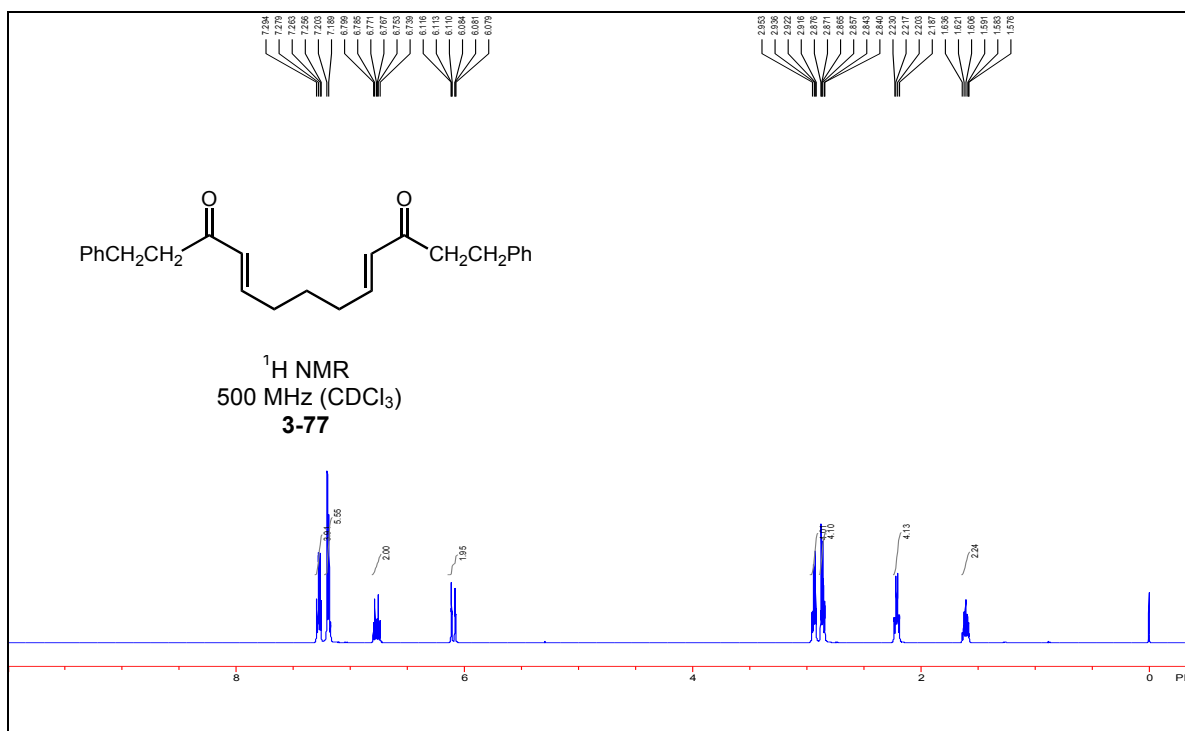
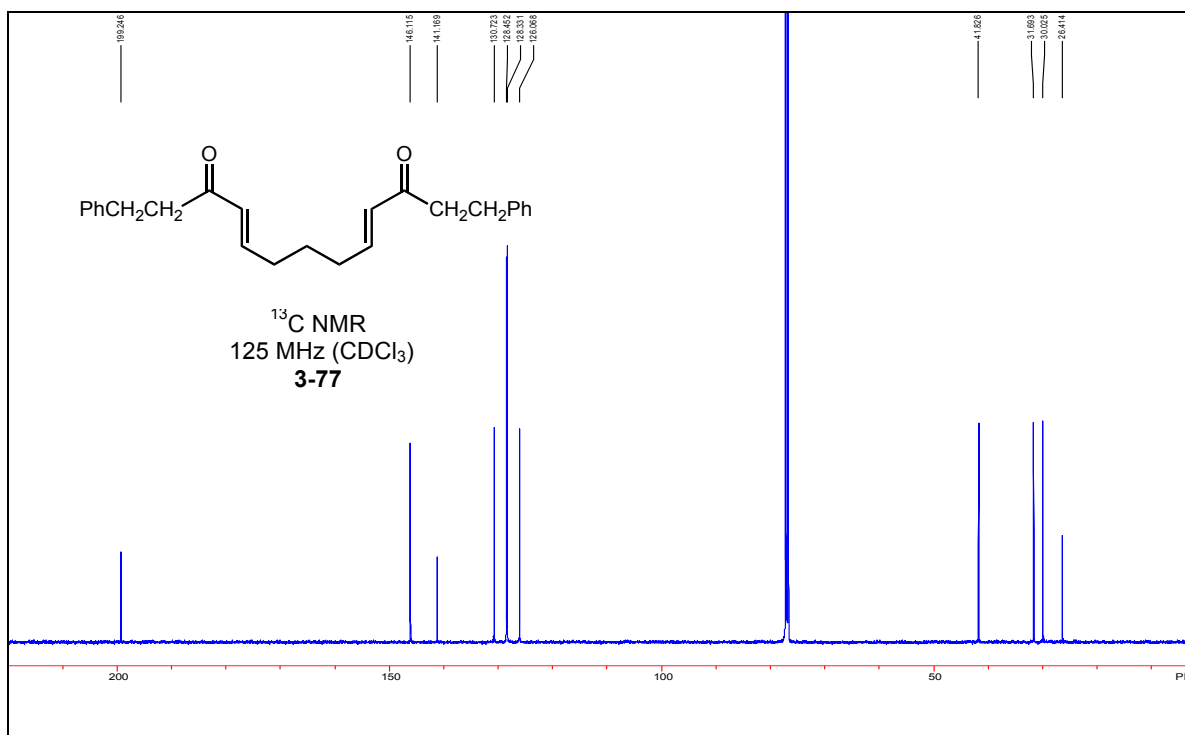


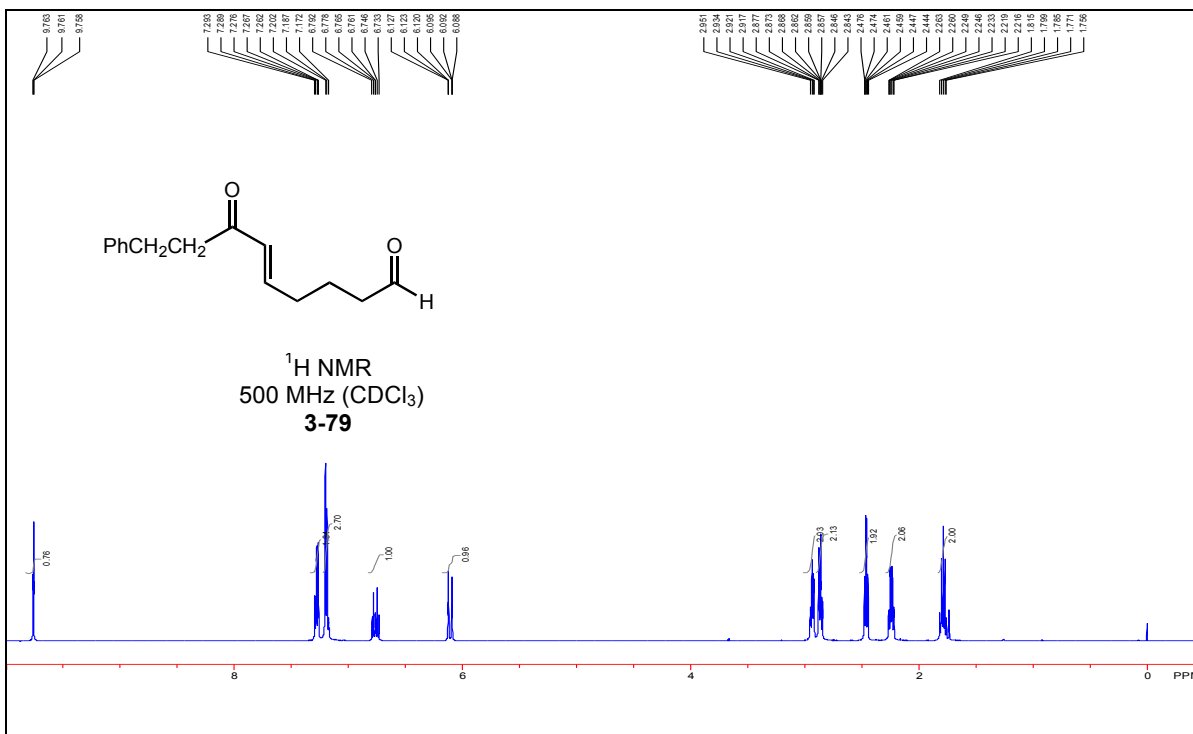


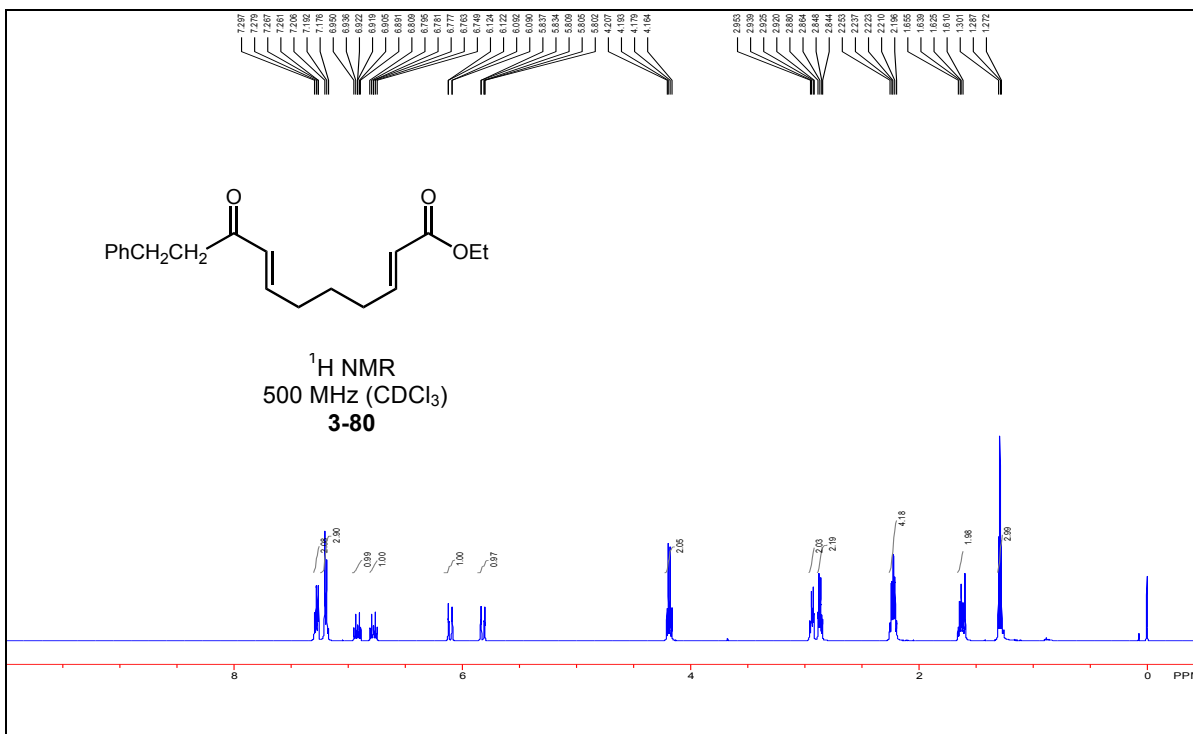


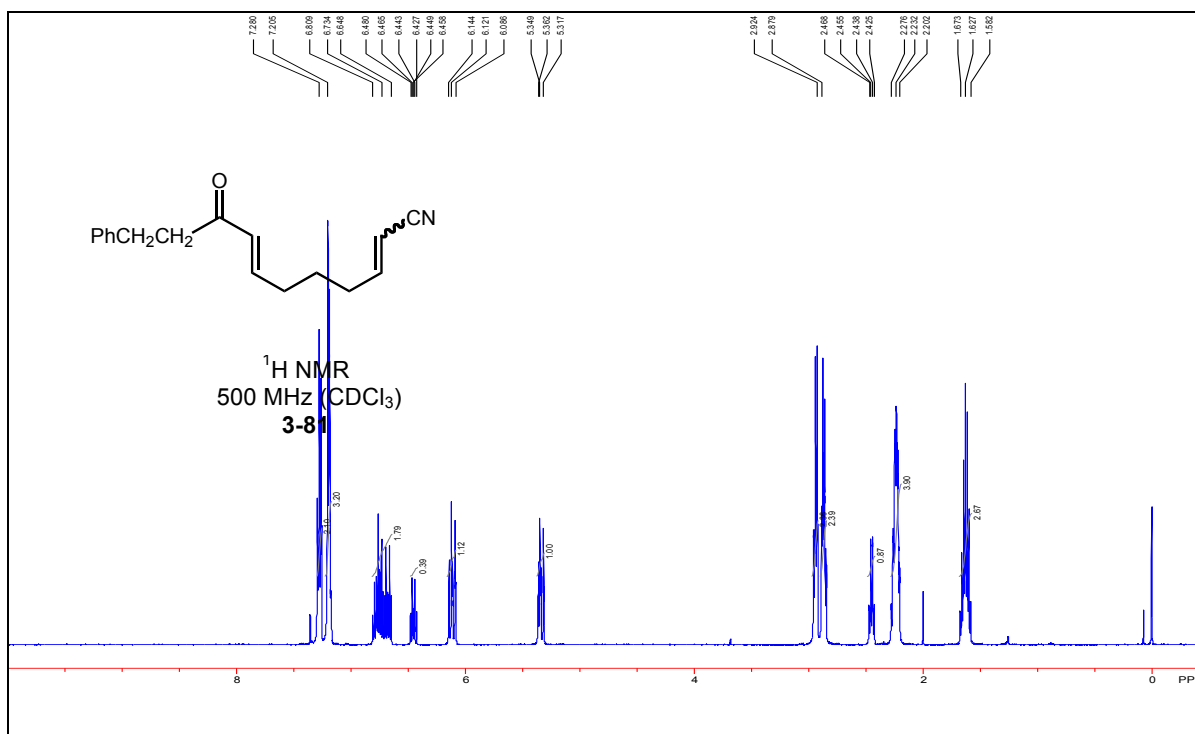
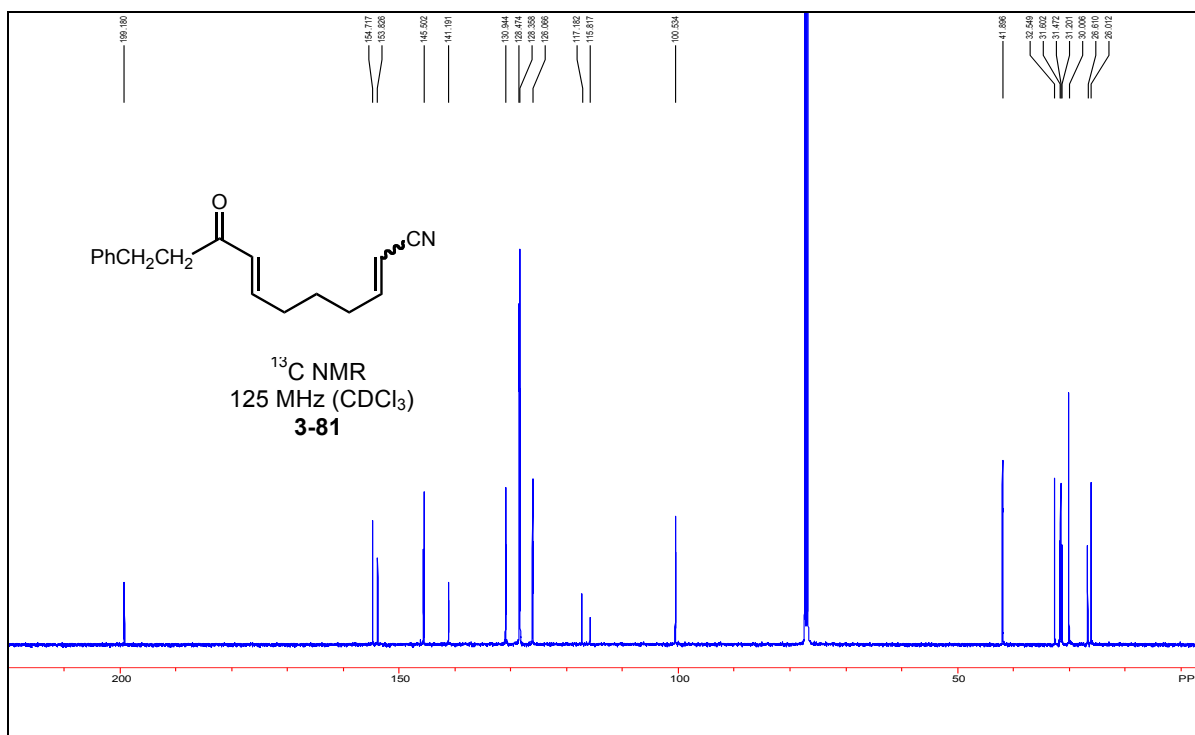


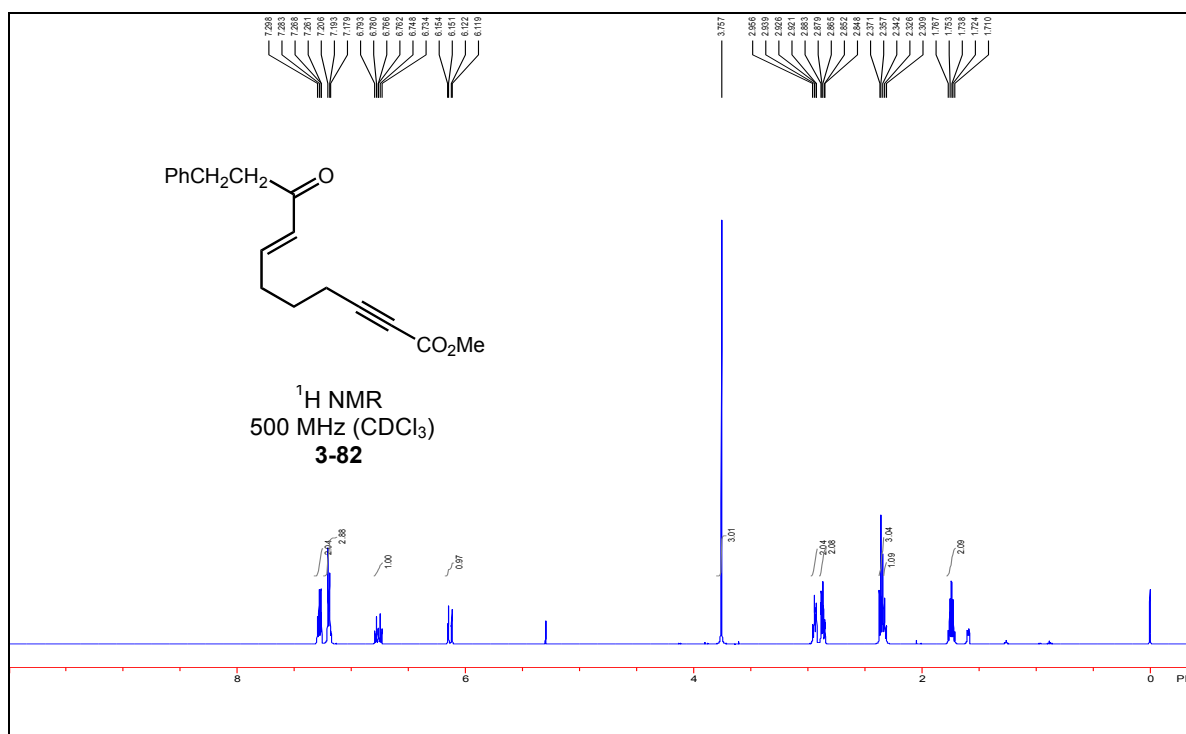
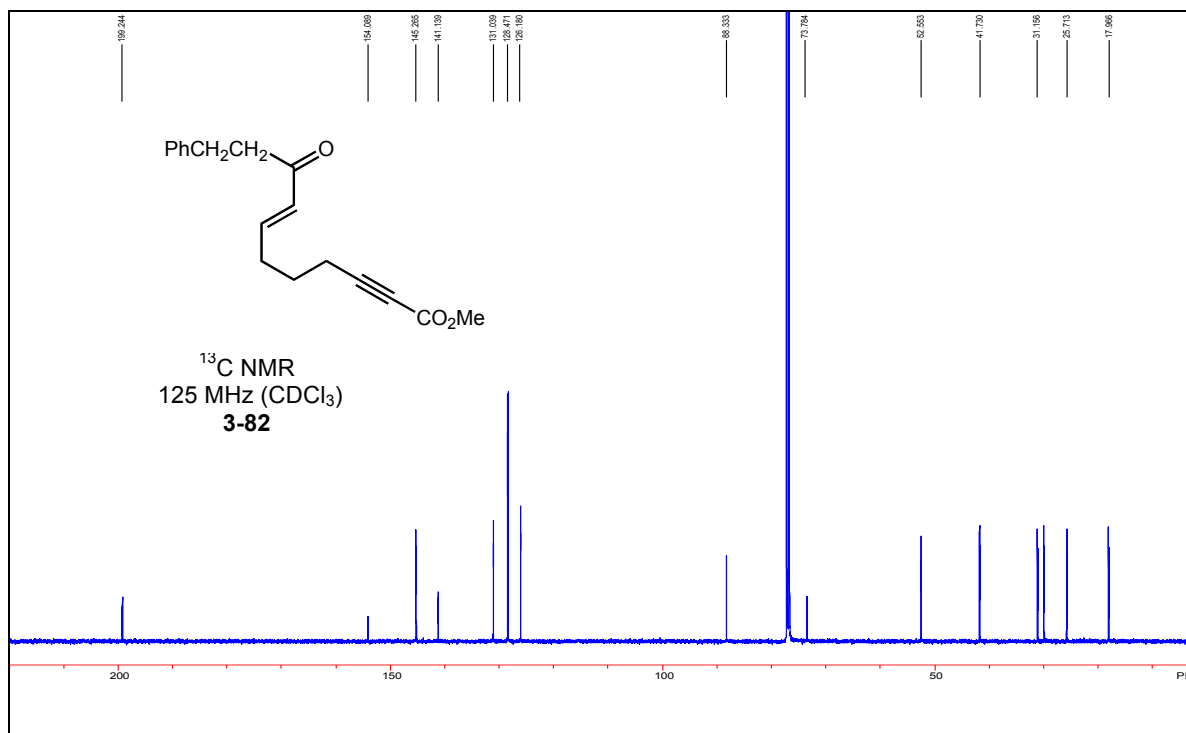


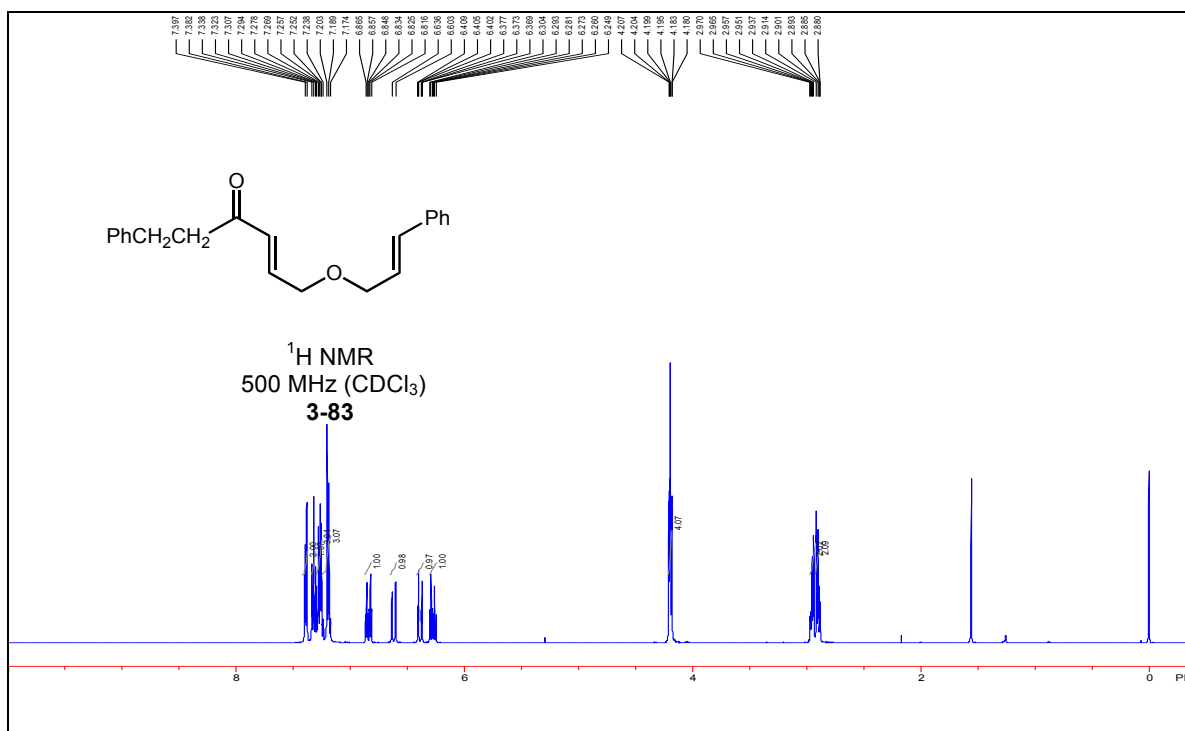
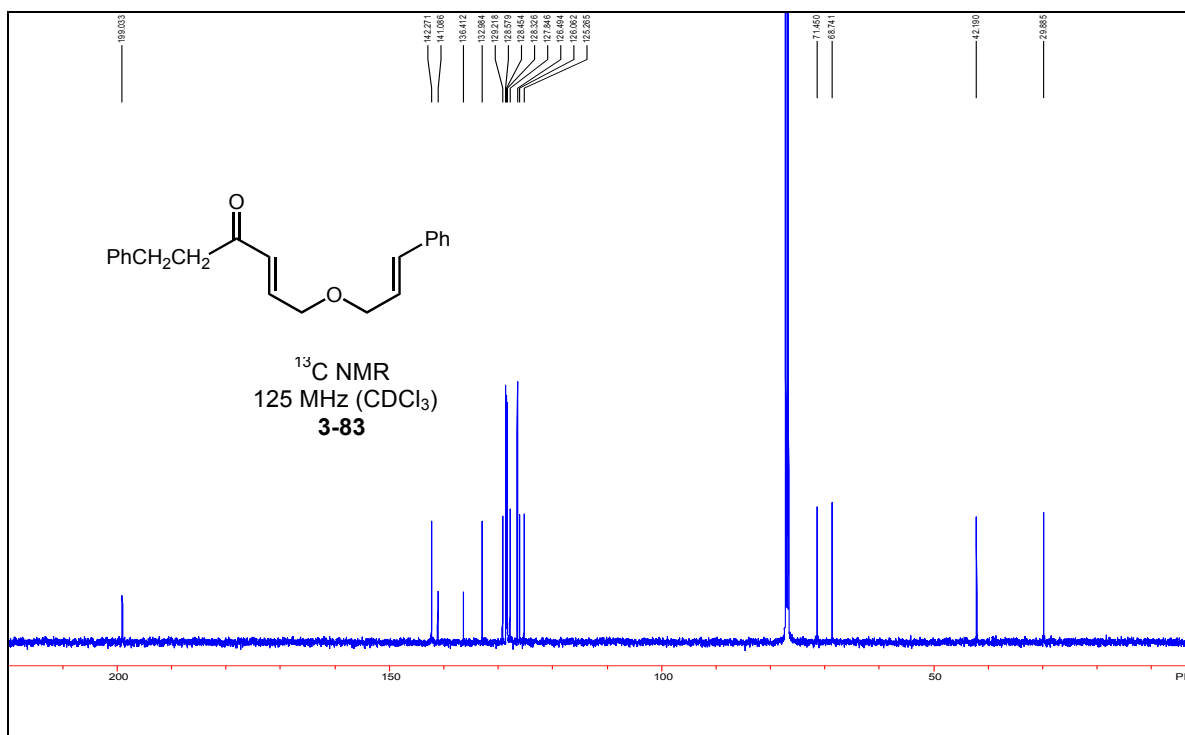


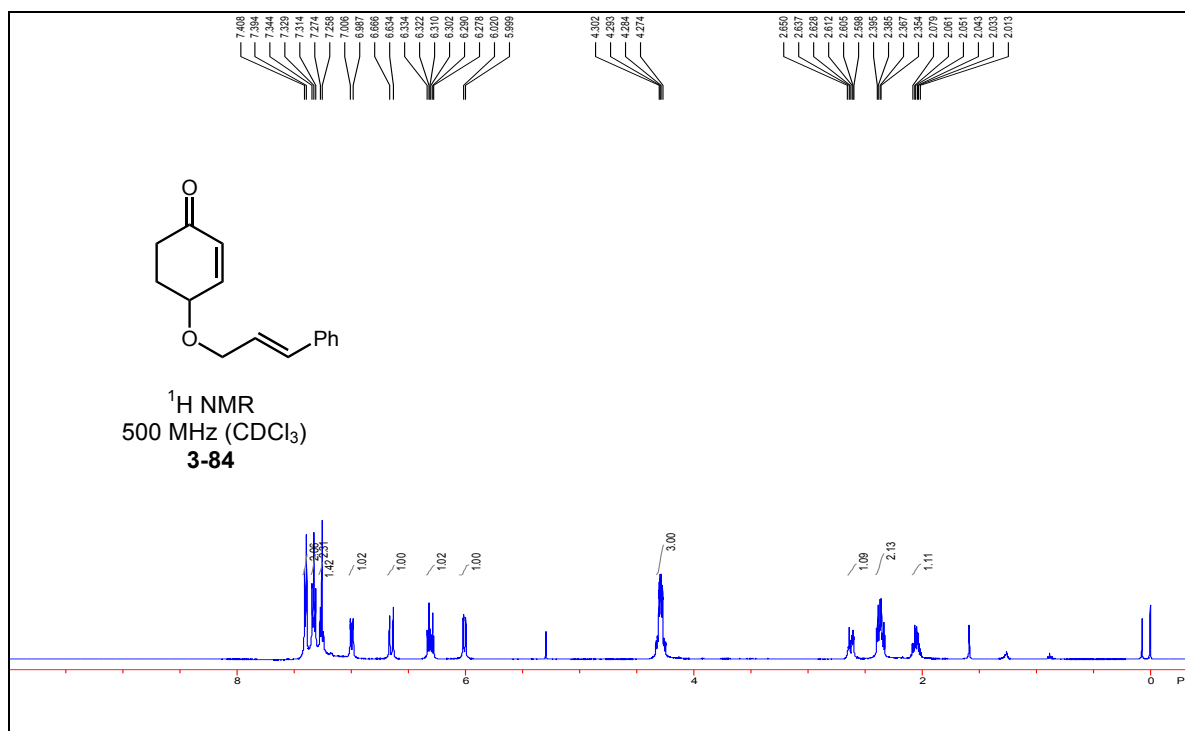
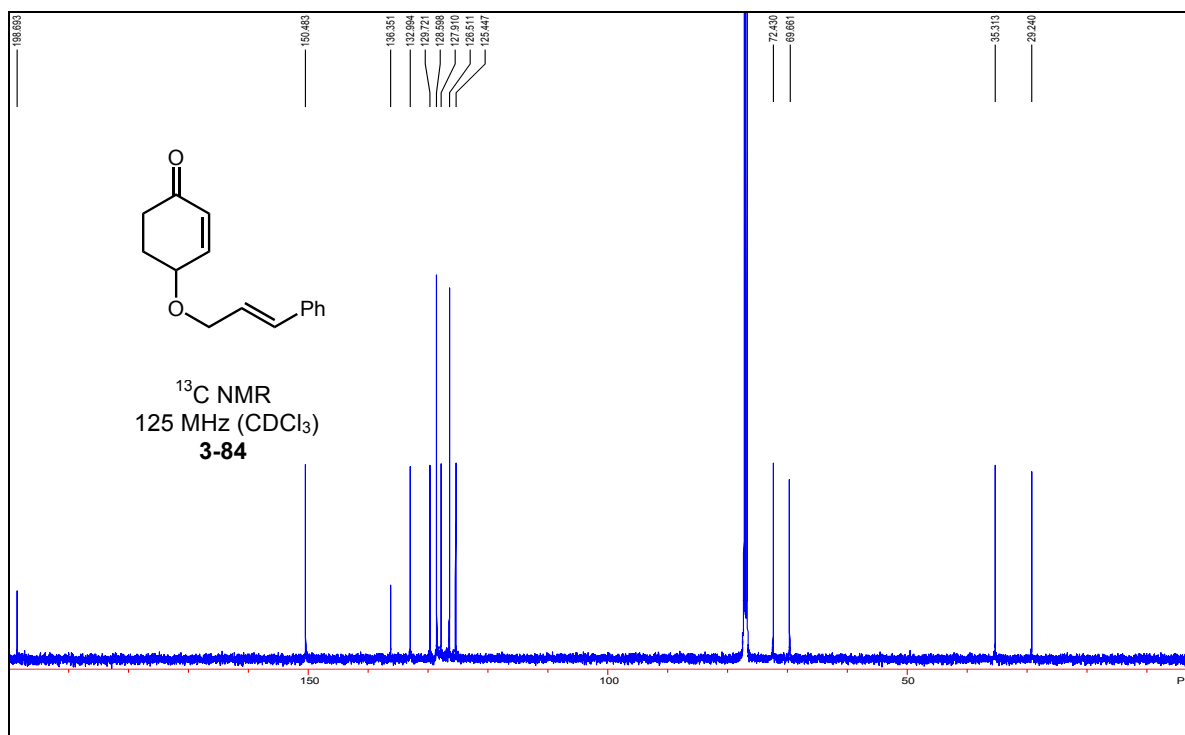


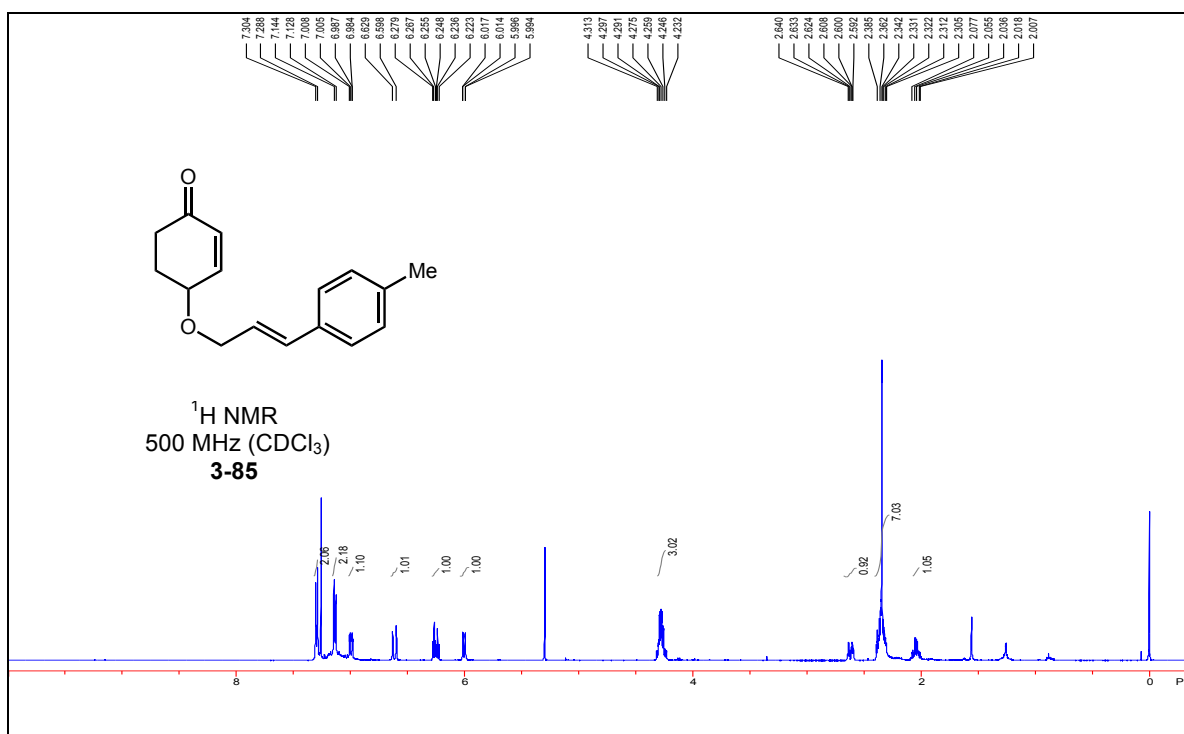
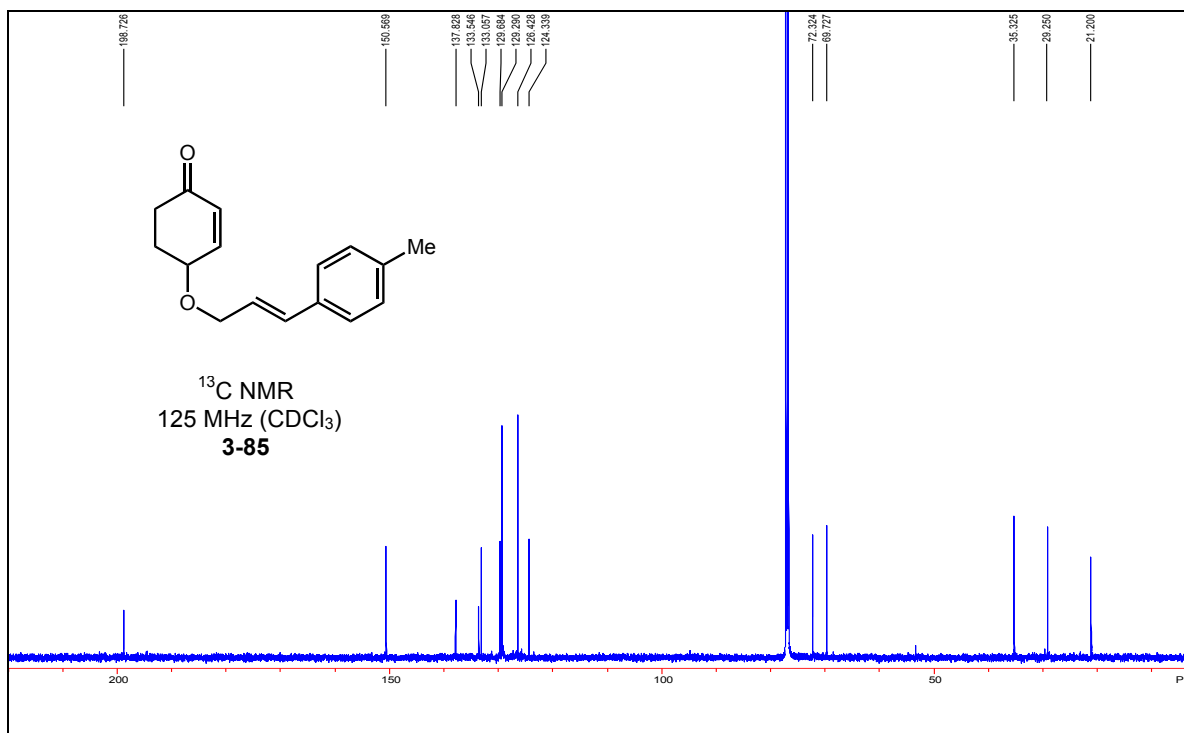




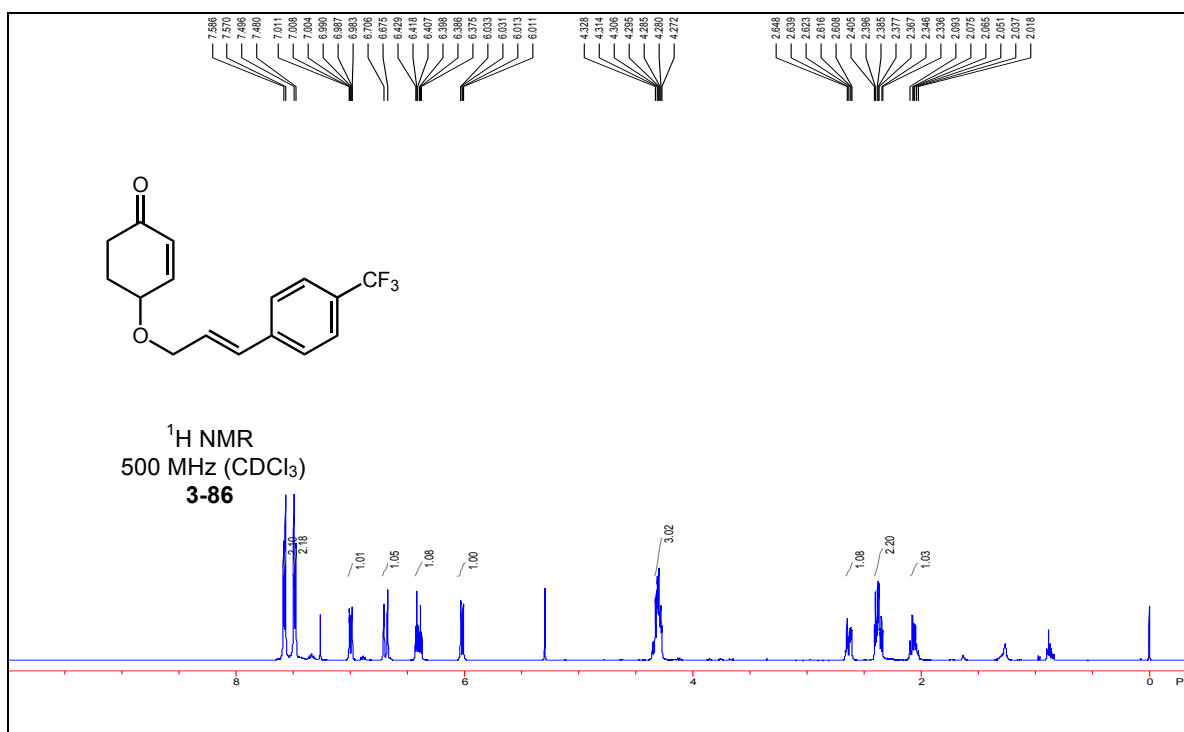
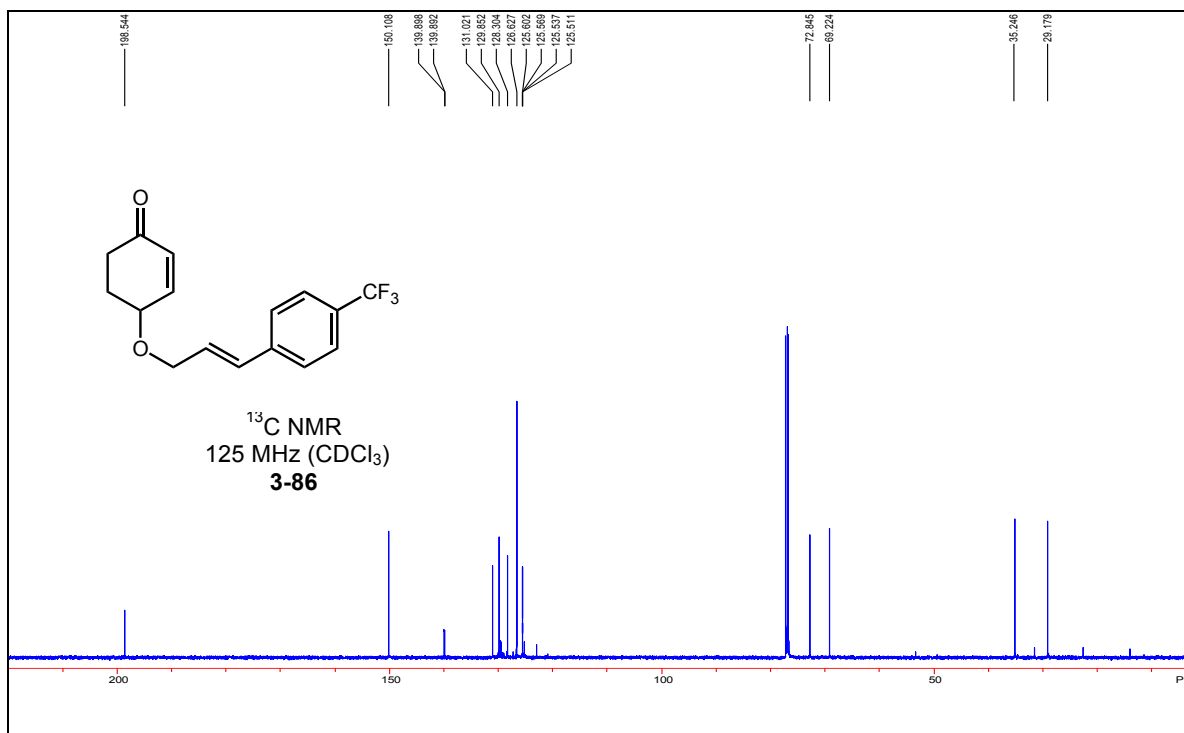


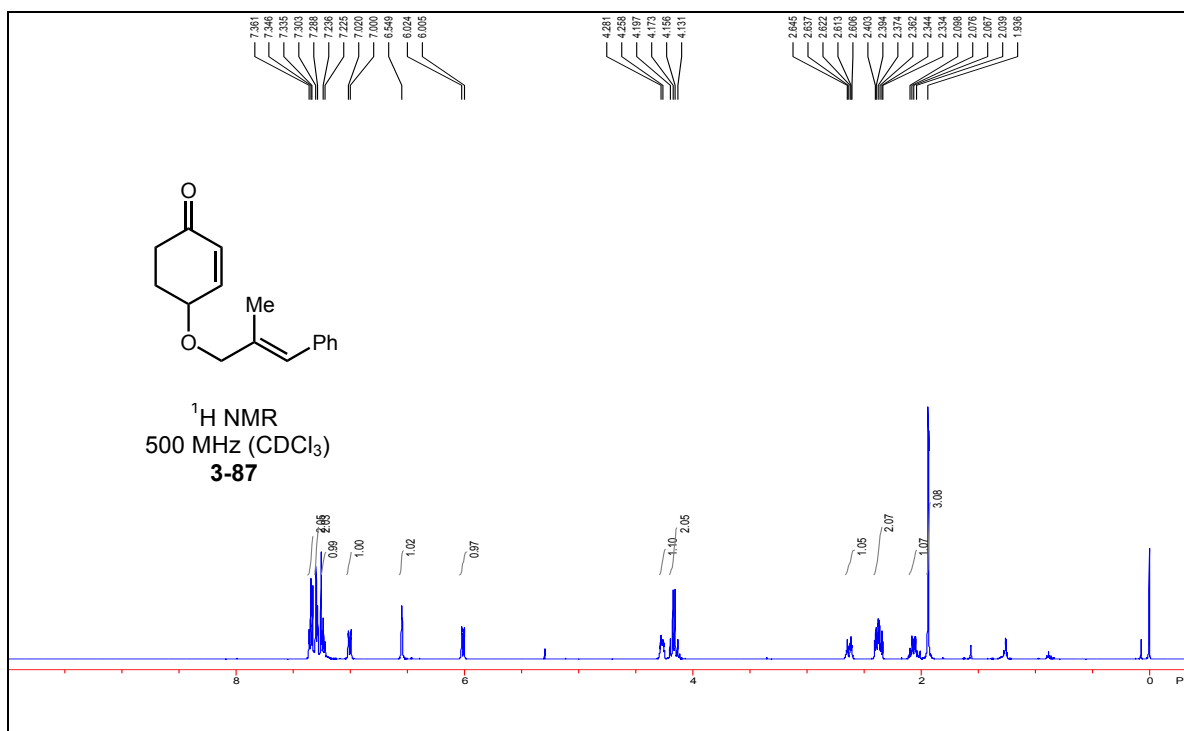
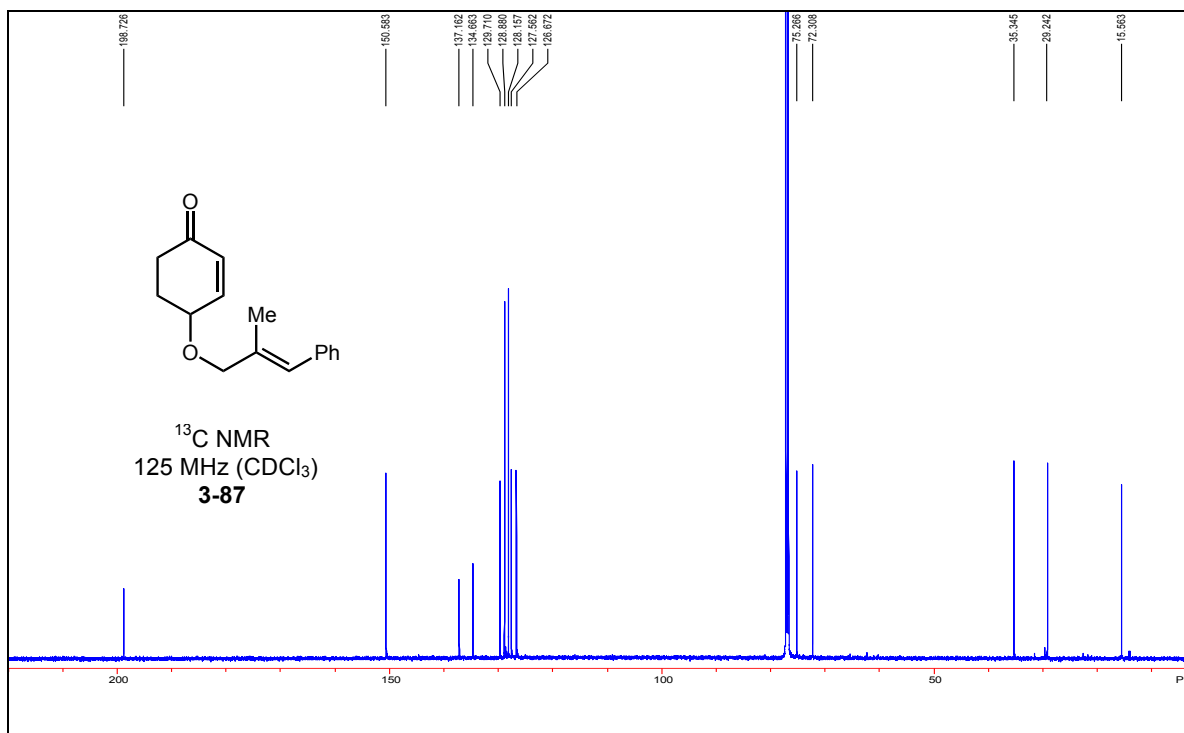


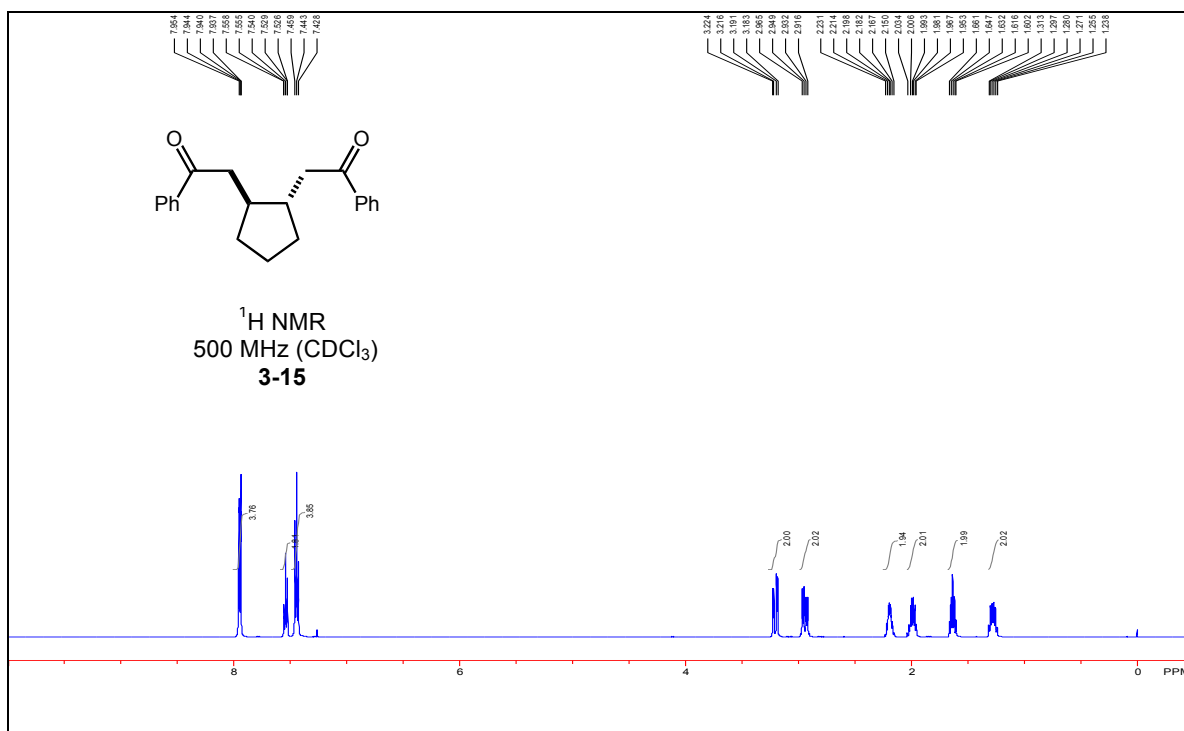
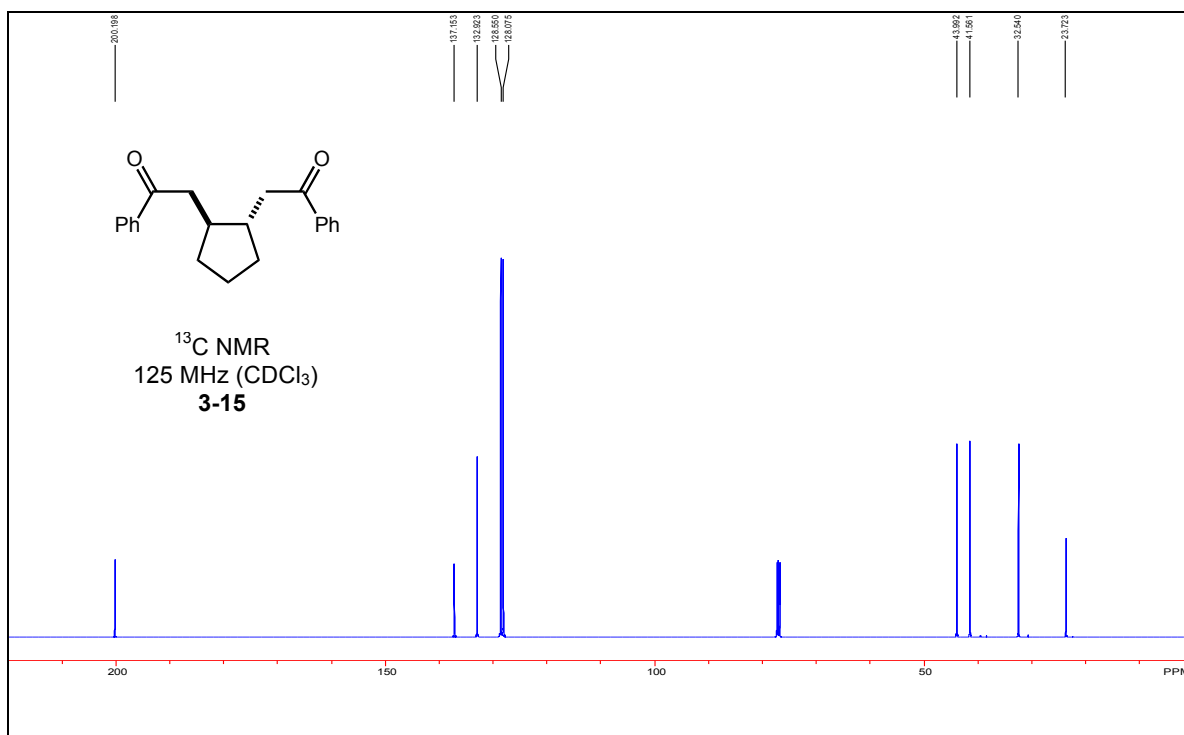


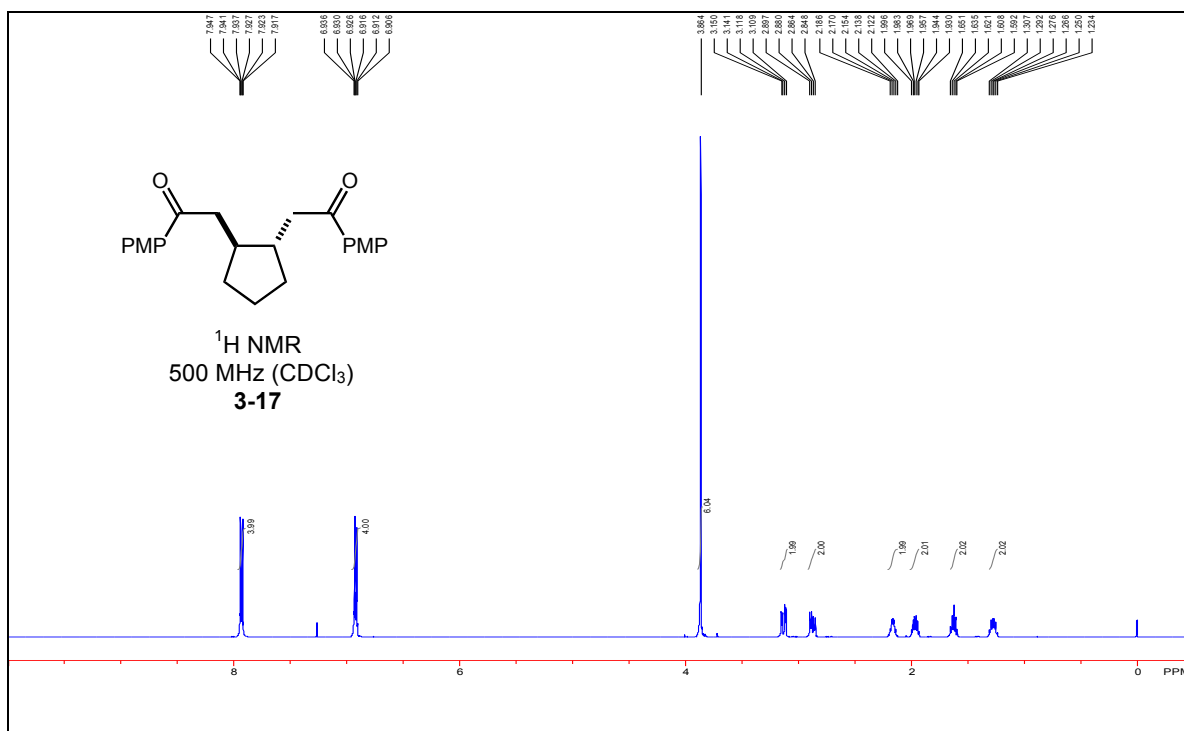
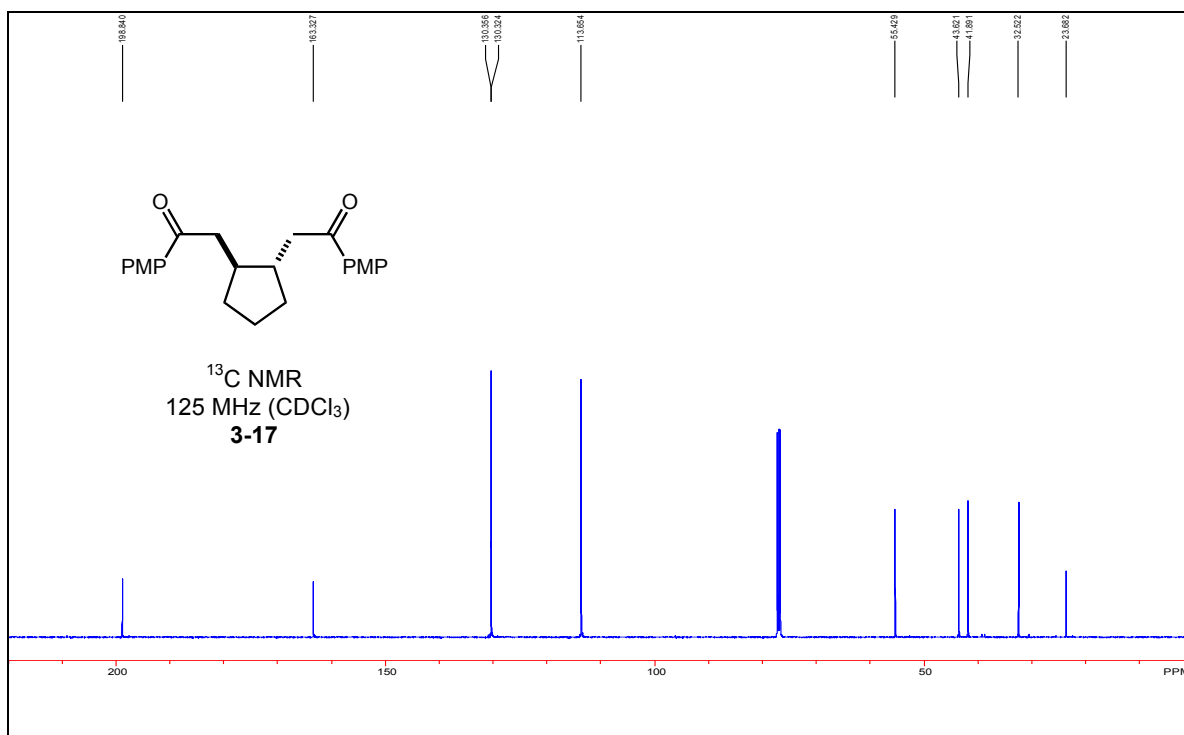


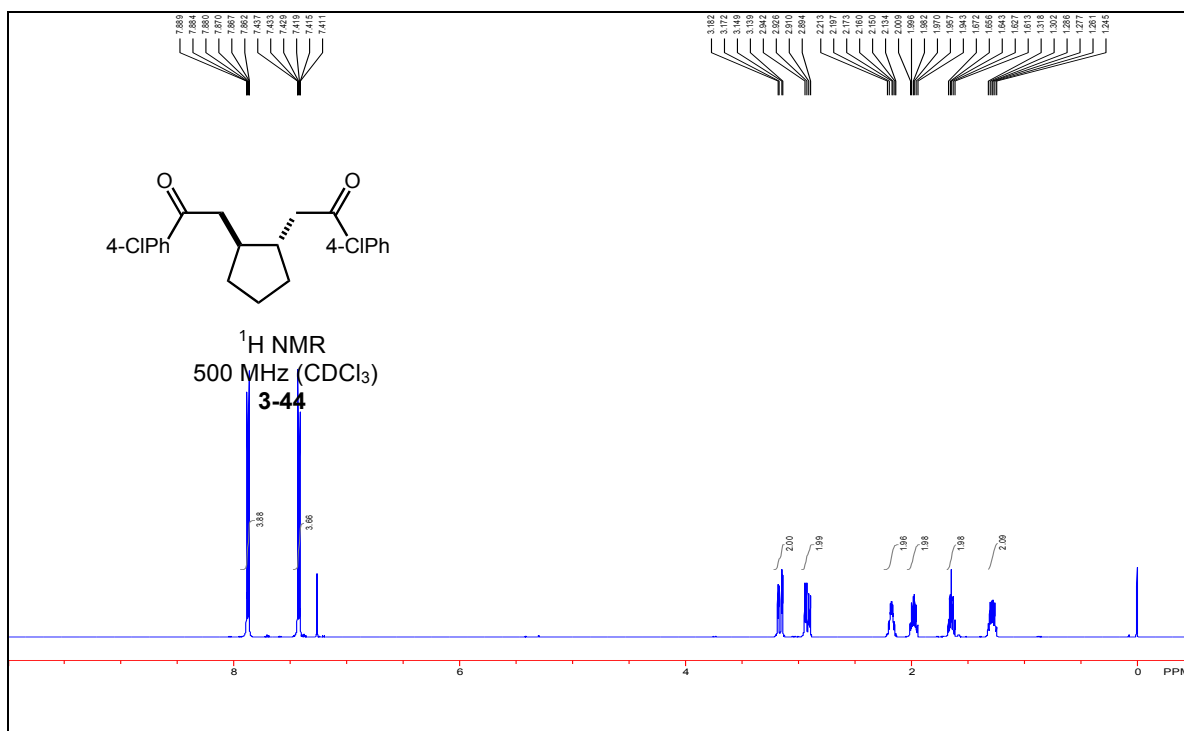
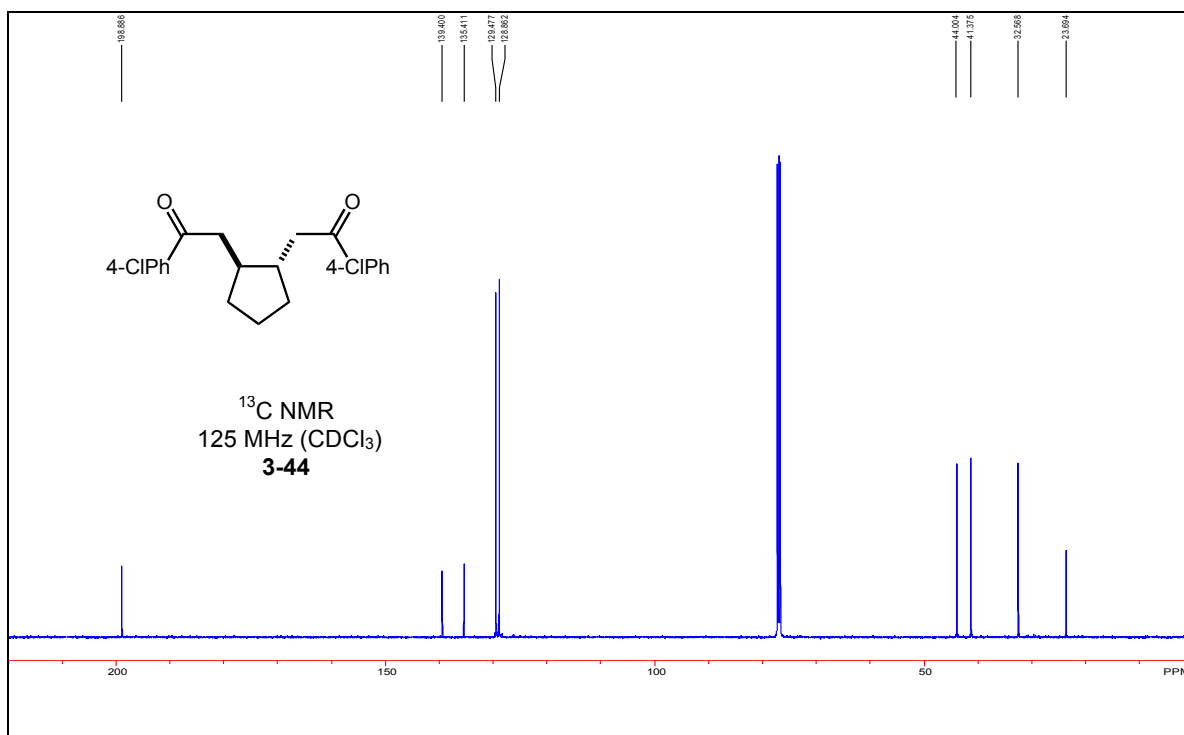


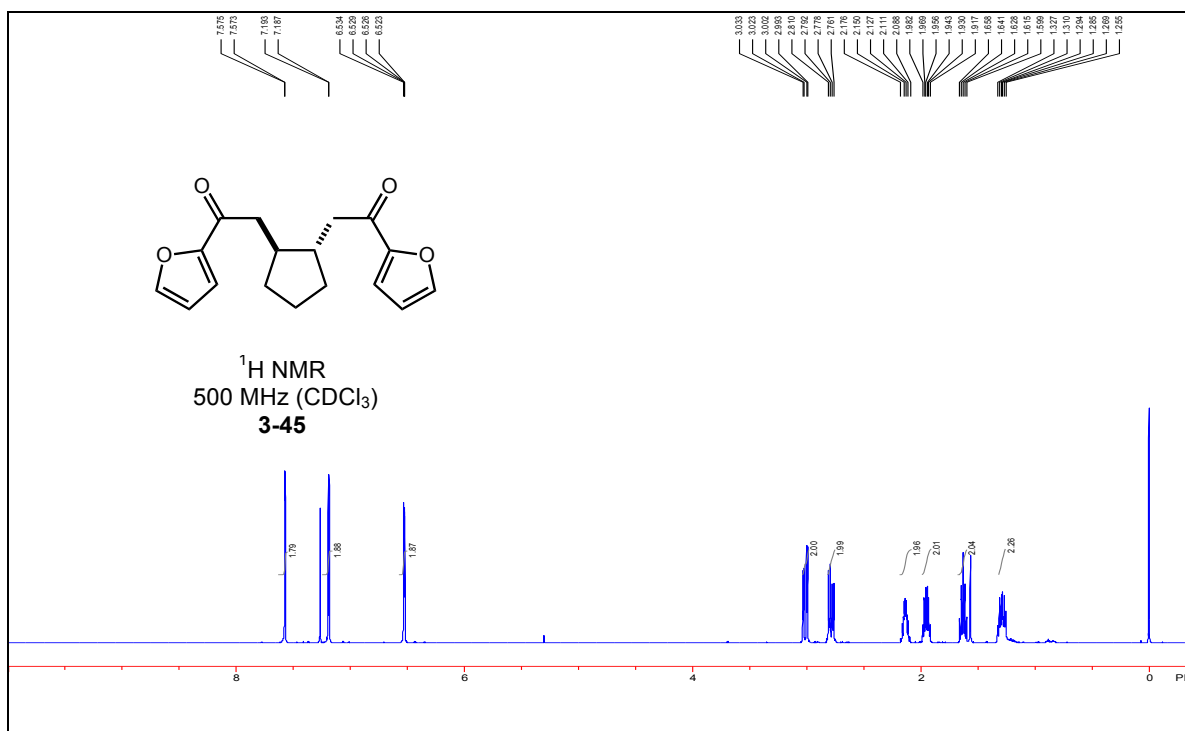
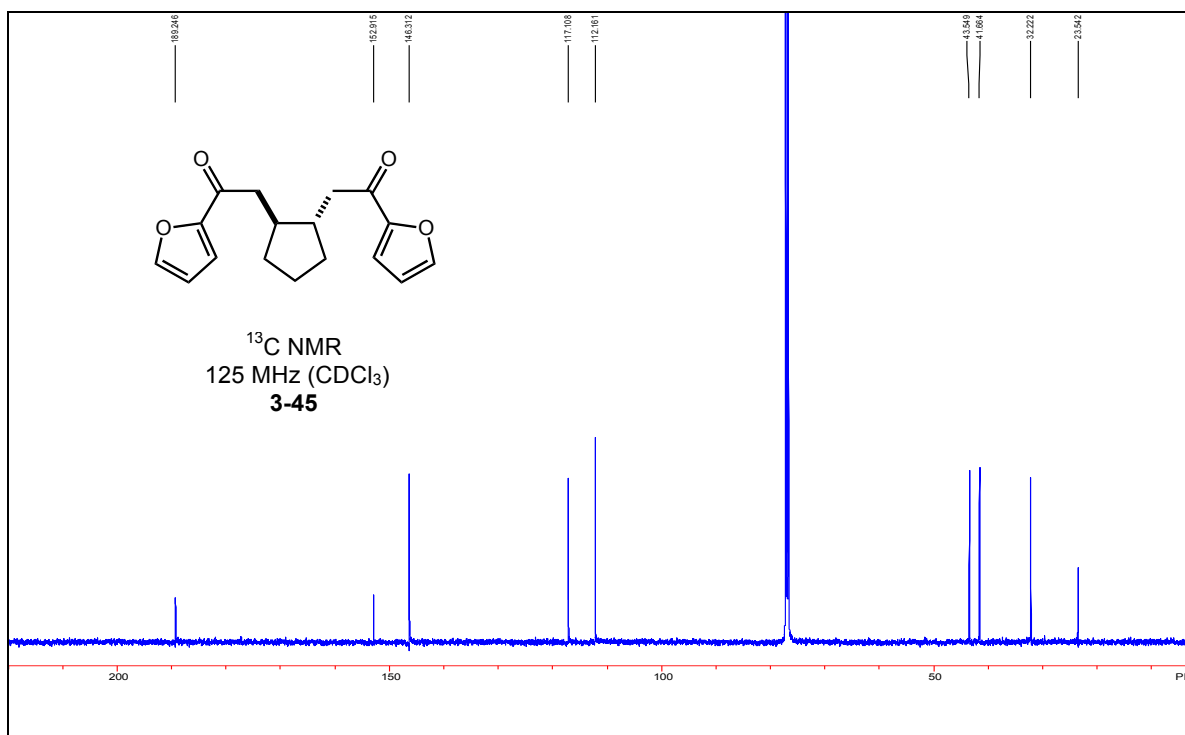


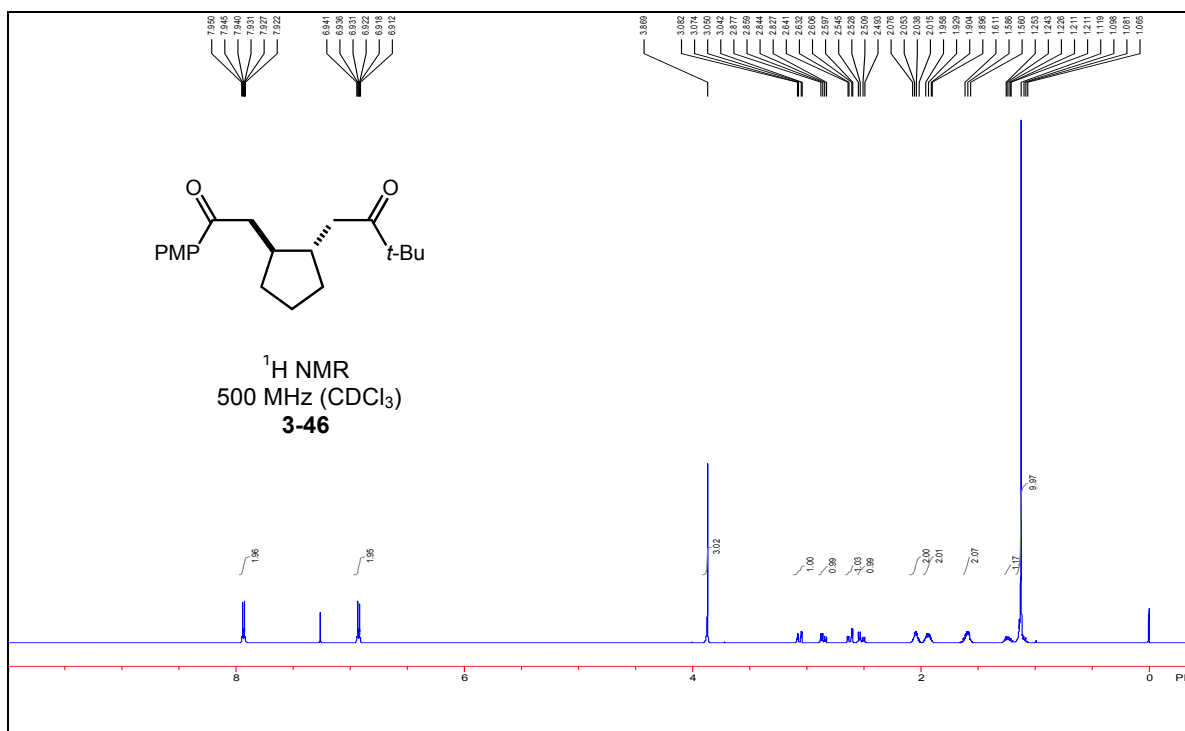
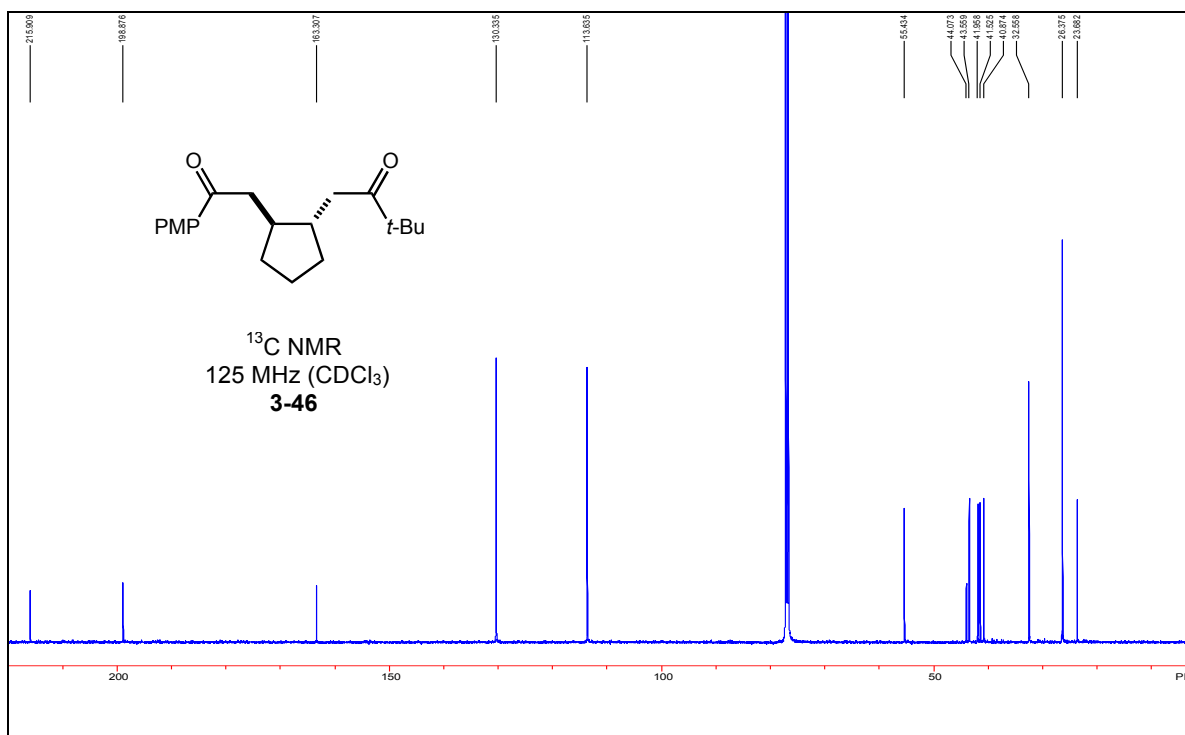


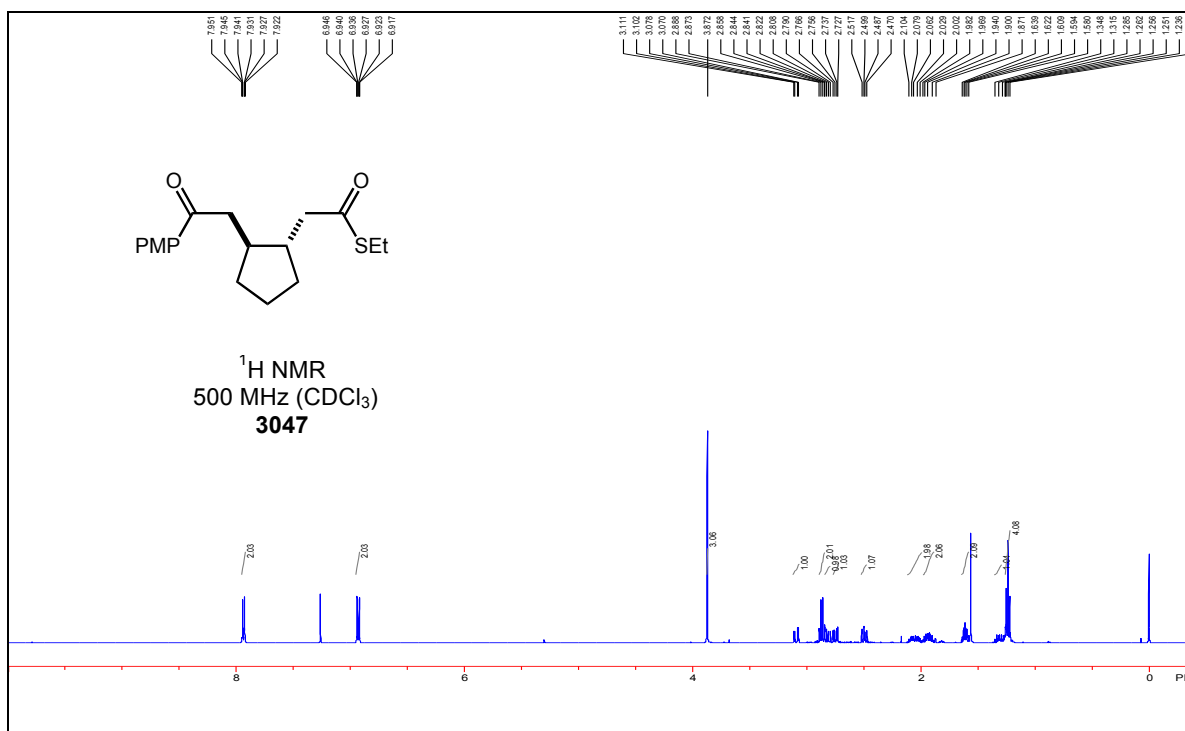
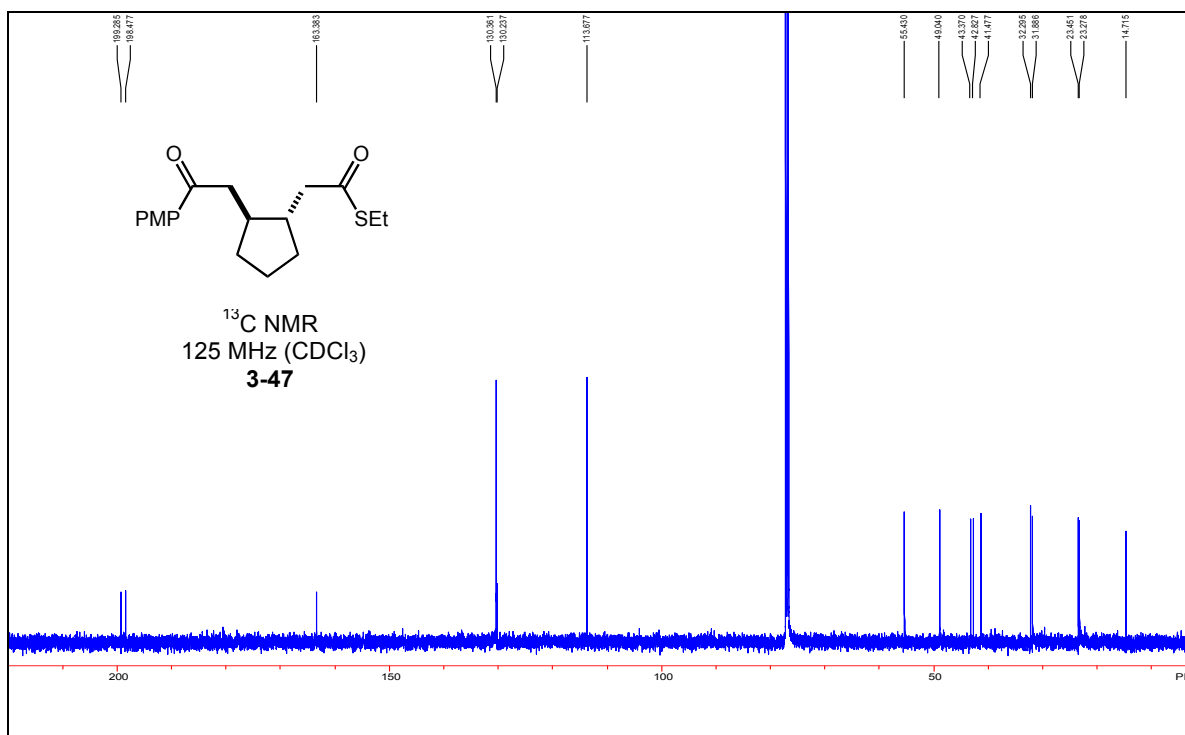




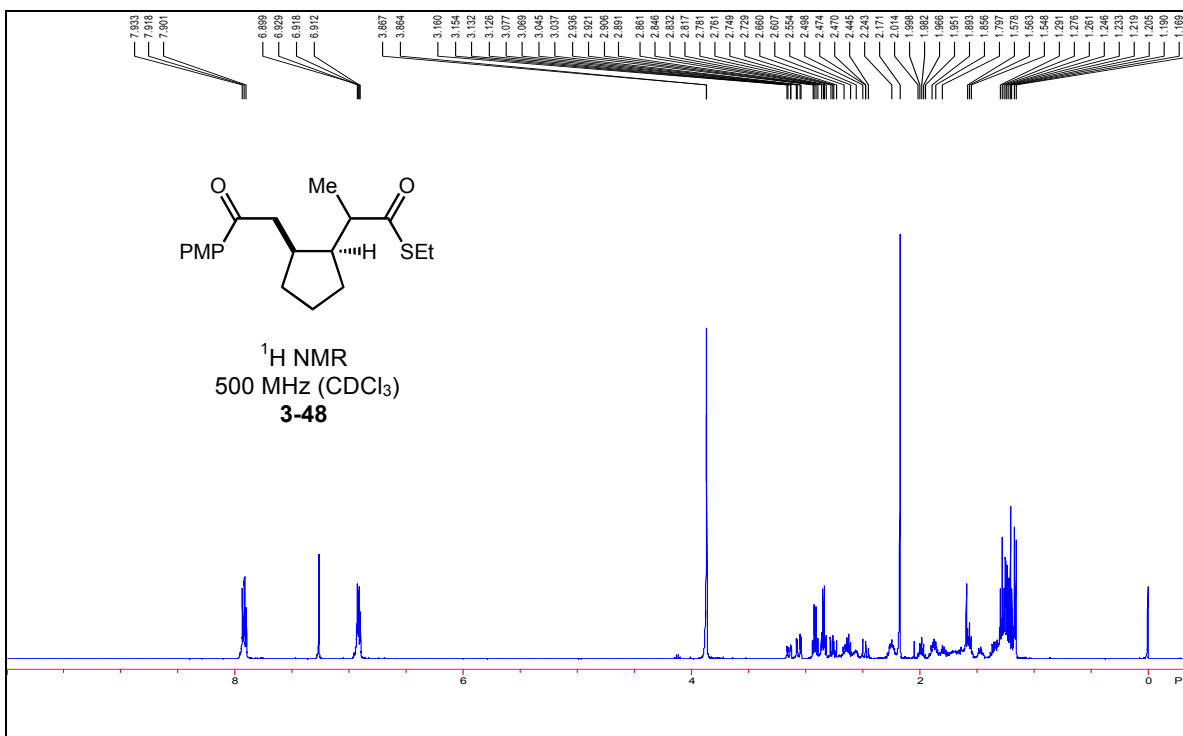
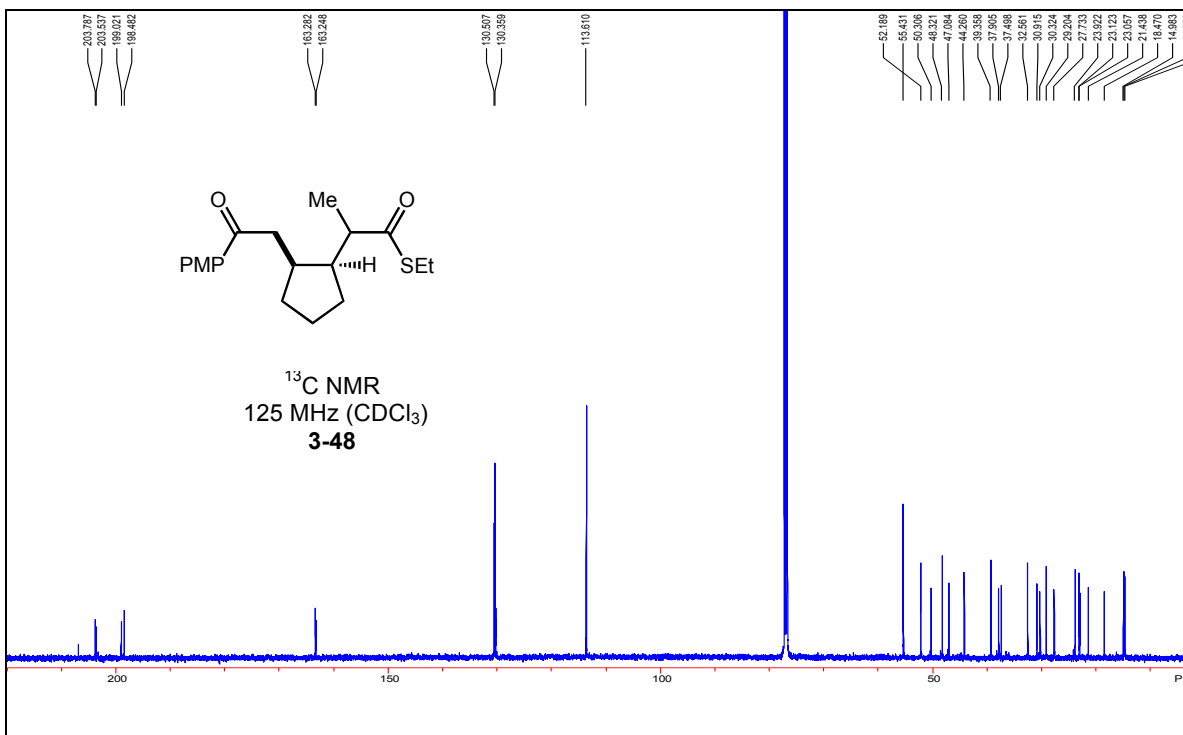


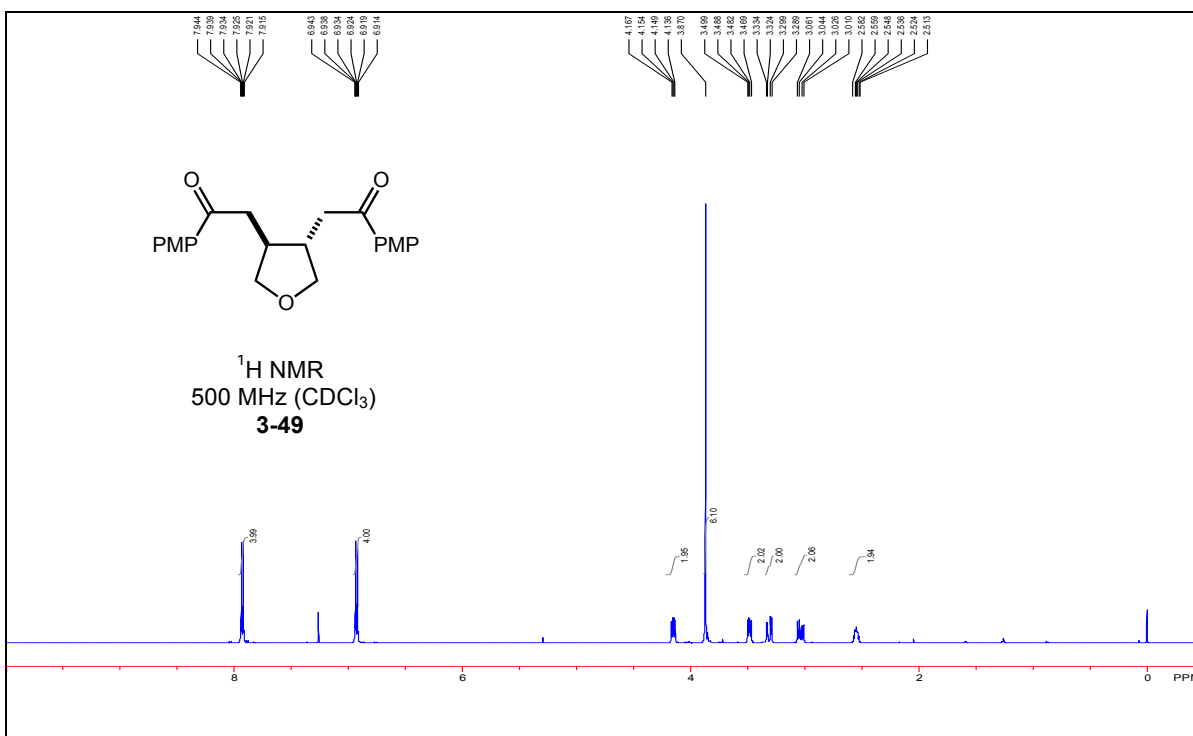


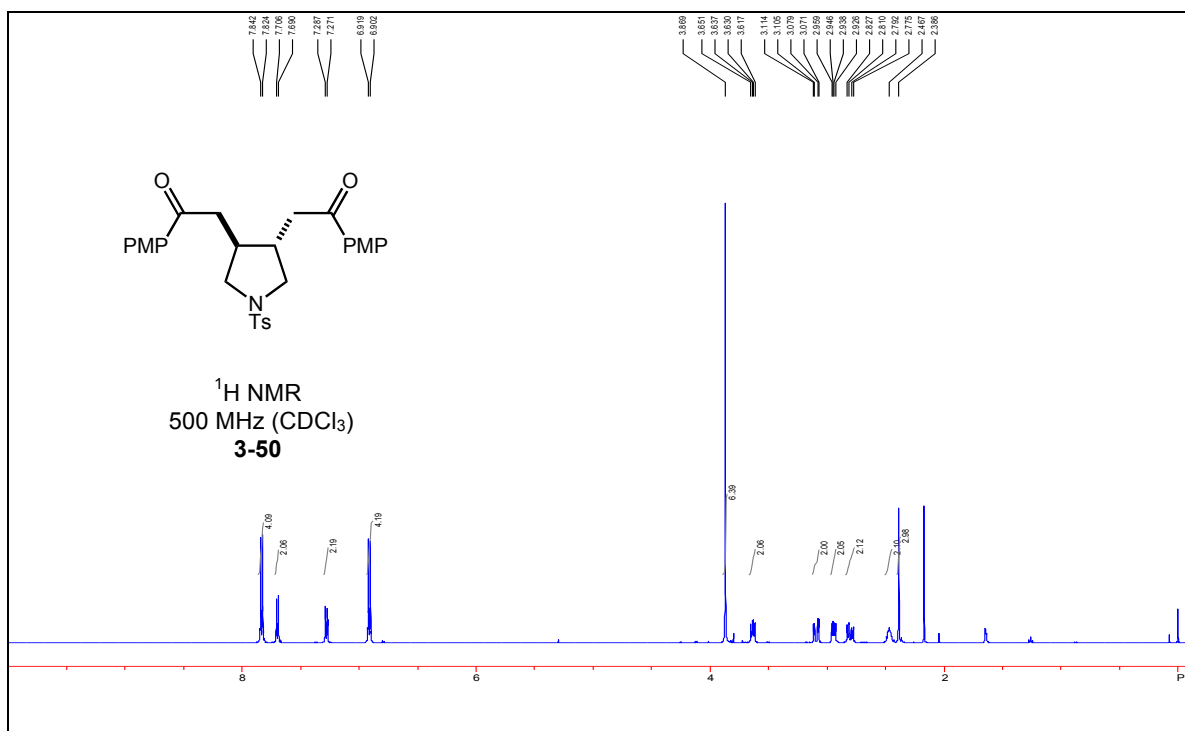
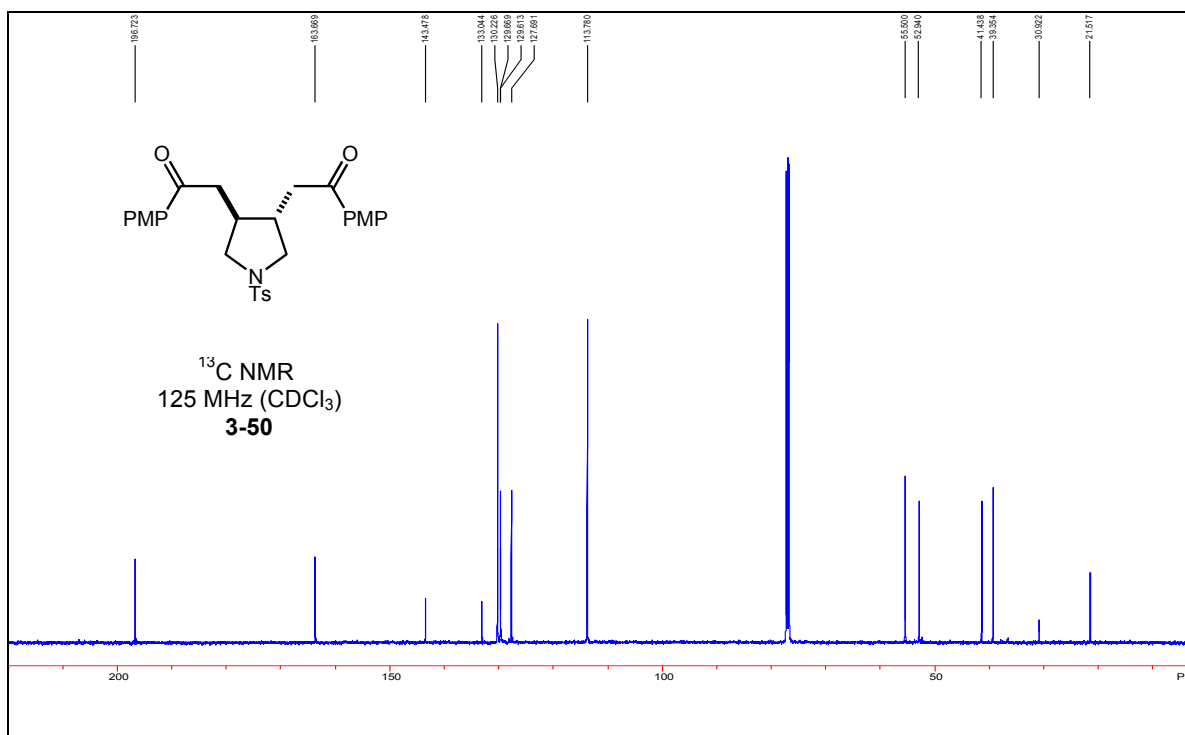


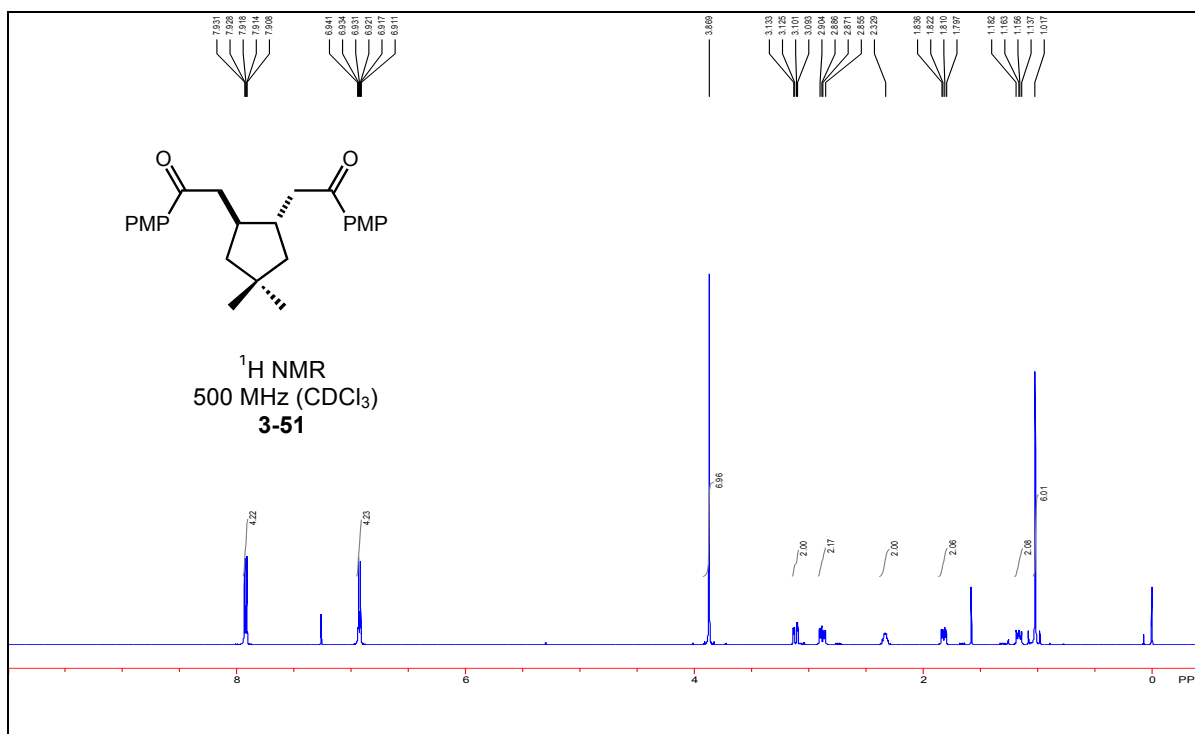
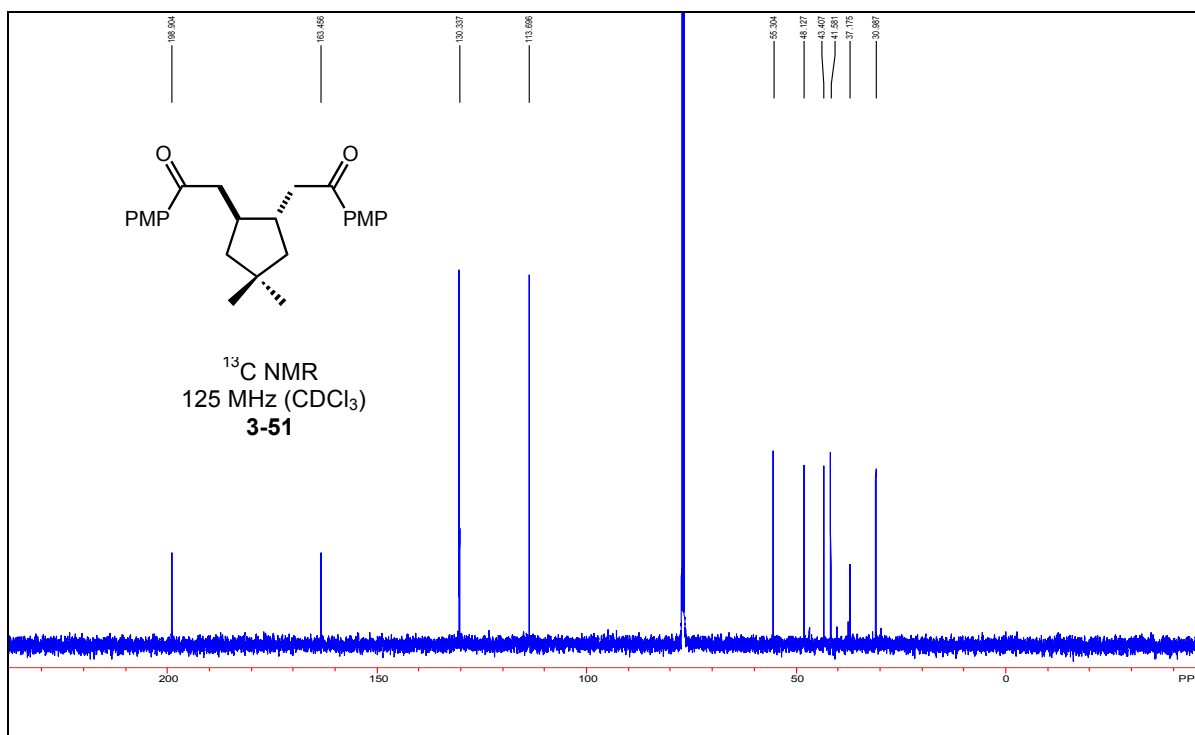


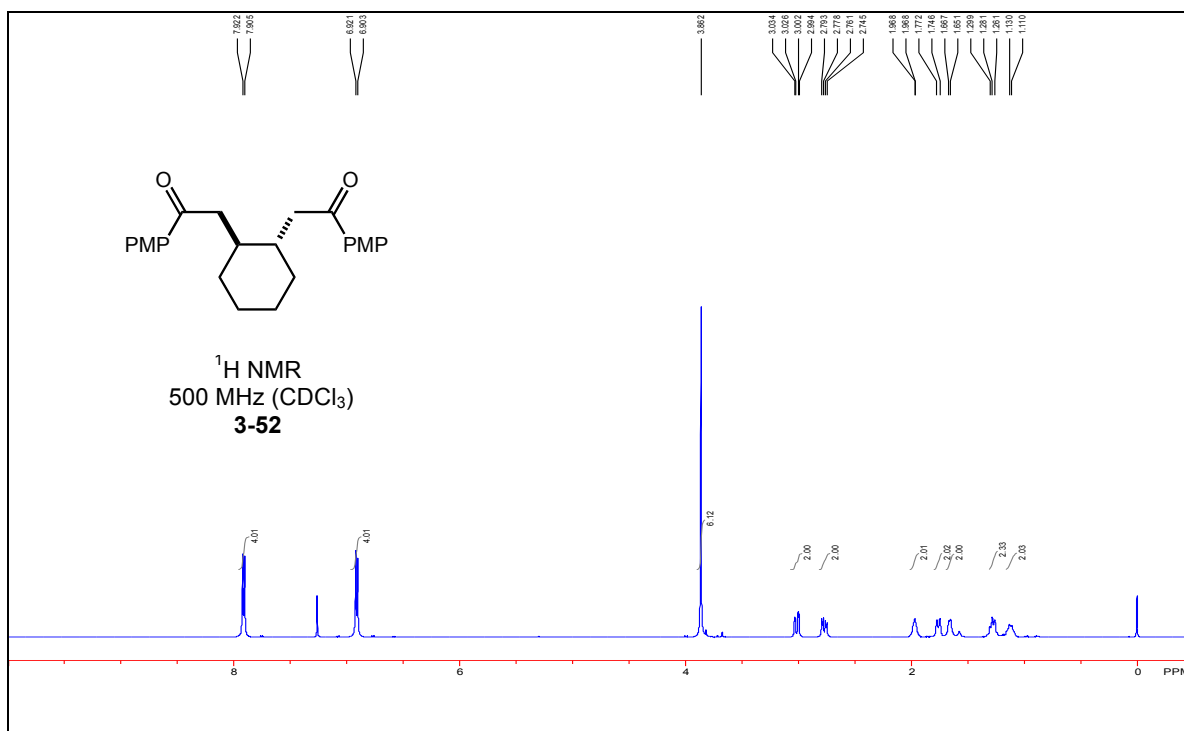
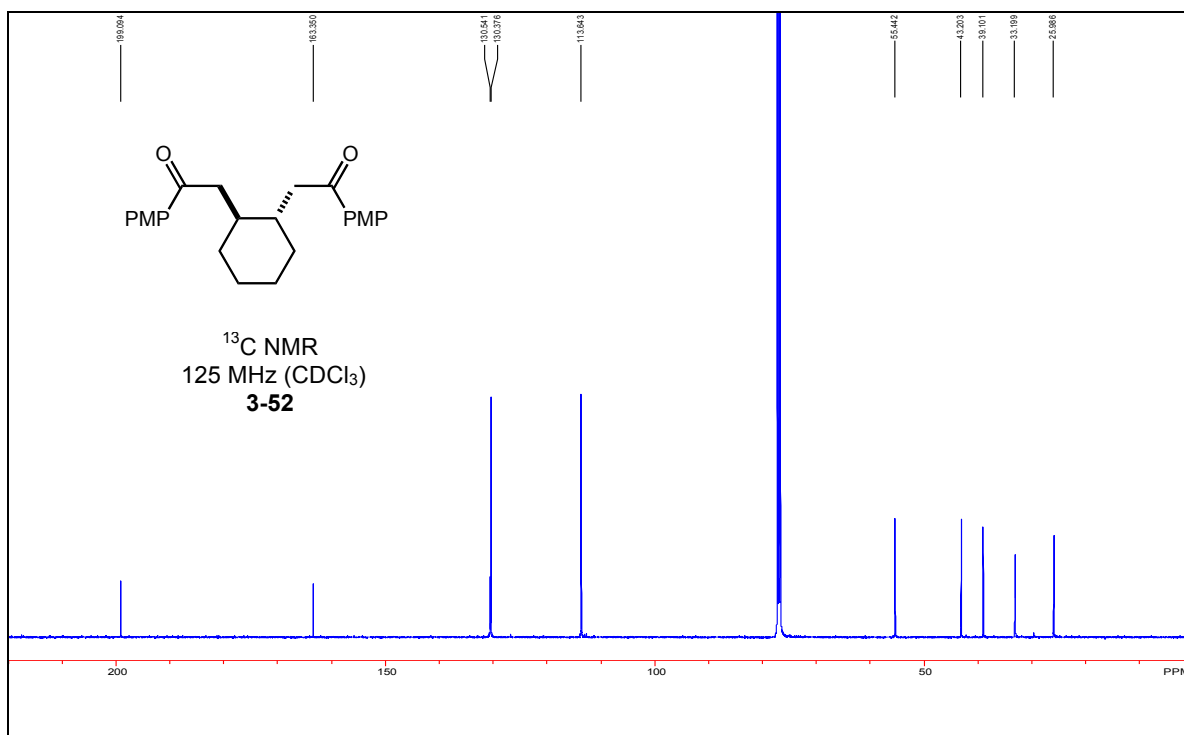


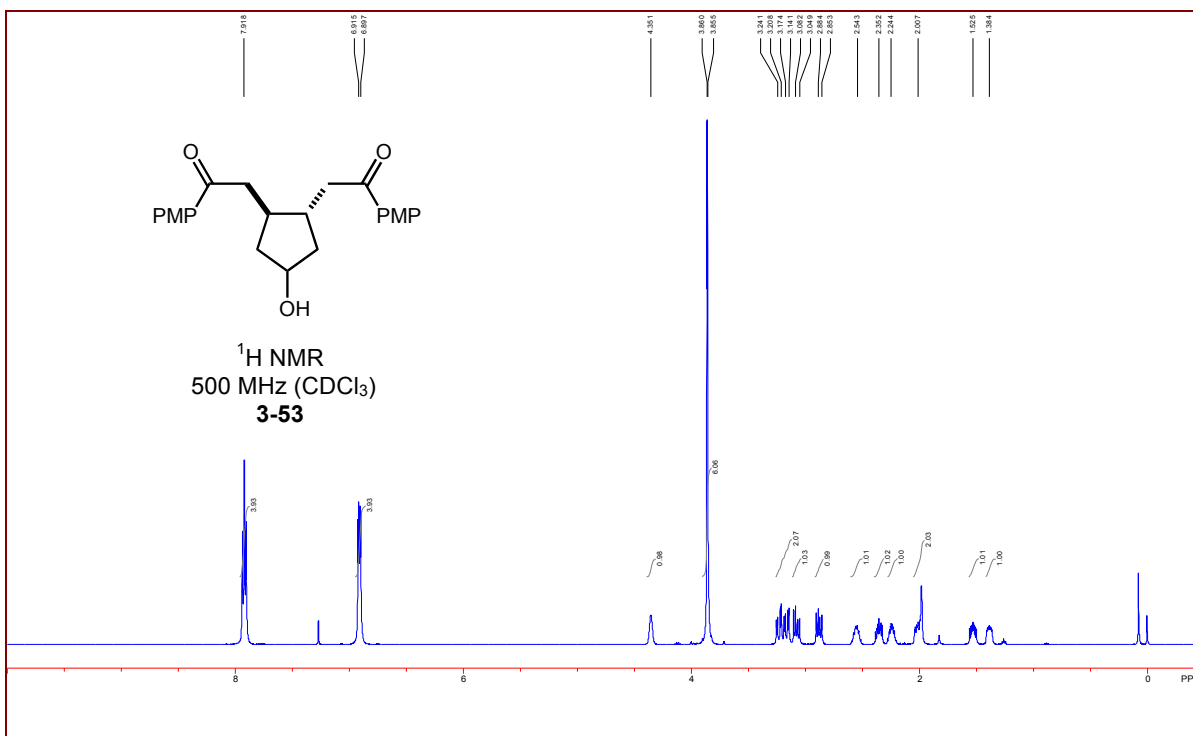


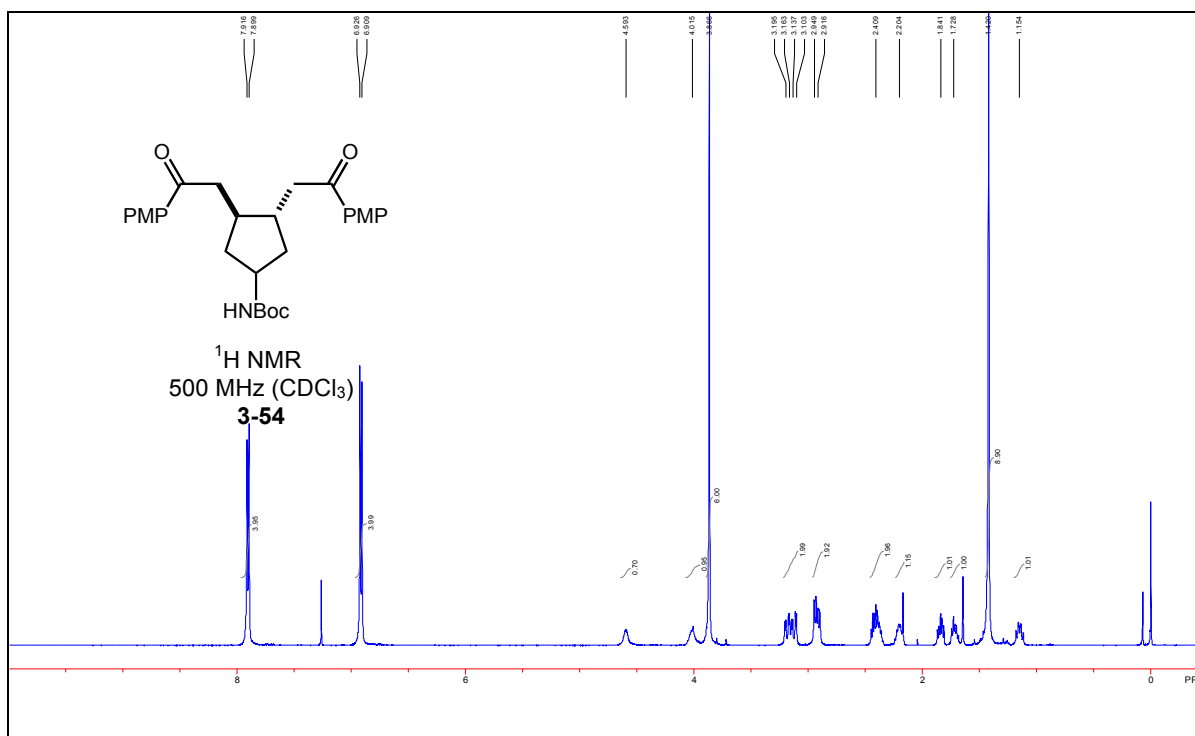
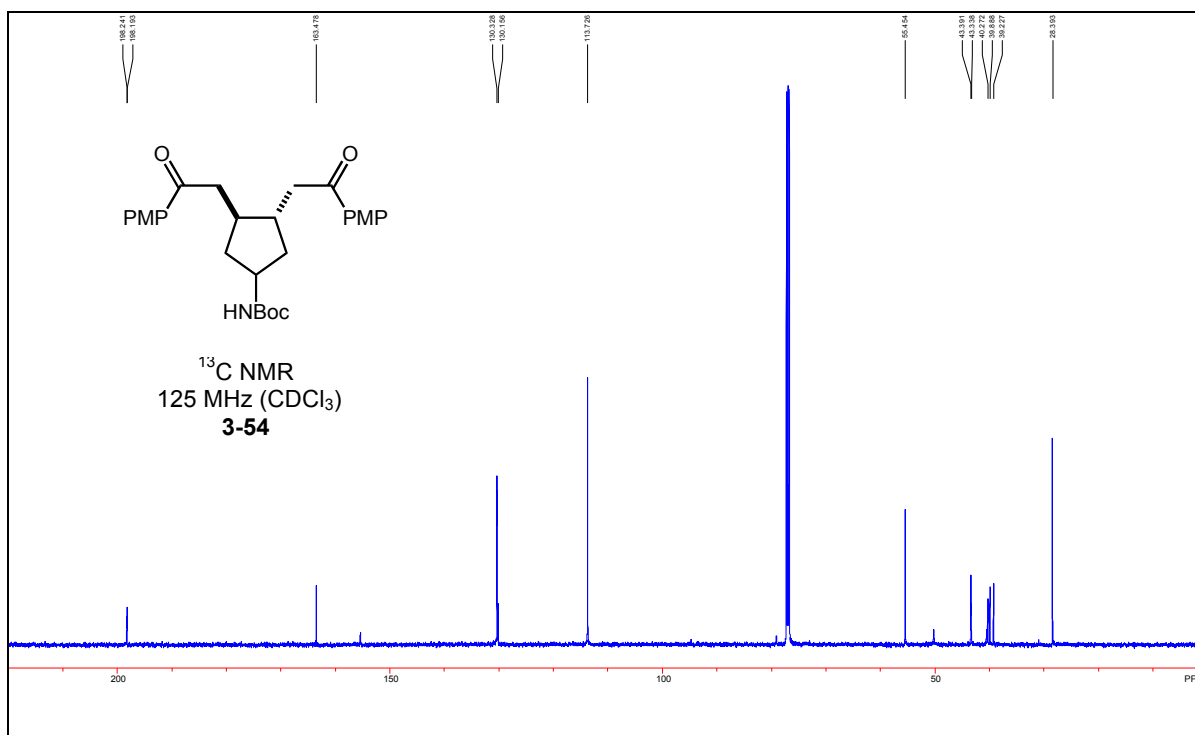


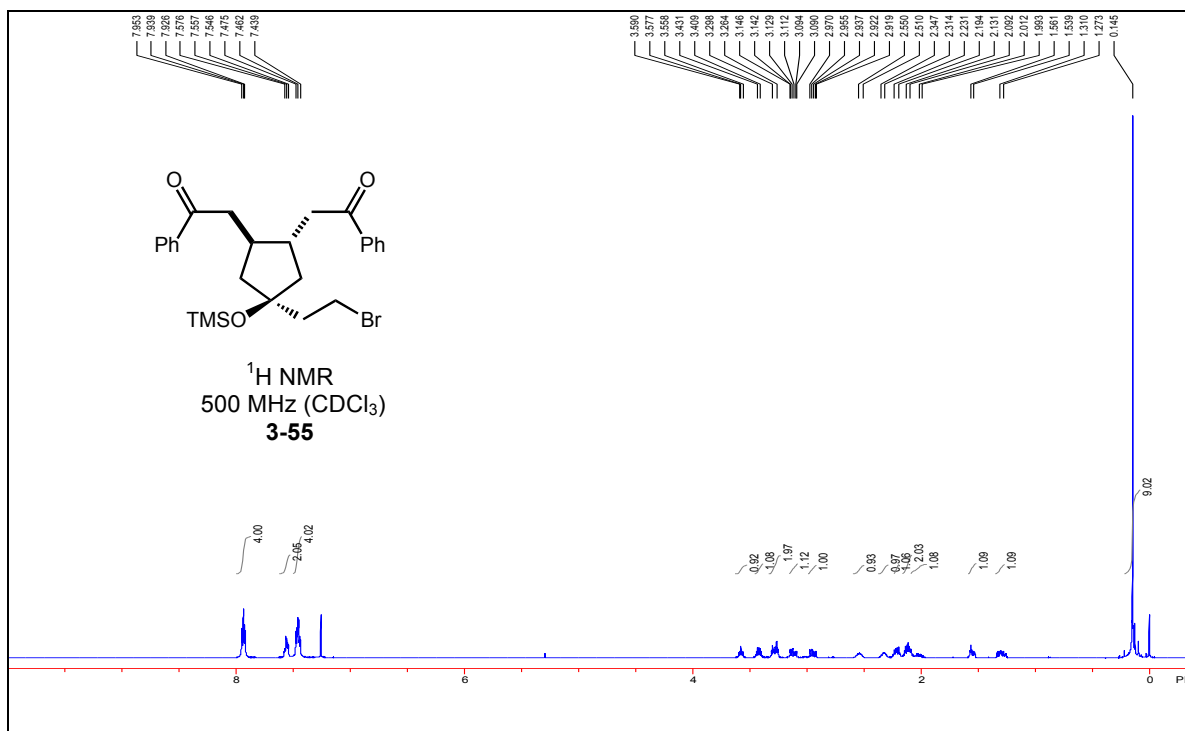
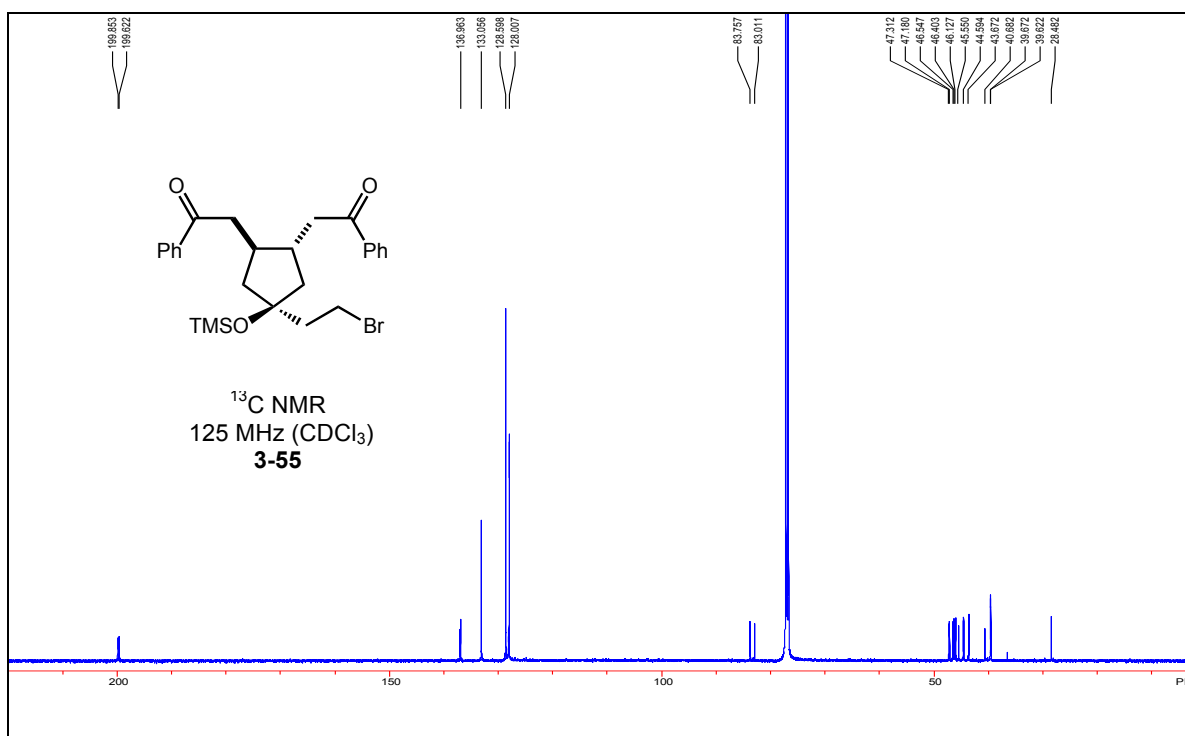




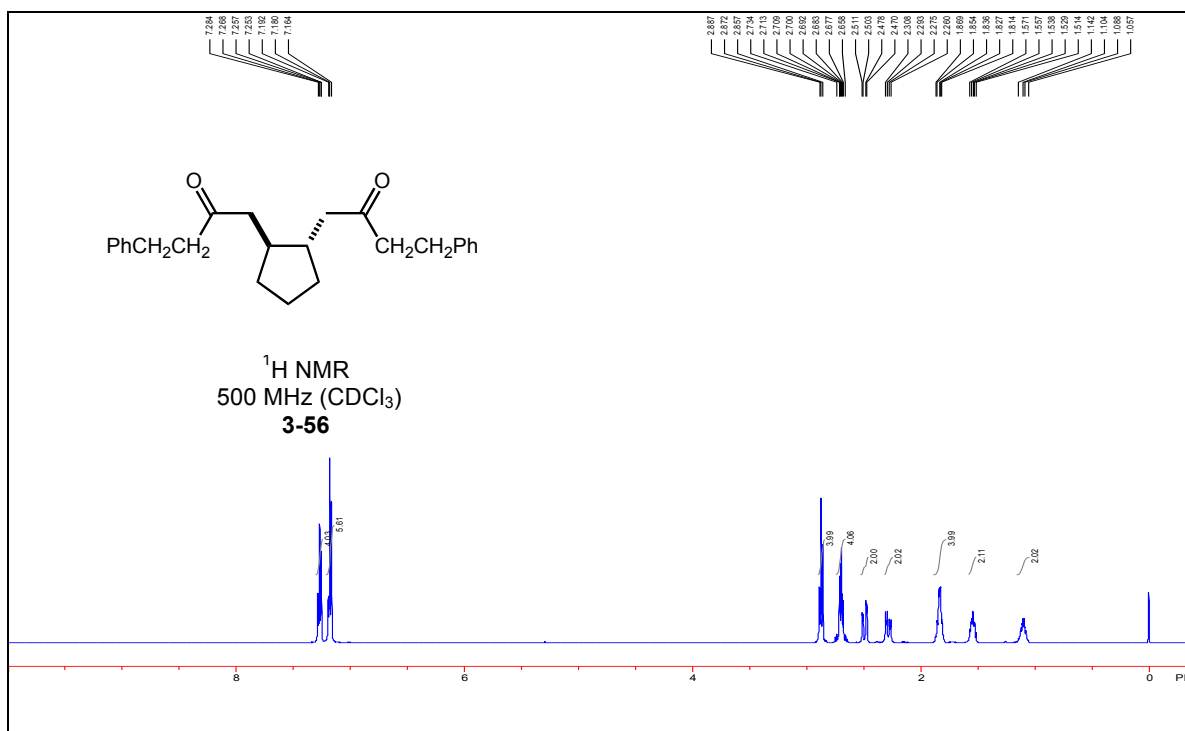
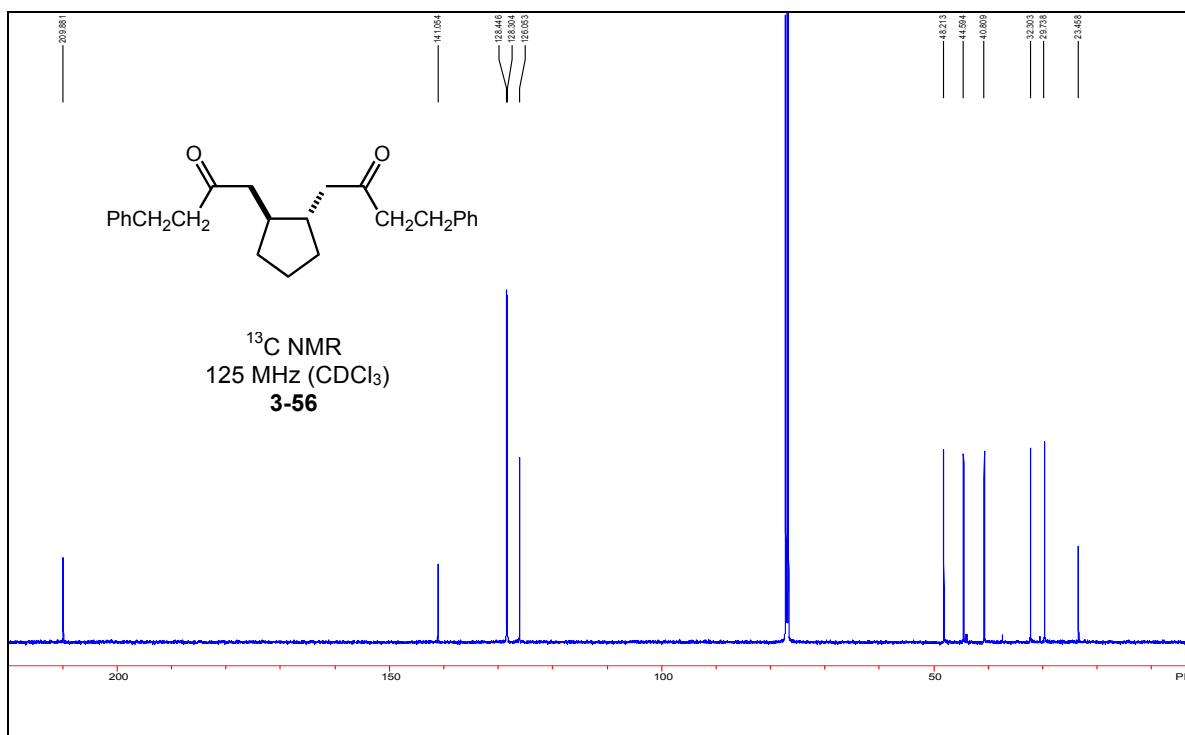


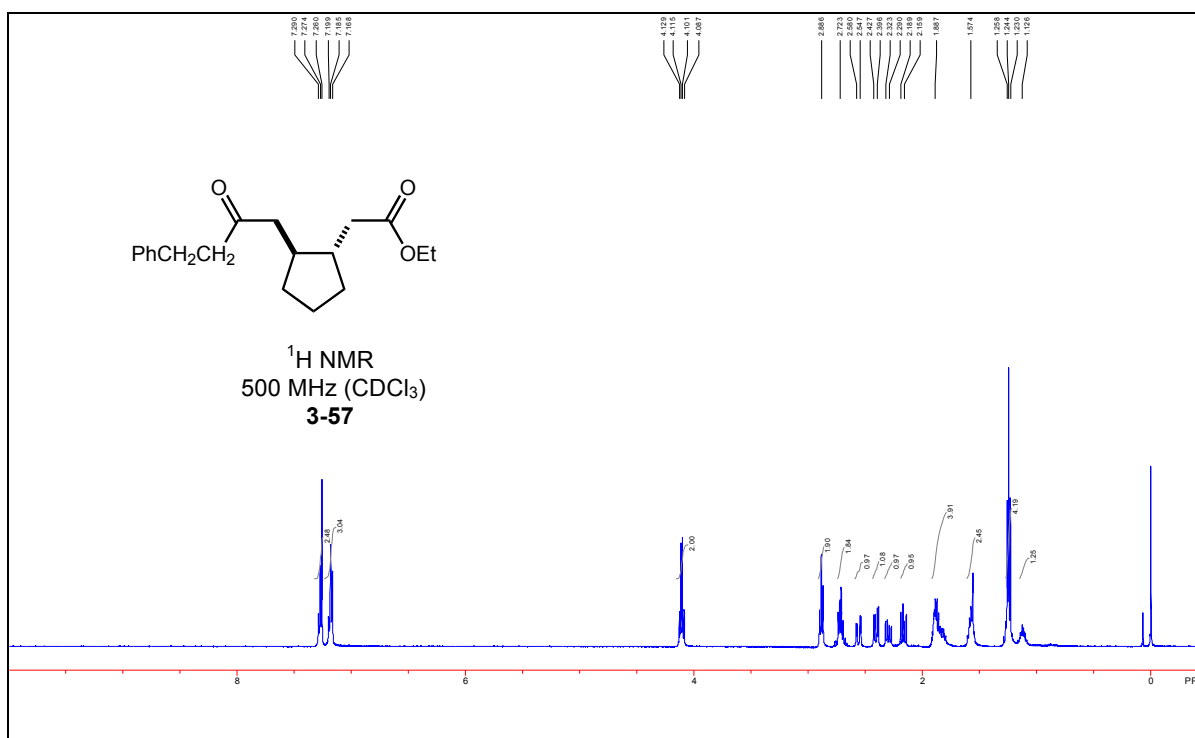
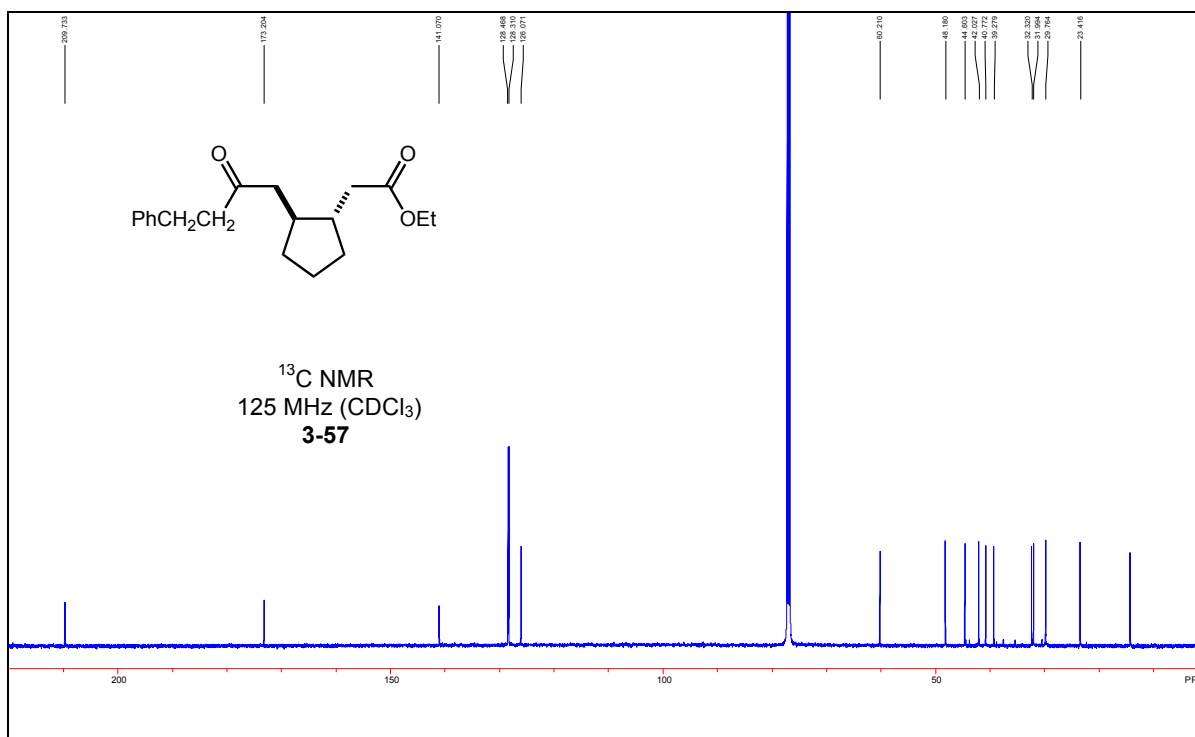


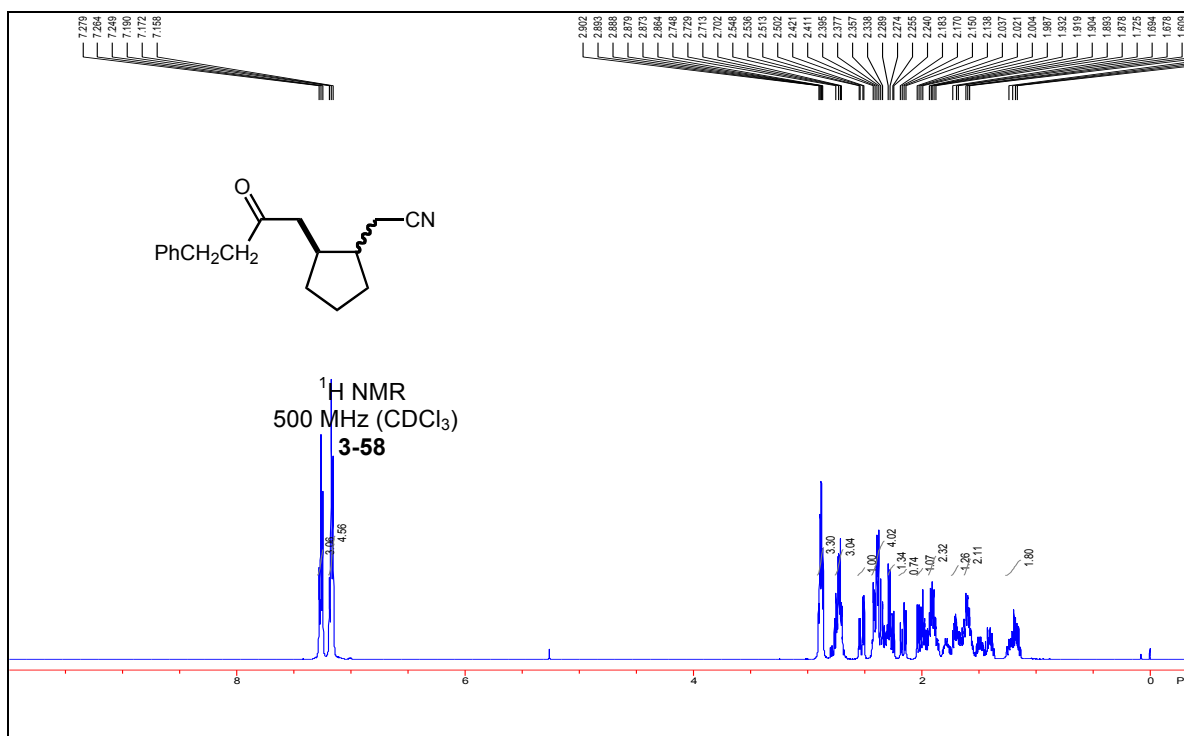
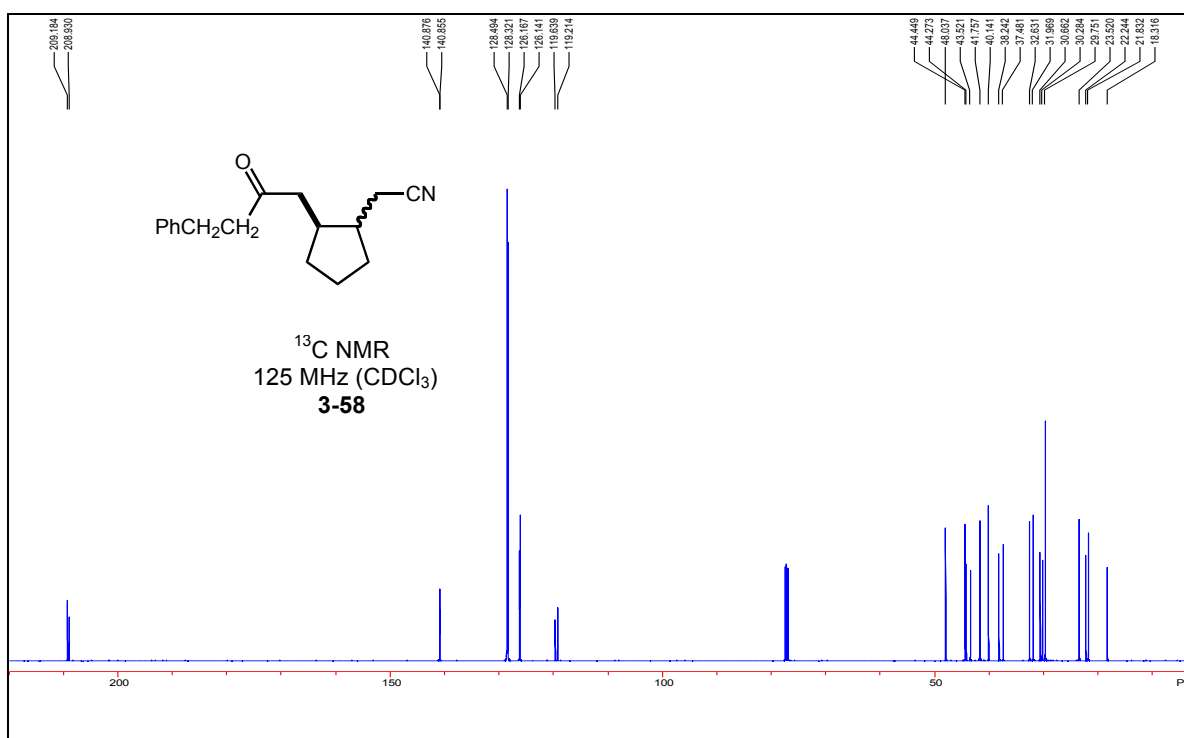


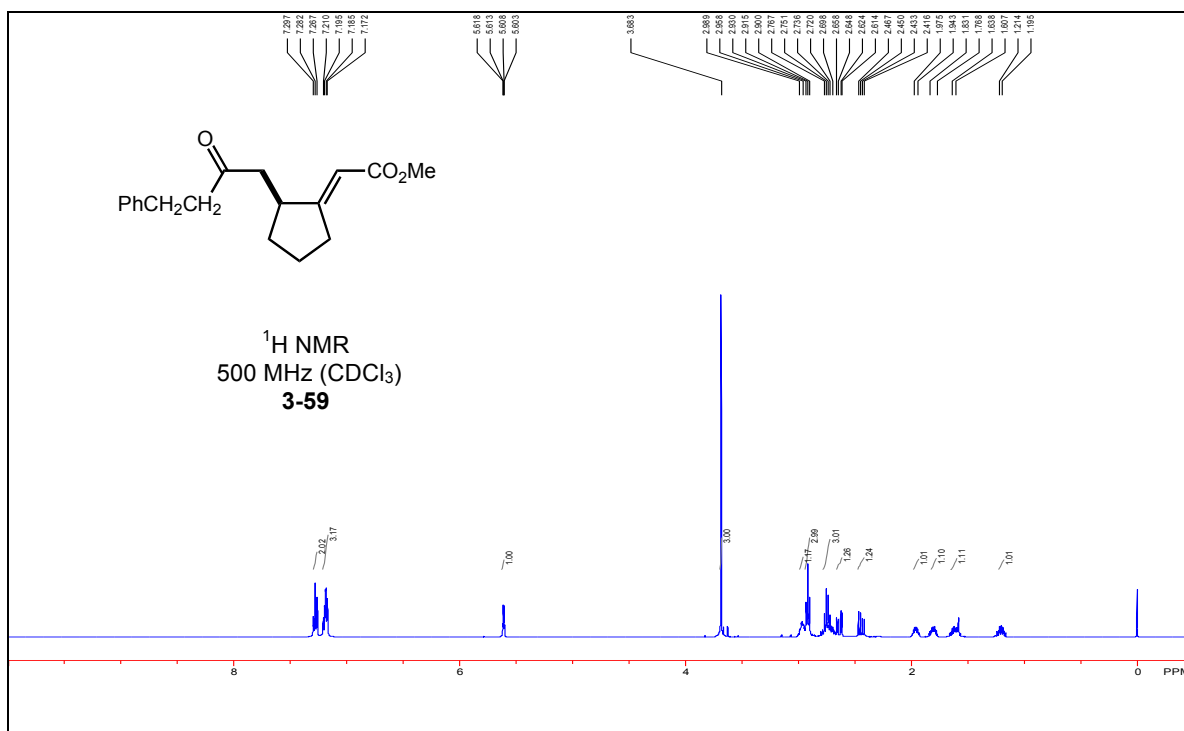
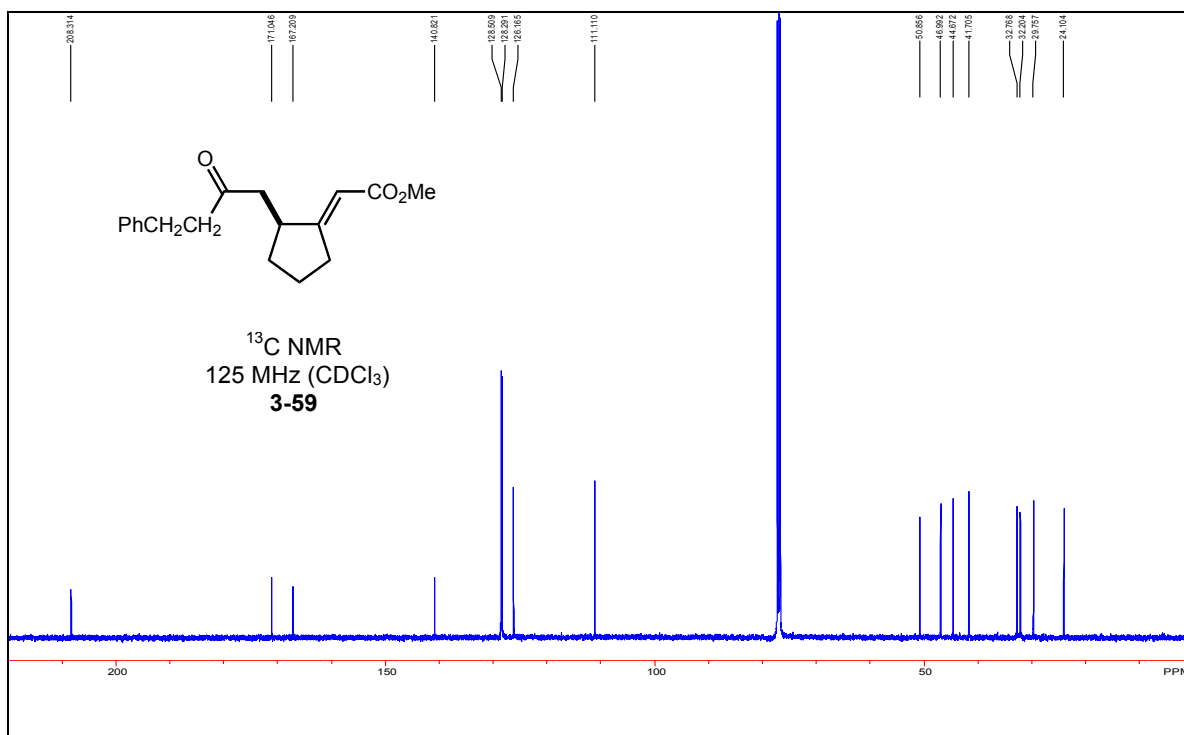


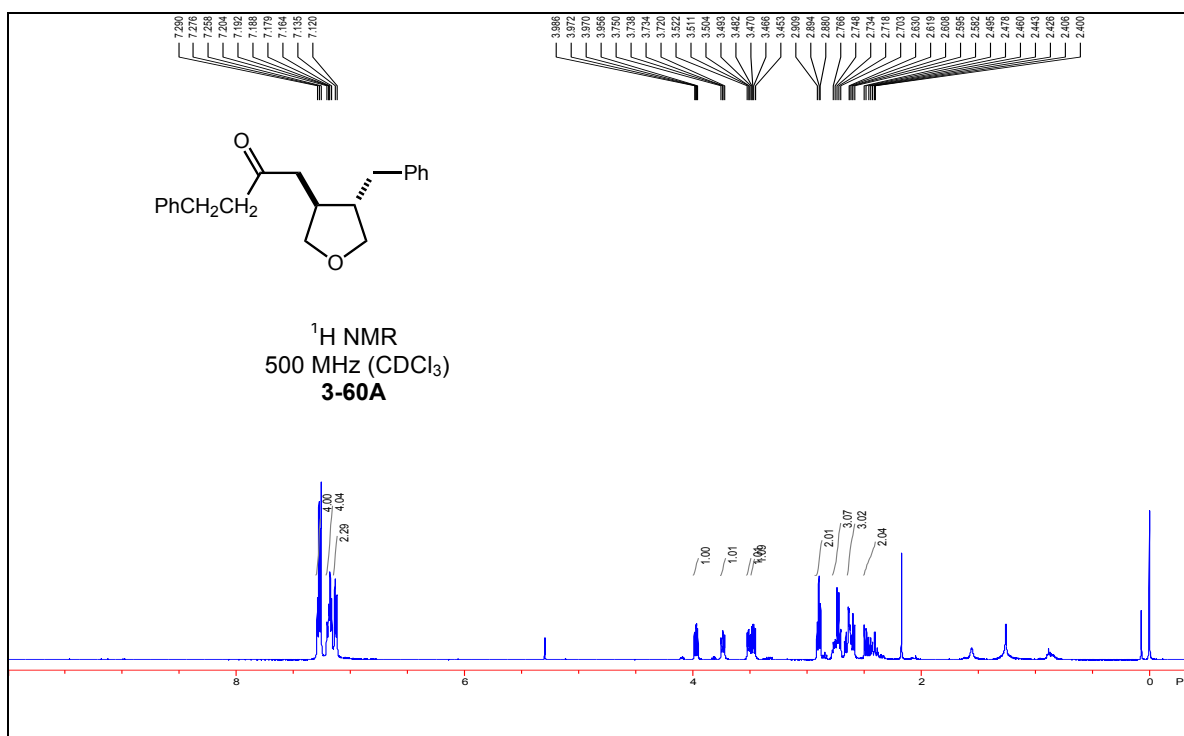
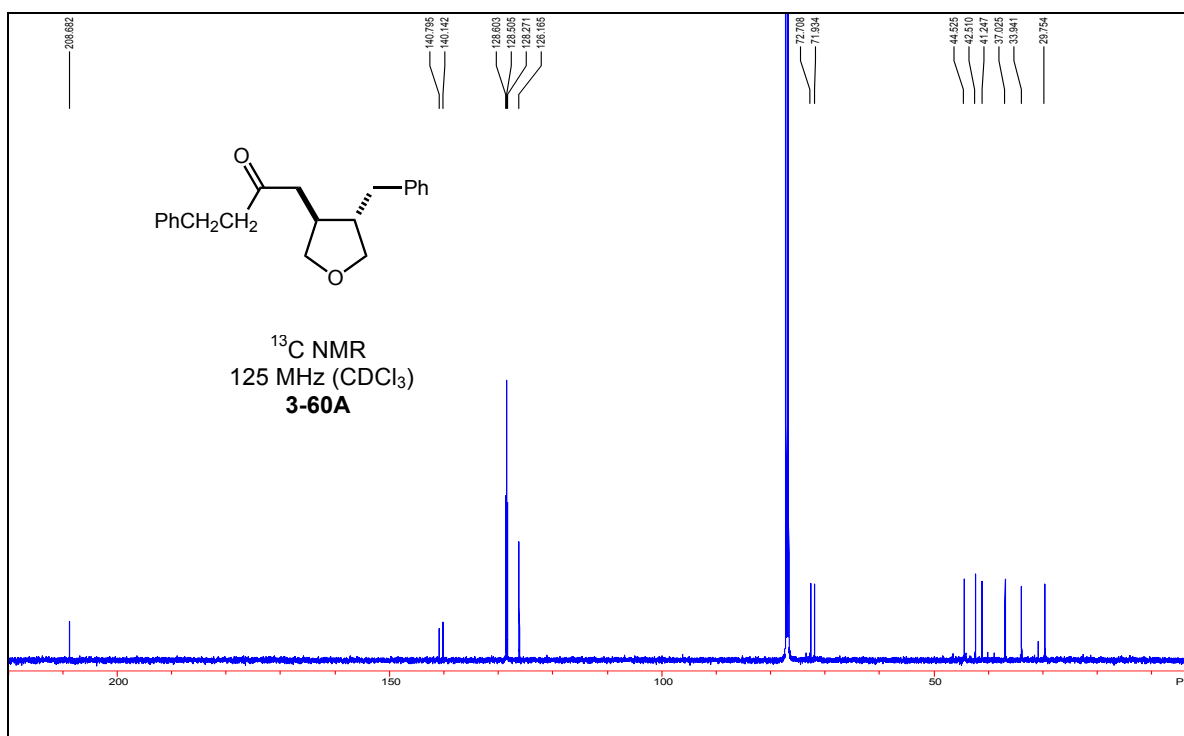


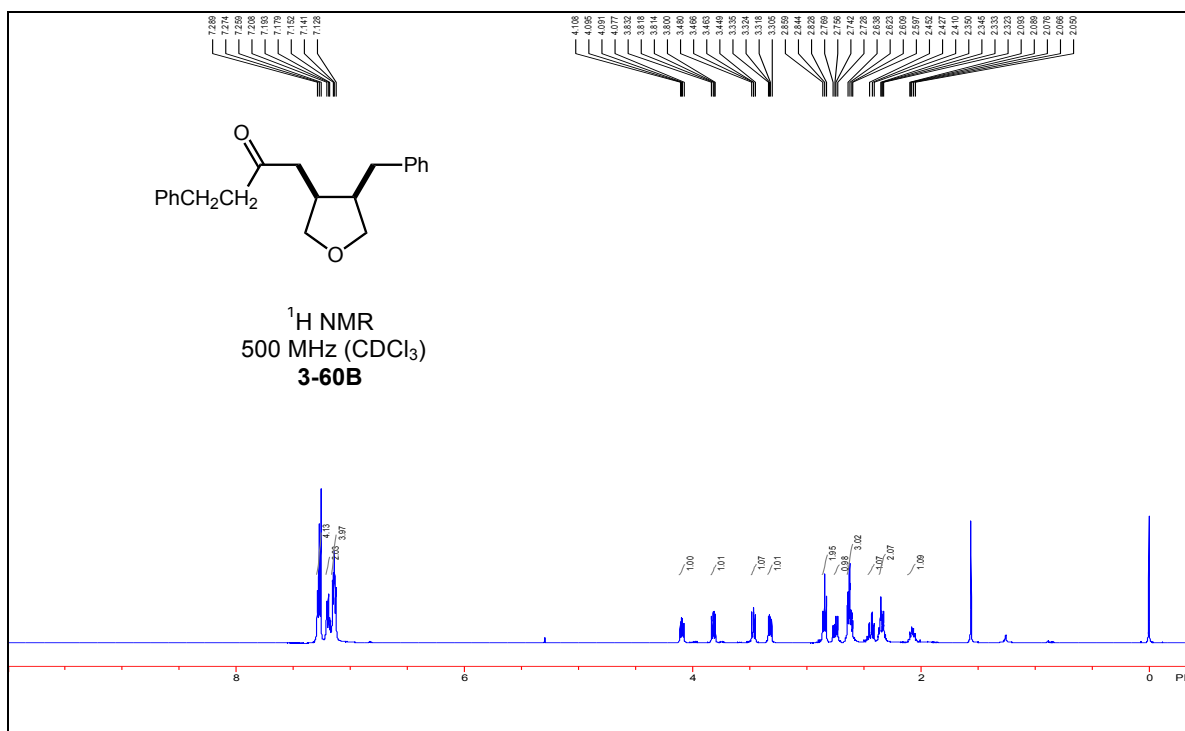
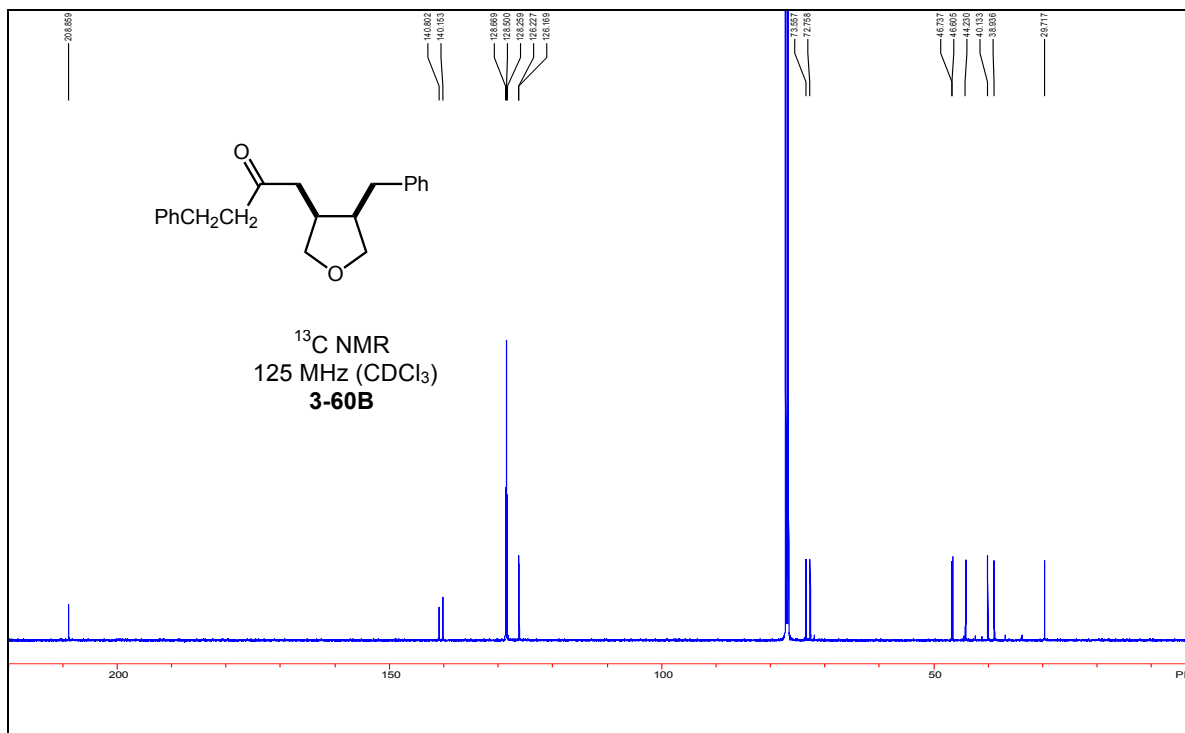


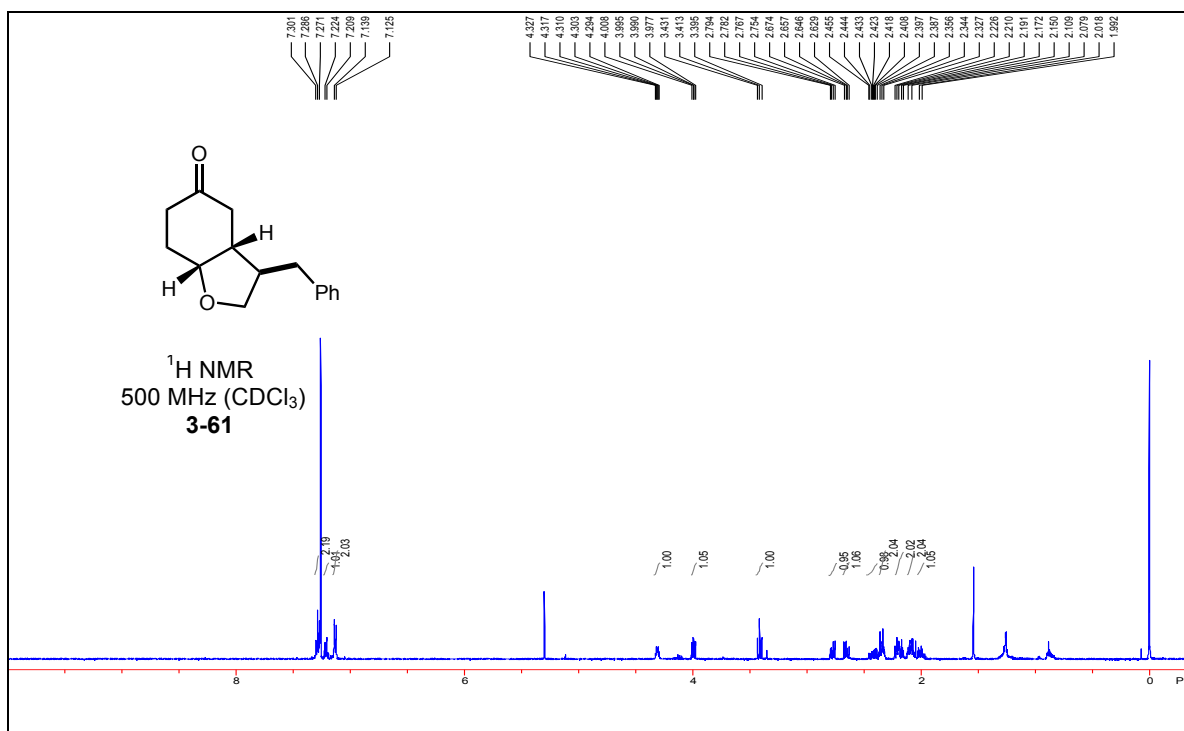
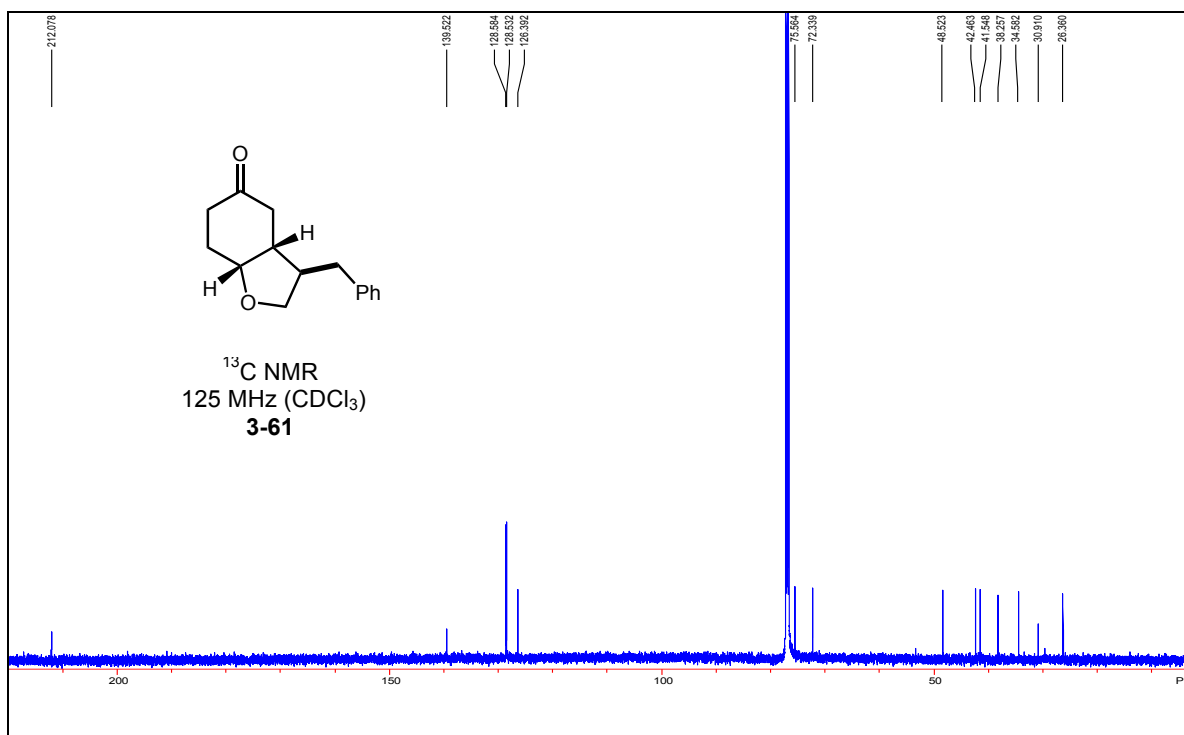


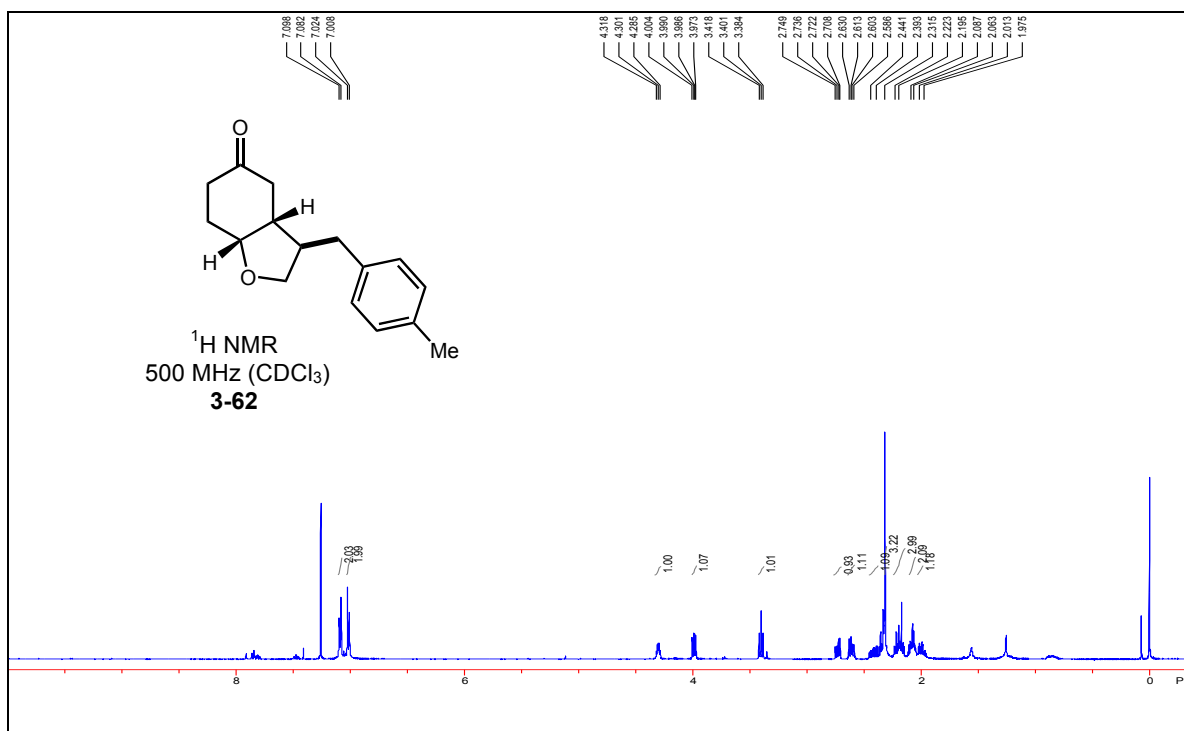
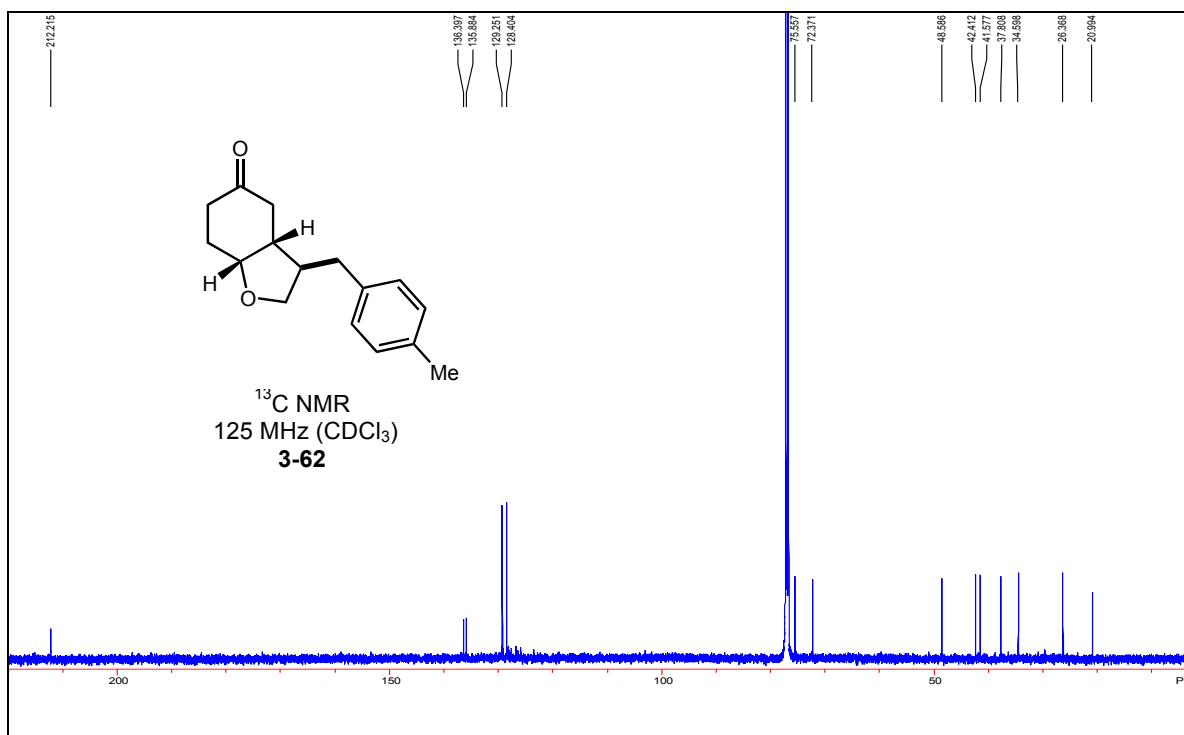




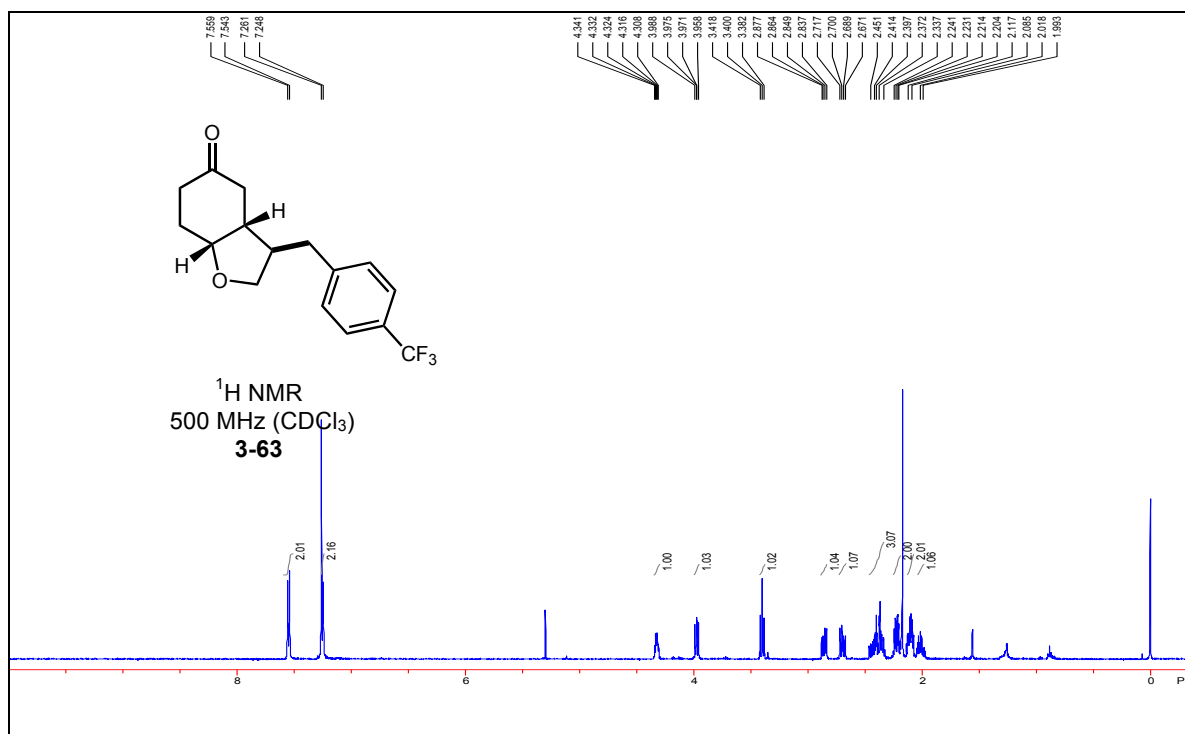
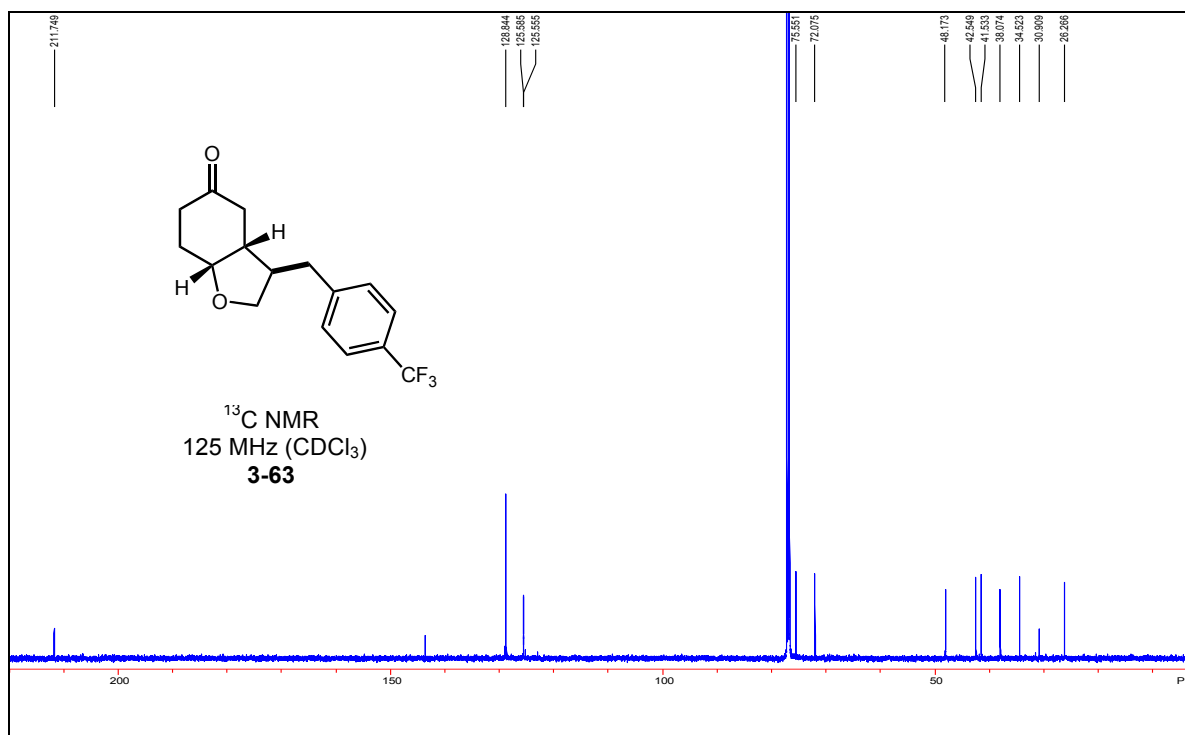


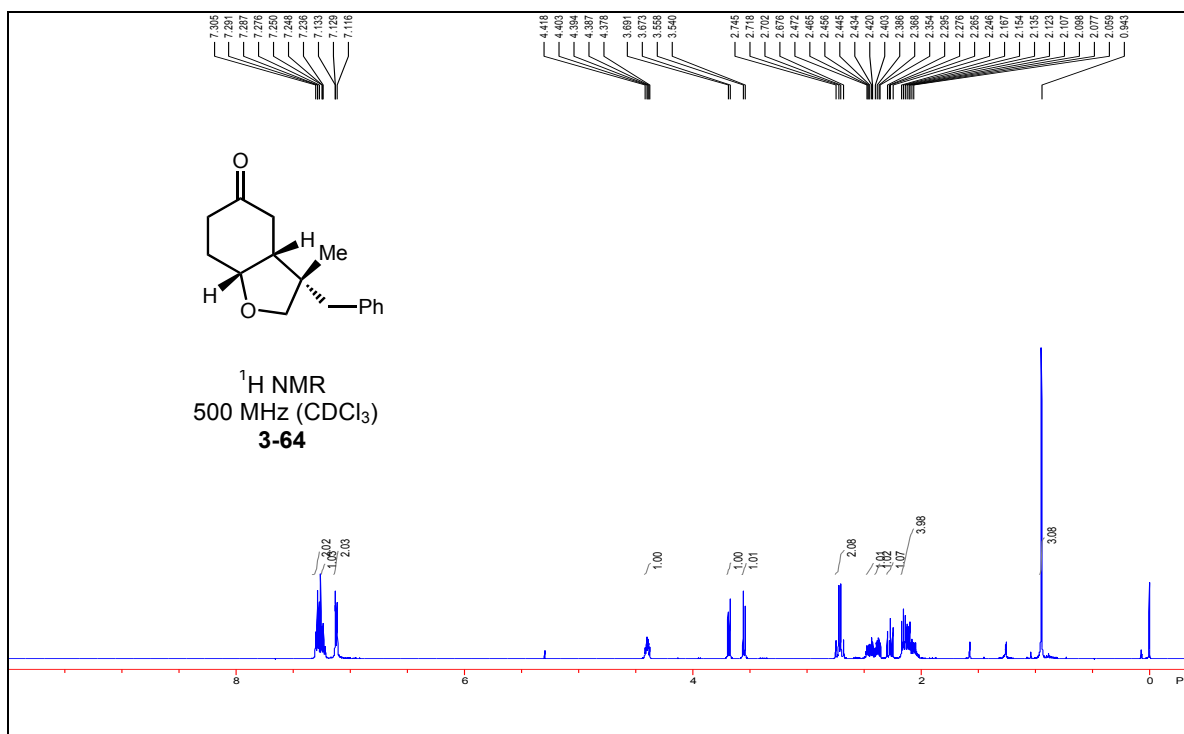
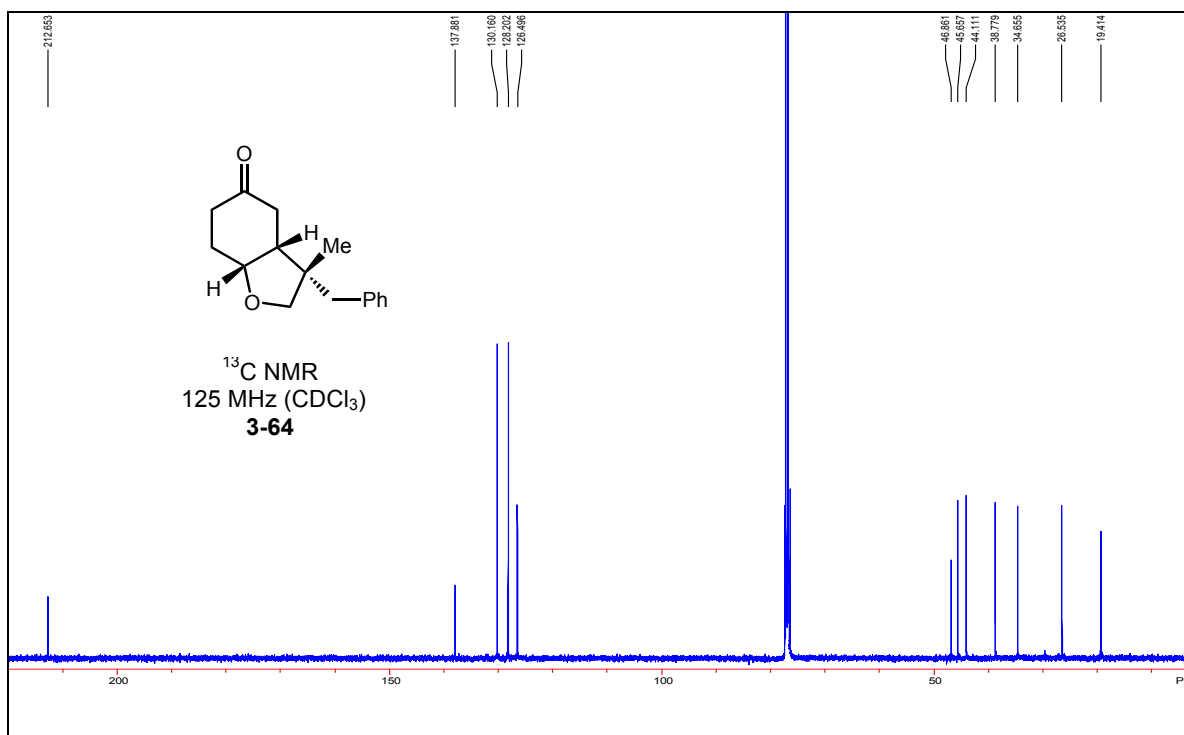


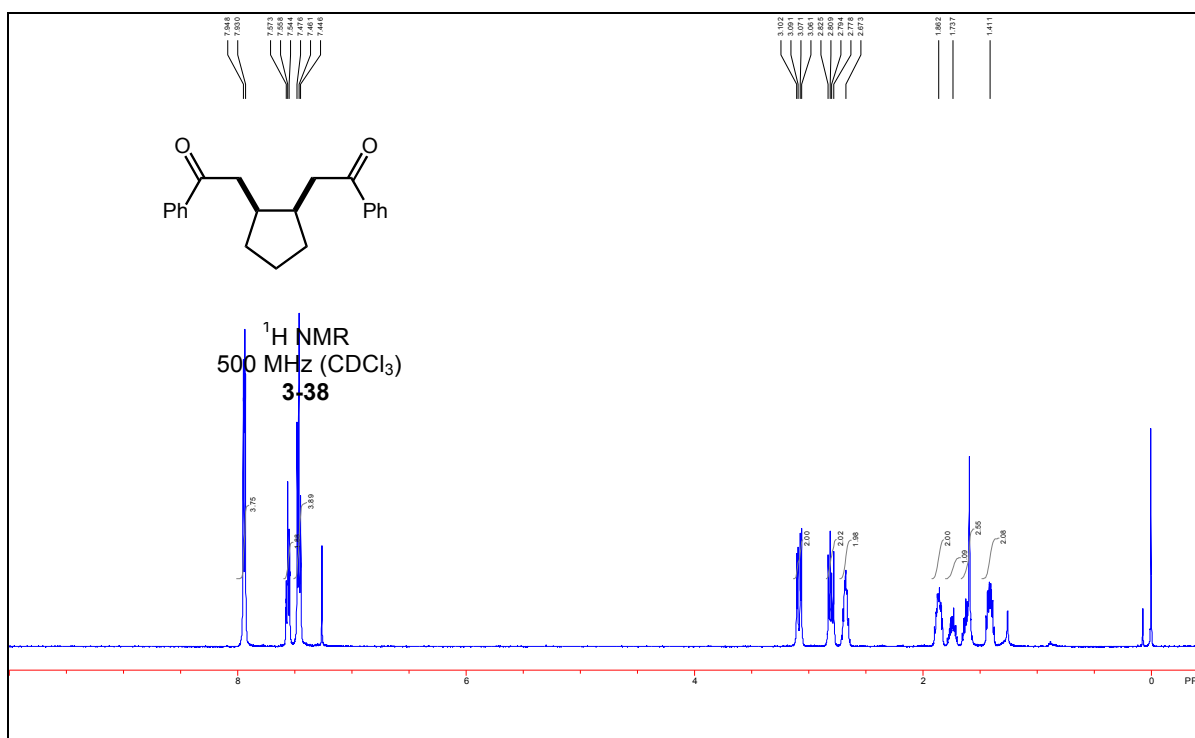
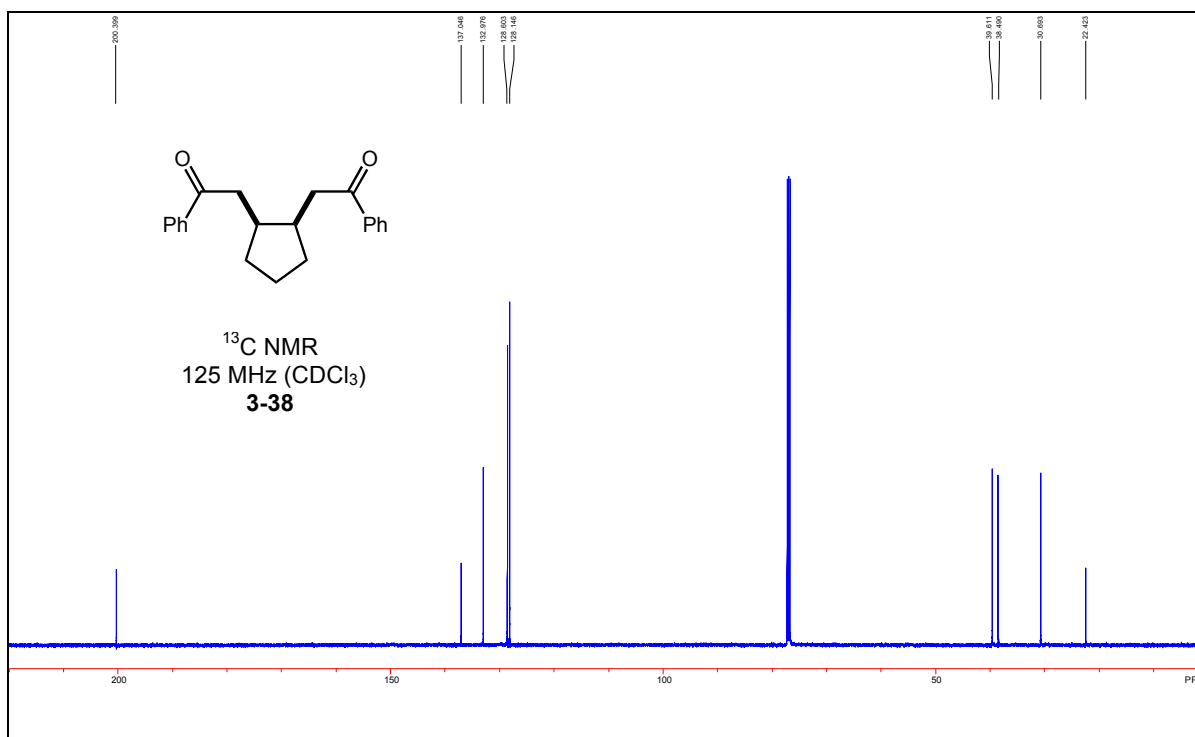


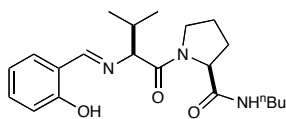


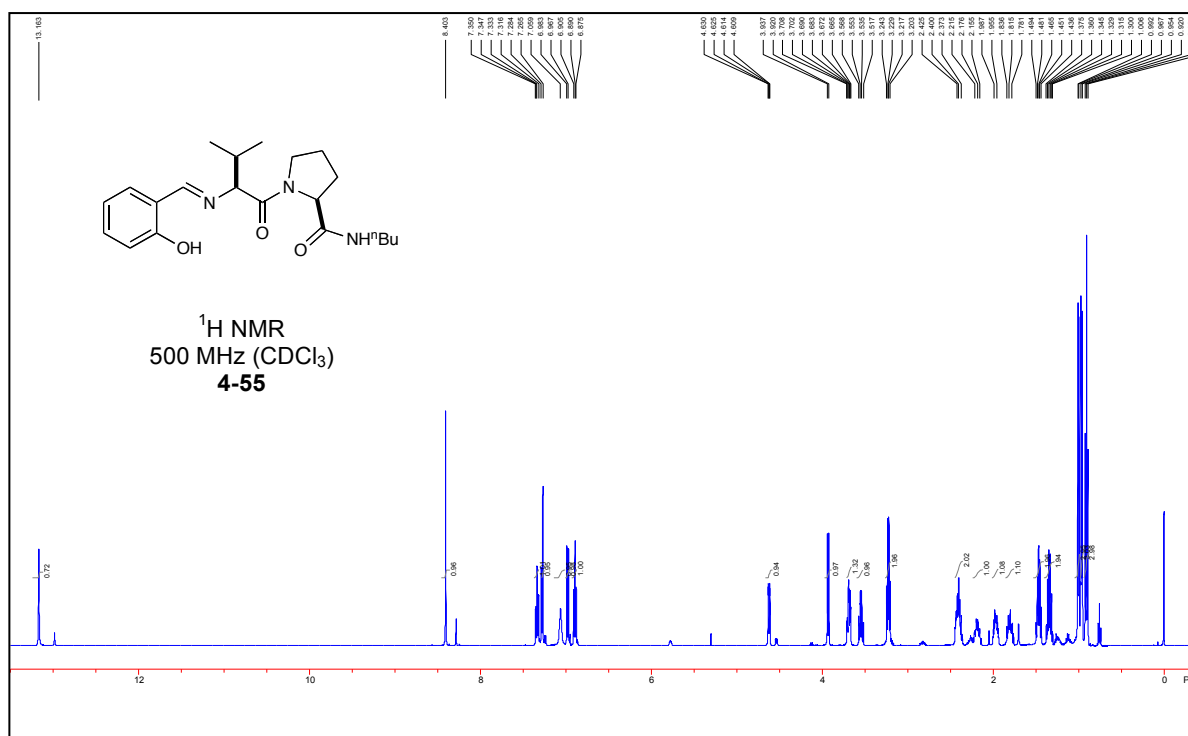


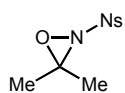
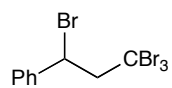
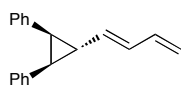
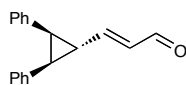
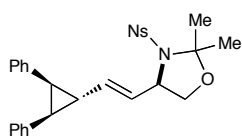
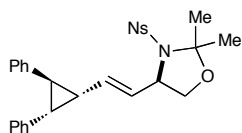
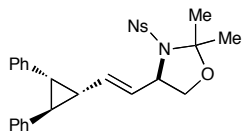


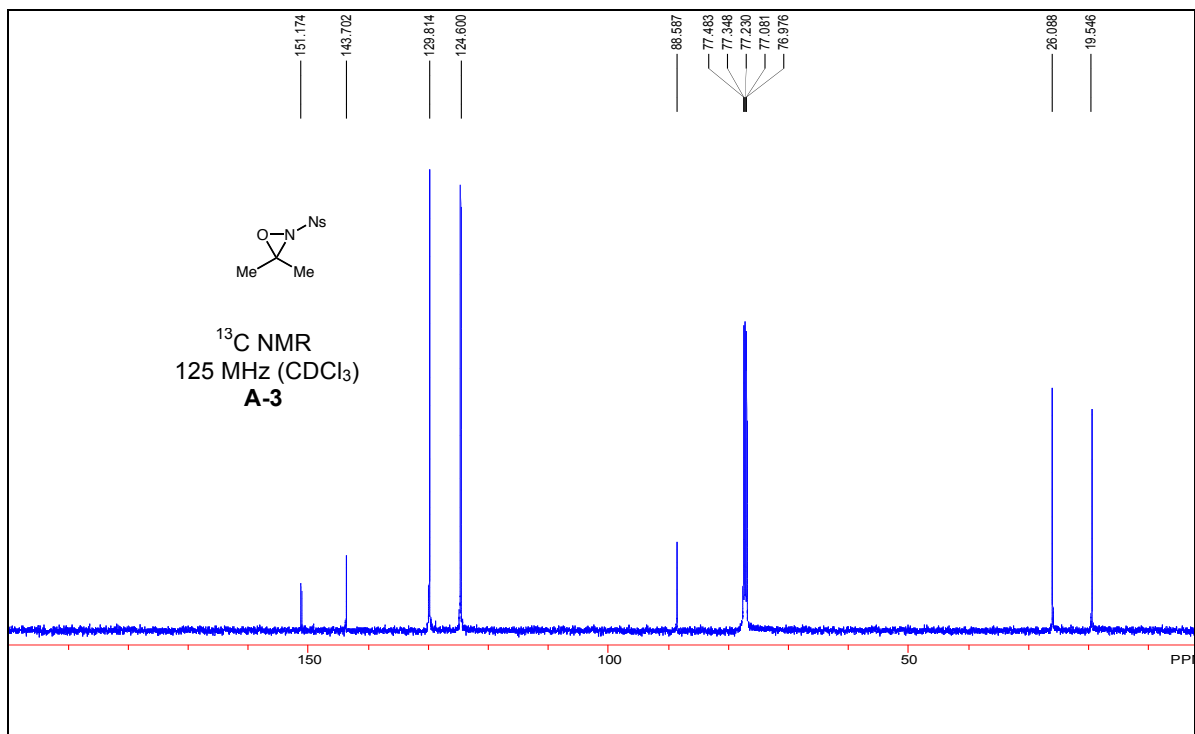
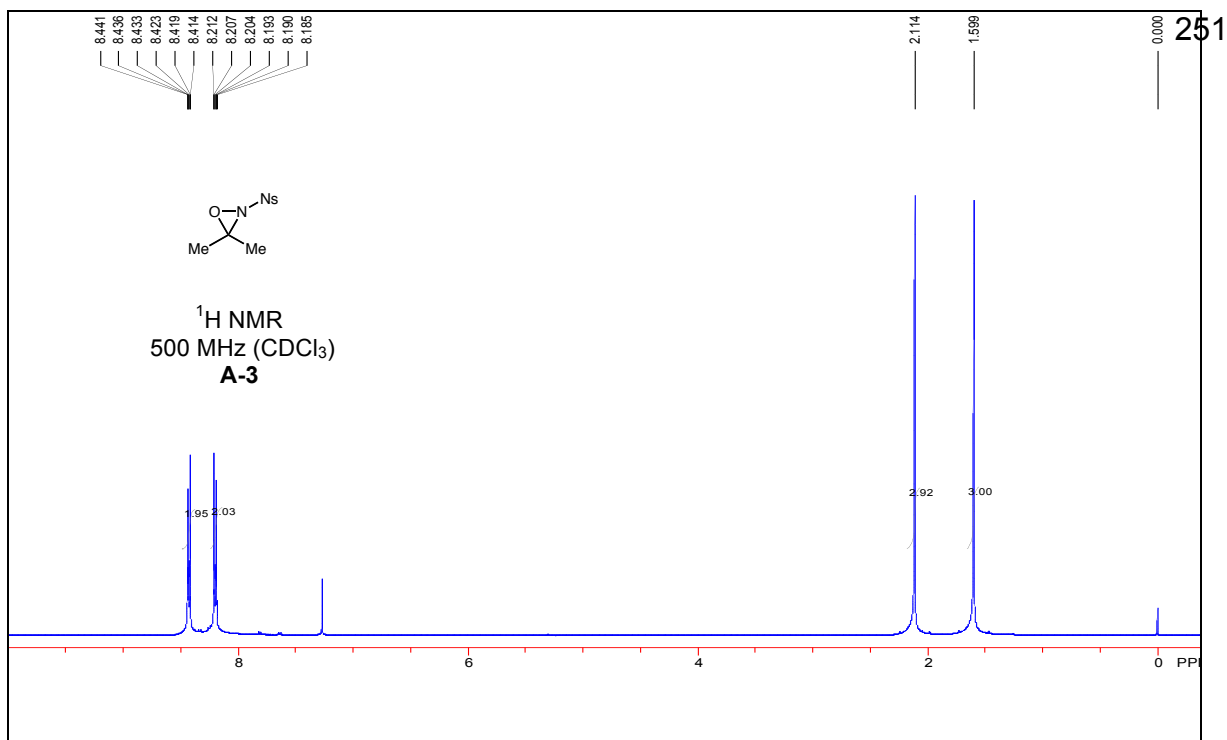


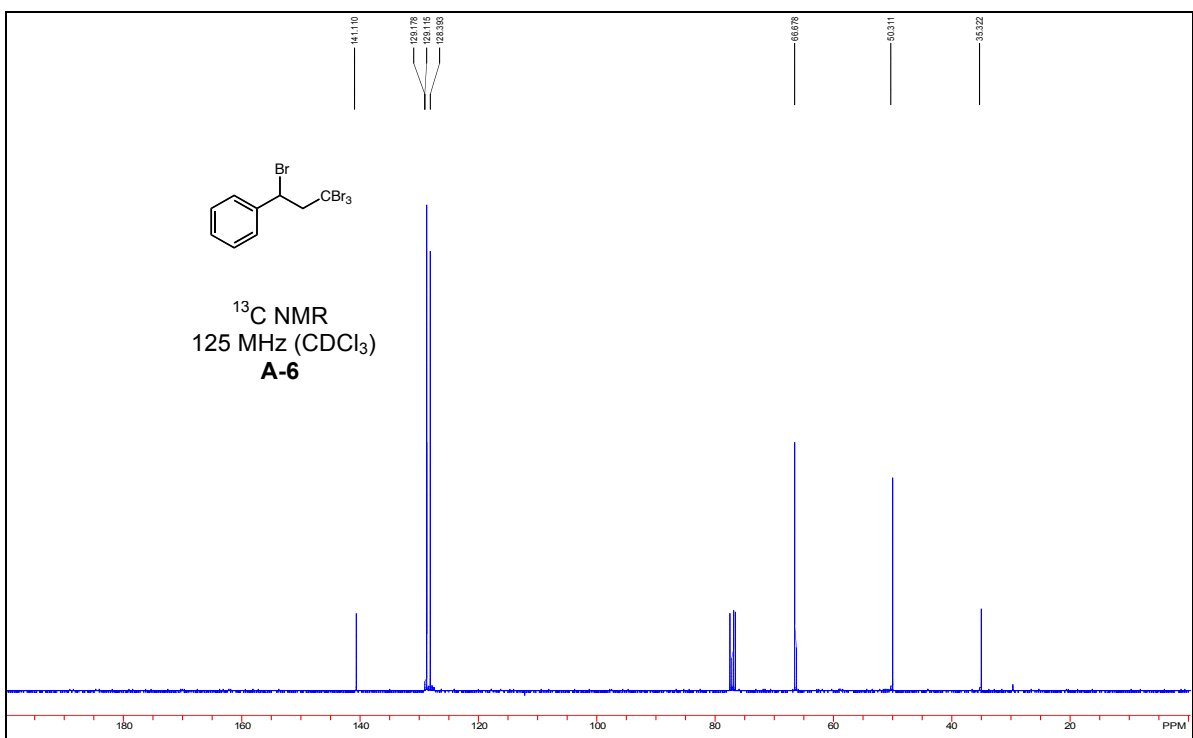


**List of Figures for Chapter 4****4-55**

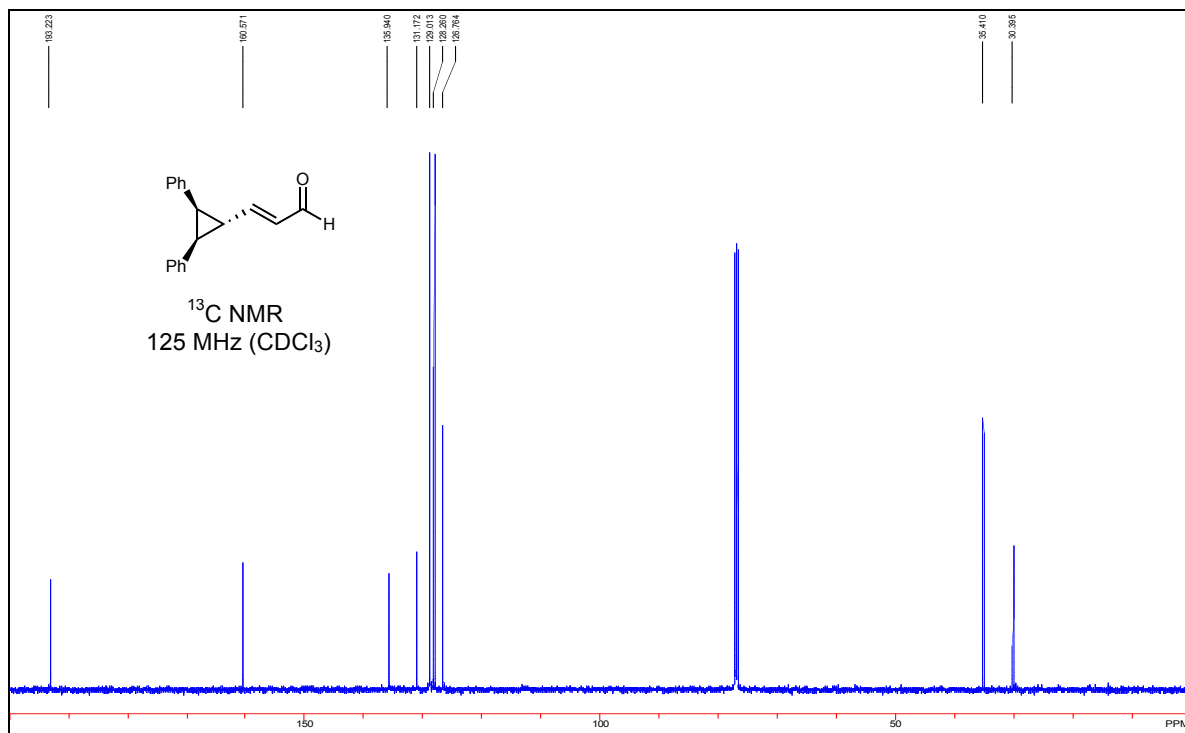
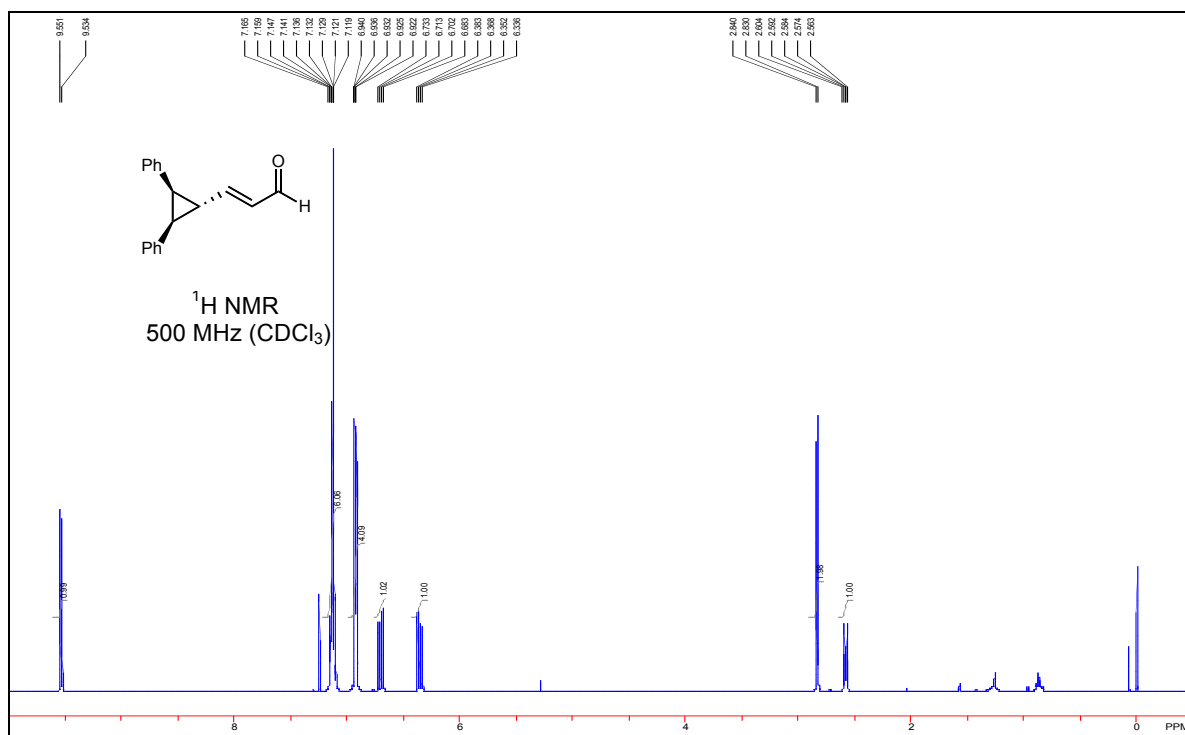


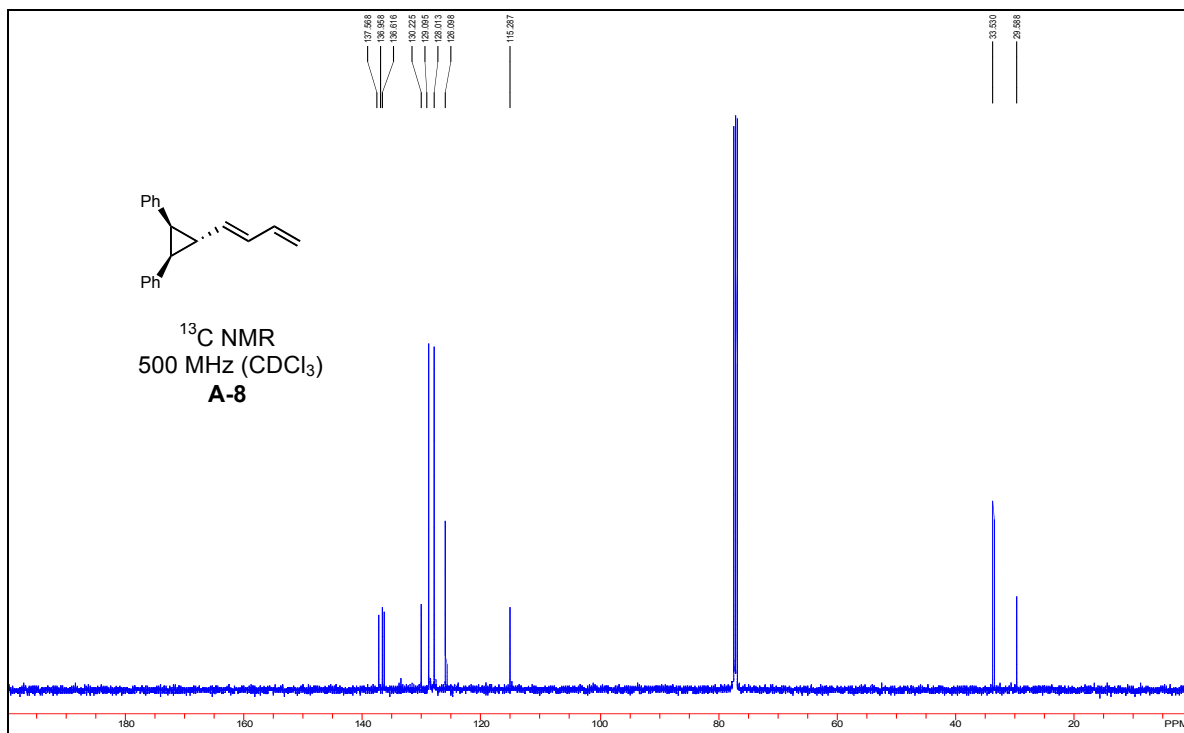
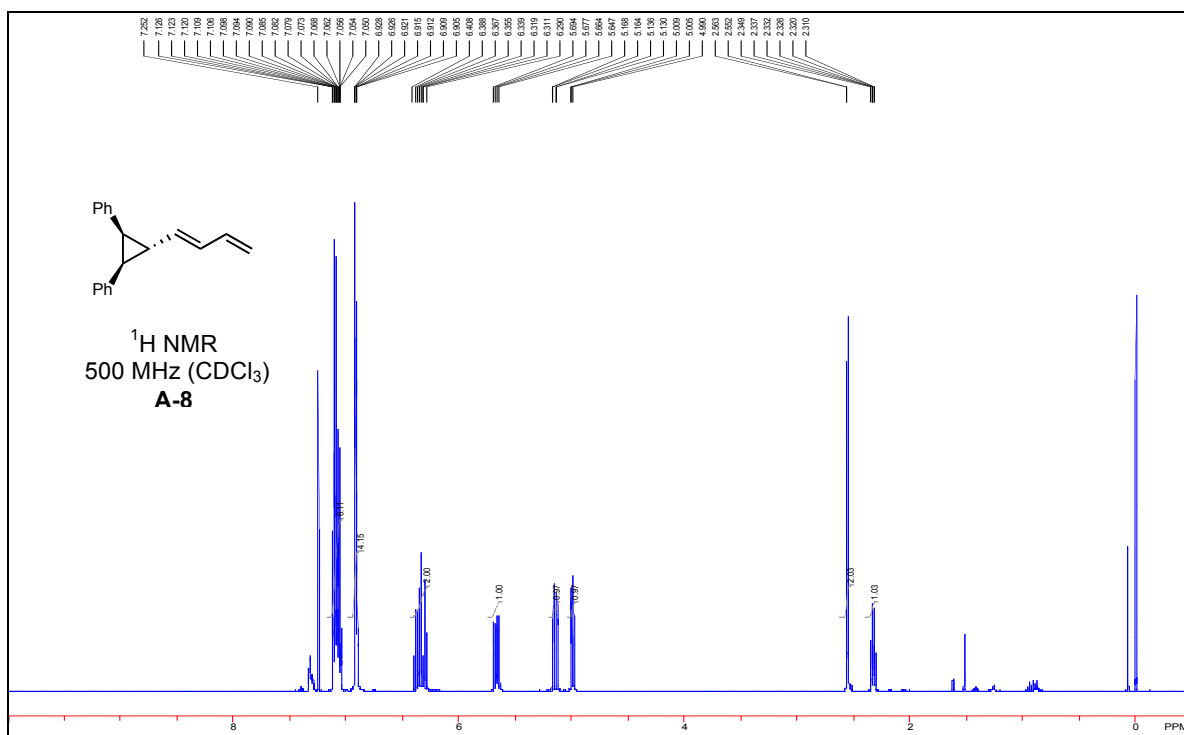
**A-3****A-6****A-8****A-9****A-10****A-11**

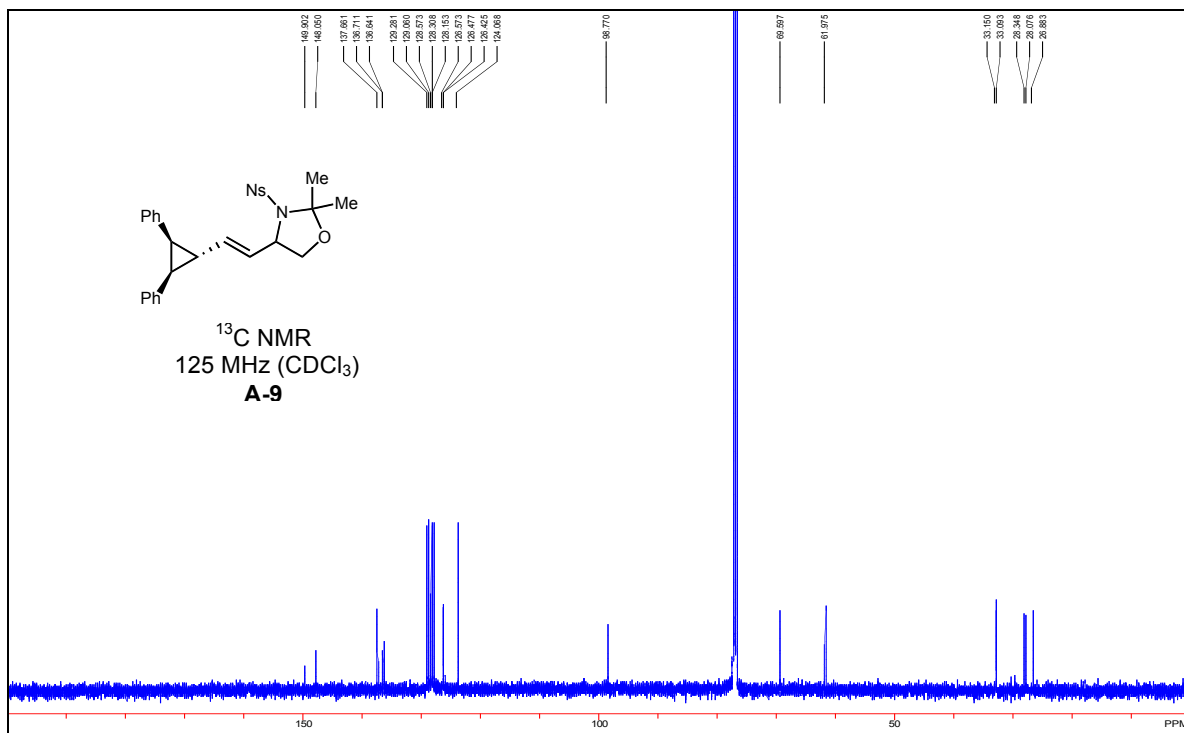
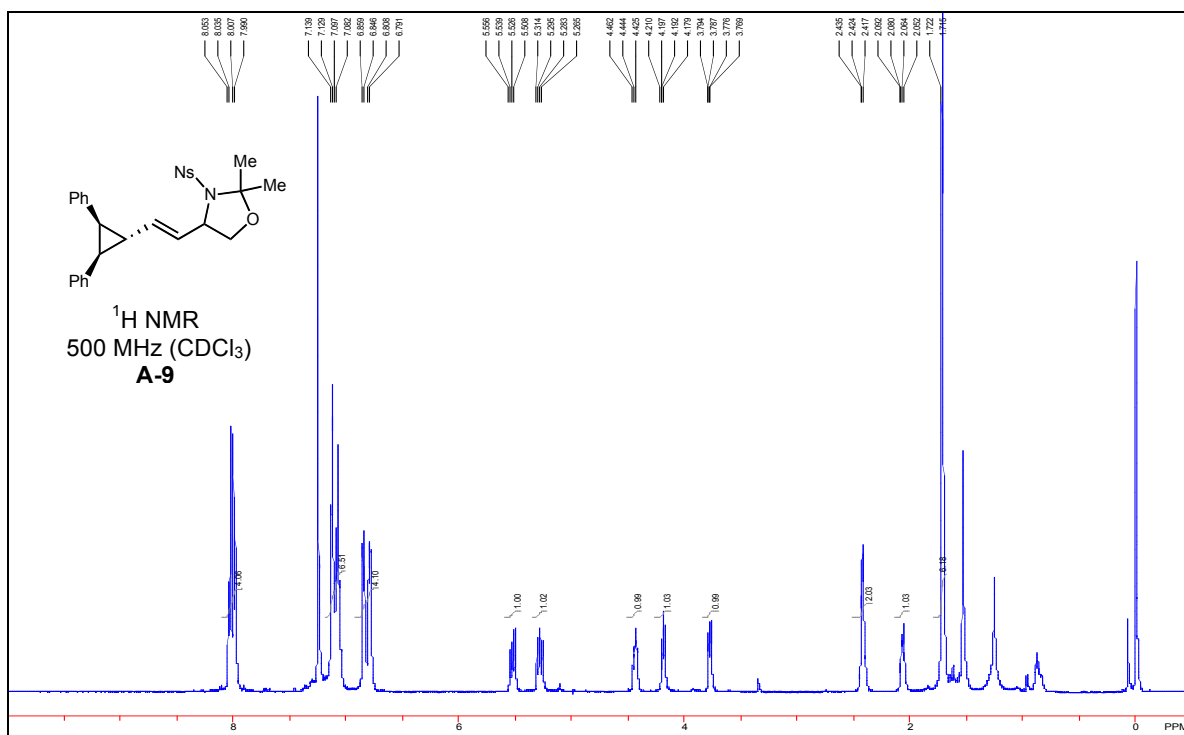


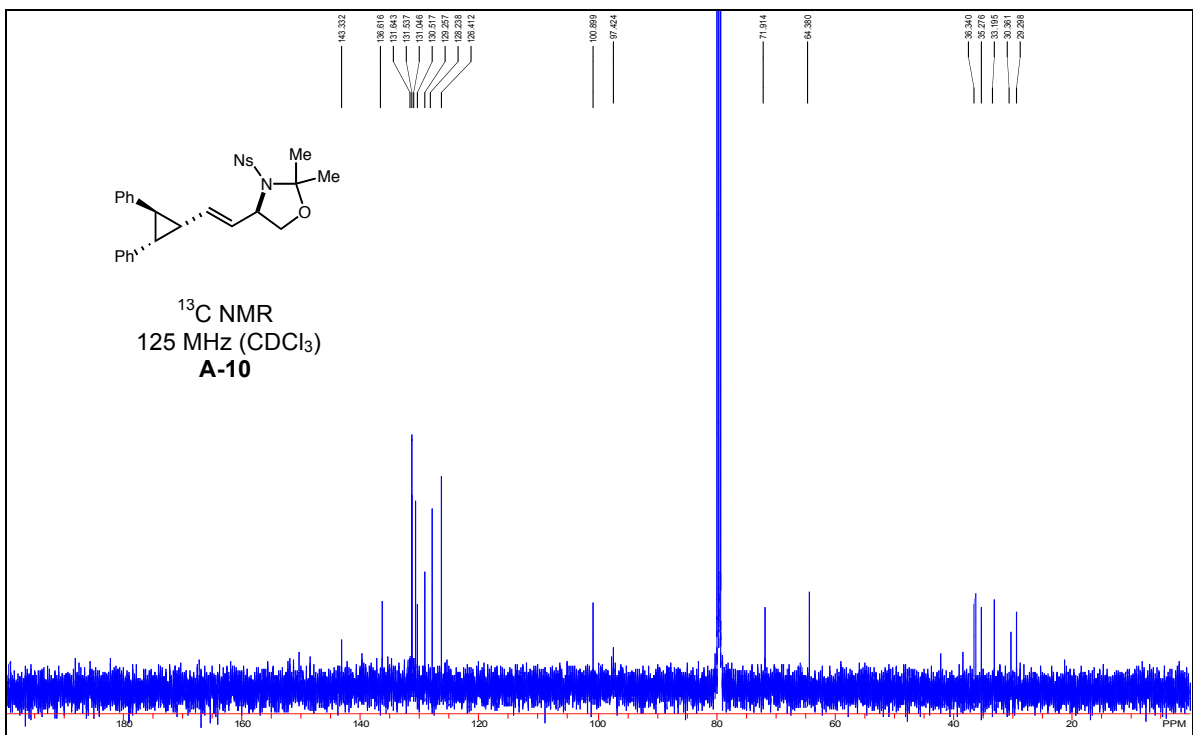


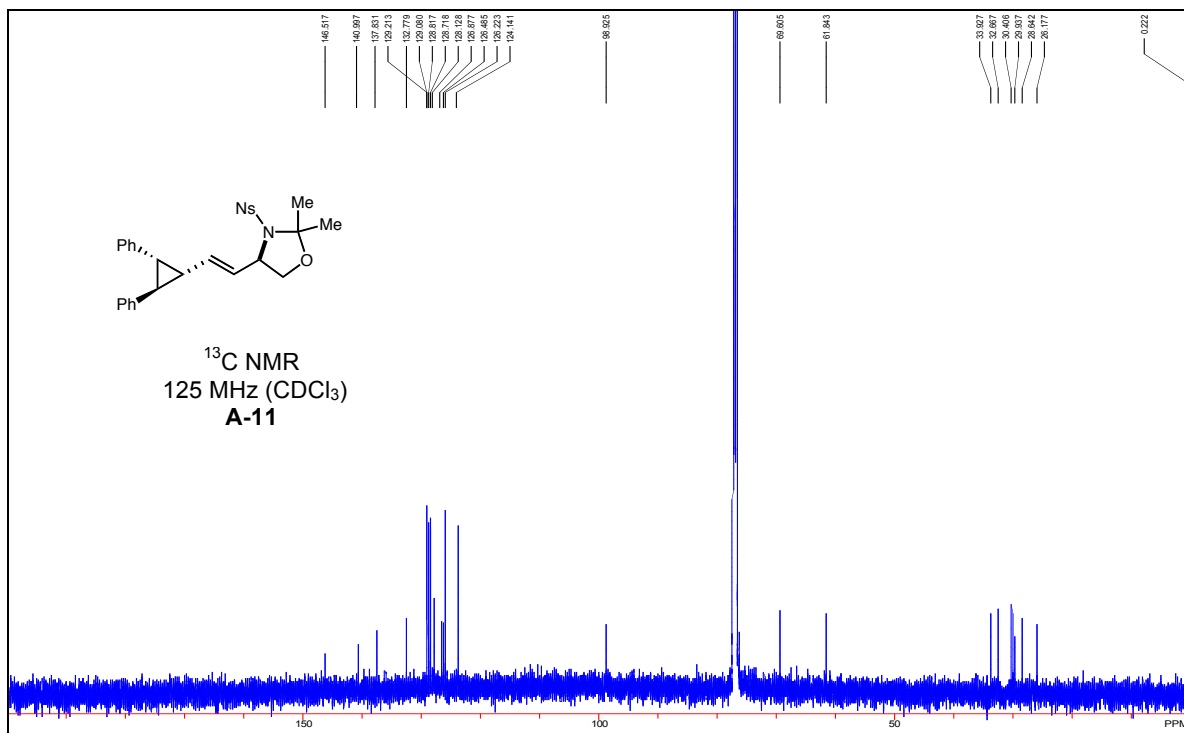
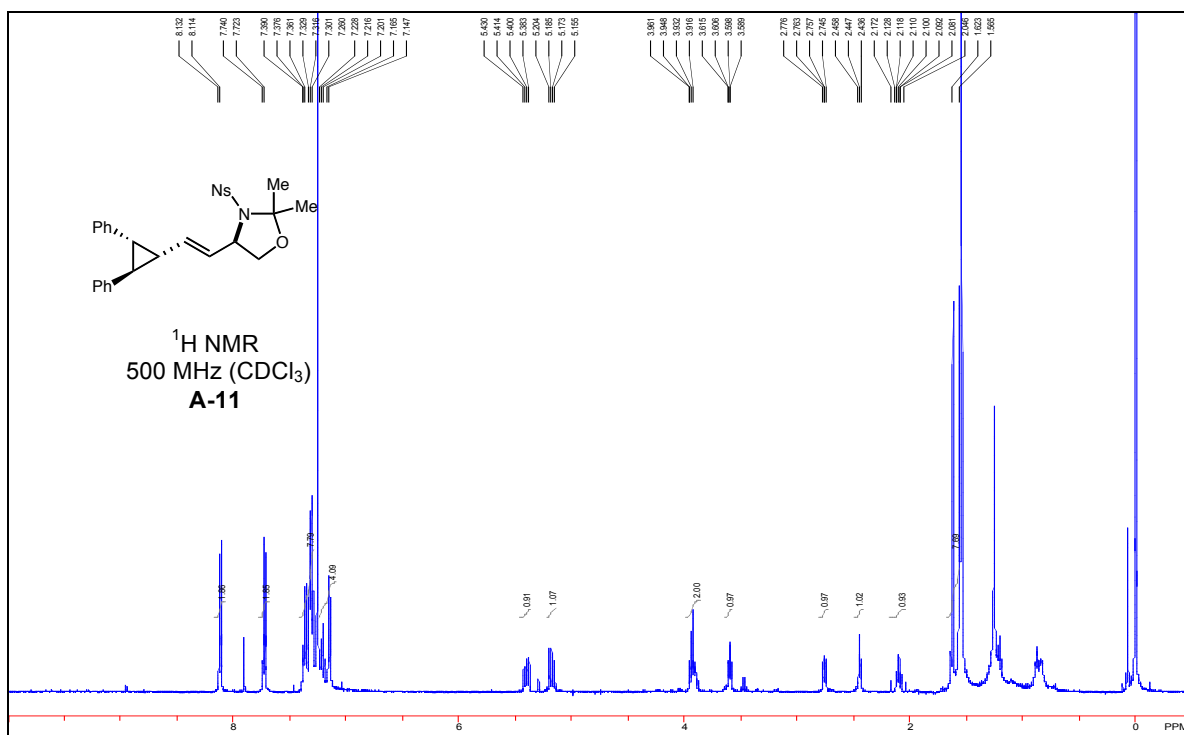




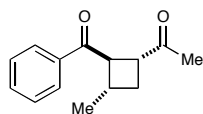






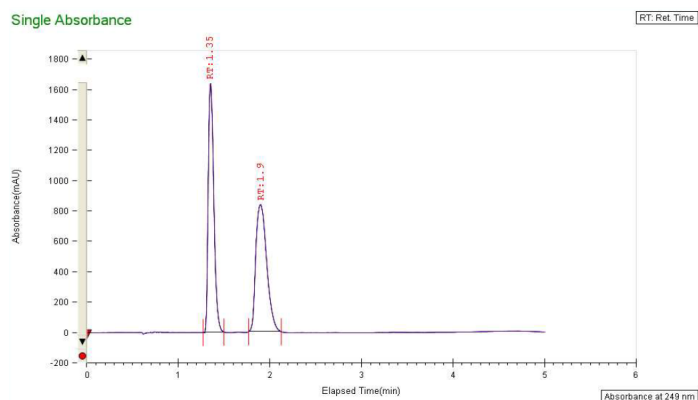


## **Appendix C. SFC Traces of New Compounds**



**Racemic:** Chiracel AD-H, 6% *i*-PrOH/CO<sub>2</sub>, 6 mL/min, 249 nm

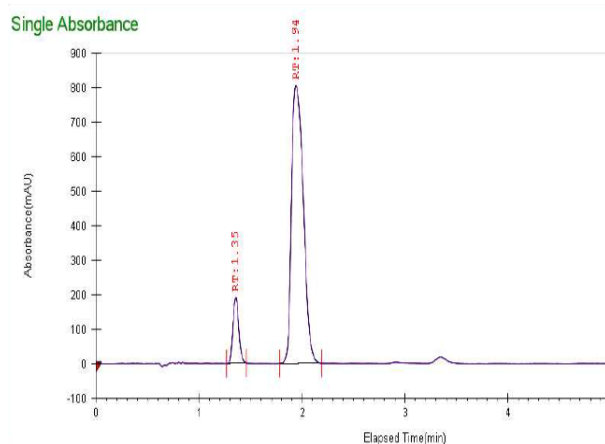
| peak  | % area  | area       | RT (min) | Height (mV) |
|-------|---------|------------|----------|-------------|
| 1     | 50.0479 | 6909.7937  | 1.35     | 1637.0582   |
| 2     | 49.9521 | 6896.5546  | 1.9      | 835.7006    |
| Total | 100     | 13806.3483 |          |             |

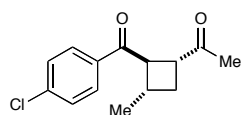


**Enantiomerically enriched:** Chiracel AD-H, 6% *i*-PrOH/CO<sub>2</sub>, 6 mL/min, 249 nm

$[\alpha]_D^{21} = -79.0$  (*c* 1.08, CH<sub>2</sub>Cl<sub>2</sub>)

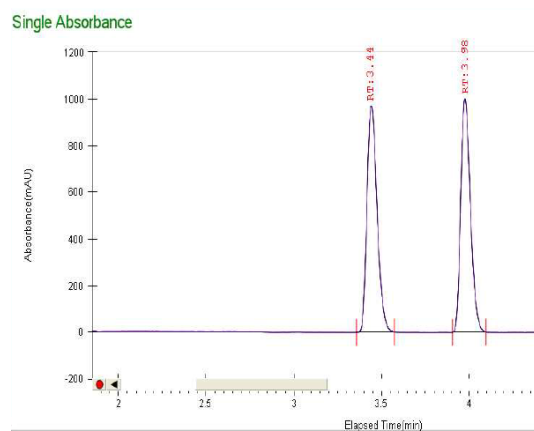
| peak  | % area  | area      | RT (min) | Height (mV) |
|-------|---------|-----------|----------|-------------|
| 1     | 10.5363 | 754.5175  | 1.35     | 190.0678    |
| 2     | 89.4637 | 6406.6247 | 1.94     | 805.9905    |
| Total | 100     | 7161.1422 |          |             |





**Racemic:** Chiracel AD-H, 5% *i*-PrOH/CO<sub>2</sub>, 3 mL/min, 249 nm

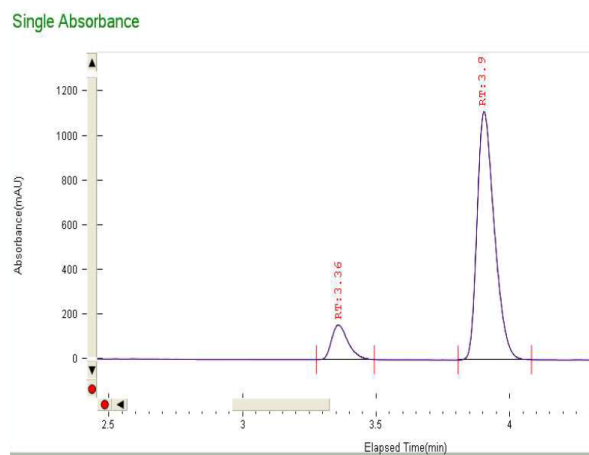
| peak  | % area  | area      | RT (min) | Height (mV) |
|-------|---------|-----------|----------|-------------|
| 1     | 50.3878 | 3885.1707 | 3.44     | 970.7744    |
| 2     | 49.6122 | 3825.3663 | 3.98     | 1000.6186   |
| Total | 100     | 7710.537  |          |             |



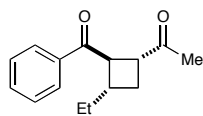
**Enantiomerically enriched:** Chiracel AD-H, 5% *i*-PrOH/CO<sub>2</sub>, 3 mL/min, 249 nm

$[\alpha]_D^{21} = -59.3$  (*c* 2.28, CH<sub>2</sub>Cl<sub>2</sub>)

| peak  | % area  | area      | RT (min) | Height (mV) |
|-------|---------|-----------|----------|-------------|
| 1     | 11.6438 | 654.5492  | 3.36     | 154.415     |
| 2     | 88.3562 | 4966.8953 | 3.9      | 1113.2996   |
| Total | 100     | 5621.4445 |          |             |

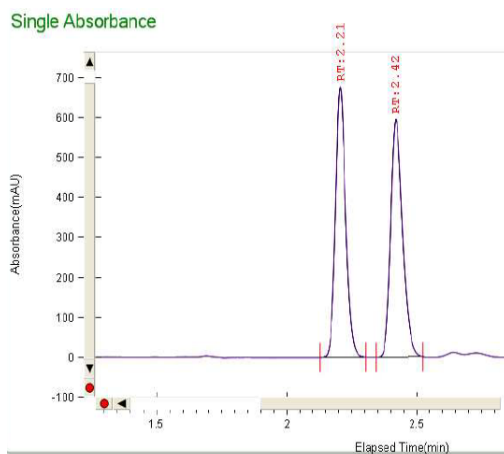






**Racemic:** Chiracel AD-H, 8% *i*-PrOH/CO<sub>2</sub>, 3 mL/min, 249 nm

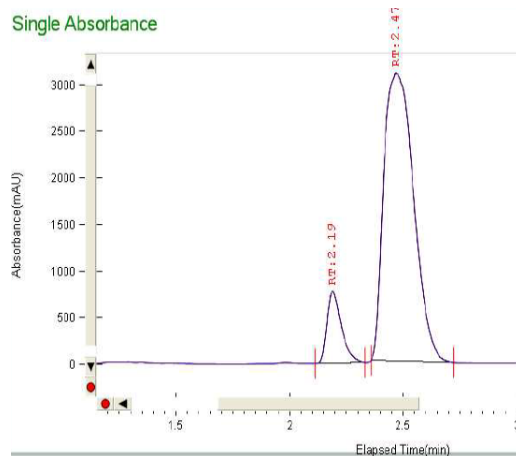
| peak  | % area  | area      | RT (min) | Height (mV) |
|-------|---------|-----------|----------|-------------|
| 1     | 49.4053 | 1849.7998 | 2.21     | 675.4549    |
| 2     | 50.5947 | 1894.3334 | 2.42     | 594.1918    |
| Total | 100     | 3744.1332 |          |             |

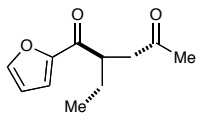


**Enantiomerically enriched:** Chiracel AD-H, 8% *i*-PrOH/CO<sub>2</sub>, 3 mL/min, 249 nm

$[\alpha]_D^{21} = -87.8$  (*c* 0.74, CH<sub>2</sub>Cl<sub>2</sub>)

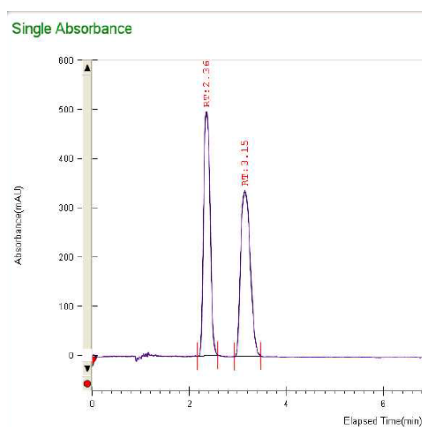
| peak  | % area  | area       | RT (min) | Height (mV) |
|-------|---------|------------|----------|-------------|
| 1     | 10.7307 | 3381.697   | 2.19     | 771.8203    |
| 2     | 89.2693 | 28132.4132 | 2.47     | 3082.8782   |
| Total | 100     | 31514.1102 |          |             |





**Racemic:** Chiracel AD-H, 6% *i*-PrOH/CO<sub>2</sub>, 4 mL/min, 249 nm

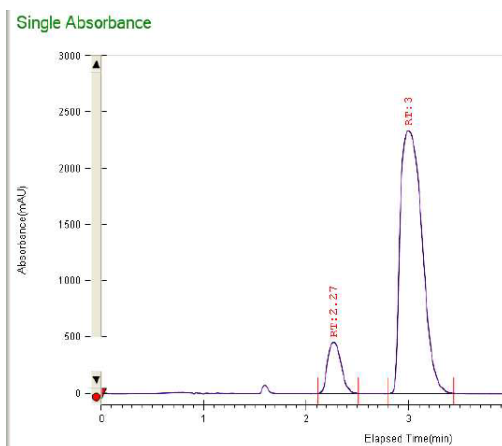
| peak  | % area  | area      | RT (min) | Height (mV) |
|-------|---------|-----------|----------|-------------|
| 1     | 49.9748 | 4586.5635 | 2.36     | 495.3304    |
| 2     | 50.0252 | 4592.1945 | 3.15     | 335.484     |
| Total | 100     | 9179.758  |          |             |

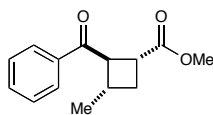


**Enantiomerically enriched:** Chiracel AD-H, 6% *i*-PrOH/CO<sub>2</sub>, 4 mL/min, 249 nm

$$[\alpha]_D^{21} = -74.3 \text{ (} c \text{ 1.48, CH}_2\text{Cl}_2 \text{)}$$

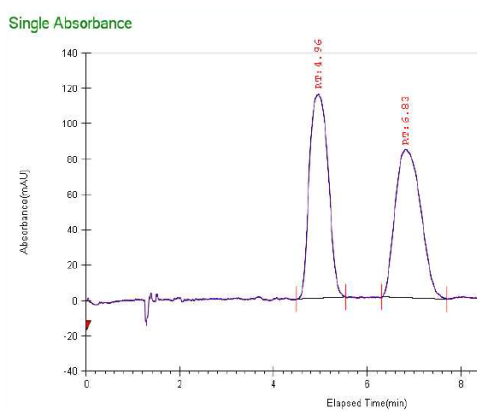
| peak  | % area  | area       | RT (min) | Height (mV) |
|-------|---------|------------|----------|-------------|
| 1     | 10.7028 | 4111.7272  | 2.27     | 450.9942    |
| 2     | 89.2972 | 34305.5514 | 3        | 2334.8298   |
| Total | 100     | 38417.2786 |          |             |





**Racemic:** Chiracel AD-H, 3% *i*-PrOH/CO<sub>2</sub>, 3 mL/min, 249 nm

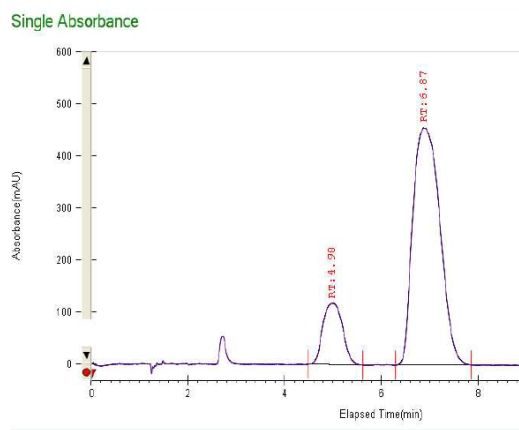
| peak  | % area  | area      | RT (min) | Height (mV) |
|-------|---------|-----------|----------|-------------|
| 1     | 50.1164 | 3201.6487 | 4.96     | 115.7922    |
| 2     | 49.8836 | 3186.7774 | 6.83     | 83.8304     |
| Total | 100     | 6388.4261 |          |             |



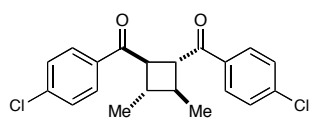
**Enantiomerically enriched:** Chiracel AD-H, 3% *i*-PrOH/CO<sub>2</sub>, 3 mL/min, 249 nm

$[\alpha]_D^{21} = -36.2$  (*c* 0.95, CH<sub>2</sub>Cl<sub>2</sub>)

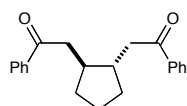
| peak  | % area  | area       | RT (min) | Height (mV) |
|-------|---------|------------|----------|-------------|
| 1     | 15.7172 | 3302.6747  | 4.98     | 117.7199    |
| 2     | 84.2828 | 17710.4497 | 6.87     | 456.9424    |
| Total | 100     | 21013.1244 |          |             |



## **Appendix D. X-ray Crystallographic Data**



**2-17**



**3-15**

### ***Data Collection***

A colorless crystal with approximate dimensions  $0.36 \times 0.30 \times 0.28 \text{ mm}^3$  was selected under oil under ambient conditions and attached to the tip of a MiTeGen MicroMount©. The crystal was mounted in a stream of cold nitrogen at 100(2) K and centered in the X-ray beam by using a video camera.

The crystal evaluation and data collection were performed on a Bruker SMART APEXII diffractometer with Cu  $K_\alpha$  ( $\lambda = 1.54178 \text{ \AA}$ ) radiation and the diffractometer to crystal distance of 4.03 cm.

The initial cell constants were obtained from three series of  $\omega$  scans at different starting angles. Each series consisted of 50 frames collected at intervals of  $0.5^\circ$  in a  $25^\circ$  range about  $\omega$  with the exposure time of 5 seconds per frame. The reflections were successfully indexed by an automated indexing routine built in the SMART program. The final cell constants were calculated from a set of 9924 strong reflections from the actual data collection.

The data were collected by using the full sphere data collection routine to survey the reciprocal space to the extent of a full sphere to a resolution of  $0.82 \text{ \AA}$ . A total of 13686 data were harvested by collecting 18 sets of frames with  $0.7^\circ$  scans in  $\omega$  and  $\phi$  with an exposure time 6-10 sec per frame. These highly redundant datasets were corrected for Lorentz and polarization effects. The absorption correction was based on fitting a function to the empirical transmission surface as sampled by multiple equivalent measurements. [1]

### **Structure Solution and Refinement**

The systematic absences in the diffraction data were consistent for the space groups  $P\bar{1}$  and  $P1$ . The  $E$ -statistics strongly suggested the centrosymmetric space group  $P\bar{1}$  that yielded chemically reasonable and computationally stable results of refinement [2].

A successful solution by the direct methods provided most non-hydrogen atoms from the  $E$ -map. The remaining non-hydrogen atoms were located in an alternating series of least-squares cycles and difference Fourier maps. All non-hydrogen atoms were refined with anisotropic displacement coefficients. All hydrogen atoms were included in the structure factor calculation

at idealized positions and were allowed to ride on the neighboring atoms with relative267 isotropic displacement coefficients.

The final least-squares refinement of 219 parameters against 3070 data resulted in residuals  $R$  (based on  $F^2$  for  $I \geq 2\sigma$ ) and  $wR$  (based on  $F^2$  for all data) of 0.0290 and 0.0782, respectively. The final difference Fourier map was featureless.

The molecular diagram is drawn with 50% probability ellipsoids.

## References

- [1] Bruker-AXS. (2007) APEX2, SADABS, and SAINT Software Reference Manuals. Bruker-AXS, Madison, Wisconsin, USA.
- [2] Sheldrick, G. M. (2008) SHELXL. *Acta Cryst.* **A64**, 112-122.
- [3] Pennington, W.T. (1999) *J. Appl. Cryst.* **32**(5), 1028-1029.

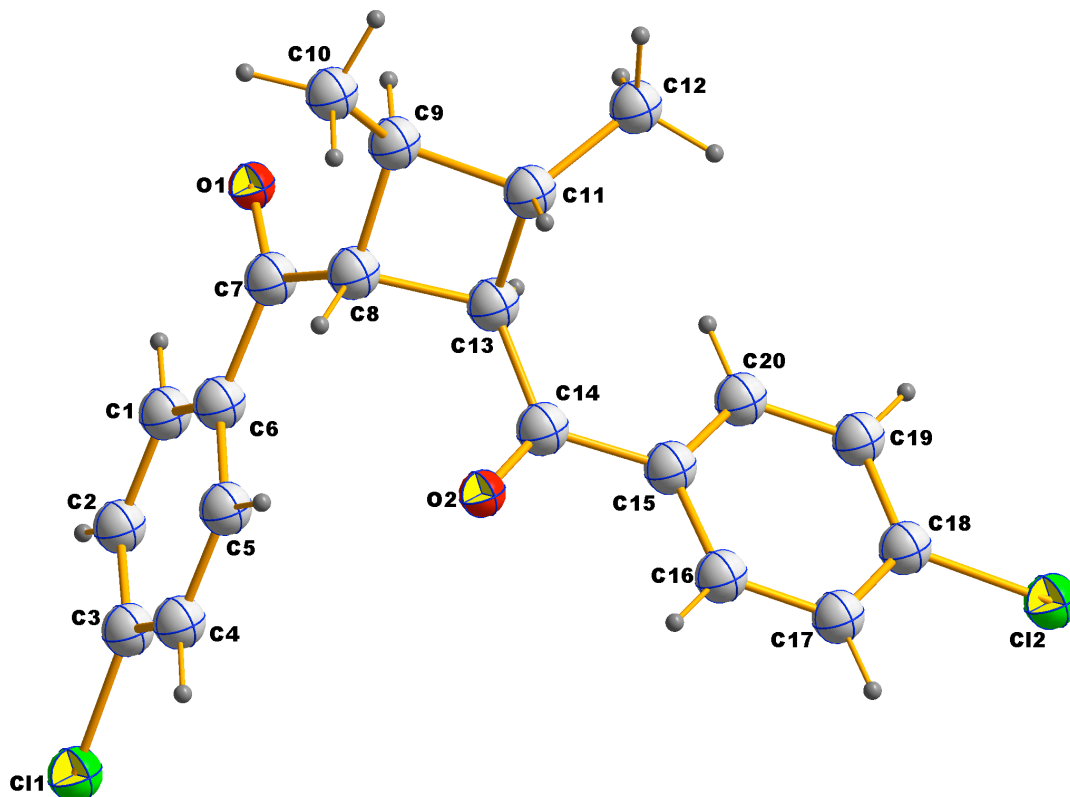


Figure 1. A molecular drawing of Yoon09 shown with 50% probability ellipsoids [3].



Table 1. Crystal data and structure refinement for Yoon09.

|                                   |  |                       |
|-----------------------------------|--|-----------------------|
| Identification code               | Yoon09   |                       |
| Empirical formula                 | C <sub>20</sub> H <sub>18</sub> Cl <sub>2</sub> O <sub>2</sub> |                       |
| Formula weight                    | 361.24   |                       |
| Temperature                       | 100(2) K   |                       |
| Wavelength                        | 1.54178 Å  |                       |
| Crystal system                    | Triclinic  |                       |
| Space group                       | P $\bar{1}$  |                       |
| Unit cell dimensions              | a = 8.400(4) Å   | $\alpha$ = 84.65(3)°. |
|                                   | b = 9.951(5) Å   | $\beta$ = 71.48(3)°.  |
|                                   | c = 11.472(7) Å  | $\gamma$ = 70.10(3)°. |
| Volume                            | 854.9(8) Å <sup>3</sup>  |                       |
| Z                                 | 2  |                       |
| Density (calculated)              | 1.403 Mg/m <sup>3</sup>  |                       |
| Absorption coefficient            | 3.485 mm <sup>-1</sup>   |                       |
| F(000)                            | 376  |                       |
| Crystal size                      | 0.36 x 0.30 x 0.28 mm <sup>3</sup>                             |                       |
| Theta range for data collection   | 4.06 to 69.88°.  |                       |
| Index ranges                      | -9 ≤ h ≤ 10, -12 ≤ k ≤ 12, -13 ≤ l ≤ 13                        |                       |
| Reflections collected             | 13686  |                       |
| Independent reflections           | 3070 [R(int) = 0.0227]   |                       |
| Completeness to theta = 69.88°    | 95.0 %   |                       |
| Absorption correction             | Empirical with SADABS  |                       |
| Max. and min. transmission        | 0.4420 and 0.3668  |                       |
| Refinement method                 | Full-matrix least-squares on F <sup>2</sup>                    |                       |
| Data / restraints / parameters    | 3070 / 0 / 219   |                       |
| Goodness-of-fit on F <sup>2</sup> | 0.998  |                       |
| Final R indices [I > 2σ(I)]       | R1 = 0.0290, wR2 = 0.0775                                      |                       |
| R indices (all data)              | R1 = 0.0297, wR2 = 0.0782                                      |                       |
| Largest diff. peak and hole       | 0.327 and -0.233 e.Å <sup>-3</sup>                             |                       |

Table 2. Atomic coordinates ( $\times 10^4$ ) and equivalent isotropic displacement parameters ( $\text{\AA}^2 \times 10^3$ ) for Yoon09.  $U(\text{eq})$  is defined as one third of the trace of the orthogonalized  $U^{ij}$  tensor.

|       | x       | y        | z       | U(eq) |
|-------|---------|----------|---------|-------|
| Cl(1) | 2557(1) | 9906(1)  | -880(1) | 19(1) |
| Cl(2) | 6594(1) | 10973(1) | 6897(1) | 22(1) |
| O(1)  | 4853(1) | 4075(1)  | 2440(1) | 20(1) |
| O(2)  | 8832(1) | 7018(1)  | 1871(1) | 18(1) |
| C(1)  | 3207(2) | 6459(2)  | 1230(1) | 16(1) |
| C(2)  | 2450(2) | 7619(2)  | 590(1)  | 17(1) |
| C(3)  | 3492(2) | 8413(1)  | -97(1)  | 15(1) |
| C(4)  | 5263(2) | 8066(2)  | -165(1) | 17(1) |
| C(5)  | 6002(2) | 6908(2)  | 489(1)  | 16(1) |
| C(6)  | 4985(2) | 6094(1)  | 1197(1) | 14(1) |
| C(7)  | 5716(2) | 4852(1)  | 1940(1) | 15(1) |
| C(8)  | 7486(2) | 4647(1)  | 2135(1) | 14(1) |
| C(9)  | 8322(2) | 3279(1)  | 2781(1) | 16(1) |
| C(10) | 9880(2) | 2114(2)  | 1993(1) | 21(1) |
| C(11) | 8711(2) | 4205(1)  | 3602(1) | 17(1) |
| C(12) | 8408(2) | 3856(2)  | 4952(1) | 22(1) |
| C(13) | 7353(2) | 5557(1)  | 3218(1) | 14(1) |
| C(14) | 7971(2) | 6840(1)  | 2916(1) | 14(1) |
| C(15) | 7620(2) | 7834(1)  | 3938(1) | 14(1) |
| C(16) | 8375(2) | 8926(1)  | 3676(1) | 16(1) |
| C(17) | 8076(2) | 9880(1)  | 4582(1) | 18(1) |
| C(18) | 7013(2) | 9741(1)  | 5764(1) | 17(1) |
| C(19) | 6279(2) | 8656(2)  | 6059(1) | 19(1) |
| C(20) | 6588(2) | 7704(2)  | 5139(1) | 17(1) |

Table 3. Bond lengths [Å] and angles [°] for Yoon09.

271

|                  |            |                     |            |
|------------------|------------|---------------------|------------|
| Cl(1)-C(3)       | 1.7426(15) | C(10)-H(10A)        | 0.9800     |
| Cl(2)-C(18)      | 1.7410(16) | C(10)-H(10B)        | 0.9800     |
| O(1)-C(7)        | 1.2200(17) | C(10)-H(10C)        | 0.9800     |
| O(2)-C(14)       | 1.2203(18) | C(11)-C(12)         | 1.515(2)   |
| C(1)-C(2)        | 1.384(2)   | C(11)-C(13)         | 1.5710(19) |
| C(1)-C(6)        | 1.400(2)   | C(11)-H(11)         | 1.0000     |
| C(1)-H(1)        | 0.9500     | C(12)-H(12A)        | 0.9800     |
| C(2)-C(3)        | 1.389(2)   | C(12)-H(12B)        | 0.9800     |
| C(2)-H(2)        | 0.9500     | C(12)-H(12C)        | 0.9800     |
| C(3)-C(4)        | 1.386(2)   | C(13)-C(14)         | 1.5080(19) |
| C(4)-C(5)        | 1.388(2)   | C(13)-H(13)         | 1.0000     |
| C(4)-H(4)        | 0.9500     | C(14)-C(15)         | 1.4955(19) |
| C(5)-C(6)        | 1.398(2)   | C(15)-C(20)         | 1.397(2)   |
| C(5)-H(5)        | 0.9500     | C(15)-C(16)         | 1.3999(19) |
| C(6)-C(7)        | 1.500(2)   | C(16)-C(17)         | 1.379(2)   |
| C(7)-C(8)        | 1.516(2)   | C(16)-H(16)         | 0.9500     |
| C(8)-C(9)        | 1.5447(19) | C(17)-C(18)         | 1.391(2)   |
| C(8)-C(13)       | 1.5588(19) | C(17)-H(17)         | 0.9500     |
| C(8)-H(8)        | 1.0000     | C(18)-C(19)         | 1.384(2)   |
| C(9)-C(10)       | 1.512(2)   | C(19)-C(20)         | 1.387(2)   |
| C(9)-C(11)       | 1.5507(19) | C(19)-H(19)         | 0.9500     |
| C(9)-H(9)        | 1.0000     | C(20)-H(20)         | 0.9500     |
| C(2)-C(1)-C(6)   | 120.91(12) | C(8)-C(9)-H(9)      | 110.2      |
| C(2)-C(1)-H(1)   | 119.5      | C(11)-C(9)-H(9)     | 110.2      |
| C(6)-C(1)-H(1)   | 119.5      | C(9)-C(10)-H(10A)   | 109.5      |
| C(1)-C(2)-C(3)   | 118.75(13) | C(9)-C(10)-H(10B)   | 109.5      |
| C(1)-C(2)-H(2)   | 120.6      | H(10A)-C(10)-H(10B) | 109.5      |
| C(3)-C(2)-H(2)   | 120.6      | C(9)-C(10)-H(10C)   | 109.5      |
| C(4)-C(3)-C(2)   | 121.77(13) | H(10A)-C(10)-H(10C) | 109.5      |
| C(4)-C(3)-Cl(1)  | 118.54(11) | H(10B)-C(10)-H(10C) | 109.5      |
| C(2)-C(3)-Cl(1)  | 119.69(11) | C(12)-C(11)-C(9)    | 118.60(12) |
| C(3)-C(4)-C(5)   | 118.91(13) | C(12)-C(11)-C(13)   | 119.08(12) |
| C(3)-C(4)-H(4)   | 120.5      | C(9)-C(11)-C(13)    | 88.54(10)  |
| C(5)-C(4)-H(4)   | 120.5      | C(12)-C(11)-H(11)   | 109.6      |
| C(4)-C(5)-C(6)   | 120.69(13) | C(9)-C(11)-H(11)    | 109.6      |
| C(4)-C(5)-H(5)   | 119.7      | C(13)-C(11)-H(11)   | 109.6      |
| C(6)-C(5)-H(5)   | 119.7      | C(11)-C(12)-H(12A)  | 109.5      |
| C(5)-C(6)-C(1)   | 118.96(13) | C(11)-C(12)-H(12B)  | 109.5      |
| C(5)-C(6)-C(7)   | 122.51(13) | H(12A)-C(12)-H(12B) | 109.5      |
| C(1)-C(6)-C(7)   | 118.53(12) | C(11)-C(12)-H(12C)  | 109.5      |
| O(1)-C(7)-C(6)   | 120.54(13) | H(12A)-C(12)-H(12C) | 109.5      |
| O(1)-C(7)-C(8)   | 120.55(12) | H(12B)-C(12)-H(12C) | 109.5      |
| C(6)-C(7)-C(8)   | 118.75(11) | C(14)-C(13)-C(8)    | 118.32(11) |
| C(7)-C(8)-C(9)   | 118.23(11) | C(14)-C(13)-C(11)   | 114.34(11) |
| C(7)-C(8)-C(13)  | 114.17(11) | C(8)-C(13)-C(11)    | 88.12(10)  |
| C(9)-C(8)-C(13)  | 89.20(10)  | C(14)-C(13)-H(13)   | 111.4      |
| C(7)-C(8)-H(8)   | 111.2      | C(8)-C(13)-H(13)    | 111.4      |
| C(9)-C(8)-H(8)   | 111.2      | C(11)-C(13)-H(13)   | 111.4      |
| C(13)-C(8)-H(8)  | 111.2      | O(2)-C(14)-C(15)    | 120.54(12) |
| C(10)-C(9)-C(8)  | 117.69(12) | O(2)-C(14)-C(13)    | 120.60(12) |
| C(10)-C(9)-C(11) | 117.75(12) | C(15)-C(14)-C(13)   | 118.73(12) |
| C(8)-C(9)-C(11)  | 89.36(10)  | C(20)-C(15)-C(16)   | 119.05(13) |
| C(10)-C(9)-H(9)  | 110.2      | C(20)-C(15)-C(14)   | 122.57(12) |

|                   |            |
|-------------------|------------|
| C(16)-C(15)-C(14) | 118.38(12) |
| C(17)-C(16)-C(15) | 120.65(13) |
| C(17)-C(16)-H(16) | 119.7      |
| C(15)-C(16)-H(16) | 119.7      |
| C(16)-C(17)-C(18) | 118.98(13) |
| C(16)-C(17)-H(17) | 120.5      |
| C(18)-C(17)-H(17) | 120.5      |
| C(19)-C(18)-C(17) | 121.78(13) |
| C(19)-C(18)-Cl(2) | 119.33(11) |
| C(17)-C(18)-Cl(2) | 118.89(11) |
| C(18)-C(19)-C(20) | 118.64(13) |
| C(18)-C(19)-H(19) | 120.7      |
| C(20)-C(19)-H(19) | 120.7      |
| C(19)-C(20)-C(15) | 120.88(13) |
| C(19)-C(20)-H(20) | 119.6      |
| C(15)-C(20)-H(20) | 119.6      |

---

Table 4. Anisotropic displacement parameters ( $\text{\AA}^2 \times 10^3$ ) for Yoon09. The anisotropic displacement factor exponent takes the form:  $-2\pi^2 [h^2 a^{*2} U^{11} + \dots + 2 h k a^* b^* U^{12}]$

|       | $U^{11}$ | $U^{22}$ | $U^{33}$ | $U^{23}$ | $U^{13}$ | $U^{12}$ |
|-------|----------|----------|----------|----------|----------|----------|
| Cl(1) | 17(1)    | 20(1)    | 19(1)    | 5(1)     | -7(1)    | -5(1)    |
| Cl(2) | 28(1)    | 19(1)    | 20(1)    | -5(1)    | -7(1)    | -6(1)    |
| O(1)  | 21(1)    | 21(1)    | 22(1)    | 6(1)     | -7(1)    | -12(1)   |
| O(2)  | 19(1)    | 21(1)    | 15(1)    | 2(1)     | -3(1)    | -10(1)   |
| C(1)  | 17(1)    | 19(1)    | 14(1)    | 0(1)     | -2(1)    | -9(1)    |
| C(2)  | 14(1)    | 22(1)    | 16(1)    | -1(1)    | -4(1)    | -6(1)    |
| C(3)  | 18(1)    | 16(1)    | 12(1)    | 0(1)     | -5(1)    | -4(1)    |
| C(4)  | 17(1)    | 18(1)    | 15(1)    | 1(1)     | -3(1)    | -8(1)    |
| C(5)  | 14(1)    | 19(1)    | 16(1)    | -1(1)    | -4(1)    | -6(1)    |
| C(6)  | 16(1)    | 16(1)    | 12(1)    | -2(1)    | -3(1)    | -6(1)    |
| C(7)  | 16(1)    | 15(1)    | 12(1)    | -2(1)    | -2(1)    | -6(1)    |
| C(8)  | 15(1)    | 13(1)    | 13(1)    | 1(1)     | -3(1)    | -5(1)    |
| C(9)  | 16(1)    | 15(1)    | 17(1)    | 2(1)     | -5(1)    | -6(1)    |
| C(10) | 20(1)    | 18(1)    | 23(1)    | 0(1)     | -5(1)    | -2(1)    |
| C(11) | 16(1)    | 15(1)    | 19(1)    | 2(1)     | -6(1)    | -5(1)    |
| C(12) | 29(1)    | 20(1)    | 21(1)    | 4(1)     | -12(1)   | -8(1)    |
| C(13) | 14(1)    | 14(1)    | 13(1)    | 1(1)     | -3(1)    | -5(1)    |
| C(14) | 10(1)    | 15(1)    | 17(1)    | 2(1)     | -6(1)    | -3(1)    |
| C(15) | 13(1)    | 14(1)    | 17(1)    | 2(1)     | -6(1)    | -4(1)    |
| C(16) | 16(1)    | 17(1)    | 16(1)    | 4(1)     | -6(1)    | -6(1)    |
| C(17) | 20(1)    | 14(1)    | 21(1)    | 4(1)     | -9(1)    | -7(1)    |
| C(18) | 18(1)    | 14(1)    | 19(1)    | -2(1)    | -8(1)    | -2(1)    |
| C(19) | 19(1)    | 21(1)    | 16(1)    | 0(1)     | -3(1)    | -7(1)    |
| C(20) | 17(1)    | 17(1)    | 18(1)    | 2(1)     | -5(1)    | -8(1)    |

Table 5. Hydrogen coordinates ( $\times 10^4$ ) and isotropic displacement parameters ( $\text{\AA}^2 \times 10^{-3}$ ) for Yoon09.

|        | x     | y     | z    | U(eq) |
|--------|-------|-------|------|-------|
| H(1)   | 2511  | 5903  | 1699 | 20    |
| H(2)   | 1241  | 7867  | 620  | 20    |
| H(4)   | 5960  | 8612  | -653 | 20    |
| H(5)   | 7211  | 6665  | 456  | 20    |
| H(8)   | 8367  | 4802  | 1358 | 17    |
| H(9)   | 7382  | 2877  | 3286 | 19    |
| H(10A) | 9467  | 1665  | 1474 | 32    |
| H(10B) | 10418 | 1393  | 2522 | 32    |
| H(10C) | 10765 | 2528  | 1472 | 32    |
| H(11)  | 9945  | 4239  | 3223 | 20    |
| H(12A) | 7198  | 3822  | 5320 | 34    |
| H(12B) | 8562  | 4595  | 5372 | 34    |
| H(12C) | 9267  | 2926  | 5038 | 34    |
| H(13)  | 6149  | 5803  | 3843 | 17    |
| H(16)  | 9100  | 9010  | 2866 | 19    |
| H(17)  | 8588  | 10621 | 4402 | 21    |
| H(19)  | 5577  | 8564  | 6875 | 23    |
| H(20)  | 6091  | 6954  | 5328 | 21    |

Table 6. Torsion angles [°] for Yoon09.

|                         |             |
|-------------------------|-------------|
| C(6)-C(1)-C(2)-C(3)     | 0.5(2)      |
| C(1)-C(2)-C(3)-C(4)     | 0.6(2)      |
| C(1)-C(2)-C(3)-Cl(1)    | -178.37(10) |
| C(2)-C(3)-C(4)-C(5)     | -1.2(2)     |
| Cl(1)-C(3)-C(4)-C(5)    | 177.84(10)  |
| C(3)-C(4)-C(5)-C(6)     | 0.6(2)      |
| C(4)-C(5)-C(6)-C(1)     | 0.4(2)      |
| C(4)-C(5)-C(6)-C(7)     | -178.68(12) |
| C(2)-C(1)-C(6)-C(5)     | -1.0(2)     |
| C(2)-C(1)-C(6)-C(7)     | 178.15(12)  |
| C(5)-C(6)-C(7)-O(1)     | -172.11(13) |
| C(1)-C(6)-C(7)-O(1)     | 8.81(19)    |
| C(5)-C(6)-C(7)-C(8)     | 12.30(19)   |
| C(1)-C(6)-C(7)-C(8)     | -166.77(12) |
| O(1)-C(7)-C(8)-C(9)     | 10.86(19)   |
| C(6)-C(7)-C(8)-C(9)     | -173.55(11) |
| O(1)-C(7)-C(8)-C(13)    | -92.05(16)  |
| C(6)-C(7)-C(8)-C(13)    | 83.53(15)   |
| C(7)-C(8)-C(9)-C(10)    | 104.86(15)  |
| C(13)-C(8)-C(9)-C(10)   | -137.94(12) |
| C(7)-C(8)-C(9)-C(11)    | -133.82(12) |
| C(13)-C(8)-C(9)-C(11)   | -16.61(10)  |
| C(10)-C(9)-C(11)-C(12)  | -99.57(16)  |
| C(8)-C(9)-C(11)-C(12)   | 139.15(13)  |
| C(10)-C(9)-C(11)-C(13)  | 137.76(12)  |
| C(8)-C(9)-C(11)-C(13)   | 16.48(10)   |
| C(7)-C(8)-C(13)-C(14)   | -105.99(14) |
| C(9)-C(8)-C(13)-C(14)   | 133.19(12)  |
| C(7)-C(8)-C(13)-C(11)   | 137.21(11)  |
| C(9)-C(8)-C(13)-C(11)   | 16.40(10)   |
| C(12)-C(11)-C(13)-C(14) | 101.01(14)  |
| C(9)-C(11)-C(13)-C(14)  | -136.74(11) |
| C(12)-C(11)-C(13)-C(8)  | -138.59(12) |
| C(9)-C(11)-C(13)-C(8)   | -16.33(10)  |
| C(8)-C(13)-C(14)-O(2)   | -12.58(18)  |
| C(11)-C(13)-C(14)-O(2)  | 89.12(15)   |
| C(8)-C(13)-C(14)-C(15)  | 171.61(11)  |
| C(11)-C(13)-C(14)-C(15) | -86.69(15)  |
| O(2)-C(14)-C(15)-C(20)  | 177.59(12)  |
| C(13)-C(14)-C(15)-C(20) | -6.60(18)   |
| O(2)-C(14)-C(15)-C(16)  | -3.13(18)   |
| C(13)-C(14)-C(15)-C(16) | 172.68(11)  |
| C(20)-C(15)-C(16)-C(17) | -1.38(19)   |
| C(14)-C(15)-C(16)-C(17) | 179.32(12)  |
| C(15)-C(16)-C(17)-C(18) | 0.1(2)      |
| C(16)-C(17)-C(18)-C(19) | 1.3(2)      |
| C(16)-C(17)-C(18)-Cl(2) | -178.46(10) |
| C(17)-C(18)-C(19)-C(20) | -1.4(2)     |
| Cl(2)-C(18)-C(19)-C(20) | 178.39(10)  |
| C(18)-C(19)-C(20)-C(15) | 0.0(2)      |
| C(16)-C(15)-C(20)-C(19) | 1.3(2)      |
| C(14)-C(15)-C(20)-C(19) | -179.42(12) |

Symmetry transformations used to generate equivalent atoms:

### ***Data Collection***

A colorless crystal with approximate dimensions 0.52 x 0.13 x 0.10 mm<sup>3</sup> was selected under oil under ambient conditions and attached to the tip of a MiTeGen MicroMount<sup>®</sup>. The crystal was mounted in a stream of cold nitrogen at 100(1) K and centered in the X-ray beam by using a video camera.

The crystal evaluation and data collection were performed on a Bruker SMART APEXII diffractometer with Cu K $\alpha$  ( $\lambda = 1.54178$  Å) radiation and the diffractometer to crystal distance of 4.03 cm.

The initial cell constants were obtained from three series of  $\omega$  scans at different starting angles. Each series consisted of 41 frames collected at intervals of 0.6° in a 25° range about  $\omega$  with the exposure time of 3 seconds per frame. The reflections were successfully indexed by an automated indexing routine built in the APEXII program. The final cell constants were calculated from a set of 9853 strong reflections from the actual data collection.

The data were collected by using the full sphere data collection routine to survey the reciprocal space to the extent of a full sphere to a resolution of 0.82 Å. A total of 22130 data were harvested by collecting 19 sets of frames with 0.6° scans in  $\omega$  with an exposure time 5/12 sec per frame. These highly redundant datasets were corrected for Lorentz and polarization effects. The absorption correction was based on fitting a function to the empirical transmission surface as sampled by multiple equivalent measurements. [1]

### **Structure Solution and Refinement**

The systematic absences in the diffraction data and the  $E$ -statistics were consistent for the space groups  $Pna2_1$  that yielded chemically reasonable and computationally stable results of refinement [2-4].

A successful solution by the direct methods provided most non-hydrogen atoms from the  $E$ -map. The remaining non-hydrogen atoms were located in an alternating series of least-squares cycles and difference Fourier maps. All non-hydrogen atoms were refined with anisotropic displacement coefficients. All hydrogen atoms were included in the structure factor calculation



at idealized positions and were allowed to ride on the neighboring atoms with relative277 isotropic displacement coefficients.

The space group is asymmetric, but S,S and R,R diastereomers are present.

The final least-squares refinement of 209 parameters against 3010 data resulted in residuals  $R$  (based on  $F^2$  for  $I \geq 2\sigma$ ) and  $wR$  (based on  $F^2$  for all data) of 0.0285 and 0.0797, respectively. The final difference Fourier map was featureless.

The molecular diagram is drawn with 50% probability ellipsoids.

## References

- [1] Bruker-AXS. (2007) APEX2, SADABS, and SAINT Software Reference Manuals. Bruker-AXS, Madison, Wisconsin, USA.
- [2] Sheldrick, G. M. (2008) SHELXL. *Acta Cryst.* **A64**, 112-122.
- [3] Dolomanov, O.V.; Bourhis, L.J.; Gildea, R.J.; Howard, J.A.K.; Puschmann, H. "OLEX2: a complete structure solution, refinement and analysis program". *J. Appl. Cryst.* (2009) **42**, 339-341.
- [4] Guzei, I.A. (2006-2008). Internal laboratory computer programs "Inserter", "FCF\_filter", "Modicifer".

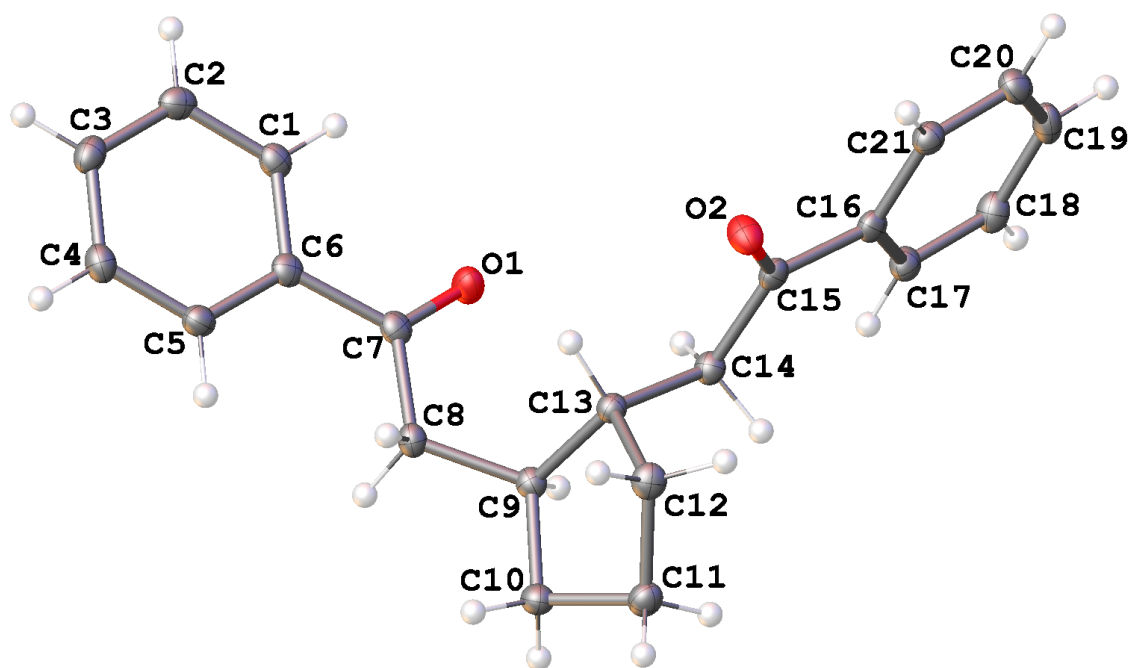


Figure 1. A molecular drawing of Yoon25.

Table 1. Crystal data and structure refinement for yoon25.

|                                      |  |          |
|--------------------------------------|--|----------|
| Identification code                  | yoon25   |          |
| Empirical formula                    | C <sub>21</sub> H <sub>22</sub> O <sub>2</sub> |          |
| Formula weight                       | 306.39   |          |
| Temperature                          | 100(1) K                                       |          |
| Wavelength                           | 1.54178 Å                                      |          |
| Crystal system                       | Orthorhombic                                   |          |
| Space group                          | Pna2 <sub>1</sub>                              |          |
| Unit cell dimensions                 | a = 18.0449(4) Å                               | α = 90°. |
|                                      | b = 16.5511(4) Å                               | β = 90°. |
|                                      | c = 5.37980(10) Å                              | γ = 90°. |
| Volume                               | 1606.75(6) Å <sup>3</sup>                      |          |
| Z                                    | 4  |          |
| Density (calculated)                 | 1.267 Mg/m <sup>3</sup>                        |          |
| Absorption coefficient               | 0.625 mm <sup>-1</sup>                         |          |
| F(000)                               | 656  |          |
| Crystal size                         | 0.10 x 0.13 x 0.52 mm <sup>3</sup>             |          |
| Theta range for data collection      | 3.62 to 69.53°.                                |          |
| Index ranges                         | -21 ≤ h ≤ 21, -19 ≤ k ≤ 17, -6 ≤ l ≤ 6         |          |
| Reflections collected                | 23965  |          |
| Independent reflections              | 3010 [R(int) = 0.0236]                         |          |
| Completeness to theta = 69.53°       | 99.8 %   |          |
| Absorption correction                | Numerical with SADABS                          |          |
| Max. and min. transmission           | 0.9379 and 0.7358                              |          |
| Refinement method                    | Full-matrix least-squares on F <sup>2</sup>    |          |
| Data / restraints / parameters       | 3010 / 1 / 209                                 |          |
| Goodness-of-fit on F <sup>2</sup>    | 1.029  |          |
| Final R indices [I > 2σ(I)]          | R1 = 0.0285, wR2 = 0.0786                      |          |
| R indices (all data)                 | R1 = 0.0292, wR2 = 0.0797                      |          |
| Absolute structure parameter Flack x | -0.05(17)                                      |          |
| Absolute structure parameter Hooft y | -0.04(4)                                       |          |
| Largest diff. peak and hole          | 0.198 and -0.176 e.Å <sup>-3</sup>             |          |

Table 2. Atomic coordinates ( $\times 10^4$ ) and equivalent isotropic displacement parameters ( $\text{\AA}^2 \times 10^3$ ) for yoon25.  $U(\text{eq})$  is defined as one third of the trace of the orthogonalized  $U^{\text{ij}}$  tensor.

|       | x       | y       | z        | U(eq) |
|-------|---------|---------|----------|-------|
| O(1)  | 7561(1) | 9379(1) | 2275(2)  | 22(1) |
| O(2)  | 5555(1) | 7847(1) | 288(2)   | 22(1) |
| C(1)  | 8544(1) | 9695(1) | -1652(2) | 18(1) |
| C(2)  | 9052(1) | 9840(1) | -3532(3) | 20(1) |
| C(3)  | 9679(1) | 9355(1) | -3749(3) | 20(1) |
| C(4)  | 9793(1) | 8725(1) | -2084(3) | 20(1) |
| C(5)  | 9282(1) | 8577(1) | -208(2)  | 18(1) |
| C(6)  | 8648(1) | 9058(1) | 20(2)    | 17(1) |
| C(7)  | 8071(1) | 8908(1) | 1983(2)  | 17(1) |
| C(8)  | 8144(1) | 8147(1) | 3540(2)  | 16(1) |
| C(9)  | 7462(1) | 7936(1) | 5081(2)  | 16(1) |
| C(10) | 7609(1) | 7167(1) | 6659(2)  | 18(1) |
| C(11) | 6880(1) | 6694(1) | 6595(2)  | 20(1) |
| C(12) | 6613(1) | 6834(1) | 3924(2)  | 19(1) |
| C(13) | 6770(1) | 7739(1) | 3447(2)  | 15(1) |
| C(14) | 6106(1) | 8272(1) | 4108(2)  | 16(1) |
| C(15) | 5493(1) | 8247(1) | 2182(2)  | 16(1) |
| C(16) | 4808(1) | 8747(1) | 2587(2)  | 16(1) |
| C(17) | 4723(1) | 9246(1) | 4654(2)  | 18(1) |
| C(18) | 4095(1) | 9733(1) | 4867(3)  | 21(1) |
| C(19) | 3556(1) | 9726(1) | 3031(3)  | 22(1) |
| C(20) | 3633(1) | 9220(1) | 984(3)   | 21(1) |
| C(21) | 4255(1) | 8731(1) | 769(2)   | 18(1) |

Table 3. Bond lengths [Å] and angles [°] for yoon25.

281

|                  |            |                     |            |
|------------------|------------|---------------------|------------|
| O(1)-C(7)        | 1.2171(14) | C(11)-C(12)         | 1.5329(18) |
| O(2)-C(15)       | 1.2207(16) | C(11)-H(11B)        | 0.9900     |
| C(1)-C(2)        | 1.3862(19) | C(11)-H(11A)        | 0.9900     |
| C(1)-C(6)        | 1.3979(17) | C(12)-C(13)         | 1.5464(16) |
| C(1)-H(1)        | 0.9500     | C(12)-H(12A)        | 0.9900     |
| C(2)-C(3)        | 1.3919(18) | C(12)-H(12B)        | 0.9900     |
| C(2)-H(2)        | 0.9500     | C(13)-C(14)         | 1.5296(15) |
| C(3)-C(4)        | 1.390(2)   | C(13)-H(13)         | 1.0000     |
| C(3)-H(3)        | 0.9500     | C(14)-C(15)         | 1.5152(16) |
| C(4)-C(5)        | 1.3886(19) | C(14)-H(14A)        | 0.9900     |
| C(4)-H(4)        | 0.9500     | C(14)-H(14B)        | 0.9900     |
| C(5)-C(6)        | 1.3984(17) | C(15)-C(16)         | 1.5040(16) |
| C(5)-H(5)        | 0.9500     | C(16)-C(21)         | 1.3970(18) |
| C(6)-C(7)        | 1.5039(17) | C(16)-C(17)         | 1.3940(18) |
| C(7)-C(8)        | 1.5188(17) | C(17)-C(18)         | 1.3951(17) |
| C(8)-C(9)        | 1.5238(16) | C(17)-H(17)         | 0.9500     |
| C(8)-H(8B)       | 0.9900     | C(18)-C(19)         | 1.3855(19) |
| C(8)-H(8A)       | 0.9900     | C(18)-H(18)         | 0.9500     |
| C(9)-C(10)       | 1.5524(16) | C(19)-C(20)         | 1.390(2)   |
| C(9)-C(13)       | 1.5624(16) | C(19)-H(19)         | 0.9500     |
| C(9)-H(9)        | 1.0000     | C(20)-C(21)         | 1.3892(17) |
| C(10)-C(11)      | 1.5299(16) | C(20)-H(20)         | 0.9500     |
| C(10)-H(10A)     | 0.9900     | C(21)-H(21)         | 0.9500     |
| C(10)-H(10B)     | 0.9900     |                     |            |
| C(2)-C(1)-C(6)   | 120.73(11) | C(10)-C(9)-C(13)    | 105.85(9)  |
| C(2)-C(1)-H(1)   | 119.6      | C(8)-C(9)-H(9)      | 109.2      |
| C(6)-C(1)-H(1)   | 119.6      | C(10)-C(9)-H(9)     | 109.2      |
| C(1)-C(2)-C(3)   | 119.91(12) | C(13)-C(9)-H(9)     | 109.2      |
| C(1)-C(2)-H(2)   | 120.0      | C(11)-C(10)-C(9)    | 105.12(9)  |
| C(3)-C(2)-H(2)   | 120.0      | C(11)-C(10)-H(10A)  | 110.7      |
| C(2)-C(3)-C(4)   | 119.89(12) | C(9)-C(10)-H(10A)   | 110.7      |
| C(2)-C(3)-H(3)   | 120.1      | C(11)-C(10)-H(10B)  | 110.7      |
| C(4)-C(3)-H(3)   | 120.1      | C(9)-C(10)-H(10B)   | 110.7      |
| C(5)-C(4)-C(3)   | 120.22(12) | H(10A)-C(10)-H(10B) | 108.8      |
| C(5)-C(4)-H(4)   | 119.9      | C(12)-C(11)-C(10)   | 102.39(10) |
| C(3)-C(4)-H(4)   | 119.9      | C(12)-C(11)-H(11B)  | 111.3      |
| C(4)-C(5)-C(6)   | 120.35(12) | C(10)-C(11)-H(11B)  | 111.3      |
| C(4)-C(5)-H(5)   | 119.8      | C(12)-C(11)-H(11A)  | 111.3      |
| C(6)-C(5)-H(5)   | 119.8      | C(10)-C(11)-H(11A)  | 111.3      |
| C(1)-C(6)-C(5)   | 118.89(11) | H(11B)-C(11)-H(11A) | 109.2      |
| C(1)-C(6)-C(7)   | 118.88(10) | C(11)-C(12)-C(13)   | 104.15(10) |
| C(5)-C(6)-C(7)   | 122.23(11) | C(11)-C(12)-H(12A)  | 110.9      |
| O(1)-C(7)-C(6)   | 120.60(11) | C(13)-C(12)-H(12A)  | 110.9      |
| O(1)-C(7)-C(8)   | 121.72(11) | C(11)-C(12)-H(12B)  | 110.9      |
| C(6)-C(7)-C(8)   | 117.67(10) | C(13)-C(12)-H(12B)  | 110.9      |
| C(7)-C(8)-C(9)   | 114.89(10) | H(12A)-C(12)-H(12B) | 108.9      |
| C(7)-C(8)-H(8B)  | 108.5      | C(14)-C(13)-C(12)   | 112.11(9)  |
| C(9)-C(8)-H(8B)  | 108.5      | C(14)-C(13)-C(9)    | 112.08(10) |
| C(7)-C(8)-H(8A)  | 108.5      | C(12)-C(13)-C(9)    | 104.75(9)  |
| C(9)-C(8)-H(8A)  | 108.5      | C(14)-C(13)-H(13)   | 109.3      |
| H(8B)-C(8)-H(8A) | 107.5      | C(12)-C(13)-H(13)   | 109.3      |
| C(8)-C(9)-C(10)  | 110.40(9)  | C(9)-C(13)-H(13)    | 109.3      |
| C(8)-C(9)-C(13)  | 112.78(10) | C(15)-C(14)-C(13)   | 113.39(10) |

|                     |            |
|---------------------|------------|
| C(15)-C(14)-H(14A)  | 108.9      |
| C(13)-C(14)-H(14A)  | 108.9      |
| C(15)-C(14)-H(14B)  | 108.9      |
| C(13)-C(14)-H(14B)  | 108.9      |
| H(14A)-C(14)-H(14B) | 107.7      |
| O(2)-C(15)-C(16)    | 119.61(11) |
| O(2)-C(15)-C(14)    | 121.29(10) |
| C(16)-C(15)-C(14)   | 119.08(10) |
| C(21)-C(16)-C(17)   | 119.41(11) |
| C(21)-C(16)-C(15)   | 118.37(11) |
| C(17)-C(16)-C(15)   | 122.17(11) |
| C(18)-C(17)-C(16)   | 119.82(12) |
| C(18)-C(17)-H(17)   | 120.1      |
| C(16)-C(17)-H(17)   | 120.1      |
| C(19)-C(18)-C(17)   | 120.41(12) |
| C(19)-C(18)-H(18)   | 119.8      |
| C(17)-C(18)-H(18)   | 119.8      |
| C(18)-C(19)-C(20)   | 120.00(12) |
| C(18)-C(19)-H(19)   | 120.0      |
| C(20)-C(19)-H(19)   | 120.0      |
| C(19)-C(20)-C(21)   | 119.83(12) |
| C(19)-C(20)-H(20)   | 120.1      |
| C(21)-C(20)-H(20)   | 120.1      |
| C(20)-C(21)-C(16)   | 120.50(12) |
| C(20)-C(21)-H(21)   | 119.7      |
| C(16)-C(21)-H(21)   | 119.7      |

---

Symmetry transformations used to generate  
equivalent atoms:

Table 4. Anisotropic displacement parameters ( $\text{\AA}^2 \times 10^3$ ) for yoon25. The anisotropic displacement factor exponent takes the form:  $-2\pi^2 [h^2 a^{*2} U^{11} + \dots + 2 h k a^* b^* U^{12}]$

|       | U <sup>11</sup> | U <sup>22</sup> | U <sup>33</sup> | U <sup>23</sup> | U <sup>13</sup> | U <sup>12</sup> |
|-------|-----------------|-----------------|-----------------|-----------------|-----------------|-----------------|
| O(1)  | 18(1)           | 20(1)           | 27(1)           | 4(1)            | 4(1)            | 3(1)            |
| O(2)  | 20(1)           | 27(1)           | 19(1)           | -7(1)           | -2(1)           | 2(1)            |
| C(1)  | 16(1)           | 15(1)           | 22(1)           | -1(1)           | -2(1)           | -2(1)           |
| C(2)  | 22(1)           | 17(1)           | 21(1)           | 2(1)            | -5(1)           | -5(1)           |
| C(3)  | 19(1)           | 24(1)           | 18(1)           | -1(1)           | 2(1)            | -6(1)           |
| C(4)  | 15(1)           | 22(1)           | 24(1)           | -2(1)           | 0(1)            | 0(1)            |
| C(5)  | 17(1)           | 17(1)           | 20(1)           | 2(1)            | -2(1)           | -1(1)           |
| C(6)  | 15(1)           | 16(1)           | 18(1)           | -2(1)           | -3(1)           | -4(1)           |
| C(7)  | 15(1)           | 17(1)           | 19(1)           | -2(1)           | -3(1)           | -2(1)           |
| C(8)  | 14(1)           | 17(1)           | 19(1)           | -1(1)           | 0(1)            | 0(1)            |
| C(9)  | 15(1)           | 16(1)           | 16(1)           | -1(1)           | 0(1)            | 0(1)            |
| C(10) | 18(1)           | 20(1)           | 17(1)           | 2(1)            | -1(1)           | 1(1)            |
| C(11) | 20(1)           | 18(1)           | 21(1)           | 2(1)            | 2(1)            | -1(1)           |
| C(12) | 20(1)           | 16(1)           | 21(1)           | -2(1)           | 0(1)            | -2(1)           |
| C(13) | 15(1)           | 15(1)           | 14(1)           | 0(1)            | 0(1)            | -1(1)           |
| C(14) | 16(1)           | 17(1)           | 16(1)           | -1(1)           | 1(1)            | -1(1)           |
| C(15) | 16(1)           | 15(1)           | 17(1)           | 1(1)            | 2(1)            | -3(1)           |
| C(16) | 15(1)           | 15(1)           | 18(1)           | 2(1)            | 1(1)            | -4(1)           |
| C(17) | 16(1)           | 20(1)           | 18(1)           | 0(1)            | 0(1)            | -3(1)           |
| C(18) | 20(1)           | 18(1)           | 24(1)           | -4(1)           | 4(1)            | -2(1)           |
| C(19) | 15(1)           | 19(1)           | 32(1)           | 2(1)            | 4(1)            | 2(1)            |
| C(20) | 17(1)           | 24(1)           | 24(1)           | 2(1)            | -3(1)           | -2(1)           |
| C(21) | 18(1)           | 18(1)           | 17(1)           | 0(1)            | 0(1)            | -3(1)           |

Table 5. Hydrogen coordinates ( $\times 10^4$ ) and isotropic displacement parameters ( $\text{\AA}^2 \times 10^{-3}$ ) for yoon25.

|        | x     | y     | z     | U(eq) |
|--------|-------|-------|-------|-------|
| H(1)   | 8120  | 10031 | -1498 | 21    |
| H(2)   | 8973  | 10270 | -4670 | 24    |
| H(3)   | 10028 | 9454  | -5034 | 25    |
| H(4)   | 10221 | 8395  | -2229 | 24    |
| H(5)   | 9363  | 8146  | 927   | 22    |
| H(8B)  | 8572  | 8211  | 4675  | 20    |
| H(8A)  | 8255  | 7688  | 2419  | 20    |
| H(9)   | 7343  | 8397  | 6213  | 19    |
| H(10A) | 8017  | 6844  | 5935  | 22    |
| H(10B) | 7741  | 7313  | 8387  | 22    |
| H(11B) | 6963  | 6112  | 6926  | 24    |
| H(11A) | 6521  | 6909  | 7819  | 24    |
| H(12A) | 6077  | 6715  | 3768  | 23    |
| H(12B) | 6890  | 6490  | 2740  | 23    |
| H(13)  | 6898  | 7818  | 1655  | 18    |
| H(14A) | 5903  | 8094  | 5728  | 20    |
| H(14B) | 6277  | 8836  | 4298  | 20    |
| H(17)  | 5092  | 9256  | 5914  | 22    |
| H(18)  | 4036  | 10071 | 6280  | 25    |
| H(19)  | 3135  | 10066 | 3171  | 26    |
| H(20)  | 3261  | 9209  | -264  | 26    |
| H(21)  | 4306  | 8383  | -626  | 21    |



Table 6. Torsion angles [ $^{\circ}$ ] for yoon25.

|                         |             |
|-------------------------|-------------|
| C(6)-C(1)-C(2)-C(3)     | -0.76(18)   |
| C(1)-C(2)-C(3)-C(4)     | 0.10(19)    |
| C(2)-C(3)-C(4)-C(5)     | 0.2(2)      |
| C(3)-C(4)-C(5)-C(6)     | 0.10(19)    |
| C(2)-C(1)-C(6)-C(5)     | 1.07(18)    |
| C(2)-C(1)-C(6)-C(7)     | -178.23(11) |
| C(4)-C(5)-C(6)-C(1)     | -0.73(17)   |
| C(4)-C(5)-C(6)-C(7)     | 178.53(12)  |
| C(1)-C(6)-C(7)-O(1)     | -7.32(17)   |
| C(5)-C(6)-C(7)-O(1)     | 173.41(11)  |
| C(1)-C(6)-C(7)-C(8)     | 171.75(11)  |
| C(5)-C(6)-C(7)-C(8)     | -7.52(16)   |
| O(1)-C(7)-C(8)-C(9)     | 11.86(16)   |
| C(6)-C(7)-C(8)-C(9)     | -167.20(10) |
| C(7)-C(8)-C(9)-C(10)    | -178.06(10) |
| C(7)-C(8)-C(9)-C(13)    | 63.77(13)   |
| C(8)-C(9)-C(10)-C(11)   | -141.42(10) |
| C(13)-C(9)-C(10)-C(11)  | -19.08(12)  |
| C(9)-C(10)-C(11)-C(12)  | 37.74(12)   |
| C(10)-C(11)-C(12)-C(13) | -42.22(11)  |
| C(11)-C(12)-C(13)-C(14) | -91.52(12)  |
| C(11)-C(12)-C(13)-C(9)  | 30.26(12)   |
| C(8)-C(9)-C(13)-C(14)   | -124.26(11) |
| C(10)-C(9)-C(13)-C(14)  | 114.93(10)  |
| C(8)-C(9)-C(13)-C(12)   | 113.95(11)  |
| C(10)-C(9)-C(13)-C(12)  | -6.86(12)   |
| C(12)-C(13)-C(14)-C(15) | -76.73(13)  |
| C(9)-C(13)-C(14)-C(15)  | 165.80(9)   |
| C(13)-C(14)-C(15)-O(2)  | -1.52(16)   |
| C(13)-C(14)-C(15)-C(16) | -179.65(10) |
| O(2)-C(15)-C(16)-C(21)  | 0.47(16)    |
| C(14)-C(15)-C(16)-C(21) | 178.63(11)  |
| O(2)-C(15)-C(16)-C(17)  | -176.78(11) |
| C(14)-C(15)-C(16)-C(17) | 1.38(16)    |
| C(21)-C(16)-C(17)-C(18) | -0.96(18)   |
| C(15)-C(16)-C(17)-C(18) | 176.27(11)  |
| C(16)-C(17)-C(18)-C(19) | -0.31(18)   |
| C(17)-C(18)-C(19)-C(20) | 1.24(19)    |
| C(18)-C(19)-C(20)-C(21) | -0.89(19)   |
| C(19)-C(20)-C(21)-C(16) | -0.39(19)   |
| C(17)-C(16)-C(21)-C(20) | 1.31(18)    |
| C(15)-C(16)-C(21)-C(20) | -176.02(11) |

Symmetry transformations used to generate equivalent atoms: